NOAA Technical Report NOS CS 34

HYDRODYNAMIC MODEL DEVELOPMENT FOR THE SAN FRANCISCO BAY OPERATIONAL FORECAST SYSTEM (SFBOFS)

Silver Spring, Maryland
June 2014

noaa National Oceanic and Atmospheric Administration

U.S. DEPARTMENT OF COMMERCE
National Ocean Service
Coast Survey Development Laboratory

Office of Coast Survey
National Ocean Service
National Oceanic and Atmospheric Administration
U.S. Department of Commerce

The Office of Coast Survey (OCS) is the Nation's only official chartmaker. As the oldest United States scientific organization, dating from 1807, this office has a long history. Today it promotes safe navigation by managing the National Oceanic and Atmospheric Administration's (NOAA) nautical chart and oceanographic data collection and information programs.

There are four components of OCS:

The Coast Survey Development Laboratory develops new and efficient techniques to accomplish Coast Survey missions and to produce new and improved products and services for the maritime community and other coastal users.

The Marine Chart Division acquires marine navigational data to construct and maintain nautical charts, Coast Pilots, and related marine products for the United States.

The Hydrographic Surveys Division directs programs for ship and shore-based hydrographic survey units and conducts general hydrographic survey operations.

The Navigational Services Division is the focal point for Coast Survey customer service activities, concentrating predominately on charting issues, fast-response hydrographic surveys, and Coast Pilot updates.

NOAA Technical Report NOS CS 34

HYDRODYNAMIC MODEL DEVELOPMENT FOR THE SAN FRANCISCO BAY OPERATIONAL FORECAST SYSTEM (SFBOFS)

Richard A. Schmalz, Jr.
Office of Coast Survey, Coast Survey Development Laboratory
Silver Spring, Maryland

June 2014

noaa National Oceanic and Atmospheric Administration

U. S. DEPARTMENT OF COMMERCE Penny Pritzker Secretary	National Oceanic and Atmospheric Administration Dr. Kathryn D. Sullivan, Under Secretary	National Ocean Service Dr. Holly A. Bamford, Assistant Administrator

Office of Coast Survey Rear Admiral Gerd F. Glang	Coast Survey Development Laboratory Dr. Jesse C. Feyen Acting Director

NOTICE

Mention of a commercial company or product does not constitute an endorsement by NOAA. Use for publicity or advertising purposes of information from this publication concerning proprietary products or the tests of such products is not authorized.

TABLE OF CONTENTS

LIST OF FIGURES

LIST OF TABLES

EXECUTIVE SUMMARY

The National Ocean Service's (NOS) San Francisco Bay Operational Forecast System (SFBOFS) has been developed using the FVCOM (Finite Volume Coastal Ocean Model) three-dimensional hydrodynamic model (Chen et al., 2006c). The domain for this new system extends from the offshore region through the entrance to San Francisco Bay and contains the entire South, Central, and North Bays, San Pablo Bay, Carquinez Strait, and Suisun Bay. It further extends to Rio Vista, California, on the Sacramento River and to Antioch, California, on the San Joaquin River in the Delta. For purpose of this report, the Delta area refers to the area shown in Figure 2.1. The system is run on the National Centers for Environmental Prediction (NCEP) supercomputers based on a recently developed High Performance Computing Coastal Ocean Modeling Framework (COMF-HPC) (Zhang et al., 2010) to allow four times daily 6-hour nowcasts and 48-hour forecasts.

Initial FVCOM tidal simulation results using a net heat flux algorithm are presented for 1-15 April 1979. Next, FVCOM modifications to enable bulk heat flux computation, a reduced minimum depth, and restart are discussed. Tidal and hindcast simulations for April – May 1979 and September – October 1980 are presented using these modifications. In an effort to further improve the results, additional experiments considering revised offshore tidal constituents, revised bottom roughness zone values, and revised stage versus flow boundary conditions are presented for 1-15 April 1979 tidal simulations. Upon further improvement of the modeled tidal dynamics as a result of these experiments, a 19-month tidal simulation as well as a 19-month hindcast were performed and are discussed. Next, the construction of the semi-operational nowcast/forecast system at NCEP is presented. Finally, conclusions are drawn and recommendations for formal skill assessment and transition to operations are advanced.

The tidal and hindcast simulation skills were evaluated using NOS skill assessment software (Zhang et al., 2006; Zhang et al. 2010). By comparing with observations, a set of performance statistics for variables of water level, currents, temperature and salinity was obtained. For example, some of the statistical parameters included in the NOS skill assessment procedures for operational forecast systems (Zhang et al., 2010) include Root Mean Square Error (RMSE) and Central Frequency (CF) for hourly water level records, high and low water levels, and time of high and low water levels.

The hindcast skill performance of RMSE for four parameters (water level, current magnitude, temperature, and salinity) is illustrated in Figure 0.1. Most of the skill assessment results show satisfactory or excellent skill and exceed the NOS criteria, with the exception of a few salinity RMSEs at several stations located in the upstream river course in the northeast part of the SFBOFS domain.

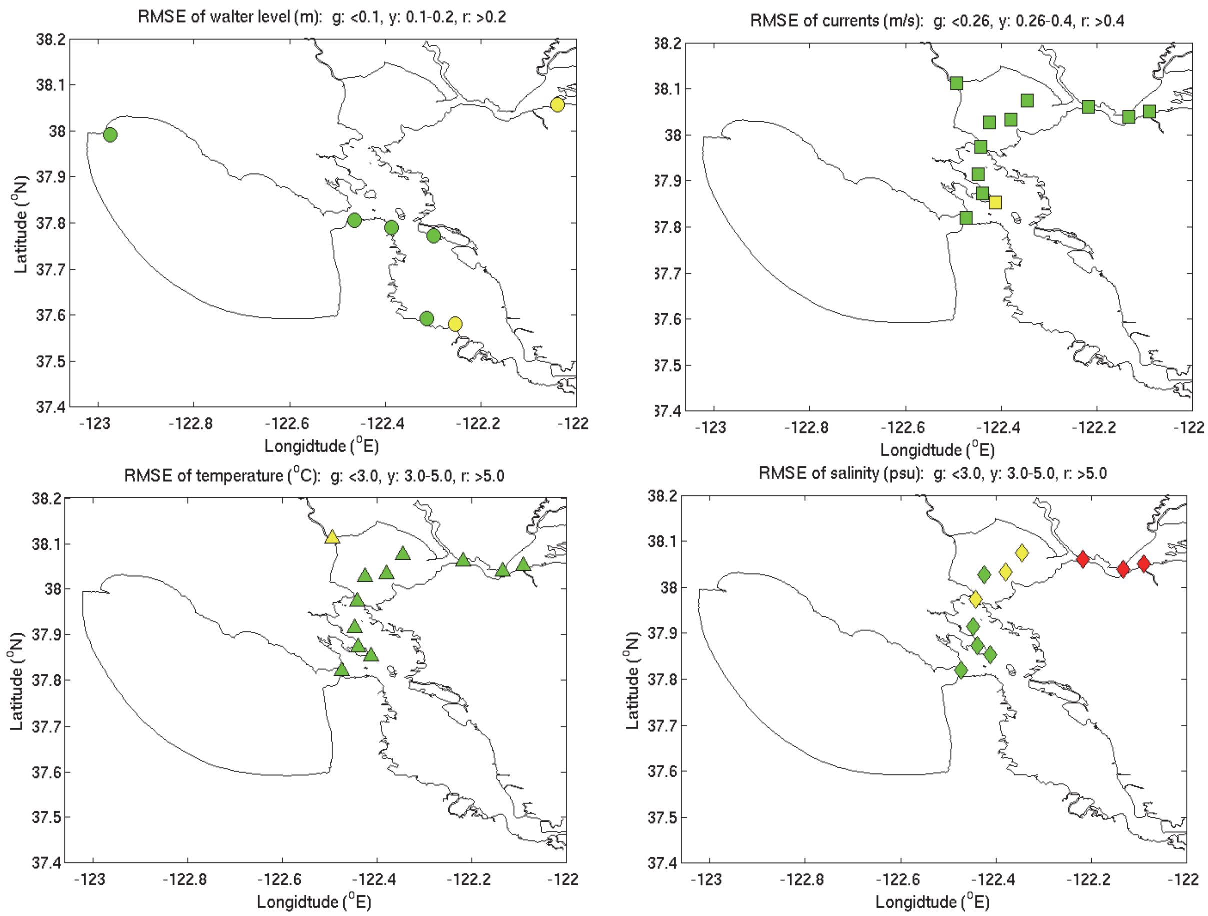

Figure 0.1. RMSEs for four parameters, water level, current magnitude, temperature, and salinity at stations spatially distributed over the SFBOFS model domain. The variable shapes are circles (water level), squares (current magnitude), triangles (temperature), and diamonds (salinity), and the skill range color in the plots are defined as:

RMSE for water levels (m): 0< Green ≤ 0.1; 0.1 ≤ Yellow ≤ 0.2; 0.2 < Red
RMSE for currents (m/s): 0 <Green ≤ 0.26; 0.26 ≤ Yellow ≤ 0.4; 0.4 < Red
RMSE for temperature/salinity (^{0}C, PSU): 0 < Green ≤ 3; 3 ≤ Yellow ≤ 5; 5 < Red

1. INTRODUCTION

The National Ocean Service's (NOS), Center for Operational Products and Services (CO-OPS), installed a Physical Oceanographic Real Time System (PORTS) during 1998 to provide observations of water surface elevation, currents at the PORTS prediction depth (4.7m below MLLW), near-surface and near-bottom temperature and salinity, and meteorological information at the locations shown in Figure 1.1. A sample PORTS screen capture is shown in Figure 1.2. To complement the PORTS, a new next generation nowcast/forecast system consistent with NOS procedures (NOS, 1999) has been developed as outlined in Aikman et al. (2008). This nowcast/forecast system is based on the Finite Volume Coastal Ocean Model (FVCOM) (Chen et al. (2003; 2006a; 2006b; 2006c) using a computational domain which extends from Rio Vista, on the Sacramento River and Antioch on the San Joaquin River through Suisun and San Pablo Bays and Upper and Lower San Francisco Bay out onto the continental shelf. Both tidal and complete meteorologically forced simulations will be performed and the results will be skill assessed using the NOS standard skill assessment software (Hess et al., 2003; Gross et al., 2006; Zhang et al., 2006; Zhang et al., 2010). Upon completion of this skill assessment, an experimental nowcast/forecast system will be constructed using the Coastal Ocean Modeling Framework for High Performance Computing (COMF-HPC) as described by Zhang et al. (2006; 2010) and exercised on a daily quasi-operational basis at the National Centers for Environmental Prediction (NCEP). This experimental nowcast/forecast system will then be run in semi-operational mode for further evaluation over a period of 3-6 months prior to official operational implementation, which will provide four times daily 6-hour nowcasts and 48 hour forecasts.

The nowcast/forecast system was developed and validated using data from the joint NOS and U.S. Geological Survey (USGS) 1979-1980 San Francisco Bay Circulation Survey (Welch et al., 1985). This survey provides additional validation data particularly for currents and density that is not available within the PORTS. Therefore as a first step, FVCOM was utilized to simulate several periods within the circulation survey timeframe to further guide the SFBOFS development.

In Chapter 2, we describe the model development process in terms of grid construction, model input requirements, and model revisions. In Chapter 3, the tidal calibration is presented. The initial 1 – 15 April 1979 tidal simulation as well as additional experimental simulations are presented to study the sensitivity of the tidal response to bottom roughness coefficients and offshore tidal constituents. An alternate boundary condition for water level in the Sacramento-San Joaquin River Delta is also considered. The results of the final configuration are presented for an extended 19-month simulation. In Chapter 4, the initial hindcast simulations are discussed. Upon further improvement of the model tidal dynamics as a result of the sensitivity analysis, results from the extended 19-month hindcast are discussed. In Chapter 5, the construction of the semi-operational nowcast/forecast system at NCEP is presented. In Chapter 6, conclusions are drawn and recommendations for formal skill assessment and transition to operations are advanced. Two additional appendices are used to discuss the SMS grid generation and simulation animation processes.

Figure 1.1 San Francisco Bay PORTS locations and measured parameters. Note cu=current meter, wl=water level, wind=wind, at=air temperature, wt=water temperature, baro=barometric pressure, and ag=air gap.

```
           San Francisco Bay PORTS, NOAA/NOS 2012-09-06 08:20 PDT

----------------------------Water Levels (above MLLW)---------------------------
Port Chicago             3.3 ft, Falling Richmond                 3.1 ft, Falling
San Francisco            *** ft,         Alameda                  3.2 ft, Falling
Redwood City             4.2 ft, Falling
--------------------------------------Winds-------------------------------------
                          Spd Dir Gusts                            Spd Dir Gusts
Port Chicago            15 kn WSW    18  Davis Point             6 kn   W     9
Pittsburg               16 kn WNW    19  Union Pacific RR Br    15 kn   W    18
Martinez-Amorco Pier    12 kn WSW    15  Richmond                3 kn WSW     5
Point Potrero Richm..    2 kn WSW     5  Oakland Middle Hbr      3 kn WSW     5
Oakland Berth 34         4 kn WNW     5  San Francisco           5 kn WNW     6
Pier 1                   3 kn   W     6  Oakland Berth 67        2 kn   W     4
Alameda                  1 kn WNW     4  Redwood City            3 kn NNW     4
----------------------------Air and Water Temperature---------------------------
                           Air   Water                             Air   Water
Port Chicago             57 °F   67 °F   Davis Point              56 °F
Pittsburg                58 °F           Martinez-Amorco Pier     56 °F
Richmond                 56 °F   62 °F   Point Potrero Richm..    57 °F
Oakland Berth 34         56 °F           San Francisco            55 °F   59 °F
Pier 1                   56 °F           Oakland Berth 67         56 °F
San Francisco Bar               *** °F   Alameda                  56 °F   66 °F
Redwood City             57 °F   69 °F
-------------------------------Barometric Pressure------------------------------
Port Chicago           1015 mb Rising    Davis Point            1015 mb Rising
Pittsburg              1014 mb Rising    Martinez-Amorco Pier   1015 mb Rising
Richmond               1016 mb Rising    Point Potrero Richm..  1016 mb Rising
Oakland Berth 34       1016 mb Rising    San Francisco          1016 mb Rising
Pier 1                 1015 mb Rising    Oakland Berth 67       1015 mb Rising
Alameda                1015 mb Rising    Redwood City           1015 mb Rising
------------------Currents (F)lood, (S)lack, (E)bb, towards °T------------------
                          Spd          Dir                           Spd          Dir
Martinez-Amorco Pier   0.3 kn (F),  53.0°T S-hampton Sh Ch LB6    0.3 kn (E), 167.0°T
Golden Gate (pred)     0.5 kn (E), 227.0°T Oakl Outer Harb LB3    0.6 kn (E),   0.0°T
--------------------------------------Waves-------------------------------------
Station                  SigHt PkDir PkPer Station                  SigHt PkDir PkPer
San Francisco Bar       *** ft ***°T *** s


*** Data not displayed as a result of quality control monitoring. For information on
missing data, go to https://corms.nos.noaa.gov/instrument_status.html or call (301) 713-2540.
```

Figure 1.2 Text-based San Francisco Bay PORTS forecast (screen capture from September 6, 2012 8:20 PDT).

2. HYDRODYNAMIC MODEL DEVELOPMENT

To support the selection of FVCOM, we first review previous and current modeling studies. Next the construction of the forecast model is discussed in terms of grid development of the hydrodynamic regimes in two separate regions: 1) San Francisco Bay and the near shelf, and 2) an offshore region to include the National Marine Sanctuaries. The specification of the upstream boundary conditions at the Delta is considered in terms of both flow and water surface elevation specification. The offshore boundary conditions are then discussed, followed by a description of the initial and forcing conditions. We next discuss plans for the pre-operational validation in terms of the tidal calibration of bottom roughness and adjustment of the open boundary conditions. We inventory available water level, current, and density validation stations. Next, the post-operational validation strategy using the NOS 2012-2013 current survey measurements is considered. Finally, model revisions required to complete the study are presented.

2.1 Review of Previous and Current Modeling Studies

Two- and three-dimensional models have been applied extensively to numerically investigate the circulation in San Francisco Bay. Barnard et al. (2006; 2007; 2009) report the existence of sand waves with heights on the order of 2 meters at the entrance of the Bay and consider coastal process evolution and the numerical prediction of severe storms on the coastline initially using the two-dimensional vertically integrated mode of the Delft3D-FLOW model (Delft Hydraulics, 2007). Uslu et al. (2010) have developed a very high resolution two-dimensional vertically integrated tsunami forecast model. Cheng and Smith (1998) have employed the two-dimensional depth-averaged model TRIM2D (Casulli, 1990) in the San Francisco Bay Marine Nowcast System with real-time nowcast model results made available for download. The TRIM3D model (Casulli and Cattani, 1994) has been most recently applied by Gross et al. (2010) to the entire San Francisco Bay. The UnTRIM model (Casulli and Walters, 2000), which is the unstructured version of TRIM3D has also been applied to San Francisco Bay by MacWilliams and Cheng (2006). Fringer et al. (2006) developed the non-hydrostatic option SUNTANS model patterned after UnTRIM. SUNTANS has also been applied in San Francisco Bay by Chua and Fringer (2011).With the recent evolution toward application of unstructured grid models in San Francisco Bay, the Finite Volume Coastal Ocean Model (FVCOM) developed by Chen et al. (2003; 2006a; 2006b; 2006c) has been selected for the NOS Nowcast/Forecast System hydrodynamic model component.

Here we characterize the application of these three-dimensional models to San Francisco Bay. In Table 2.1 we note the major application features and consider the validation characteristics in Table 2.2. As the last row in Tables 2.1 and 2.2, we contrast the NOS San Francisco Bay Model characteristics.

Table 2.1. Characteristics of 3D Model Applications to San Francisco Bay. Note H and V denote horizontal and vertical resolution. W/D corresponds to wetting/drying, OBL corresponds to open ocean boundary distance from the coastline, DBC corresponds to Delta boundary condition with (Q,WL)=(Flow, Water level) specification, and Inflow notes the additional inflows with STP being sewage treatment plant.

Model	Reference	Resolution	W/D	OBL	DBC	Inflow
TRIM3D	Gross et al. (2010)	H:200m V:1m	Yes	22km	Q-Limited False Deltas	5 Rivers 3 STP
SI3D	Zameni et al. (2010)	H:500m V:2m	No	17km	WL-No False Deltas	None
UnTRIM	MacWilliams and Cheng (2006)	H:25-5000m V:(1m)	Yes	17km	WL-No False Deltas	None
UnTRIM	MacWilliams et al. (2007)	H:50-400m V:(1m)	Yes	17km	Q-Limited False Deltas	4 Rivers 1 STP
UnTRIM	MacWilliams et al. (2008)	H:10-1000m V: 1m	Yes	40km	Q-Delta Included	4 Rivers 1 STP
SUNTANS	Chua and Fringer (2011)	H:50-200m V: 0.27-82m	Yes	40km Pt Reyes	Q-False Deltas	2 Rivers
FVCOM	Chen et al. (2003)	H:50-2000m V: 20 σ levels	Yes	40km Pt Reyes	Q-No False Deltas	5 Rivers

Table 2.1. (Cont.) Characteristics of 3D Model Applications to San Francisco Bay. Note TSP corresponds to the turbulence closure scheme with vertical and eddy viscosity and diffusivity. WF corresponds to wind forcing with # s indicating number (#) of met stations used to generate the windfield. NARR represents the use of the North American Regional Reanalysis as the windfield. HF corresponds to heat flux and EP corresponds to evaporation/precipitation. BR corresponds to z_0 bottom roughness. Note that a dash ('–') designates information was not available in the reference.

Model	Reference	TSP	WF	HF	EP	BR
TRIM3D	Gross et al. (2010)	GLS-MY2.5 V: 10-4 m^2/s	3 s	No	Yes	0.1-2 mm
SI3D	Zameni et al. (2010)	-	-	-	-	-
UnTRIM	MacWilliams and Cheng (2006)	Algebraic	-	-	-	0.1-2mm
UnTRIM	MacWilliams et al. (2007)	GLS-MY2.5 V:0.5x10-4 m^2/s	3 s	No	Yes	0.1-2 mm
UnTRIM	MacWilliams et al. (2008)	GLS-MY2.5 V:0.5x10-4 m^2/s	3 s	No	Yes	0.1-2 mm
SUNTANS	Chua and Fringer (2010)	GLS	-	-	-	0.001m-1 mm
FVCOM	Chen et al. (2003)	MY 2.5 V:10-4m^2/s	NARR	Yes	No	5-30 mm

Table 2.2. Validation Characteristics of 3D Model Applications to San Francisco Bay. Note [η, (u,v),(U,V)] correspond to water surface elevation, East and North horizontal velocity components, East and North vertically-averaged horizontal velocity components, and S and T correspond to salinity and temperature. TC corresponds to the tidal calibration period with DC corresponding to the density validation period. Within the validation metrics, AE denotes average error, SE denotes the standard error, RMSE denotes the root mean square error, R denotes the correlation coefficient, AR is the amplitude ratio, and LG is the lag. LR is a linear regression y=mx+b of model, y, on data, x. Note CF equals central frequency and NOS denotes NOS standard skill assessment metrics.

Model	Reference	Variables	TC	DC	Metrics
TRIM3D	Gross et al. (2010)	η, (u,v), (U,V),S	1/1997-3/1998	1/1997-3/1998	AE,SE, R^2,AR,LG, LR(m,b)
SI3D	Zameni et al. (2010)	(u,v),S	2/17/2008-2/22/2008	2/3/2008-3/4/2008	Graphical
UnTRIM	MacWilliams and Cheng (2006)	η, (u,v)	6/1998	9/18/1980-10/18/1980	Graphical
UnTRIM	MacWilliams et al. (2007)	η, (U,V),S	5/7/2002-7/31/2002	1994	AE,SE, RMSE
UnTRIM	MacWilliams et al. (2008)	η, (U,V)	2007	1999 2002	R^2,AR,LG, LR(m,b)
SUNTANS	Chua and Fringer (2011)	η, (U,V),S	1/1/2005-1/30/2005	1/14/2005-2/14/2005	RMSE,ME,R
FVCOM	Chen et al. (2003)	η, (u,v),S,T	3/-4/1979 9/-10/1980	3/-4/1979 9/-10/1980	RMSE, CF, NOS

2.2 Model Grid Construction

We first consider the development of the initial grid, which is used in the subsequent computations and for SFBOFS. Next, the development of two supplemental grids is presented. The use of these grids in future studies will enable the consideration of inundation (overland flooding events) and Bay plume dynamics on the adjacent continental shelf. Modifications to the initial SFBOFS grid to increase numerical stability are finally considered. In each of these grid systems, a uniform 20-layer sigma level vertical discretization was used.

2.2.1 Initial Grid

The initial grid shown in Figure 2.1 was developed using Surface Water Modeling System (SMS) Version 10.1 as described by Brigham Young University Surface Modeling Laboratory

(2006) and was based on the VDatum grid developed by Xu et al. (2009) for the coastal waters of North/Central California, Oregon and western Washington. The open boundary of the San Francisco Bay grid was developed from this grid in the near shelf region external to the Bay. It was necessary to modify the VDatum grid such that the outer boundary of the San Francisco Bay grid follows an approximate circular arc with one of the element sides nearly orthogonal to the boundary arc. The grid then extends through the entrance and includes the South and Central San Francisco Bay, San Pablo Bay, Carquinez Strait, Suisun Bay, and the Delta entrance region. The VDatum grid was extended in the Delta entrance region up the Sacramento River to Rio Vista and up the San Joaquin River past Antioch. The grid contains 102,264 elements and 54,120 nodes with a minimum depth of 0.2m and maximum depth of 106.8m as shown in Figure 2.1 and Figure 2.2. Hydrographic survey data over the entire grid are shown in Figure 2.3. The model grid in lower South San Francisco Bay and bathymetry are shown in Figure 2.4 and Figure 2.5, with the hydrosurvey data coverage shown in Figure 2.6. The model grid in the lower portion of the San Francisco Bay Delta and bathymetry are shown in Figure 2.7 and Figure 2.8, with the hydrographic survey data coverage shown in Figure 2.9.

The following element quality checks were used: 1) minimum and maximum interior angles of 10 and 130 degrees, respectively, 2) maximum slope of 0.1, 3) maximum adjacent element area change ratio of 0.5, and 4) maximum number of elements connected to a node of 8. Note the slope corresponds to the maximum allowed gradient of the edge length inside the domain. The slope determines how fast the mesh size will increase toward the middle of the region. A small slope order 0.1 means small meshes. The paving method was used, which uses an advancing front technique to fill the polygon with elements. Based on the vertex distribution on the boundaries, equilateral triangles are created on the interior to define a smaller interior polygon. Overlapping regions are removed and the process is repeated until the region is filled. Interior nodal locations are relaxed to create better quality elements.

Sounding datasets were obtained from CSDL's Cartographic and Geospatial Technology Programs (CGTP) branch. The sounding datasets were interpolated to both model grids using a new interpolation program. The program interpolate_xyz_to_mesh.f90 was modified to consider the Tracer Element Control Volume used in FVCOM in addition to the ADCIRC procedure. In addition, the bathy2all.f90 program was included in the revised mesh program, interpolate_xyz_to_mesh_fill.f90, to fill in all grid nodes for which no data were available from the soundings. SMS grid development procedures are documented in Appendix A.

Figure 2.1. San Francisco Bay model grid.

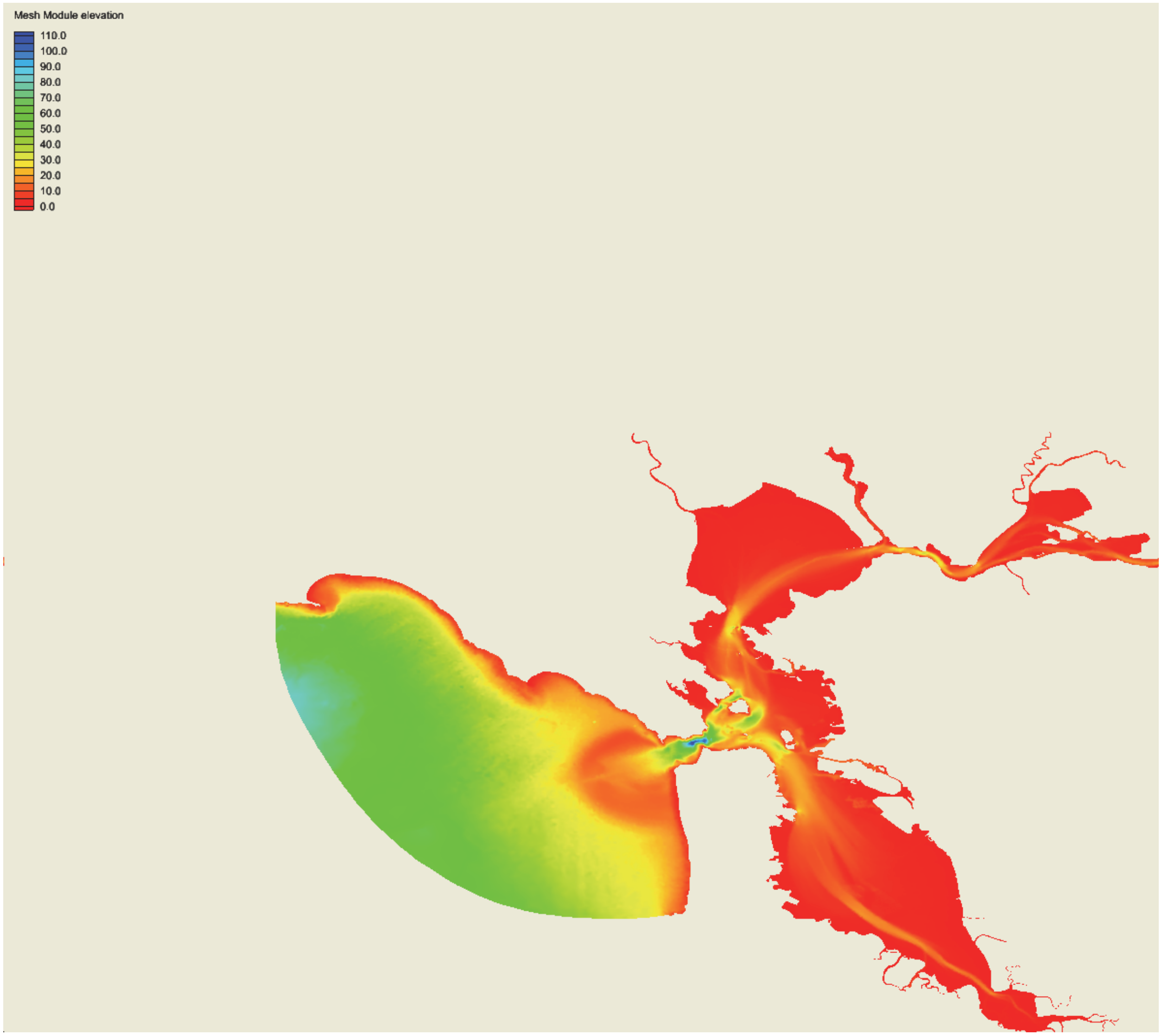

Figure 2.2. San Francisco Bay model bathymetry in meters.

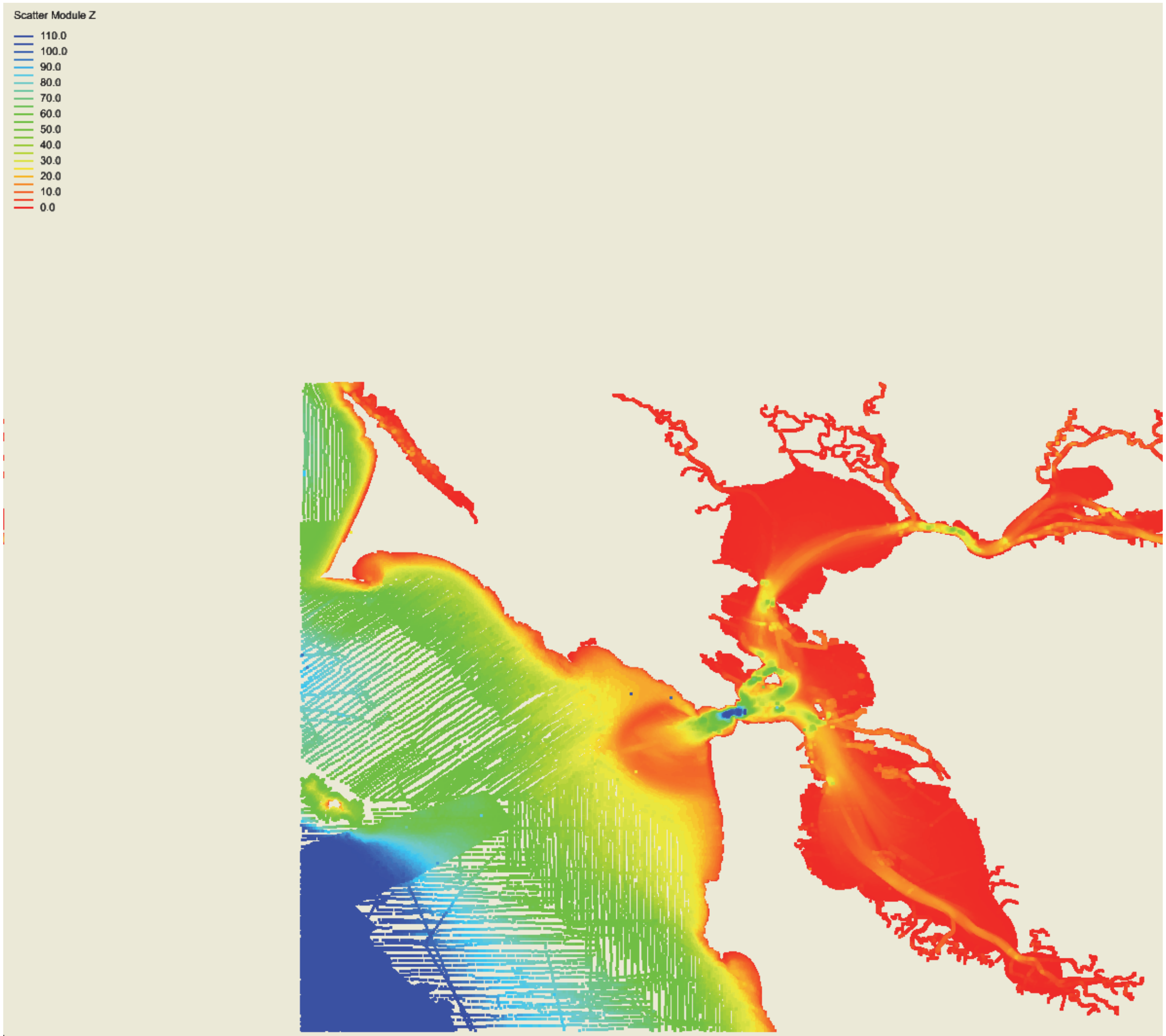

Figure 2.3. San Francisco Bay hydrographic survey data in meters.

Figure 2.4. SouthSan Francisco Bay Model Grid.

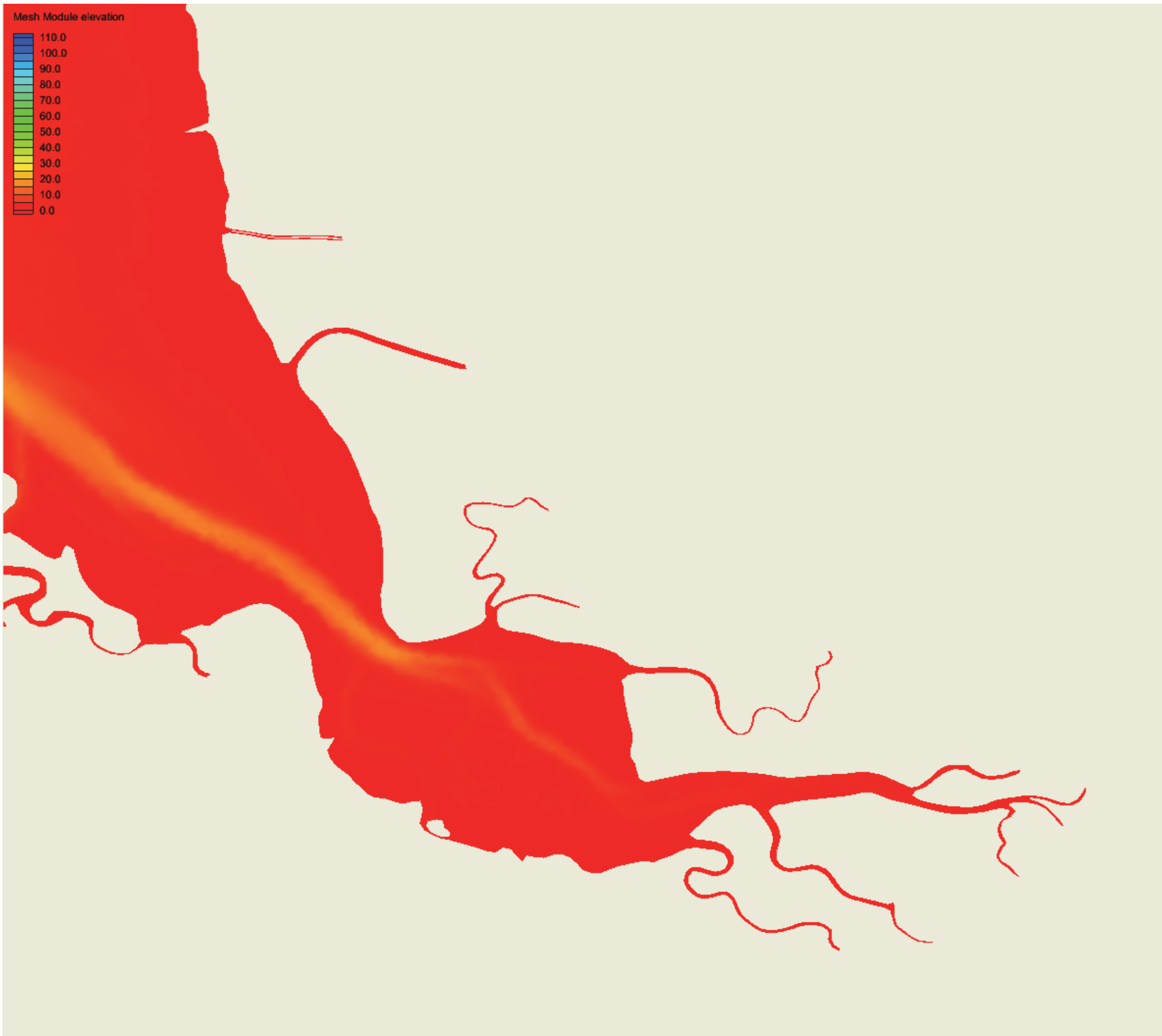

Figure 2.5. SouthSan Francisco Bay Model Bathymetry in meters.

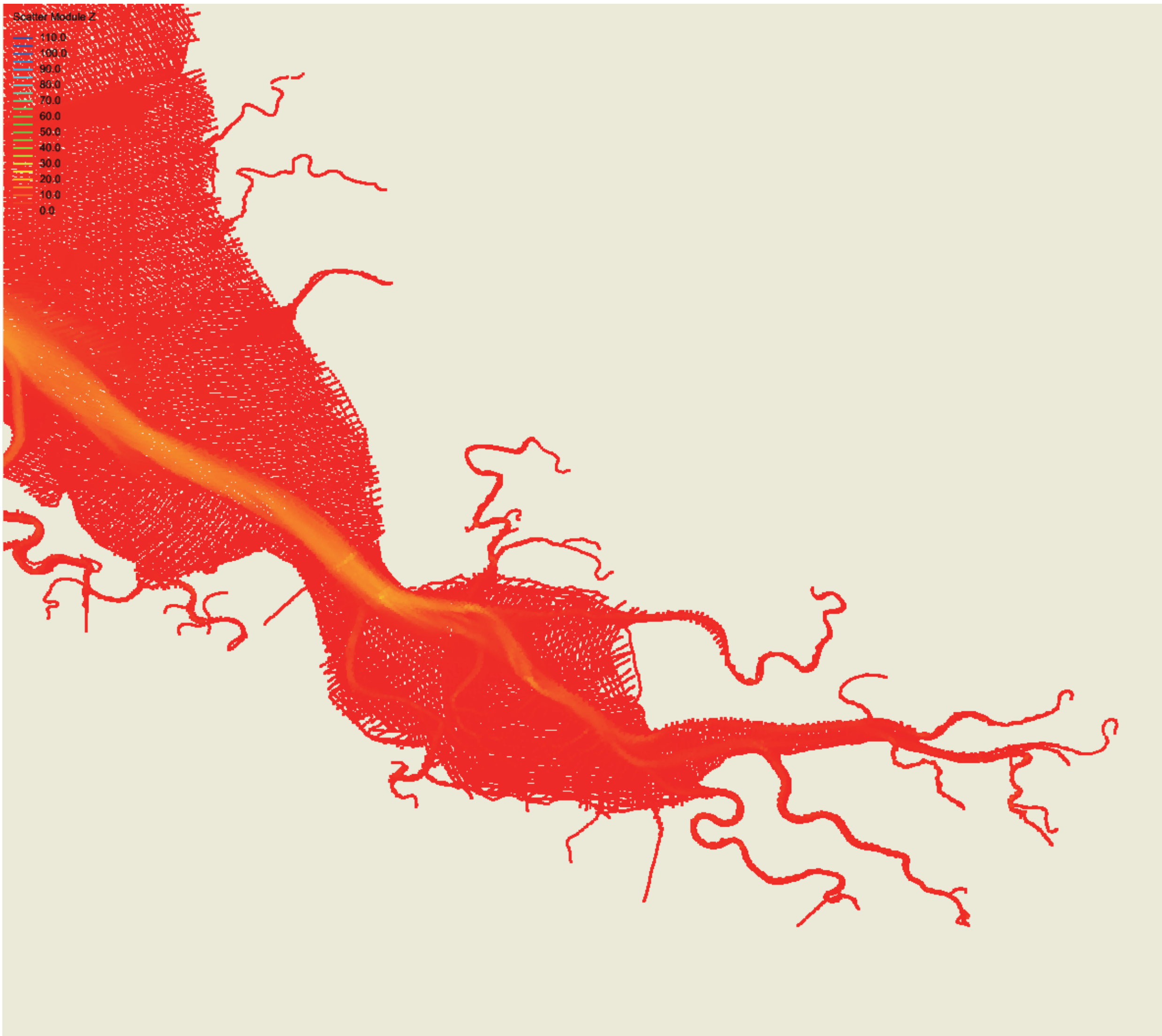

Figure 2.6. SouthSan Francisco Bay Hydrographic Survey Data in meters. (ZYANG)

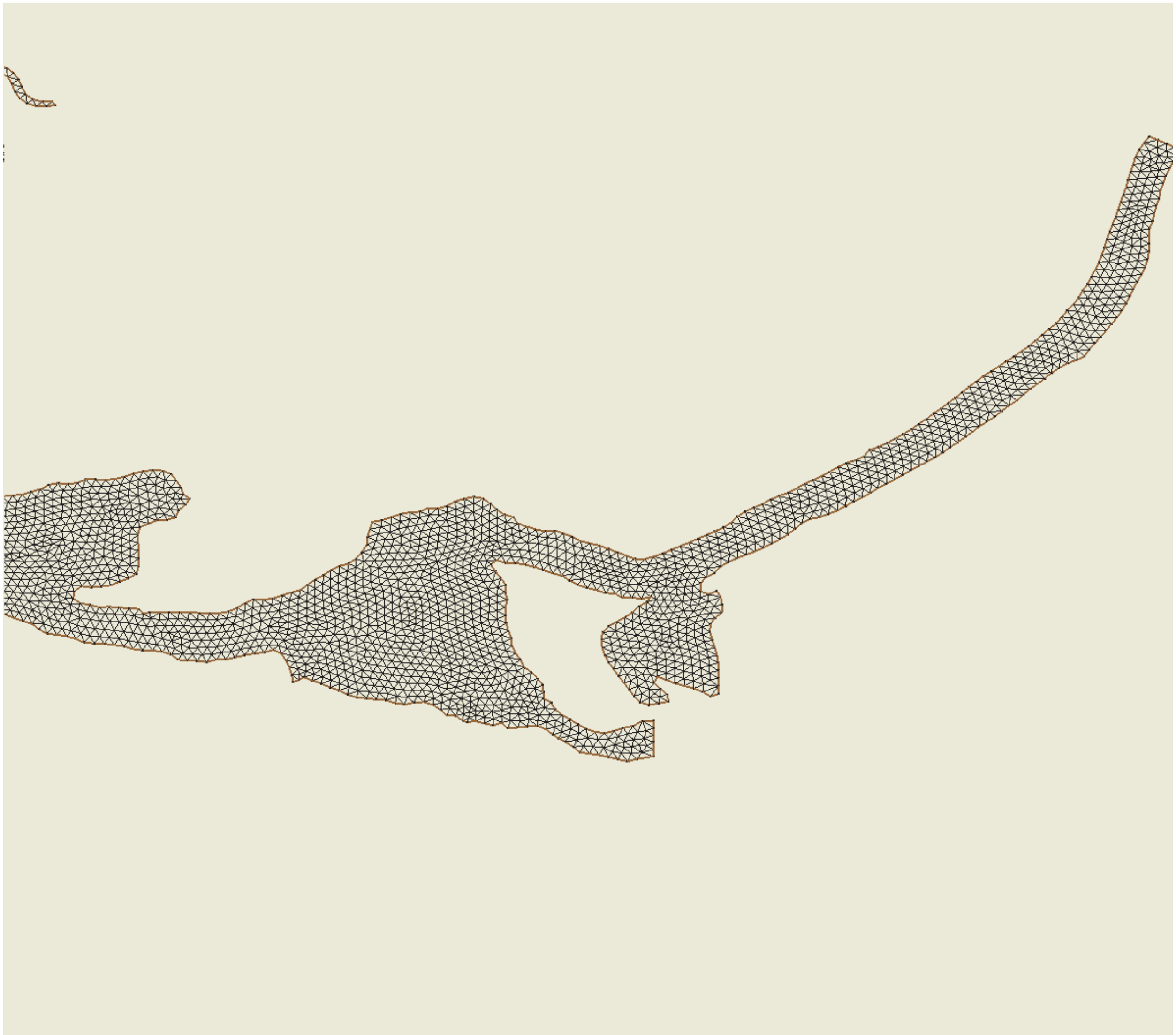

Figure 2.7. San Francisco Bay Delta Grid. (ZYANG)

Figure 2.8. San Francisco Bay Delta Model Bathymetry in meters.

Figure 2.9. San Francisco Bay Delta Hydrographic Survey Data in meters.

2.2.2 Supplemental Grids

Two additional grids were developed for further consideration. An inundation grid shown in Figure 2.104 was developed by modifying the original grid to include inundation to the 5m mean high water (MHW) level. The offshore grid shown in Figure 2.11 was developed by extending the inundation grid to include the offshore regions of the Gulf of the Farallones/Cordell Bank National Marine Sanctuaries. Sounding datasets were obtained from the Coast Survey Development Laboratory’s VDatum group and the National Geophysical Data Center (NOS Hydrographic Survey Data; San Francisco Bay, Californai 1/3 Arc-Second MHW DEM; Carignan et al., 2010). Water depths and land topography were interpolated to the three grids using a new interpolation program, which considered the tracer element control volume used in FVCOM. The program was used to determine nodal values and to fill grid nodes for which no values were assigned.

2.2.3 Initial Grid Modifications and Computational Resources

While working with the initial grid in consultation with the FVCOM modeling group, several triangles were adjusted such that the minimum interior angle was at least 30 degrees. In addition, along the open boundaries, it was necessary to adjust the element topology, such that each boundary element contained only one boundary side. In addition, the side lengths of several of the smaller elements were increased to allow a larger external mode time step. Time step limits were determined in a Subroutine cfl.f, which was added to the bathymetry program. It should be noted that the above supplemental grids would require similar minimum interior angle adjustment.

Initial simulations on the original grid, without the inclusion of the river inflows, indicate a ratio of approximately 60:1 simulation to real time using 256 processors on the NCEP Central Computing System (CCS). Thus to complete a 54 hour nowcast/forecast cycle, 54 minutes of CPU time would be required. This computational requirement is near the upper limit of the present operational time allotment. Therefore under the present resources, SFBOFS will utilize the original grid.

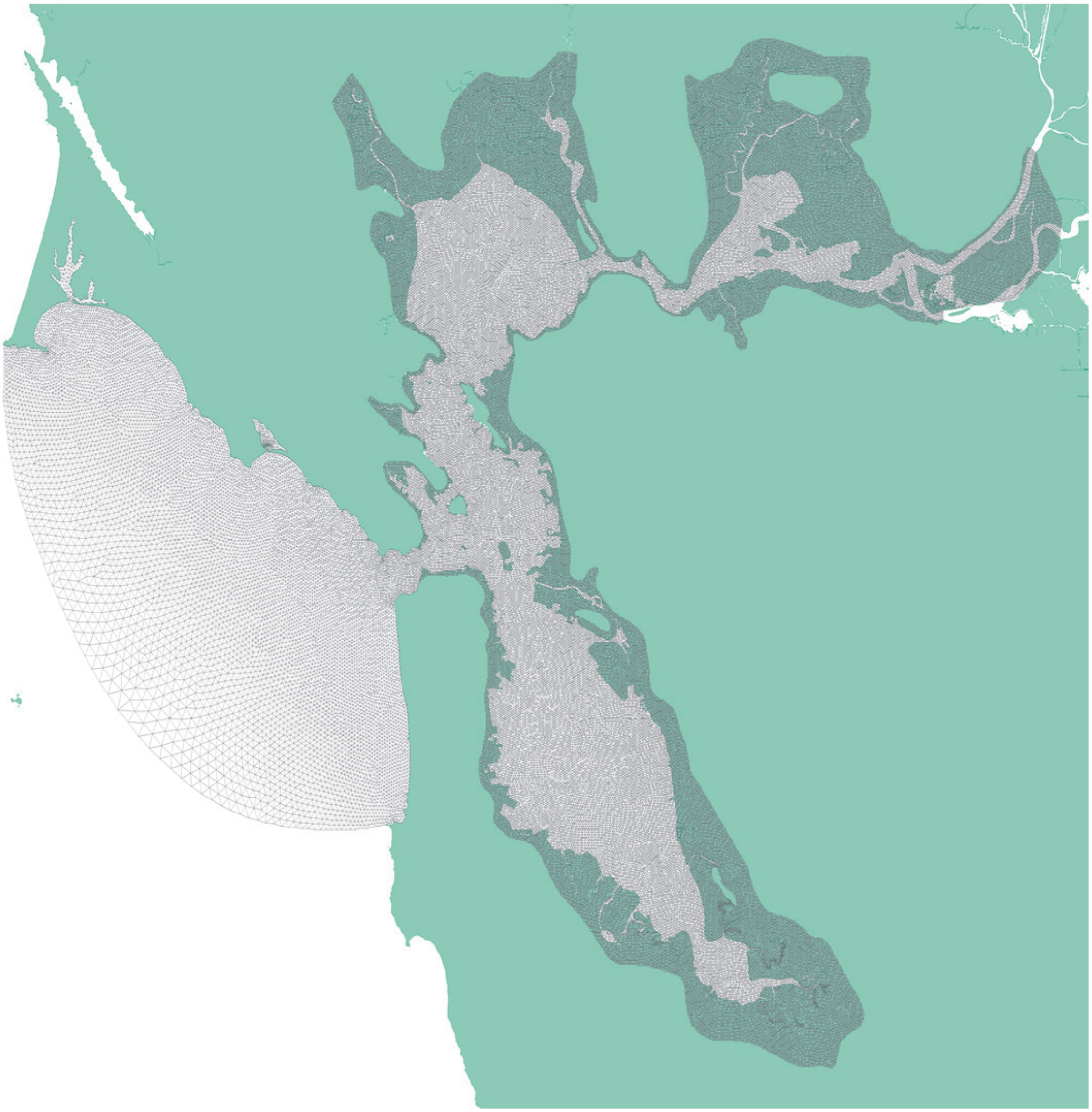

Figure 2.10. San Francisco Bay Inundation Grid-5m MHW. Number of elements: 147683; Number of nodes: 75489; Range of edge lengths (m): 130–1770.

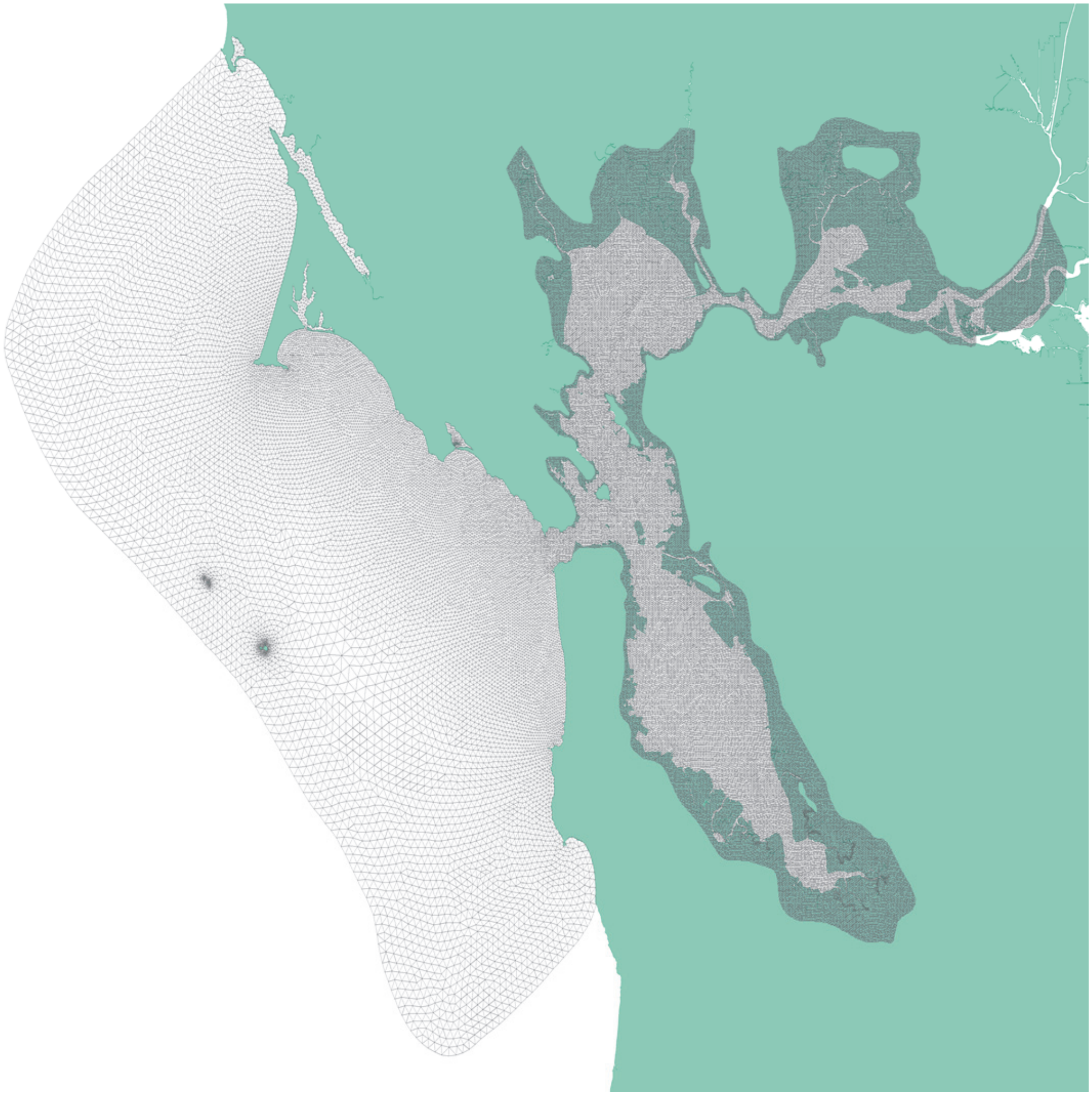

Figure 2.11. Offshore Inundation Grid -5m MHW. Number of elements: 158380; Number of nodes: 81065; Range of edge lengths (m): 34-1770.

2.3 Model Setup

The setup of the three-dimensional hydrodynamic model is discussed in terms of the following phases: 1) Delta inflow boundary condition specification, 2) open ocean boundary condition specification, 3) initial condition specification, and 4) surface forcing specification. Each of these model elements is discussed in turn below.

2.3.1 Delta Inflow Boundary Specification

Two different upstream boundary condition types were considered. In type one, the average daily flow as reported by the California Department of Natural Resources' DAYFLOW project (http://www.water.ca.gov/dayflow/output) were used to specify the flow at Rio Vista (RIO), while the San Joaquin River flow will be estimated at the total Delta outflow (OUT) minus the Rio Vista flow (RIO). DAYFLOW average daily flows (note negative flow indicate flow into the Delta from the Bay) will be used during the hindcast and the nowcast with persistence used during the forecast. Note one might assign the minimum inflow and the salinity as zero, since during low flow conditions DAYFLOW estimates may be suspect (Oltmann, 1998).

In type two, the water level surface elevations were specified at Rio Vista and Antioch. To investigate this boundary condition, flow and stage data were obtained to derive the flow-stage relationships at the Delta inflow points at Rio Vista Bridge and Antioch based on the DAYFLOW data. The subtidal stage data obtained from a 30-hr low-pass Fourier filter were regressed on the DAYFLOW total Delta outflow. The regression coefficients were determined on a monthly basis over 1990 and exhibited considerable variability from month to month. Correlation coefficients between regressed and observed subtidal water levels ranged from 0.2 to 0.5. The regression of the subtidal water levels on the flow yielded an improvement of order 1 cm RMSE with respect to the tidal prediction alone. However, the tidal predictions yielded RMSEs of order 10 cm for each month of 1990. As a result, one might use tidal predictions during the hindcast, observed stage during the nowcast and tidal predictions plus persisted subtidal water levels during the forecast. The specification of salinity is more problematic during period of inflow to the Delta, in which the salinity is not zero.

2.3.2 Open Ocean Boundary Condition Specification

The Oregon State University Tidal Data Inversion, OTIS Regional Tide Solutions (2010) West Coast tidal data (wc2010 1/30$^{o)}$ is used to provide offshore boundary conditions for the M_2, S_2, N_2, K_2, K_1, O_1, P_1, and Q_1 tidal constituents. The NOS harmonically-analyzed Ssa and Sa long period constituent values at station 941-5020 at Point Reyes, California were used along the entire open ocean boundary. Four boundary locations were selected; their harmonic constants are given in Table 2.3. These locations correspond to open ocean nodes 1 (37.959 ^{o}N, 123.027^{o}W), 40 (37.814^{o}N, 122.970^{o}W), 59 (37.613^{o}N, 122.763^{o}W), and 91 (37.587^{o}N, 122.526^{o}W), respectively. For nodes 2 through 39, the tidal signal was computed based on a linear spatial interpolation from the reconstructed tidal signals at nodes 1 and 40. Similar procedures were used for the other open ocean boundary nodes. For the specification of stage, additional harmonic constants were used (Table 3.8) as discussed in Chapter 3.

Table 2.3 Open Ocean Boundary Signals 1-4 Harmonic Constituents. Note in each cell amplitude (m) and Greenwich phase in (^{o}) are given. Results are obtained from the Oregon State University Tidal Data Inversion, OTIS Regional Tide Solutions (2010) West Coast of USA tidal data (wc2010). Note: Ssa and Sa tidal constituents are based on values at 941-5020, Point Reyes, CA. Signals 1- 4 were applied at open ocean boundary nodes 1, 40, 59, and 91, respectively.

Constituent	Signal 1	Signal 2	Signal 3	Signal 4
M2	0.527 190.8	0.531 189.7	0.554 188.9	0.599 188.2
S2	0.132 197.1	0.131 195.6	0.133 193.5	0.141 192.9
N2	0.117 163.7	0.116 162.8	0.117 161.6	0.122 161.0
K1	0.357 220.4	0.354 220.2	0.355 218.9	0.355 216.9
O1	0.220 205.0	0.219 205.0	0.221 203.9	0.220 202.1
Q1	0.039 199.2	0.039 199.0	0.039 198.2	0.039 197.4
P1	0.110 220.0	0.110 219.8	0.110 219.0	0.110 218.2
K2	0.037 188.8	0.037 187.4	0.037 184.7	0.039 183.2
SSA	0.029 285.3	0.029 284.6	0.029 283.9	0.029 283.3
SA	0.058 217.6	0.058 217.3	0.058 217.0	0.058 216.6

2.3.3 Initial Condition Specification

The salinity and temperature fields were developed for 1 April 1979 and 1 September 1980 using the joint NOS and USGS historical circulation survey conductivity-temperature-depth (CTD) datasets (Welch et al., 1985; Cheng and Gartner, 1984). These datasets were quality controlled using the methods of Loeper (2006) and Richardson and Schmalz (2006) as discussed in Richardson and Schmalz (2008). The location of the CTD casts were used to construct a coarse unstructured triangular mesh, with the nodal points assigned the values of the CTD casts. Utilizing this coarse grid, each nodal point in the original FVCOM grid was assigned a salinity and temperature value at the appropriate sigma level depth via an interpolation procedure. The horizontal interpolation of the vertical profiles was conducted by using a linear interpolation of the three surrounding nodal profile values of the coarse element in which the FVCOM grid node was located. A linear vertical interpolation was used to compute the FVCOM sigma level depth from the horizontally interpolated profile.

2.3.4 Surface Forcing Specification

The North American Regional Reanalysis (NARR, 2007) datasets were used to provide 3- and 6-hourly values of 10-m winds, sea-level atmospheric pressure, and fluxes of downward shortwave radiation and net total heat flux. The initial simulations for 1-15 April 1979 employed these two fluxes at 6-hour intervals and did not consider the bulk flux formulation. All subsequent simulations employed the 3-hour fluxes and used the bulk flux formulation.

2.4 Model Validation

To validate the SFBOFS setup, the following set of two-month hindcasts were used for April -

May 1979 and Sept-Oct 1980 based on the NOS and USGS historical circulation survey data inventories given in Tables 2.4 and 2.5, respectively. Station locations are shown in Figures 2.12 – 2.16.

Table 2.4. NOS and USGS San Francisco Historical Data, April – May 1979, Julian Dates 92 – 152. Refer to Welch et al. (1985), and Cheng and Gartner (1984) for measurement station locations and depths. Note the asterisk marked stations were added from the USGS survey datasets. Note no stations in the Delta are available.

Region	**Salinity**	**Temperature**	**Current**
Entrance	C-1	C-1	C-1
Mid Bay)	C-5, C-17, C-18	C-5, C-17, C-18, C-323	C-5, C-17, C-18, C-323
South Bay			
San Pablo Bay	C-19, C-20, C-22, C-18*, C-23*	C-19, C-20, C-22, C-18*, C-23*	C-19, C-20, C-22, C-18*, C-23*
Carquinez Strait	C-24, C-24, C-24, C-25*	C-24, C-24, C-24	C-24, C-24, C-24
Suisun Bay	C-25, C-26, C-28, C-29, C-30, C-31, C-32, C-33	C-25, C-26, C-28, C-29, C-30, C-31, C-32, C-33	C-25, C-26, C-28, C-29, C-30, C-31, C-32, C-33

Table 2.5. NOS and USGS San Francisco Historical Data, September – October 1980, Julian Dates 245-305. Refer to Welch et al. (1985), and Cheng and Gartner (1984) for measurement station locations and depths. Note the asterisk marked stations were added from the USGS survey datasets.

Region	**Salinity**	**Temperature**	**Current**
Entrance	C-211, C-1, C-1	C-1, C-211, C-1, C-1, C-1	C-1, C-211, C-1, C-1, C-1
Mid Bay	C-16, C-323, C-215, C-216, C-16, C-215, C-216, C-16, C-18, C-211, C-211, C-211	C-16, C-323, C-215, C-216, C-16, C-323, C-215, C-216, C-16, C-18, C-211, C-211, C-211	C-16, C-323, C-215, C-216, C-16, C-323, C-215, C-216, C-16, C-18, C-211, C-16, C-211, C-211
South Bay	C-13*, C-9*	C-10, C-13*, C-9*	C-10, C-13*, C-9*
San Pablo Bay	C-18, C-316, C-18, C-316, C-19, C-316, C-22, C-23, C-19, C-316, C-18, C-23, C315, C-18, C-320	C-18, C-316, C-22, C-18, C-316, C-19, C-316, C-22, C-23, C-19, C-316, C-314, C-18, C-23, C315, C-18	C-18, C-316, C-22, C-18, C-316, C-19, C-316, C-22, C-23, C-19, C-316, C-314, C-23, C315, C-18, C-320
Carquinez Strait	C-24, C-317, C-24, C-24, C-24, C-24	C-24, C-317, C-24, C-317, C-24, C-317, C-24, C-24	C-24, C-317, C-24, C-317, C-24, C-317, C-24, C-24
Suisun Bay	C-26, C32*, C-237*	C-26, C32*, C-237*	C-26, C32*, C-237*, C-235*
Delta	C-34	C-34	C-34, C-246

The initial effort was to organize, recover, and process the historical water level, CT and current, and CTD data that were collected during the joint NOS and USGS circulation survey of 1979-1980 (Welch et al., 1985; Cheng and Gartner, 1984). Harmonic analysis results for water levels at the stations shown in Table 2.6 were obtained from CO-OPS. Water level station locations are shown in Figures 2.17 – 2.19. The majority of the CTD data were unusable due to time stamp issues; however, data were available in September and October 1980 (Richardson and Schmalz, 2008). These data were used to check the CT time series data.

Table 2.6. NOS Historical Circulation Survey Water Level Stations. Refer to Welch et al. (1985), and Cheng and Gartner (1984) for water level station locations.

NOS Station No/ Location	Latitude N (D-M-S)	Longitude W (D-M-S)
941-4317 Pier 22.5, San Francisco, CA	37 47 24	122 23 12
941-4290 San Francisco, CA	37 48 24	122 27 54
941-4358 Hunters Point	37 43 48	122 21 24
941-4392 Oyster Point Marina	37 35 30	122 18 48
941-4458 San Mateo Bridge	37 34 48	122 15 12
941-4509 Dumbarton Bridge	37 30 24	122 07 06
941-4575 Coyote Creek	37 27 48	122 01 24
941-4523 Redwood City, CA	37 30 24	122 12 36
941-4750 Alameda, CA	37 46 18	122 17 54
941-4863 Richmond, CA	37 55 42	122 24 0
941-5020 Point Reyes, CA	37 59 48	122 58 30
941-5144 Port Chicago, CA	38 3 24	122 2 24

Following the techniques described in Richardson and Schmalz (2006), the filter program was used to remove S and T spikes and limit current directions. Program harm15.f was used to develop control and data files for the NOS 15 day harmonic analysis program. The 15 day harmonic analysis script, harm15.sh, was used to perform the harmonic analysis of all current stations with at least 15 days of data using the methods of Shureman (1958). All 15 day harmonic analyses of the current data at the stations in Table 2.4 and 2.5 were performed using the techniques described in Richardson and Schmalz (2006).

To develop initial salinity and temperature conditions on 1 April 1979 and 1 September 1980, the available CTD and CT time series data were placed on the unstructured grid shown in Figure 2.26. An interpolation program was developed in which each FVCOM grid node was assigned a given element and the salinity/temperature value interpolated from the node values at the appropriate depths. This program allows the initial density condition to be developed for the April-May 1979 and September-October 1980 tidal and hindcast simulations.

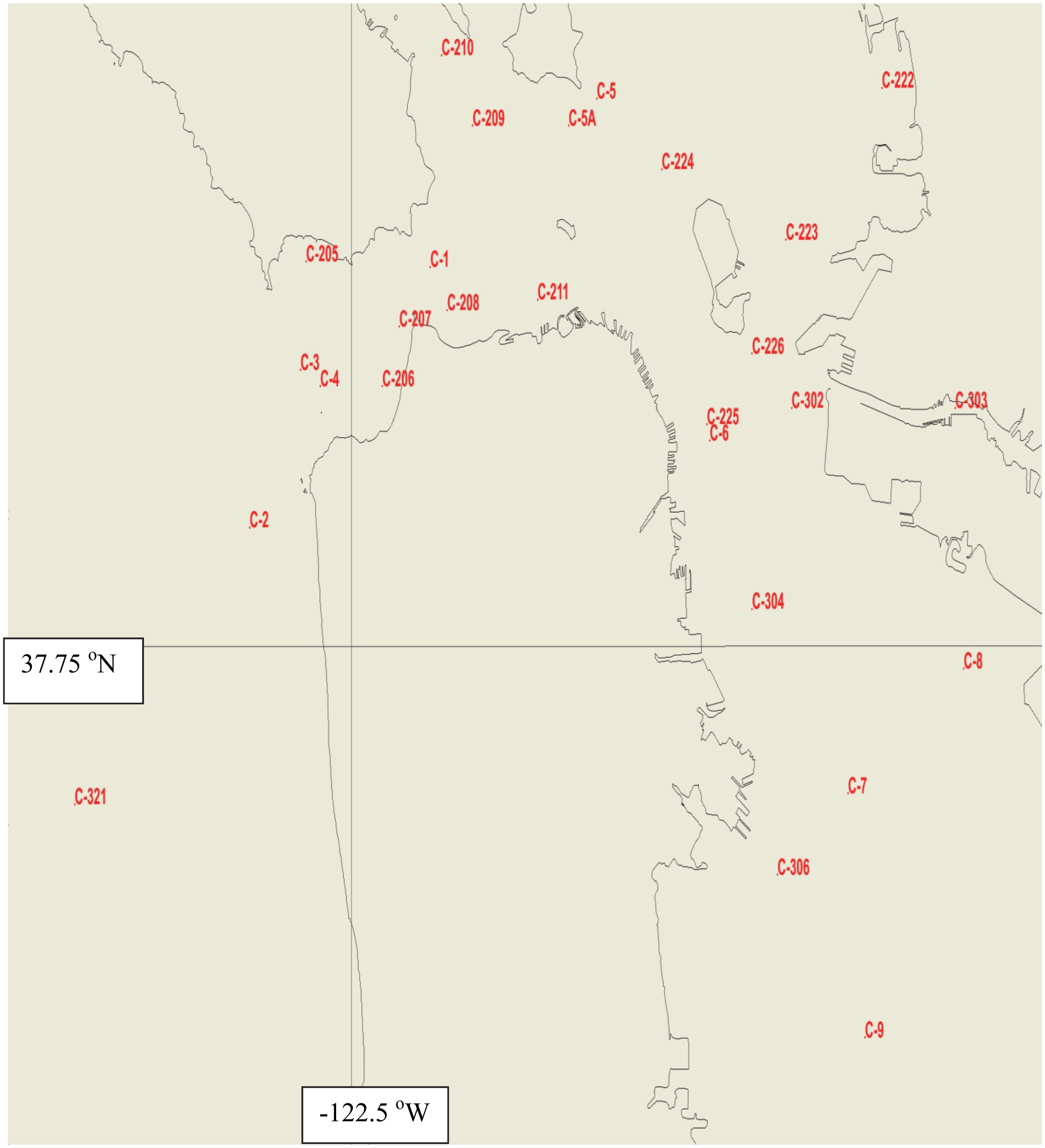

Figure 2.12. NOS Current Meter Stations Offshore and in Central and South San Francisco Bay.

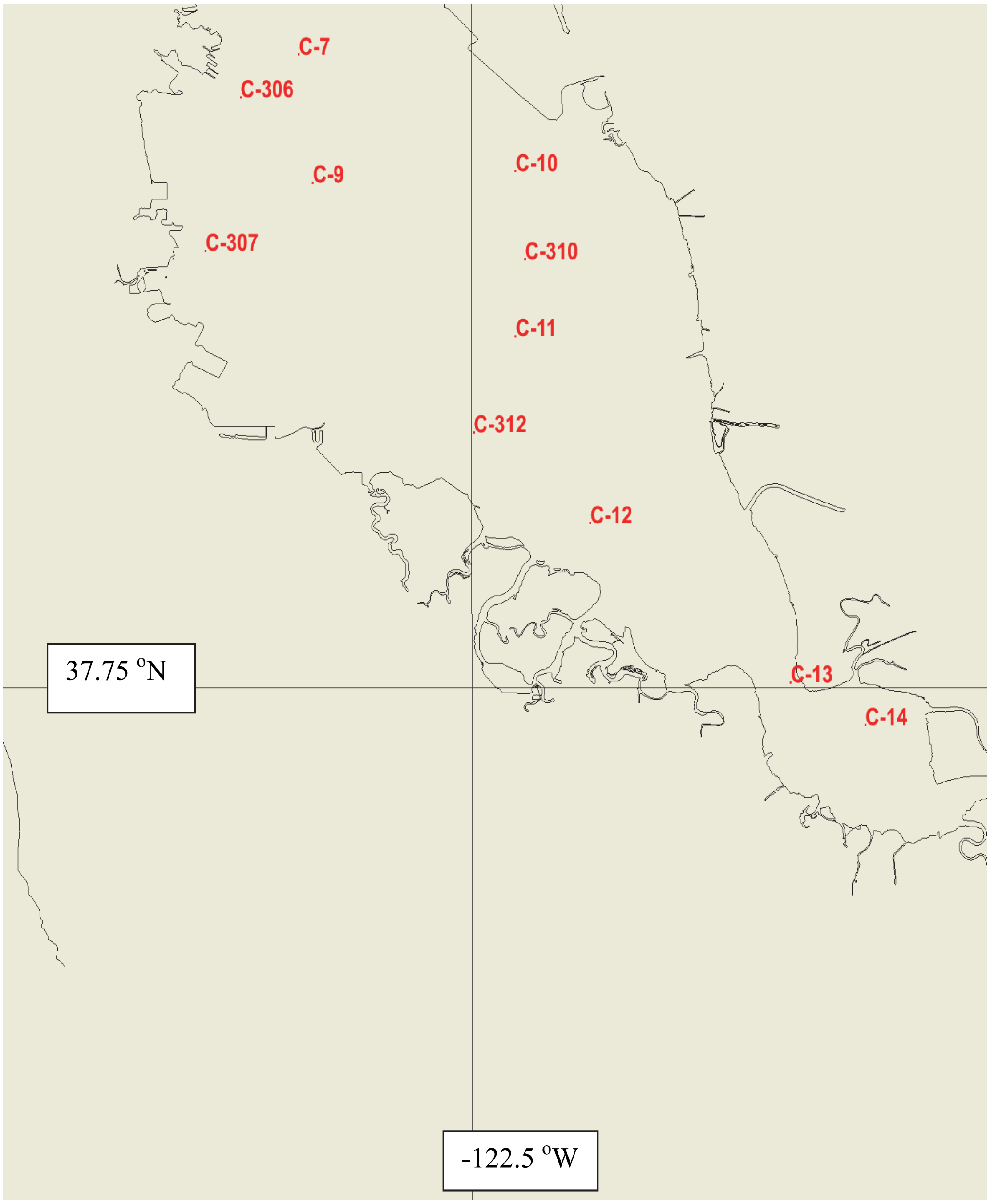

Figure 2.13. NOS Current Meter Stations in South San Francisco Bay.

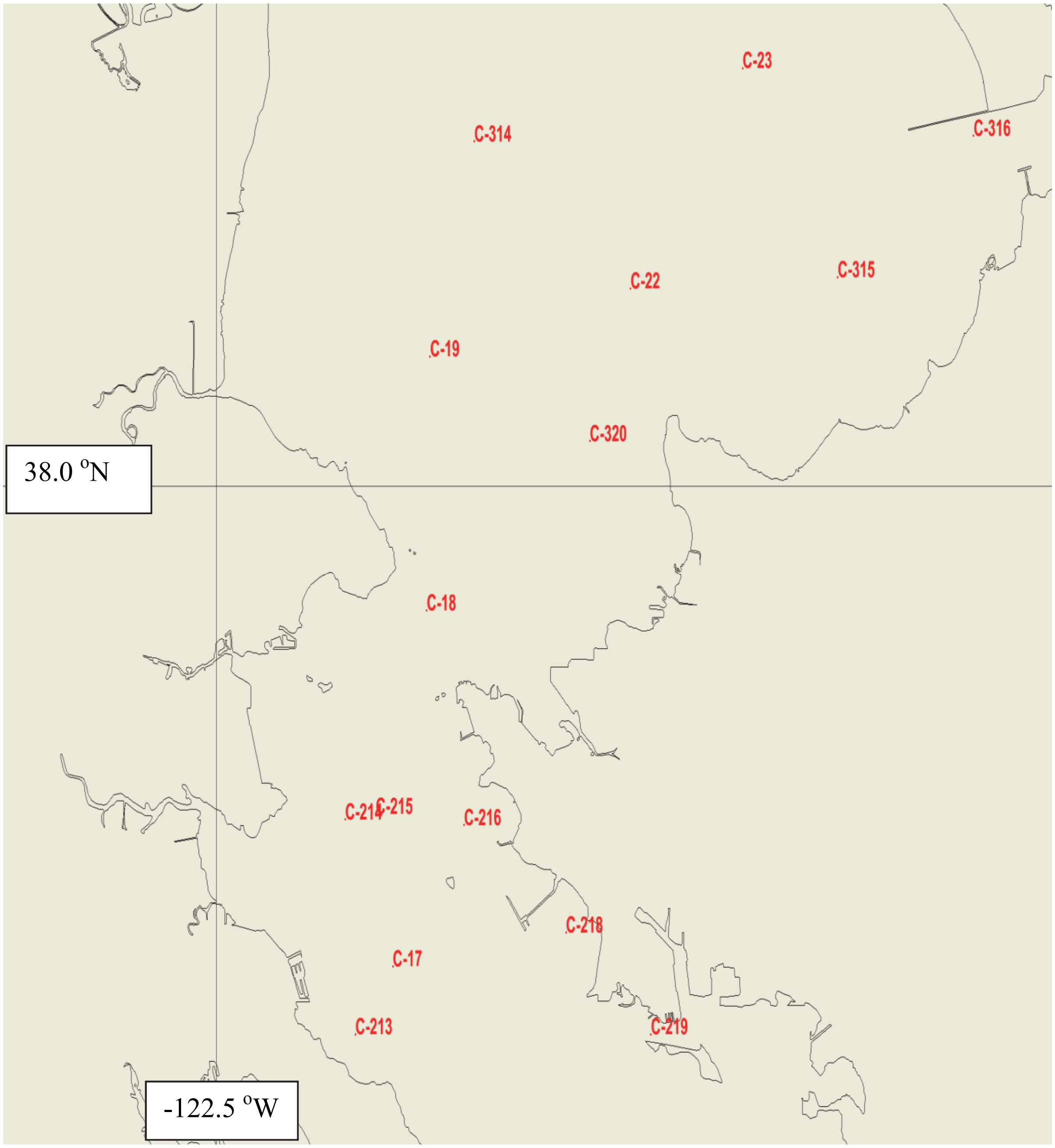

Figure 2.14. NOS Current Meter Stations in North San Francisco Bay and San Pablo Bay.

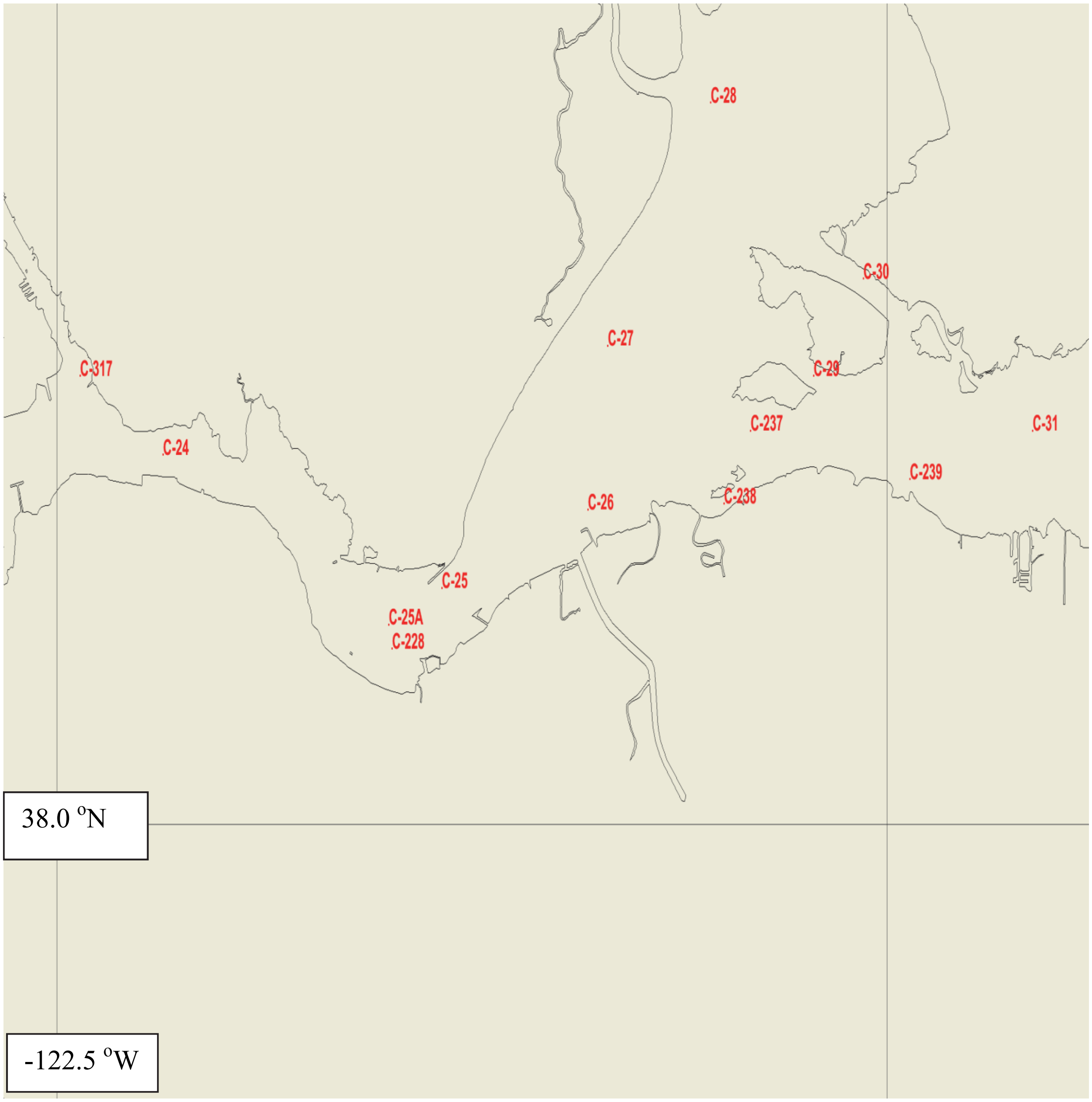

Figure 2.15. NOS Current Meter Stations in Carquinez Strait and in Suisun Bay.

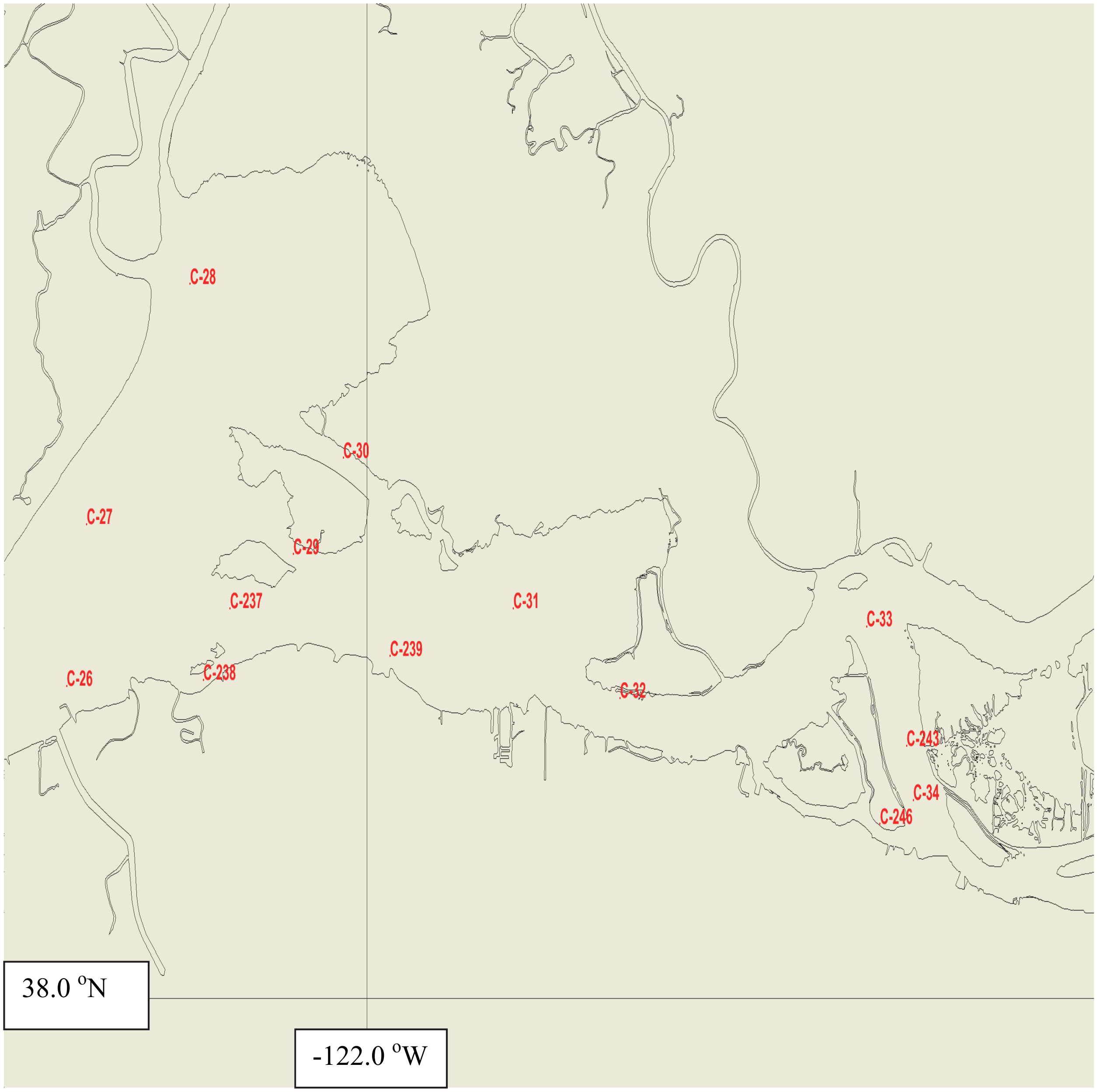

Figure 2.16. NOS Current Meter Stations in in the lower Delta.

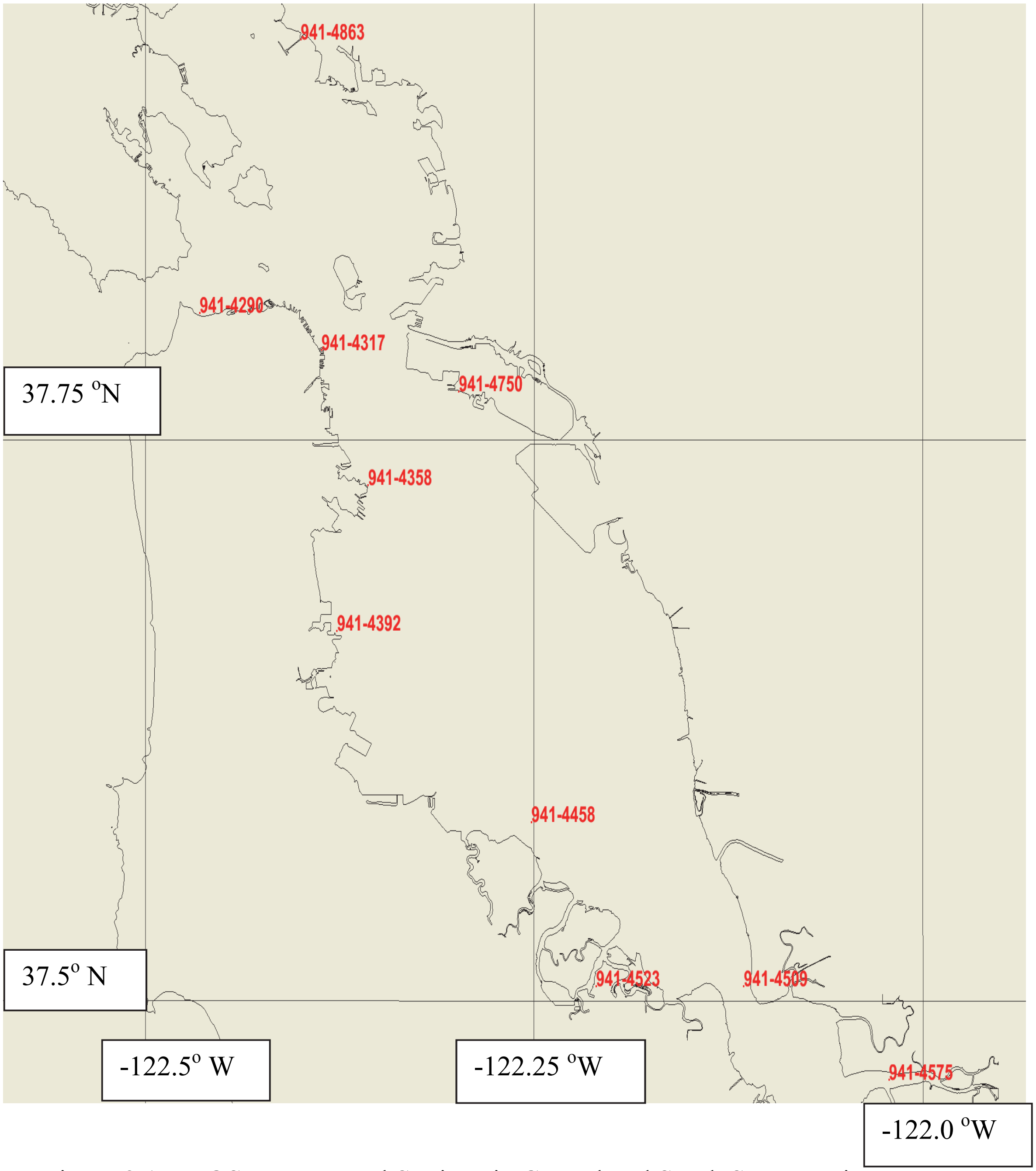

Figure 2.17. NOS Water Level Stations in Central and South San Francisco Bay.

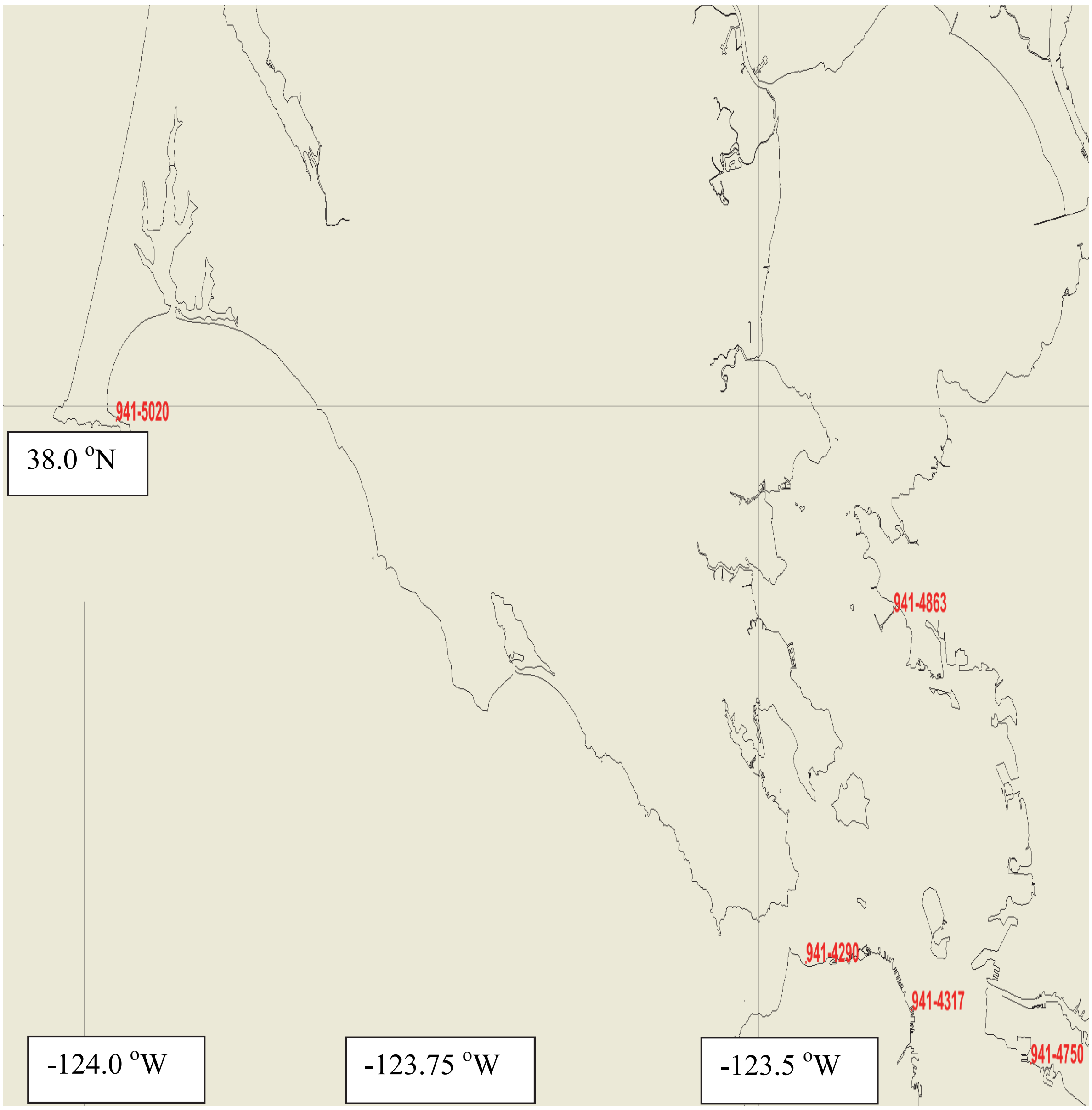

Figure 2.18. NOS Water Level Stations outside and in the Central and North Bays of San Francisco Bay.

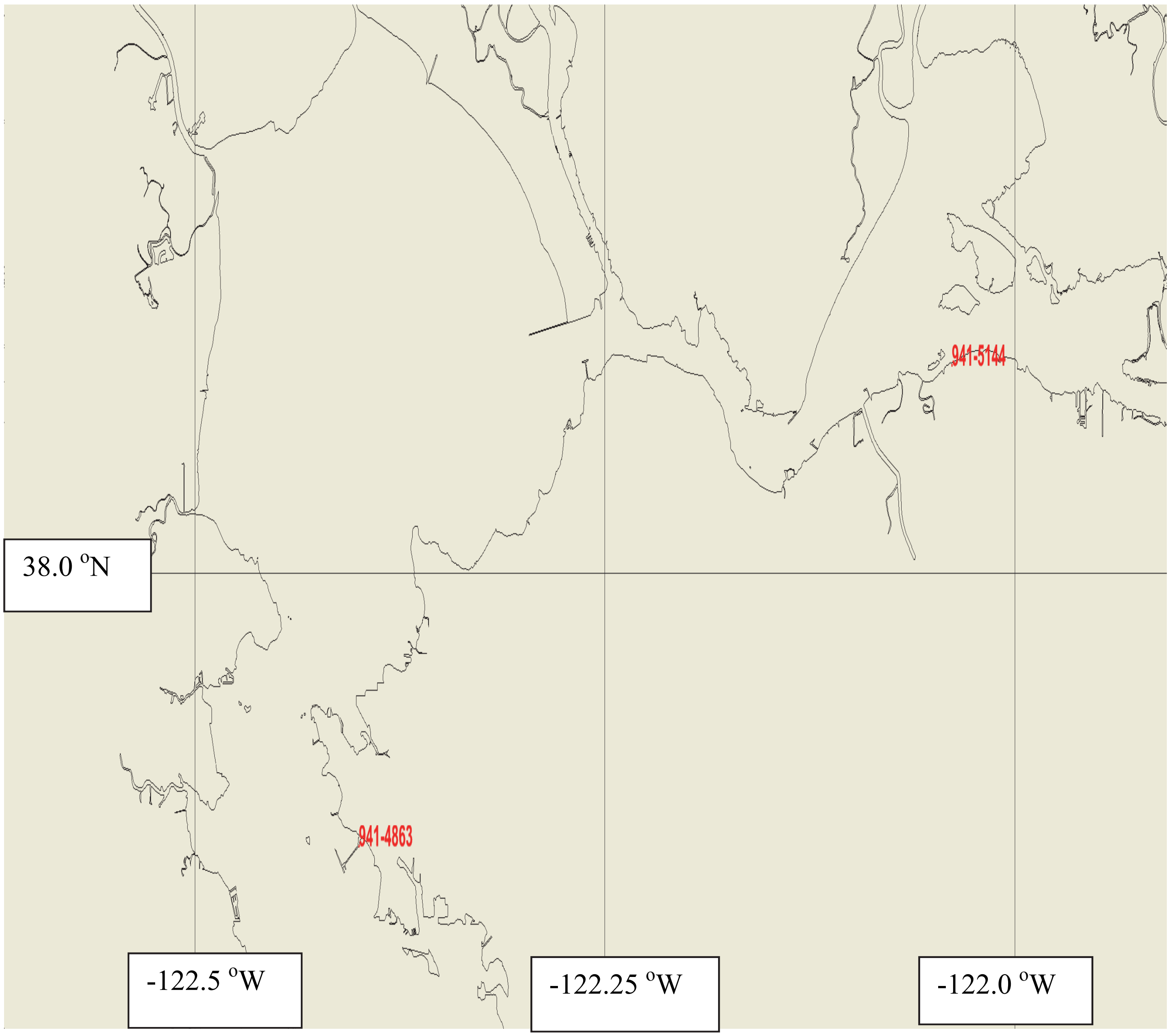

Figure 2.19. NOS Water Level Stations in North and Suisun Bays in San Francisco Bay.

The bottom roughness, z_0, was specified as a function of stilled water depth as shown in Table 2.7 after Cheng et al. (1993). A netCDF file was developed to specify the roughness value at the center of each element based on the average of the nodal still water depths.

Table 2.7. Bottom Roughness Zones.

Roughness Zone Number	Lower Depth (m)	Upper Depth (m)	Bottom Roughness z_0 (mm)
1	0	1	30
2	1	3	20
3	3	10	10
4	10	50	7
5	50	1000	5

Initially, purely tidal simulations were performed to calibrate these bottom roughness values. Next the set of two-month simulations was extended to include meteorological effects to further validate the bottom roughness calibration. Model evaluation used NOS standard skill metrics (Hess et al., 2003) and additional statistics as reported by Schmalz (2011).

The system will then be transferred to the NOS Center for Operational Oceanographic Products and Services (CO-OPS) to run at NOAA's National Centers for Environmental Prediction (NCEP) under the Coastal Ocean Modeling Framework for High Performance Computing (COMF-HPC) for an extended test period (NOS, 1999). Over the last three months of this test period, this pre-operational model version will be evaluated using the NOS standard skill assessment software (Hess et al., 2003; Zhang et al., 2006; Zhang et al., 2010). Upon final evaluation, the model will be transferred to operational status.

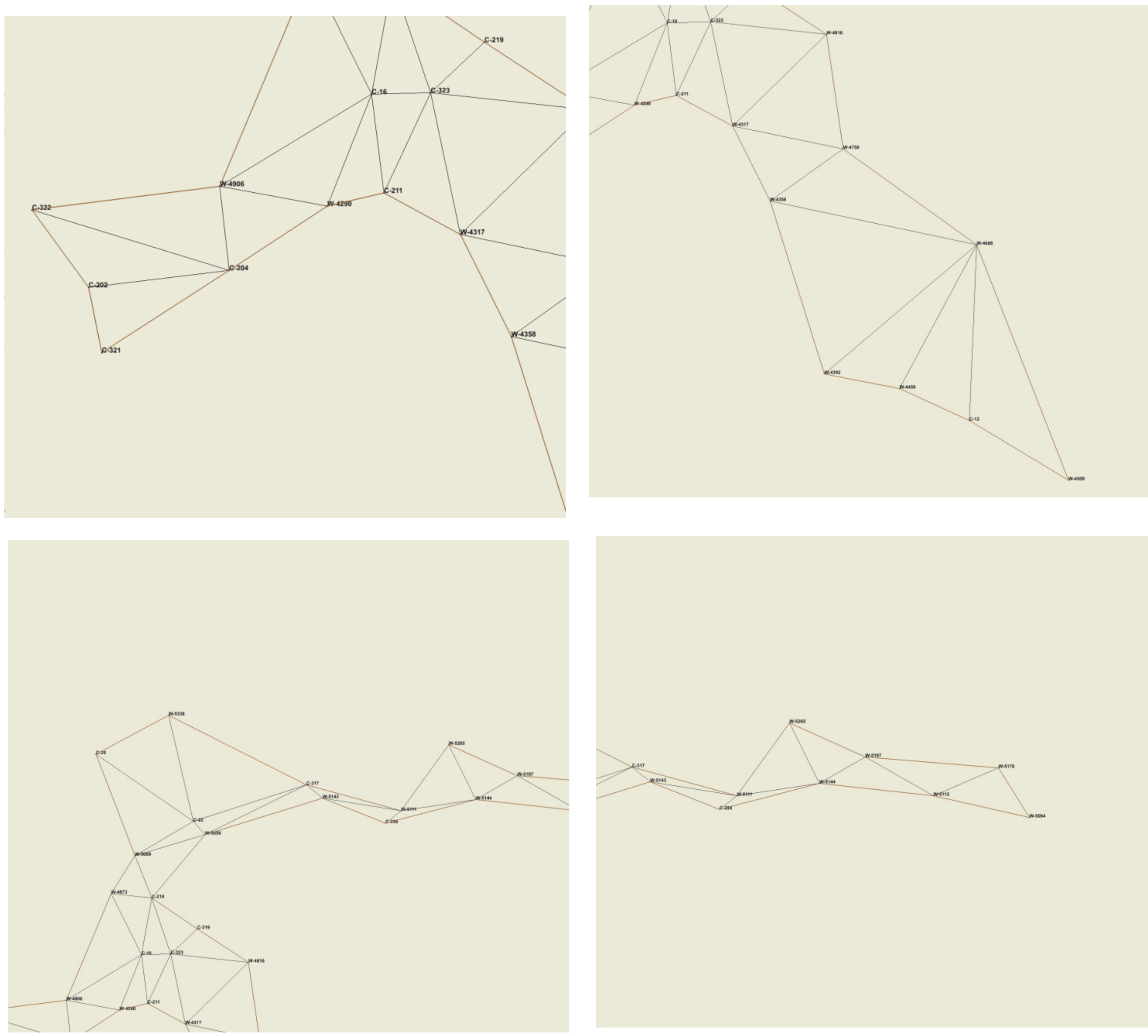

Figure 2.20. Unstructured Salinity and Temperature Initial Condition Grid, with the appropriate water level and CT stations assigned. Note it was necessary to assign synthetic CTD profiles to each station based on CT and CTD data.

2.5 Post-Operational Model Validation

CO-OPS is conducting a current meter survey in San Francisco Bay during the summers of 2012 and 2013. Approximately 45 stations will be occupied in total for 30-35 days with half of the stations occupied split between 2012 and 2013 at the locations shown in Figures 2.20-2.25. CTD profiles will be measured during deployment and retrieval of all current meters, thereby providing additional density information. SFBOFS will save current and density information at the final 45 selected stations to enable further model evaluation after the measurements have been quality controlled. This will enable post-operational validation and further model improvements.

As an additional source of post-operational model validation data, the following additional PORTS measurements are listed in priority order.

I. Salinity measurement locations:
PORTS Redwood City
PORTS Alameda
PORTS San Francisco
PORTS Richmond
PORTS Port Chicago

II. Current meter measurement locations from Welch et al. (1985):
C-211, C-6, C-7, C-312, C-13, C-18, C-22, C-24, and C-32

III. New PORTS station for water levels: 941-
4816, 4818, 5056, 5143, 5112, 4358, 4392, 4688, and 4509

IV. Near shelf salinity, temperature, and current measurement locations from Welch et al. (1985): Station T1

These additional PORTS measurements would need to be implemented over time with the highest priority being given to the acquisition of salinity information to further validate the operational model salinity structure within the Bay. The near-shelf measurements will support the development of the proposed, future NOS West Coast Operational Forecast System (WCOFS), which would address the cross and along shelf processes described by Marchesiello et al. (2003) and Penven et al. (2006)

A future WCOFS could be used in addition to Global-RTOFS (Global-RTOFS, NWS, http://polar.ncep.noaa.gov/global/about) to provide the open ocean boundary conditions for SFBOFS. During this process the SFBOFS grid will need modification and it will be useful to further consider the inundation and offshore grids shown in Figures 2.10 and 2.11, respectively.

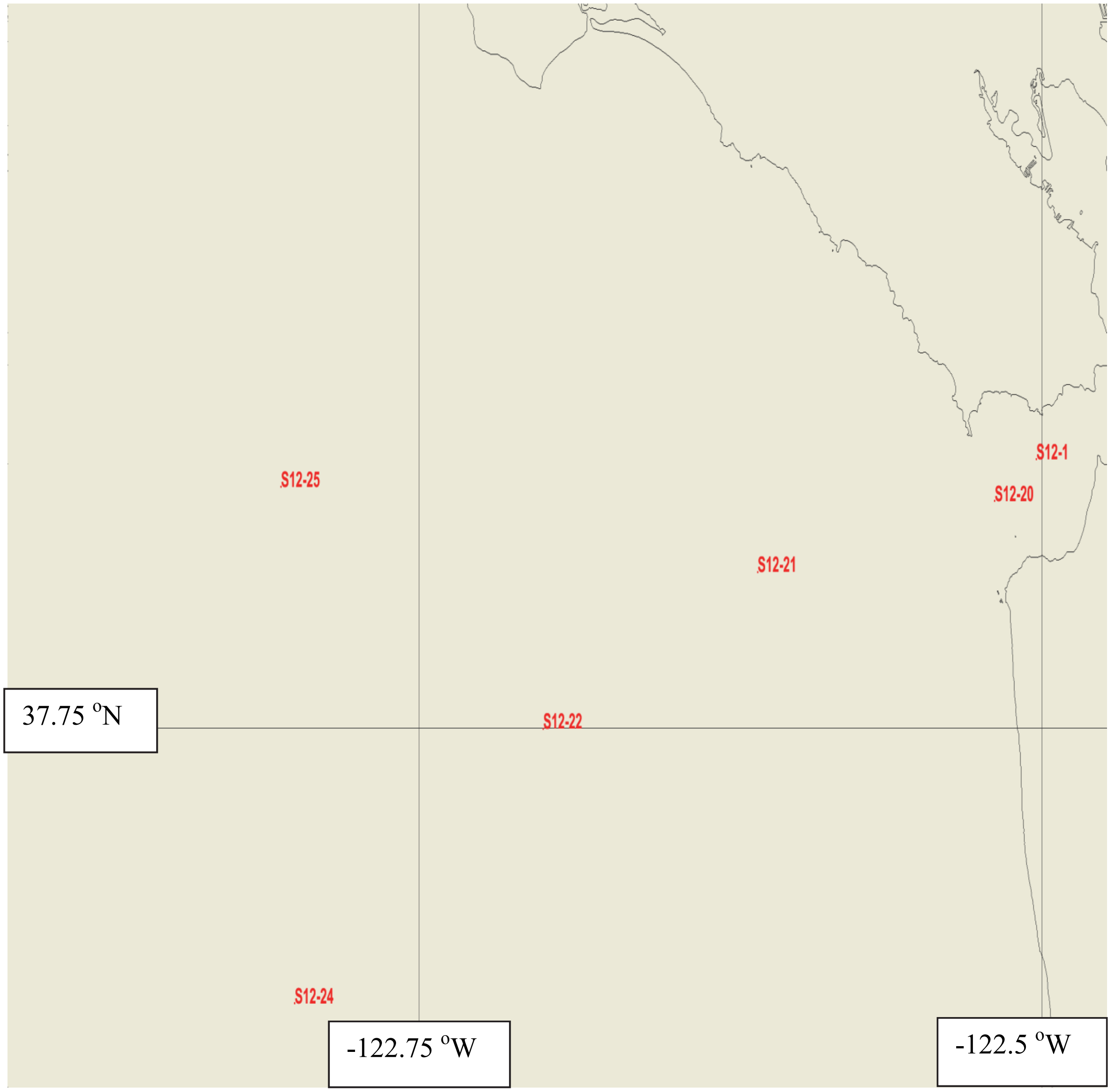

Figure 2.21. NOS 2012 Current Survey Locations in the offshore and entrance to San Francisco Bay.

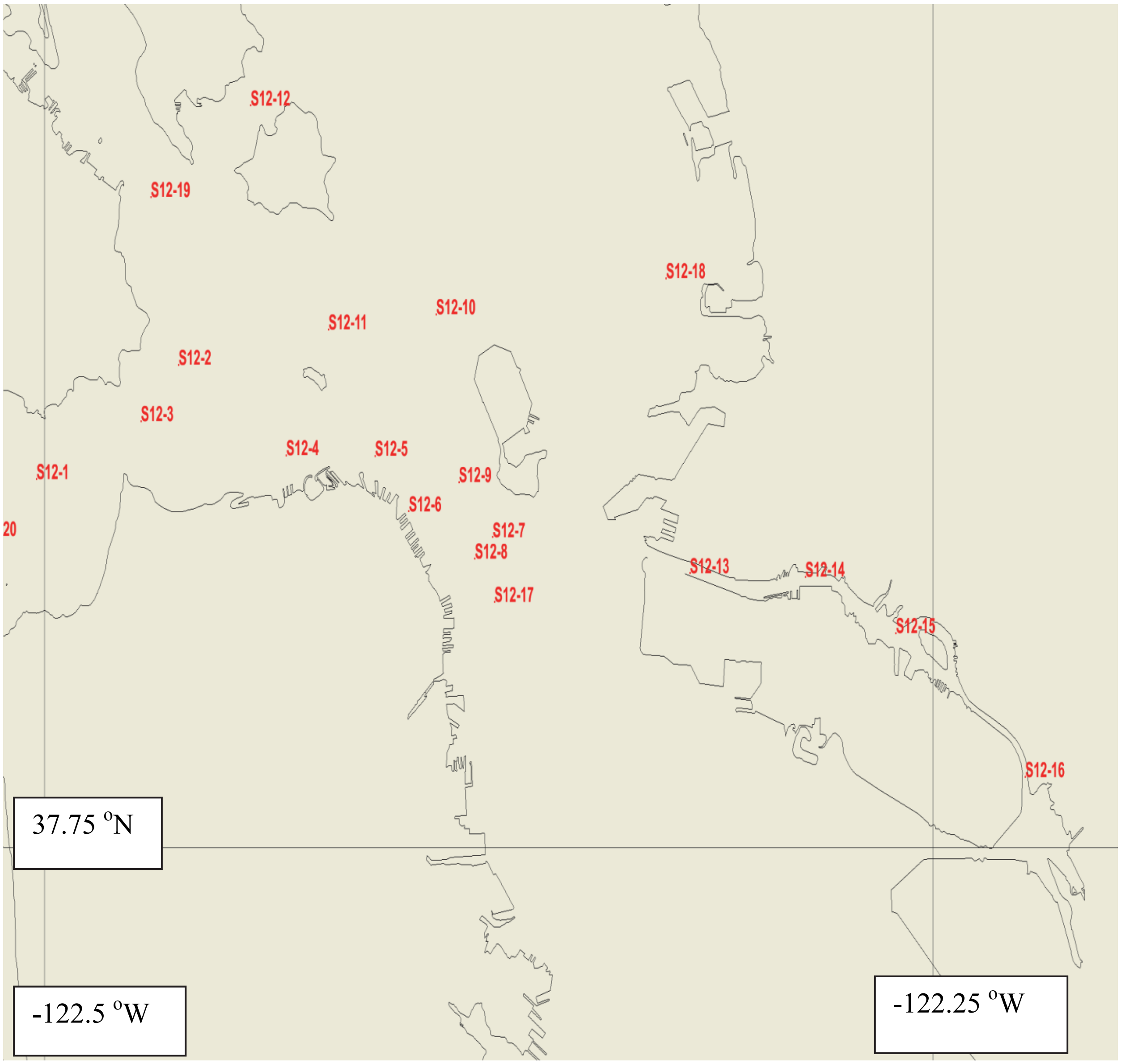

Figure 2.22. NOS 2012 Current Survey Station Locations in Central San Francisco Bay.

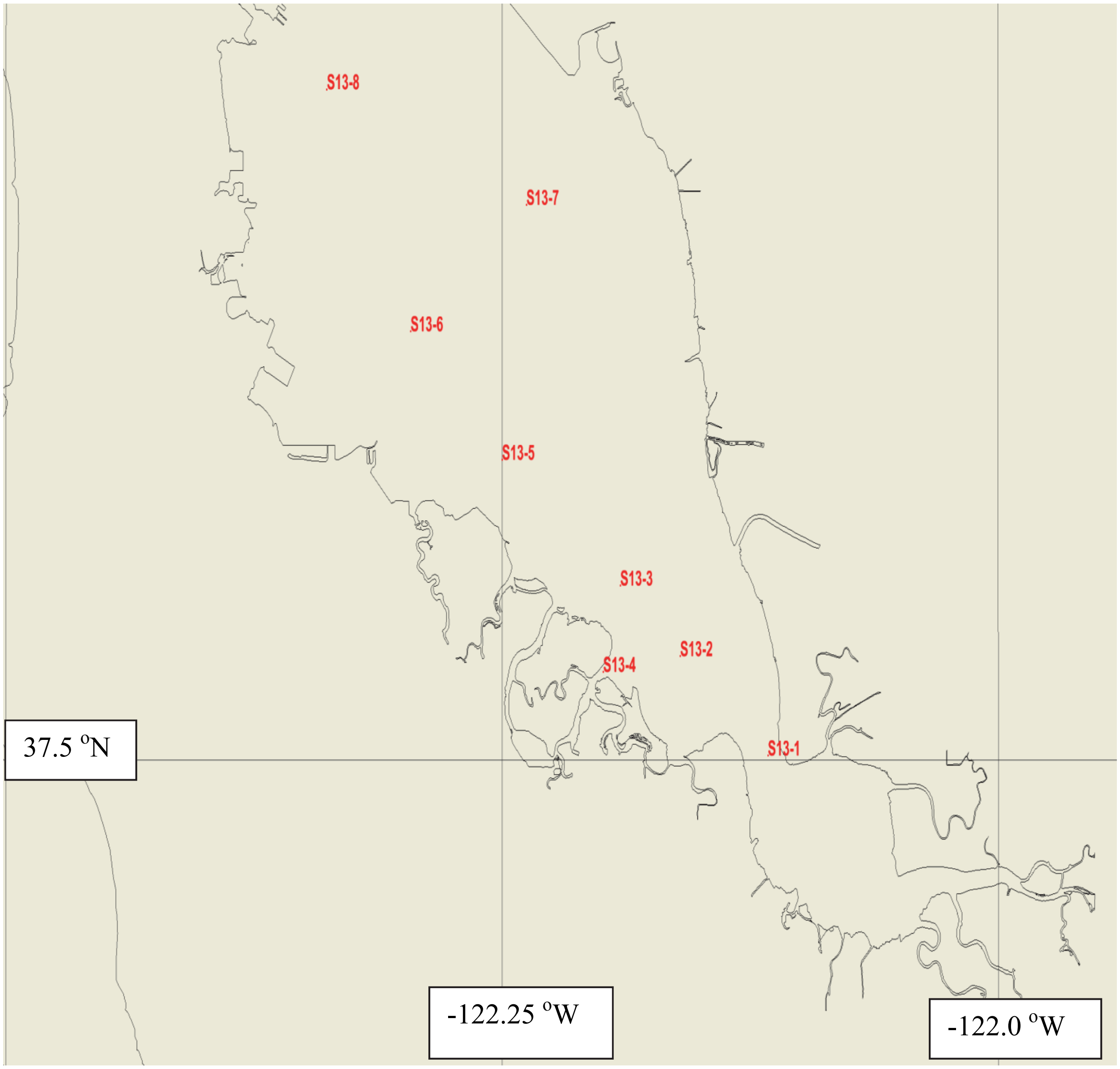

Figure 2.23. NOS 2013 Current Survey Locations in South San Francisco Bay.

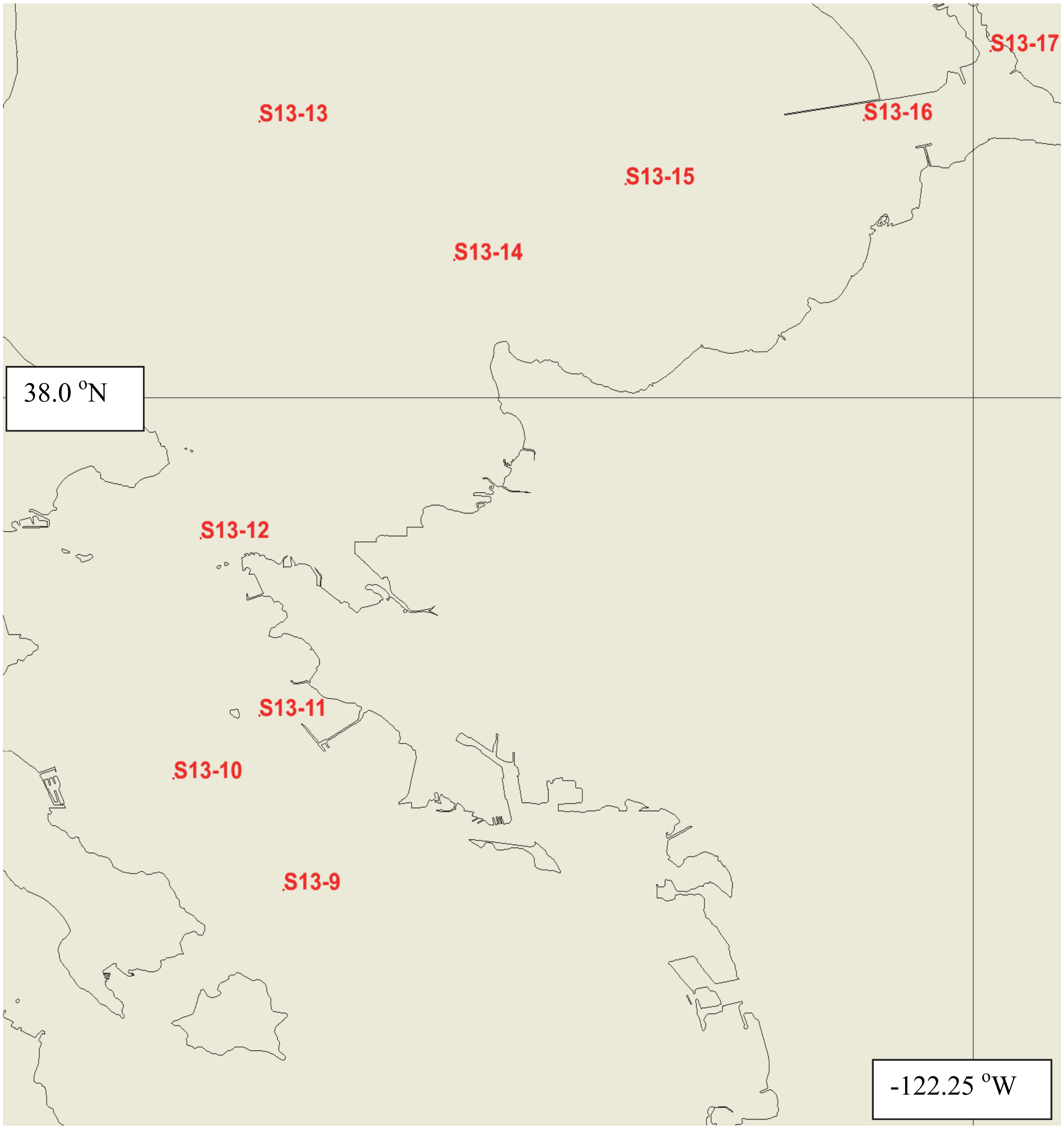

Figure 2.24. NOS 2013 Current Survey Locations in North San Francisco and San Pablo Bays.

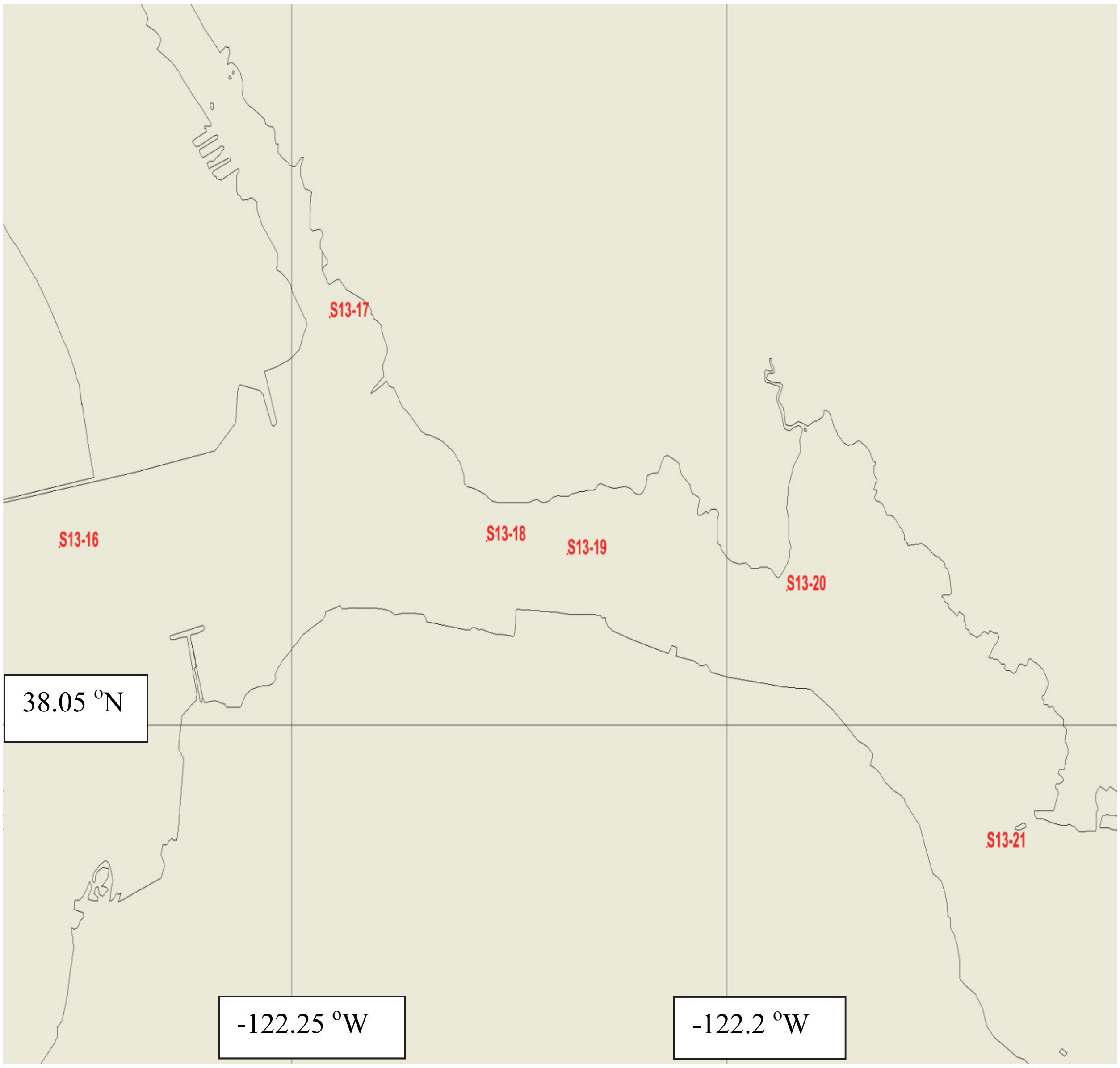

Figure 2.25. NOS 2013 Current Survey Locations in Carquinez Strait.

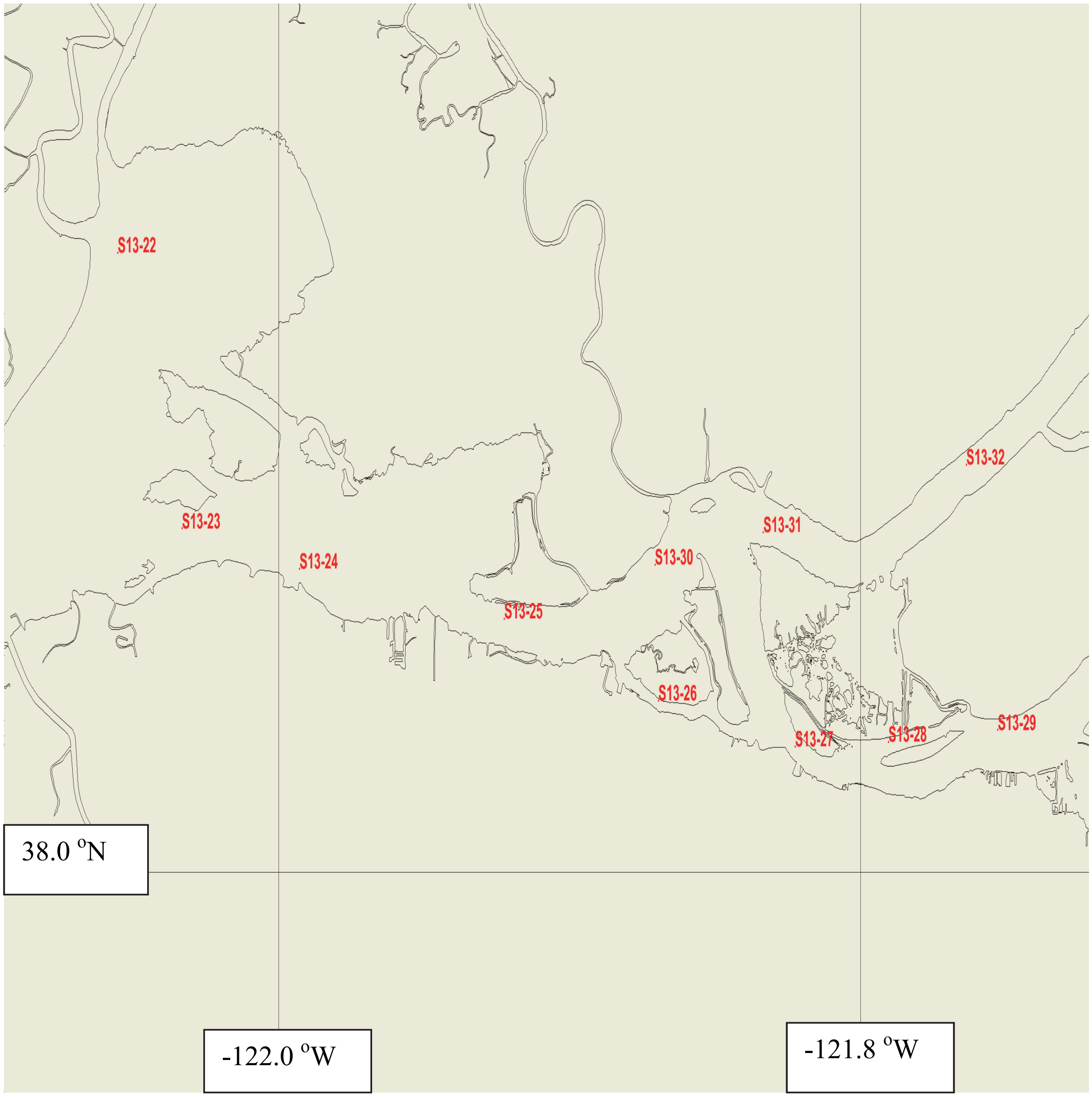

Figure 2.26. NOS 2013 Current Survey Locations in Suisun Bay and the Delta Entrance.

2.6 Model Revisions

FVCOM 3.1.6 was used as the initial version. However several additions were made in the development of SFBOFS. The draft version of the FVCOM 3.1.6 User Manual was reviewed and provided several insights into running the code. It should be noted that if the HEATING_CALCULATED_ON options is selected than the AIR_PRESSURE_ON option must be selected. While the sea level atmospheric pressure field is needed for the heating calculations, its gradient does not need to be applied in the momentum equations. In fact for tidal simulations this is not correct. For tidal simulations with the heat flux calculations selected, it is necessary to provide a constant sea level atmospheric pressure field (1013 mb). Also if one selects AIRPRESSURE_ON = F in namelist, the flag FLAG_28 = -DAIR_PRESSURE in file make.inc should be commented.

The bottom roughness fix reported by Warner (2012) for wetting/drying was added in file brough.F. In model testing, with the *min_depth* as 0.05 m the model ran successfully and works for the wetting/drying case in San Francisco Bay. A Newtonian damping sponge layer was implemented by Lettmann (2012), which provides a more robust implementation of the clamped water level open ocean boundary condition. This formulation was used on both the open ocean boundary and for the Delta river inflow boundary river stage specification.

In the shallow mud flat regions of the Bay there also was an issue with overheating. As a result, subroutine vdif_ts.F was modified to limit the short wave radiation and total heat flux as a function of depth. For depths less than 10m the fluxes were set to zero. In this manner, the heat transfer is due to only advection and diffusion. There the zeta1_eff and zeta2_eff parameters which control the attenuation of the short wave radiation are set never to be less than 30% of the water depth and therefore always allow attenuation

In total, the following routines are involved in the above modifications:

1. fvcom.F, mod_ncdio.F, mod_timeseries.F-----air_pressure option or heating_calculated_on option.

2. brough.F-----bottom roughness with the Warner (2012) wet/dry treatment.

3. advave_edge_gcn.F, advave_edge_gcy.F, extuv_edge.F, mod_semi_implicit.F and vdif_uv.F--- Lettmann (2012) sponge boundary.

4. vdif_ts.F and vdif_ts_gom.F----revised heat flux in shallow water.

All code changes were coordinated with the FVCOM Group at the University of Massachusetts at Dartmouth. The final version of the code was obtained on 22 July 2012 from the FVCOM Group.

The interaction between the hydrodynamic and the sediment-water interface, particularly in the shallow water mudflat areas, which occupy some 16% of the Bay surface area, is an area where further research is needed. Fang and Stefan (1996) considered the dynamics of heat exchange between the sediment and the bottom boundary layer for several hypothetical lakes. They found that the direction of the heat transfer reverses frequently on daily timescales as well as following an overall seasonal cycle based on weather conditions at Minneapolis-St. Paul, Minnesota. Smith (2002) performed a series of heat budget studies in Indian River Lagoon, Florida, to estimate the water-sediment heat exchanges using assumed values for conductivity and density. The study sought to characterize intra-seasonal heat fluxes and temperature changes in the sediment and overlying estuarine waters.

The bottom stress formulation in shallow water for wetting and drying has received continuing interest. Research by Xue and Due (2010), Uchiyama (2005), Oey (2005; 2006), and Oey et al. (2007) has indicated that the bottom drag coefficient must be adjusted if the water depth approaches the bottom roughness height. How to perform this adjustment is an area for further consideration. In the present version of FVCOM, the effective water depth used in the bottom friction formulation is limited to 3m; e.g., when the actual water depth is less than 3m, the depth used in the bottom friction formulation is set to 3m. We have recently developed a Fortran code, Program Cdform.f, to compute the bottom drag coefficient as the water depth is reduced using several different formulations.

The computation of rx0 and rx1 is recommended to provide a measure of bathymetric gradients to assist in studying the numerical stability. This was done in ROMS but is not done in FVCOM.

3. TIDAL CALIBRATION

Here we include the salinity and temperature in fully three-dimensional tidal simulations to enable the prediction of the density structure and the internal tides. Carter et al. (2010) note that the inclusion of internal tides in a baroclinic model can significantly alter the sea surface height field as compared to a barotropic model as observed in simulations of Monterey Bay tidal dynamics (Carter, 2010). In fact, it was necessary to include the salinity and temperature in the simulation to replicate the tidal dynamics in Monterey Bay.

First we present the results of the initial tidal simulation in Section 3.1. Next we discuss the two 2-month tidal simulations for April – May 1979 in Section 3.2 and September – October 1980 in Section 3.3. The intent was to consider two different tidal regimes with respect to the longer period tidal constituents. Additional experimental tidal simulations are then discussed in in Section 3.4, in an effort to improve the tidal response in the lower South Bay and at Port Chicago in Suisun Bay. A stage boundary condition specification was used at the Delta, which greatly improved the tidal response at Port Chicago relative to the flow specification. Using the Delta stage boundary condition an extended 19-month simulation was performed over the period April 1979 – October 1980 with the results presented in Section 3.5. Finally in Section 3.6, we summarize results and discuss additional considerations with respect to the simulation of the tidal dynamics.

3.1 Initial April 1–15, 1979 Tidal Simulation

An initial 15-day baroclinic simulation was performed using 6-hour NARR, downward long wave radiation and net heat flux. The salinity and temperature offshore boundary condition was determined by setting the normal gradients to zero. Flows were specified at 21 inflow locations (with the majority of the inflows from the Sacramento River at Rio Vista and the San Joaquin River at Antioch) using average daily flows from the California Department of Natural Resources' DAYFLOW program as shown in Figure 3.1. Inflows were also specified for the Napa River, Petaluma River, Guadalupe River, and Coyote Creek using USGS average daily values. Initial salinity and temperature fields were developed based on CT data collected during the joint NOS-USGS historical circulation survey. Offshore tidal elevations were developed from the Oregon State University Tidal Data Inversion, OTIS Regional Tide Solutions (2010) tidal constituents. The Sa and Ssa constituents were specified using the San Francisco accepted constants. The net-heat flux and downward short wave radiation using the HEATING_ON option were interpolated to the model grid using bi-linear interpolation from the NARR fields at 6 hour intervals. The sea level atmospheric pressure field was estimated from the surface fields.

Simulation results for water surface elevation and principal component direction currents, vertically integrated and mid layer (k=10), are compared to harmonic predictions in terms of RMS error and Willmott et al. (1985) relative error in Tables 3.1 and 3.2, respectively. In addition model and predicted means with respect to station MLLW are compared as well. In Figure 3.2 simulated water levels at Port Chicago and Coyote Creek are considered since these stations are located in Suisun Bay near the Delta and at the southern end of South Bay, respectively. One notes the simulated water levels are over predicted at Port Chicago and under predicted at Coyote Creek. In Figure 3.3 simulated water levels at Point Reyes near the offshore boundary and at San Francisco are in close agreement with predictions. One notes the spike just prior to Julian day 96 at Point Reyes. It appears that there is some reflection from the boundary, where a pure water level specification is employed, despite the fact that a sponge layer is utilized. In Figures 3.4 and 3.5, points immediately inside the offshore boundary are compared with predictions at Point Reyes. In Figure 3.5, one notes the spike just prior to Julian day 96. In Figure 3.6, the simulated water levels are shown immediately inside the inflow boundaries for the Sacramento and San Joaquin Rivers. Amplitudes are considerably larger than those of the M_2 tidal components at both locations. In Figure 3.7, vertically integrated principal component currents are under predicted at C-1 at the Golden Gate Bridge and are over predicted at C-17 in mid-Bay.

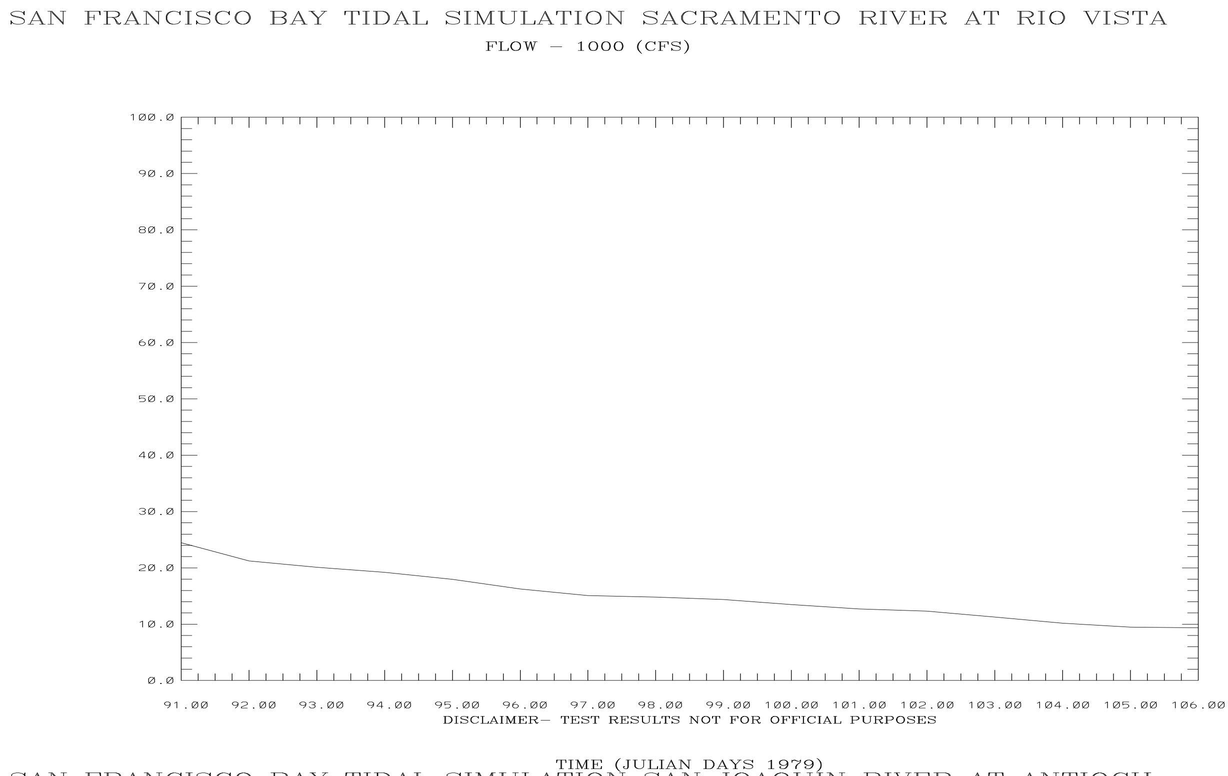

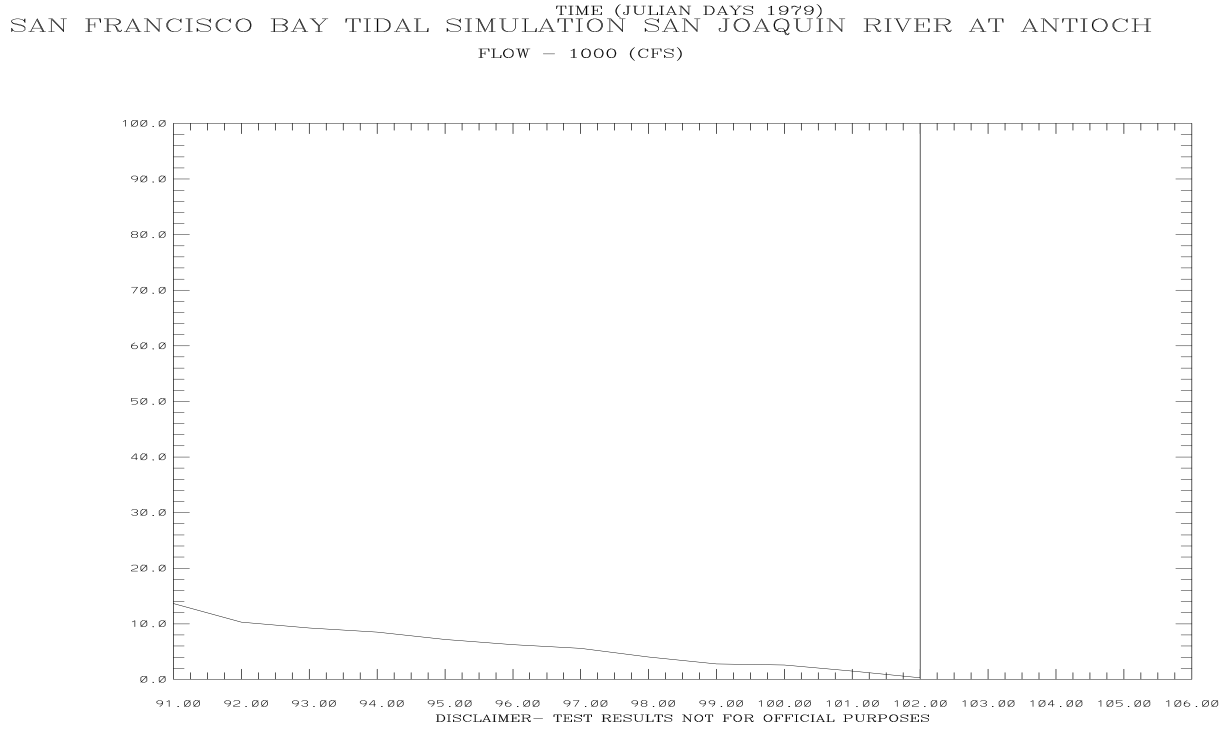

Figure 3.1. DAYFLOW inflows for the Sacramento and San Joaquin Rivers 1-15 April 1979. The flow after Julian Day 102 is negative and is set to zero.

Table 3.1. Water Surface Elevation Tidal Simulation: April 1-15, 1979. Note model and predicted means are with respect to station MLLW.

Station	RMSE (cm)	Willmott RE (%)	Model mean (cm)	Predicted mean (cm)
Alameda 941-4750	13	1	105	102
Dumbarton Bridge 941-4509	23	3	141	135
Oyster Point Marina 941-4392	16	2	116	111
Port Chicago 941-5144	25	7	147	130
Point Reyes 941-5020	9	1	90	88
San Francisco 941-4290	11	1	91	91
Pier 22.5 941-4317	12	1	97	95
San Mateo Bridge 941-4458	18	2	126	121
Coyote Creek 941-4575	25	3	155	150

Table 3.2. Principal Flood Direction Current Speed Tidal Simulation: April 1-15, 1979. Note the first entry in each cell corresponds to the vertically integrated current, while the second entry corresponds to the current in mid-level layer k=10.

Station	RMSE (cm/s)	Willmott RE (%)	Model mean (cm/s)	Predicted mean (cm/s)
C-1 GG	37 50	6 12	6 8	28
C-5 MB	20 26	6 10	-2 10	14
C-17 MB	17 15	3 5	-2 8	12
C-18 MB	18 28	3 7	4 15	13
C-19 SPB	12 10	4 4	1 3	8
C-20 SPB	24 27	31 43	-3 3	10
C-22 SPB	30 18	11 6	-2 6	11
C-23 SPB	5 6	3 3	1 1	5
C-24 CS	35 33	7 9	3 -8	-4
C-25 CS	38 25	13 8	-8 1	7
C-26 SB	37 34	12 11	-7 -3	5
C-28 SB	10 10	8 9	-1 0	7
C-29 SB	31 30	27 30	4 2	0
C-30 SB	33 30	29 30	2 0	0
C-31 SB	17 17	25 25	0 0	0
C-33 SB	35 36	46 52	1 0	0

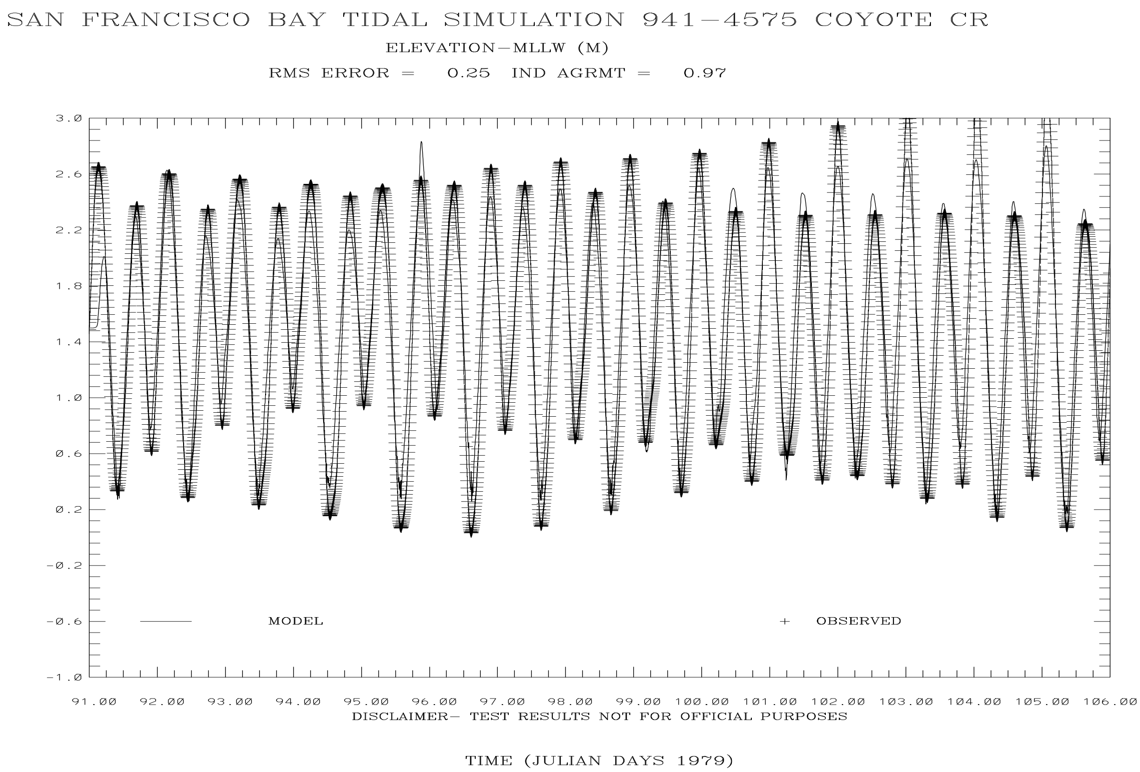

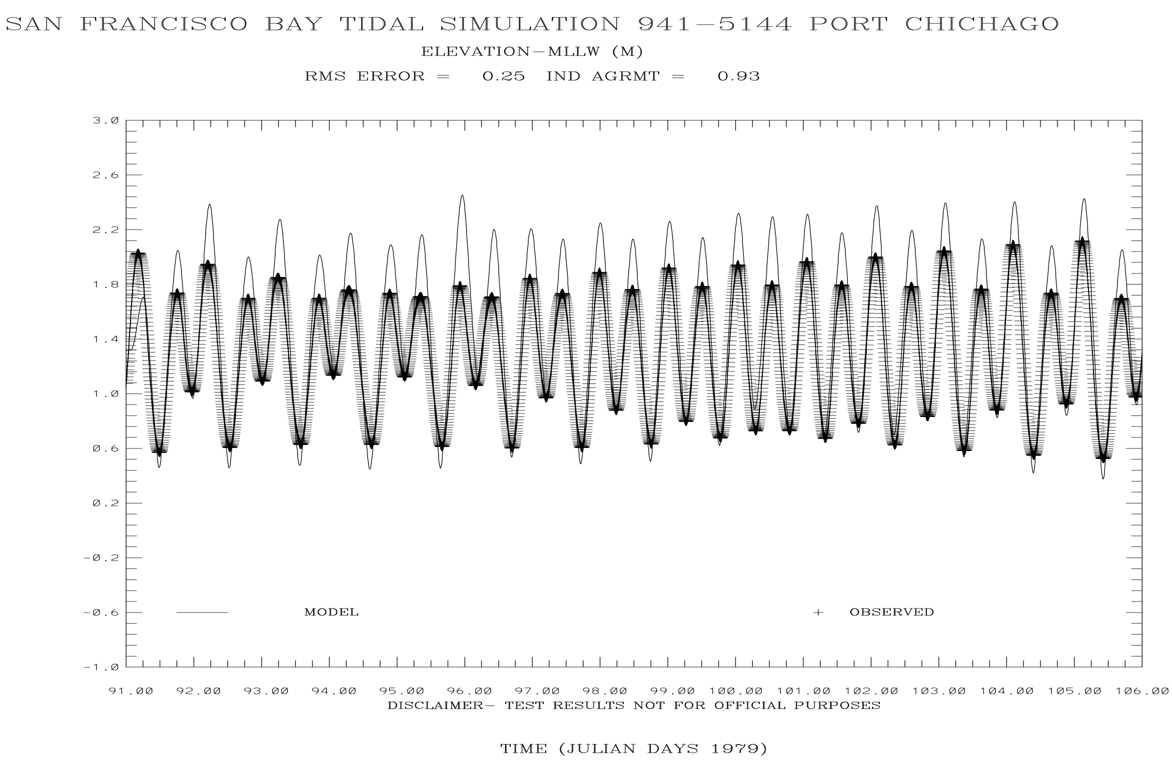

Figure 3.2. April 1-15, 1979 Initial Tidal Simulation: Coyote Creek and Port Chicago Water Level Comparisons. Note IND AGRMT equals one minus Willmott et al. (1985) relative error.

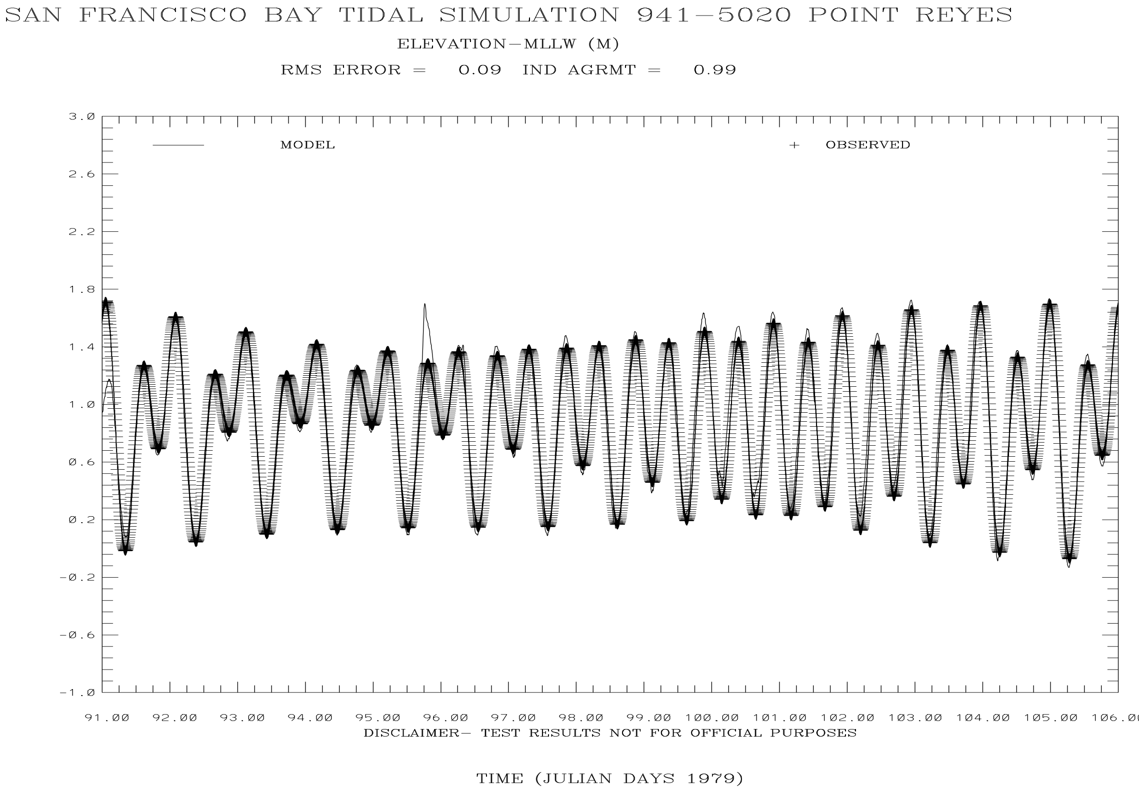

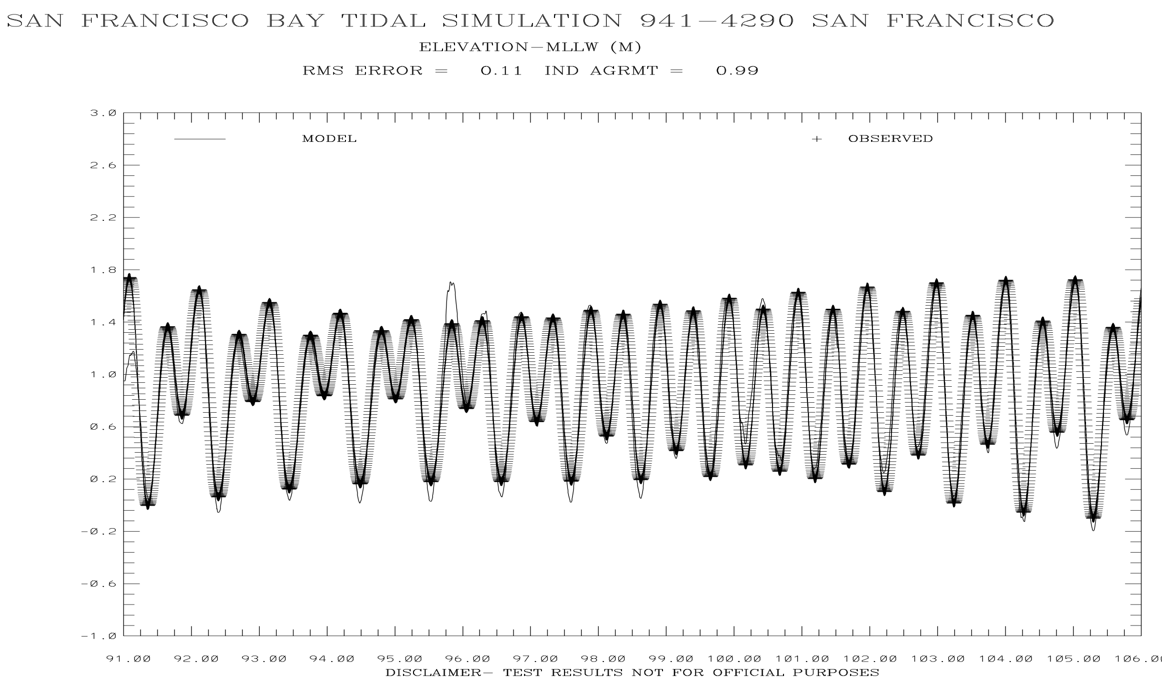

Figure 3.3. April 1-15, 1979 Initial Tidal Simulation: Point Reyes and San Francisco Water Level Comparisons. Note IND AGRMT equals one minus Willmott et al. (1985) relative error.

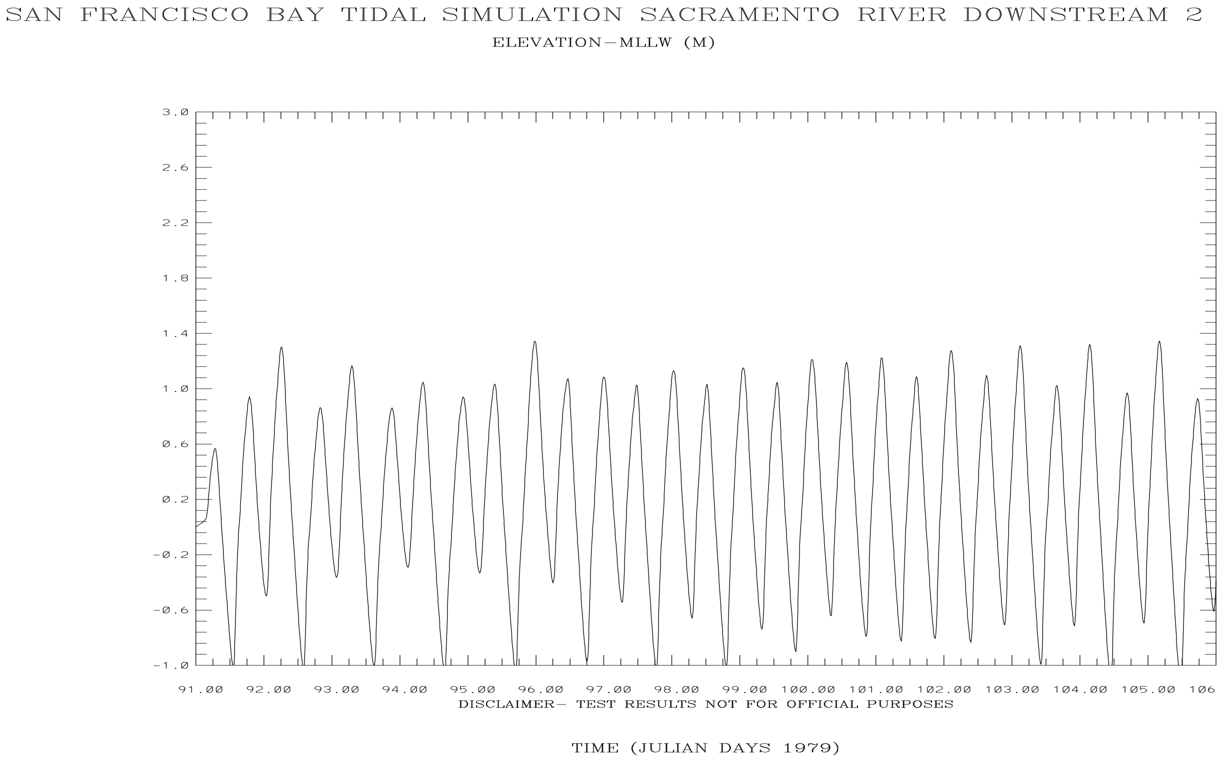

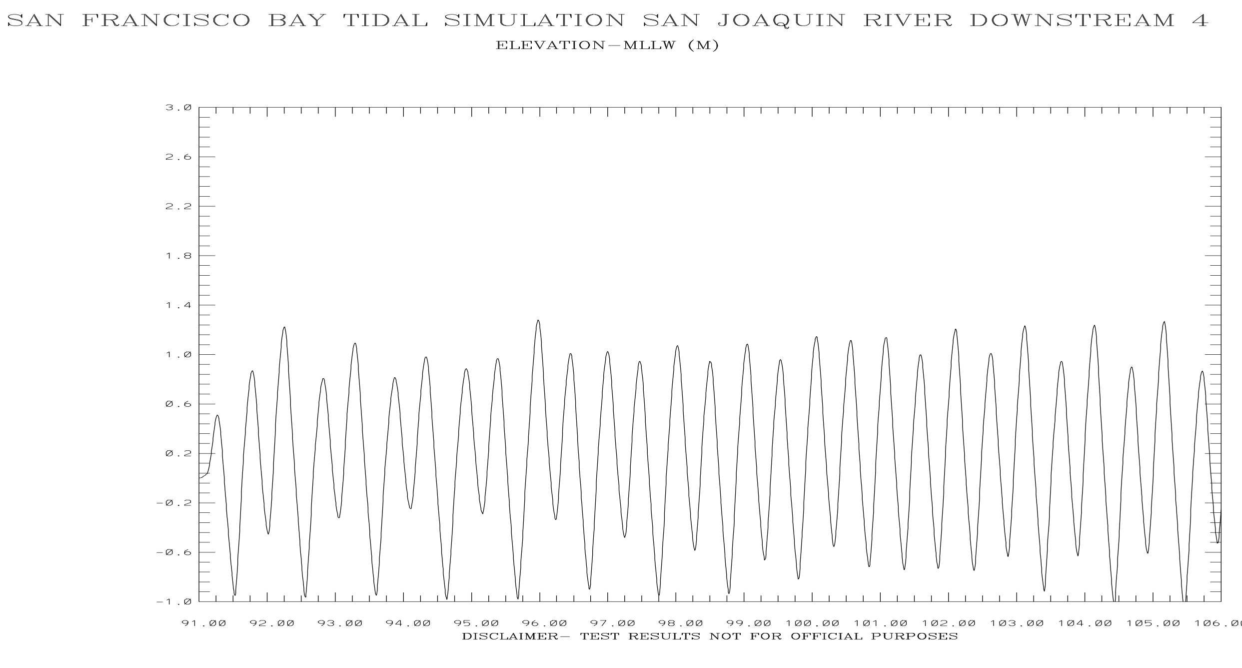

Figure 3.4. April 1-15, 1979 Initial Tidal Simulation: Sacramento River and San Joaquin River Inflow Water Levels. Note IND AGRMT equals one minus Willmott et al. (1985) relative error.

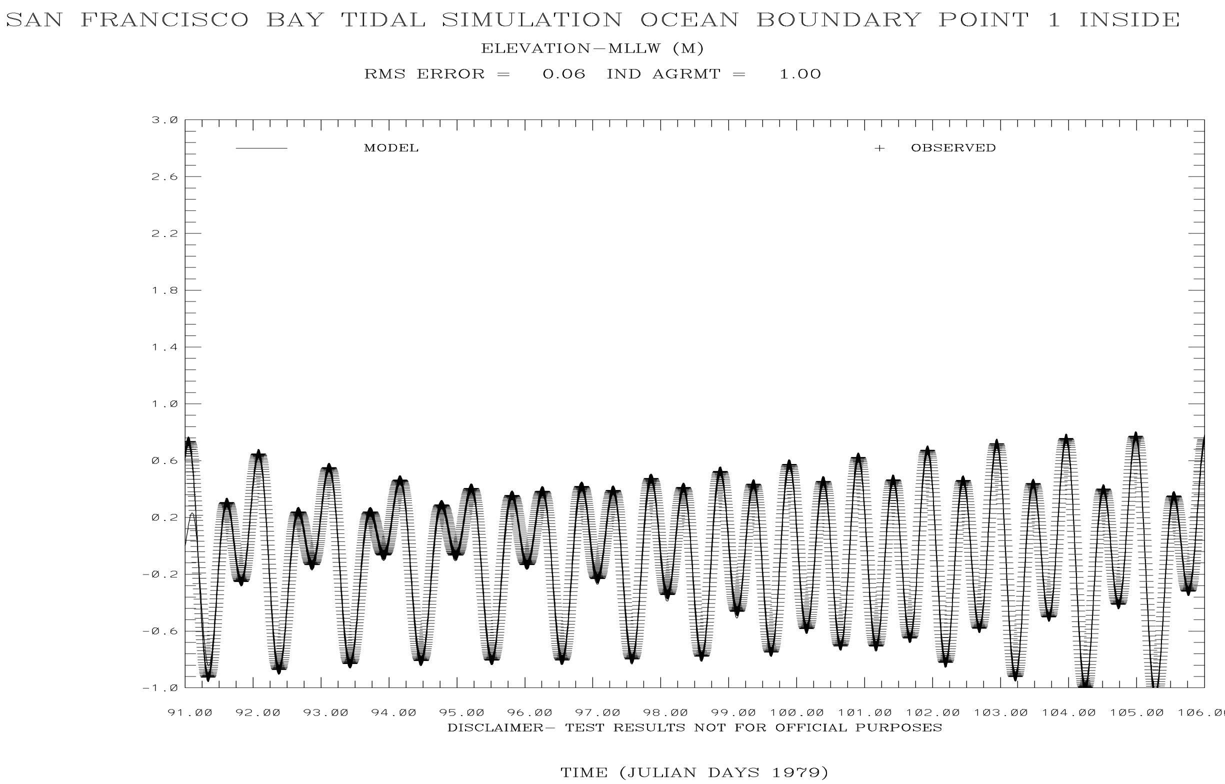

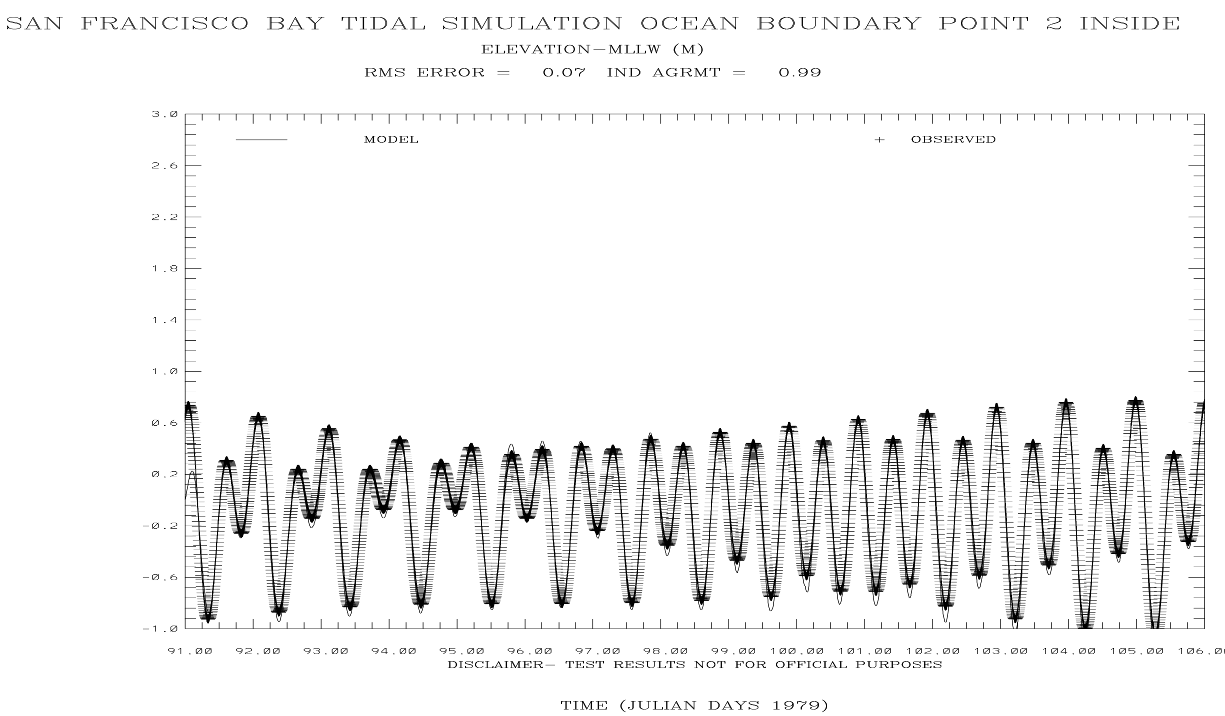

Figure 3.5. April 1-15, 1979 Initial Tidal Simulation: Boundary Point 1 and 2 Inside Water Level Comparisons. Note IND AGRMT equals one minus Willmott et al. (1985) relative error.

SAN FRANCISCO BAY TIDAL SIMULATION OCEAN BOUNDARY POINT 3 INSIDE

ELEVATION–MLLW (M)

RMS ERROR = 0.13 IND AGRMT = 0.98

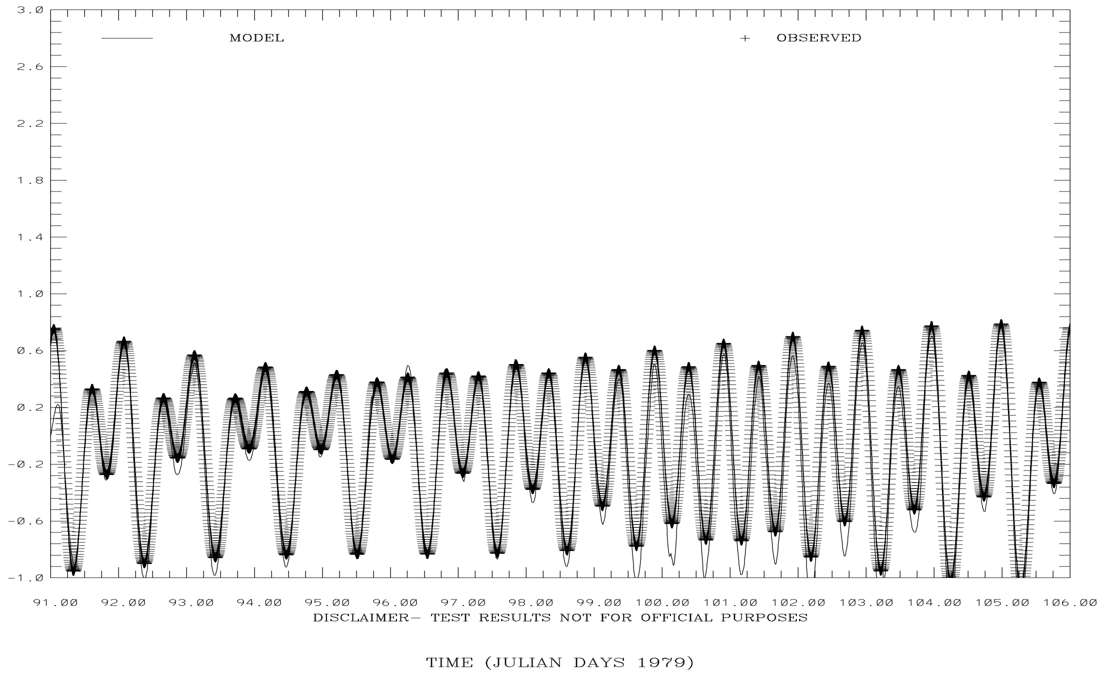

SAN FRANCISCO BAY TIDAL SIMULATION OCEAN BOUNDARY POINT 4 INSIDE

ELEVATION–MLLW (M)

RMS ERROR = 0.09 IND AGRMT = 0.99

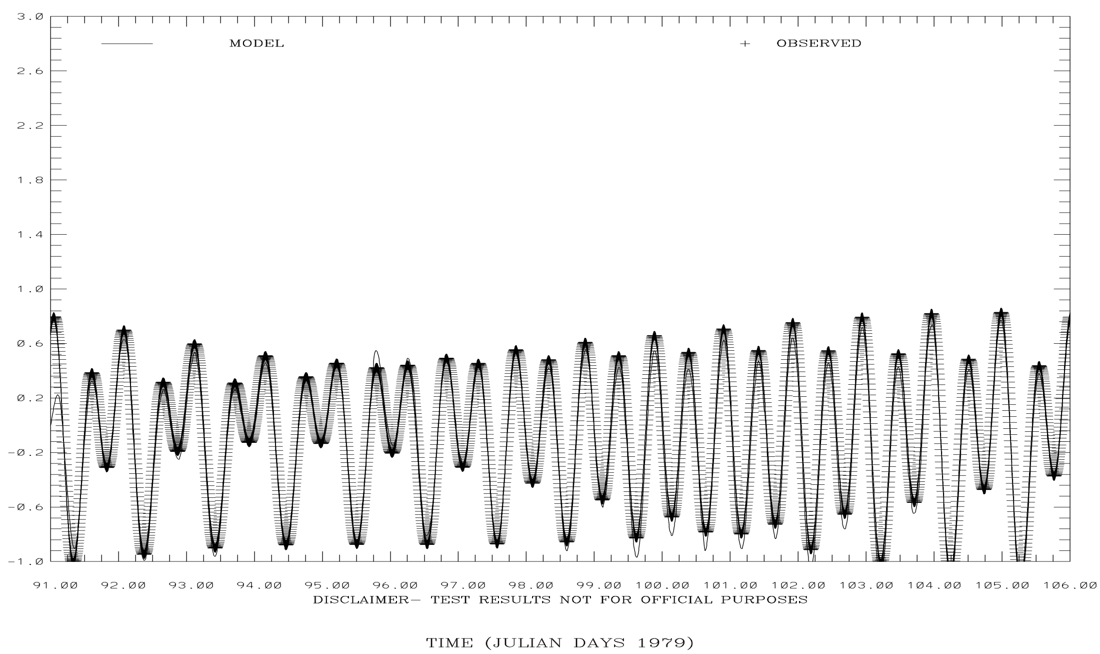

Figure 3.6. April 1-15, 1979 Initial Tidal Simulation: Boundary Point 3 and 4 Inside Water Level Comparisons. Note IND AGRMT equals one minus Willmott et al. (1985) relative error.

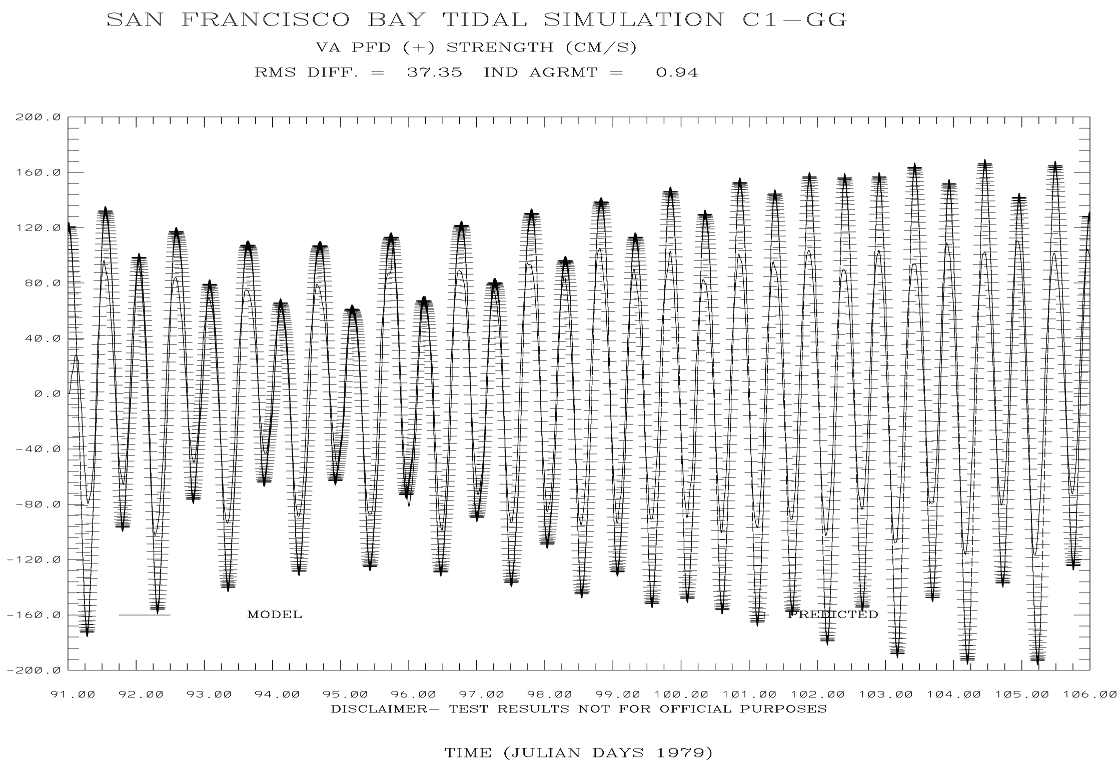

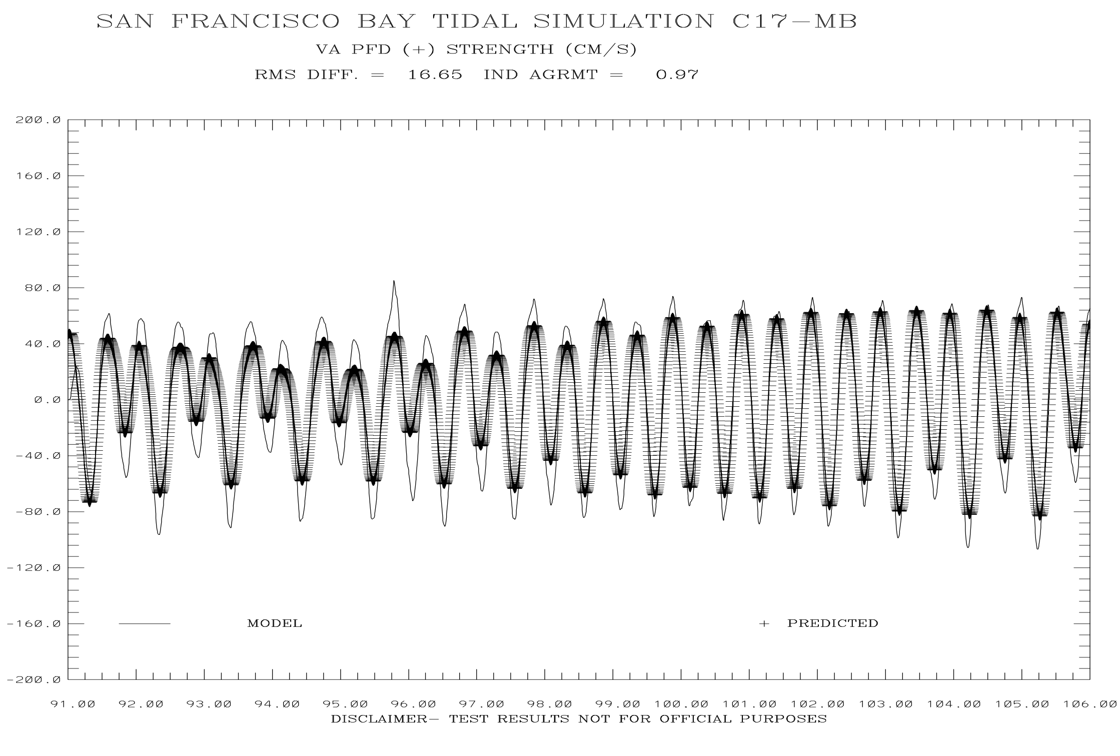

Figure 3.7. April 1-15, 1979 Initial Tidal Simulation: C-1 and C-17 Vertically Integrated Principal Current Component Comparisons**.** Note IND AGRMT equals one minus Willmott et al. (1985) relative error.

3.2 April-May 1979 Tidal Simulation

In an effort to improve the heat flux specification, the latent and sensible heat fluxes were dynamically coupled to the sea surface temperature using the HEATING_CALCULATED_ON option. The NARR fields were interpolated to the model grid using the Barnes (1963) algorithm at 3 hour intervals and the sea level atmospheric pressure field was directly used. The downward radiation and total heat flux were set to zero in the shallow water regions less than 10m in depth. A revised sponge layer treatment near the open ocean boundary was considered. A zero gradient temperature and salinity condition was invoked along the open ocean boundary. The Oregon State University Tidal Data Inversion, OTIS Regional Tide Solutions (2010) harmonic constant set was used as given in Table 2.3. River inflows were specified as previously discussed in Section 3.1. The two month simulation was completed in four segments of 15, 15, 15, and 16 day duration. Each segment required approximately 3.5 CPU hours on the NCEP-CCS using 256 processors.

In Tables 3.3 and 3.4, simulation results for water surface elevation and principal component direction currents vertically integrated and mid layer (k=10) respectively are compared to harmonic predictions in terms of RMS error and Willmott et al. (1985) relative error. In addition model and predicted means with respect to station MLLW are compared as well. In Figures 3.8 and 3.12 simulated water levels at Port Chicago and Coyote Creek are considered since these stations are located in Suisun Bay near the Delta and at the southern end of South Bay, respectively. The simulated water levels are overpredicted at Port Chicago and underpredicted at Coyote Creek. In Figures 3.9 and 3.13 simulated water levels at Point Reyes near the offshore boundary and at Richmond are considered with simulated water levels in close agreement with predictions. The spike just prior to Julian day 96 at Point Reyes is no longer present. It appears that the revised sponge layer improves the water level response. In Figures 3.10 and 3.14 vertically integrated principal component currents are under predicted at C-1 at the Golden Gate Bridge and over predicted at C-6 in mid-Bay. In Figures 3.11 and 3.15 vertically integrated principal component currents are over predicted at C-19 in San Pablo Bay and at CS-24 at the entrance to Carquinez Strait.

Table 3.3. Water Surface Elevation Tidal Simulation: April- May, 1979. Note there are four entries in each cell corresponding to the results of the 15 day simulation segments. Model and predicted means are with respect to station MLLW.

Station	RMSE (cm)	Willmott RE (%)	Model mean (cm)	Predicted mean (cm)
Alameda 941-4750	10 7 6 7	1 0 0 0	98 97 96 99	102 100 98 98
Dumbarton Bridge 941-4509	13 10 9 11	1 0 0 0	132 132 130 134	135 133 132 132
Oyster Point Marina 941-4392	10 8 7 9	1 0 0 0	108 108 106 110	111 109 108 108
Port Chicago 941-5144	20 20 18 21	5 4 4 4	71 72 69 76	76 74 72 73
Point Reyes 941-5020	8 6 5 7	1 0 0 0	86 85 84 87	88 86 86 86
San Francisco 941-4290	9 7 6 7	1 0 0 0	87 85 85 88	91 89 88 88
Pier 22.5 941-4317	9 6 5 6	1 0 0 0	92 90 90 93	95 93 92 92
San Mateo Bridge 941-4458	10 7 5 7	1 0 0 0	119 118 116 120	121 119 118 118
Coyote Creek 941-4575	18 20 15 20	1 1 1 1	144 144 142 146	146 144 142 143

Table 3.4. Principal Flood Direction Current Speed Tidal Simulation: April –May, 1979. Note there are four entries in each row of each cell corresponding to the results of the 15 day simulation segments. Note the first row in each cell corresponds to the vertically integrated current, while the second row corresponds to the current in mid-level layer k=10.

Station	RMSE (cm/s)	Willmott RE (%)	Model mean (cm/s)	Predicted mean (cm/s)
C-1 GG	27 32 29 31 41 48 43 47	3 3 3 3 7 8 8 7	8 9 7 9 9 11 8 9	0 0 0 0
C-5 MB	15 16 15 17 25 29 27 30	3 3 3 3 9 10 10 11	0 0 0 0 11 11 10 11	0 0 0 0
C-17 MB	20 20 18 22 11 10 10 11	5 3 3 4 2 1 2 2	-3 -4 -3 -4 7 5 6 5	0 0 0 0
C-18 MB	14 13 12 14 24 22 22 23	2 1 1 1 4 3 3 3	4 3 3 3 15 14 14 14	0 0 0 0
C-19 SPB	13 12 12 13 8 10 9 10	4 2 3 3 2 2 2 3	0 1 1 0 3 4 3 4	0 0 0 0
C-20 SPB	14 17 15 17 17 20 18 20	8 9 9 8 12 13 14 13	-1 -1 -1 -1 0 0 1 1	0 0 0 0
C-22 SPB	33 32 31 33 16 15 15 16	11 8 10 9 4 3 3 3	-2 -3 -1 -3 6 5 6 5	0 0 0 0
C-23 SPB	6 6 6 6 5 5 5 5	3 2 3 2 3 2 3 2	1 0 1 0 1 1 2 1	0 0 0 0
C-24 CS	27 32 27 33 26 36 32 35	4 5 4 5 6 9 8 8	3 1 2 3 -9 -11 -12 -10	0 0 0 0
C-25 CS	34 34 32 35 18 19 19 20	10 8 8 8 4 4 4 4	-8 -7 -7 -8 2 7 8 6	0 0 0 0
C-26 SB	27 30 27 31 25 28 25 28	7 6 6 7 6 6 6 7	-5 -4 -4 -5 -2 0 0 -1	0 0 0 0
C-28 SB	9 9 9 9 9 9 9 10	6 4 5 4 6 5 6 6	0 0 0 0 0 0 0 0	0 0 0 0
C-29 SB	26 31 28 31 26 31 28 32	18 19 19 20 21 22 22 23	3 2 2 3 2 1 1 2	0 0 0 0
C-30 SB	27 32 28 32 26 31 28 31	21 22 22 22 24 25 25 25	1 -1 0 1 -1 -2 -1 0	0 0 0 0
C-31 SB	15 17 16 17 15 18 16 18	17 18 18 18 18 19 19 20	0 1 1 1 0 1 1 1	0 0 0 0
C-33 SB	33 40 35 39 35 42 37 41	41 44 43 44 50 52 52 54	2 0 1 1 1 0 0 1	0 0 0 0

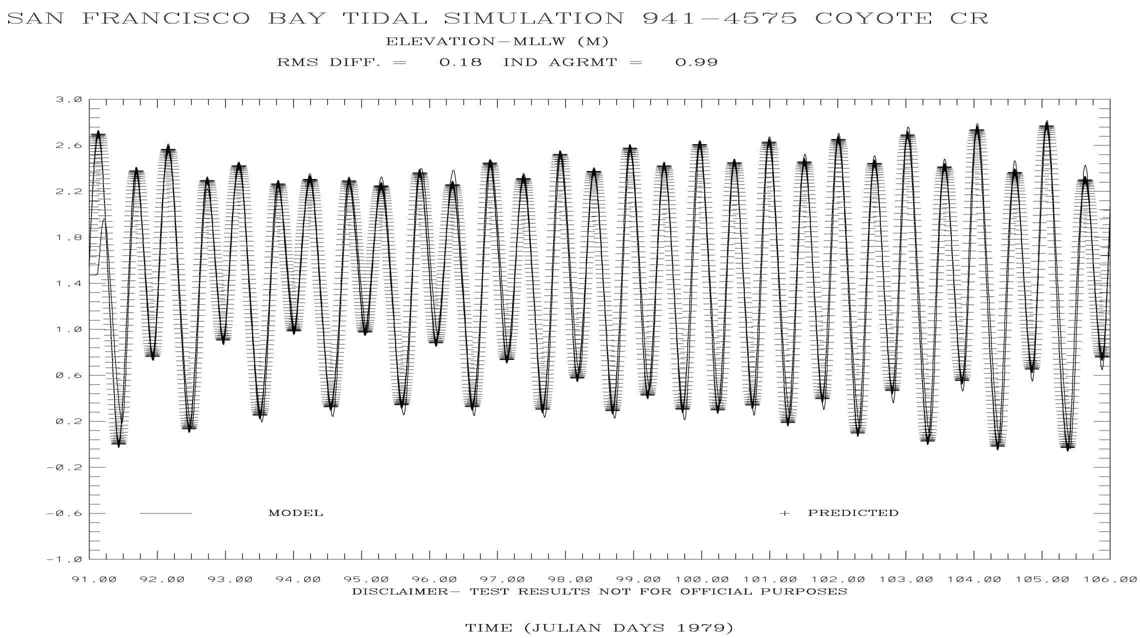

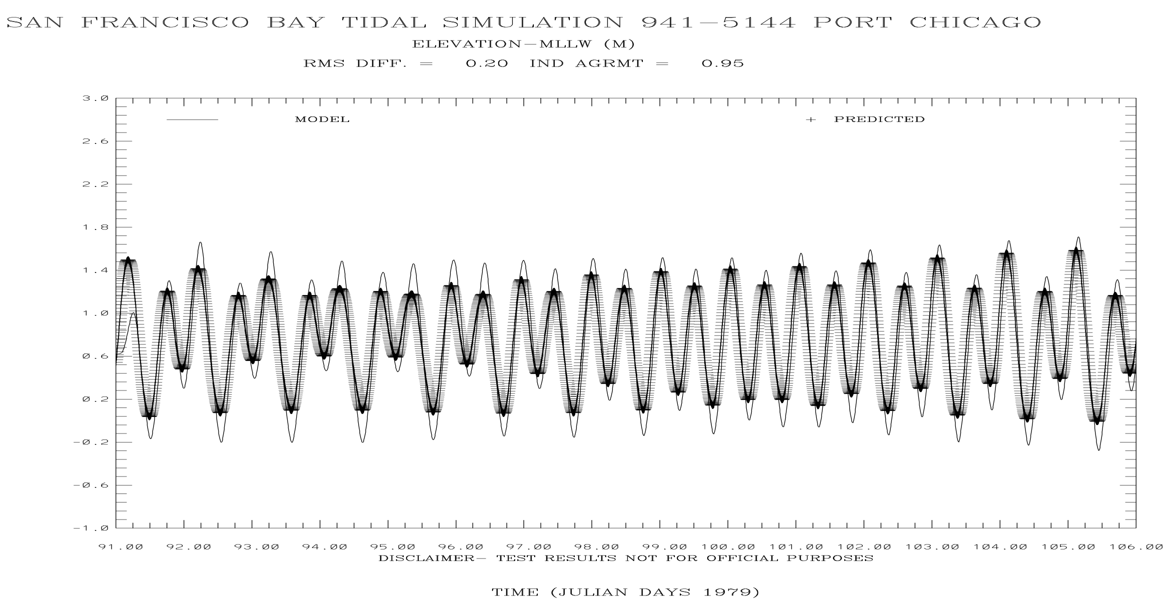

Figure 3.8. April 1-15, 1979 Tidal Simulation: Coyote Creek and Port Chicago Water Level Comparisons. Note IND AGRMT equals one minus Willmott et al. (1985) relative error.

SAN FRANCISCO BAY TIDAL SIMULATION 941−5020 POINT REYES
ELEVATION−MLLW (M)
RMS DIFF. = 0.08 IND AGRMT = 0.99

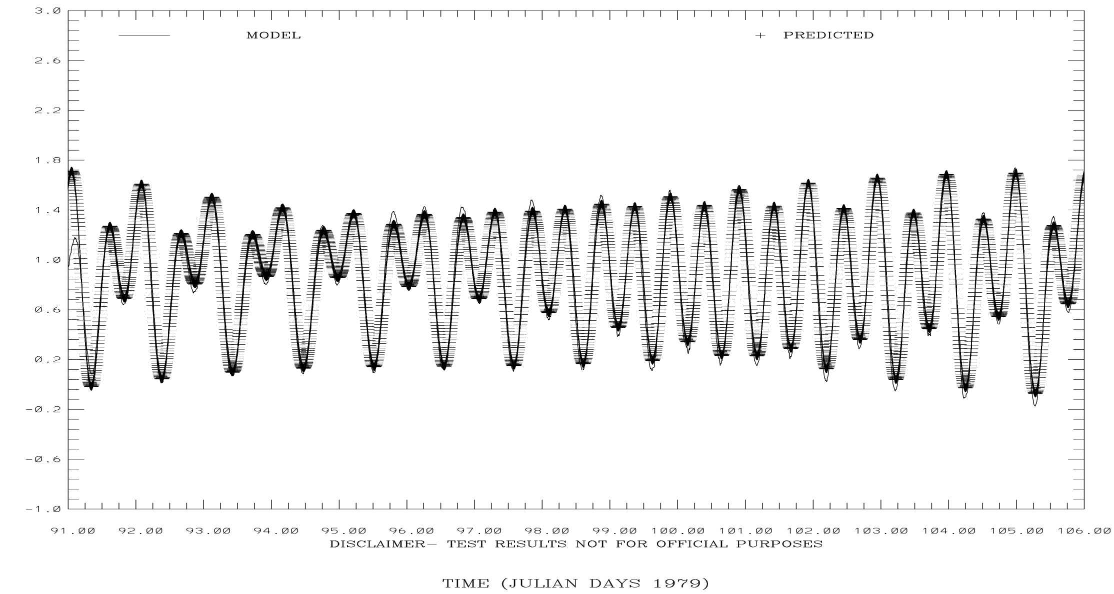

SAN FRANCISCO BAY TIDAL SIMULATION 941−4863 RICHMOND
ELEVATION−MLLW (M)
RMS DIFF. = 0.08 IND AGRMT = 0.99

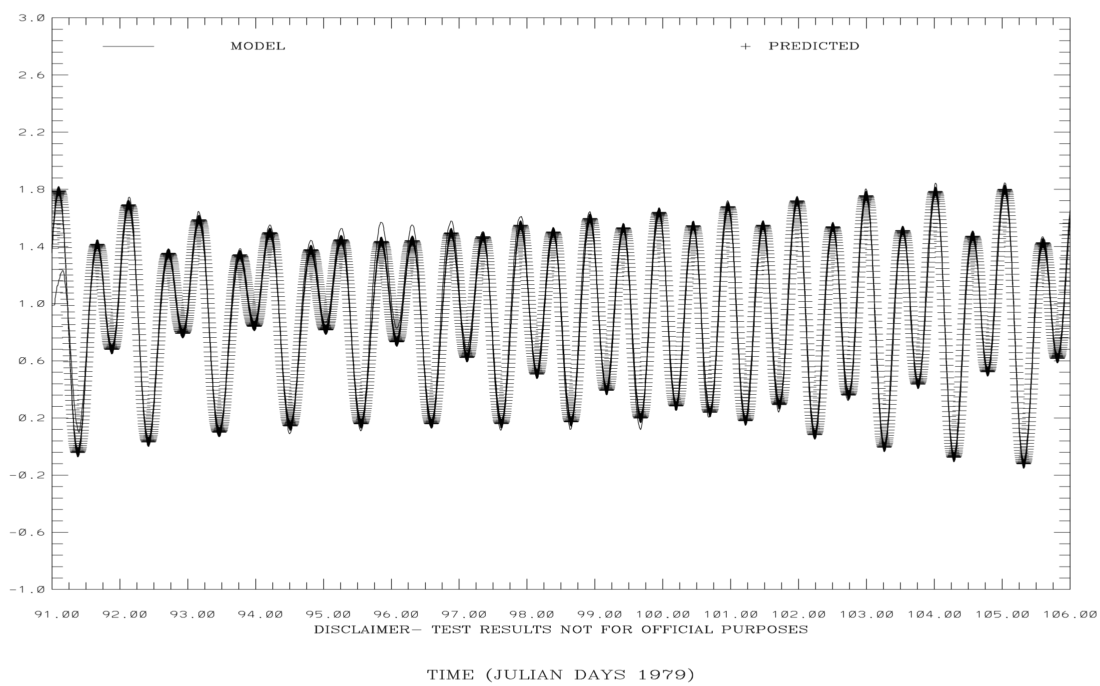

Figure 3.9. April 1-15, 1979 Tidal Simulation: Point Reyes and San Francisco Water Level Comparisons. Note IND AGRMT equals one minus Willmott et al. (1985) relative error.

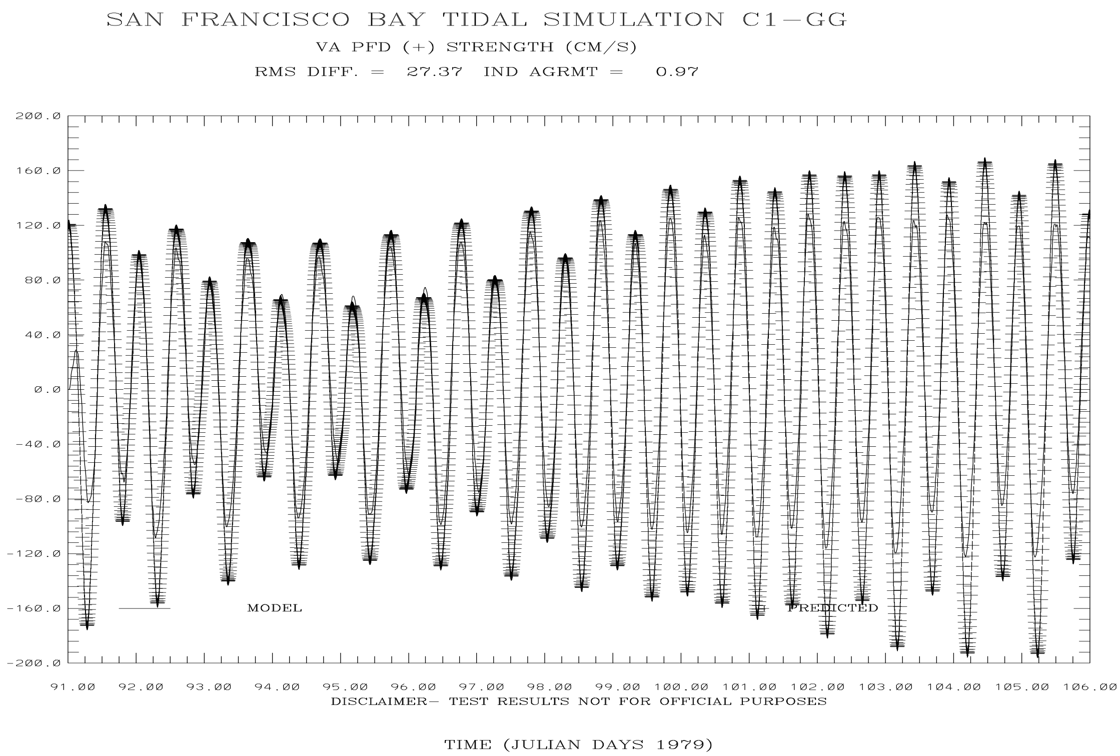

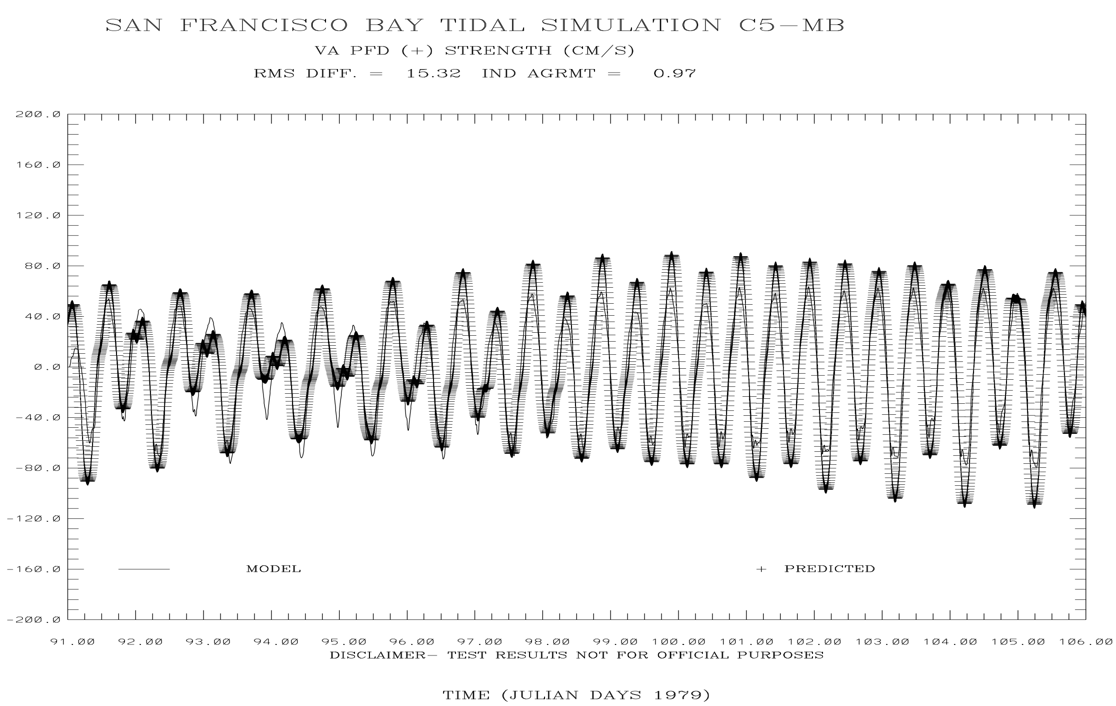

Figure 3.10. April 1-15, 1979 Tidal Simulation: C-1 and C-6 Vertically Integrated Principal Current Component Comparisons. Note IND AGRMT equals one minus Willmott et al. (1985) relative error.

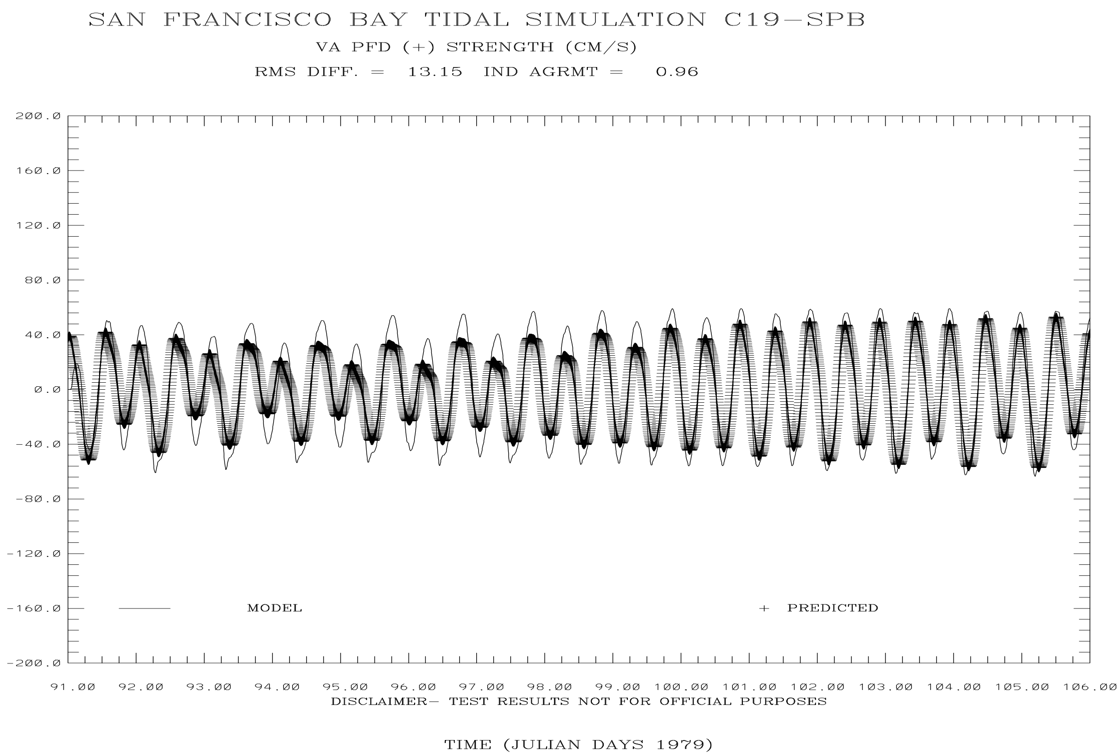

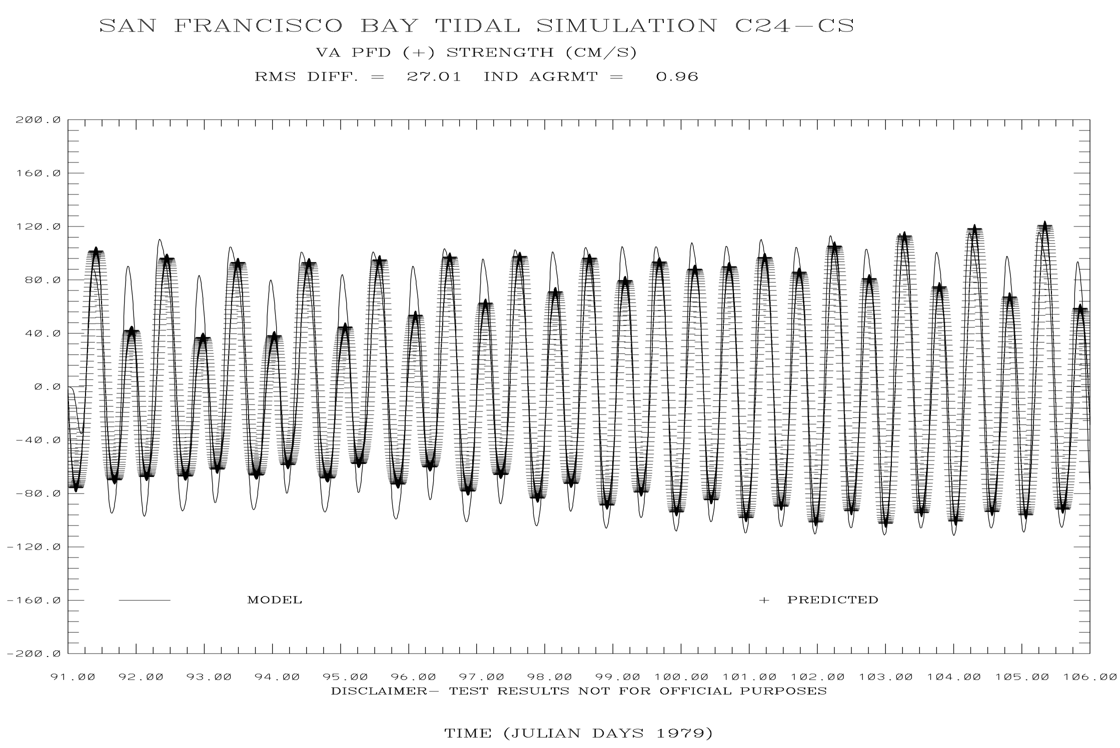

Figure 3.11. April 1-15, 1979 Tidal Simulation: C-19 and C-24 Vertically Integrated Principal Current Component Comparisons. Note IND AGRMT equals one minus Willmott et al. (1985) relative error.

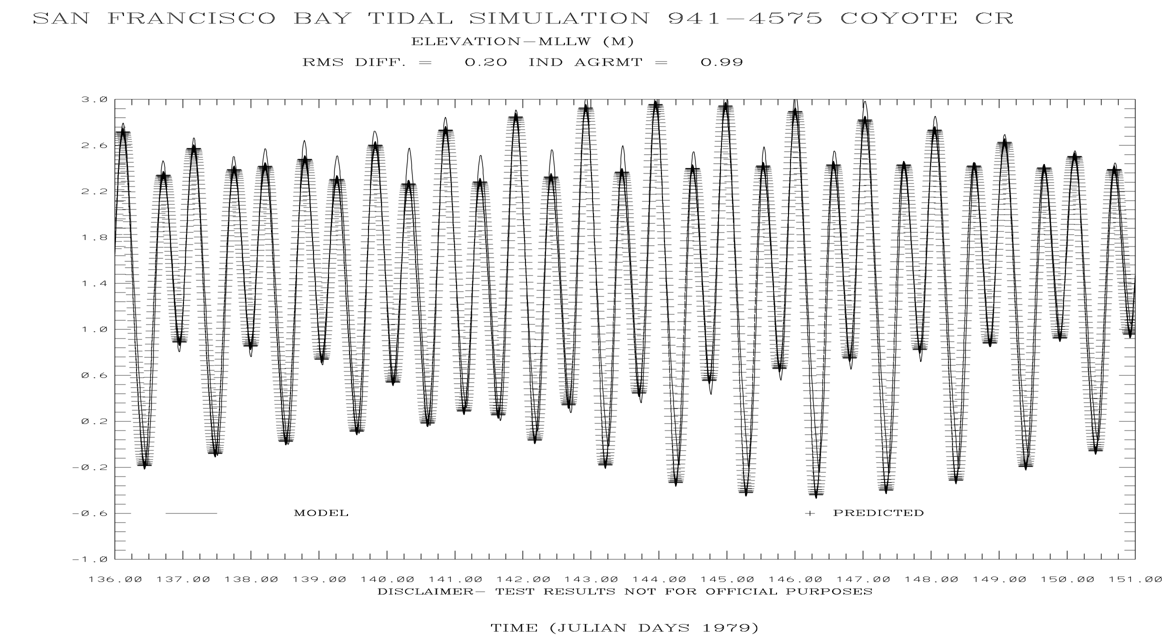

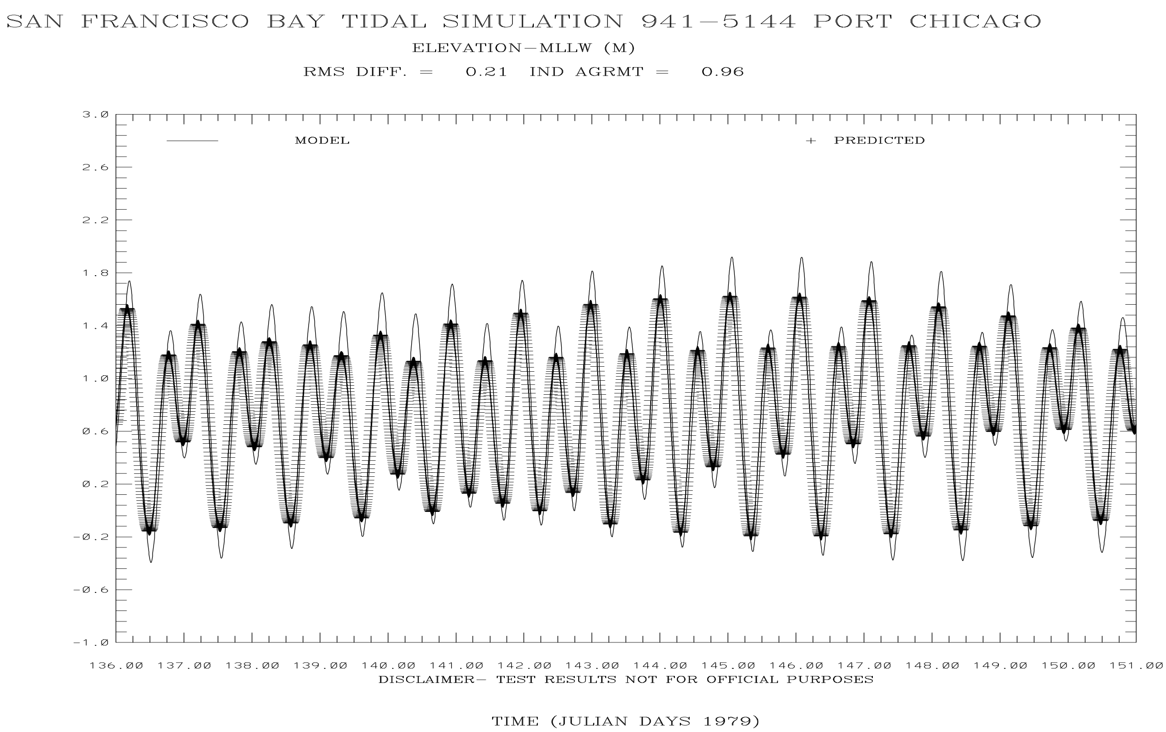

Figure 3.12. May 15-31, 1979 Tidal Simulation: Coyote Creek and Port Chicago Water Level Comparisons. Note IND AGRMT equals one minus Willmott et al. (1985) relative error.

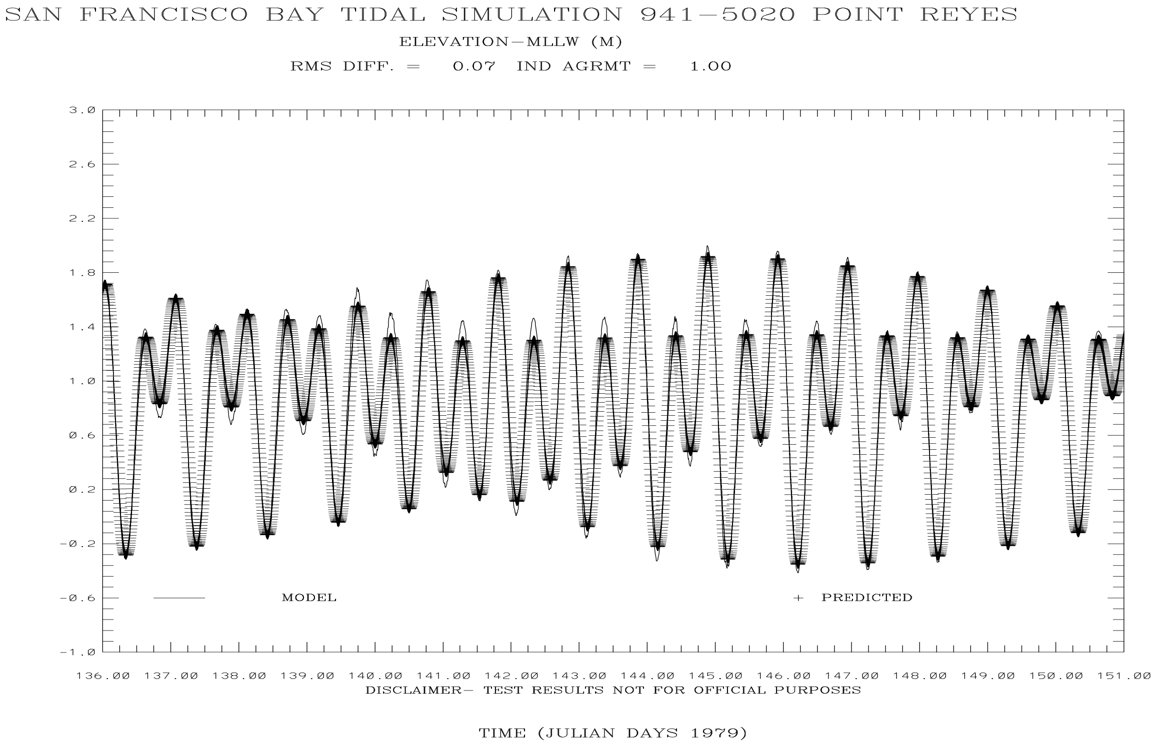

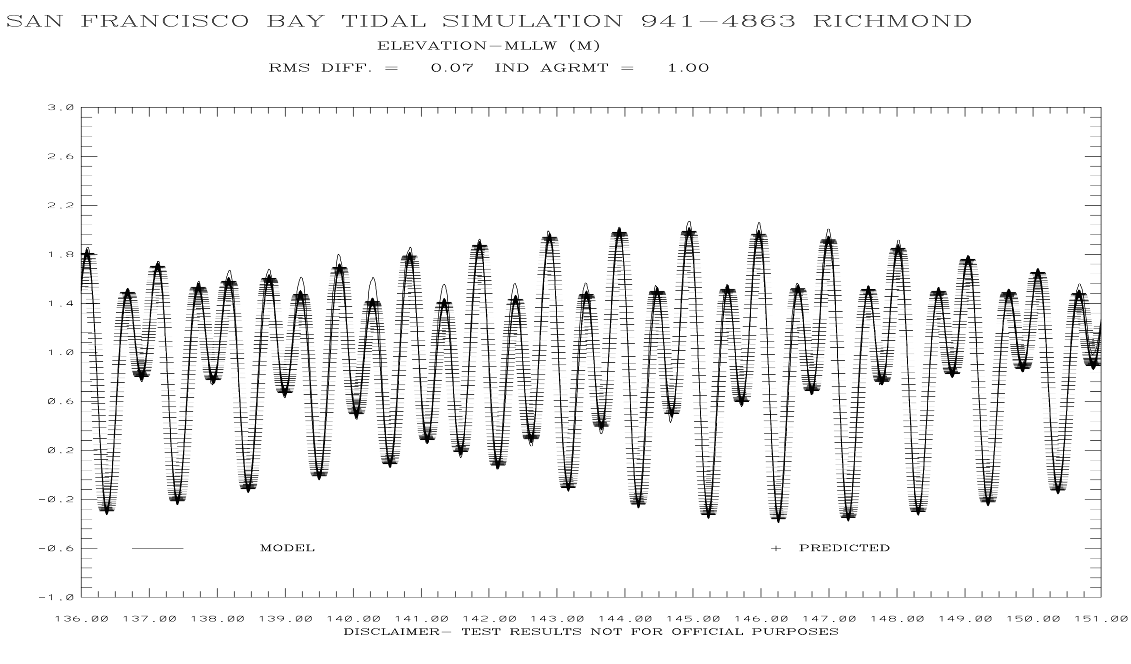

Figure 3.13. May 15-31, 1979 Tidal Simulation: Point Reyes and Richmond Water Level Comparisons. Note IND AGRMT equals one minus Willmott et al. (1985) relative error.

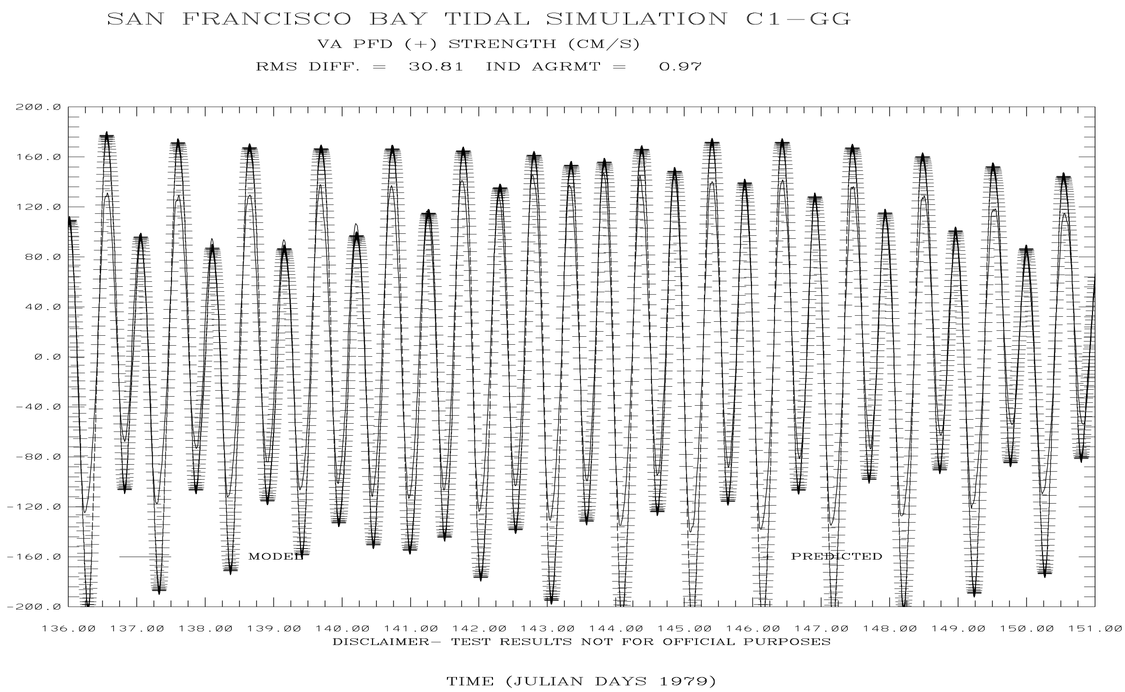

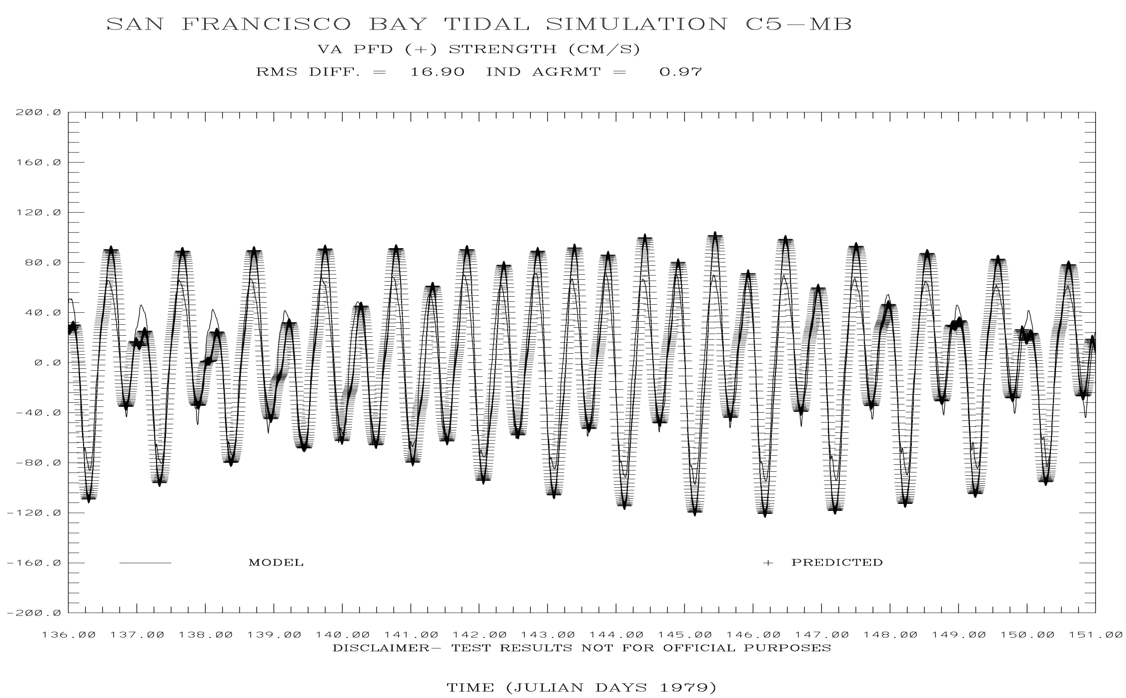

Figure 3.14. May 15-31, 1979 Tidal Simulation: C-1 and C-6 Vertically Integrated Principal Current Component Comparisons. Note IND AGRMT equals one minus Willmott et al. (1985) relative error.

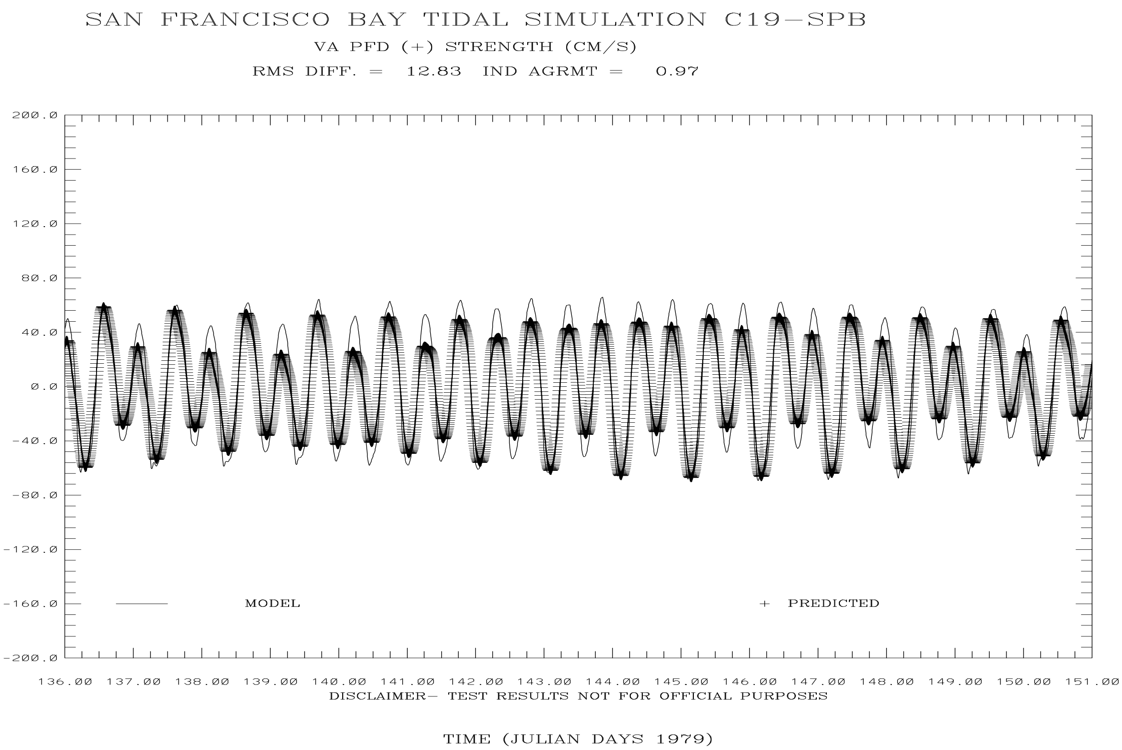

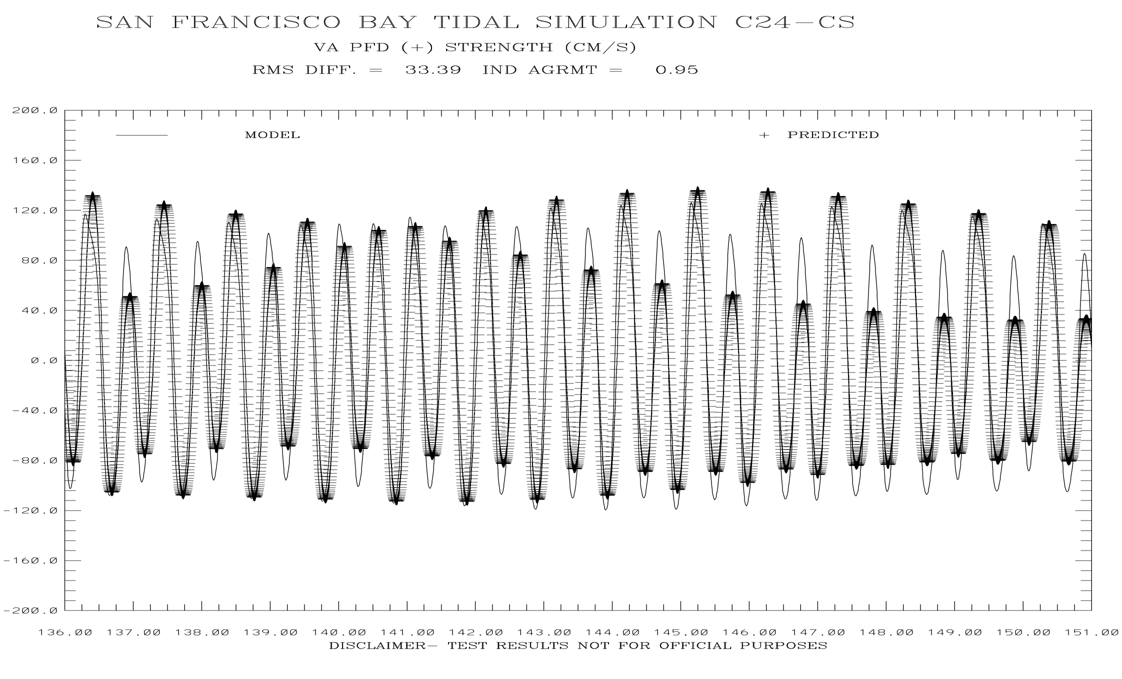

Figure 3.15. May 15-31, 1979 Tidal Simulation: C-19 and C-24 Vertically Integrated Principal Current Component Comparisons. Note IND AGRMT equals one minus Willmott et al. (1985) relative error.

3.3 September-October 1980 Simulation

To further test the heat flux and tidal dynamics, the latent and sensible heat fluxes were dynamically coupled to the sea surface temperature using the HEATING_CALCULATED_ON option in FVCOM. The NARR fields were interpolated to the model grid using the Barnes (1963) method at 3 hour intervals and the sea level atmospheric pressure field was directly used. A revised sponge layer treatment at the open ocean boundary was considered. The downward radiation and total heat flux were set to zero in the shallow water regions less than 10m in depth. A zero gradient temperature and salinity condition was invoked along the open ocean boundary. The Oregon State University Tidal Data Inversion, OTIS Regional Tide Solutions (2010) harmonic constant set was used as given in Table 2.3. River inflows were specified as previously discussed in Section 3.1. The two month simulation was completed in four segments of 15, 15, 15, and 16 day duration. Each segment required approximately 3.5 CPU hours on the NCEP-CCS using 256 processors.

In Tables 3.5 and 3.6, simulation results for water surface elevation and principal component direction currents vertically integrated and mid layer (k=10) are compared respectively to harmonic predictions in terms of RMS error and Willmott et al. (1985) relative error. In addition model and predicted means with respect to station MLLW are compared as well. In Figures 3.16 and 3.20 simulated water levels at Port Chicago and Coyote Creek are considered since these stations are located in Suisun Bay near the Delta and at the southern end of South Bay, respectively. The simulated water levels are over predicted at Port Chicago and under predicted at Coyote Creek. In Figure 3.17 and 3.21 simulated water levels at Point Reyes near the offshore boundary and at Richmond are considered with simulated water levels in close agreement with predictions. There are no spikes in water levels using the revised sponge layer. In Figures 3.18 and 3.22 vertically integrated principal component currents are under predicted at C-1 at the Golden Gate Bridge and over predicted at C-6 in mid-Bay. In Figures 3.19 and 3.23 vertically integrated principal component currents are over predicted at C-19 in San Pablo Bay and at CS-24 at the entrance to Carquinez Strait.

Table 3.5. Water Surface Elevation Tidal Simulation: September-October, 1980. Note there are four entries in each cell corresponding to the results of the 15 day simulation segments. Model and predicted means are with respect to station MLLW.

Station	RMSE (cm)	Willmott RE (%)	Model mean (cm)	Predicted mean (cm)
Alameda 941-4750	8 7 7 6	0 0 0 0	109 110 110 107	109 108 107 106
Dumbarton Bridge 941-4509	11 11 8 11	1 1 0 0	143 144 144 141	143 143 141 141
Oyster Point Marina 941-4392	10 9 8 8	1 0 0 0	119 120 120 117	120 119 117 116
Port Chicago 941-5144	19 21 20 22	4 4 4 5	80 84 83 80	82 79 76 74
Point Reyes 941-5020	7 5 6 5	1 0 0 0	99 99 99 96	100 100 99 98
San Francisco 941-4290	7 5 7 5	1 0 1 0	98 99 99 96	100 99 97 96
Pier 22.5 941-4317	7 6 7 5	0 0 0 0	103 104 104 100	104 103 102 101
San Mateo Bridge 941-4458	9 8 6 5	0 0 0 0	130 131 130 128	130 129 127 127
Coyote Creek 941-4575	17 17 14 18	1 1 1 1	155 157 156 154	154 154 152 151

Table 3.6. Principal Flood Direction Current Speed Tidal Simulation: September-October, 1980. Note there are four entries in each row of each cell corresponding to the results of the 15 day simulation segments. Note the first row in each cell corresponds to the vertically integrated current, while the second row corresponds to the current in mid-level layer k=10.

Station	RMSE (cm/s)	Willmott RE (%)	Model mean (cm/s)	Predicted mean (cm/s)
C-1 GG	26 35 24 36 37 48 36 50	2 3 2 3 5 7 5 8	7 8 8 8 7 7 8 9	0 0 0 0 0
C-5 MB	15 16 14 17 24 28 25 30	3 2 2 3 8 10 9 11	0 0 1 1 9 10 11 11	0 0 0 0 0
C-17 MB	22 19 21 19 10 9 9 11	5 3 5 3 2 1 1 1	-3 -4 -3 -3 3 3 4 4	0 0 0 0 0
C-18 MB	15 13 14 14 20 21 21 22	2 1 1 1 3 3 3 3	1 2 2 3 11 13 13 14	0 0 0 0 0
C-19 SPB	13 11 13 11 9 9 8 10	4 2 4 2 2 2 2 2	1 1 1 1 3 4 3 4	0 0 0 0 0
C-20 SPB	15 19 14 19 17 21 16 21	8 10 7 10 11 14 11 14	-1 -1 -1 -1 0 0 0 0	0 0 0 0 0
C-22 SPB	32 30 32 30 17 15 17 14	10 8 11 7 4 3 4 2	-3 -3 -2 -2 4 4 5 5	0 0 0 0 0
C-23 SPB	7 6 7 6 5 5 5 5	3 2 3 2 3 2 3 2	0 0 1 0 1 1 1 1	0 0 0 0 0
C-24 CS	31 34 30 34 28 38 28 39	5 5 5 5 6 9 6 10	2 2 1 1 -8 -10 -11 -11	0 0 0 0 0
C-25 CS	35 33 35 33 21 20 20 23	10 7 10 7 5 4 5 5	-7 -7 -7 -6 6 7 9 10	0 0 0 0 0
C-26 SB	29 30 28 31 27 29 25 30	7 7 7 7 7 7 6 7	-4 -4 -4 -3 0 0 1 2	0 0 0 0 0
C-28 SB	10 8 9 9 10 8 9 9	6 4 6 4 7 4 6 5	0 0 0 0 0 0 0 1	0 0 0 0 0
C-29 SB	28 31 27 32 29 32 27 33	20 21 19 21 24 24 21 24	2 2 2 1 -1 0 1 0	0 0 0 0 0
C-30 SB	30 32 28 32 32 34 28 32	25 24 23 23 36 32 26 28	-3 -2 -1 -2 -8 -6 -4 -4	0 0 0 0 0
C-31 SB	16 18 15 18 16 18 15 18	18 19 17 19 19 20 17 19	0 1 1 2 0 1 1 1	0 0 0 0 0
C-33 SB	34 40 33 41 37 42 35 43	43 46 41 46 58 53 49 54	-2 0 0 0 -4 -1 0 -1	0 0 0 0 0

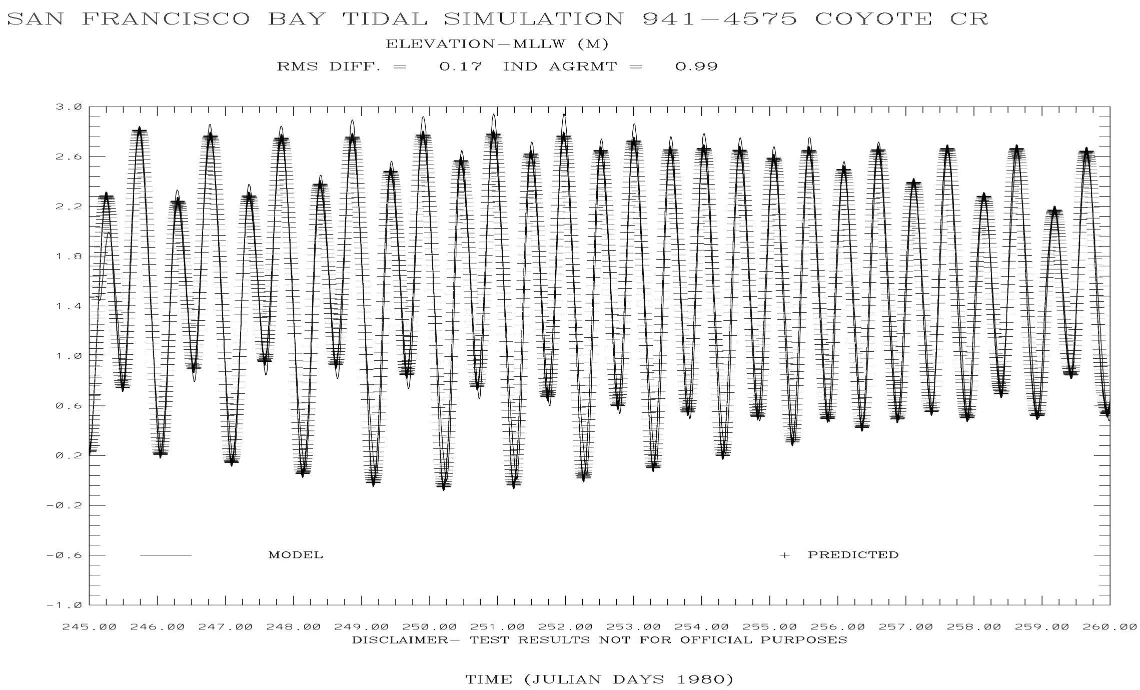

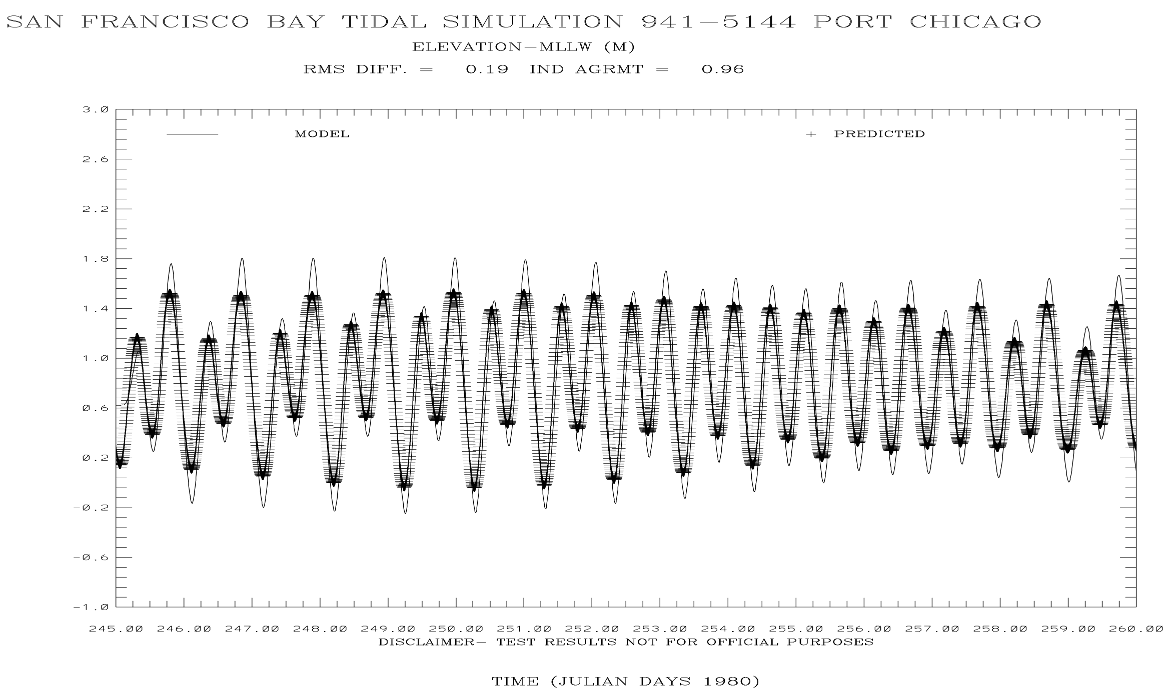

Figure 3.16. September 1-15, 1980 Tidal Simulation: Coyote Creek and Port Chicago Water Level Comparisons. Note IND AGRMT equals one minus Willmott et al. (1985) relative error.

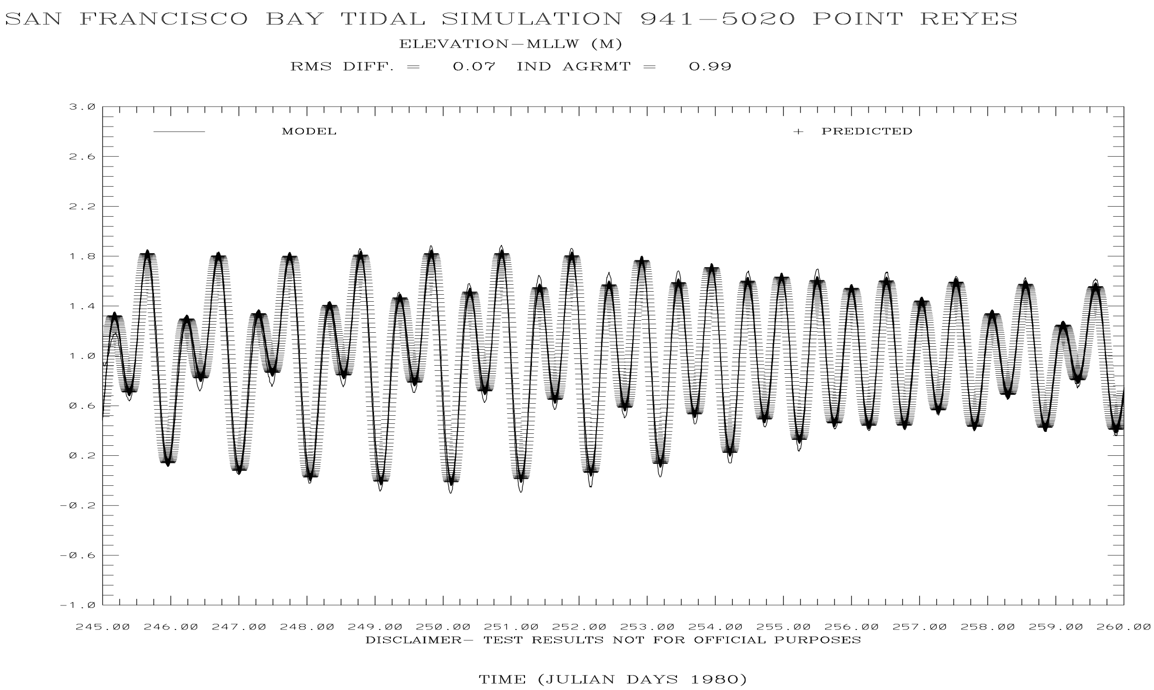

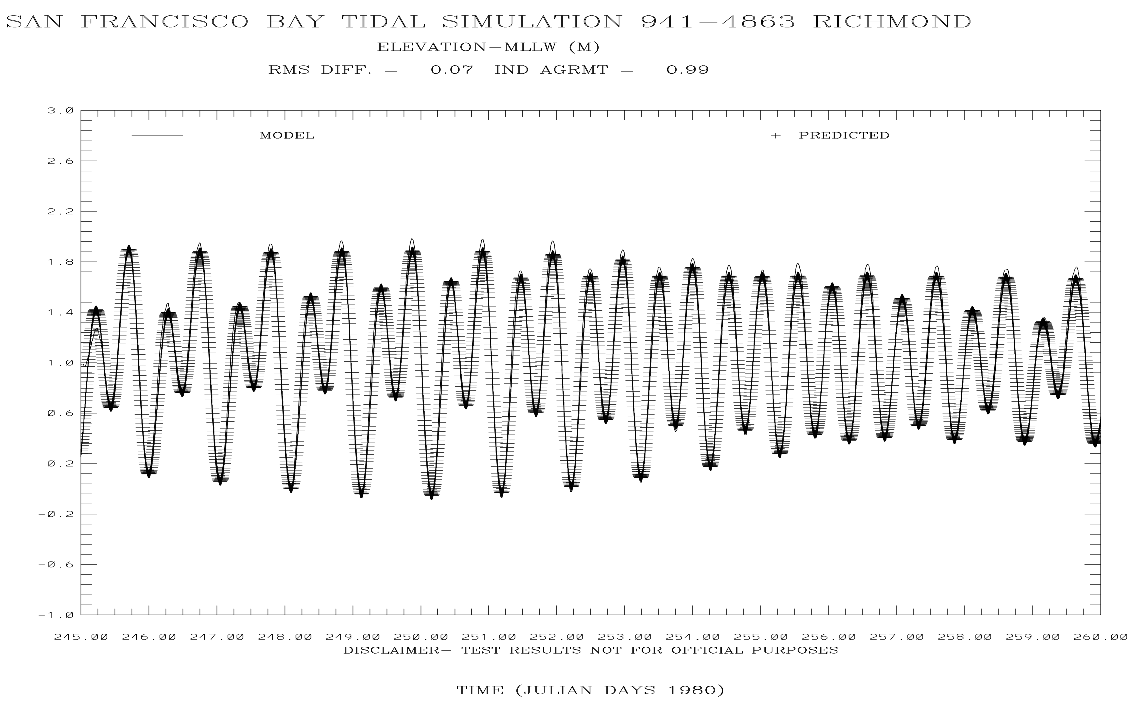

Figure 3.17. September 1-15, 1980 Tidal Simulation: Point Reyes and Richmond Water Level Comparisons. Note IND AGRMT equals one minus Willmott et al. (1985) relative error.

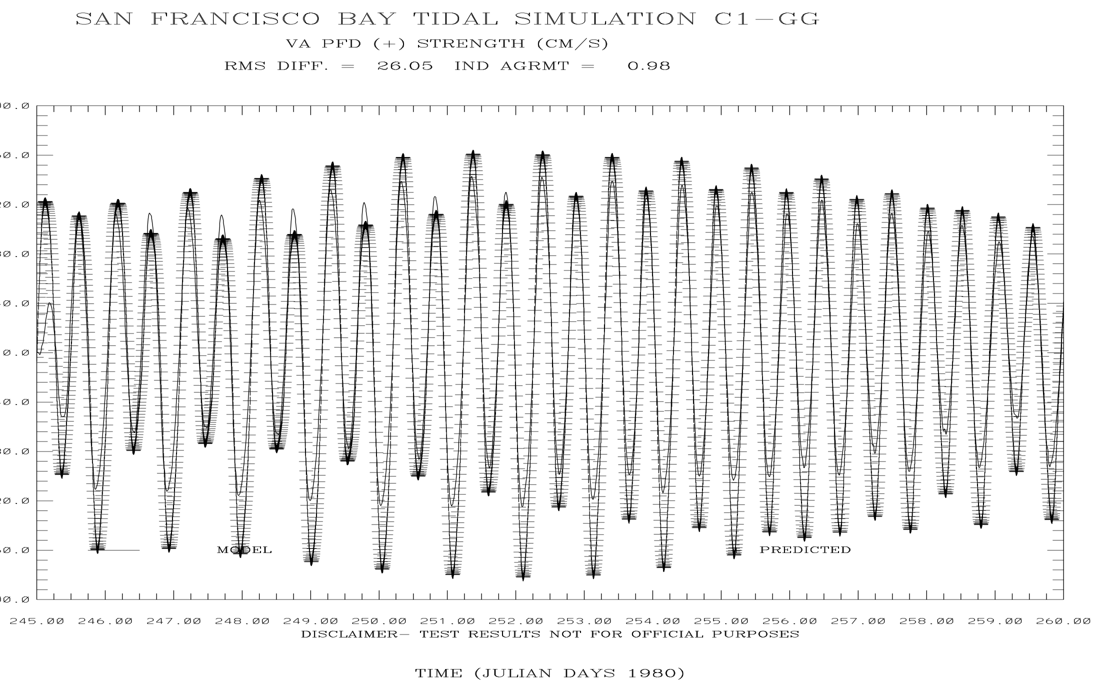

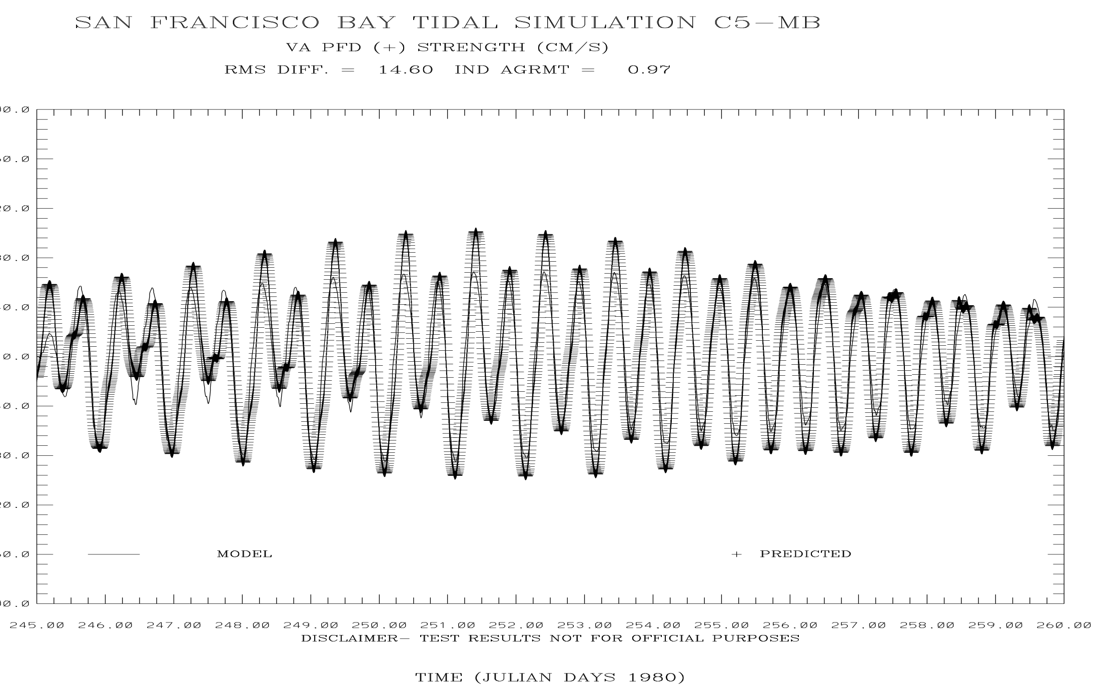

Figure 3.18. September 1-15, 1980 Tidal Simulation: C-1 and C-6 Vertically Integrated Principal Current Component Comparisons. Note IND AGRMT equals one minus Willmott et al. (1985) relative error.

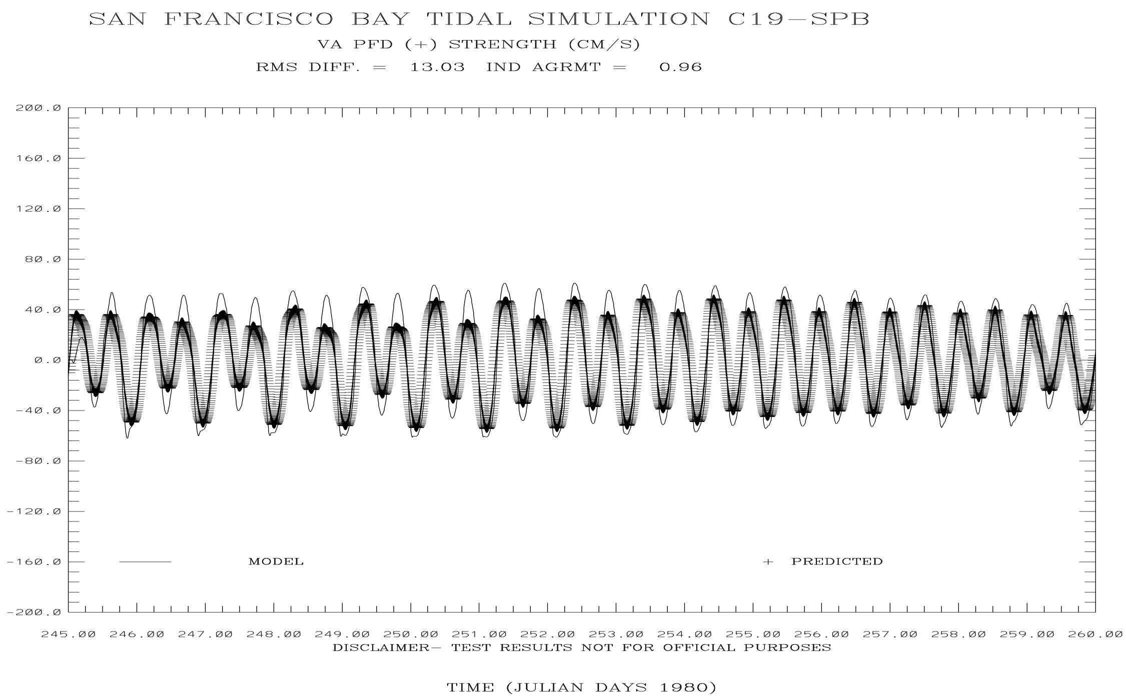

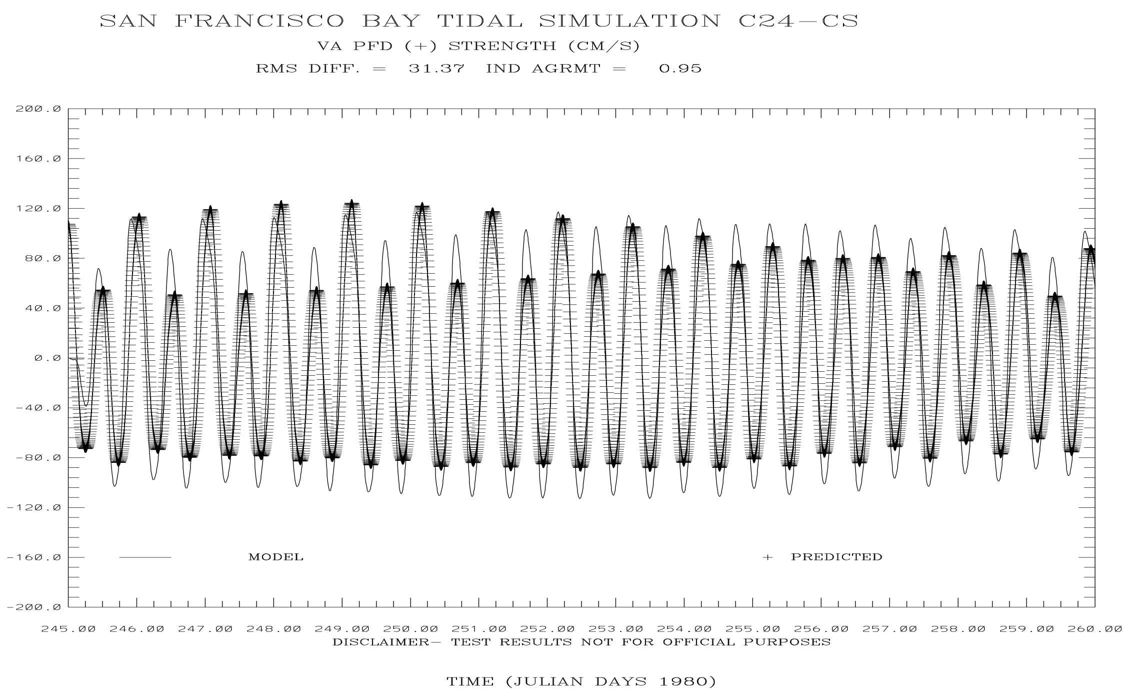

Figure 3.19. September 1-15, 1980 Tidal Simulation: C-19 and C-24 Vertically Integrated Principal Current Component Comparisons. Note IND AGRMT equals one minus Willmott et al. (1985) relative error.

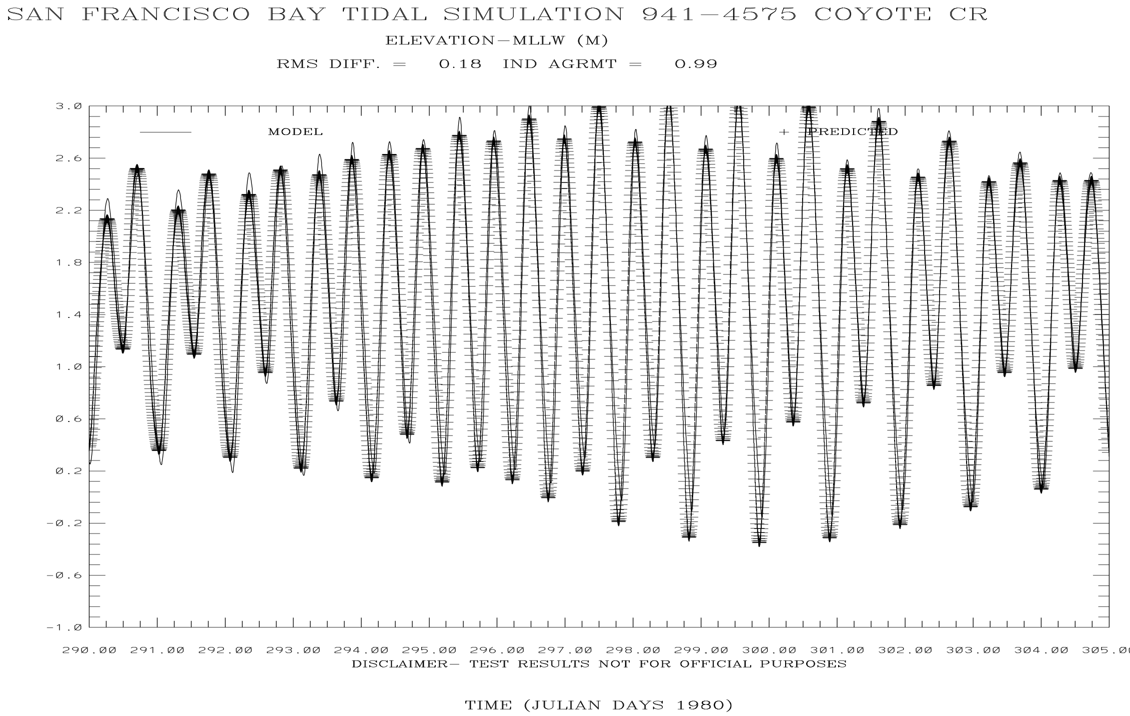

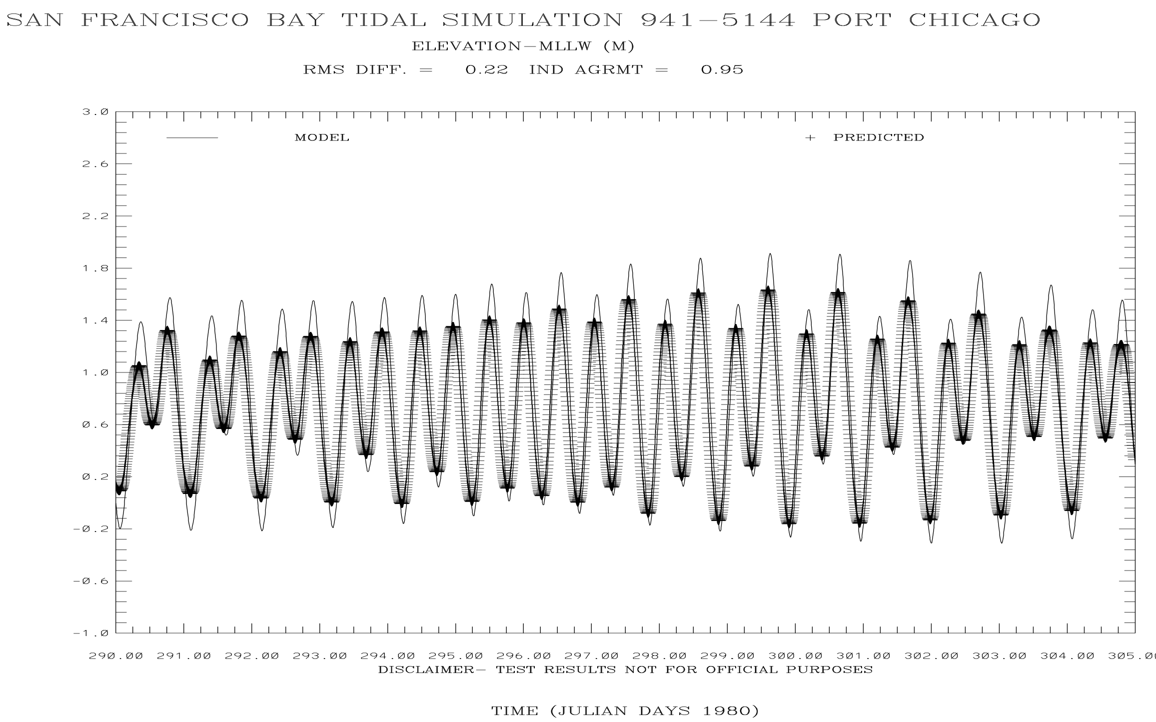

Figure 3.20. October 15-31 1980 Tidal Simulation: Coyote Creek and Port Chicago Water Level Comparisons. Note IND AGRMT equals one minus Willmott et al. (1985) relative error.

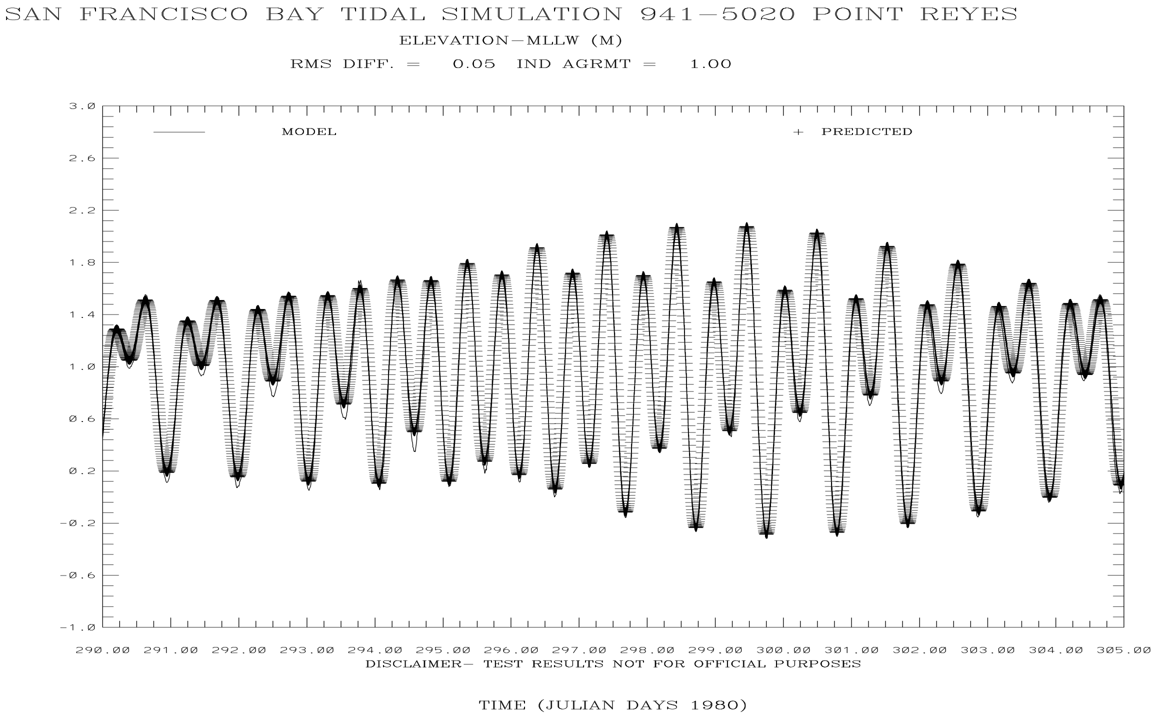

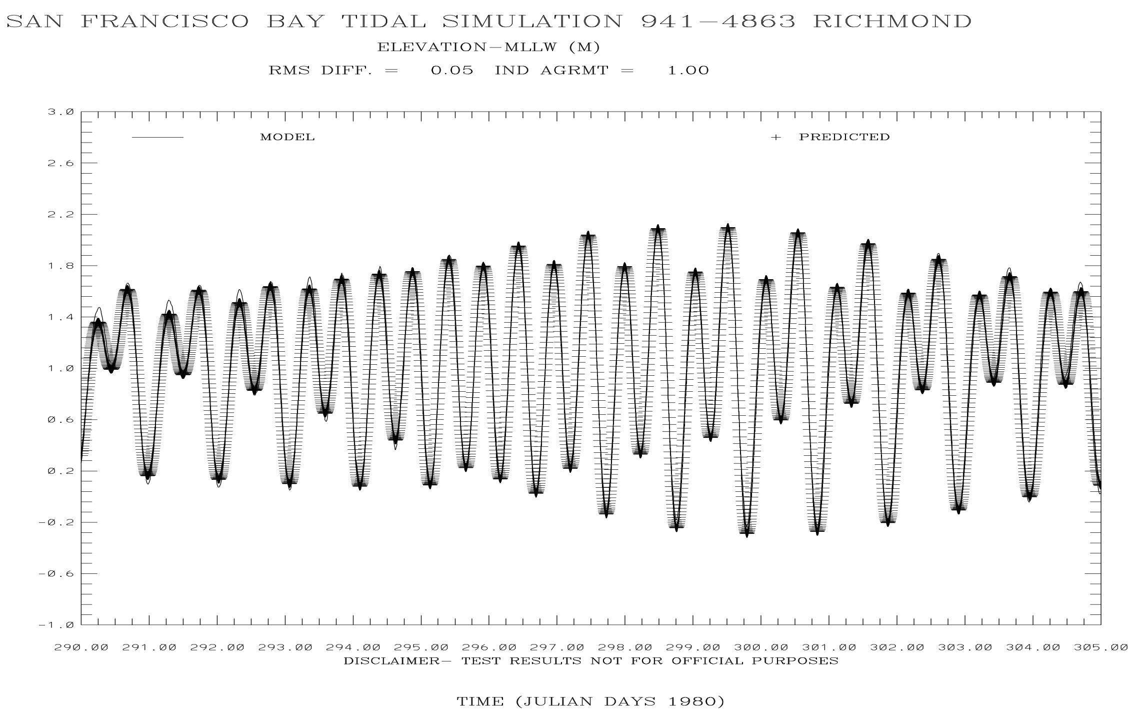

Figure 3.21. October 15-31, 1980 Tidal Simulation: Point Reyes and Richmond Water Level Comparisons. Note IND AGRMT equals one minus Willmott et al. (1985) relative error.

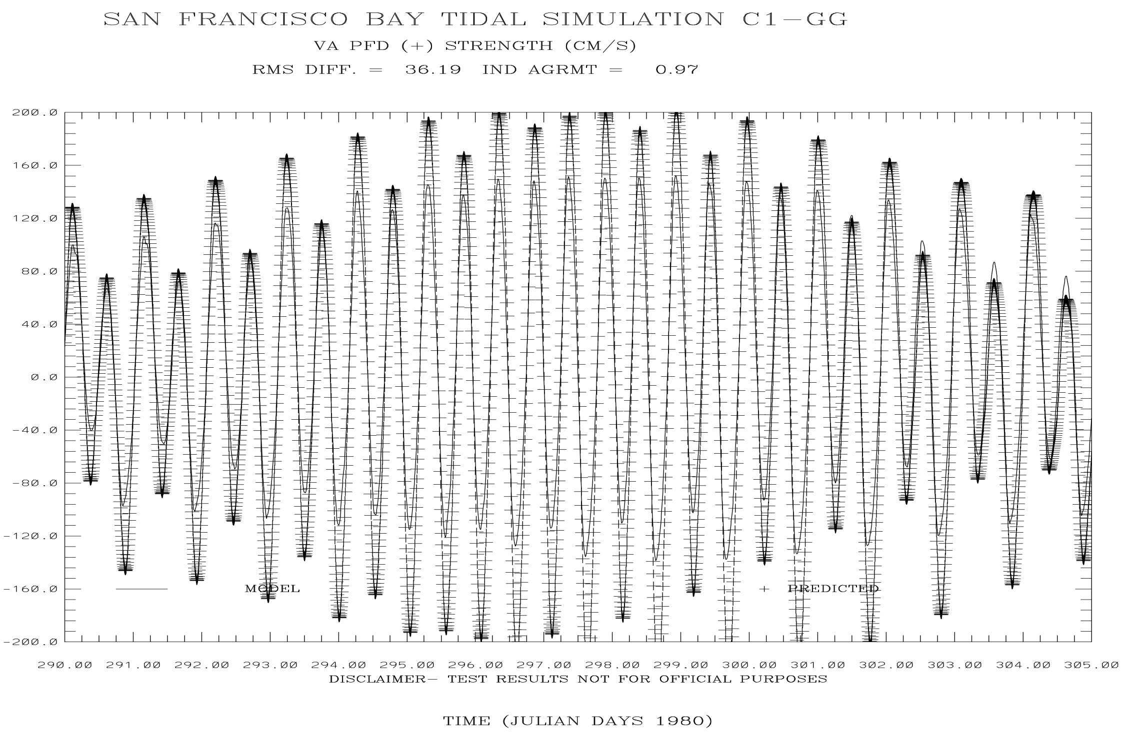

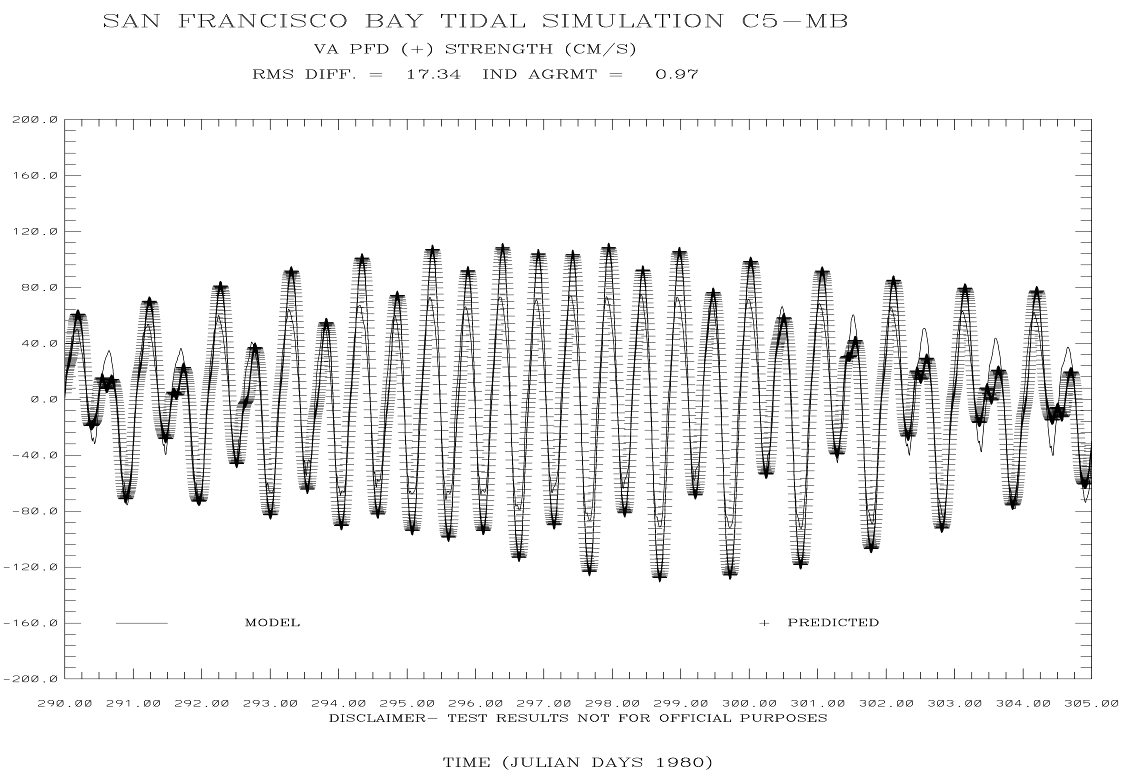

Figure 3.22. October 15-31, 1980 Tidal Simulation: C-1 and C-6 Vertically Integrated Principal Current Component Comparisons. Note IND AGRMT equals one minus Willmott et al. (1985) relative error.

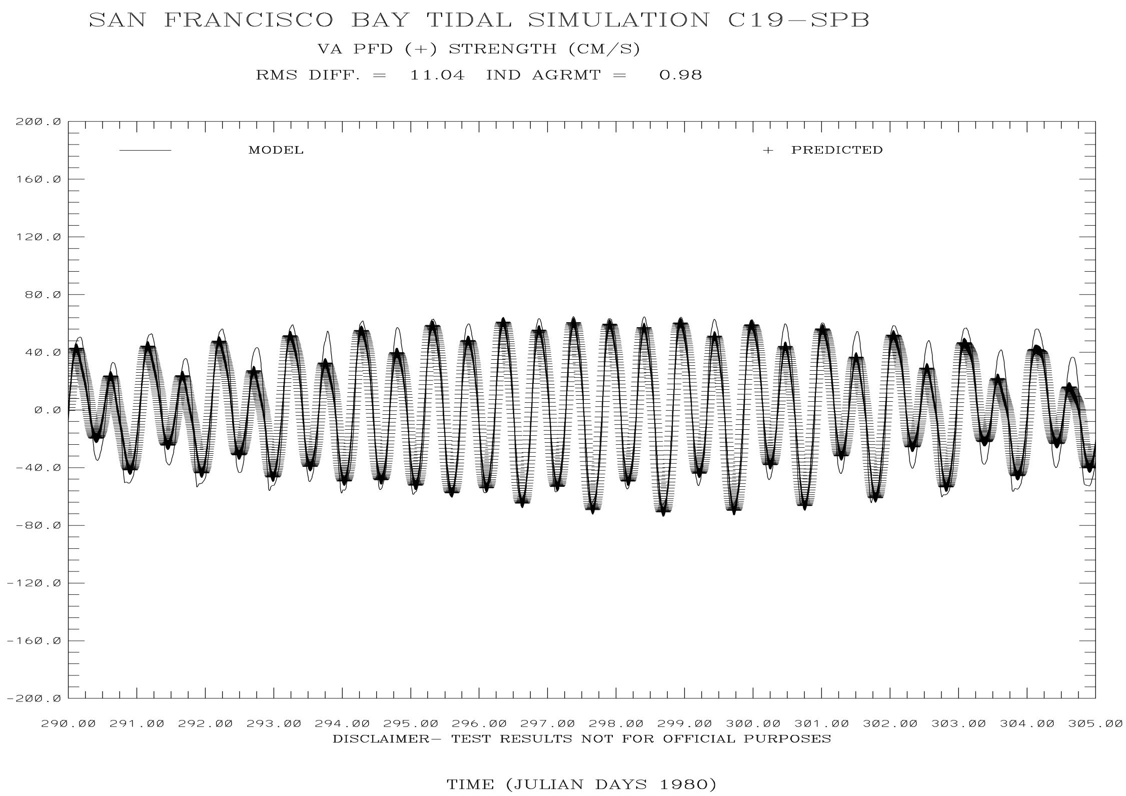

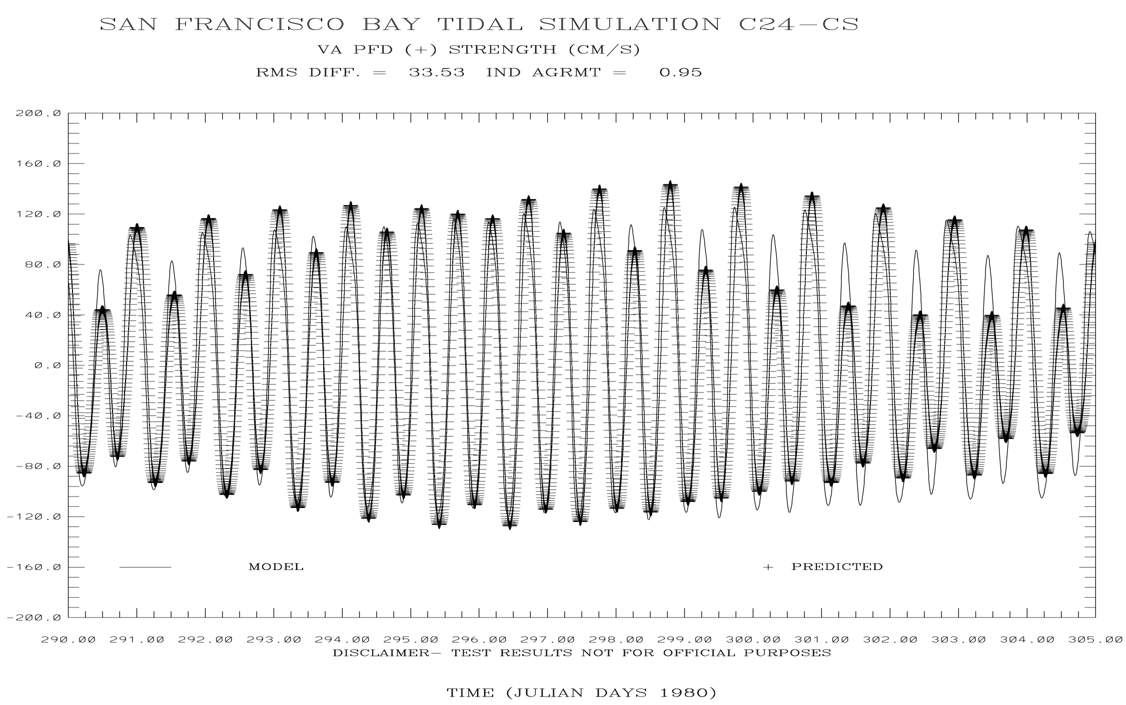

Figure 3.23. October 15-31, 1980 Tidal Simulation: C-19 and C-24 Vertically Integrated Principal Current Component Comparisons. Note IND AGRMT equals one minus Willmott et al. (1985) relative error.

3.4 Additional April 1-15, 1979 Tidal Simulation Experiments

As noted in the tidal simulations (Section 3.2 for the April-May 1979 and in Section 3.3 for the September-October 1980), the simulated water level response at Port Chicago in Suisun Bay is over predicted. In an effort to reduce the amplitude of the simulated water level response at Port Chicago, above the entrance to Carquinez Strait and up through the Delta, the bottom friction was increased using either a constant scale factor or a tapered scale factor as a linear function of longitude as noted in Table 3.7. The water level response with respect to MLLW at Port Chicago for experiments 1 and 2 is shown in Figure 3.24 and for experiments 5 and 7 in Figure 3.25. Experiments 3, 4, and 6 were unstable, due to large horizontal gradients in bottom roughness during the wetting/drying cycle.

Three additional Experiments 8-10 were conducted in which the river stage was reconstructed from the harmonic constituents given in Table 3.8. Experiment 8 used the Experiment 7 bottom roughness specification. Experiment 9 included a 20 cm offset for the San Joaquin River and a 22 cm offset for the Sacramento River. In Experiment 10, the offsets were retained with the original bottom roughness specification. Note in these stage experiments the Oregon State University Tidal Data Inversion, OTIS Regional Tide Solutions (2010) harmonic analysis results were reduced by 5% for the four ocean open boundary stations. Note Sa and Ssa harmonic constituents from San Francisco were used at these stations. The water level response at Port Chicago with respect to MLLW is shown in Figure 3.26 with the offsets improving the agreement from 17 cm to 9 cm RMSE. The results for Experiments 9 and 10 were nearly identical.

Table 3.7 Delta Inflow Bottom Friction Experiment Summary. The scale factor was used to multiply bottom roughness in model domain above Carquinez Strait. The tapered scale factor is ranges from 1 to the full value in a linear fashion from Carquinez Strait to the river inflows based on longitude. The bottom roughness sets are given in the second table. The HA amplitude reduction corresponds to reducing the amplitudes of the offshore boundary harmonic constants.

Experiment	Scale Factor	Bottom Roughness Set	HA Amplitude Reduction (%)
Exp1	2	1	0
Exp2	5	1	0
Exp3	10 tapered	1	0
Exp4	10	1	0
Exp5	5	1	5
Exp6	5	2	10
Exp7	1.2	2	10

Bottom Roughness Zone Set 1 and Set 2.

Roughness Zone Number	Lower Depth (m)	Upper Depth (m)	Set 1 Bottom Roughness z_0 (mm)	Set 2 Bottom Roughness z_0 (mm)
1	0	1	30	40
2	1	3	20	30
3	3	10	10	20
4	10	50	7	17
5	50	1000	5	15

Table 3.8 River Stage Harmonic Constituents. Note Amp1 and Phase1 correspond to Station 941-5064 Antioch, San Joaquin River, CA and Amp2 and Phase2 correspond to Station 941-5316 Rio Vista, CA.

Constituent	Amp1 (m)	Phase1 (^{o}G)	Amp2 (m)	Phase2 (^{o}G)
M2	0.400	318.1	0.369	338.5
S2	0.068	325.1	0.066	355.9
N2	0.073	293.6	0.068	304.3
K1	0.231	298.1	0.221	302.5
M4	0.018	166.3	0.026	213.0
O1	0.128	278.5	0.111	294.2
M6	0.015	328.0	0.009	17.3
MK3	0.029	170.0	0.032	199.8
S4			0.002	238.6
MN4	0.006	143.3	0.010	191.8
NU2	0.020	297.3	0.009	333.2
S6				
MU2	0.021	129.8	0.020	151.5
2N2	0.006	246.4	0.010	311.7
OO1	0.006	342.8	0.003	62.5
LAM2	0.008	300.5	0.014	326.5
S1	0.010	118.2	0.023	267.7
M1			0.004	209.4
J1	0.003	37.3	0.009	43.6
MM				
SSA	0.060	285.0	0.060	285.7
SA				
MSF				
MF				
RHO	0.011	280.5	0.005	287.0
Q1	0.021	290.3	0.016	295.7
T2			0.007	352.4
R2			0.007	65.6
2Q1	0.004	316.4	0.005	315.9
P1	0.068	283.8	0.082	308.1
2SM2	0.005	154.0	0.004	171.2
M3	0.009	258.8	0.010	280.7
L2	0.030	350.5	0.031	355.6
2MK3	0.033	159.2	0.029	191.3
K2	0.029	311.0	0.029	337.0
M8			0.002	251.6
MS4	0.010	193.0	0.012	240.5

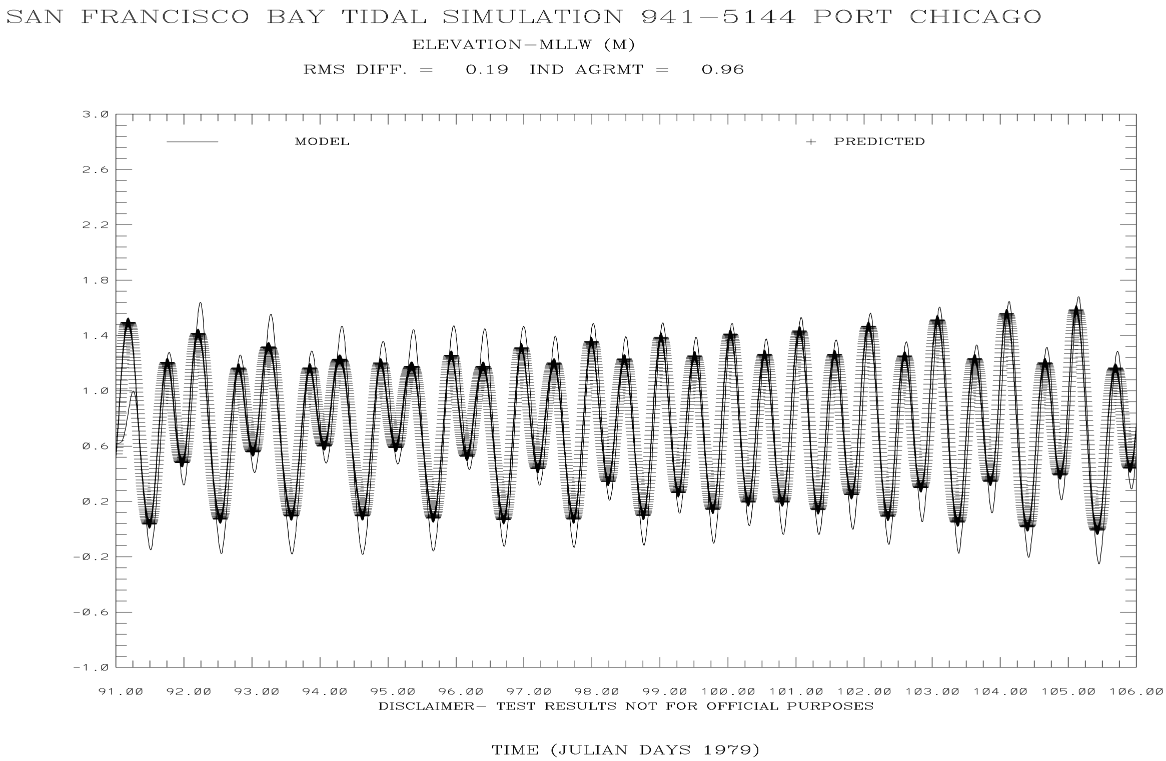

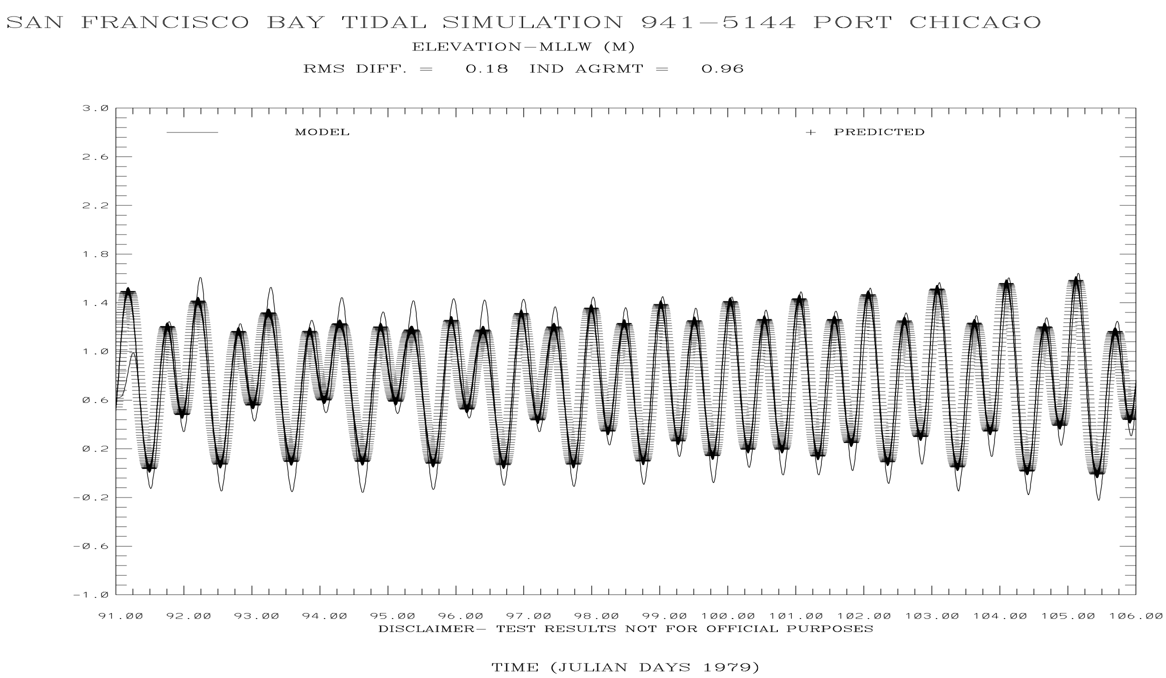

Figure 3.24. Port Chicago Water Level Response for Inflow Experiments 1 and 2. Note IND AGRMT equals one minus Willmott et al. (1985) relative error.

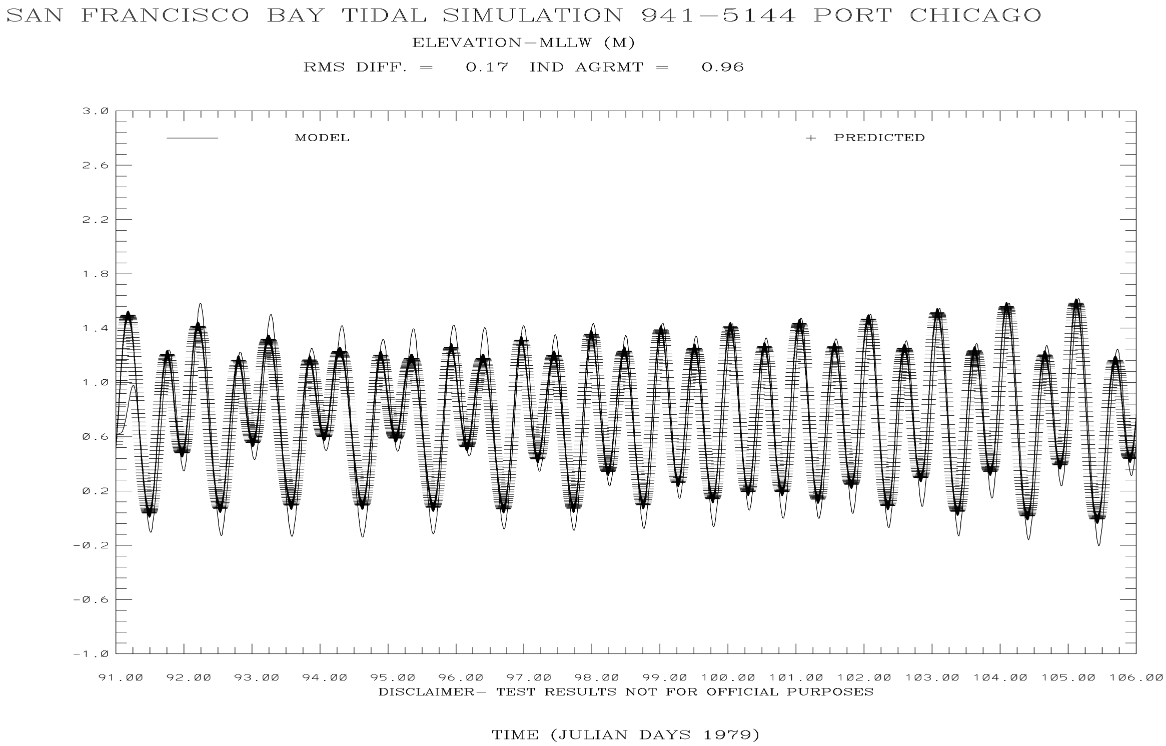

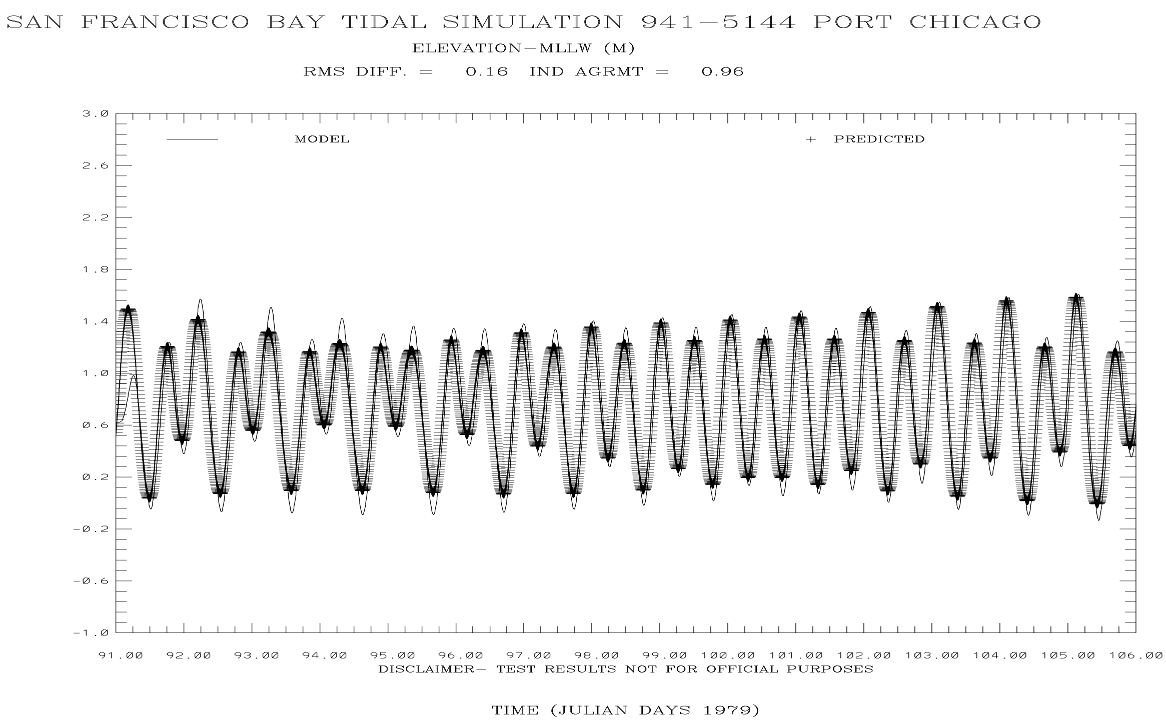

Figure 3.25. Port Chicago Water Level Response for Inflow Experiments 5 and 7. Note IND AGRMT equals one minus Willmott et al. (1985) relative error.

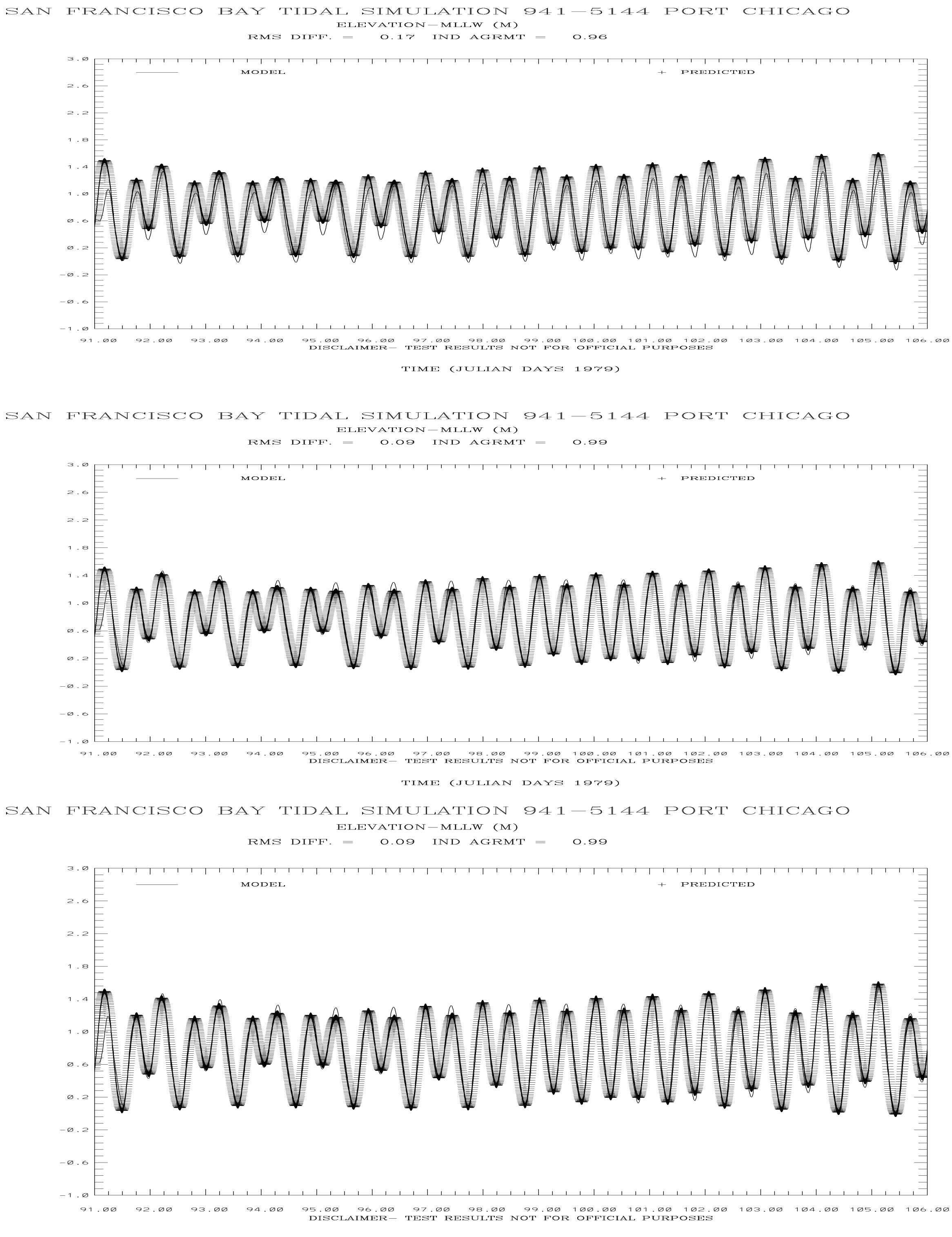

Figure 3.26. Port Chicago Water Level Response for Stage Experiments 8, 9, and 10. Note IND AGRMT equals one minus Willmott et al. (1985) relative error.

3.5 April 1979 - October 1980 Extended Simulation

Based on the performance of the Experiment 10 stage boundary conditions for the Delta, this boundary condition was used over the extended 19-month simulation from April 1979 through October 1980. The HEATING_CALCULATED_ON option was used with the NARR fields updated at 3 hour intervals. The sea level atmospheric pressure field was directly used from these fields. A revised sponge layer treatment at the open ocean boundary was considered. The downward radiation and total heat flux were set to zero in the shallow water regions less than 10m in depth. A nudging of both salinity and temperature to specified climatological values was used along the open ocean boundary. The Oregon State University Tidal Data Inversion, OTIS Regional Tide Solutions (2010) harmonic constant set was used with 5% reduction in tidal constituent amplitudes. River inflows were specified as previously discussed in Section 3.1. The nineteen month simulation was completed in thirty eight segment of approximately 15 days duration. Each segment required approximately 3.5 CPU hours on the NCEP-CCS using 256 processors with each segment restarted from the previous segment's final fields.

In Tables 3.9-3.11 simulation segment results for water surface elevation and principal component direction currents vertically integrated and at mid layer (k=10) are compared respectively to harmonic predictions in terms of RMS error and Willmott et al. (1985) relative error. In addition model and predicted means are compared with respect to station MLLW.

Time series comparisons for water levels and principal component currents are shown for the following three two-month segments with results discussed in turn below.

April and May 1979: In Figures 3.27 and 3.31 simulated water levels at Port Chicago and Coyote Creek are compared with tidal predictions. The simulated water levels are in close agreement at Port Chicago and at Coyote Creek with RMSEs of order 10 and 15 cm, respectively. In Figures 3.28 and 3.32 simulated water levels at Point Reyes near the offshore boundary and at Richmond are evaluated with simulated water levels in close agreement with predictions. There are no spikes in water levels using the revised sponge layer. In Figures 3.29 and 3.33 vertically integrated principal component current comparisons at C-1 at the Golden Gate Bridge and at C-6 in mid-Bay are shown. Figures 3.30 and 3.34 show vertically integrated principal component current comparisons at C-19 in San Pablo Bay and at CS-24 at the entrance to Carquinez Strait.

December 1979 and January 1980: In Figures 3.35 and 3.39 simulated water levels at Port Chicago and Coyote Creek are compared with tidal predictions. One notes the simulated water levels are in close agreement at Port Chicago and at Coyote Creek with RMSEs of order 10 and 15 cm, respectively. In Figures 3.36 and 3.40 simulated segment water levels at Point Reyes near the offshore boundary and at Richmond are considered with simulated water levels in close agreement with predictions. One notes that there are no spikes in water levels using the revised sponge layer. In Figures 3.37 and 3.41 vertically integrated principal component current comparisons at C-1 at the Golden Gate Bridge and at C-6 in mid-Bay are shown, while in Figures 3.38 and 3.42 vertically integrated principal component current comparisons at C-19 in San Pablo Bay and at CS-24 at the entrance to Carquinez Strait are presented.

September and October 1980: In Figures 3.43 and 3.47 simulated water levels at Port Chicago and Coyote Creek are compared with tidal predictions. One notes the simulated water levels are in close agreement at Port Chicago and at Coyote Creek with RMSEs of order 10 and 15 cm, respectively. In Figures 3.44 and 3.48 simulated segment water levels at Point Reyes near the offshore boundary and at Richmond are considered with simulated water levels in close agreement with predictions. One notes that there are no spikes in water levels using the revised sponge layer. In Figures 3.45 and 3.49 vertically integrated principal component current comparisons at C-1 at the Golden Gate Bridge and at C-6 in mid-Bay are shown, while in Figures 3.46 and 3.50 vertically integrated principal component current comparisons at C-19 in San Pablo Bay and at CS-24 at the entrance to Carquinez Strait are presented.

In general, the water level RMS errors do not exceed 15 cm and are consistent from month to month from Port Chicago in Suisun Bay through San Pablo and mid-Bay regions, as well as in the offshore and southern regions of San Francisco Bay. Current amplitude RMS errors are consistent from month to month and are generally less than 35 cm/s. The heat flux algorithm generates no excessive temperatures and produces accurate seasonal heating and cooling.

While meteorological effects were not considered, we still compared the tidal simulation salinity reponse versus observations and climatology. The salinity response is summarized in Table 3.12 and was overestimated in the northern portion of San Pablo Bay and throughout Suisun Bay, due to the fact that the offsets were held constant and did not reflect the increased levels during the high flow months. This in effect, limited the amount of freshwater entering the Bay through the Delta. From the open ocean boundary into the Bay entrance, the salinity response was in agreement with observations and climatology.

While no wind effects were included, the temperature response is summarized in Table 3.13 and exhibited a normal seasonal response, but in October 1980 there was some evidence of overheating by about 2 ^{o}C in Suisun Bay.

Table 3.9. Water Surface Elevation Tidal Validation: April 1979-October 1980. For each row in each month, the first entry corresponds to the first 15 days of the month, with the second entry denoting the remaining portion of the month. Row 1 corresponds to the RMSE in cm. Row 2 corresponds to the Willmott Relative Error in percent. Row 3 corresponds to the model mean in cm with row 4 denoting the predicted water level mean in cm.

Station	Apr	May	Jun	Jul	Aug	Sep	Oct	Nov	Dec
Alameda 941-4750	9 6 1 0 101 101 102 100	5 6 0 0 100 101 98 99	5 6 0 0 102 104 100 102	6 6 0 0 107 110 104 107	7 6 0 0 112 113 109 109	8 7 8 0 113 112 109 108	7 7 0 0 111 109 107 105	6 6 0 0 108 108 104 105	6 5 0 0 107 108 105 106
Dumbarton Bridge 941-4509	13 11 1 1 135 135 135 132	9 10 0 0 134 135 132 132	10 10 0 0 136 139 134 136	11 9 0 0 142 144 139 141	12 8 1 0 147 147 144 144	12 8 1 0 148 146 144 143	11 8 0 0 145 143 141 140	10 8 0 0 142 142 139 139	9 8 0 0 141 142 140 141
Oyster Point Marina 941-4392	10 7 1 0 111 111 111 109	4 7 0 0 110 111 108 108	7 7 0 0 112 114 109 112	8 7 0 0 117 120 115 117	9 7 0 0 123 123 120 120	9 8 0 0 123 122 120 119	8 8 0 0 121 119 117 116	7 8 0 0 118 118 115 115	6 8 0 0 117 118 115 116
Port Chicago 941-5144	9 7 1 0 76 76 76 74	7 7 1 1 74 74 72 73	7 7 1 1 76 78 74 77	8 7 1 1 81 84 80 82	8 7 1 1 86 85 84 84	7 7 1 1 84 82 82 79	6 7 0 1 79 76 76 73	6 7 0 1 74 74 72 72	6 8 1 1 75 78 74 77
Point Reyes 941-5020	7 4 1 0 89 88 88 86	4 4 0 0 88 88 86 86	4 4 0 0 90 93 88 90	5 4 0 0 95 98 93 96	6 3 0 0 100 101 99 100	5 3 0 0 102 101 101 100	5 3 0 0 100 99 99 98	4 4 0 0 98 98 97 97	4 5 0 0 98 98 97 97
San Francisco 941-4290	7 4 1 0 91 89 91 89	4 4 0 0 89 89 88 88	4 5 0 0 90 93 89 92	4 5 0 0 96 99 94 97	5 5 0 0 101 102 99 100	5 5 0 0 102 101 100 99	5 5 0 0 100 99 97 96	4 5 0 0 98 97 95 95	3 5 0 0 97 97 95 97
Pier 22.5 941-4317	8 5 1 0 96 94 95 93	4 5 0 0 94 94 92 92	4 5 0 0 96 98 94 96	5 5 0 0 101 104 99 102	6 5 0 0 106 107 104 104	6 5 0 0 107 106 104 103	5 5 0 0 104 103 102 100	4 5 0 0 102 101 99 99	4 4 0 0 101 101 100 101
San Mateo Bridge 941-4458	10 8 1 0 122 122 121 119	6 7 0 0 121 121 118 118	7 7 0 0 122 125 119 122	8 6 0 0 128 130 125 127	9 6 0 0 133 133 130 130	9 6 0 0 134 133 130 129	5 6 0 0 131 130 127 126	7 6 0 0 128 128 125 125	7 5 0 0 128 128 126 127
Coyote Creek 941-4575	17 20 1 1 147 148 146 144	15 19 1 1 146 148 142 143	17 19 1 1 148 151 144 147	17 16 1 1 154 156 150 152	17 14 1 1 159 159 154 155	16 14 1 1 160 158 155 154	16 15 1 1 157 155 152 151	17 16 1 1 154 154 150 150	18 16 1 1 153 154 150 151

Table 3.9 (Cont.). Water Surface Elevation Tidal Validation April 1979 –October 1980. For each row in each month, the first entry corresponds to the first 15 days of the month, with the second entry denoting the remaining portion of the month. Row 1 corresponds to the RMSE in cm. Row 2 corresponds to the Willmott Relative Error in percent. Row 3 corresponds to the model mean in cm with row 4 denoting the predicted water level mean in cm.

Station	Jan	Feb	Mar	Apr	May	Jun	Jul	Aug	Sep	Oct
Alameda 941-4750	6 5 0 0 108 109 108 109	6 5 0 0 109 108 109 108	6 5 0 0 106 104 106 104	7 4 0 0 102 101 101 100	7 4 0 0 100 100 98 99	7 5 0 0 98 105 100 102	7 5 0 0 107 110 104 107	7 6 0 0 112 113 109 109	7 7 0 0 113 112 109 108	6 7 0 0 110 110 107 106
Dumbarton Bridge 941-4509	9 10 0 0 142 143 142 143	9 9 0 0 143 142 143 142	10 9 0 0 141 138 140 137	11 8 1 0 137 135 135 133	12 8 1 0 134 134 132 132	13 8 1 0 133 139 133 136	11 9 0 0 142 144 139 141	9 10 0 0 146 147 144 145	8 11 0 0 147 147 144 143	7 11 0 1 144 144 141 141
Oyster Point Marina 941-4392	7 8 0 0 118 119 118 118	7 8 0 0 119 118 118 118	7 6 0 0 117 115 116 113	8 5 0 0 113 111 111 109	8 6 0 0 110 110 107 108	8 6 0 0 108 115 109 112	8 6 0 0 117 120 114 117	8 7 0 0 122 123 119 120	8 8 0 0 123 122 120 119	7 8 0 0 120 120 117 116
Port Chicago 941-5144	7 8 1 1 81 84 80 83	6 8 1 1 84 84 84 84	6 7 1 1 82 80 82 79	6 7 1 1 77 75 76 74	7 7 1 1 74 74 72 73	7 7 1 1 75 79 74 77	8 7 1 1 82 84 80 82	8 7 1 1 86 86 84 84	7 7 1 1 84 82 82 79	7 6 1 1 78 76 76 74
Point Reyes 941-5020	3 6 0 0 98 98 98 97	4 6 0 0 98 96 97 95	4 5 0 0 95 92 93 90	5 5 0 0 90 89 88 86	5 4 0 0 88 88 86 86	6 4 0 0 86 93 88 91	4 4 0 0 95 98 93 96	4 4 0 0 100 101 99 100	4 5 0 0 102 101 100 100	4 5 0 0 100 99 99 99
San Francisco 941-4290	3 5 0 0 98 98 98 98	3 6 0 0 98 97 99 98	3 5 0 0 96 93 96 93	4 4 0 0 91 89 91 89	4 4 0 0 88 89 88 88	6 3 0 0 86 94 89 92	5 4 0 0 96 98 94 97	6 4 0 0 101 102 99 100	6 5 0 0 102 101 100 99	6 5 0 0 100 99 97 96
Pier 22.5 941-4317	4 5 0 0 103 102 102 103	4 6 0 0 104 102 103 102	4 5 0 0 101 98 100 98	5 4 0 0 97 95 95 93	5 4 0 0 94 94 92 92	6 4 0 0 91 99 94 96	5 4 0 0 100 104 99 102	6 5 0 0 105 107 104 105	6 5 0 0 107 106 104 103	6 6 0 0 104 103 102 101
San Mateo Bridge 941-4458	6 7 0 0 129 129 128 129	7 7 0 0 129 129 129 128	7 6 0 0 127 125 126 123	8 5 0 0 123 121 121 119	9 5 0 0 121 121 118 118	9 6 0 0 119 125 119 122	8 6 0 0 128 130 125 127	7 7 0 0 133 134 130 131	6 8 0 0 133 133 130 129	6 9 0 0 131 130 127 127
Coyote Creek 941-4575	17 18 1 1 154 155 153 153	17 15 1 1 155 154 153 153	17 14 1 1 153 151 151 148	19 14 1 1 149 147 145 144	21 15 2 1 146 147 142 143	22 15 2 1 145 151 144 147	20 15 1 1 154 156 150 152	16 15 1 1 158 160 154 155	14 16 1 1 159 159 154 154	13 17 1 1 156 156 152 151

Table 3.10 Principal Flood Direction Vertically Integrated Current Speed Tidal Validation: April 1979-October 1980. For each row in each month, the first entry corresponds to the first 15 days of the month, with the second entry denoting the remaining portion. Row 1 corresponds to the RMSE in cm/s. Row 2 corresponds to the Willmott Relative Error in percent. Row 3 corresponds to the model mean in cm/s. Note the predicted mean current speed is zero.

Station	Apr 1979	May 1979	Sep 1980	Oct 1980
C-1	30 35	32 33	27 39	27 38
GG	3 3	4 3	3 4	3 4
	7 9	7 9	9 9	8 9
C-5	17 19	18 19	17 19	16 19
MB	4 4	4 4	4 4	4 4
	-1 0	-1 0	0 0	1 1
C-17	15 16	13 16	16 14	14 14
MB	3 2	2 3	3 2	3 2
	-2 -3	-2 -3	-2 -2	-2 -2
C-18	13 15	13 15	13 16	11 15
MB	2 2	1 1	1 2	1 2
	4 3	3 3	2 3	2 3
C-19	11 10	10 10	10 8	9 8
MB	3 2	2 2	2 1	2 1
	1 1	1 1	1 1	1 2
C-20	14 17	15 16	14 18	14 18
SPB	7 8	8 7	7 9	7 9
	-1 -1	-1 -1	-1 -1	-1 -1
C-22	24 23	22 23	22 20	20 18
SPB	7 5	6 5	6 4	5 4
	-3 -3	-2 -3	-2 -2	-2 -2
C-23	4 4	4 4	4 4	4 4
SPB	2 1	1 1	1 1	1 1
	1 0	1 0	1 0	0 0

Table 3.10 (Cont.). Principal Flood Direction Vertically Integrated Current Speed Tidal Validation April 1979 –October 1980. For each row in each month, the first entry corresponds to the first 15 days of the month, with the second entry denoting the remaining portion. Row 1 corresponds to the RMSE in cm/s. Row 2 corresponds to the Willmott Relative Error in percent. Row 3 corresponds to the model mean in cm/s. Note the predicted mean current speed is zero.

Station	Apr 1979	May 1979	Sep 1980	Oct 1980
C-24 CS	14 19 1 2 5 2	16 18 2 2 3 1	15 23 2 3 1 -1	13 22 1 3 0 -2
C-25 CS	18 16 4 2 -9 -6	16 17 3 2 -6 -5	18 16 3 2 -5 -3	17 16 3 2 -3 -1
C-26 SB	15 16 2 2 -8 -6	14 16 2 2 -6 -5	13 18 2 3 -5 -3	11 18 1 3 -3 -2
C-28 SB	9 9 7 6 0 0	9 10 7 7 0 0	10 9 8 6 0 0	10 9 8 6 0 0
C-29 SB	11 11 2 2 3 1	10 12 2 3 2 0	10 13 2 3 0 -1	8 13 1 3 -1 -2
C-30 SB	15 13 5 2 4 1	13 14 3 3 2 0	17 16 5 4 0 -2	17 15 5 5 -2 -3
C-31 SB	8 10 4 5 0 2	8 10 4 5 1 2	7 10 3 5 1 2	7 11 3 7 0 0
C-33 SB	22 27 13 15 0 -1	24 27 14 15 -1 -2	21 28 11 16 -3 -4	21 29 11 16 -5 -6

Table 3.11 Principal Current Direction Mid-Level Current Speed Tidal Validation: April 1979-October 1980. For each row in each month, the first entry corresponds to the first 15 days of the month, with the second entry denoting the remaining portion. Row 1 corresponds to the RMSE in cm/s. Row 2 corresponds to the Willmott Relative Error in percent. Row 3 corresponds to the model mean in cm/s. Note the predicted mean current speed is zero.

Station	Apr 1979	May 1979	Sep 1980	Oct 1980
C-1 GG	44 51 9 9 8 10	48 49 10 8 8 9	39 52 6 9 8 8	38 51 6 8 7 7
C-5 MB	25 31 10 11 11 12	27 30 11 12 11 11	25 29 10 11 10 10	24 28 9 10 9 7
C-17 MB	14 14 4 3 9 6	14 13 4 3 8 5	12 13 2 2 5 4	9 13 2 2 3 2
C-18 MB	25 26 5 4 16 15	24 24 5 4 15 13	20 22 3 3 11 12	16 20 2 3 11 10
C-19 MB	9 11 3 3 3 4	10 11 3 3 3 4	8 10 2 2 4 4	7 10 2 3 3 4
C-20 SPB	17 20 12 12 0 0	18 19 13 12 1 1	16 21 10 13 0 0	16 21 11 14 1 1
C-22 SPB	13 10 3 1 6 4	11 10 2 1 6 4	11 9 2 1 4 3	10 9 2 1 2 2
C-23 SPB	5 5 2 2 1 2	5 5 2 2 2 2	4 5 2 2 1 1	4 5 2 2 1 2

Table 3.11 (Cont.). Principal Current Direction Mid-Level Current Speed Tidal Validation April 1979 –October 1980. For each row in each month, the first entry corresponds to the first 15 days of the month, with the second entry denoting the remaining portion. Row 1 corresponds to the RMSE in cm/s. Row 2 corresponds to the Willmott Relative Error in percent. Row 3 corresponds to the model mean in cm/s. Note the predicted mean current speed is zero.

Station	Apr 1979	May 1979	Sep 1980	Oct 1980
C-24 CS	30 38 9 12 -10 -12	35 36 11 11 -12 -12	29 39 8 11 -11 -11	25 36 6 9 -9 -8
C-25 CS	15 21 3 5 6 11	20 22 6 6 12 13	20 23 6 7 14 14	17 20 5 5 11 10
C-26 SB	15 19 3 3 -4 -1	16 19 3 4 -1 1	14 22 2 5 1 3	14 22 2 5 2 3
C-28 SB	9 10 9 7 0 1	9 11 8 9 1 1	10 9 10 7 1 2	10 10 10 8 2 2
C-29 SB	12 14 3 4 1 -1	13 15 4 4 0 -2	11 16 3 5 -3 -4	10 17 3 5 -4 -5
C-30 SB	11 11 3 2 2 -1	11 12 2 3 0 -2	13 15 4 4 -3 -5	13 15 4 4 -5 -6
C-31 SB	8 10 4 6 1 3	9 11 5 6 2 3	7 11 3 6 3 3	7 12 4 8 2 2
C-33 SB	24 30 18 20 0 -2	26 29 19 20 -1 -2	24 32 16 24 -4 -7	25 33 19 24 -8 -9

Table 3.12 Salinity Tidal Simulation Validation: April 1979-October 1980. For each row in each month, the first entry corresponds to the first 15 days of the month, with the second entry denoting the remaining portion. Row 1 corresponds to the RMSE in PSU. Row 2 corresponds to the Willmott Relative Error in percent. Row 3 corresponds to the model mean in PSU with row 4 denoting the observed salinity mean in PSU. Note n/a denotes not applicable.

Station	Apr 1979	Oct 1980
C-1 (46) GG	2 2 39 48 30 30 31 32	0 n/a 22 n/a 32 32 32 n/a
C-5 (25) MB	2 n/a 21 n/a 28 30 28 n/a	n/a n/a n/a n/a n/a n/a n/a n/a
C-17 (5) MB	2 n/a 12 n/a 25 26 25 n/a	n/a n/a n/a n/a n/a n/a n/a n/a
C-18 (15) MB	2 2 15 19 22 23 22 25	2 3 37 47 29 30 27 26
C-19 (1) MB	2 n/a 16 n/a 18 19 18 n/a	n/a n/a n/a n/a 27 28 n/a n/a
C-20 (1) SPB	n/a n/a n/a n/a 17 14 n/a n/a	n/a n/a n/a n/a n/a n/a n/a n/a
C-22 (2) SPB	3 n/a 26 n/a 20 20 22 n/a	n/a n/a n/a n/a n/a n/a n/a n/a
C-23 (1) SPB	n/a n/a n/a n/a 12 14 n/a n/a	5 8 81 94 26 28 21 19

Table 3.12 (Cont.). Salinity Tidal SimulationValidation April 1979-October 1980. For each row in each month, the first entry corresponds to the first 15 days of the month, with the second entry denoting the remaining portion. Row 1 corresponds to the RMSE in PSU. Row 2 corresponds to the Willmott Relative Error in percent. Row 3 corresponds to the model mean in PSU with row 4 denoting the observed salinity mean in PSU. Note n/a denotes not applicable.

Station	Apr 1979	Oct 1980
C-24 (17,12) CS	5 5 44 41 7 10 11 14	4 n/a 42 n/a 24 27 19 n/a
C-25 (8) CS	4 5 33 33 3 6 7 10	n/a n/a n/a n/a n/a n/a n/a n/a
C-26 (2) SB	n/a n/a n/a n/a 2 3 n/a n/a	n/a 13 n/a 68 18 23 n/a 13
C-28 (1) SB	n/a 3 n/a 57 1 0 n/a 3	n/a n/a n/a n/a n/a n/a n/a n/a
C-29 (2) SB	n/a 3 n/a 56 0 0 n/a 3	n/a n/a n/a n/a n/a n/a n/a n/a
C-30 (2) SB	n/a 6 n/a 58 0 0 n/a 5	n/a n/a n/a n/a n/a n/a n/a n/a
C-31 (1) SB	n/a 2 n/a 54 0 0 n/a 2	n/a n/a n/a n/a n/a n/a n/a n/a
C-33 (2) SB	n/a 0 n/a 56 0 0 n/a 0	n/a n/a n/a n/a n/a n/a n/a n/a

Table 3.13 Temperature Tidal Simulation Validation: April 1979- October 1980. For each row in each month, the first entry corresponds to the first 15 days of the month, with the second entry denoting the remaining portion. Row 1 corresponds to the RMSE in ^{o}C. Row 2 corresponds to the Willmott Relative Error in percent. Row 3 corresponds to the model mean in ^{o}C with row 4 denoting the observed temperature mean in ^{o}C. Note n/a denotes not applicable.

Station	Apr 1979	Oct 1980
C-1 (46) GG	1 2 68 69 13 14 12 11	2 n/a 69 n/a 17 17 15 n/a
C-5 (25) MB	1 n/a 49 n/a 13 14 13 n/a	n/a n/a n/a n/a n/a n/a n/a n/a
C-17 (5) MB	0 n/a 26 n/a 13 14 13 n/a	n/a n/a n/a n/a n/a n/a n/a n/a
C-18 (15) MB	1 1 41 51 14 15 14 14	1 2 41 73 19 18 18 16
C-19 (1) MB	0 n/a 41 n/a 14 15 14 n/a	1 n/a 31 n/a 19 19 19 n/a
C-20 (1) SPB	4 n/a 59 n/a 13 13 17 n/a	n/a n/a n/a n/a n/a n/a n/a n/a
C-22 (2) SPB	0 n/a 22 n/a 14 15 13 n/a	n/a n/a n/a n/a 19 18 n/a n/a
C-23 (1) SPB	n/a n/a n/a n/a 15 16 n/a n/a	1 3 50 91 20 19 19 17

Table 3.13 (Cont.). Temperature Tidal Simulation Validation April 1979–October 1980. For each row in each month, the first entry corresponds to the first 15 days of the month, with the second entry denoting the remaining portion. Row 1 corresponds to the RMSE in ^{o}C. Row 2 corresponds to the Willmott Relative Error in percent. Row 3 corresponds to the model mean in ^{o}C with row 4 denoting the observed temperature mean in ^{o}C. Bold italics indicate measurement errors and their associated model discrepancies. Note n/a denotes not applicable.

Station	Apr 1979	Oct 1980
C-24 (17,12) CS	1 1 49 76 15 17 15 15	1 n/a 68 n/a 20 19 19 n/a
C-25 (8) CS	1 2 77 83 16 17 15 15	n/a n/a n/a n/a n/a n/a n/a n/a
C-26 (2) SB	2 2 80 83 16 18 15 15	n/a 3 n/a 93 21 20 n/a 16
C-28 (1) SB	n/a 2 n/a 62 16 18 n/a 16	n/a n/a n/a n/a n/a n/a n/a n/a
C-29 (2) SB	n/a 2 n/a 64 16 18 n/a 16	n/a n/a n/a n/a n/a n/a n/a n/a
C-30 (2) SB	n/a 2 n/a 66 16 18 n/a 16	n/a n/a n/a n/a n/a n/a n/a n/a
C-31 (1) SB	n/a 2 n/a 63 17 18 n/a 16	n/a n/a n/a n/a n/a n/a n/a n/a
C-33 (2) SB	n/a 2 n/a 58 17 18 n/a 16	n/a n/a n/a n/a n/a n/a n/a n/a

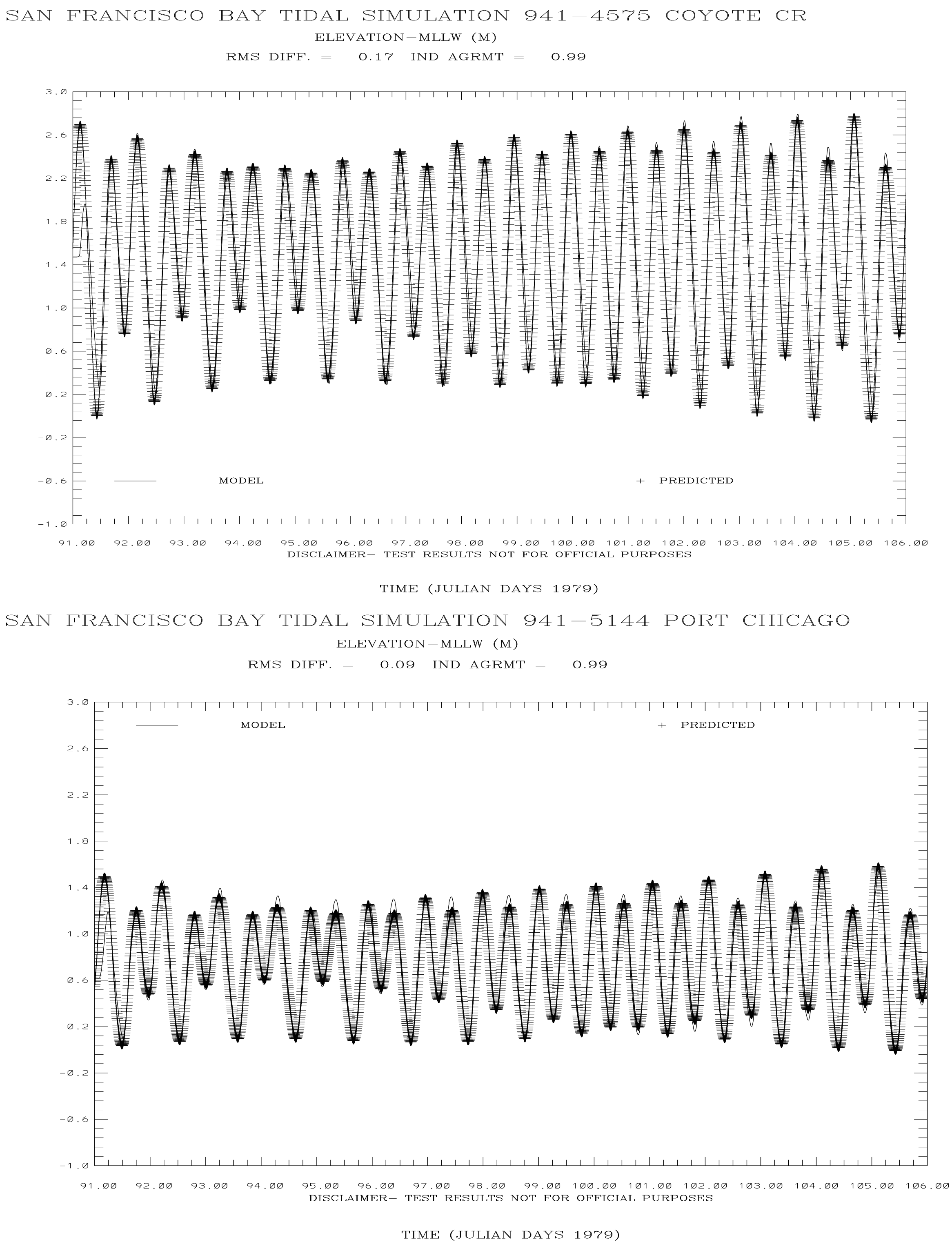

Figure 3.27. April 1-15, 1979 Tidal Simulation: Coyote Creek and Port Chicago Water Level Comparisons. Note IND AGRMT equals one minus Willmott et al. (1985) relative error.

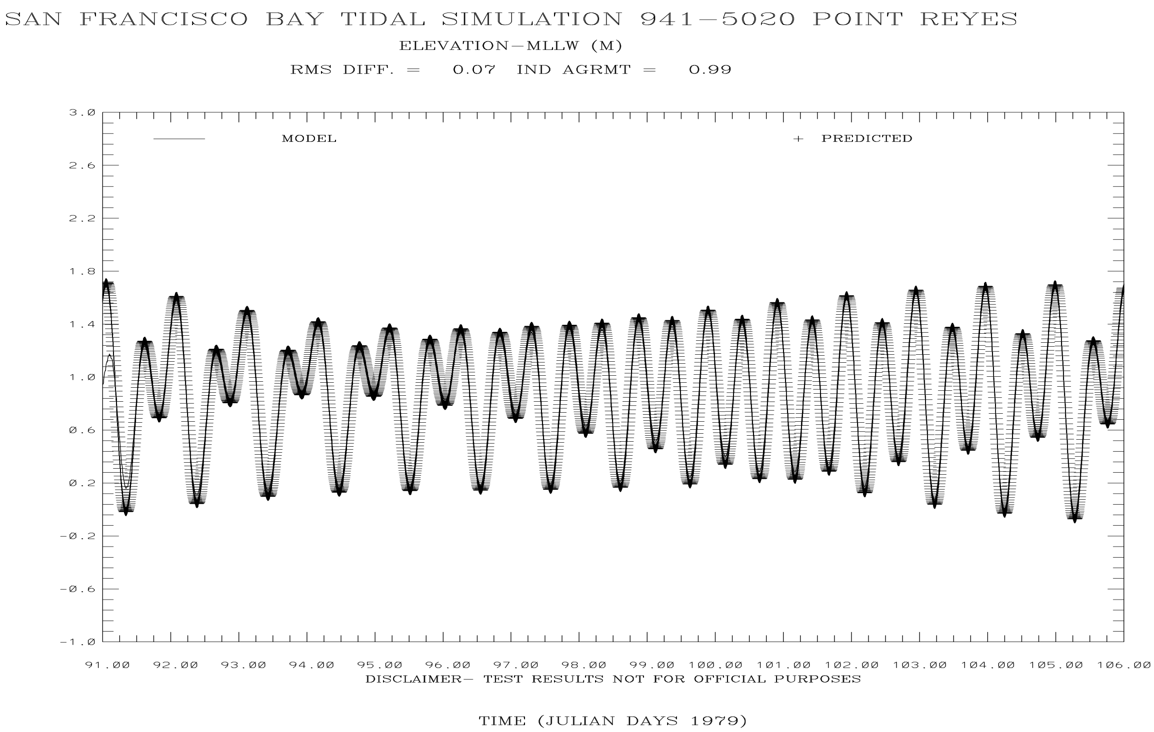

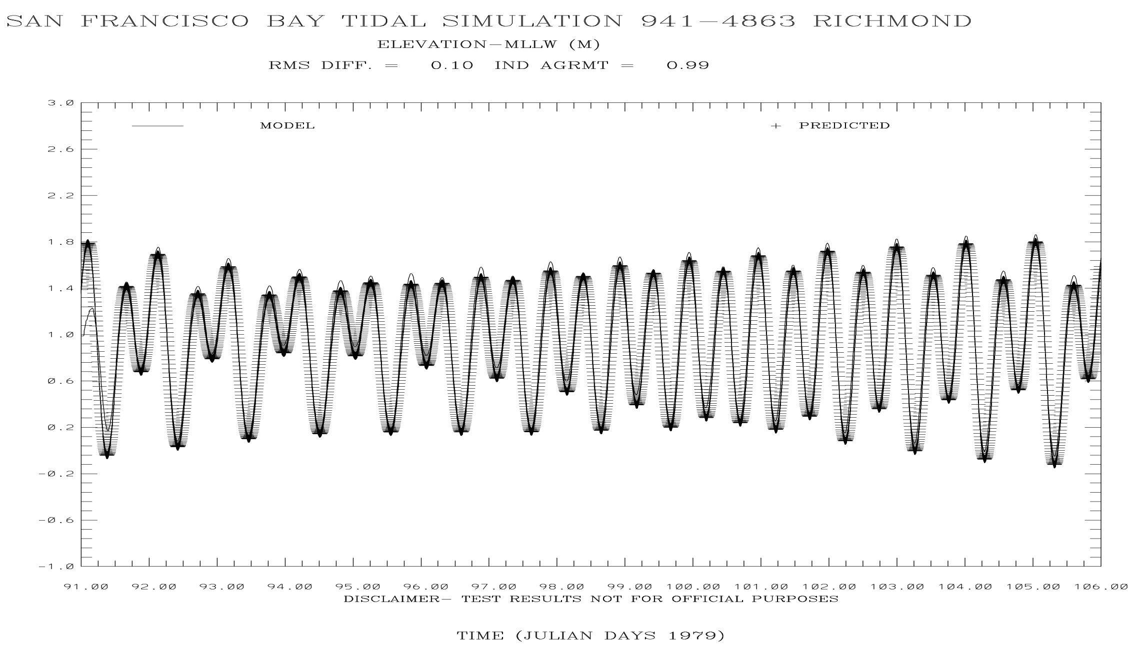

Figure 3.28. April 1-15, 1979 Tidal Simulation: Point Reyes and Richmond Water Level Comparisons. Note IND AGRMT equals one minus Willmott et al. (1985) relative error.

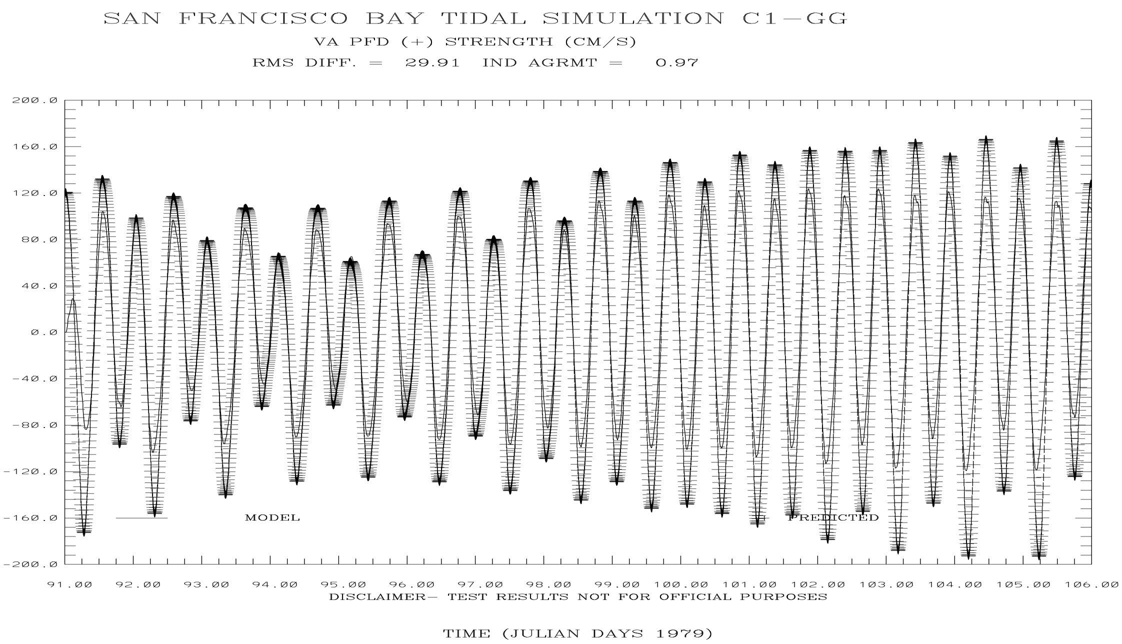

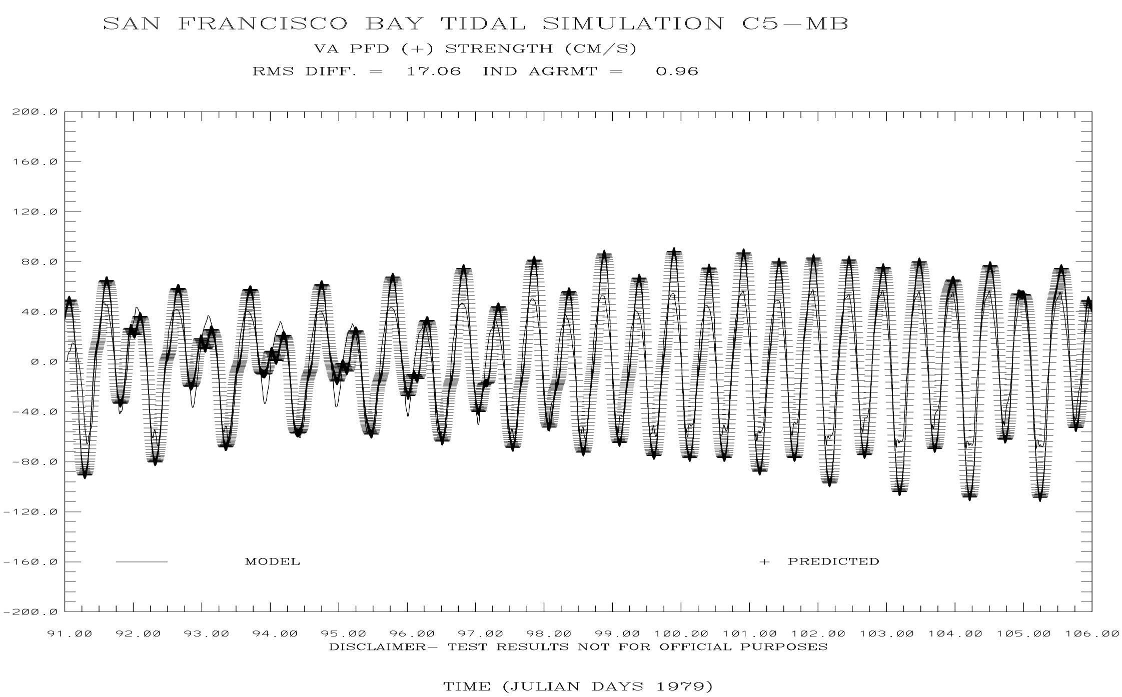

Figure 3.29. April 1-15, 1979 Tidal Simulation: C-1 and C-6 Vertically Integrated Principal Current Component Comparison. Note IND AGRMT equals one minus Willmott et al. (1985) relative error.

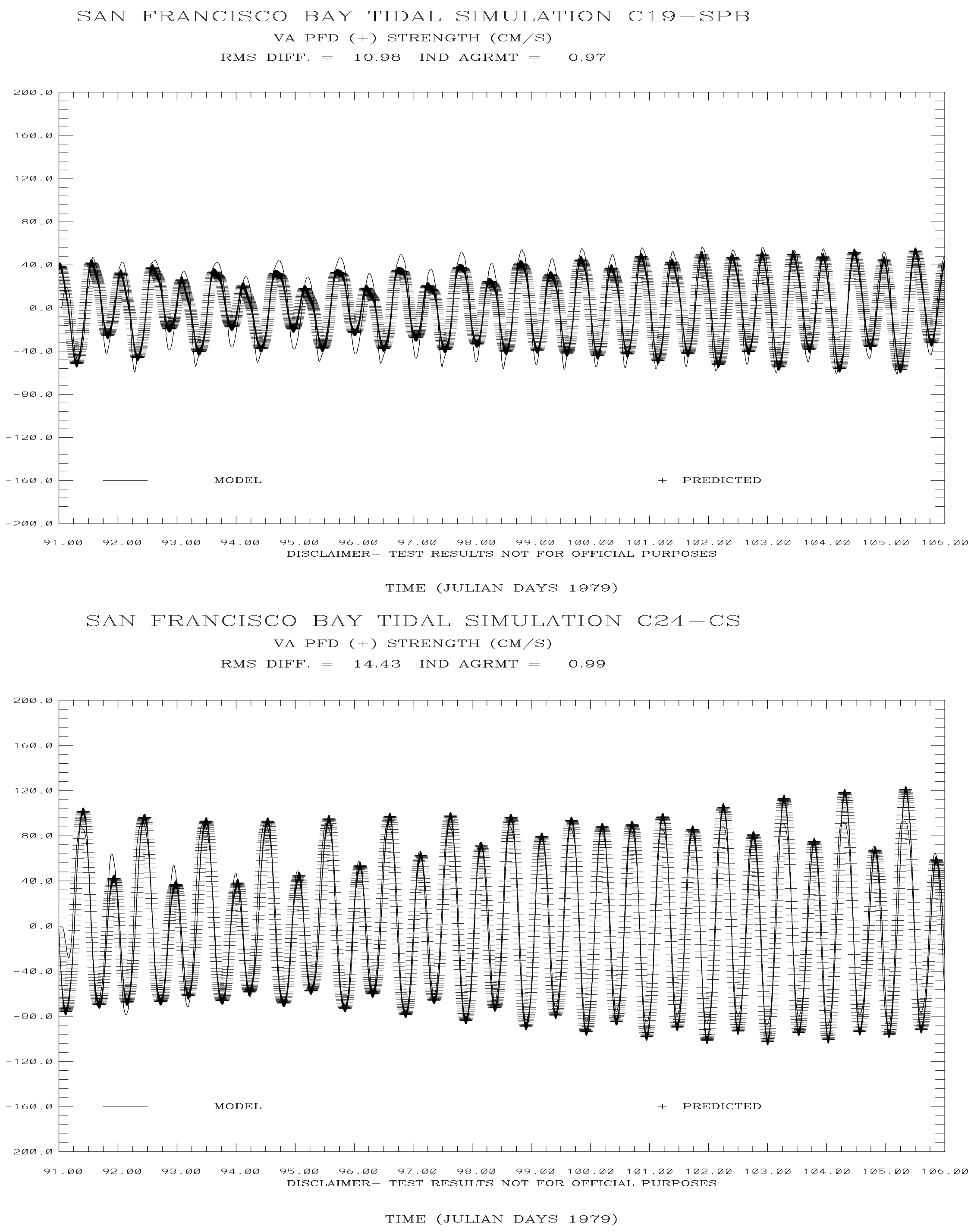

Figure 3.30. April 1-15, 1979 Tidal Simulation: C-19 and C-24 Vertically Integrated Principal Current Component Comparison. Note IND AGRMT equals one minus Willmott et al. (1985) relative error.

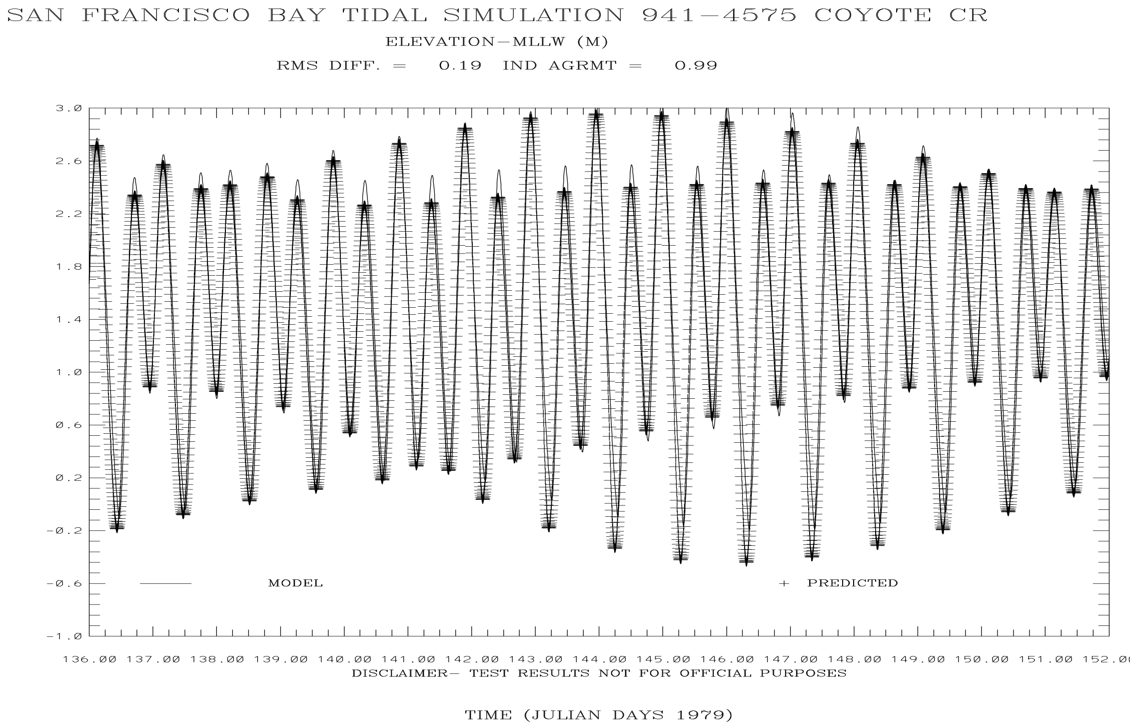

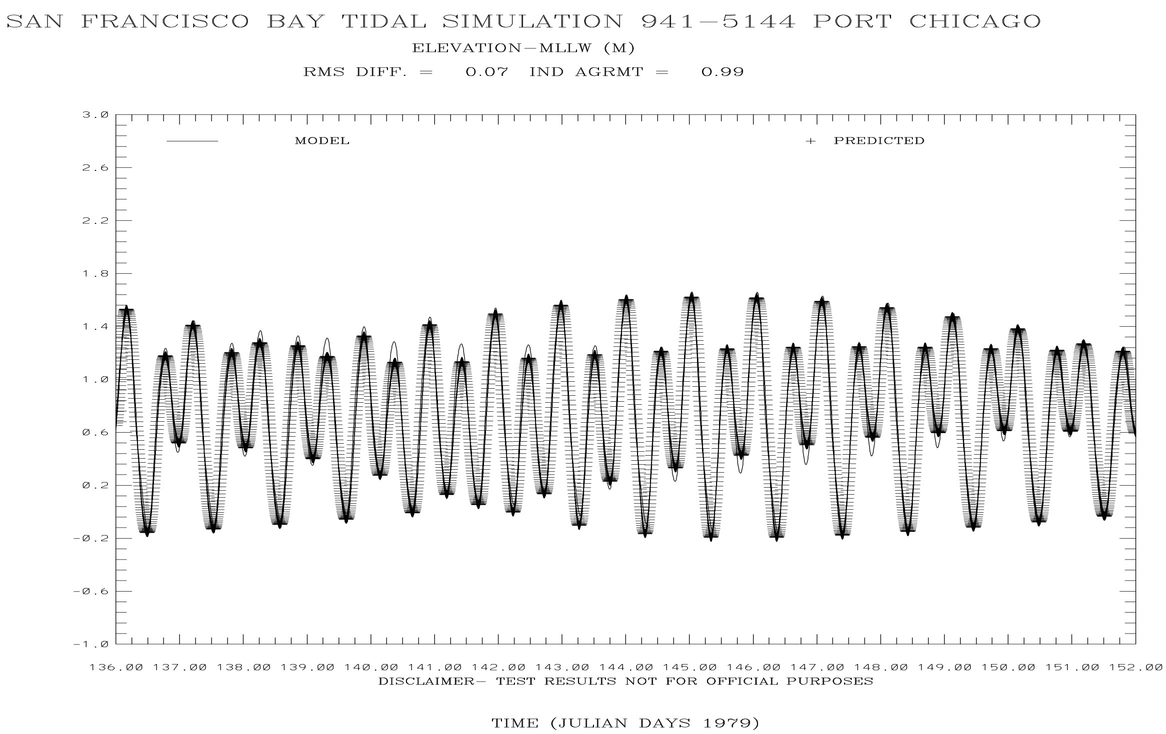

Figure 3.31. May 15-31, 1979 Tidal Simulation: Coyote Creek and Port Chicago Water Level Comparisons. Note IND AGRMT equals one minus Willmott et al. (1985) relative error.

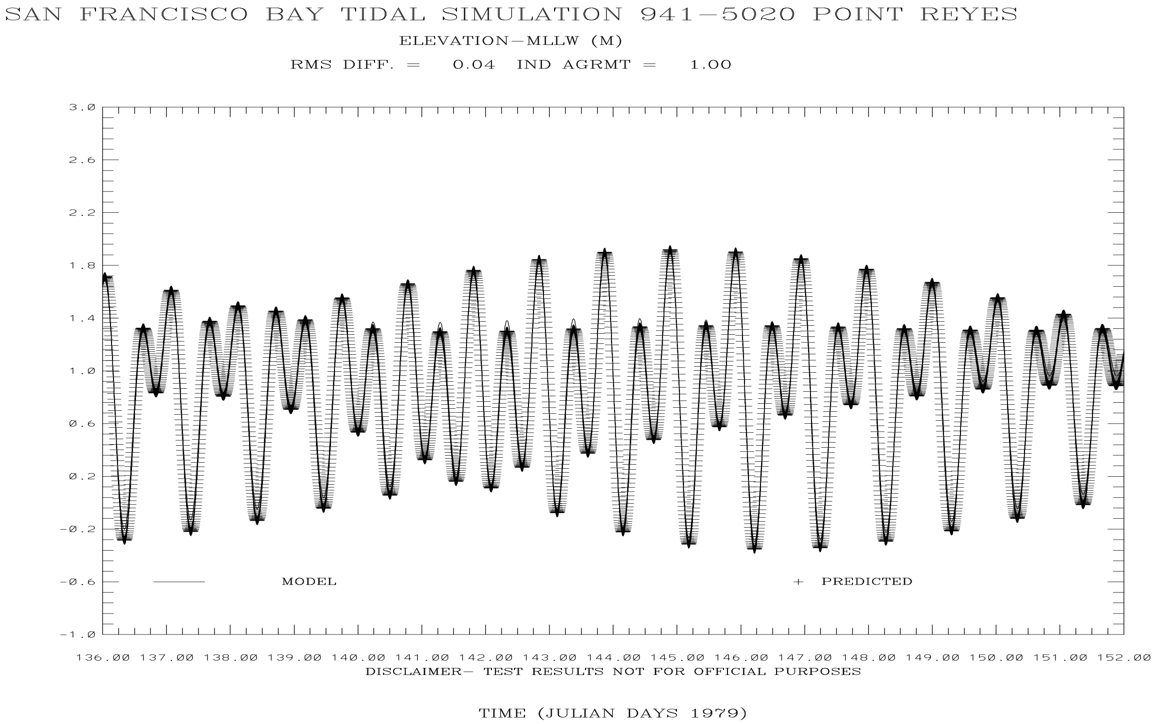

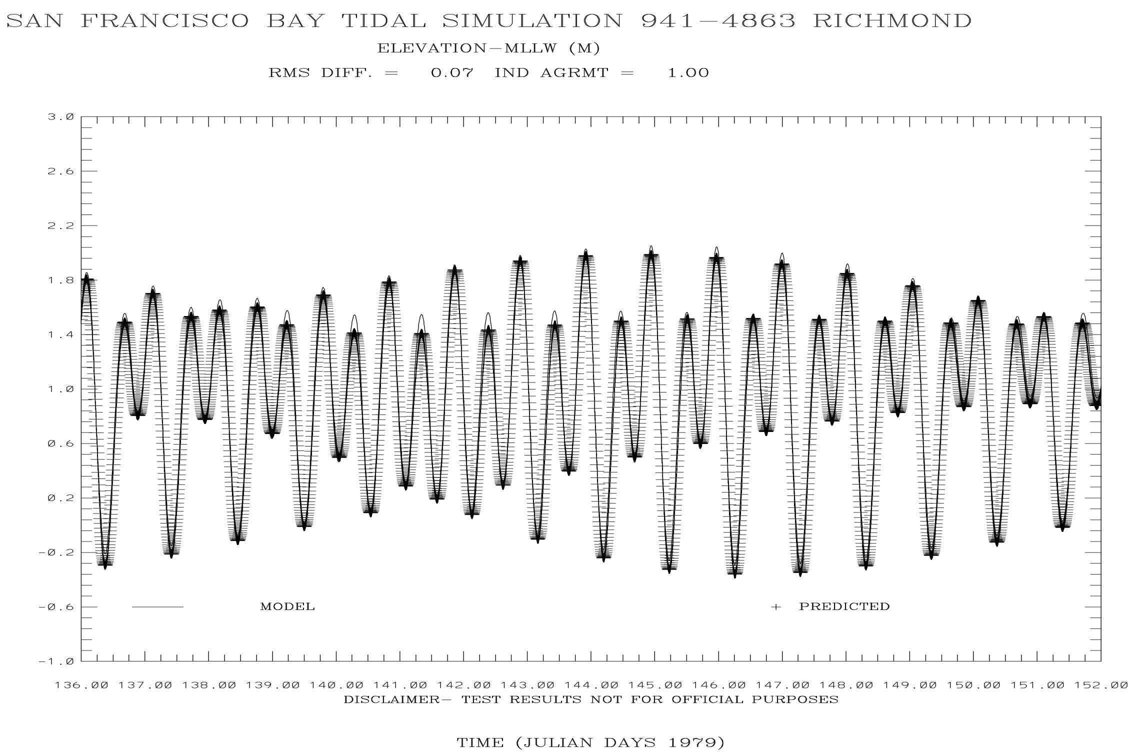

Figure 3.32. May 15-31, 1979 Tidal Simulation: Point Reyes and Richmond Water Level Comparisons. Note IND AGRMT equals one minus Willmott et al. (1985) relative error.

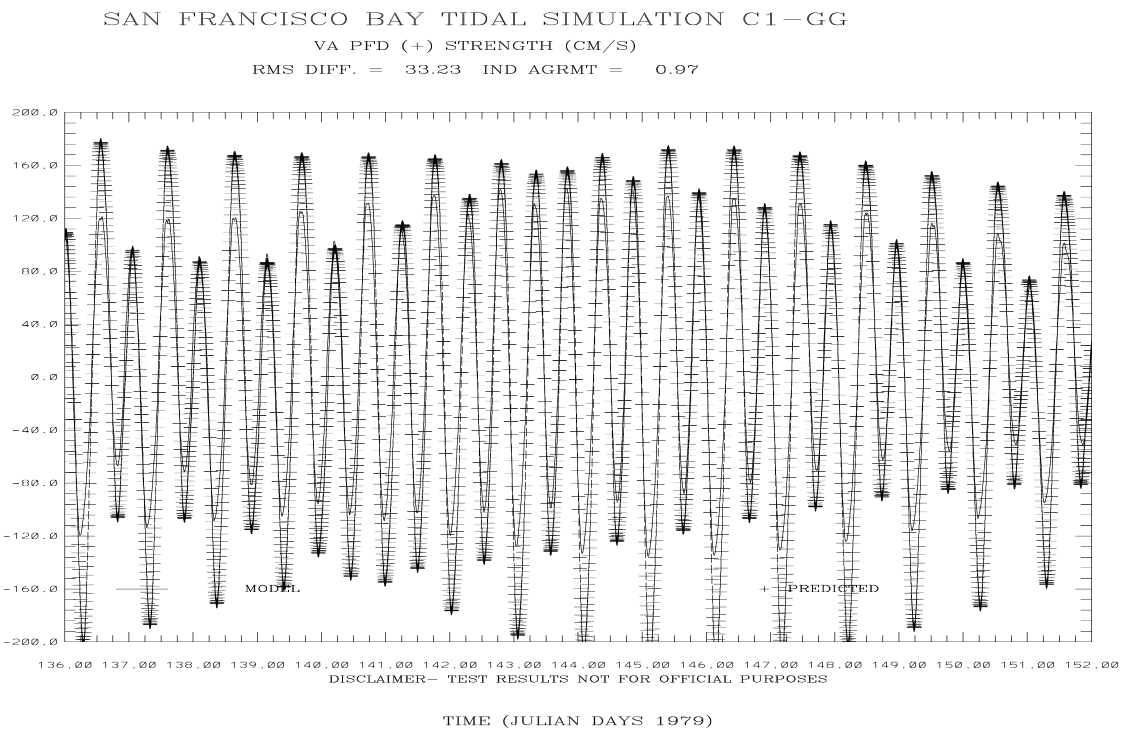

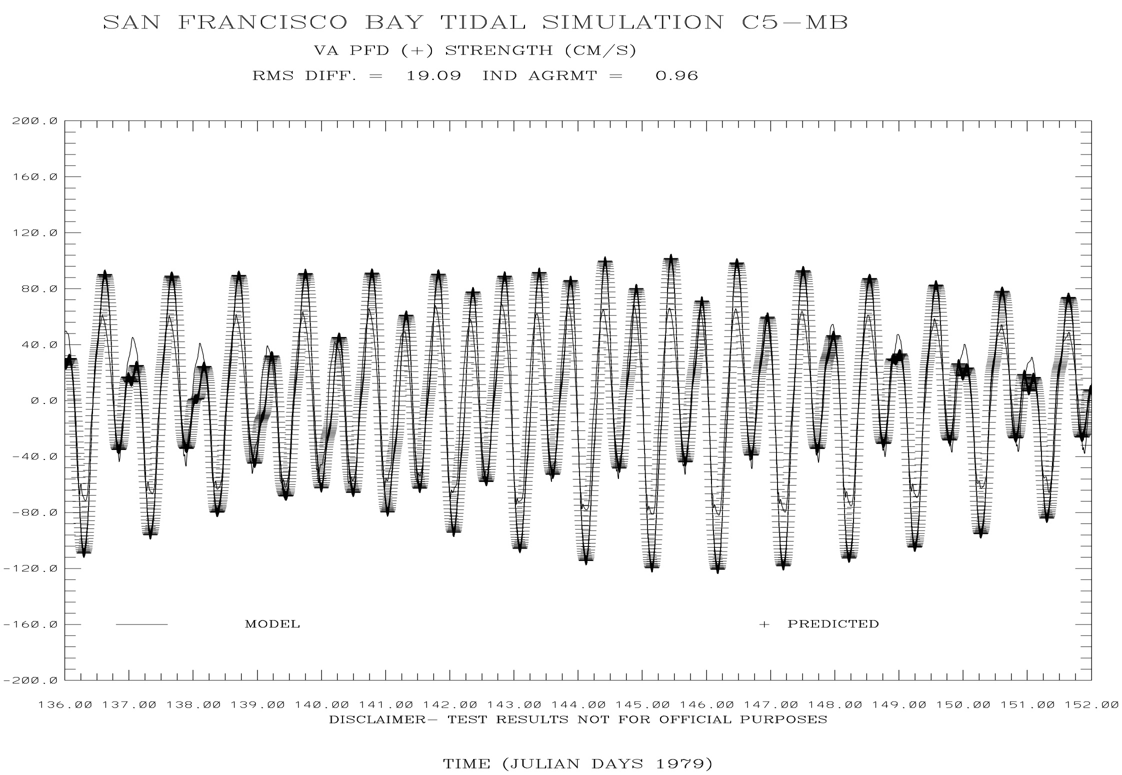

Figure 3.33. May 15-31, 1979 Tidal Simulation: C-1 and C-6 Vertically Integrated Principal Current Component Comparisons. Note IND AGRMT equals one minus Willmott et al. (1985) relative error.

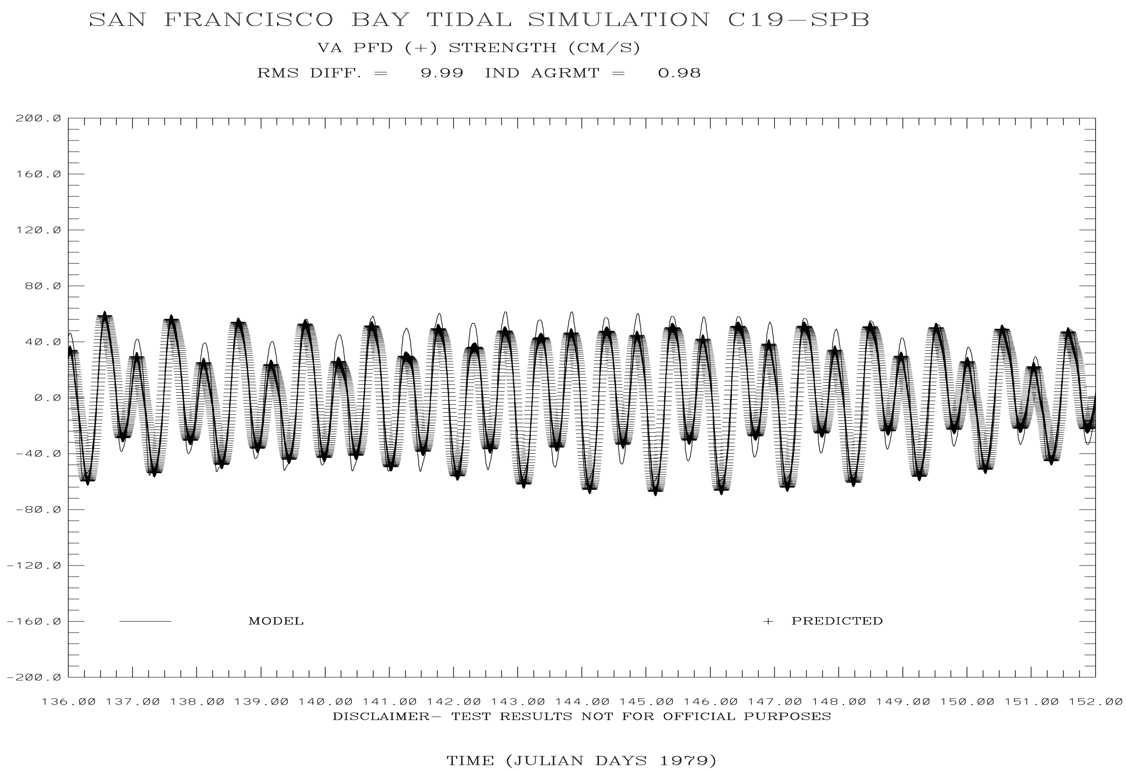

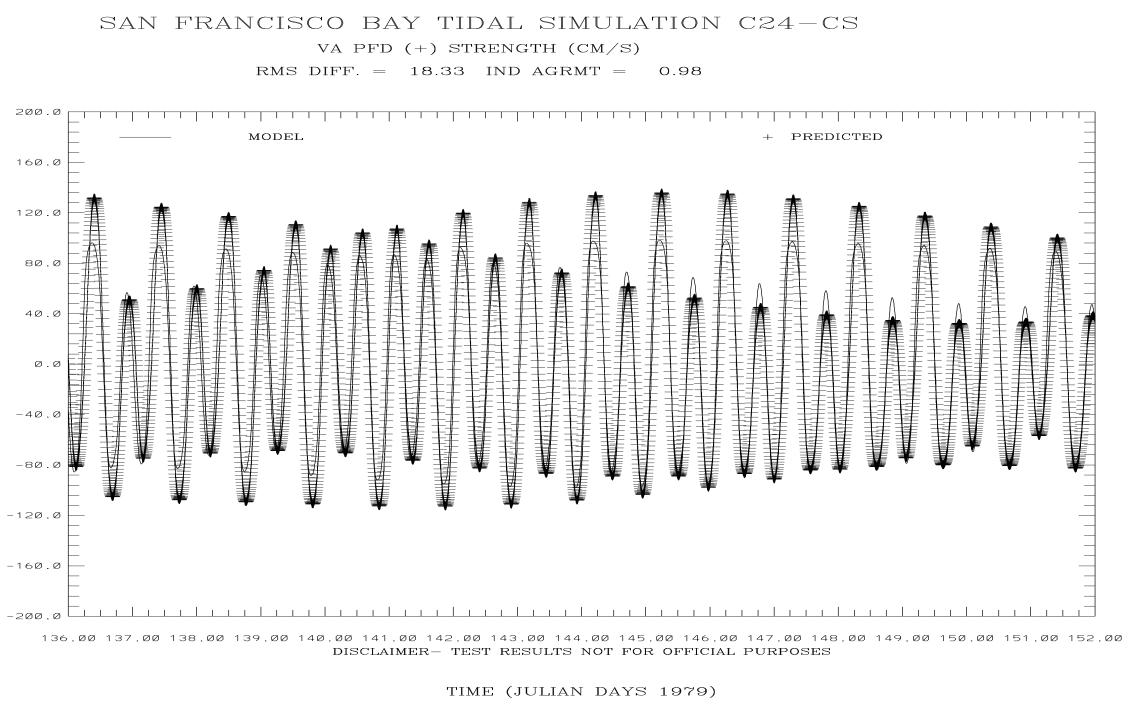

Figure 3.34. May 15-31, 1979 Tidal Simulation: C-19 and C-24 Vertically Integrated Principal Current Component Comparisons. Note IND AGRMT equals one minus Willmott et al. (1985) relative error.

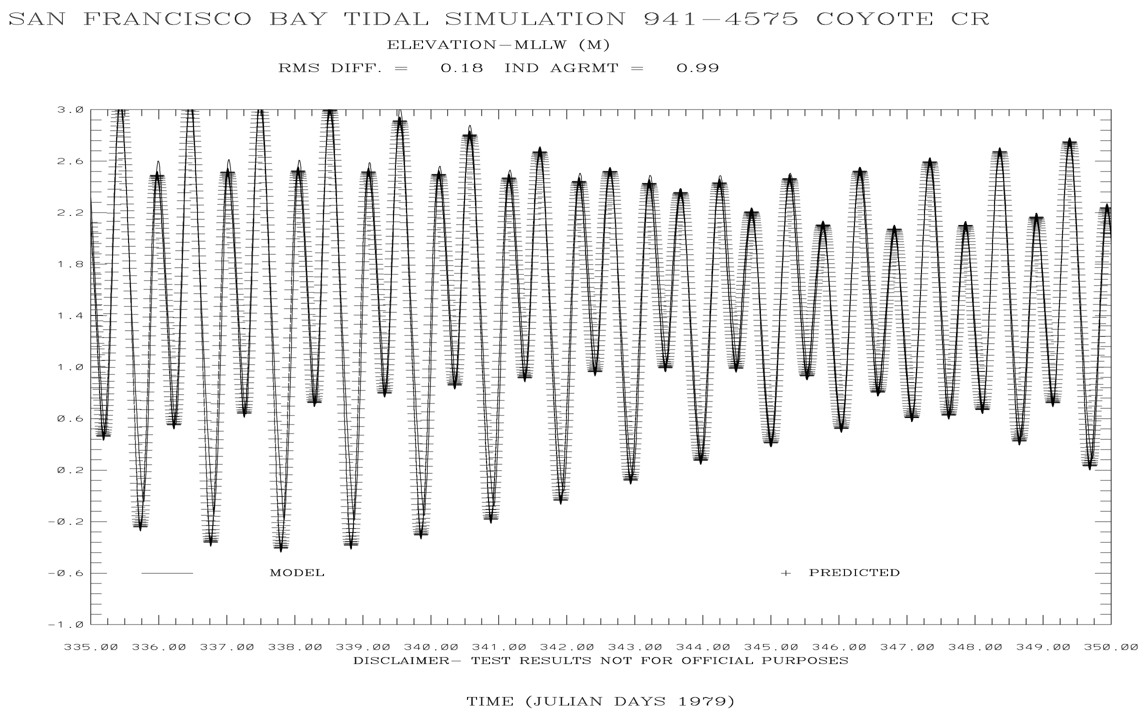

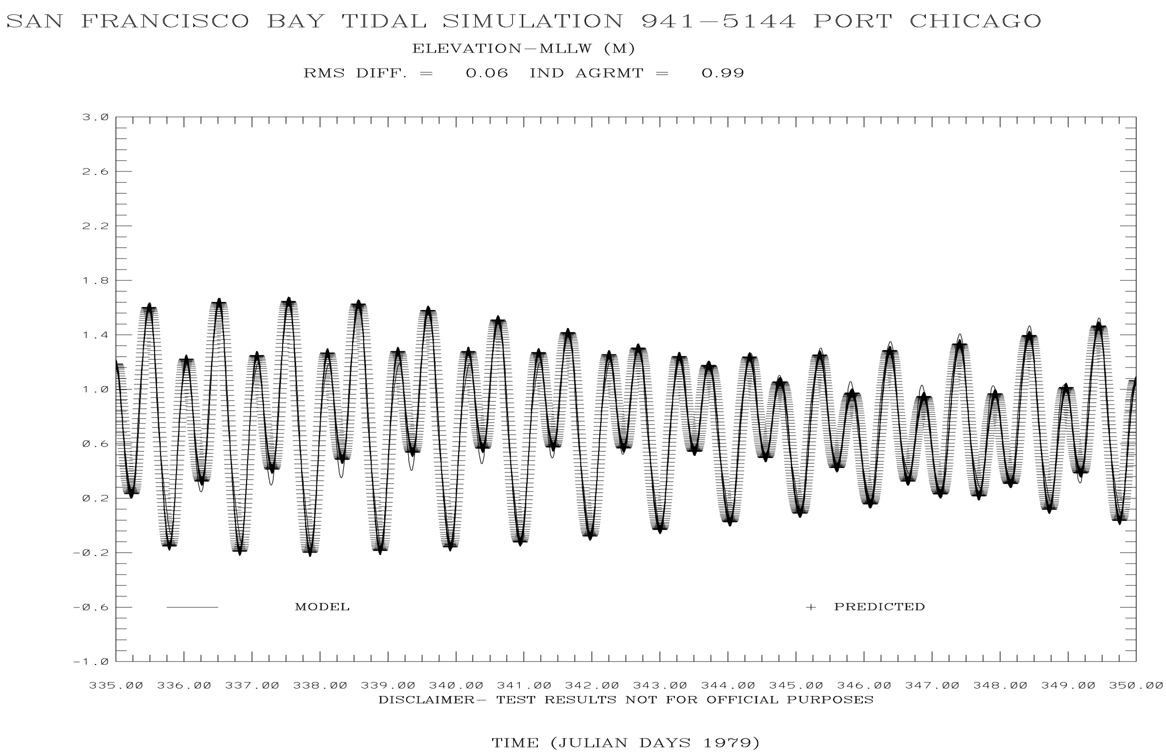

Figure 3.35. December 1-15, 1979 Tidal Simulation: Coyote Creek and Port Chicago Water Level Comparisons. Note IND AGRMT equals one minus Willmott et al. (1985) relative error.

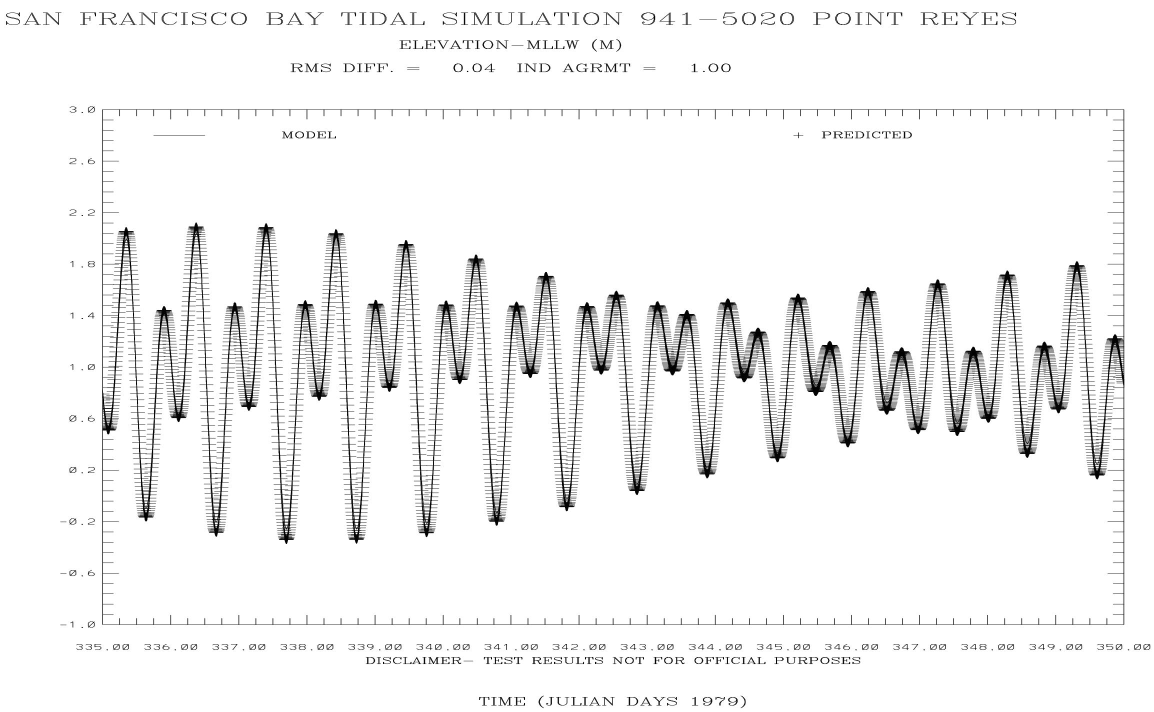

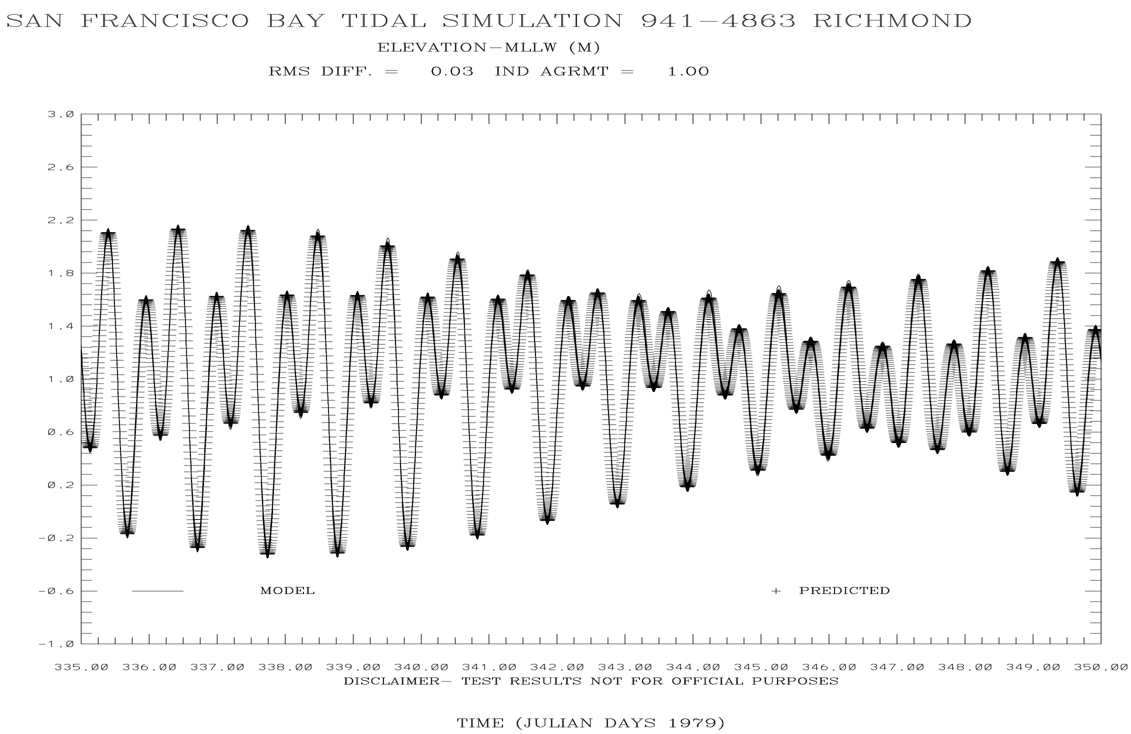

Figure 3.36. December 1-15, 1979 Tidal Simulation: Point Reyes and Richmond Water Level Comparisons. Note IND AGRMT equals one minus Willmott et al. (1985) relative error.

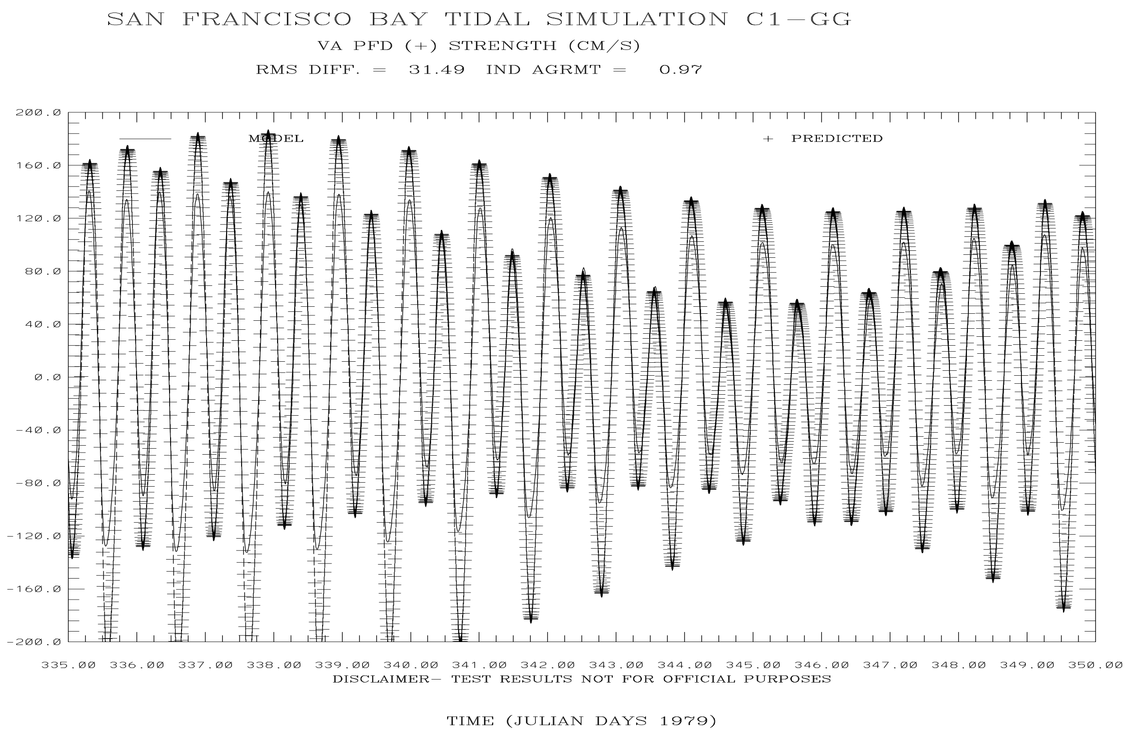

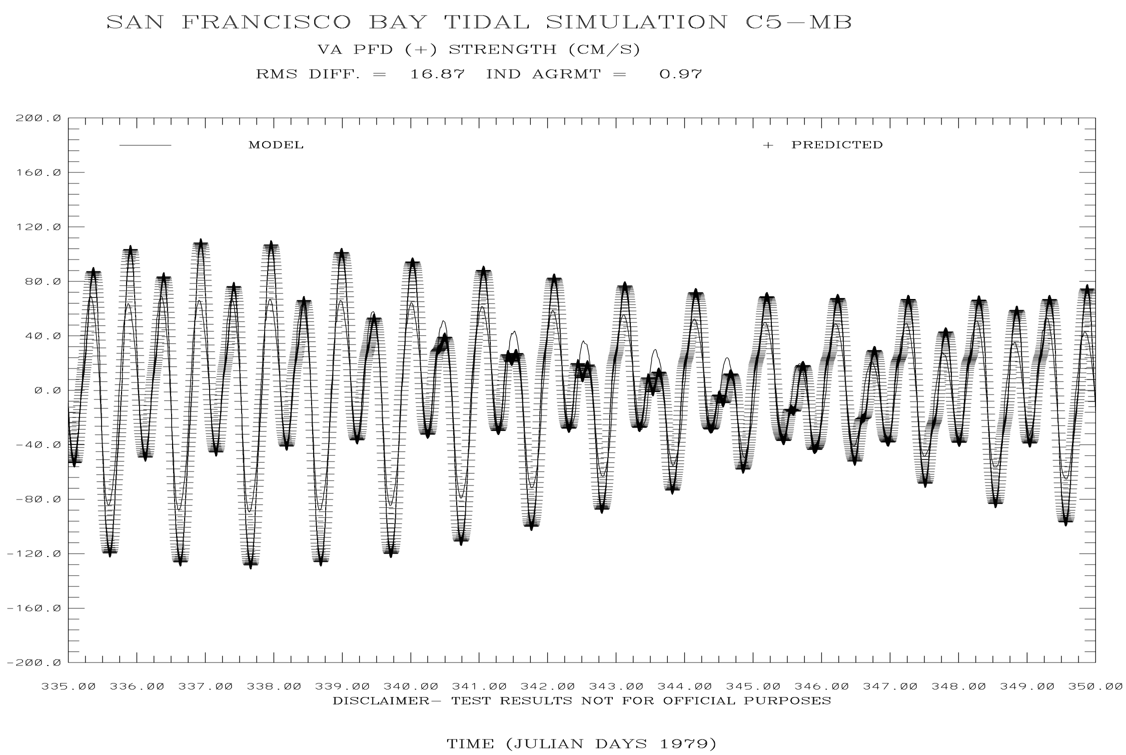

Figure 3.37. December 1-15, 1979 Tidal Simulation: C-1 and C-6 Vertically Integrated Principal Current Component Comparisons. Note IND AGRMT equals one minus Willmott et al. (1985) relative error.

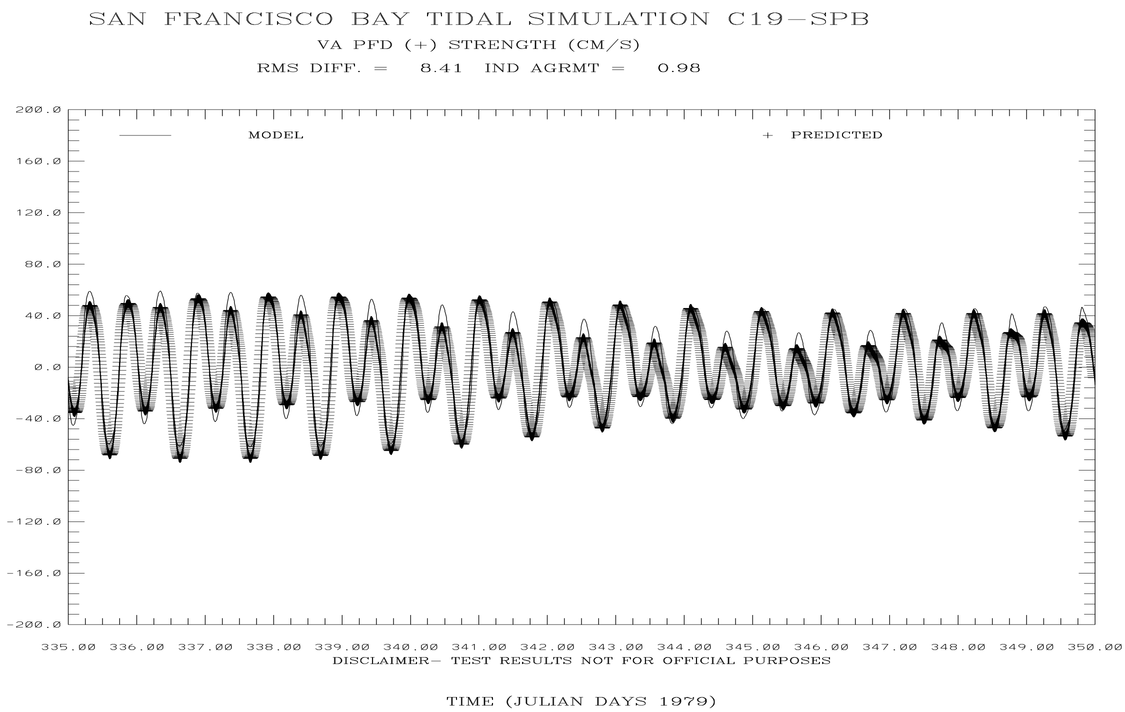

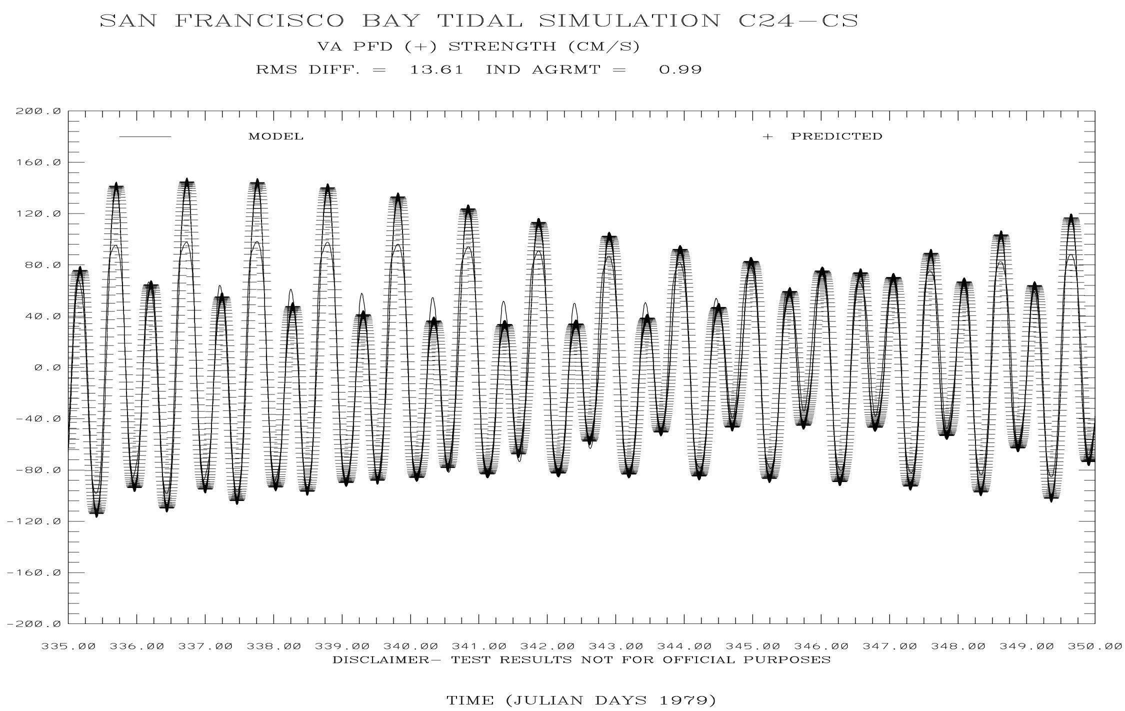

Figure 3.38. December 1-15, 1979 Tidal Simulation: C-19 and C-24 Vertically Integrated Principal Current Component Comparisons. Note IND AGRMT equals one minus Willmott et al. (1985) relative error.

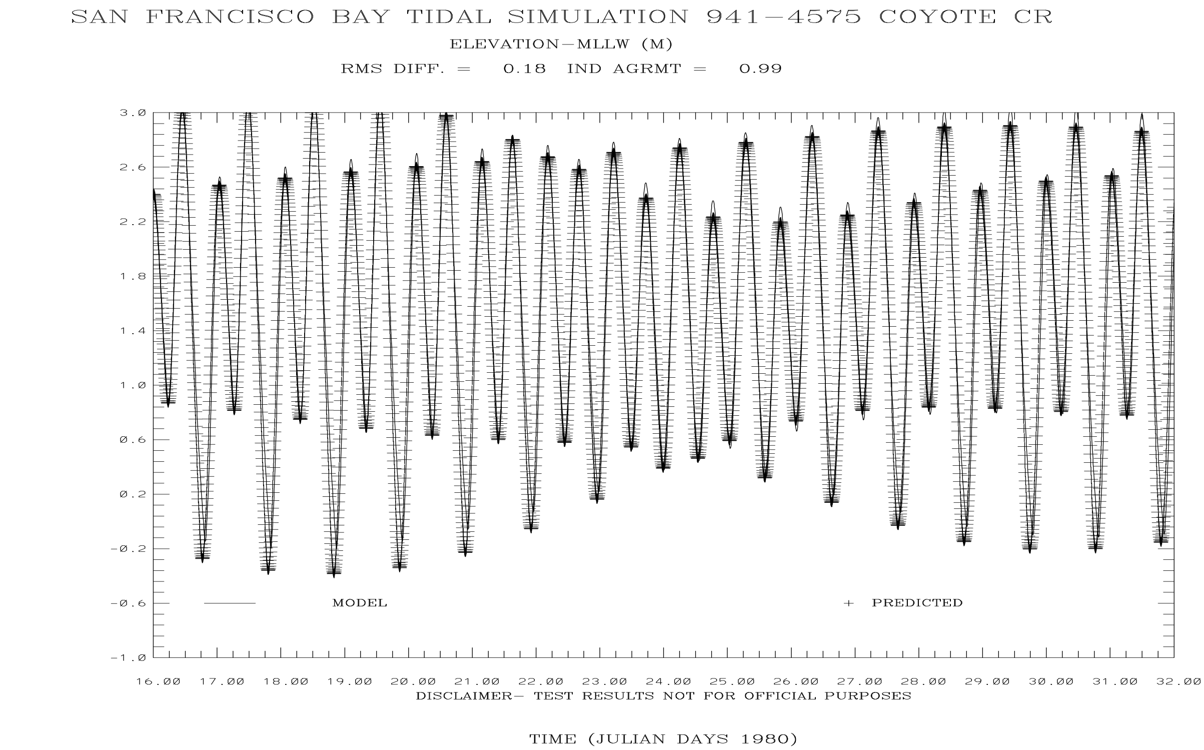

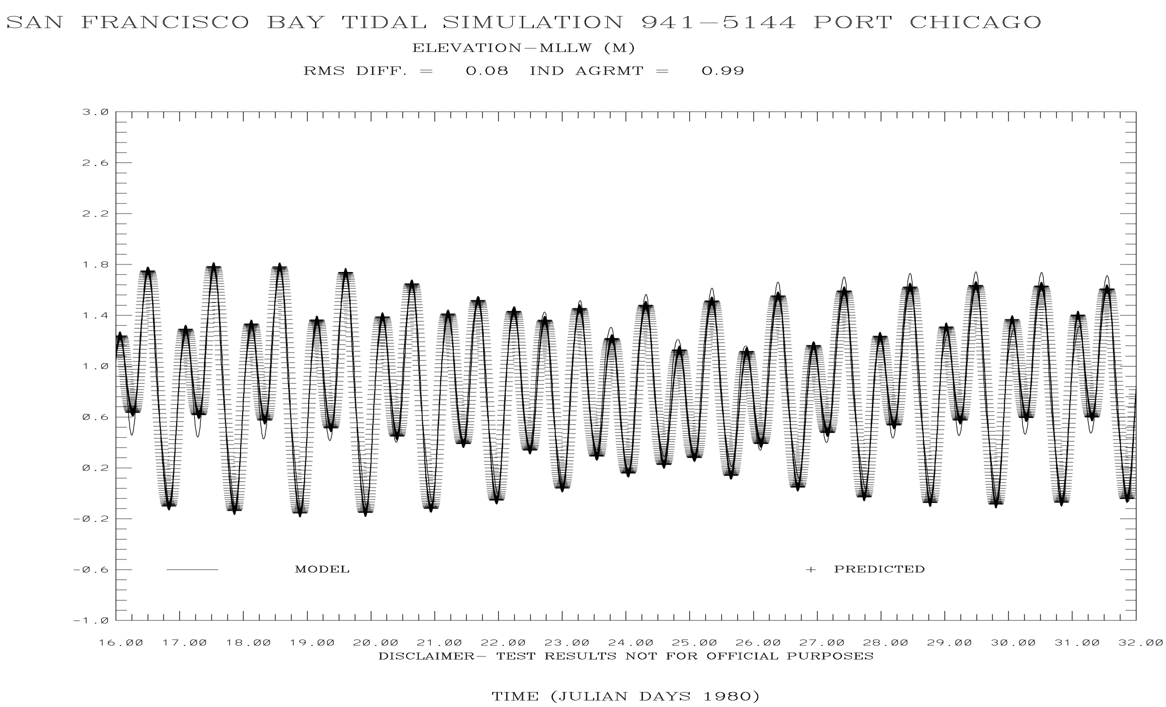

Figure 3.39. January 15-31, 1980 Tidal Simulation: Coyote Creek and Port Chicago Water Level Comparisons. Note IND AGRMT equals one minus Willmott et al. (1985) relative error.

SAN FRANCISCO BAY TIDAL SIMULATION 941−5020 POINT REYES

ELEVATION−MLLW (M)

RMS DIFF. = 0.06 IND AGRMT = 1.00

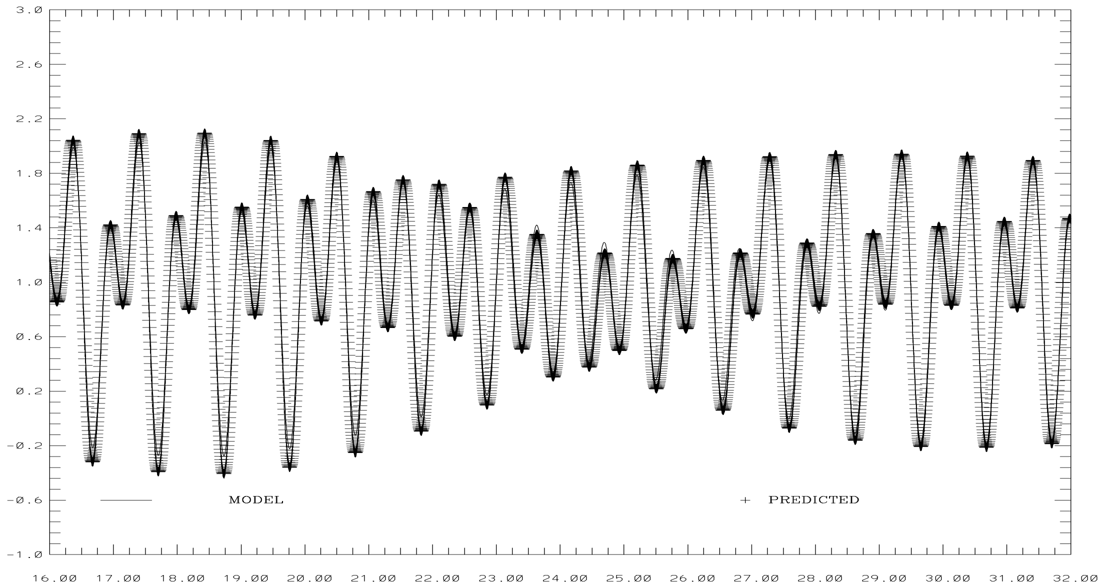

DISCLAIMER− TEST RESULTS NOT FOR OFFICIAL PURPOSES

TIME (JULIAN DAYS 1980)

SAN FRANCISCO BAY TIDAL SIMULATION 941−4863 RICHMOND

ELEVATION−MLLW (M)

RMS DIFF. = 0.06 IND AGRMT = 1.00

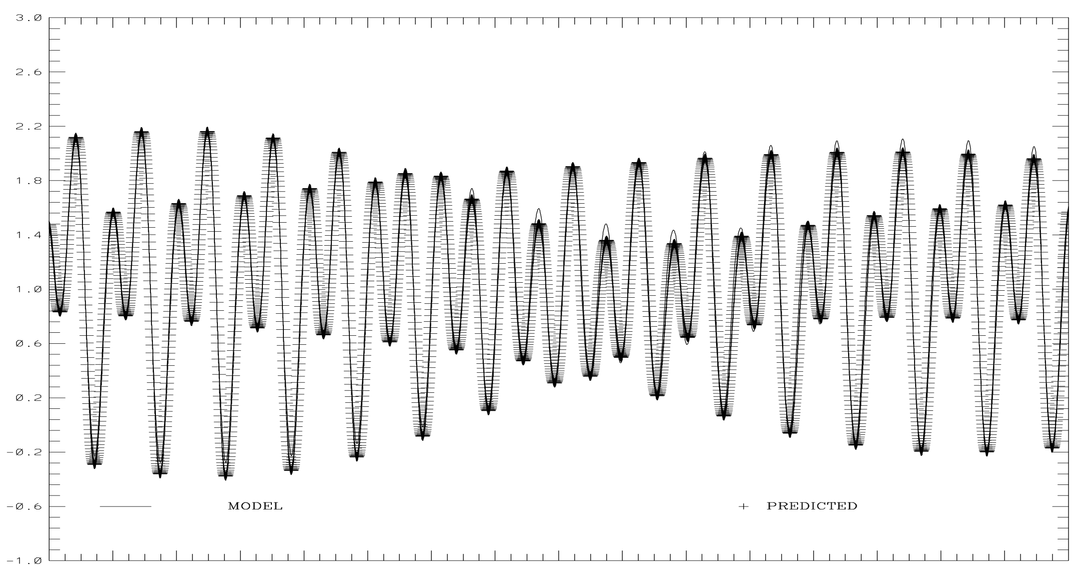

DISCLAIMER− TEST RESULTS NOT FOR OFFICIAL PURPOSES

TIME (JULIAN DAYS 1980)

Figure 3.40. January 15-31, 1980 Tidal Simulation: Point Reyes and Richmond Water Level Comparisons. Note IND AGRMT equals one minus Willmott et al. (1985) relative error.

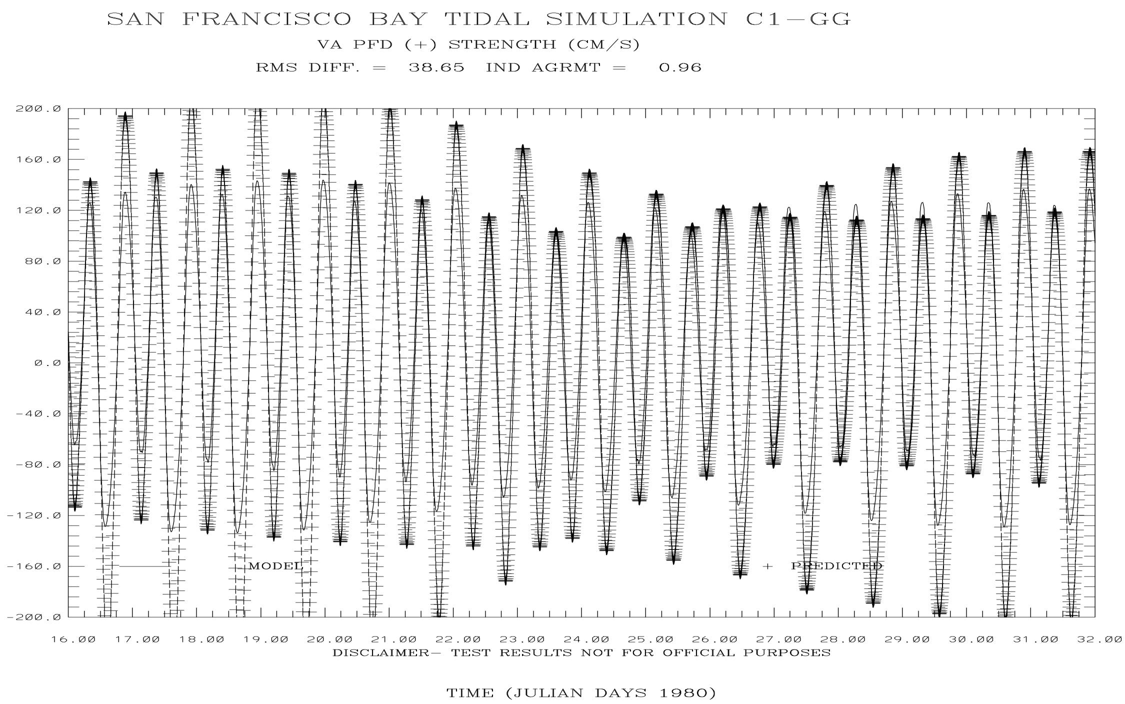

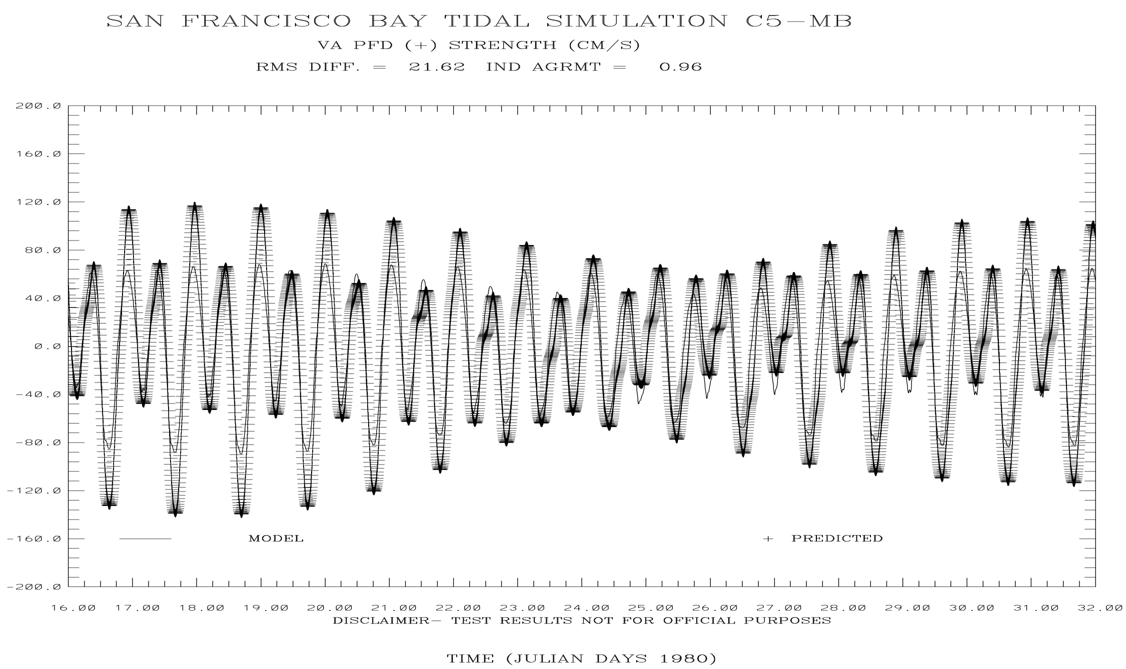

Figure 3.41. January 15-31, 1980 Tidal Simulation: C-1 and C-6 Vertically Integrated Principal Current Component Comparisons. Note IND AGRMT equals one minus Willmott et al. (1985) relative error.

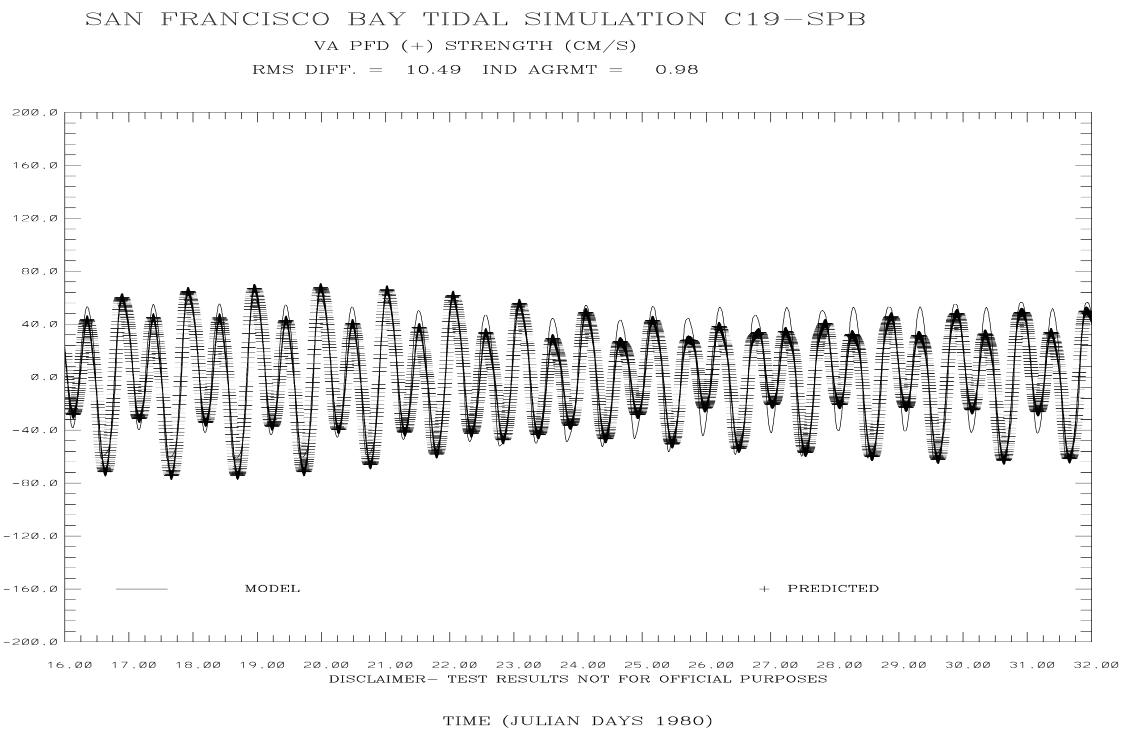

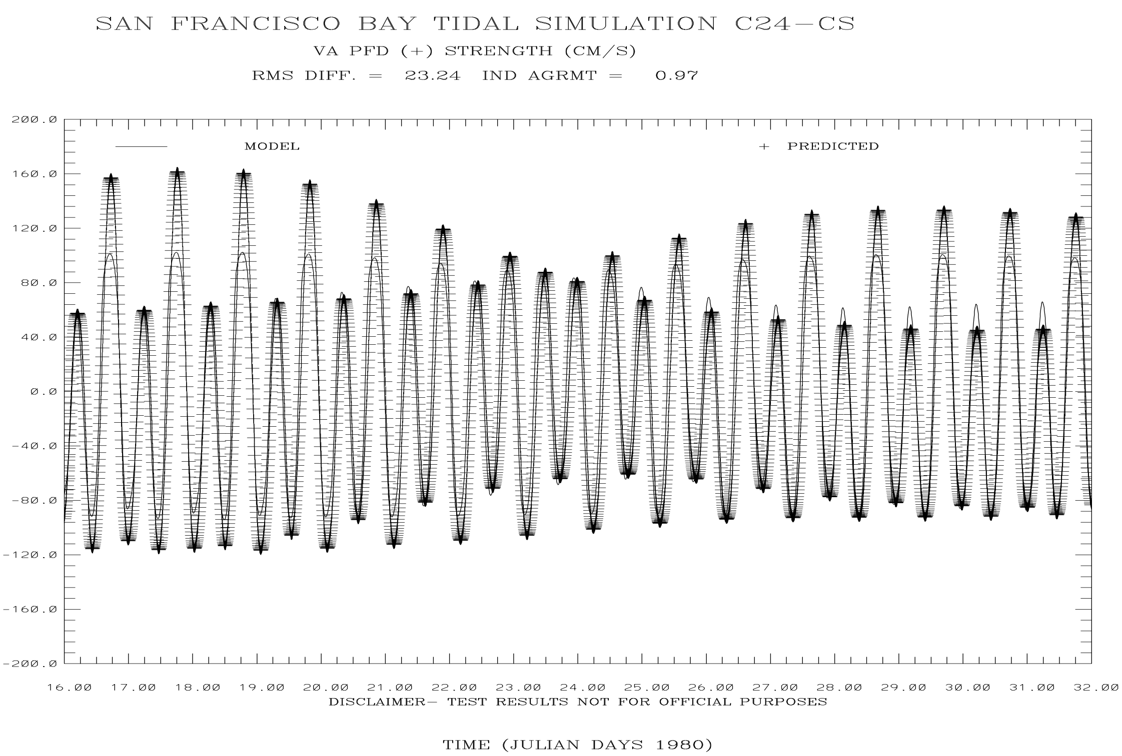

Figure 3.42. January 15-31, 1980 Tidal Simulation: C-19 and C-24 Vertically Integrated Principal Current Component Comparisons. Note IND AGRMT equals one minus Willmott et al. (1985) relative error.

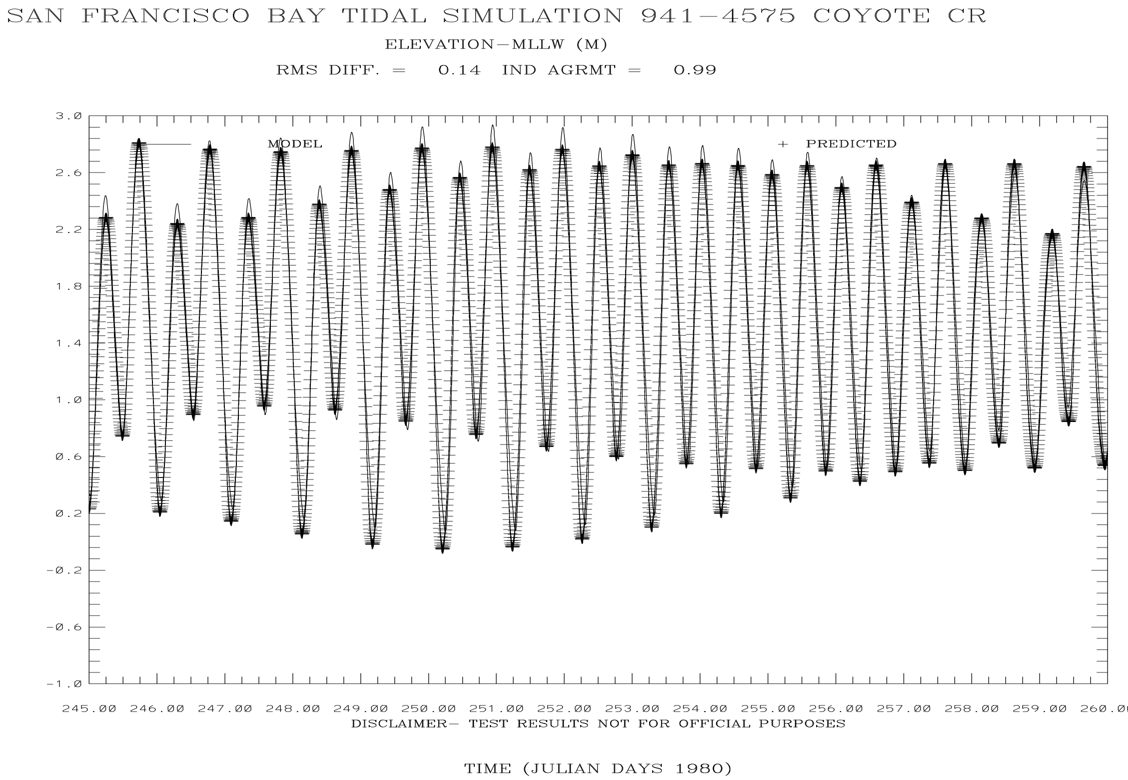

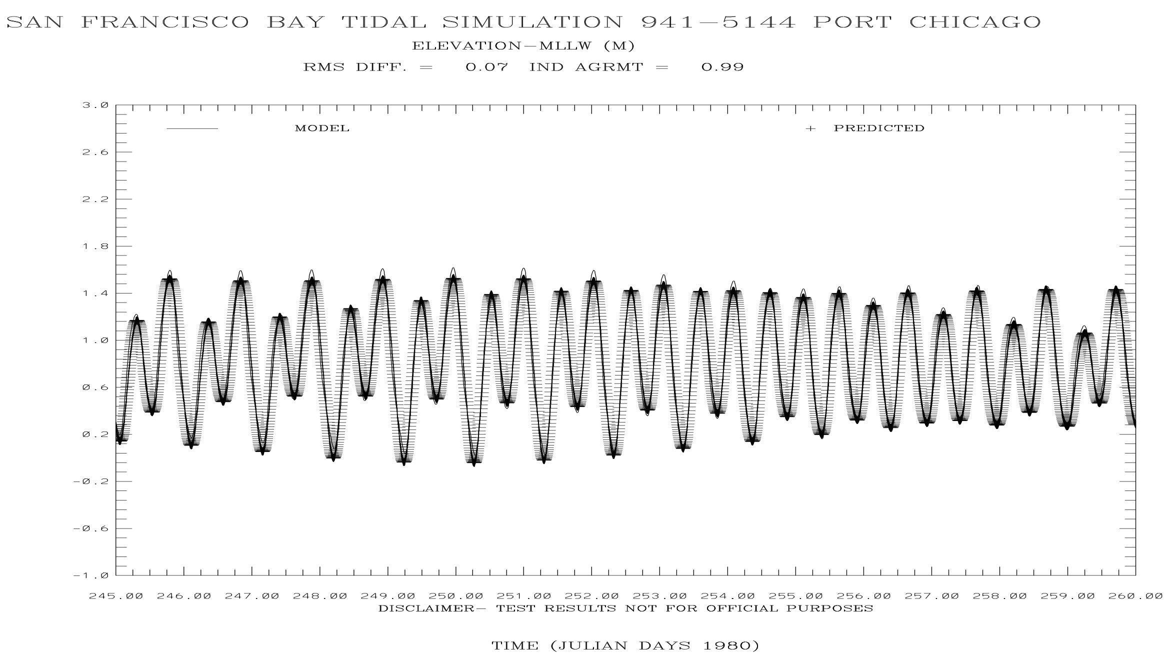

Figure 3.43. September 1-15, 1980 Tidal Simulation: Coyote Creek and Port Chicago Water Level Comparisons. Note IND AGRMT equals one minus Willmott et al. (1985) relative error.

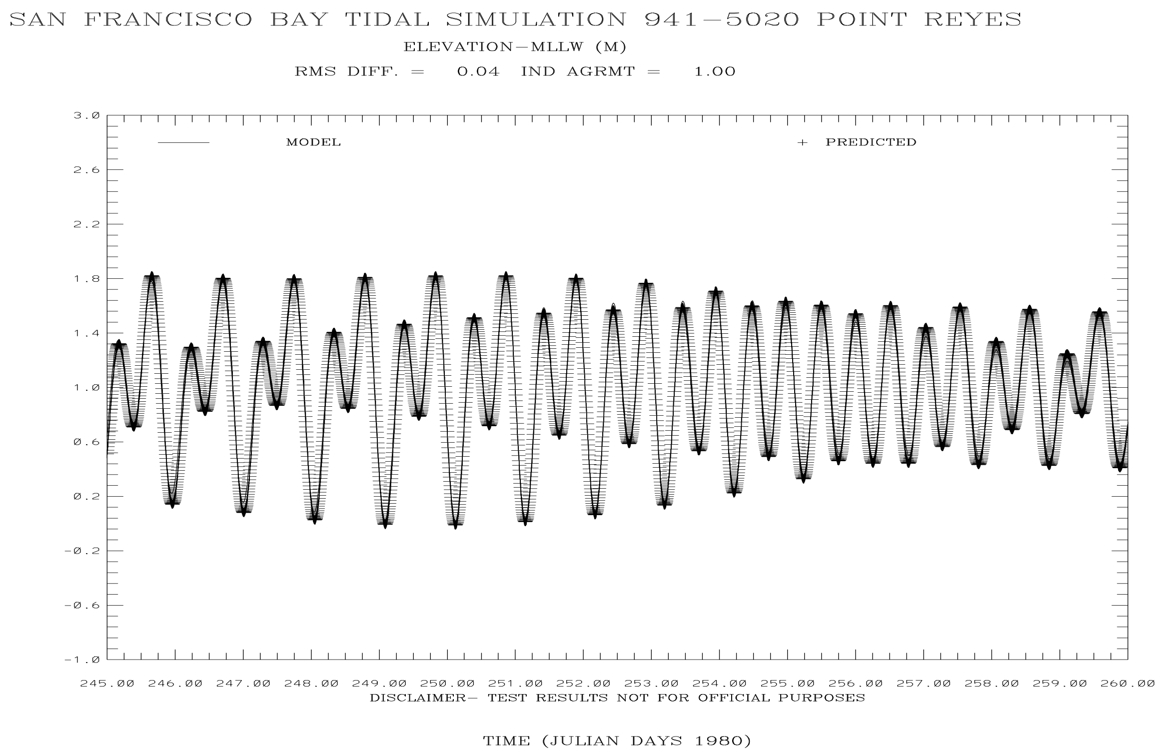

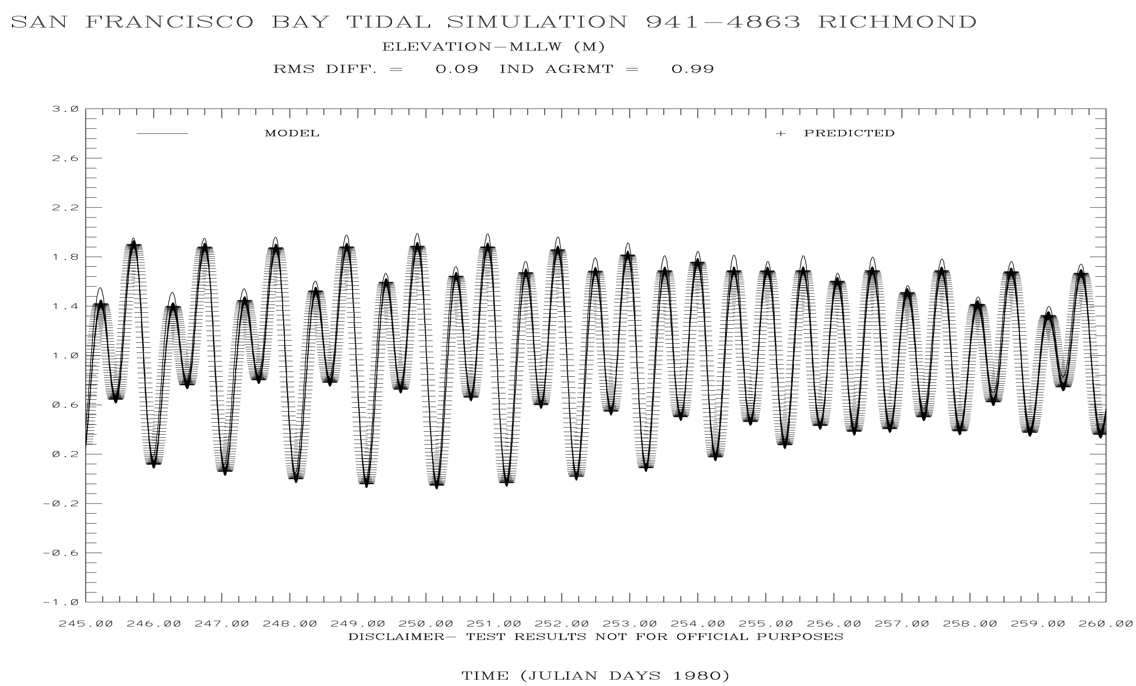

Figure 3.44. September 1-15, 1980 Tidal Simulation: Point Reyes and Richmond Water Level Comparisons. Note IND AGRMT equals one minus Willmott et al. (1985) relative error.

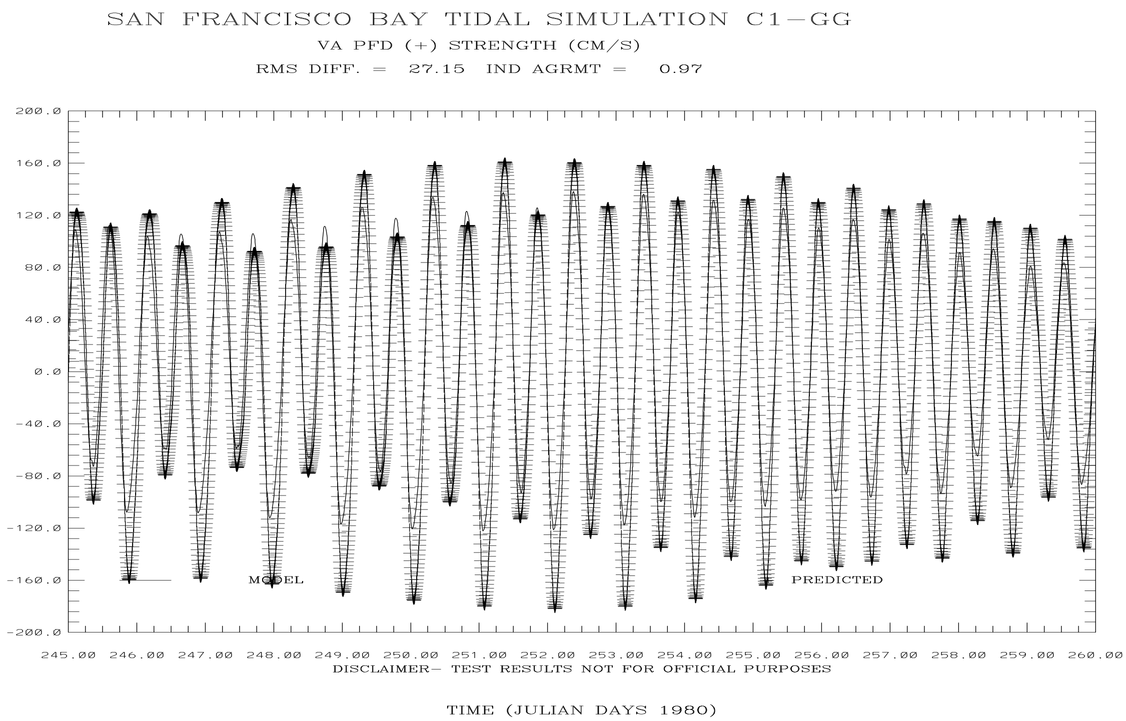

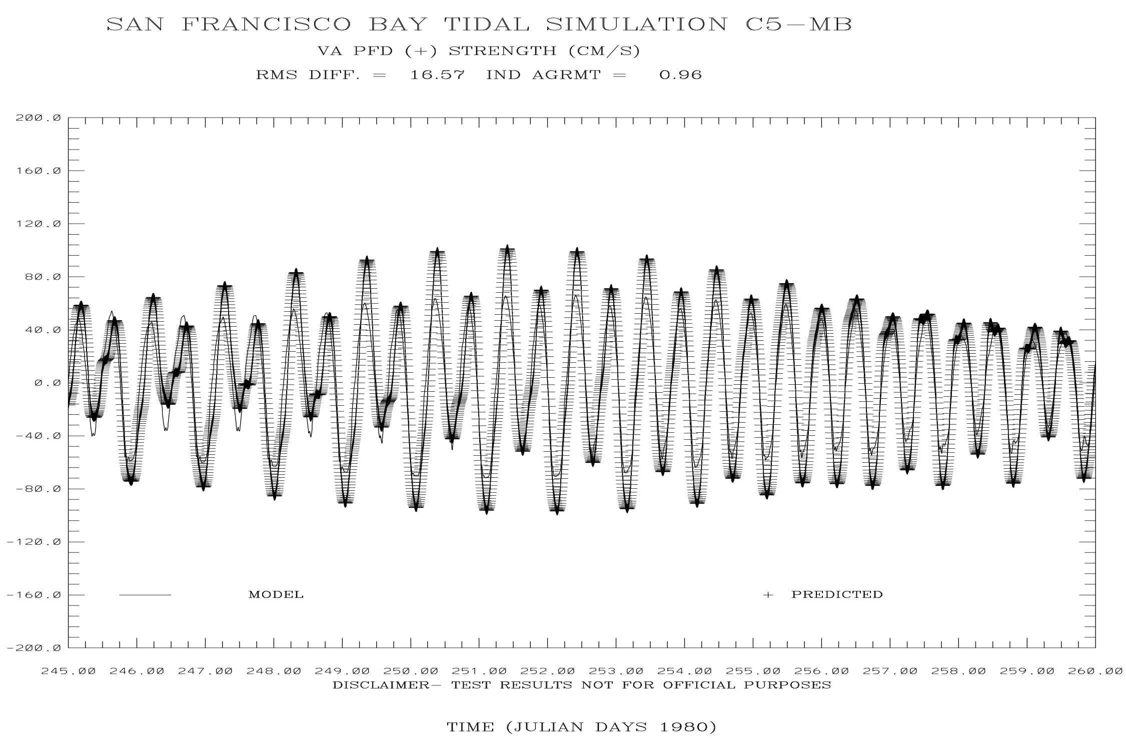

Figure 3.45. September 1-15, 1980 Tidal Simulation: C-1 and C-6 Vertically Integrated Principal Current Component Comparisons. Note IND AGRMT equals one minus Willmott et al. (1985) relative error.

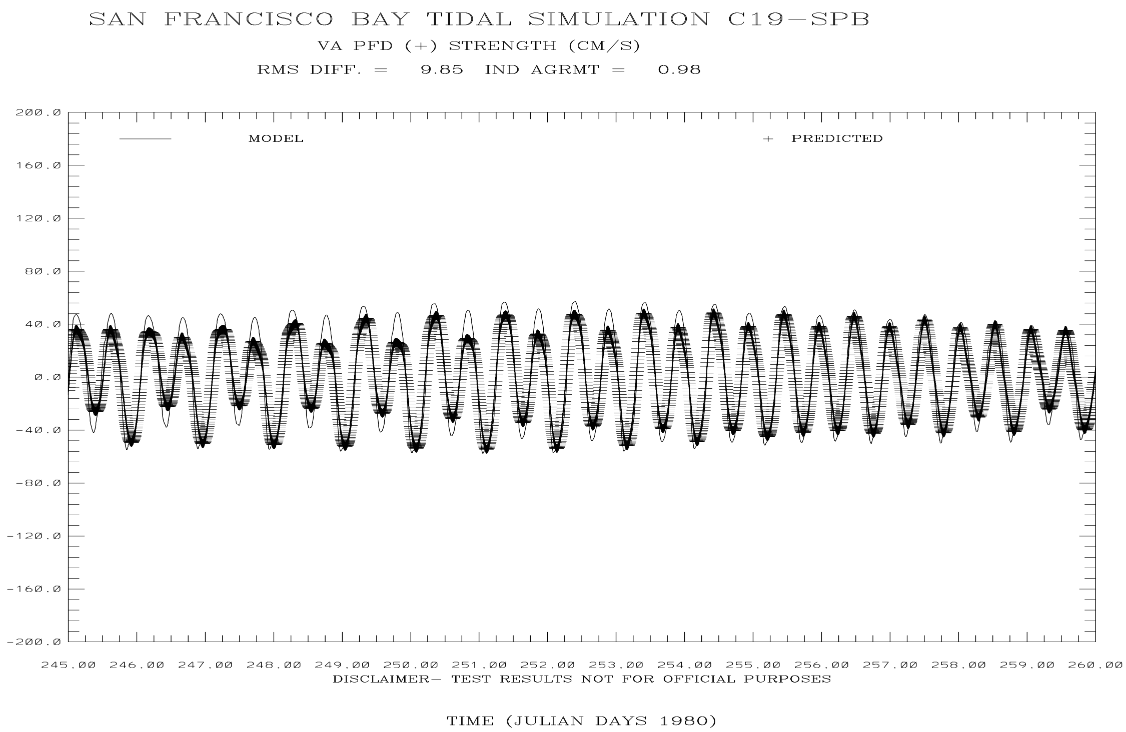

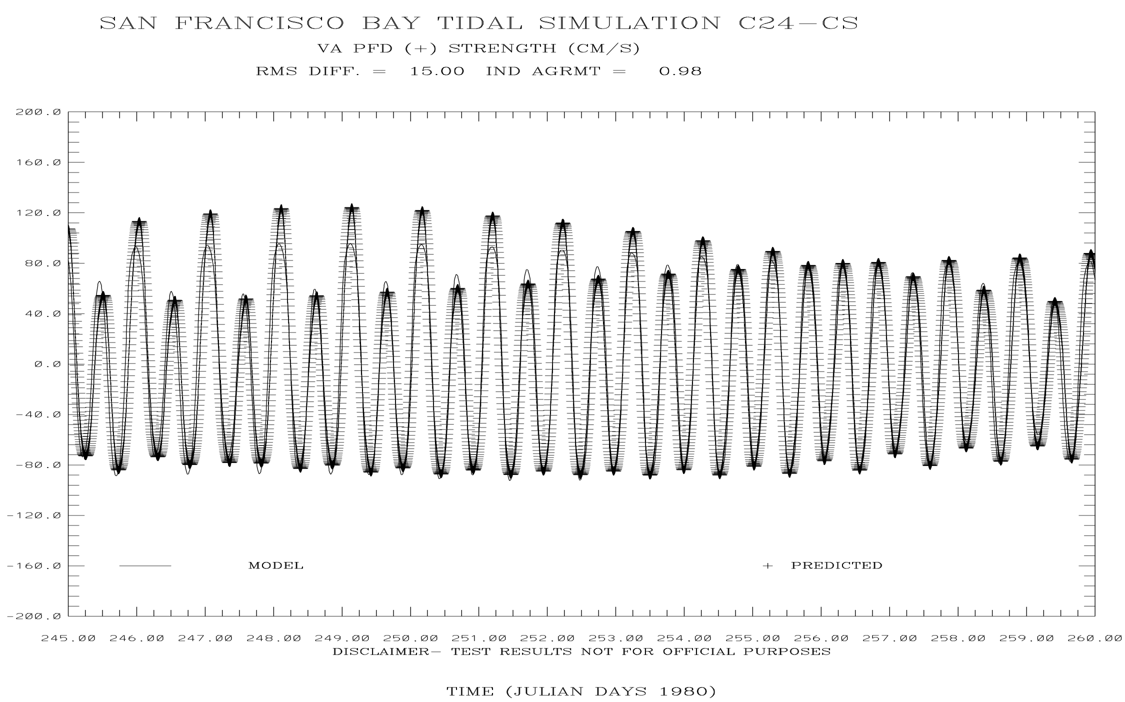

Figure 3.46. September 1-15, 1980 Tidal Simulation: C-19 and C-24 Vertically Integrated Principal Current Component Comparisons. Note IND AGRMT equals one minus Willmott et al. (1985) relative error.

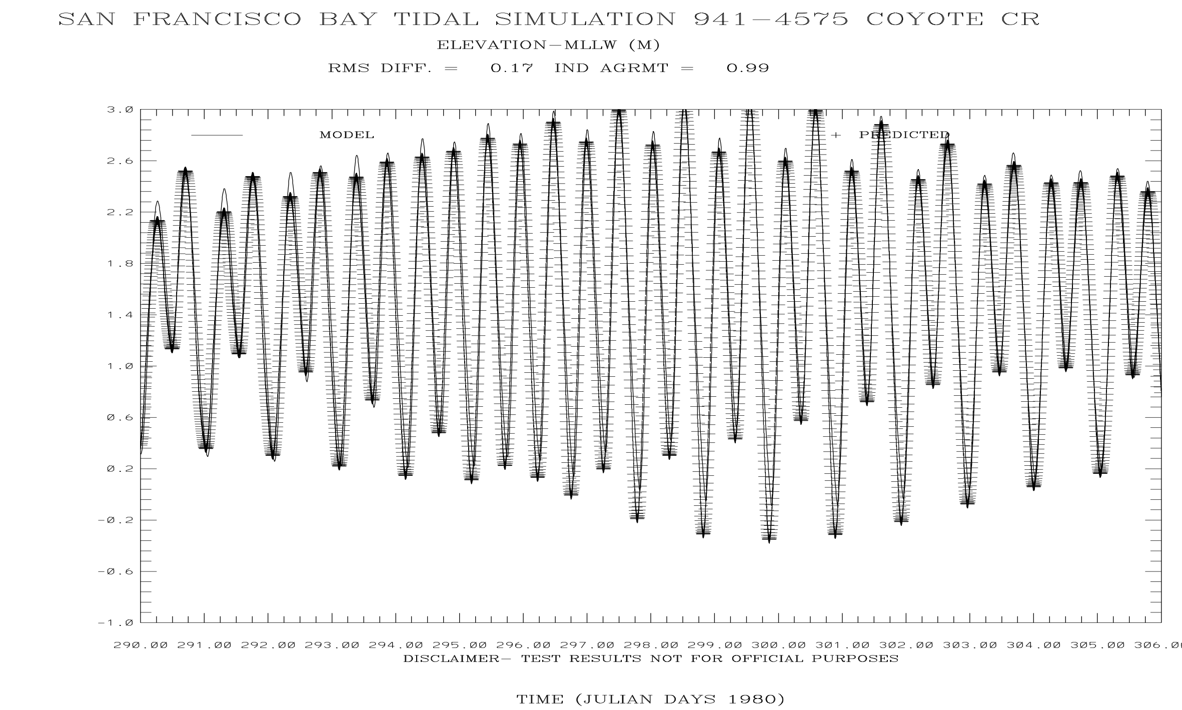

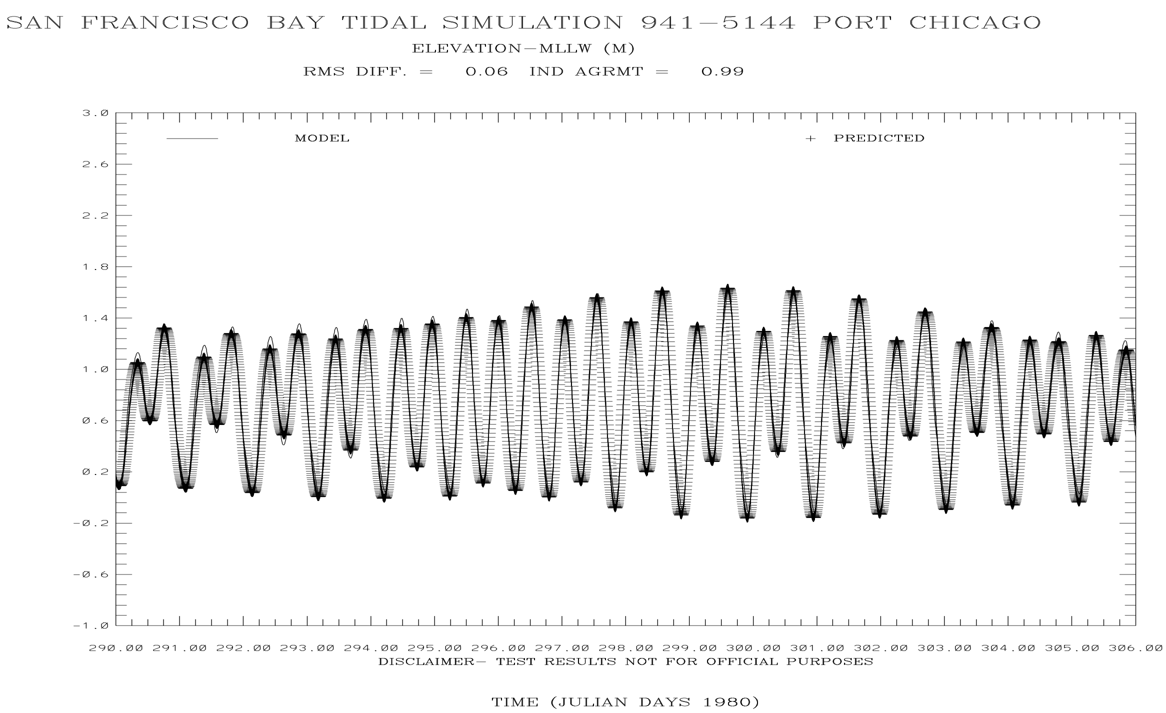

Figure 3.47. October 15-31, 1980 Tidal Simulation: Coyote Creek and Port Chicago Water Level Comparisons. Note IND AGRMT equals one minus Willmott et al. (1985) relative error.

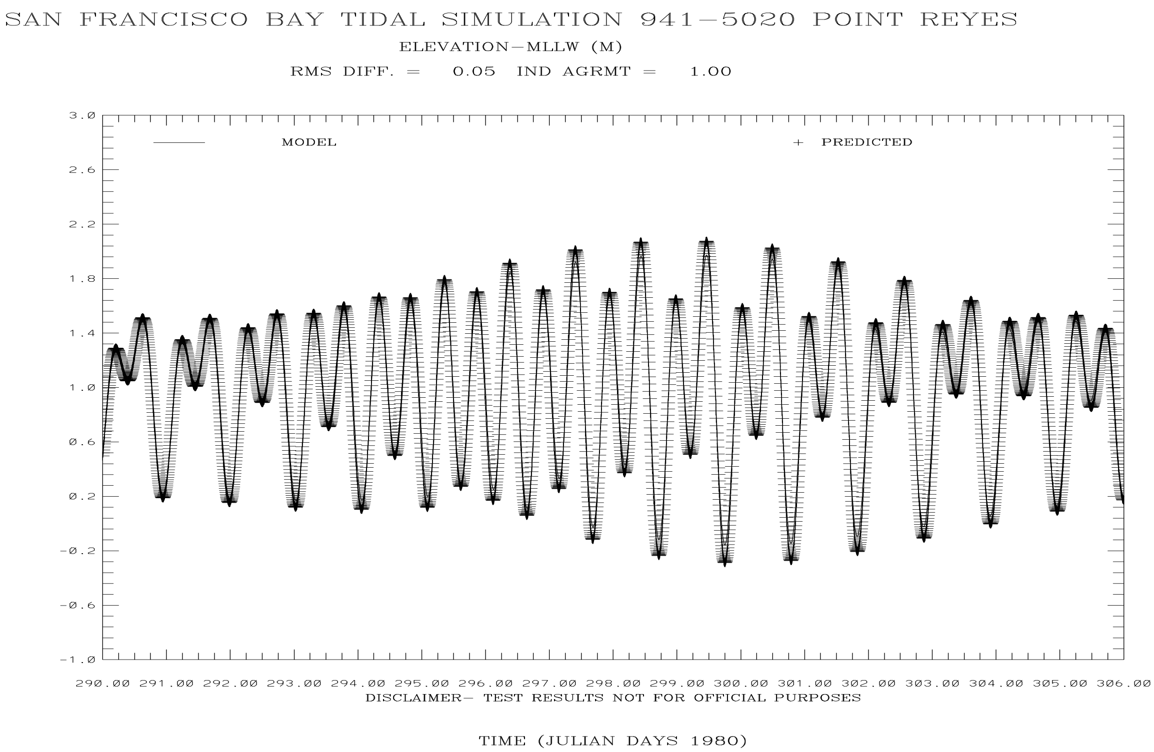

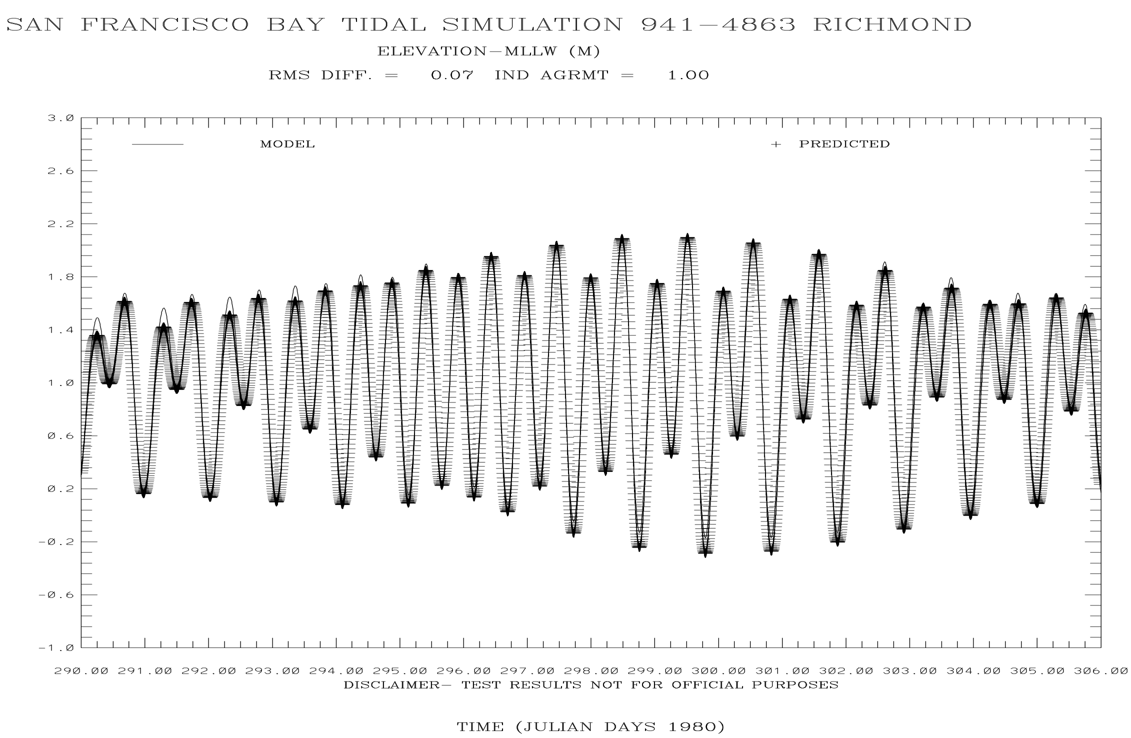

Figure 3.48. October 15-31, 1980 Tidal Simulation: Point Reyes and Richmond Water Level Comparisons. Note IND AGRMT equals one minus Willmott et al. (1985) relative error.

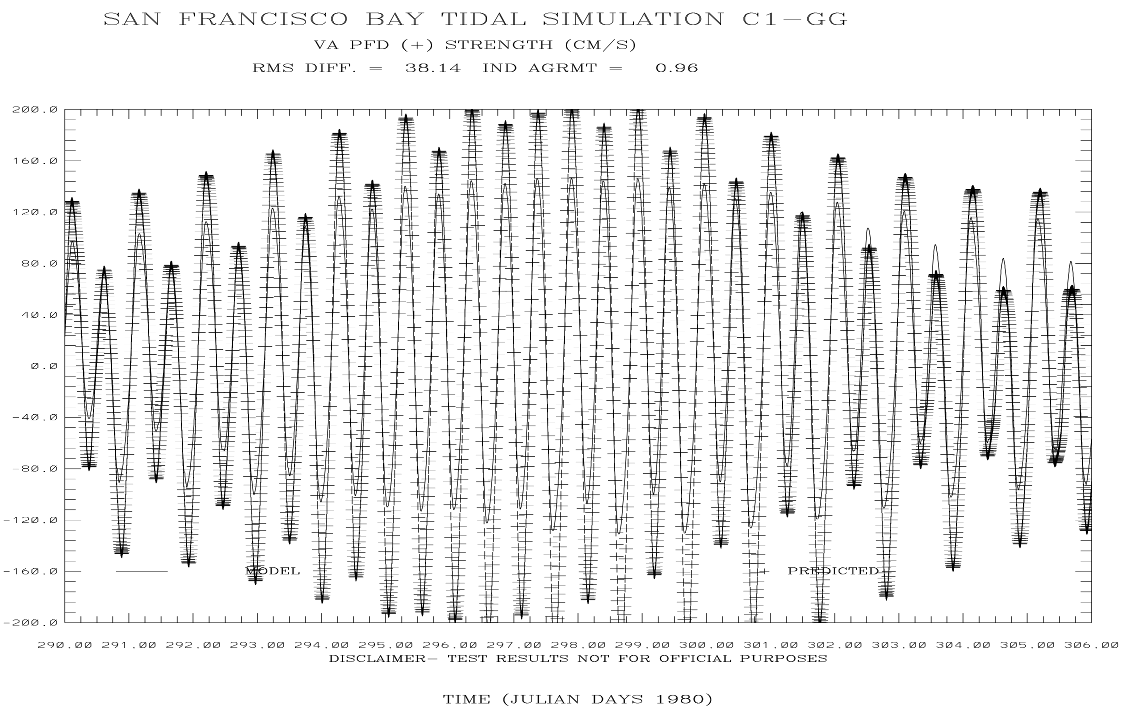

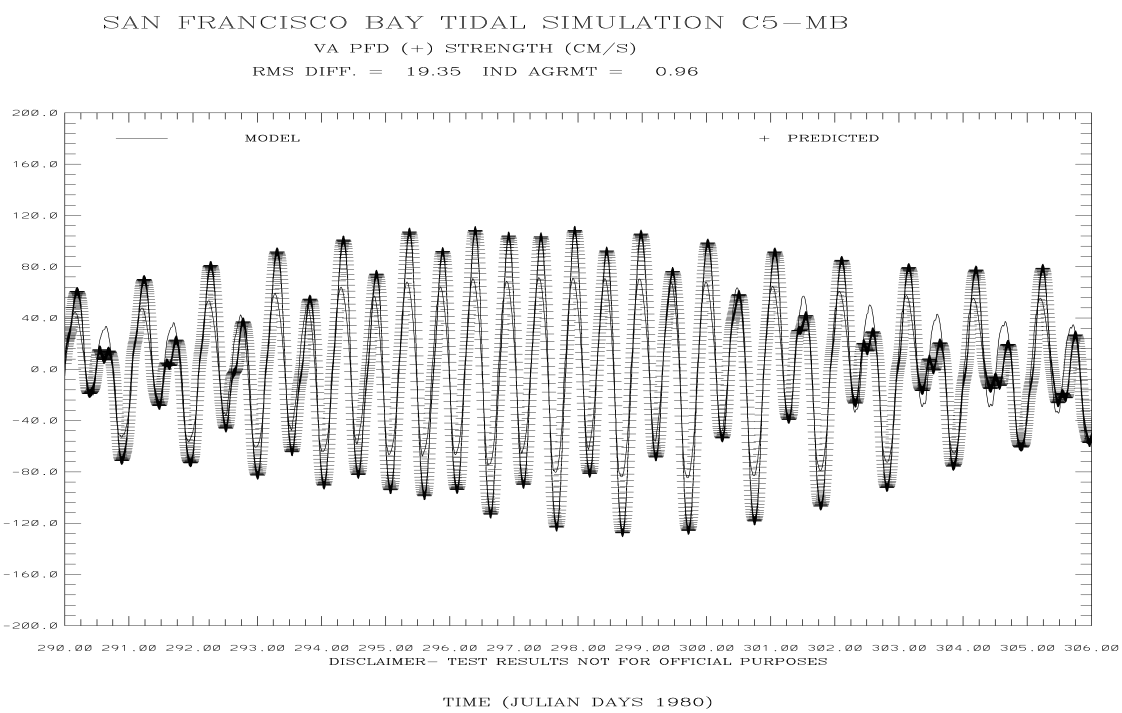

Figure 3.49. October 15-31, 1980 Tidal Simulation: C-1 and C-6 Vertically Integrated Principal Current Component Comparisons. Note IND AGRMT equals one minus Willmott et al. (1985) relative error.

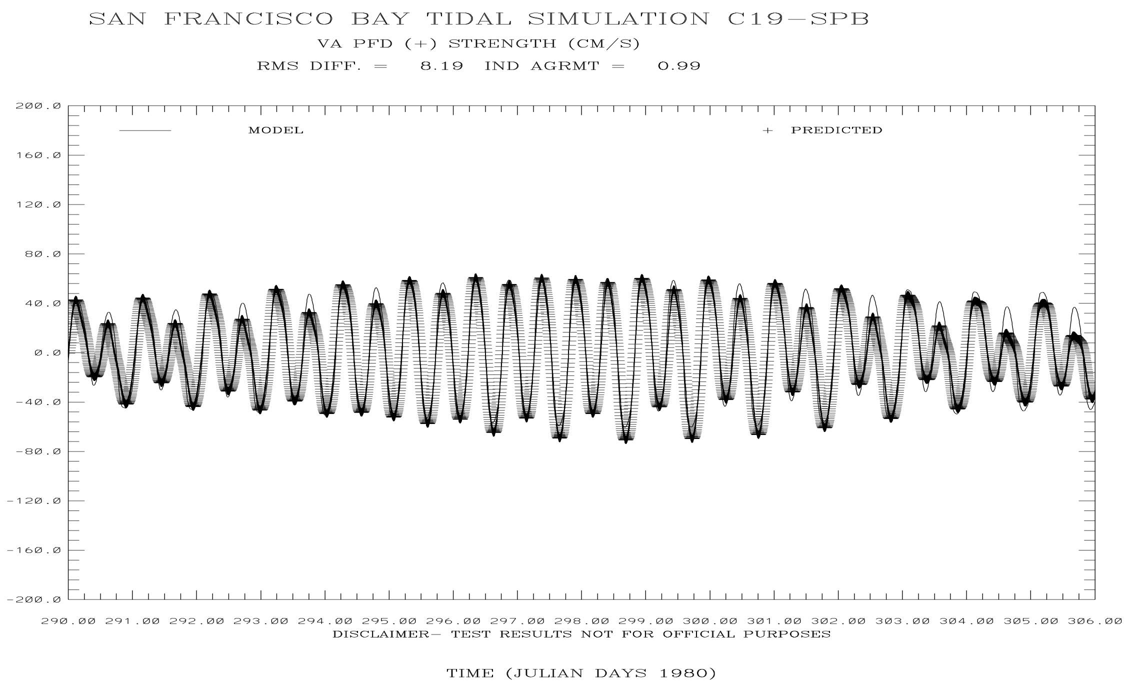

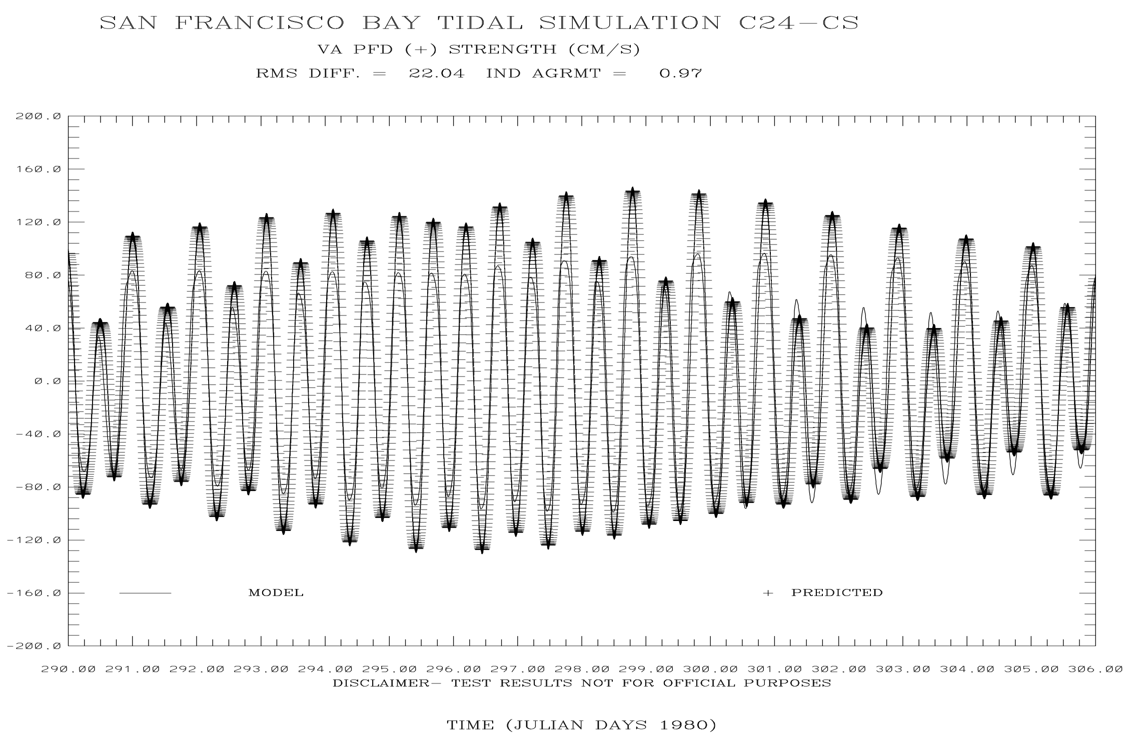

Figure 3.50. October 15-31, 1980 Tidal Simulation: C-19 and C-24 Vertically Integrated Principal Current Component Comparisons. Note IND AGRMT equals one minus Willmott et al. (1985) relative error.

3.6 Summary and Discussion

Work was presented for the initial April 1-15, 1979 simulation, which used the 6 hour NARR heat flux fields with no reduction in shallow water. The water surface response at Port Chicago was over predicted resulting in an RMS error of order 20 cm using the Delta flow boundary condition. In addition, a water level spike near Julian Day 96 was excited from the reflection at the open boundary.

During the April-May 1979 and September-October 1980 tidal simulations, the use of the 3 hour NARR fields with a reduction of the heat fluxes in shallow water did not produce an adverse impact on seasonal heating and cooling. However with the Delta flow boundary condition the water level response at Port Chicago was not improved. A revised sponge layer treatment at the open ocean boundary eliminated the water level spike near Julian Day 96 and no subsequent spikes were generated.

Additional experiments over the period 1-15 April 1979 in which the bottom friction above Carquinez Strait was increased exhibited some improvement, but the errors were above the 15 cm NOS error target. Utilizing the tidal stage boundary conditions at the Delta inflow locations (with a 22 cm water level offset at Rio Vista on the Sacramento River and a 20 cm water level offset at Antioch on the San Joaquin River) the water level response at Port Chicago was in close agreement with tidal predictions with an RMS error under 10 cm.

As a result, this Delta stage boundary condition and set of water level offsets were used for an extended 19-month simulation from April 1979 through October 1980. For this extended simulation a nudging to climatological salinity and temperature was used for the offshore boundary condition. Water level RMS errors were consistent from month to month and were below 15 cm at the majority of the stations. Principal component current strengths were in close agreement with predictions with RMS errors less than 35 cm/s at the majority of the stations.

Despite the inclusion of the meteorological effects, the salinity was overestimated in the northern portion of San Pablo Bay and throughout Suisun Bay. Due to the fact that the offsets were held constant and did not reflect the increased levels during the high flow months, the amount of freshwater entering the Bay through the Delta was limited.

The temperature response exhibited a normal seasonal response, but at the end of the simulation in October 1980 there was some evidence of overheating by about 2 ^{o}C in the shallow water areas in Suisun Bay even with the inclusion of the surface wind forcings.

4. HINDCAST VALIDATION

Here, we first present in Section 4.1, the results of the two-month hindcast for April – May 1979. In Section 4.2, the results of the September – October 1980 hindcast are discussed. The intent is to consider two different tidal and heating/cooling regimes. These two hindcasts were completed prior to the improved Delta stage boundary condition and thus used the Delta flow specification. Using the improved Delta stage boundary condition, an extended 19-month simulation was performed over the period April 1979 – October 1980 with the results presented in Section 4.3.

It should be noted that the NARR three-hourly winds and sea level atmospheric pressure fields are interpolated to the model grid and used to provide the surface forcings. In addition, three-hourly NARR downward short wave radiation, relative humidity, and air temperature fields are used to calculate the surface heat fluxes. A reduction of the fluxes to zero is used for all stilled water depths less than 10m. It should be noted that in Sections 4.1 and 4.2 comparisons of the NARR winds and atmospheric pressure are made at San Francisco International Airport. In general RMS wind speed errors are less than 5 m/s with direction RMS errors of order 50 degrees. For sea level atmospheric pressure, the RMS errors are near 2 mb. The water level residual at Point Reyes is small relative to the tidal amplitude and is less than 20 cm. River inflow from the Delta into San Francisco Bay ranged from 30,000 to 40,000 cfs.

Finally, in Section 4.4, we summarize results and discuss additional considerations with respect to the simulation of the combined river inflow, meteorological forcing, and tidal dynamics.

4.1 April – May 1979 Simulation

Results are presented in 15 day increments in Table 4..1 for water surface elevation, in Table 4.2 and 4.3 for current speed and direction, in Table 4.4 for salinity, and in Table 4.5 for temperature. The NARR atmospheric forcings are compared with meteorological data at San Francisco International Airport in Table 4.6 for wind speed, wind direction and sea level atmospheric pressure. Note the observed winds have not been corrected to 10 m and are stronger than the NARR sea level winds. Wind directions are in general agreement as are the NARR atmospheric pressure values. In general, there are fewer stations available with measured data for comparison than for the tidal simulation. For the offshore temperature and salinity a zero gradient boundary condition is used.

Water levels at Port Chicago and Point Reyes are shown in Figures 4.1 and 4.14 and at San Francisco and at the San Mateo Bridge in Figures 4.2 and 4.15.

Current speed and direction are shown at Station C-1 (Golden Gate Bridge) in Figures 4.3 and 4.16, at Station C-18 (mid-Bay) in Figures 4.4 and 4.17, at Station C-19 (San Pablo Bay) in Figures 4.5 and 4.18, and at C-24 (Carquinez Strait) in Figures 4.6 and 4.19.

Salinity is shown at Stations C-1 (Golden Gate Bridge) and C-18 (mid-Bay) in Figures 4.7 and 4.20 and at Stations C-22 (San Pablo Bay) and C-24 (Carquinez Strait) in Figures 4.8 and 4.21.

Temperature is shown at Stations C-1 (Golden Gate Bridge) and C-18 (mid-Bay) in Figures 4.9 and 4.22 and at Stations C-22 (San Pablo Bay) and C-24 (Carquinez Strait) in Figures 4.10 and 4.23.

Wind speed and direction at San Francisco International Airport are shown in Figures 4.11 and 4.24. Sea level atmospheric pressure at San Francisco International Airport and water level residual at Point Reyes are shown in Figures 4.12 and 4.25, respectively.

Flows on the Sacramento River at Rio Vista, CA and on the San Joaquin River at Antioch, CA are shown in Figures 4.13 and 4.26, respectively.

We briefly characterize each simulation month in turn.

April 1979: There are datum issues associated with the observed water levels at San Francisco and at San Mateo Bridge. At Point Reyes the RMS error in water level is 7 cm with a Willmott relative error of 0.01. At San Francisco the RMS error in water level is near 20 cm with a Willmott et al. (1985) relative error of 0.03 for the second simulation segment. For salinity, temperature, and currents, the model response is examined at Station C-1 at the Golden Gate Bridge, at Stations C-5, C-17, and C-18 in the mid-Bay, at Stations C-19 and C-22 in San Pablo Bay, and at C-24 and C-25 in Carquinez Strait. For the San Pablo Bay stations the RMS errors are order 3 PSU, while in Carquinez Strait the RMS errors are above 4.5 PSU. In this region, there are large horizontal salinity gradients and the model tends to be too fresh by order 3 PSU. Temperature comparisons are uniform throughout the Bay with RMS errors less than 1 ^{o}C. There are potential measurement issues at Stations C-20 and C-23. RMS errors in current speeds are near 26 cm/s. At Station C-1 at the Golden Gate Bridge near surface current strength is underestimated in the model by order 10 cm/s. Mean current directions are within 45 degrees, with similar or reduced RMS errors. In general, RMS wind speed errors are less than 5 m/s with direction RMS errors order 50 degrees. For sea level atmospheric pressure, the RMS errors are near 2 mb. The water level residual at Point Reyes is small relative to the tidal amplitude and is less than 20 cm. River inflow from the Delta into San Francisco Bay ranged from 30,000 to 40,000 cfs during the first simulation segment and was near zero during the second simulation segment.

May 1979: At Point Reyes, San Francisco, and San Mateo Bridge the RMS errors in water levels are near 5 cm with a Willmott et al. (1985) relative error of near zero. For salinity, temperature, and currents, the model response is examined at Station C-18 in the mid-Bay, at Stations C-28, C-29, C-30, C-31, and C-33 in Suisun Bay, and at C-24 in Carquinez Strait. For the Suisun Bay stations the RMS errors range from 0.5 to 6.0 PSU, while in Carquinez Strait the RMS errors are above 4.5 PSU. In this region, there are large horizontal salinity gradients and the model tends to be too fresh by order 3 PSU. Temperature comparisons are uniform throughout the Bay with RMS errors less than 1 ^{o}C. RMS errors in current speeds are near 26 cm/s at most stations. Mean current directions are within 45 degrees with similar or reduced RMS errors. In general, RMS wind speed errors are less than 5 m/s, with direction RMS errors order 70 degrees. For sea level atmospheric pressure, the RMS errors are less than 3 mb. The water level residual at Point Reyes is small relative to the tidal amplitude and is less than 20 cm. River inflow from the Delta into San Francisco Bay ranged from 8,000 to 12,000 cfs.

Table 4.1. Water Surface Elevation Hindcast Validation: April -May 1979. For each row in each month, the first entry corresponds to the first 15 days of the month, with the second entry denoting the remaining portion of the month. Row 1 corresponds to the RMSE in cm. Row 2 corresponds to the Willmott Relative Error in percent. Row 3 corresponds to the model mean in cm relative to station MLLW with row 4 denoting the observed water level mean in cm with respect to station MLLW. Bold italics indicate measurement errors and their associated model discrepancies. Note n/a denotes not applicable due to lack of measurements.

Station	Apr	May
Alameda 941-4750	7 n/a 1 n/a 94 93 n/a n/a	n/a n/a n/a n/a 92 99 n/a n/a
Dumbarton Bridge 941-4509	n/a n/a n/a n/a 130 129 n/a n/a	n/a n/a n/a n/a 128 134 n/a n/a
Oyster Point Marina 941-4392	n/a n/a n/a n/a 105 104 n/a n/a	n/a n/a n/a n/a 102 109 n/a n/a
Port Chicago 941-5144	n/a n/a n/a n/a 68 69 n/a n/a	n/a n/a n/a n/a 66 76 n/a n/a
Point Reyes 941-5020	7 6 1 0 81 81 80 79	5 7 0 0 79 86 78 85
San Francisco 941-4290	16 20 3 3 83 82 85 82	5 7 0 0 81 87 79 86
Pier 22.5 941-4317	n/a n/a n/a n/a 88 87 n/a n/a	n/a n/a n/a n/a 86 92 n/a n/a
San Mateo Bridge 941-4458	***303 146*** ***69 39*** 117 115 ***419 180***	6 8 0 0 113 120 110 117

Table 4.2. Current Speed Hindcast Validation: April – May 1979. For each row in each month, the first entry corresponds to the first 15 days of the month, with the second entry denoting the remaining portion. Row 1 corresponds to the RMSE in cm/s. Row 2 corresponds to the Willmott Relative Error in percent. Row 3 corresponds to the model mean in cm/s with row 4 denoting the observed mean current speed in cm/s. Note n/a denotes not applicable.

Station	Apr 1979	May 1979
C-1 (76) GG	n/a n/a n/a n/a n/a n/a n/a n/a	n/a n/a n/a n/a n/a n/a n/a n/a
C-1 (91) GG	37 n/a 24 n/a 67 80 80 n/a	n/a n/a n/a n/a 67 80 n/a n/a
C-5 (2) MB	31 n/a 51 n/a 35 38 29 n/a	n/a n/a n/a n/a 35 39 n/a n/a
C-5 (8) MB	35 n/a 44 n/a 48 52 34 n/a	n/a n/a n/a n/a 48 53 n/a n/a
C-5 (25) MB	29 n/a 38 n/a 47 55 35 n/a	n/a n/a n/a n/a 47 55 n/a n/a
C-17 (2) MB	12 n/a 14 n/a 35 40 33 n/a	n/a n/a n/a n/a 35 40 n/a n/a
C-17 (5) MB	21 n/a 19 n/a 45 52 49 n/a	n/a n/a n/a n/a 46 52 n/a n/a
C-18 (9) MB	17 13 8 4 64 67 68 63	n/a n/a n/a n/a 64 69 n/a n/a
C-18 (15) MB	20 19 7 6 77 85 75 74	22 n/a 10 n/a 77 84 55 n/a

Table 4.2 (Cont.). Current Speed Hindcast Validation April – May 1979. For each row in each month, the first entry corresponds to the first 15 days of the month, with the second entry denoting the remaining portion. Row 1 corresponds to the RMSE in cm/s. Row 2 corresponds to the Willmott Relative Error in percent. Row 3 corresponds to the model mean in cm/s with row 4 denoting the observed mean current speed in cm/s. Note n/a denotes not applicable.

Station	Apr 1979	May 1979
C-19 (1) SPB	10 n/a 21 n/a 26 29 23 n/a	n/a n/a n/a n/a 26 29 n/a n/a
C-20 (1) SPB	17 n/a 37 n/a 15 17 27 n/a	n/a n/a n/a n/a 15 16 n/a n/a
C-22 (2) SPB	17 n/a 22 n/a 41 47 29 n/a	n/a n/a n/a n/a 42 46 n/a n/a
C-23 (1) SPB	6 n/a 24 n/a 17 19 16 n/a	n/a n/a n/a n/a 17 19 n/a n/a
C-24 (2,6) CS	28 27 32 29 46 51 26 32	33 n/a 37 n/a 46 51 n/a n/a
C-24 (17,11) CS	37 30 23 16 82 90 81 80	44 n/a 37 n/a 83 91 n/a n/a
C-25 (2) CS	14 13 13 12 46 49 41 42	n/a n/a n/a n/a 44 49 n/a n/a
C-25 (8) CS	28 27 22 19 64 70 65 68	n/a n/a n/a n/a 65 71 n/a n/a
C-26 (2) SB	25 31 37 40 47 51 36 26	n/a n/a n/a n/a 47 51 n/a n/a

Table 4.3 Current Direction Hindcast Validation: April - May 1979. For each row in each month, the first entry corresponds to the first 15 days of the month, with the second entry denoting the remaining portion. Row 1 corresponds to the RMSE in degrees. Row 2 corresponds to the Willmott Relative Error in percent. Row 3 corresponds to the model mean in degrees with row 4 denoting the observed mean current direction in degrees. Note n/a denotes not applicable.

Station	Apr 1979	May 1979
C-1 (76) GG	n/a n/a n/a n/a n/a n/a n/a n/a	n/a n/a n/a n/a n/a n/a n/a n/a
C-1 (91) GG	37 n/a 4 n/a 177 182 152 n/a	n/a n/a n/a n/a 178 185 n/a n/a
C-5 (2) MB	51 n/a 7 n/a 123 117 162 n/a	n/a n/a n/a n/a 123 117 n/a n/a
C-5 (8) MB	44 n/a 6 n/a 119 121 145 n/a	n/a n/a n/a n/a 118 120 n/a n/a
C-5 (25) MB	35 n/a 5 n/a 131 n/a 146 n/a	n/a n/a n/a n/a 132 132 n/a n/a
C-17 (2) MB	20 n/a 1 n/a 247 245 227 n/a	n/a n/a n/a n/a 245 243 n/a n/a
C-17 (5) MB	21 n/a 1 n/a 233 235 243 n/a	n/a n/a n/a n/a 230 232 n/a n/a
C-18 (9) MB	12 11 0 0 99 101 101 97	n/a n/a n/a n/a 100 101 n/a n/a
C-18 (15) MB	19 12 1 0 117 122 13 118	22 n/a 10 n/a 122 122 126 n/a

Table 4.3 (Cont.). Current Direction Hindcast Validation April – May 1979. For each row in each month, the first entry corresponds to the first 15 days of the month, with the second entry denoting the remaining portion. Row 1 corresponds to the RMSE in degrees. Row 2 corresponds to the Willmott Relative Error in percent. Row 3 corresponds to the model mean in degrees with row 4 denoting the observed mean current direction in degrees. Note n/a denotes not applicable.

Station	Apr 1979	May 1979
C-19 (1) SPB	10 n/a 0 n/a 109 111 105 n/a	n/a n/a n/a n/a 110 107 n/a n/a
C-20 (1) SPB	13 n/a 1 n/a 185 181 172 n/a	n/a n/a n/a n/a 185 184 n/a n/a
C-22 (2) SPB	17 n/a 1 n/a 135 138 139 n/a	n/a n/a n/a n/a 135 137 n/a n/a
C-23 (1) SPB	25 n/a 4 n/a 146 147 80 n/a	n/a n/a n/a n/a 146 147 n/a n/a
C-24 (2,6) CS	23 24 2 2 180 179 181 175	33 n/a 37 n/a 177 180 n/a n/a
C-24 (17,11) CS	39 26 5 2 200 198 197 197	44 n/a 37 n/a 200 199 208 n/a
C-25 (2) CS	10 11 0 0 149 146 141 132	n/a n/a n/a n/a 144 148 n/a n/a
C-25 (8) CS	25 17 2 1 151 150 164 157	n/a n/a n/a n/a 149 150 n/a n/a
C-26 (2) SB	21 13 1 1 158 157 152 127	n/a n/a n/a n/a 157 158 n/a n/a

Table 4.4 Salinity Hindcast Validation: April – May 1979. For each row in each month, the first entry corresponds to the first 15 days of the month, with the second entry denoting the remaining portion. Row 1 corresponds to the RMSE in PSU. Row 2 corresponds to the Willmott Relative Error in percent. Row 3 corresponds to the model mean in PSU with row 4 denoting the observed salinity mean in PSU. Note n/a denotes not applicable.

Station	Apr 1979	May 1979
C-1 (46) GG	1 3 34 39 30 30 31 32	n/a n/a n/a n/a 30 30 n/a n/a
C-1 (91,76) GG	2 2 40 43 29 29 30 31	n/a n/a n/a n/a 29 29 n/a n/a
C-5 (2) MB	1 n/a 35 n/a 29 29 30 n/a	n/a n/a n/a n/a 30 29 n/a n/a
C-5 (8) MB	1 n/a 35 n/a 29 29 29 n/a	n/a n/a n/a n/a 30 29 n/a n/a
C-5 (25) MB	2 n/a 20 n/a 29 29 28 n/a	n/a n/a n/a n/a 29 29 n/a n/a
C-17 (2) MB	2 n/a 12 n/a 26 27 26 n/a	n/a n/a n/a n/a 27 27 n/a n/a
C-17 (5) MB	2 n/a 12 n/a 26 26 25 n/a	n/a n/a n/a n/a 27 26 n/a n/a
C-18 (9) MB	1 2 10 16 24 24 25 26	2 2 32 32 25 24 27 27
C-18 (15) MB	1 2 6 9 23 23 22 25	2 2 16 16 24 23 25 25

Table 4.4 (Cont.). Salinity Hindcast Validation April – May 1979. For each row in each month, the first entry corresponds to the first 15 days of the month, with the second entry denoting the remaining portion. Row 1 corresponds to the RMSE in PSU. Row 2 corresponds to the Willmott Relative Error in percent. Row 3 corresponds to the model mean in PSU with row 4 denoting the observed salinity mean in PSU. Note n/a denotes not applicable.

Station	Apr 1979	May 1979
C-19 (1) SPB	2 n/a 17 n/a 19 20 18 n/a	n/a n/a n/a n/a 20 20 n/a n/a
C-20 (1) SPB	n/a n/a n/a n/a 17 13 n/a n/a	n/a n/a n/a n/a 12 12 n/a n/a
C-22 (2) SPB	3 n/a 32 n/a 20 21 22 n/a	n/a n/a n/a n/a 21 21 n/a n/a
C-23 (1) SPB	n/a n/a n/a n/a 12 14 n/a n/a	n/a n/a n/a n/a 14 14 n/a n/a
C-24 (2,6) CS	7 6 47 51 9 11 15 13	6 n/a 41 n/a 11 10 n/a n/a
C-24 (17,11) CS	5 6 43 39 7 10 11 14	5 n/a 33 n/a 10 9 14 n/a
C-25 (2) CS	n/a n/a n/a n/a 4 5 n/a n/a	n/a n/a n/a n/a 5 4 n/a n/a
C-25 (8) CS	5 6 36 35 4 5 7 10	n/a n/a n/a n/a 5 4 n/a n/a
C-26(2) SB	n/a n/a n/a n/a 2 2 n/a n/a	n/a n/a n/a n/a 2 2 n/a n/a

Table 4.5 Temperature Hindcast Validation: April - May 1979. For each row in each month, the first entry corresponds to the first 15 days of the month, with the second entry denoting the remaining portion. Row 1 corresponds to the RMSE in ^oC. Row 2 corresponds to the Willmott Relative Error in percent. Row 3 corresponds to the model mean in ^oC with row 4 denoting the observed temperature mean in ^oC. Note n/a denotes not applicable.

Station	Apr 1979	May 1979
C-1 (46,76) GG	1 2 59 61 13 13 12 12	n/a n/a n/a n/a 13 14 n/a n/a
C-1 (91) GG	1 2 58 62 13 13 12 12	n/a n/a n/a n/a 14 15 n/a n/a
C-5 (2) MB	1 n/a 63 n/a 13 13 12 n/a	n/a n/a n/a n/a 14 15 n/a n/a
C-5 (8) MB	1 n/a 60 n/a 13 13 12 n/a	n/a n/a n/a n/a 14 15 n/a n/a
C-5 (25) MB	0 n/a 41 n/a 13 13 13 n/a	n/a n/a n/a n/a 14 15 n/a n/a
C-17 (2) MB	0 n/a 33 n/a 13 14 13 n/a	n/a n/a n/a n/a 14 15 n/a n/a
C-17 (5) MB	0 n/a 23 n/a 13 14 13 n/a	n/a n/a n/a n/a 14 15 n/a n/a
C-18 (9) MB	0 1 22 31 13 14 13 13	0 n/a 19 n/a 15 16 14 n/a
C-18 (15) MB	0 1 27 26 14 14 14 14	0 n/a 18 n/a 15 16 15 n/a

Table 4.5 (Cont.). Temperature Hindcast Validation April – May 1979. For each row in each month, the first entry corresponds to the first 15 days of the month, with the second entry denoting the remaining portion. Row 1 corresponds to the RMSE in ^{o}C. Row 2 corresponds to the Willmott Relative Error in percent. Row 3 corresponds to the model mean in ^{o}C with row 4 denoting the observed temperature mean in ^{o}C. Bold italics indicate measurement errors and their associated model discrepancies. Note n/a denotes not applicable.

Station	Apr 1979	May 1979
C-19 (1) SPB	0 n/a 37 n/a 14 14 14 n/a	n/a n/a n/a n/a 15 16 n/a n/a
C-20 (1) SPB	4 n/a 59 n/a 13 14 17 n/a	n/a n/a n/a n/a 14 15 n/a n/a
C-22 (2) SPB	0 n/a 20 n/a 14 14 13 n/a	n/a n/a n/a n/a 15 16 n/a n/a
C-23 (1) SPB	***11*** n/a ***93*** n/a 14 15 ***3*** n/a	n/a n/a n/a n/a 16 17 n/a n/a
C-24 (2,6) CS	1 1 35 49 15 15 14 14	0 n/a 46 n/a 16 17 n/a n/a
C-24 (17,11) CS	0 0 27 38 15 15 15 15	0 n/a 58 n/a 16 17 16 n/a
C-25 (2) CS	1 1 58 63 15 16 15 15	n/a n/a n/a n/a 16 18 n/a n/a
C-25 (8) CS	0 1 51 60 15 16 15 15	n/a n/a n/a n/a 16 18 n/a n/a
C-26 (2) SB	1 1 55 57 15 16 15 15	n/a n/a n/a n/a 17 18 n/a n/a

Table 4.6 NARR Atmospheric Forcings April – May 1979 at San Francisco International Airport. In each cell, row 1 corresponds to the RMSE, row 2 corresponds to the Willmott Relative Error, row 3 corresponds to the NARR model mean, and row 4 denotes the observed mean.

Parameter	1-15 April	15-30 April	1-15 May	15-31 May
Wind Speed (m/s)	5 50 4 7	4 50 3 6	4 53 4 6	5 57 3 6
Wind Direction (^{o}T)	53 61 115 116	60 18 133 120	46 42 106 111	67 41 111 110
Atmospheric Pressure (mb)	2 13 1019 1019	1 6 1018 1018	1 6 1017 1016	1 8 1015 1014

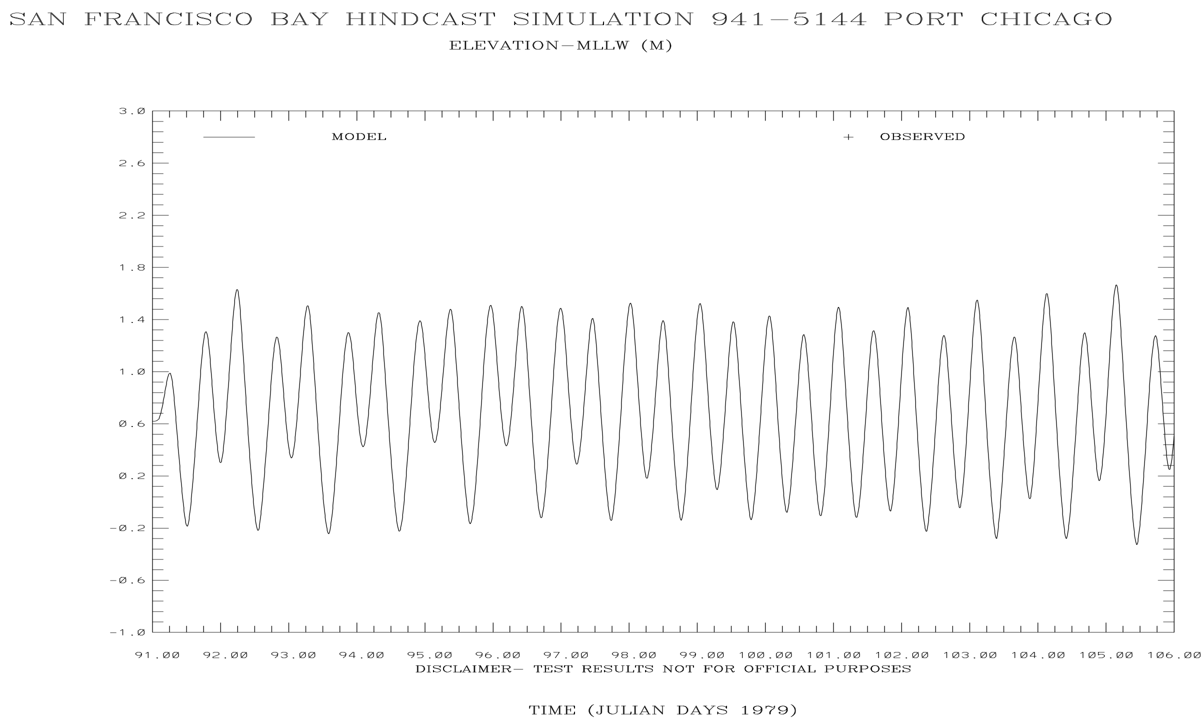

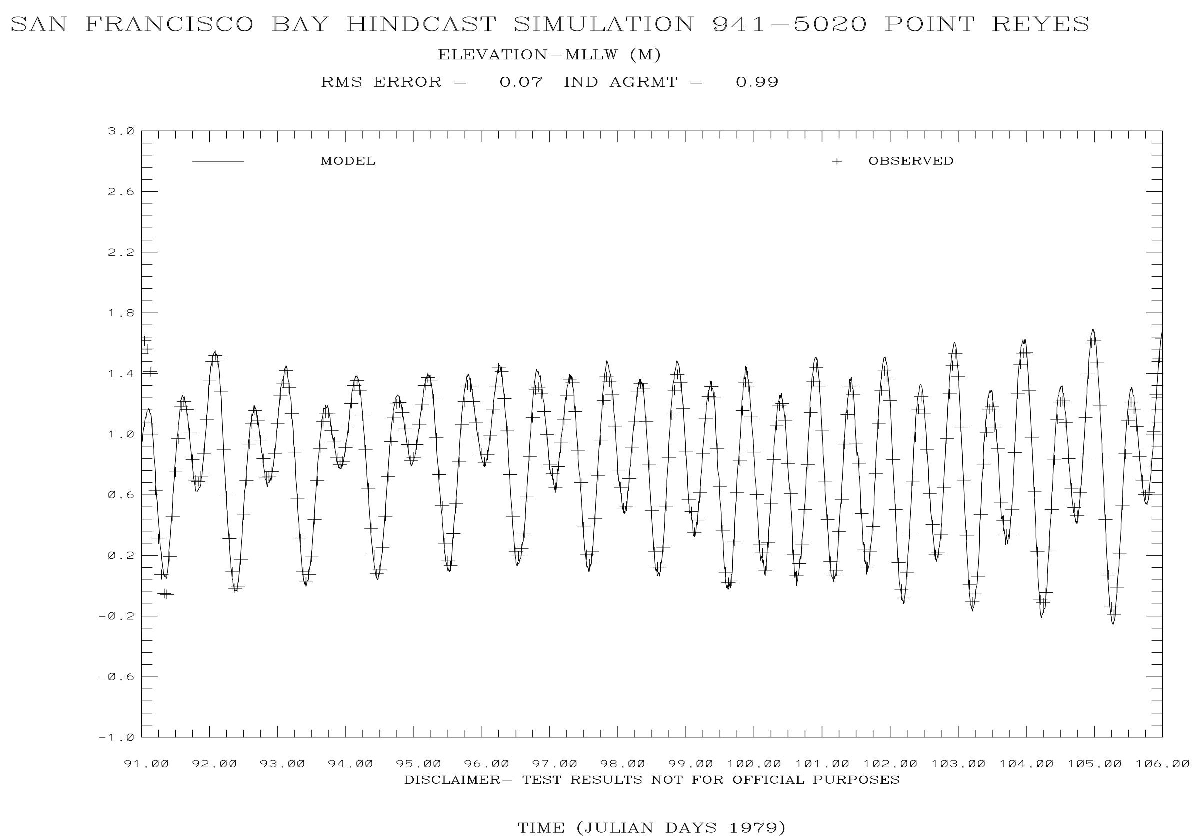

Figure 4.1. April 1-15, 1979 Hindcast: Port Chicago and Point Reyes Water Level Comparisons. Note IND AGRMT equals one minus Willmott et al. (1985) relative error.

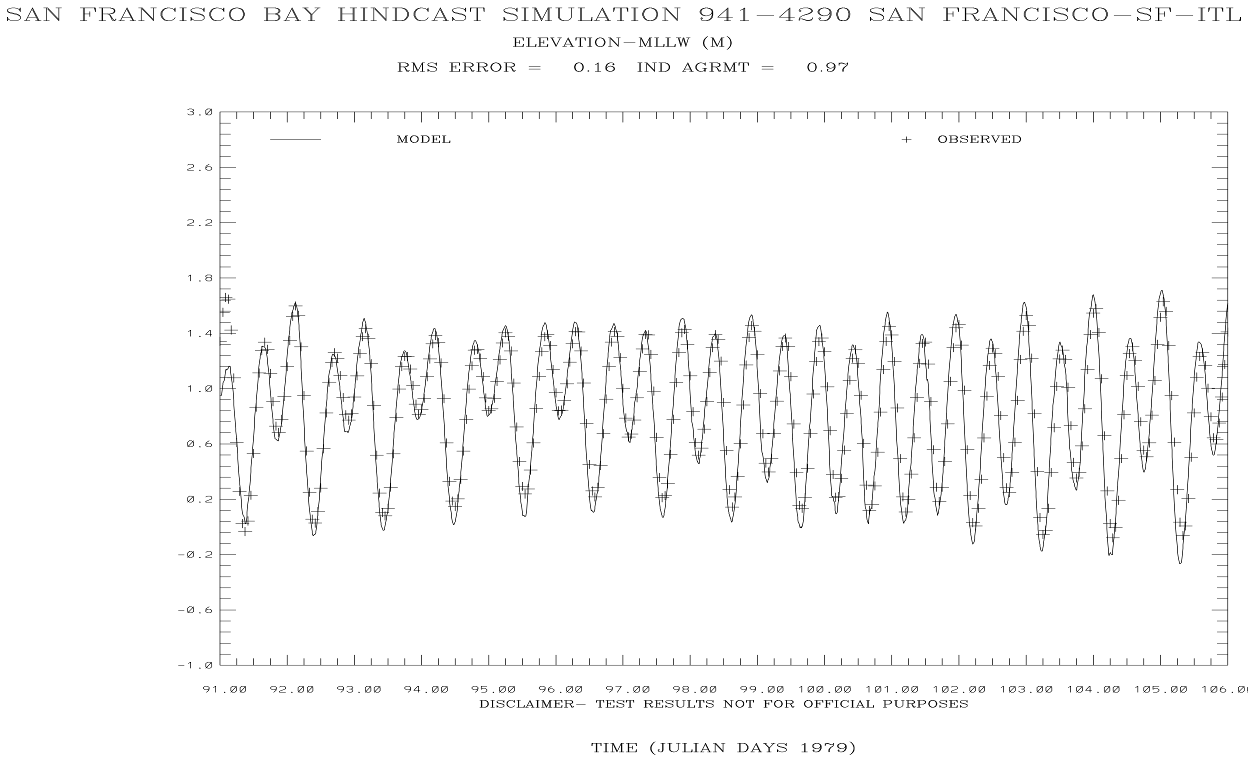

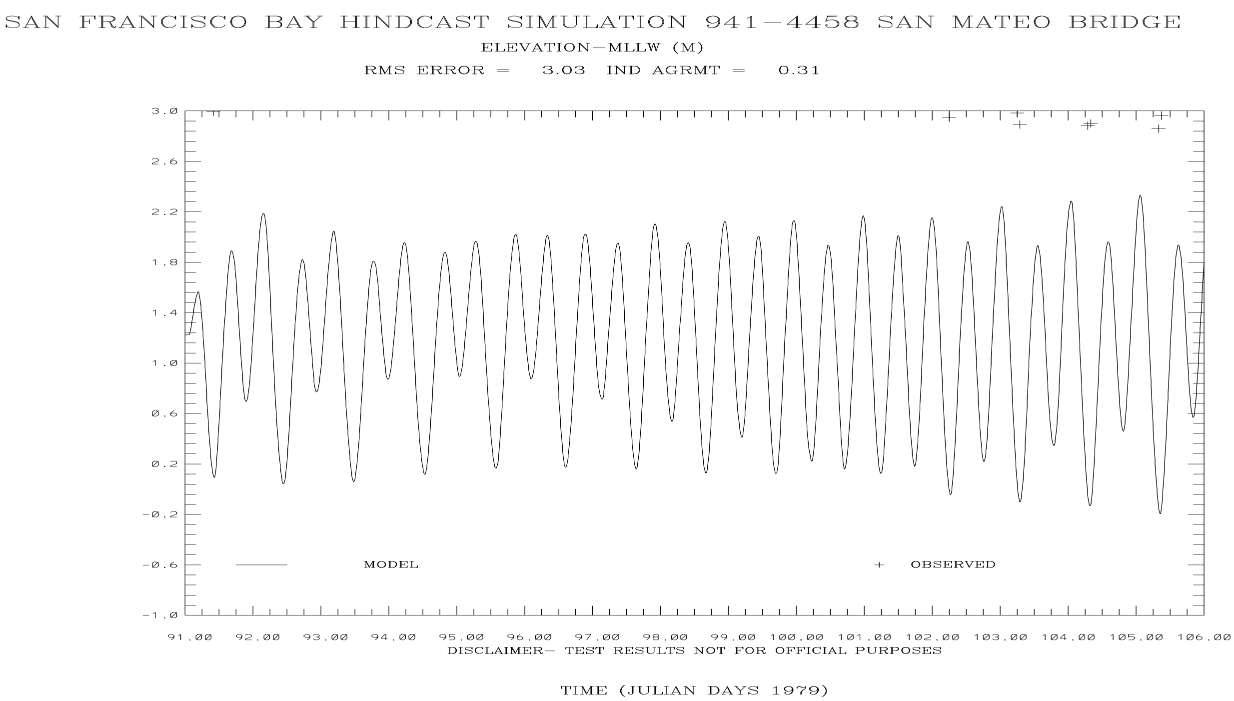

Figure 4.2. April 1-15, 1979 Hindcast: San Francisco and San Mateo Bridge Water Level Comparisons. Note IND AGRMT equals one minus Willmott et al. (1985) relative error.

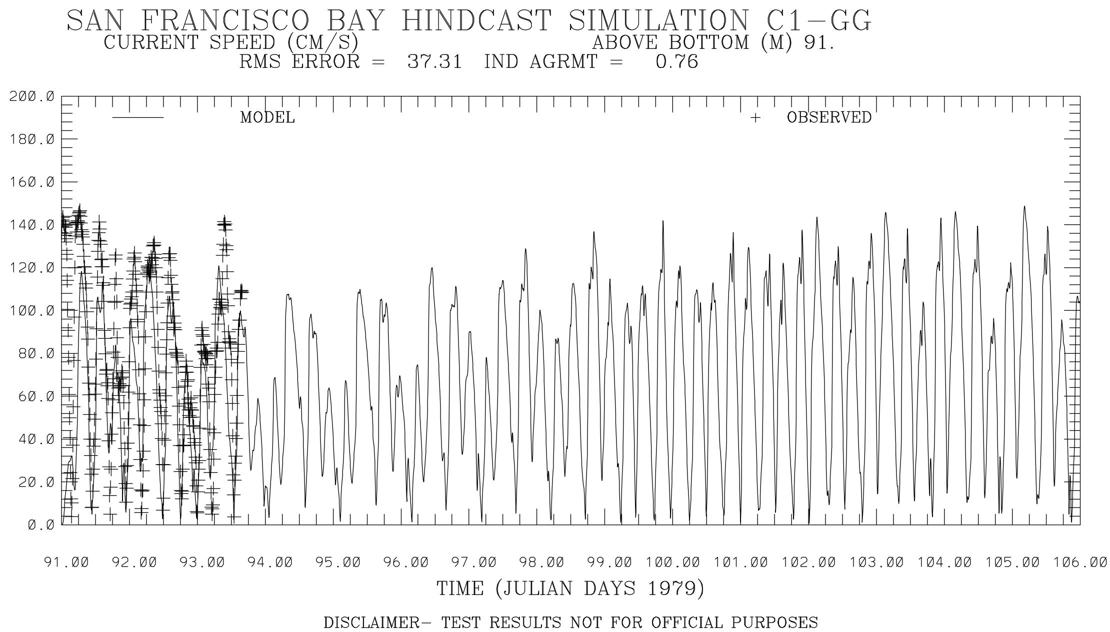

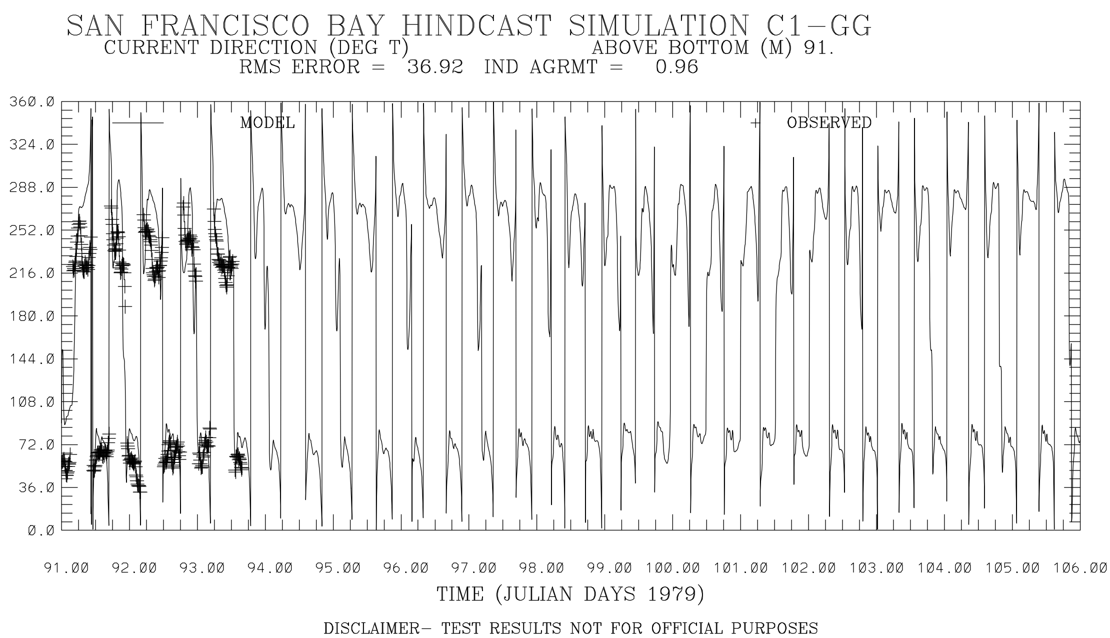

Figure 4.3. April 1-15, 1979 Hindcast: C-1 Current Speed and Direction at 91m above the bottom. Note IND AGRMT equals one minus Willmott et al. (1985) relative error.

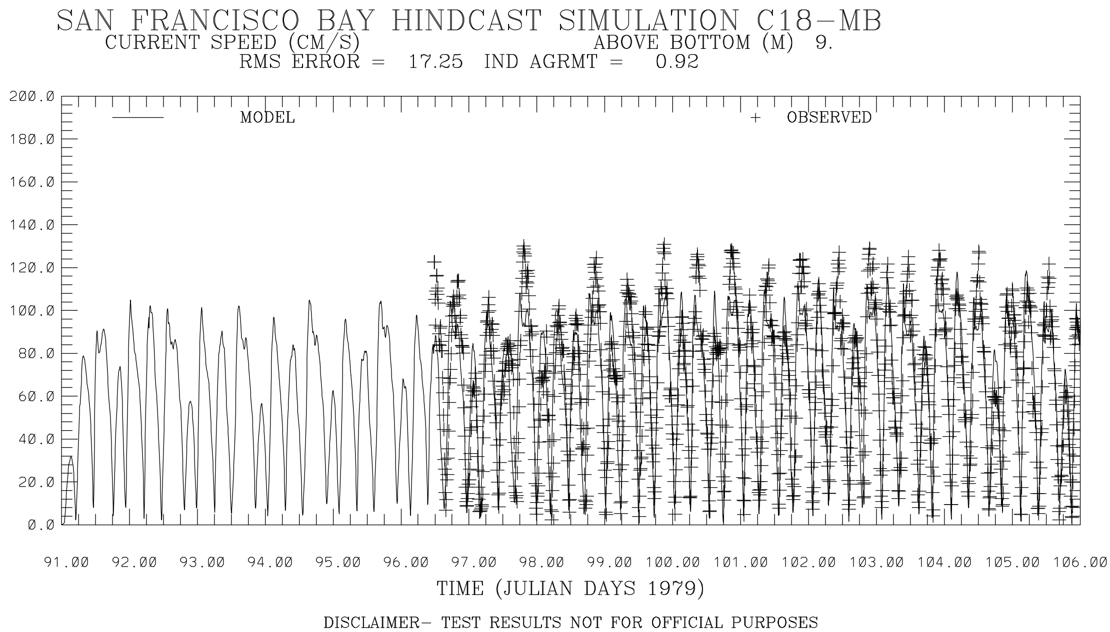

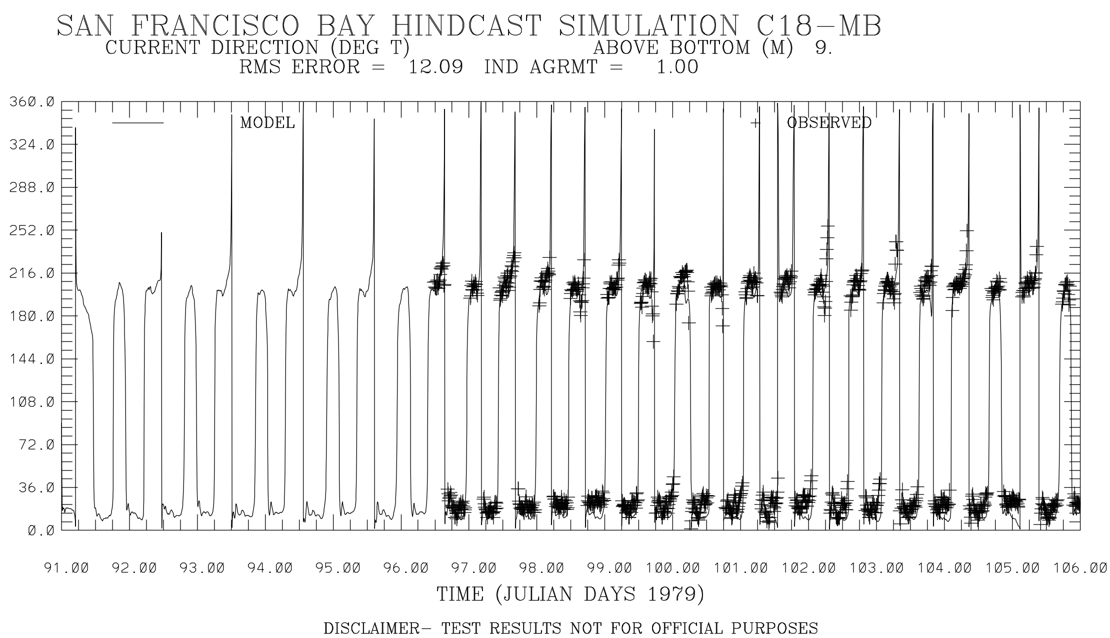

Figure 4.4. April 1-15, 1979 Hindcast: C-18 Current Speed and Direction at 9m above the bottom. Note IND AGRMT equals one minus Willmott et al. (1985) relative error.

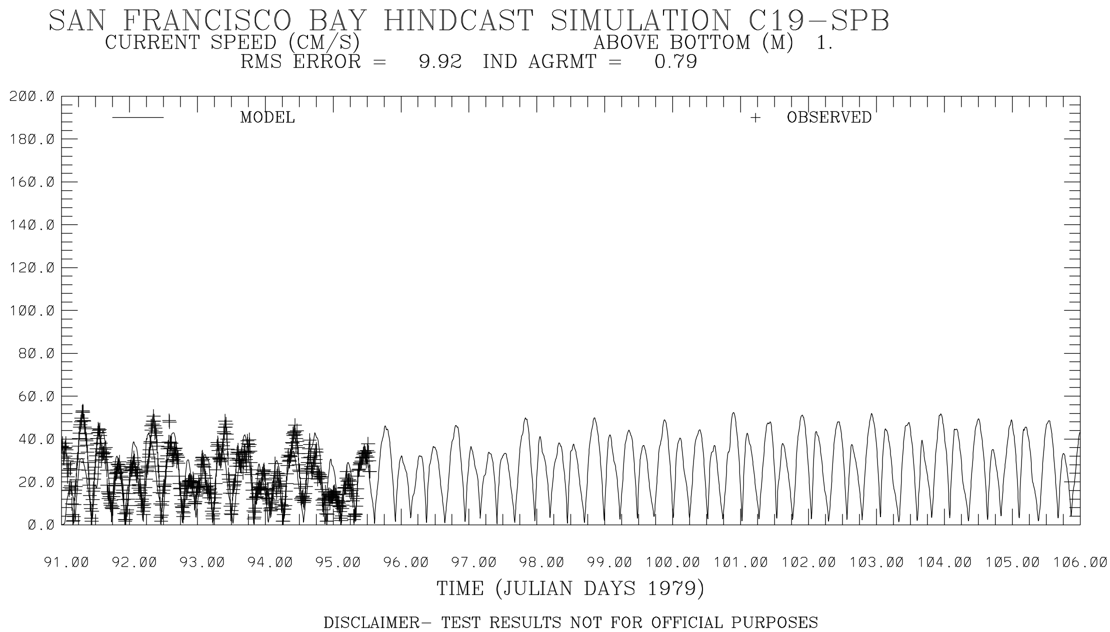

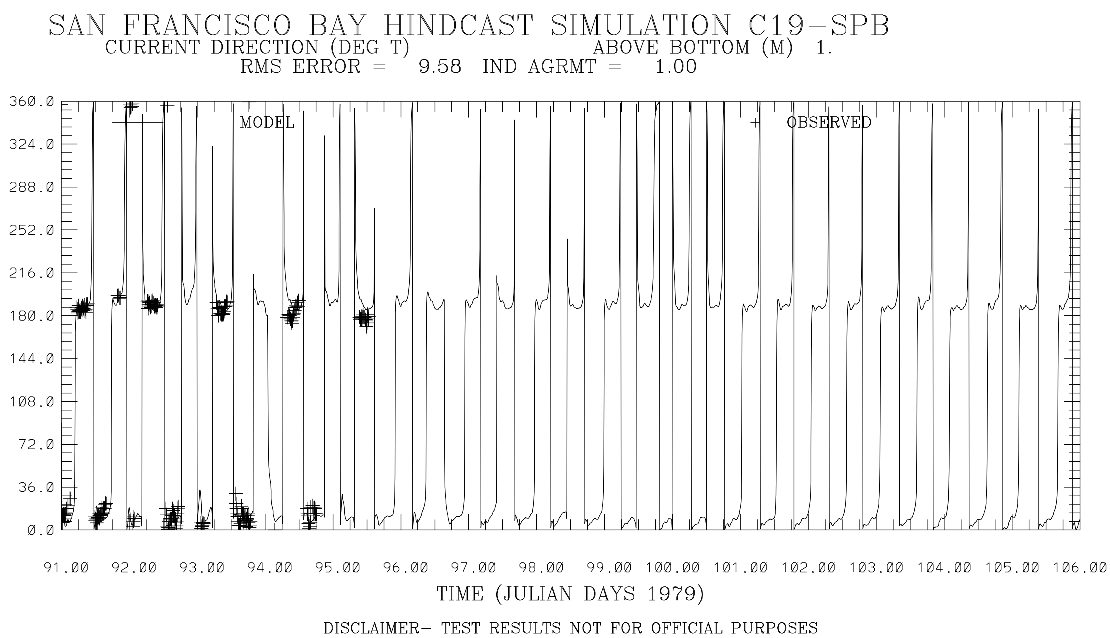

Figure 4.5. April 1-15, 1979 Hindcast: C-19 Current Speed and Direction at 1m above the bottom. Note IND AGRMT equals one minus Willmott et al. (1985) relative error.

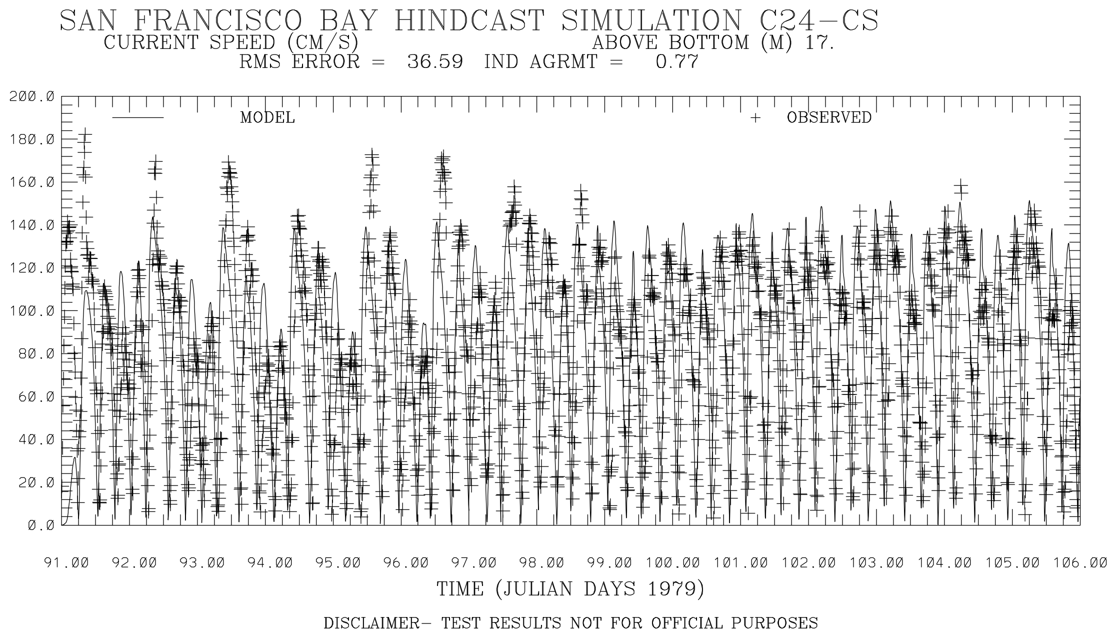

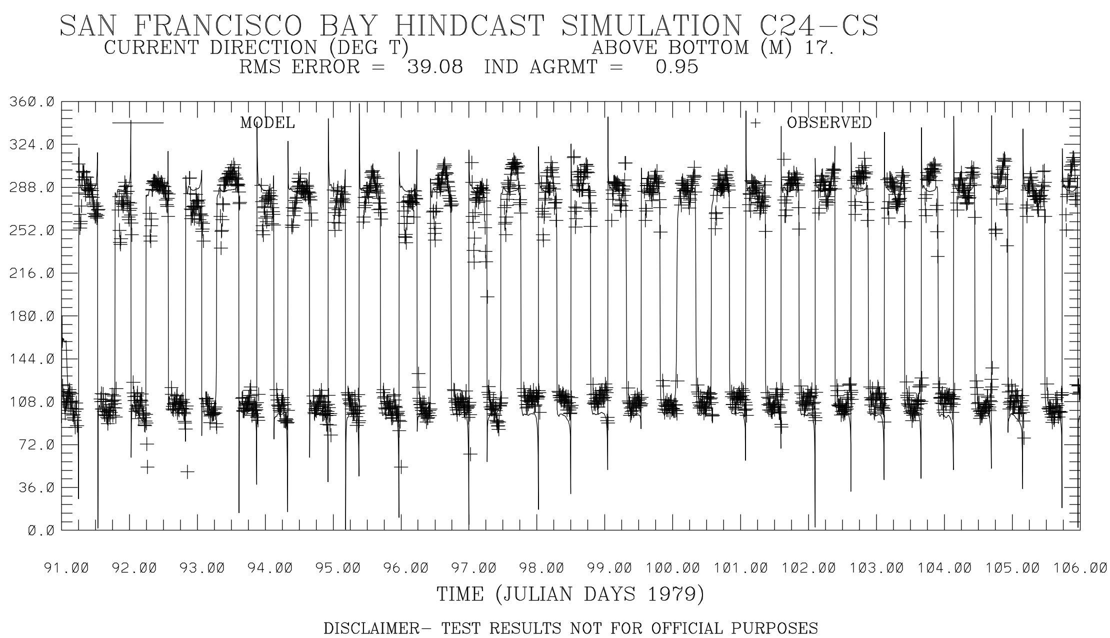

Figure 4.6. April 1-15, 1979 Hindcast: C-24 Current Speed and Direction at 17m above the bottom. Note IND AGRMT equals one minus Willmott et al. (1985) relative error.

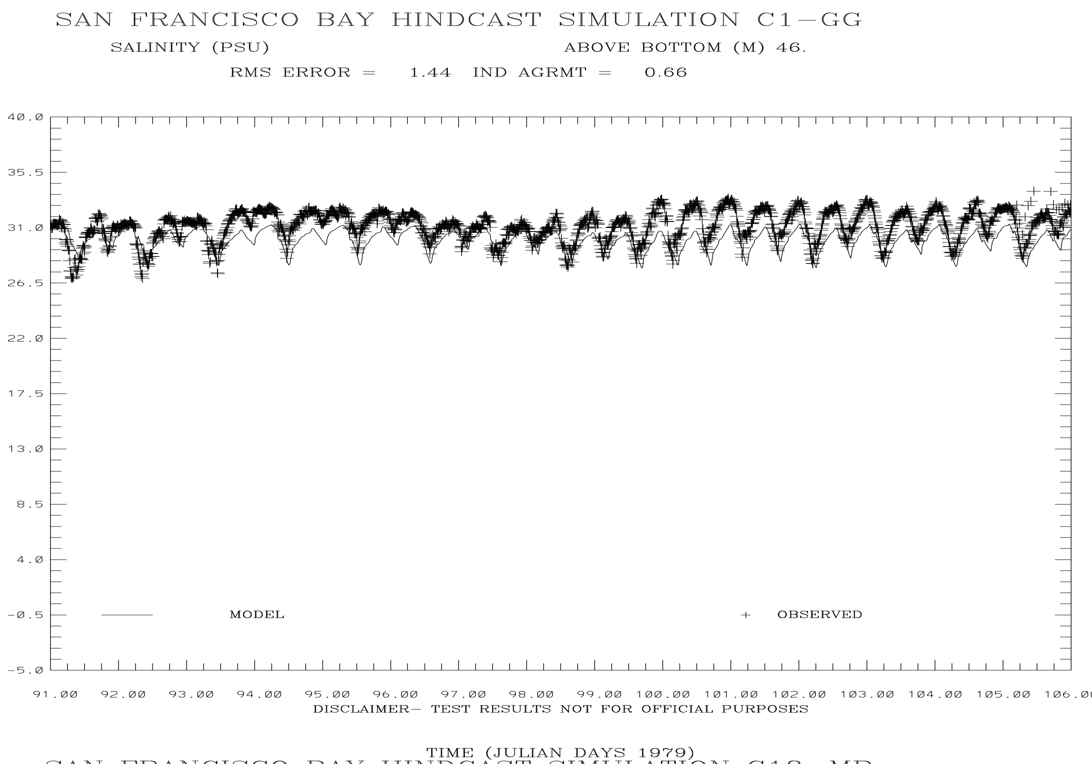

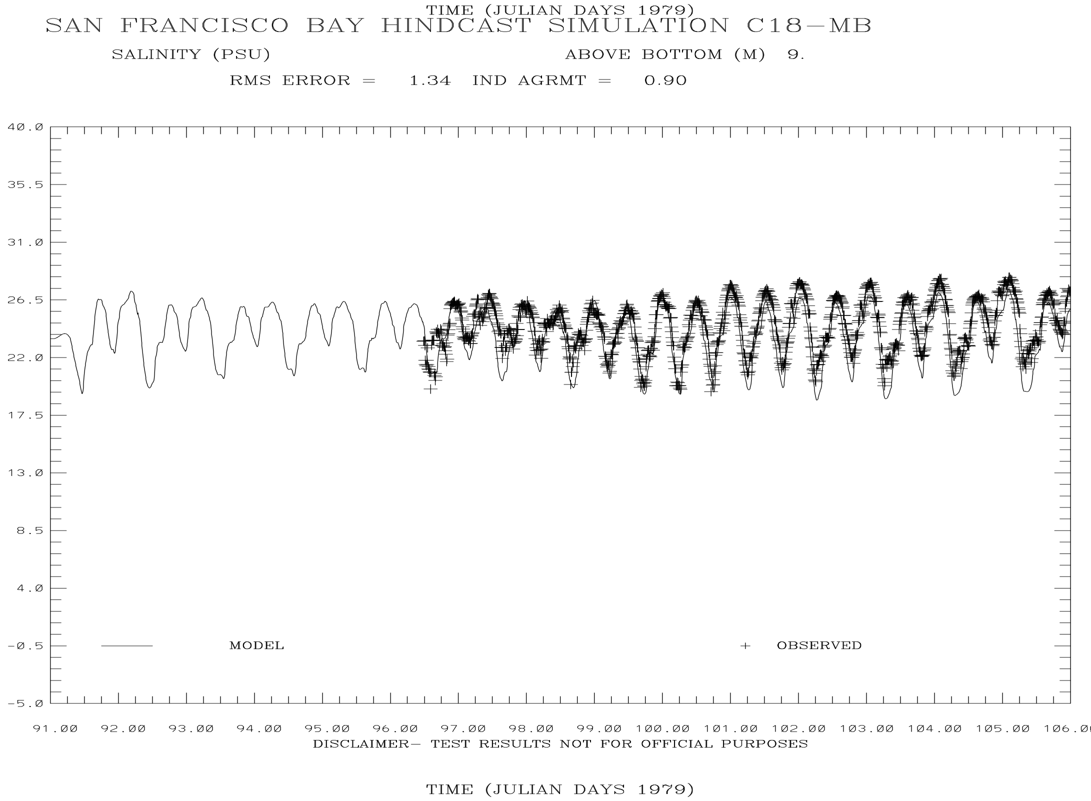

Figure 4.7. April 1-15, 1979 Hindcast: Salinity at C-1 at 46m and C-18 at 9m above the bottom. Note IND AGRMT equals one minus Willmott et al. (1985) relative error.

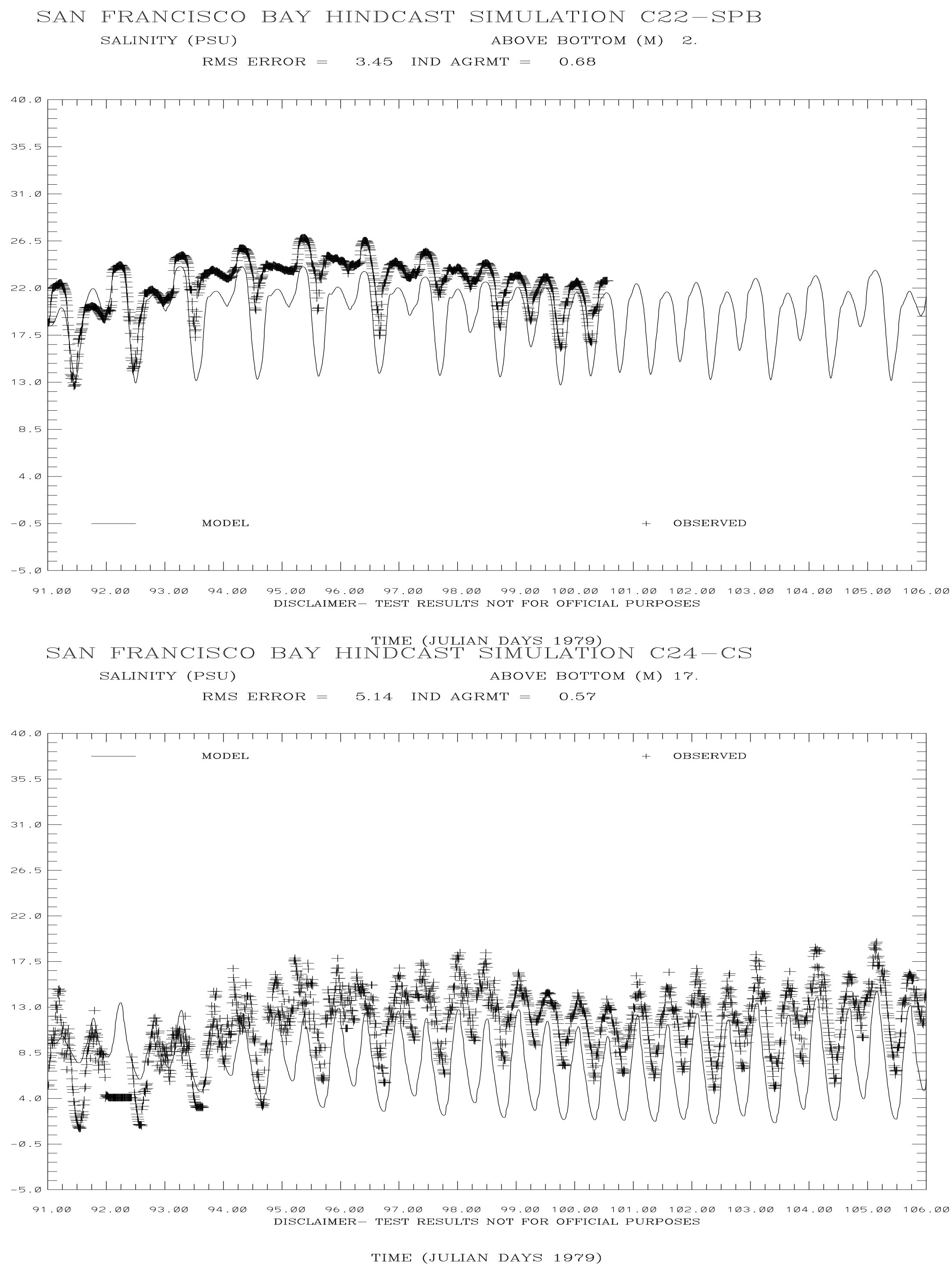

Figure 4.8. April 1-15, 1979 Hindcast: Salinity at C-22 at 2m and C-24 at 17m above the bottom. Note IND AGRMT equals one minus Willmott et al. (1985) relative error.

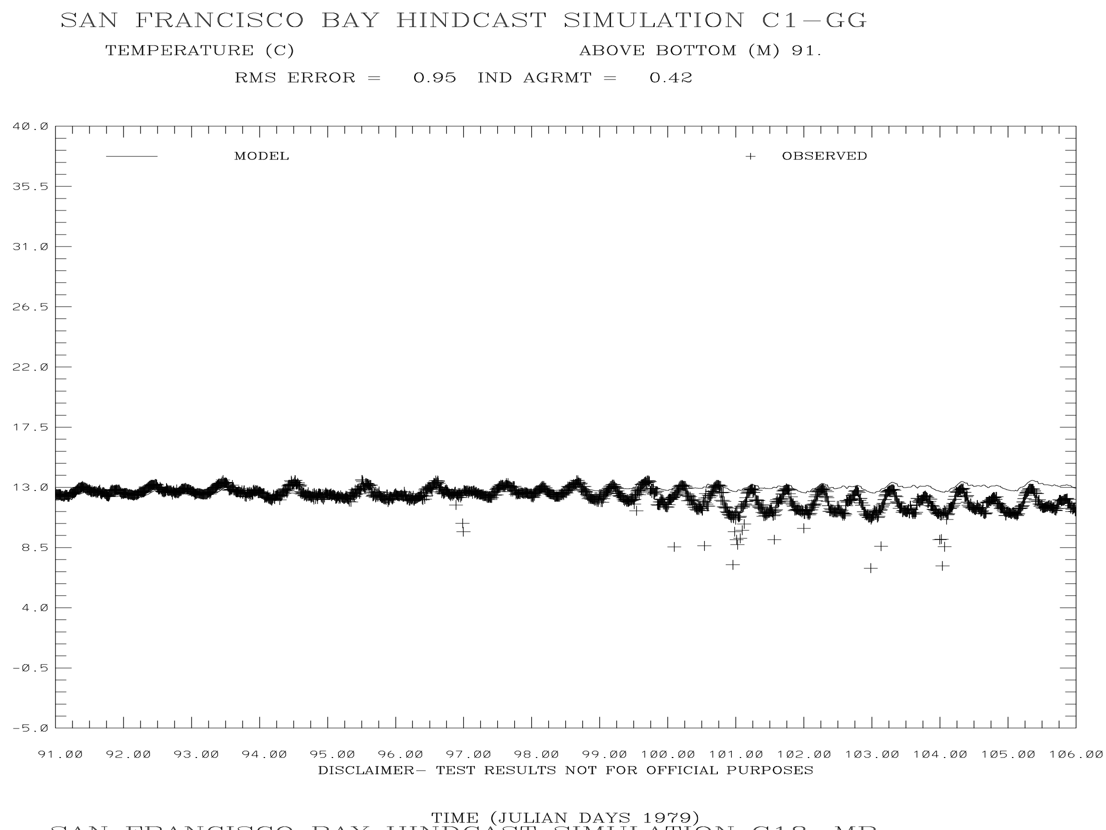

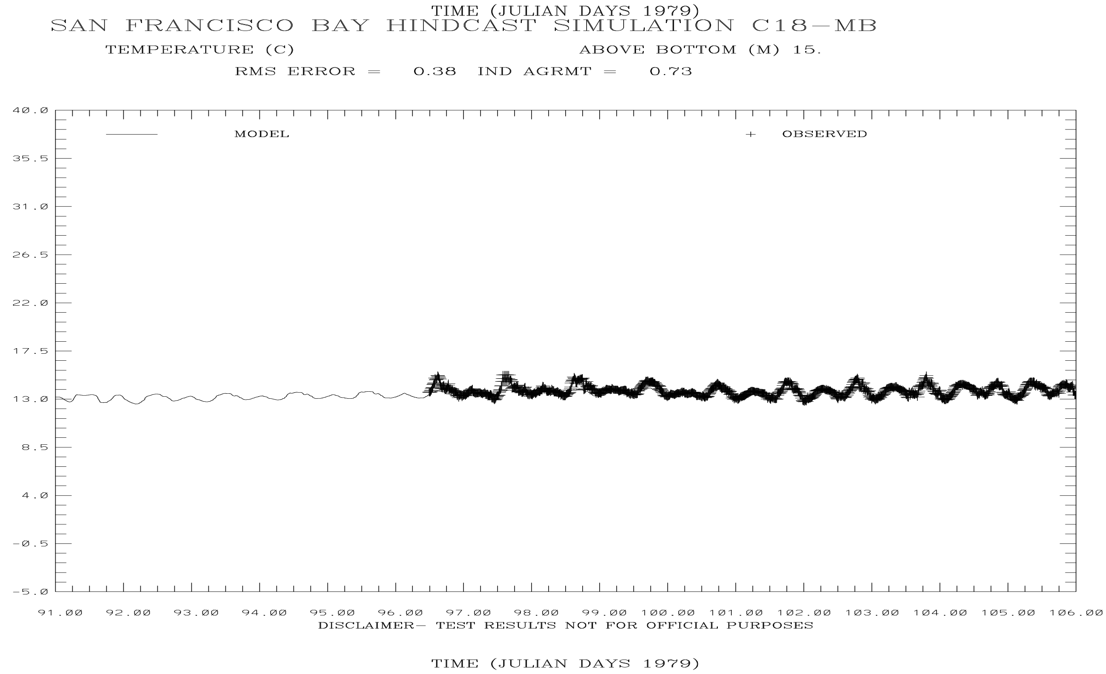

Figure 4.9. April 1-15, 1979 Hindcast: Temperature at C-1 at 91m and C-18 at 15m above the bottom. Note IND AGRMT equals one minus Willmott et al. (1985) relative error.

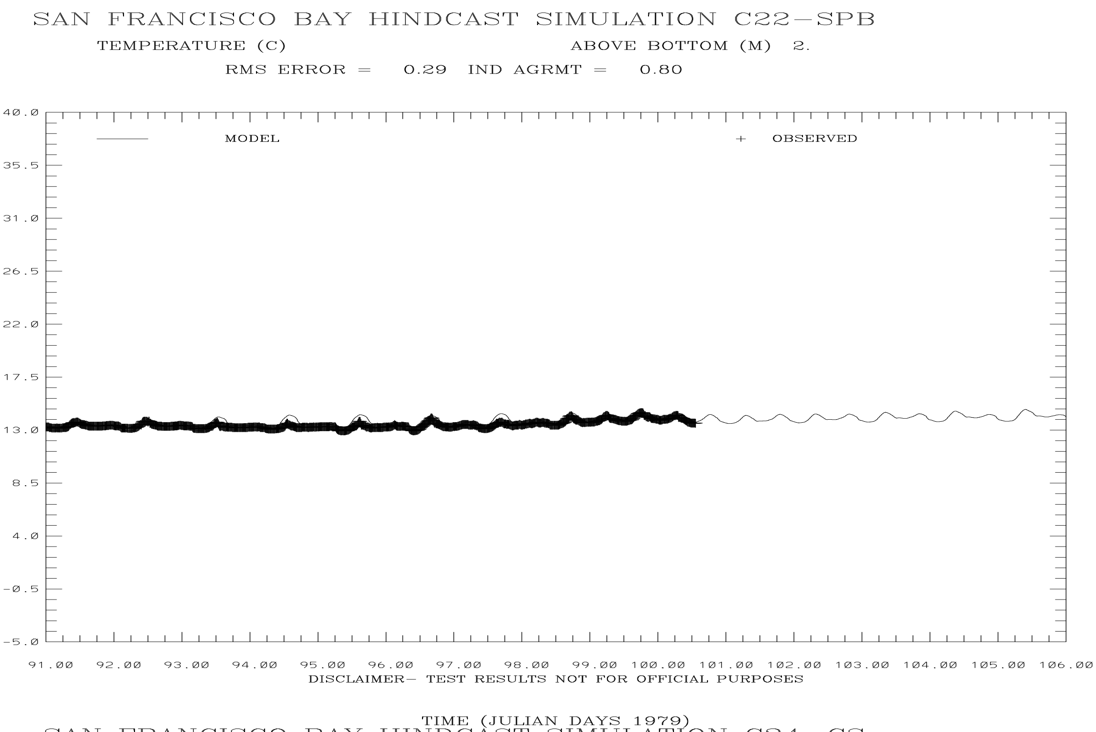

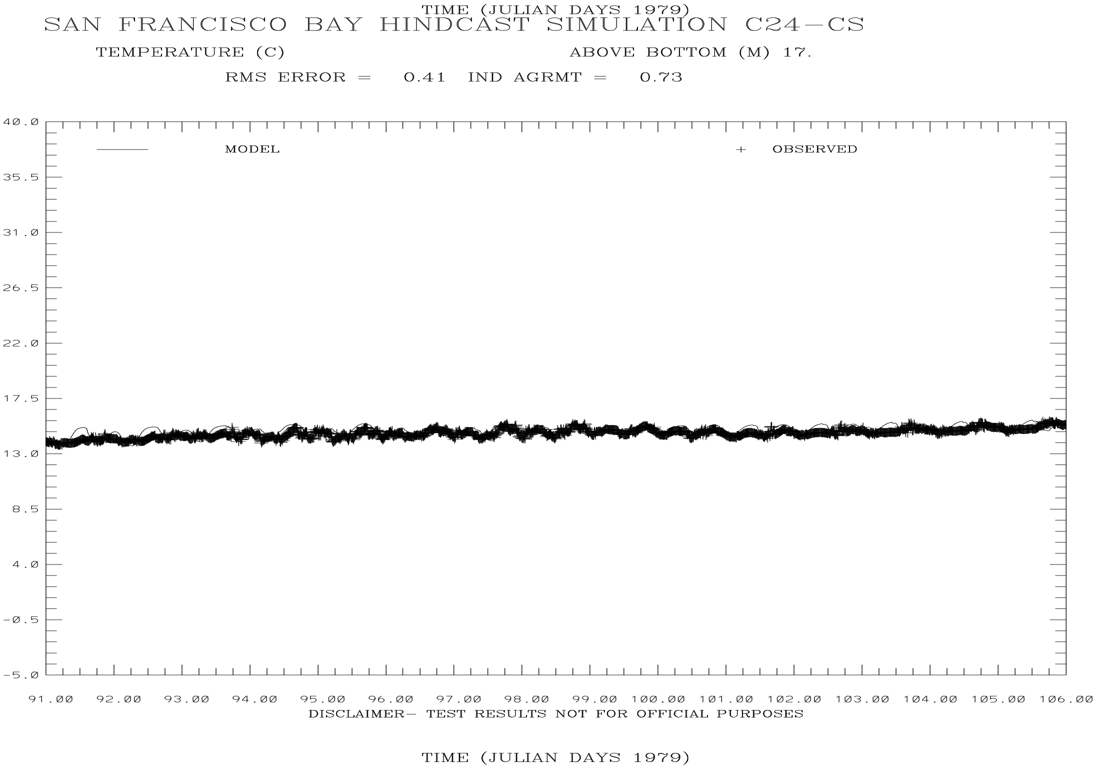

Figure 4.10. April 1-15, 1979 Hindcast: Temperature at C-22 at 2m and C-24 at 17m above the bottom. Note IND AGRMT equals one minus Willmott et al. (1985) relative error.

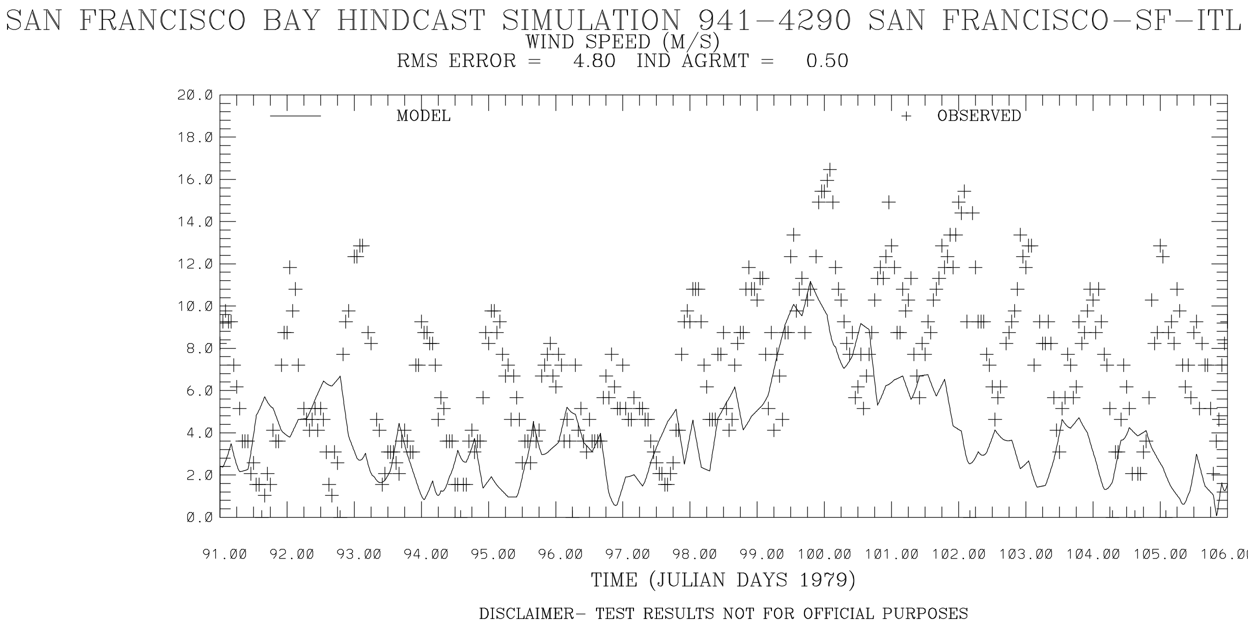

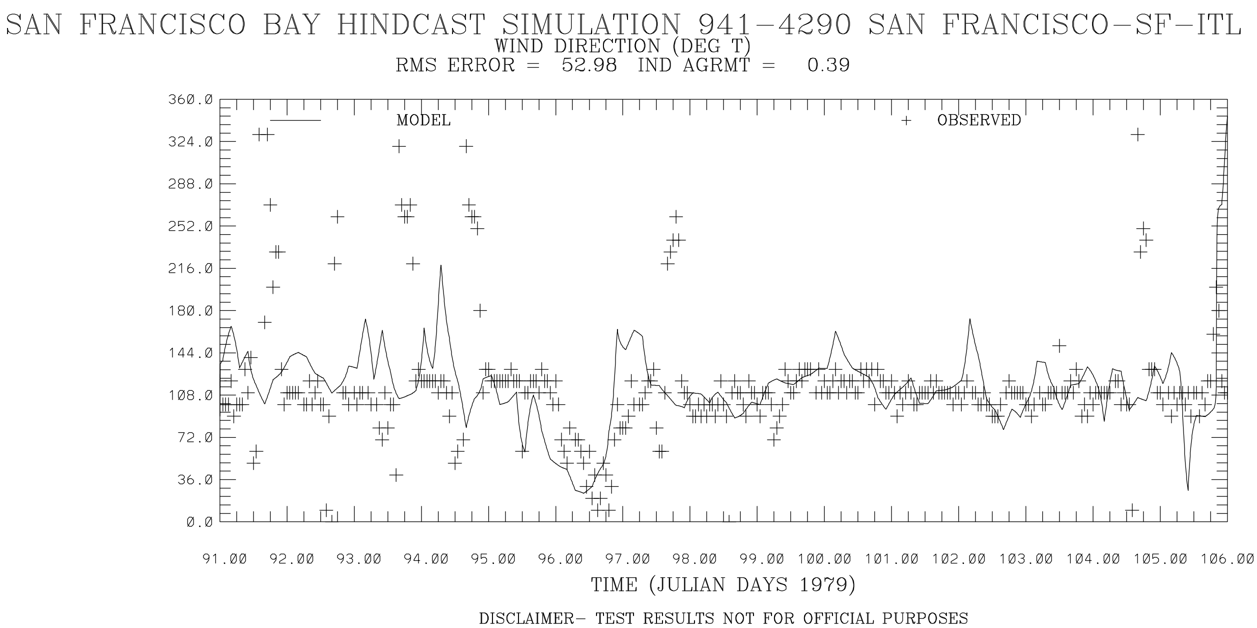

Figure 4.11. April 1-15, 1979 Hindcast: Wind speed and direction at San Francisco International Airport. Note IND AGRMT equals one minus Willmott et al. (1985) relative error.

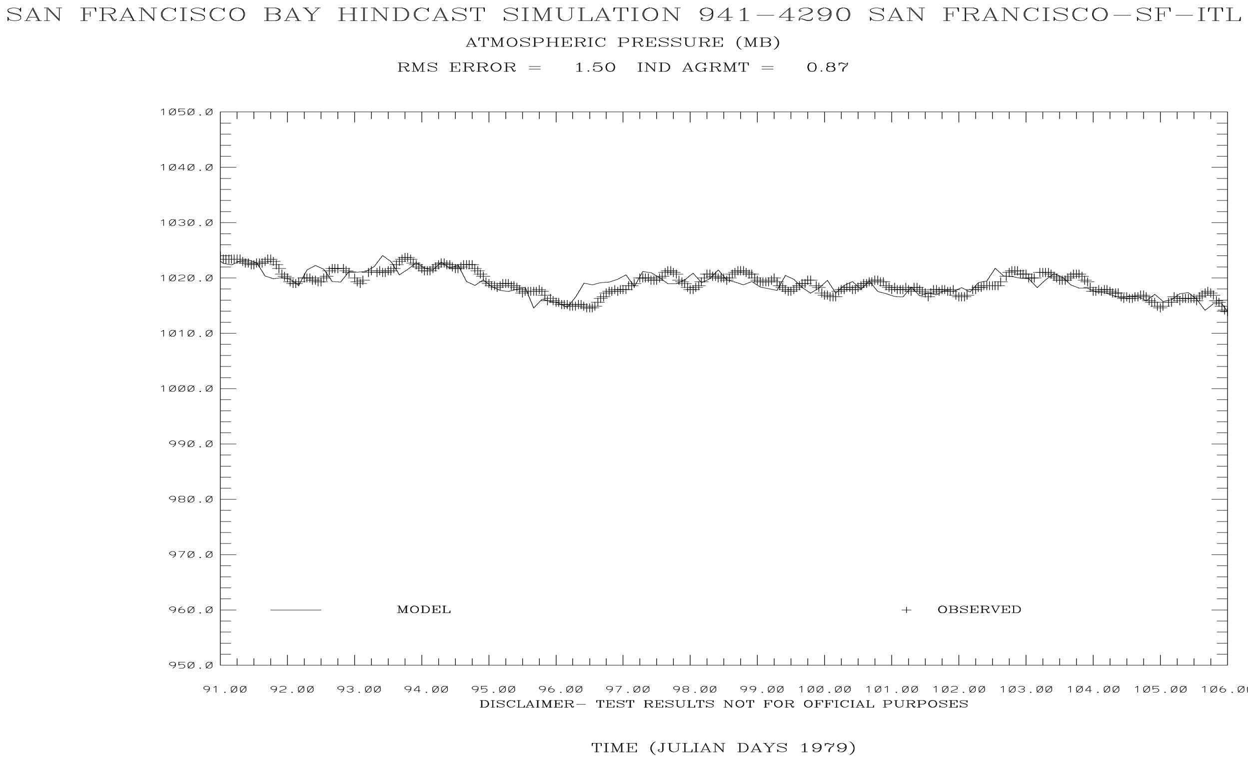

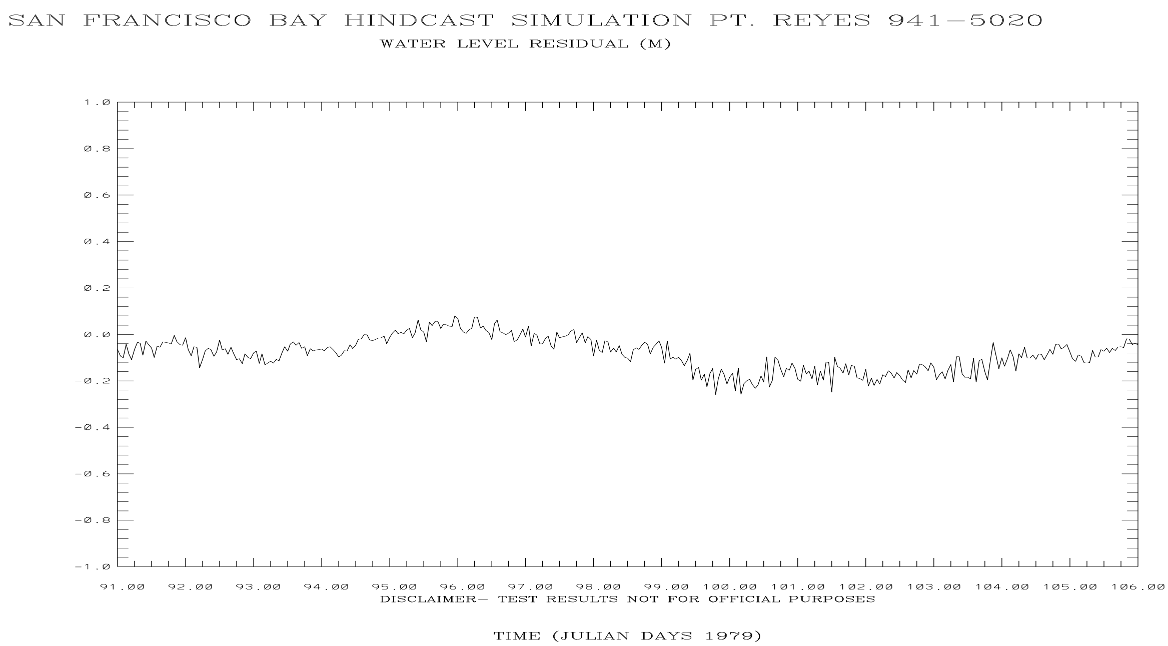

Figure 4.12. April 1-15, 1979 Hindcast: Atmospheric Pressure at San Francisco International Airport and Water Level Residual at Point Reyes. Note IND AGRMT equals one minus Willmott et al. (1985) relative error.

SAN FRANCISCO BAY HINDCAST SIMULATION SACRAMENTO RIVER AT RIO VISTA

FLOW – 1000 (CFS)

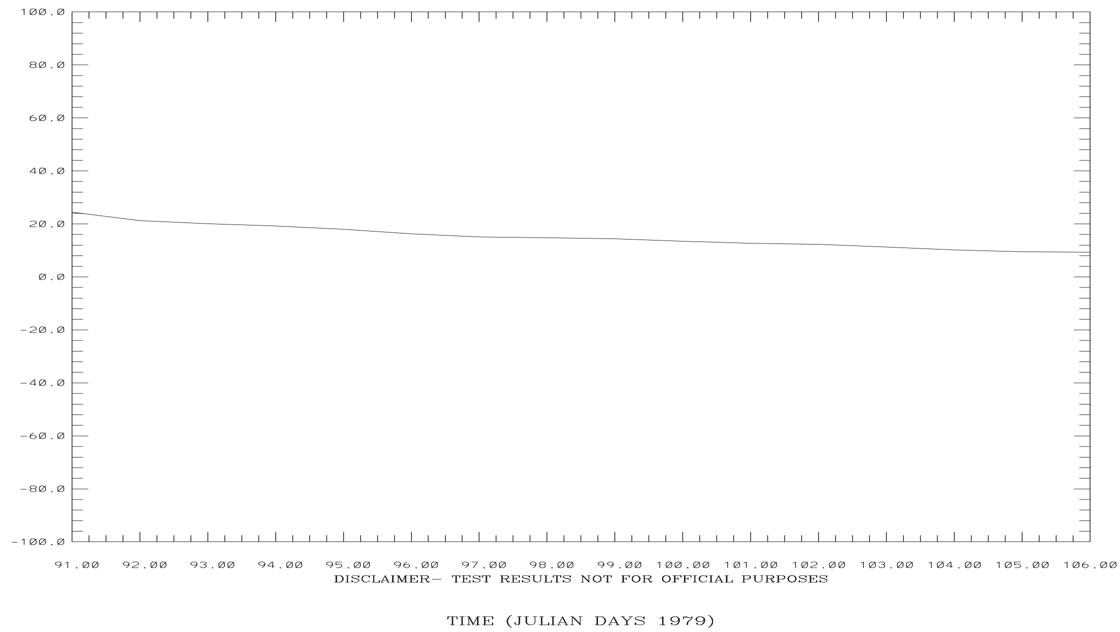

SAN FRANCISCO BAY HINDCAST SIMULATION SAN JOAQUIN RIVER AT ANTIOCH

FLOW – 1000 (CFS)

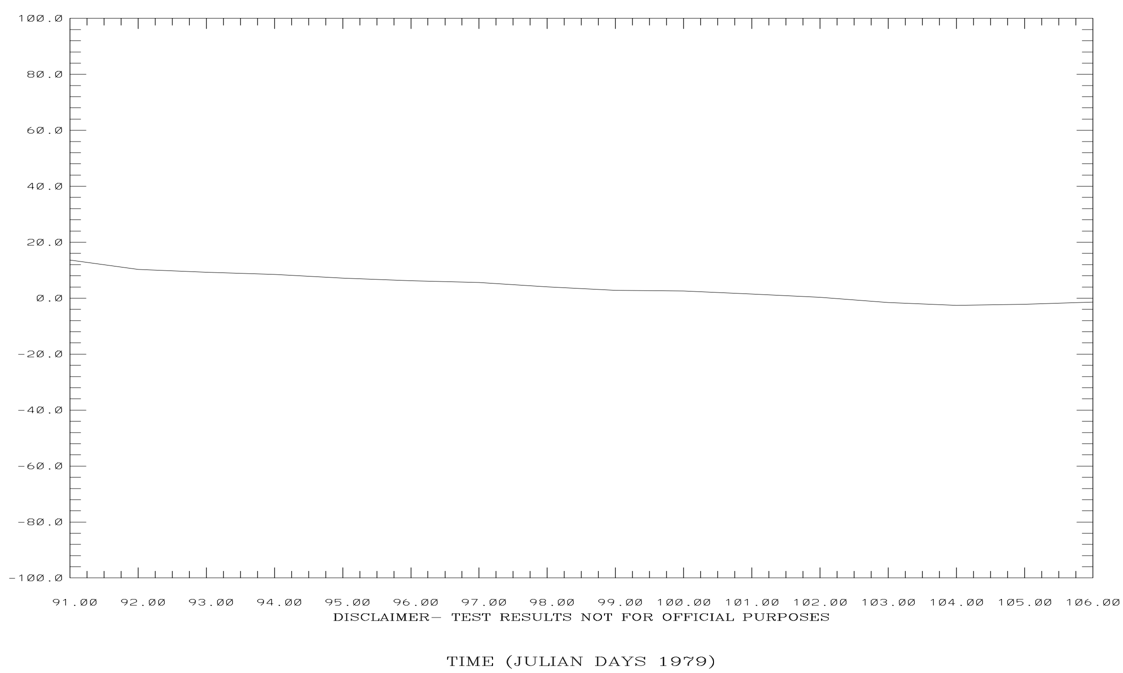

Figure 4.13. April 1-15, 1979 Hindcast: Flow (Thousands of CFS) on the Sacramento River at Rio Vista, CA and on the San Joaquin River at Antioch, CA.

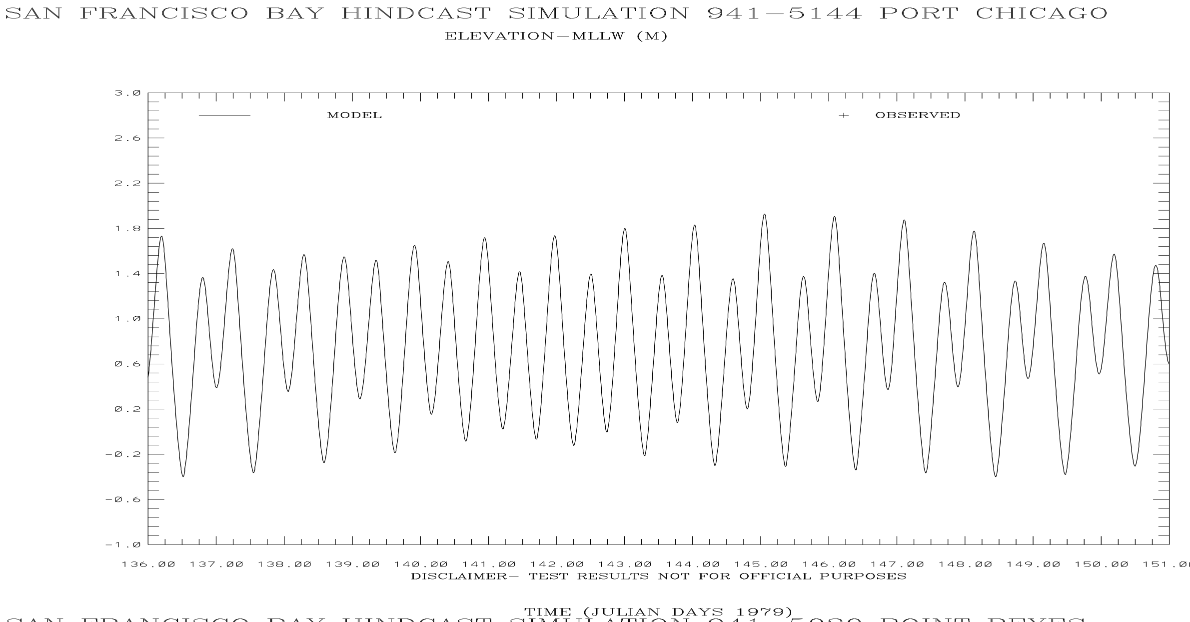

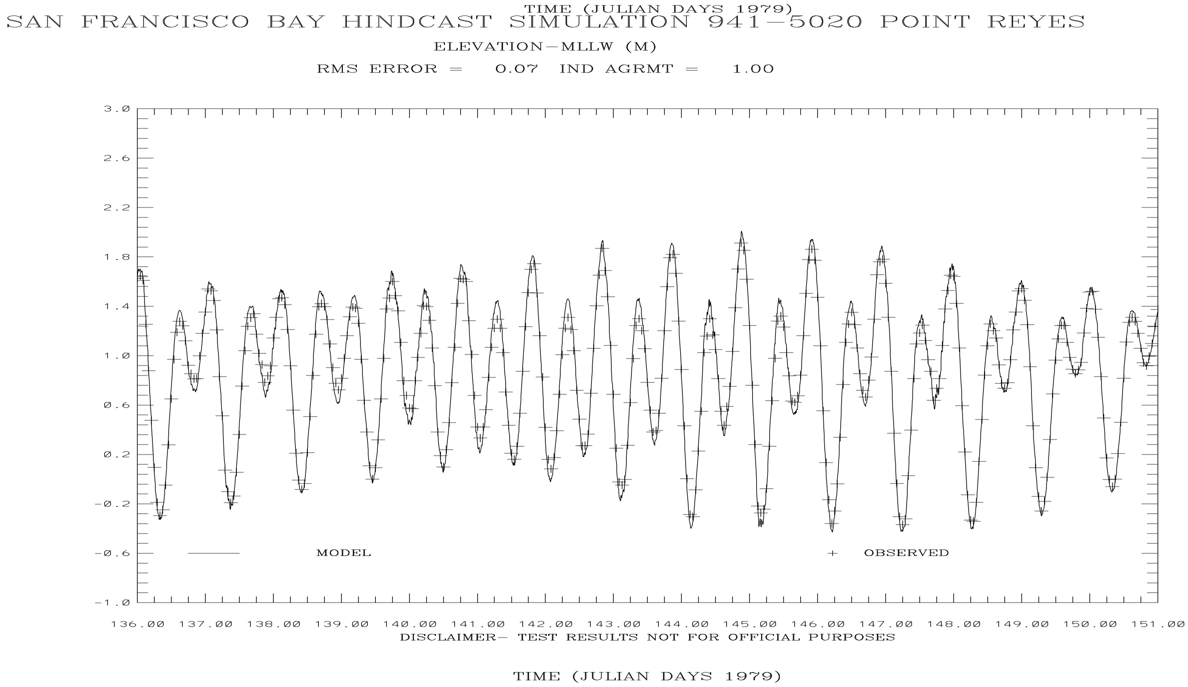

Figure 4.14. May 15-31, 1979 Hindcast: Port Chicago and Point Reyes Water Level Comparisons. Note IND AGRMT equals one minus Willmott et al. (1985) relative error.

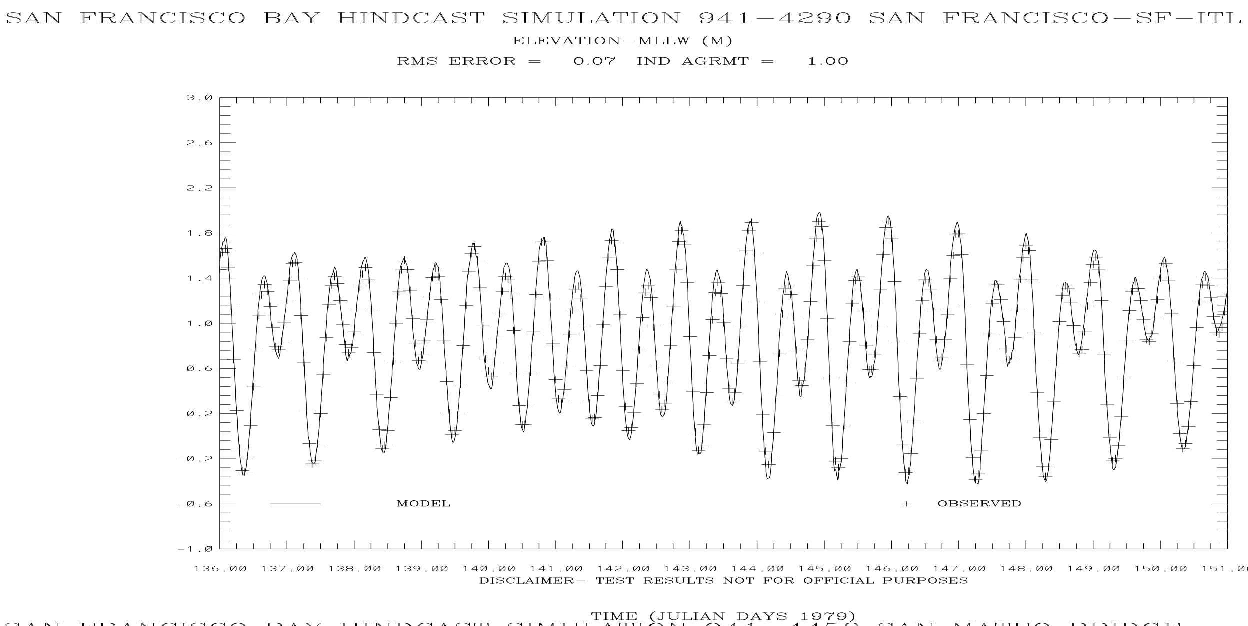

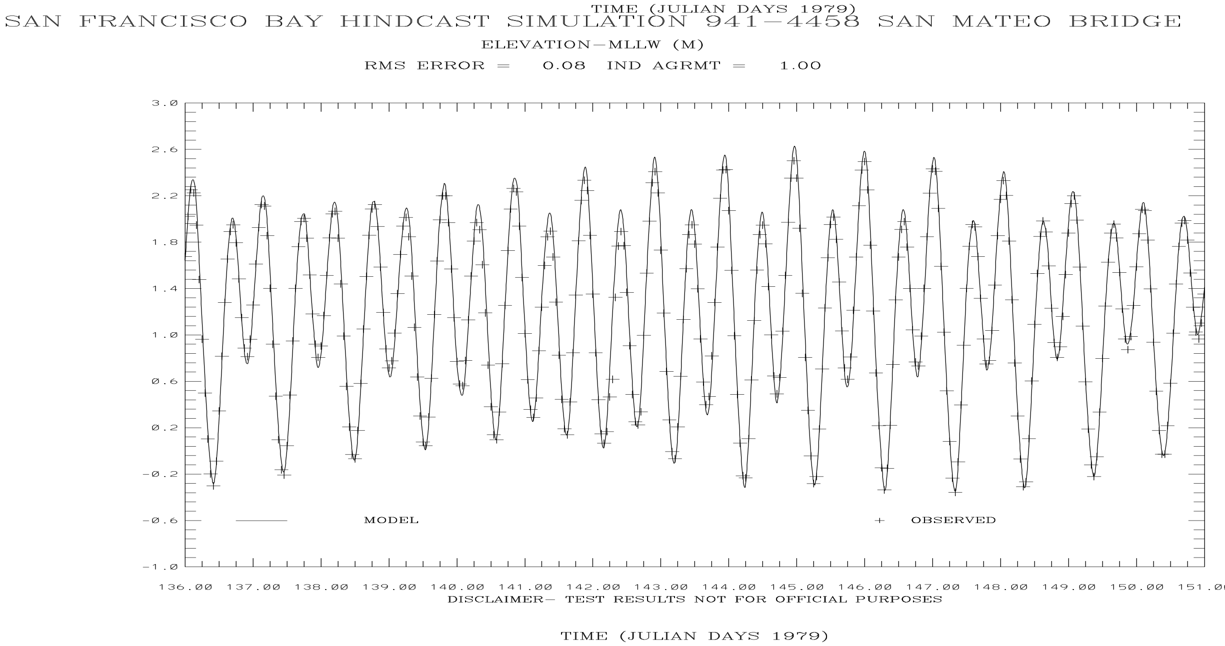

Figure 4.15. May 15-31, 1979 Hindcast: San Francisco and San Mateo Bridge Water Level Comparisons. Note IND AGRMT equals one minus Willmott et al. (1985) relative error.

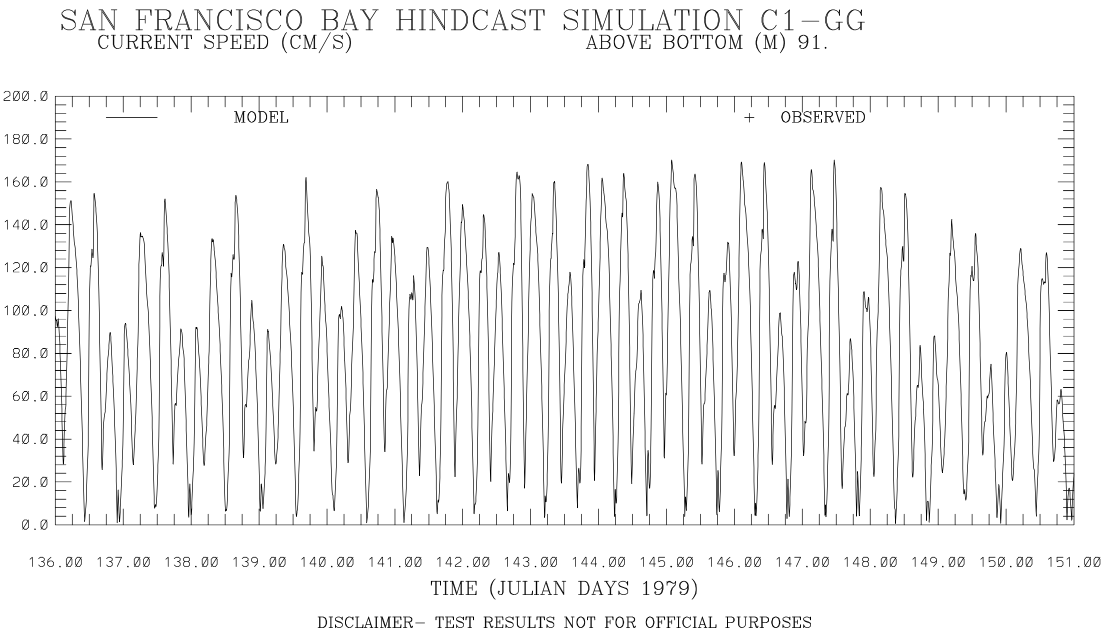

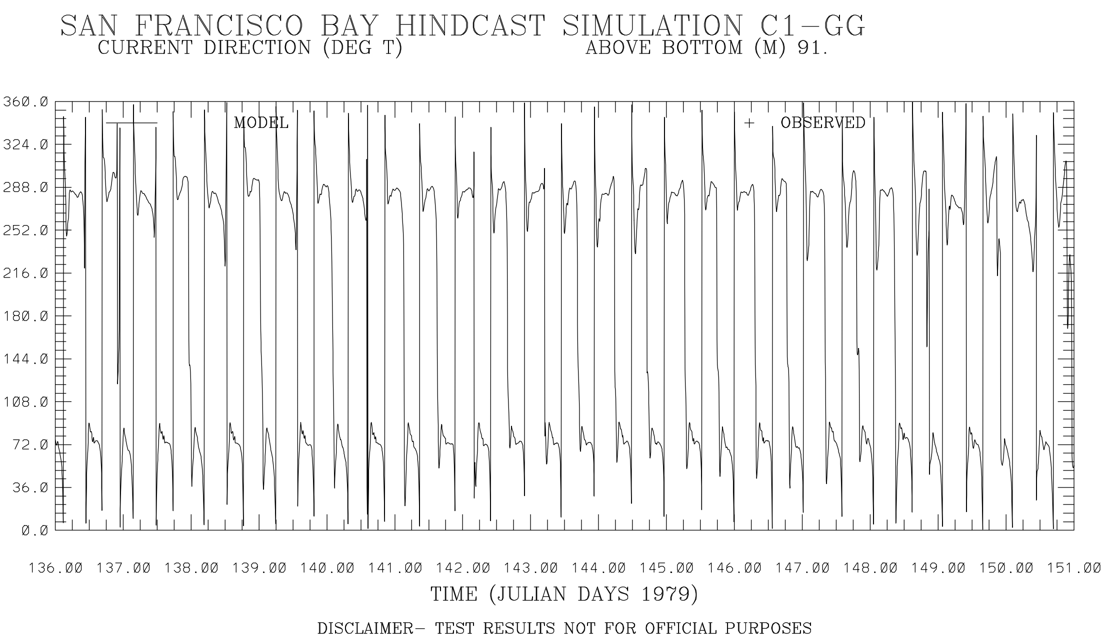

Figure 4.16. May 15-31, 1979 Hindcast: C-1 Current Speed and Direction at 91m above the bottom. Note IND AGRMT equals one minus Willmott et al. (1985) relative error.

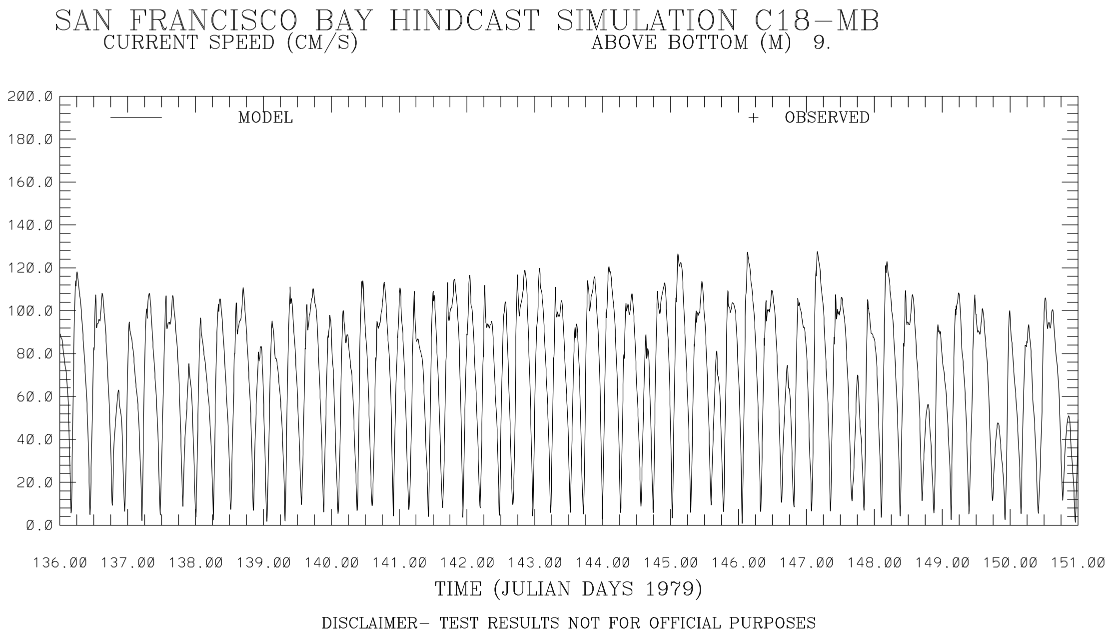

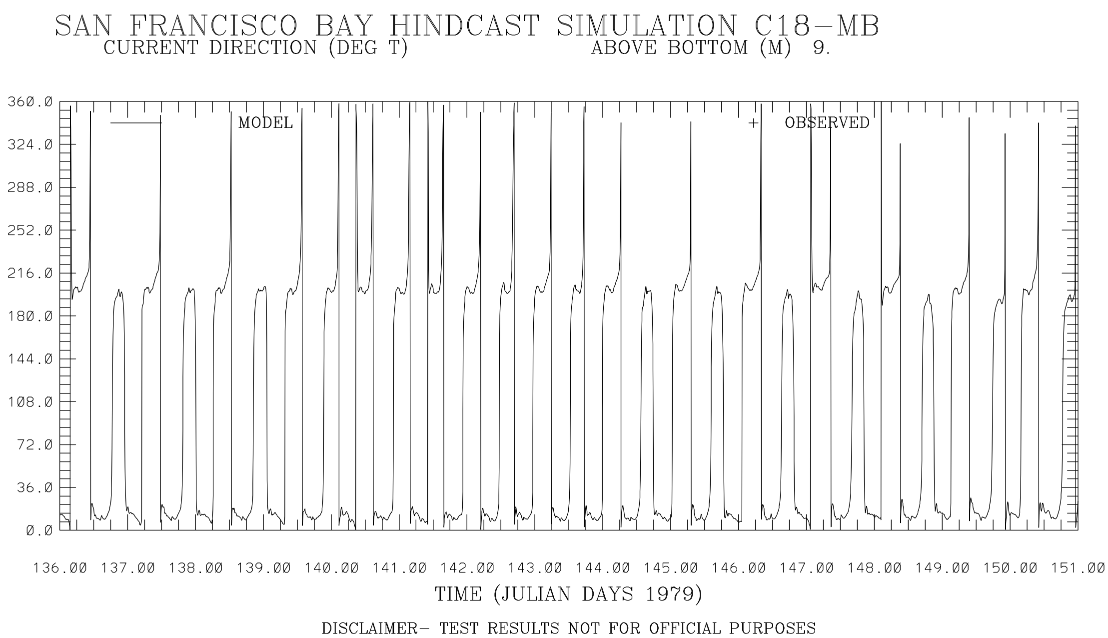

Figure 4.17. May 15-31, 1979 Hindcast: C-18 Current Speed and Direction at 9m above the bottom. Note IND AGRMT equals one minus Willmott et al. (1985) relative error.

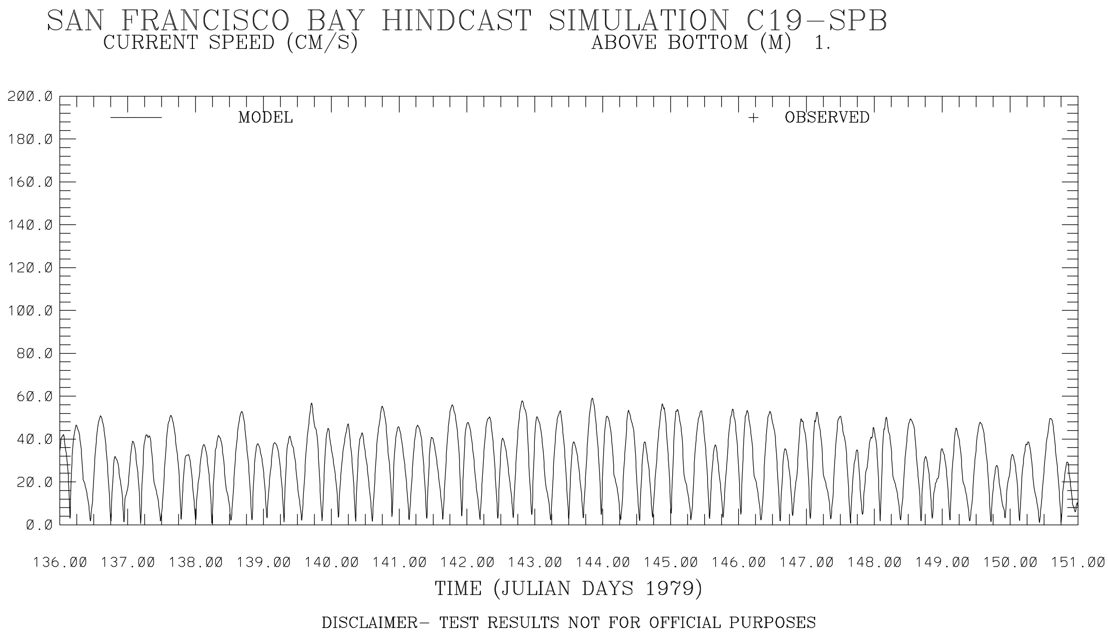

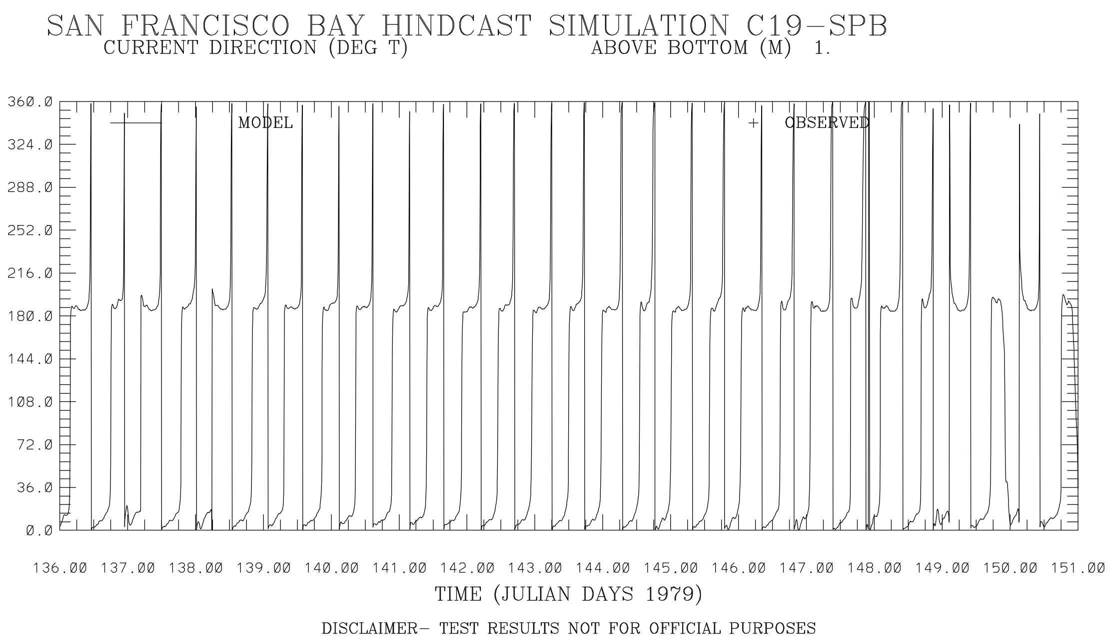

Figure 4.18. May 15-31, 1979 Hindcast: C-19 Current Speed and Direction at 1m above the bottom. Note IND AGRMT equals one minus Willmott et al. (1985) relative error.

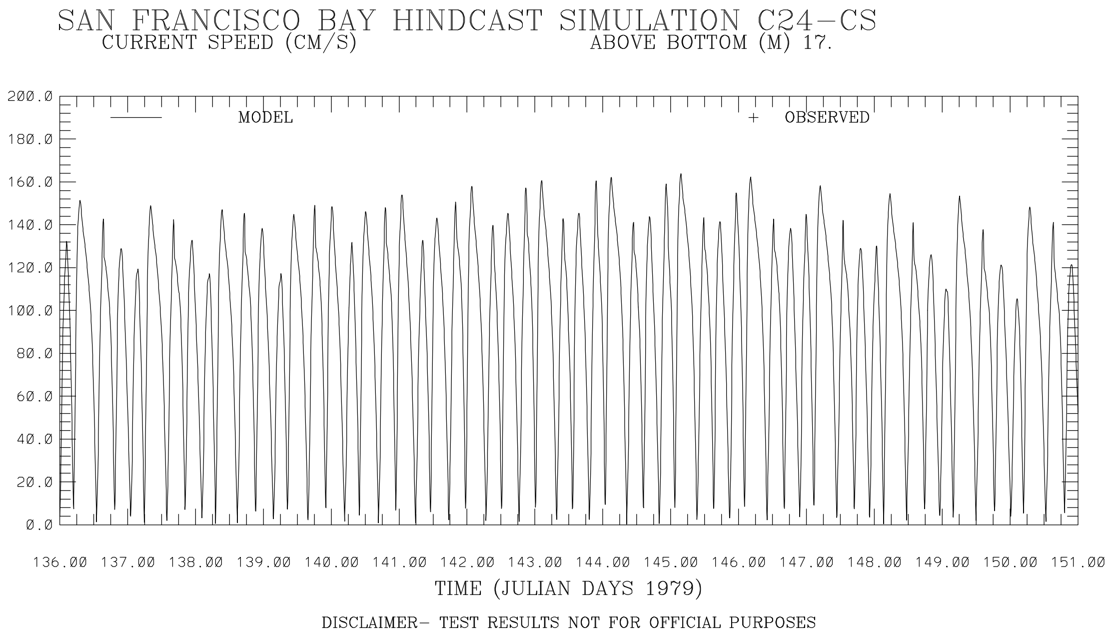

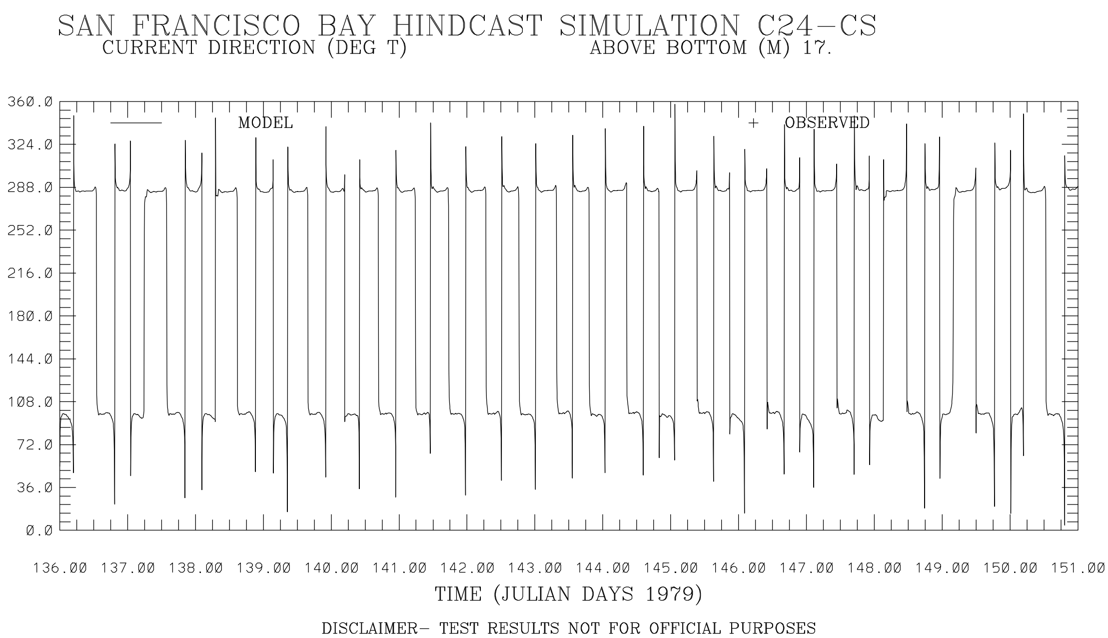

Figure 4.19. May 15-31, 1979 Hindcast: C-24 Current Speed and Direction at 17m above the bottom. Note IND AGRMT equals one minus Willmott et al. (1985) relative error.

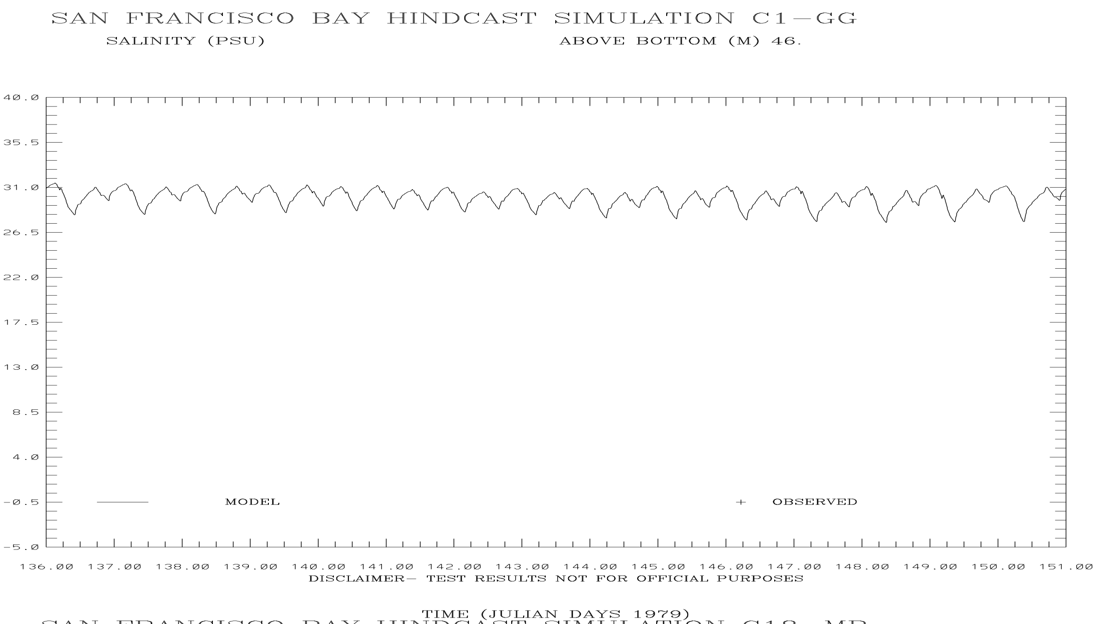

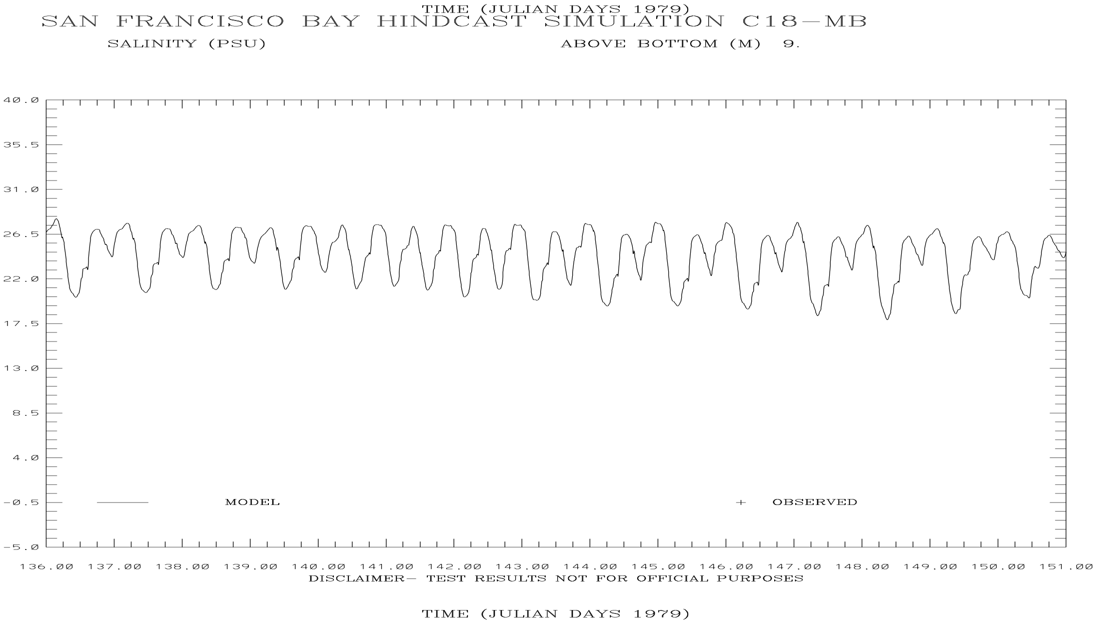

Figure 4.20. May 15-31, 1979 Hindcast: Salinity at C-1 at 91m and C-18 at 9m above the bottom. Note IND AGRMT equals one minus Willmott et al. (1985) relative error.

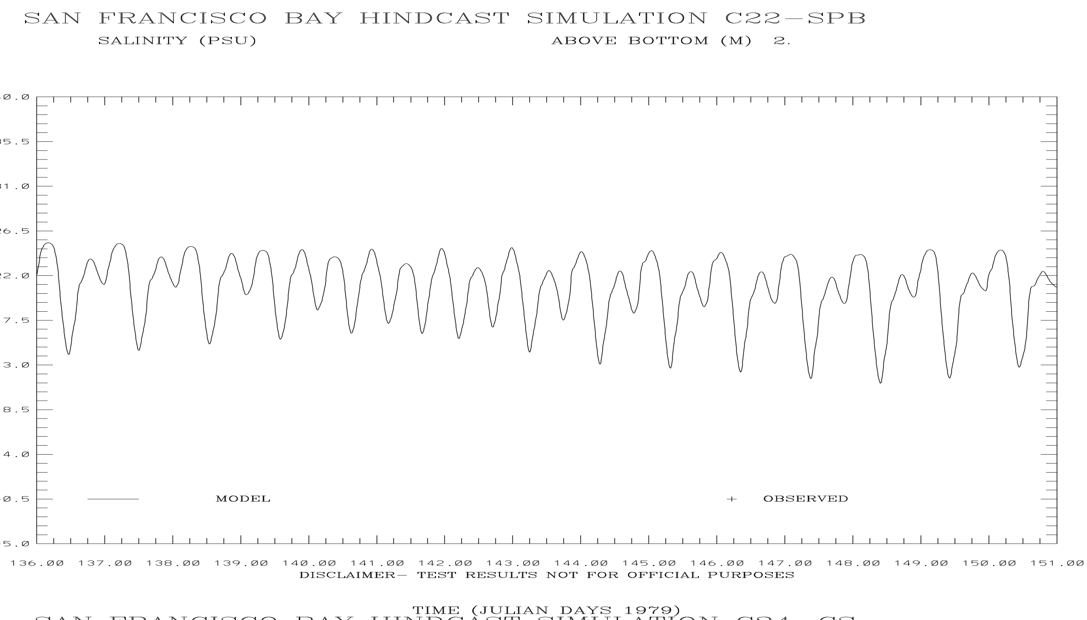

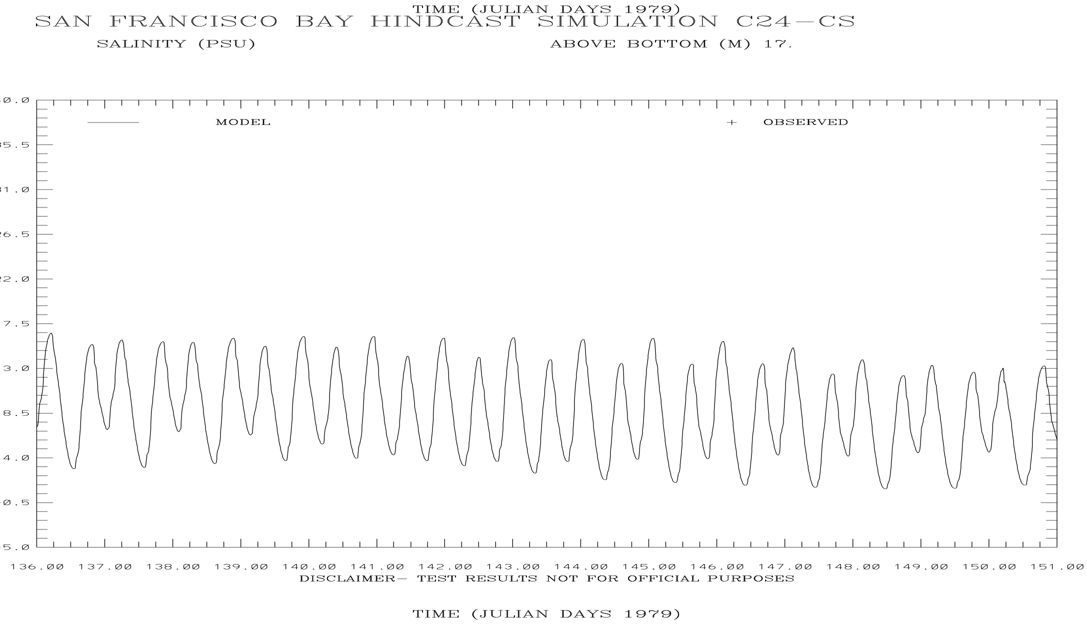

Figure 4.21. May 15-31, 1979 Hindcast: Salinity at C-22 at 2m and C-24 at 17m above the bottom. Note IND AGRMT equals one minus Willmott et al. (1985) relative error.

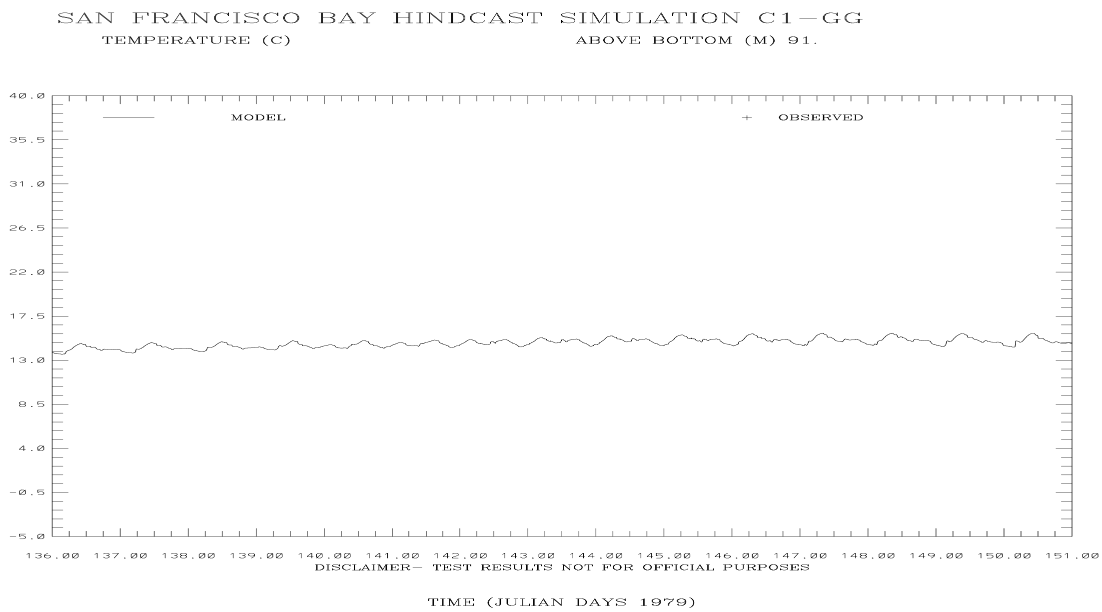

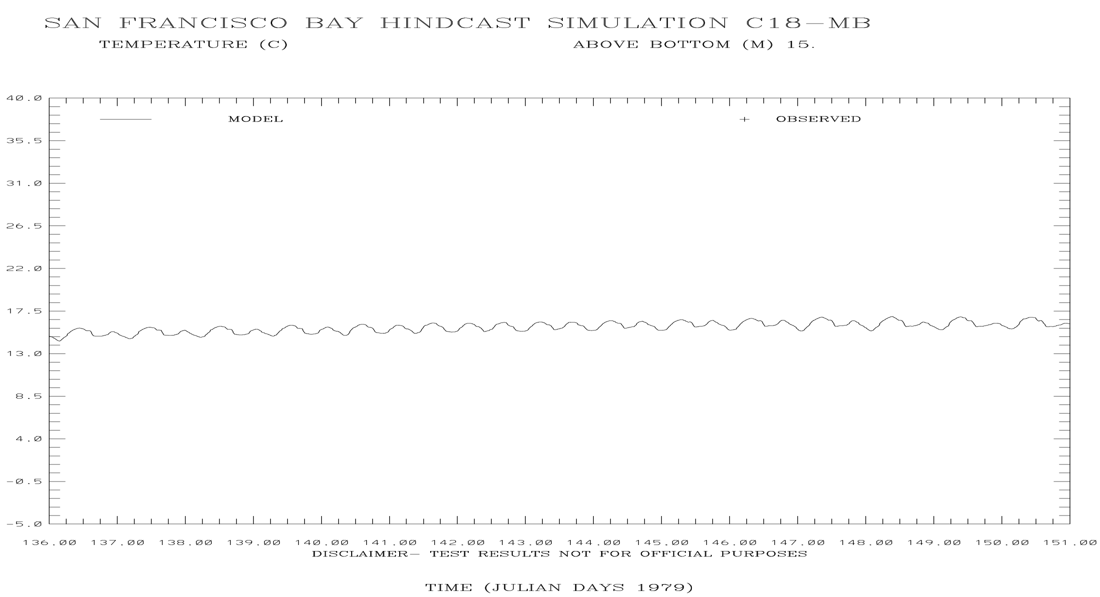

Figure 4.22. May 15-31, 1979 Hindcast: Temperature at C-1 at 91m and C-18 at 15m above the bottom. Note IND AGRMT equals one minus Willmott et al. (1985) relative error.

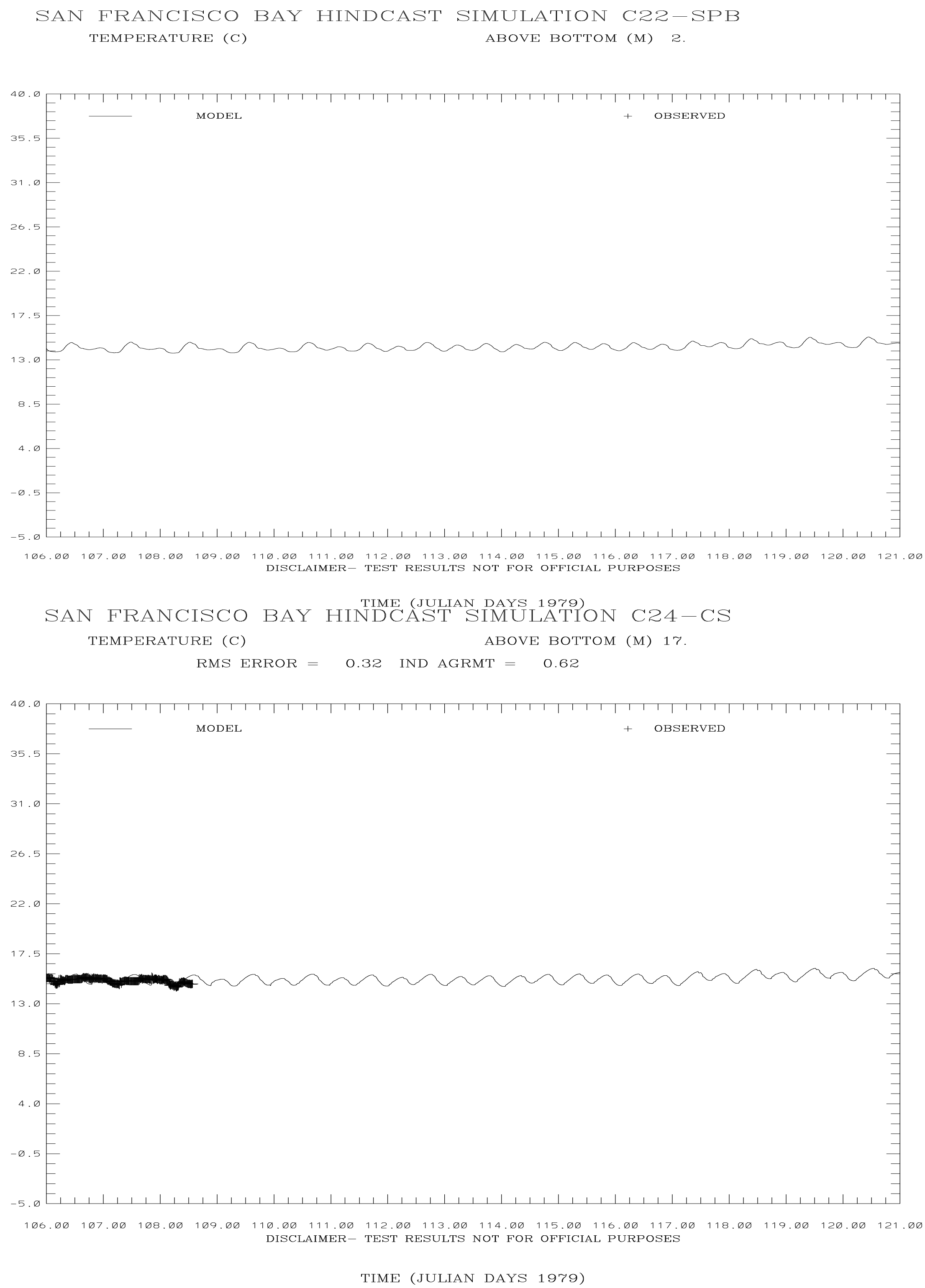

Figure 4.23. May 15-31, 1979 Hindcast: Temperature at C-22 at 2m and C-24 at 17m above the bottom. Note IND AGRMT equals one minus Willmott et al. (1985) relative error.

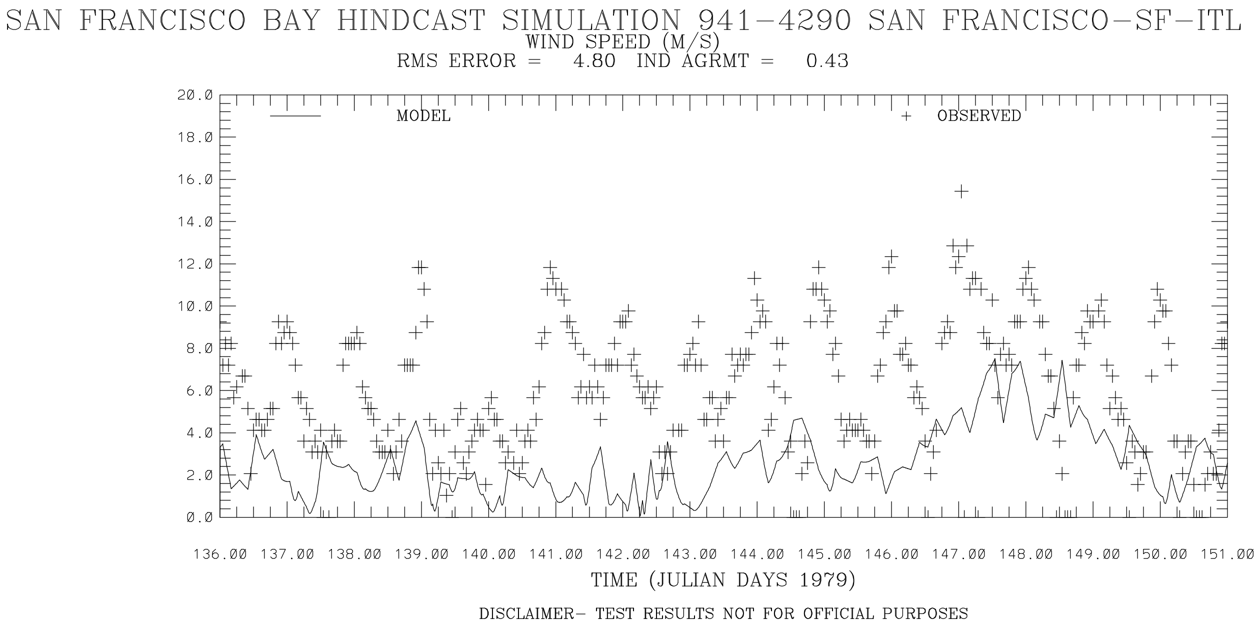

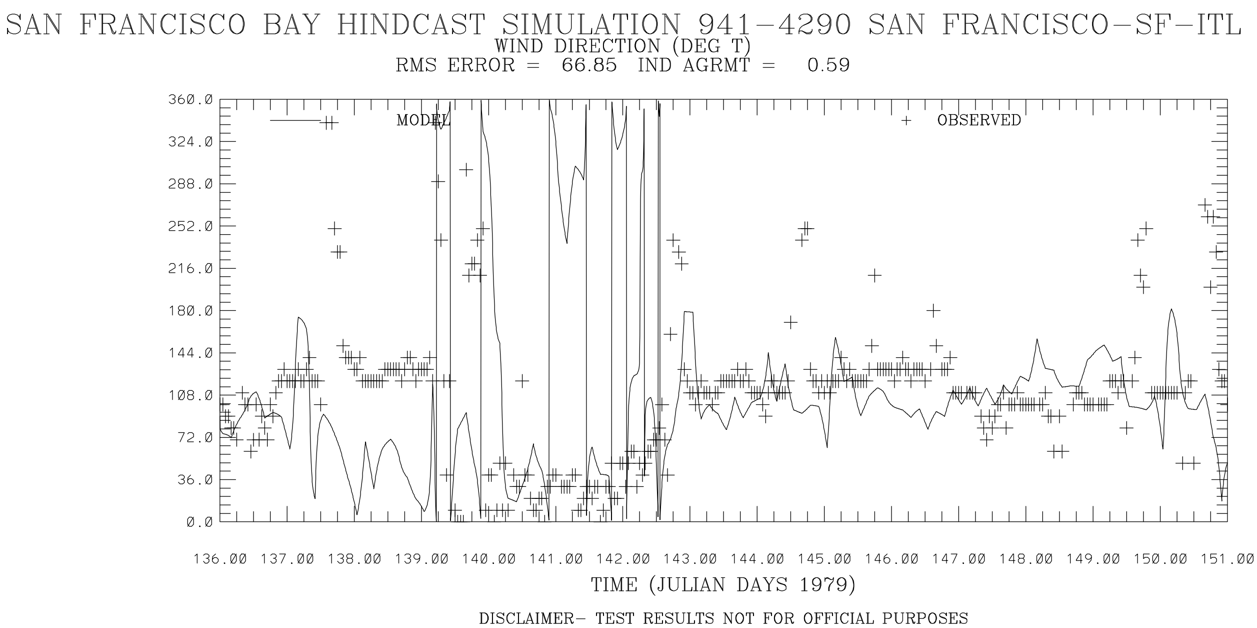

Figure 4.24. May 15-31, 1979 Hindcast: Wind speed and direction at San Francisco International Airport. Note IND AGRMT equals one minus Willmott et al. (1985) relative error.

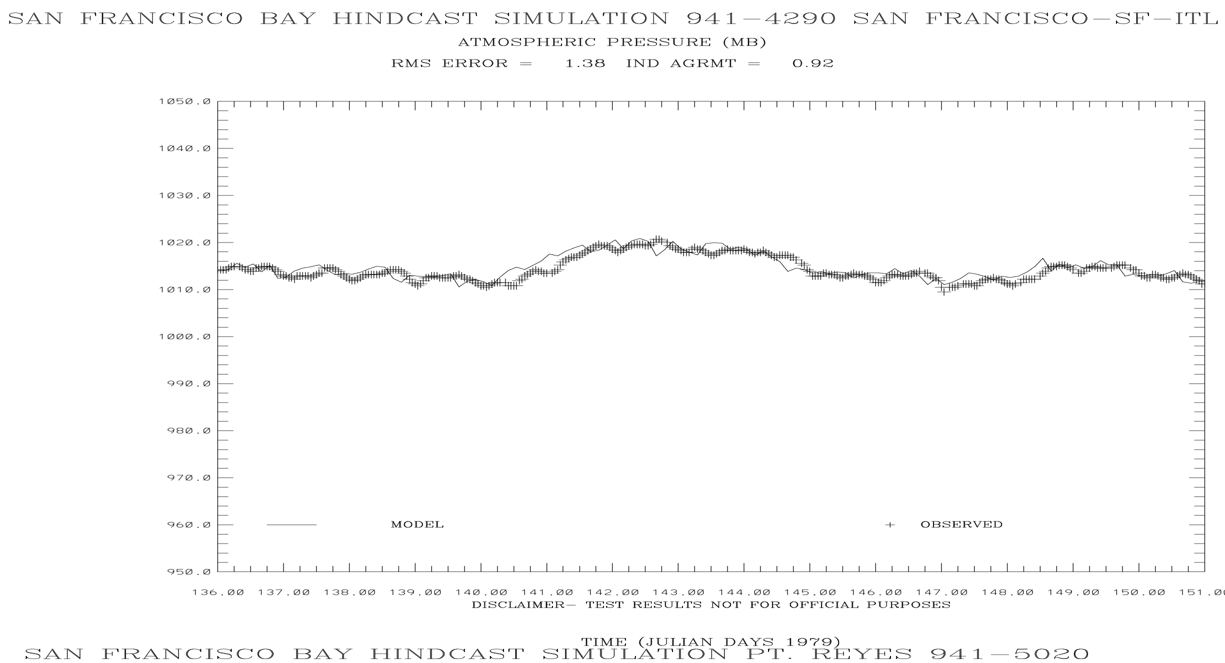

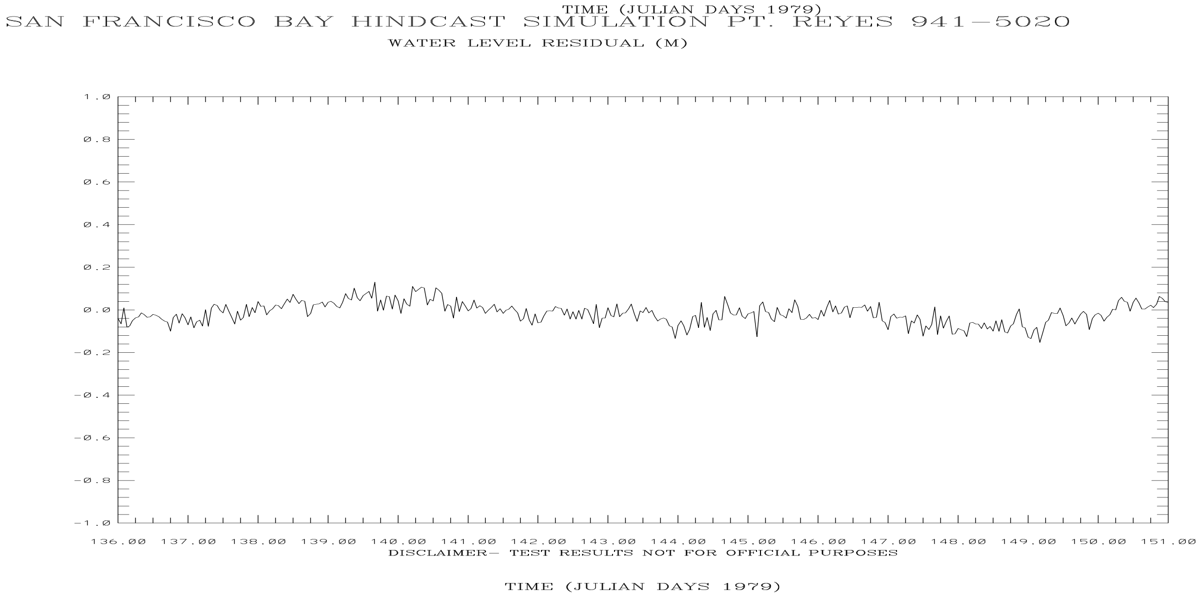

Figure 4.25. May 15-31, 1979 Hindcast: Atmospheric Pressure at San Francisco International Airport and Water Level Residual at Point Reyes. Note IND AGRMT equals one minus Willmott et al. (1985) relative error.

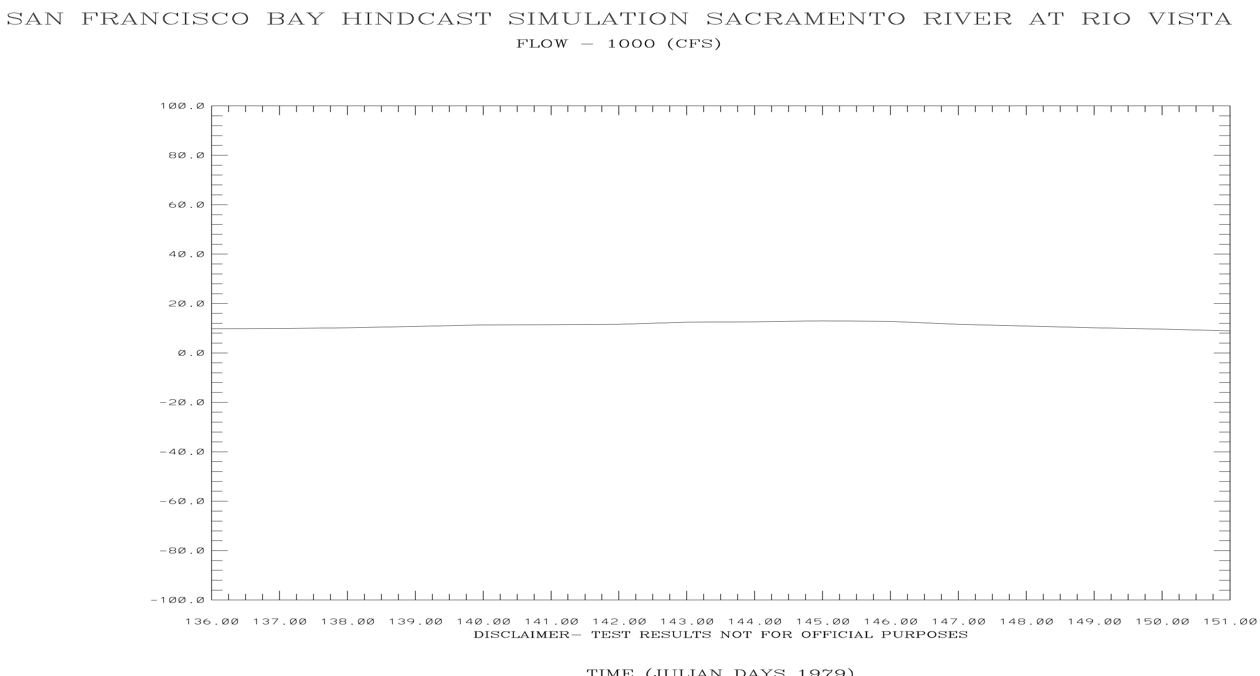

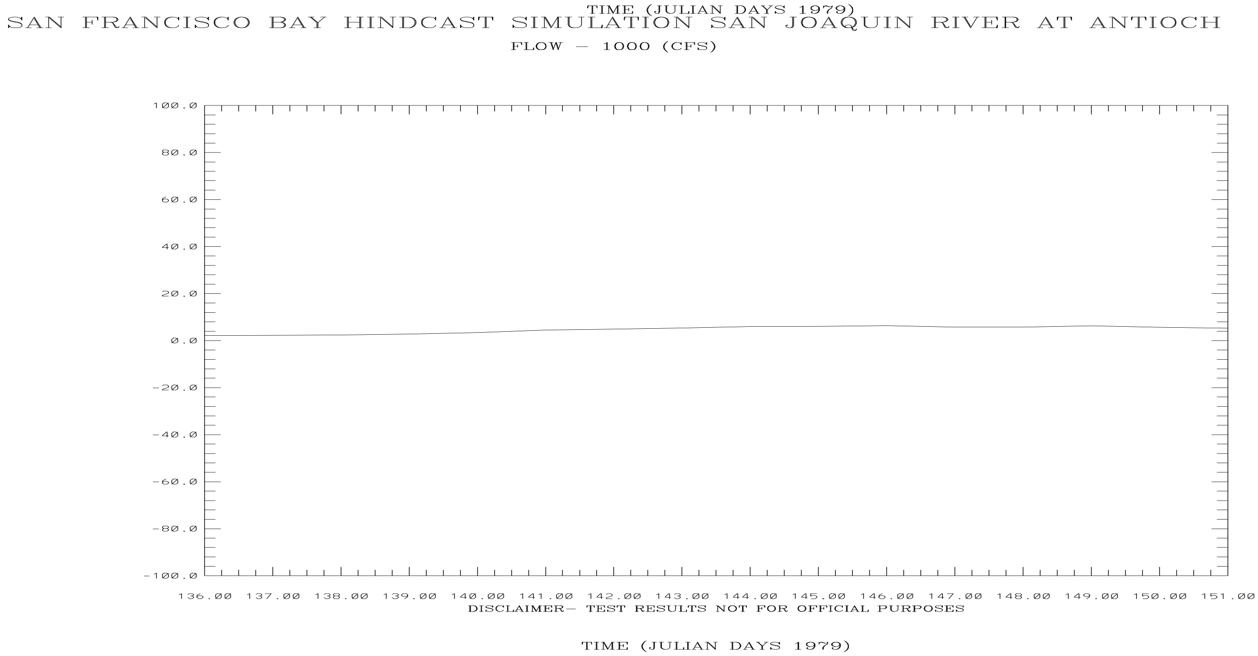

Figure 4.26. May 15-31, 1979 Hindcast: Flow (Thousands of CFS) on the Sacramento River at Rio Vista, CA and on the San Joaquin River at Antioch, CA.

4.2 September – October 1980 Simulation

Results are presented in 15 day increments in Table 4.7 for water levels, in Tables 4.8 and 4.9 for current speed and direction, in Table 4.10 for salinity, and in Table 4.11 for temperature. The NARR atmospheric forcing variables are compared to meteorological observations at San Francisco International Airport in Table 4.12. Note winds have not been corrected to 10 m and are stronger than the NARR model winds. Wind directions and sea level atmospheric pressure observations correspond well with the NARR model predictions. In general, there are fewer stations available with measured data for comparison than for the tidal simulation. For the offshore temperature and salinity, a zero gradient boundary condition is used.

Water levels at Port Chicago and Point Reyes are shown in Figures 4.27 and 4.40. Water levels at San Francisco and San Mateo Bridge are displayed in Figures 4.28 and 4.41.

Current speed and direction are shown at Station C-1 (Golden Gate Bridge) in Figures 4.29 and 4.42, at Station C-18 (mid-Bay) in Figures 4.30 and 4.43, at Station C-19 (San Pablo Bay) in Figures 4.31 and 4.44, and at C-24 (Carquinez Strait) in Figures 4.32 and 45.

Salinity is shown at Stations C-1 (Golden Gate Bridge) and C-18 (mid-Bay) in Figures 4.33 and 4.46, and at Stations C-22 (San Pablo Bay) and C-24 (Carquinez Strait) in Figures 4.34 and 4.47.

Temperature is shown at Stations C-1 (Golden Gate Bridge) and C-18 (mid-Bay) in Figures 4.35 and 4.48, and at Stations C-22 (San Pablo Bay) and C-24 (Carquinez Strait) in Figures 4.36 and 4.49.

Wind speed and wind direction at San Francisco International Airport are shown in Figures 4.37 and 4.50. Sea level atmospheric pressure at San Francisco International Airport and water level residual at Point Reyes are shown in Figures 4.38 and 4.51.

Flows on the Sacramento River at Rio Vista, CA and on the San Joaquin River at Antioch, CA are shown in Figures 4.39 and 4.52.

We briefly characterize each simulation month in turn.

September 1980: There are datum issues associated with the observed water levels at Oyster Point Marina, Pier 22.5, and at Dumbarton Bridge. At Point Reyes, San Francisco, and Alameda the RMS errors in water levels are near 8 cm with a Willmott et al. (1985) relative error of 0.01. At Port Chicago in Suisun Bay, the simulated water level range exceeds the observed range by 15 to 20 cm with a resulting RMS error from 20 to 23 cm. For salinity, temperature, and currents, the model response is examined at Stations C-16. C-211, and C-323 in the mid-Bay and at Station C-22 in San Pablo Bay. Salinity RMS errors are less than 0.5 PSU at most stations with temperature RMS errors less than 1.5 ^{o}C. Currents speed and direction RMS errors could not be assessed due to lack of observational data. In general, RMS wind speed errors are less than 5 m/s and direction RMS errors order 70 degrees. For sea level atmospheric pressure, the RMS errors are less than 3.3 mb. The water level residual at Point Reyes is small relative to the tidal amplitude and is less than 15 cm. River inflow from the Delta into San Francisco Bay ranged from 8,000 to 12,000 cfs.

October 1980: There are datum issues associated with the observed water levels at Dumbarton Bridge. At Point Reyes, San Francisco, and Alameda the RMS errors in water levels are near 7 cm with a Willmott et al. (1985) relative error of 0.01. At Port Chicago in Suisun Bay, the simulated water level range exceeds the observed range by 15 to 20 cm with a resulting RMS error from 20 to 23 cm. For salinity, temperature, and currents, the model response is examined at Station C-1 at the Golden Gate Bridge, at Station C-18 in the mid-Bay, at Stations C-19, C-23, and C-316 in San Pablo Bay, and at Station C-24 in Carquinez Strait. Salinity RMS errors are less than 1.0 PSU at all stations outside of Suisun Bay and Carquinez Strait, where the model prediction is too fresh by order 3 to 4 PSU. Temperature RMS errors are less than 1.0 ^{o}C at most stations. Currents speed and direction RMS errors are order 26 cm/s and 30 degrees, respectively. In general, RMS wind speed errors are less than 5 m/s, with direction RMS errors order 70 degrees. For sea level atmospheric pressure, the RMS errors are less than 3.3 mb. The water level residual at Point Reyes is small relative to the tidal amplitude and is less than 15 cm. River inflow from the Delta into San Francisco Bay ranged from 6,000 to 10,000 cfs.

Table 4.7 Water Surface Elevation Hindcast Validation September –October 1980. For each row in each month, the first entry corresponds to the first 15 days of the month, with the second entry denoting the remaining portion of the month. Row 1 corresponds to the RMSE in cm. Row 2 corresponds to the Willmott Relative Error in percent. Row 3 corresponds to the model mean in cm relative to MLLW with row 4 denoting the observed water level mean in cm relative to MLLW. Bold italics indicate measurement errors and their associated model discrepancies. Note n/a denotes not applicable due to lack of measurements.

Station	Sep		Oct	
Alameda	8	7	7	6
941-4750	1	0	0	0
	107	109	109	101
	105	107	107	98
Dumbarton	***335***	***336***	***336***	***337***
Bridge	***68***	***66***	***69***	***66***
941-4509	142	143	143	135
	-193	***-192***	***-192***	***-201***
Oyster Point	***77***	n/a	n/a	n/a
Marina	***35***	n/a	n/a	n/a
941-4392	117	119	119	111
	89	n/a	n/a	n/a
Port Chicago	20	23	20	23
941-5144	4	5	4	5
	79	83	82	74
	77	77	76	66
Point Reyes	7	5	7	6
941-5020	1	0	0	0
	96	97	97	89
	95	96	96	87
San	8	6	7	8
Francisco	1	0	0	0
941-4290	97	98	98	89
	95	96	96	87
Pier 22.5	***59***	n/a	n/a	n/a
941-4317	***22***	n/a	n/a	n/a
	101	102	103	94
	146	n/a	n/a	n/a
San Mateo	n/a	n/a	n/a	n/a
Bridge	n/a	n/a	n/a	n/a
941-4458	128	130	130	122
	n/a	n/a	n/a	n/a

Table 4.8 Current Speed Hindcast Validation: September - October 1980. For each row in each month, the first entry corresponds to the first 15 days of the month, with the second entry denoting the remaining portion. Row 1 corresponds to the RMSE in cm/s. Row 2 corresponds to the Willmott Relative Error in percent. Row 3 corresponds to the model mean in cm/s with row 4 denoting the observed mean current speed in cm/s. Note n/a denotes not applicable.

Station	Sep 1980	Oct 1980
C-1 (76) GG	16 12 4 5 73 77 77 50	n/a n/a n/a n/a 70 77 n/a n/a
C-16 (8) MB	15 17 12 14 47 49 45 47	n/a n/a n/a n/a 47 50 n/a n/a
C-16 (17) MB	12 15 6 8 51 54 49 49	n/a n/a n/a n/a 51 52 n/a n/a
C-16 (23) MB	13 16 7 9 52 55 50 50	n/a n/a n/a n/a 53 55 n/a n/a
C-18 (9) MB	n/a 19 n/a 8 63 67 n/a 74	17 15 8 6 64 67 64 52
C-18 (15) MB	n/a 17 n/a 4 77 82 n/a 83	19 14 6 4 79 83 71 55

Table 4.8 (Cont.). Current Speed Hindcast Validation September –October 1980. For each row in each month, the first entry corresponds to the first 15 days of the month, with the second entry denoting the remaining portion. Row 1 corresponds to the RMSE in cm/s. Row 2 corresponds to the Willmott Relative Error in percent. Row 3 corresponds to the model mean in cm/s with row 4 denoting the observed mean current speed in cm/s. Note n/a denotes not applicable.

Station	Sep 1980	Oct 1980
C-19 (1) SPB	9 15 11 18 36 38 28 29	11 n/a 14 n/a 36 38 25 n/a
C-22 (2) SPB	17 18 18 13 48 51 36 37	n/a n/a n/a n/a 48 51 n/a n/a
C-23 (1) SPB	n/a 6 n/a 22 18 19 n/a 18	6 4 23 17 18 19 17 12
C-24 (2) CS	n/a 16 n/a 14 50 51 n/a 44	22 n/a 29 n/a 49 51 37 n/a
C-24 (17,11) CS	n/a 28 n/a 14 n/a 83 n/a 77	35 n/a 28 n/a 81 83 72 n/a
C-26 (2) SB	n/a n/a n/a n/a 48 50 n/a n/a	n/a 25 n/a 38 48 50 n/a 37

Table 4.9 Current Direction Hindcast Validation: September-October 1980. For each row in each month, the first entry corresponds to the first 15 days of the month, with the second entry denoting the remaining portion. Row 1 corresponds to the RMSE in degrees. Row 2 corresponds to the Willmott Relative Error in percent. Row 3 corresponds to the model mean in degrees with row 4 denoting the observed mean current direction in degrees. Note n/a denotes not applicable.

Station	Sep 1980	Oct 1980
C-1 (76) GG	28 33 2 5 173 172 152 104	n/a n/a n/a n/a 171 171 n/a n/a
C-16 (8) MB	15 17 12 1 147 145 139 130	n/a n/a n/a n/a 140 143 n/a n/a
C-16 (17) MB	12 18 6 1 147 146 158 148	n/a n/a n/a n/a 140 143 n/a n/a
C-16 (23) MB	13 22 7 1 149 148 162 155	n/a n/a n/a n/a 147 148 n/a n/a
C-18 (9) MB	n/a 15 n/a 1 112 105 n/a 102	13 15 0 6 104 102 97 ***31***
C-18 (15) MB	n/a 12 n/a 0 119 120 n/a 106	14 14 1 4 120 121 109 ***22***

Table 4.9 (Cont.). Current Direction Hindcast Validation September –October 1980. For each row in each month, the first entry corresponds to the first 15 days of the month, with the second entry denoting the remaining portion. Row 1 corresponds to the RMSE in degrees. Row 2 corresponds to the Willmott Relative Error in percent. Row 3 corresponds to the model mean in degrees with row 4 denoting the observed mean current direction in degrees. Note n/a denotes not applicable.

Station	Sep 1980	Oct 1980
C-19 (1) SPB	9 16 11 1 113 112 237 246	16 n/a 1 n/a 113 112 227 n/a
C-22 (2) SPB	17 34 18 4 139 139 149 156	n/a n/a n/a n/a 137 143 n/a n/a
C-23 (1) SPB	n/a 11 n/a 78 151 149 n/a 242	16 4 1 17 150 147 143 n/a
C-24 (2) CS	n/a 26 n/a 3 179 179 n/a 187	29 n/a 3 n/a 178 178 172 n/a
C-24 (17,11) CS	n/a 19 n/a 1 193 194 n/a 194	36 n/a 4 n/a 195 194 191 n/a
C-26 (2) SB	n/a n/a n/a n/a 155 156 n/a n/a	n/a 25 n/a 38 156 155 n/a 129

Table 4.10 Salinity Hindcast Validation: September-October 1980. For each row in each month, the first entry corresponds to the first 15 days of the month, with the second entry denoting the remaining portion. Row 1 corresponds to the RMSE in PSU. Row 2 corresponds to the Willmott Relative Error in percent. Row 3 corresponds to the model mean in PSU with row 4 denoting the observed salinity mean in PSU. Note n/a denotes not applicable.

Station	Sep 1980	Oct 1980
C-1 (46) GG	n/a 1 n/a 36 32 31 n/a 32	1 n/a 41 n/a 31 31 32 n/a
C-1 (91,76) GG	n/a n/a n/a n/a 32 31 n/a n/a	n/a n/a n/a n/a 31 31 n/a n/a
C-16 (8) MB	0 3 12 61 31 31 32 32	n/a n/a n/a n/a 30 29 n/a n/a
C-16 (17) MB	0 0 8 5 31 31 31 31	n/a n/a n/a n/a 30 30 n/a n/a
C-16 (23) MB	0 0 4 4 31 30 31 31	n/a n/a n/a n/a 30 30 n/a n/a
C-18 (9) MB	n/a 1 n/a 4 29 27 n/a 27	1 1 11 22 26 26 27 28
C-18 (15) MB	n/a 1 n/a 4 28 27 n/a 27	1 1 8 4 26 26 27 26

Table 4.10 (Cont.). Salinity Hindcast Validation September-October 1980. For each row in each month, the first entry corresponds to the first 15 days of the month, with the second entry denoting the remaining portion. Row 1 corresponds to the RMSE in PSU. Row 2 corresponds to the Willmott Relative Error in percent. Row 3 corresponds to the model mean in PSU with row 4 denoting the observed salinity mean in PSU. Note n/a denotes not applicable.

Station	Sep 1980	Oct 1980
C-19 (1) SPB	13 n/a 0 n/a 25 24 n/a n/a	n/a n/a n/a n/a 23 22 n/a n/a
C-22 (2) SPB	1 1 34 4 26 25 27 25	n/a n/a n/a n/a 23 23 n/a n/a
C-23 (1) SPB	n/a 3 n/a 89 22 19 n/a 21	3 2 73 81 18 18 21 19
C-24 (2,6) CS	n/a 5 n/a 34 19 16 n/a 20	7 n/a 47 n/a 14 15 20 n/a
C-24 (17,11) CS	n/a 4 n/a 28 18 16 n/a 19	6 n/a 42 n/a 13 14 19 n/a
C-26(2) SB	n/a n/a n/a n/a 11 7 n/a n/a	n/a 7 n/a 47 4 5 n/a 12

Table 4.11 Temperature Hindcast Validation: September- October 1980. For each row in each month, the first entry corresponds to the first 15 days of the month, with the second entry denoting the remaining portion. Row 1 corresponds to the RMSE in ^oC. Row 2 corresponds to the Willmott Relative Error in percent. Row 3 corresponds to the model mean in ^oC with row 4 denoting the observed temperature mean in ^oC. Note n/a denotes not applicable.

Station	Sep 1980	Oct 1980
C-1 (46,76) GG	1 2 64 57 16 17 15 15	2 n/a 60 n/a 16 16 15 n/a
C-16 (8) MB	1 1 63 59 17 17 16 16	n/a n/a n/a n/a 17 16 n/a n/a
C-16 (17) MB	1 1 57 52 17 17 16 16	n/a n/a n/a n/a 17 16 n/a n/a
C-16 (23) MB	1 1 54 48 17 17 16 16	n/a n/a n/a n/a 17 16 n/a n/a
C-18 (9) MB	n/a 1 n/a 25 17 18 n/a 17	1 1 25 57 18 17 17 16
C-18 (15) MB	n/a 0 n/a 20 18 18 n/a 18	1 1 23 49 18 17 18 16

Table 4.11 (Cont.). Temperature Hindcast Validation September–October 1980. For each row in each month, the first entry corresponds to the first 15 days of the month, with the second entry denoting the remaining portion. Row 1 corresponds to the RMSE in ^oC. Row 2 corresponds to the Willmott Relative Error in percent. Row 3 corresponds to the model mean in ^oC with row 4 denoting the observed temperature mean in ^oC. Bold italics indicate measurement errors and their associated model discrepancies. Note n/a denotes not applicable.

Station	Sep 1980	Oct 1980
C-19 (1) SPB	0 2 27 28 18 18 18 18	1 n/a 30 n/a 18 17 19 n/a
C-22 (2) SPB	0 1 25 35 18 18 18 18	n/a n/a n/a n/a 18 17 n/a n/a
C-23 (1) SPB	n/a 1 n/a 55 19 19 n/a 19	1 2 68 87 19 18 19 17
C-24 (2,6) CS	n/a 1 n/a 50 19 19 n/a 18	0 n/a 25 n/a 19 20 19 n/a
C-24 (17,11) CS	n/a 1 n/a 52 19 19 n/a 19	0 n/a 23 n/a 19 18 19 n/a
C-26 (2) SB	n/a n/a n/a n/a 19 19 n/a n/a	n/a 3 n/a 92 20 19 n/a 16

Table 4.12 NARR Atmospheric Forcings September-October 1980 at San Francisco International Airport. In each cell, row 1 corresponds to the RMSE, row 2 corresponds to the Willmott Relative Error, row 3 corresponds to the NARR model mean, and row 4 denotes the observed mean.

Parameter	1-15 September	15-30 September	1-15 October	15-31 October
Wind Speed (m/s)	5 58 2 6	5 57 2 5	4 56 2 5	4 60 2 4
Wind Direction (^{o}T)	70 53 87 123	79 73 125 126	74 46 120 125	74 61 142 134
Atmospheric Pressure (mb)	1 18 1015 1015	2 13 1015 1015	1 13 1016 1015	2 8 1020 1019

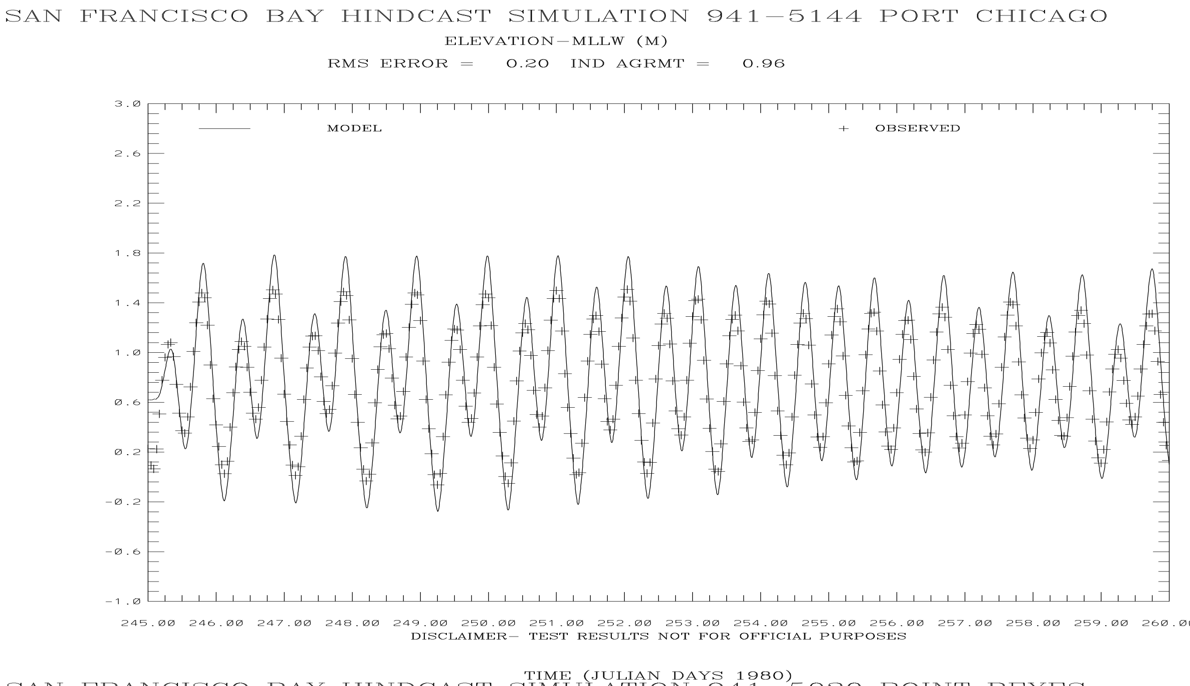

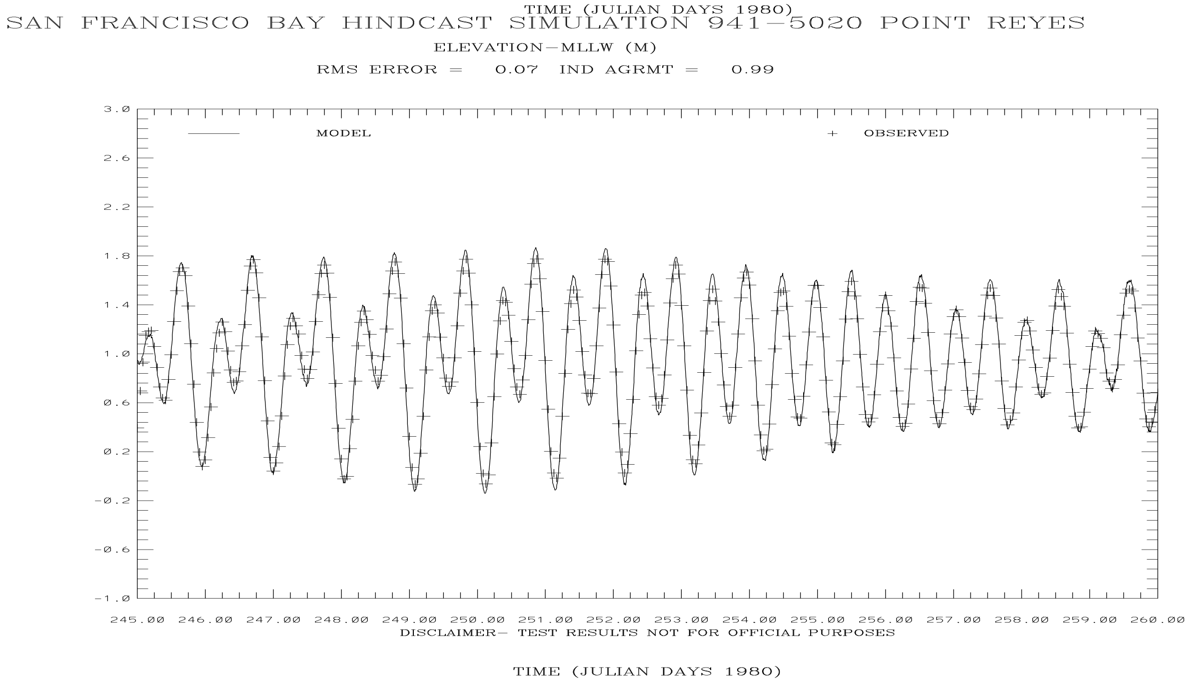

Figure 4.27. September 1-15, 1980 Hindcast: Port Chicago and Point Reyes Water Level Comparisons. Note IND AGRMT equals one minus Willmott et al. (1985) relative error.

SAN FRANCISCO BAY HINDCAST SIMULATION 941-4290 SAN FRANCISCO-SF-ITL
ELEVATION-MLLW (M)
RMS ERROR = 0.08 IND AGRMT = 0.99

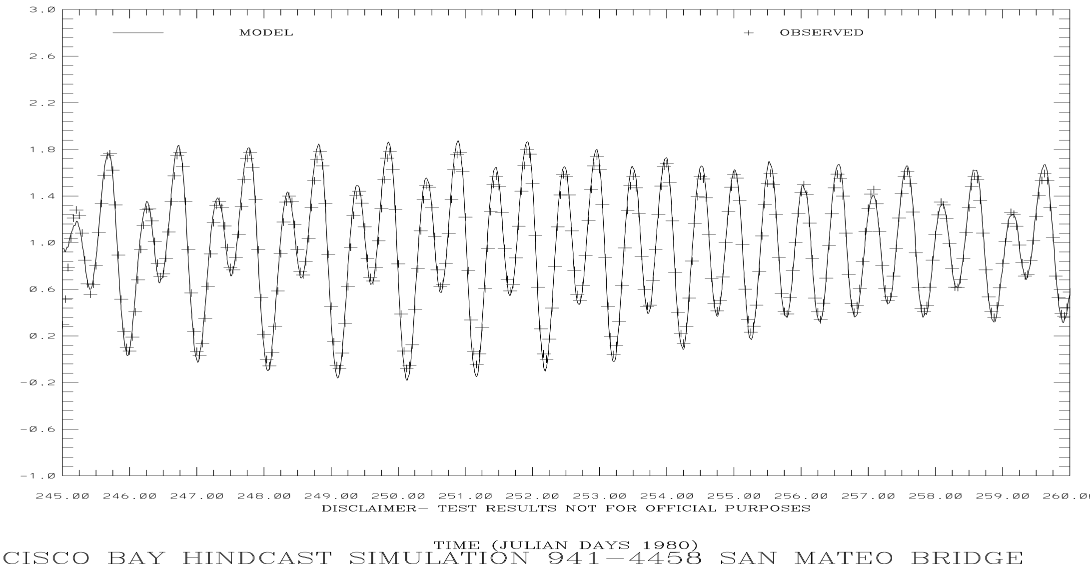

SAN FRANCISCO BAY HINDCAST SIMULATION 941-4458 SAN MATEO BRIDGE
ELEVATION-MLLW (M)

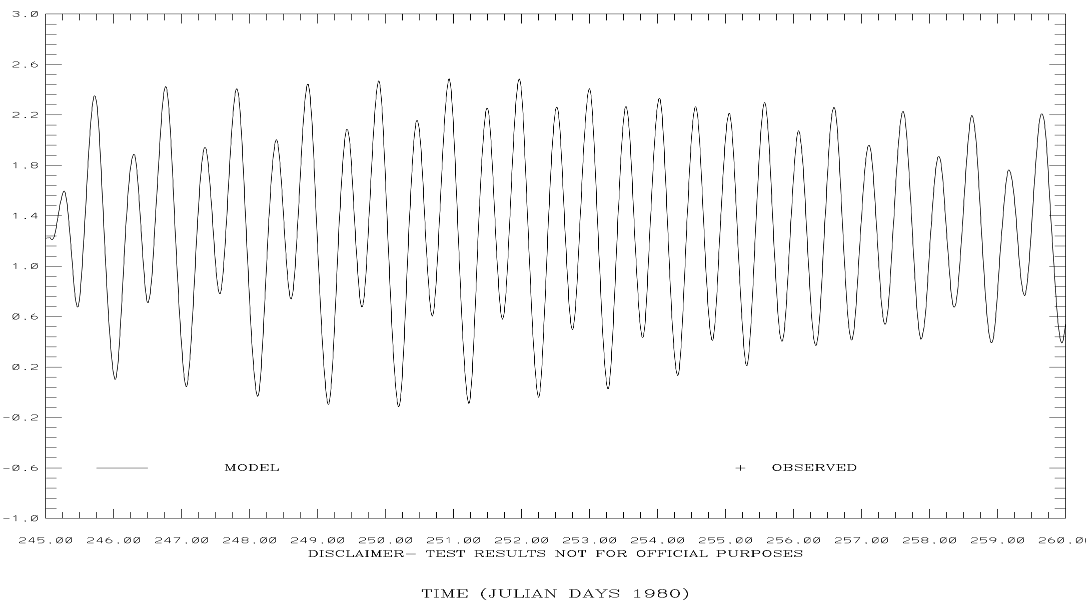

Figure 4.28. September 1-15, 1980 Hindcast: San Francisco and San Mateo Bridge Water Level Comparisons. Note IND AGRMT equals one minus Willmott et al. (1985) relative error.

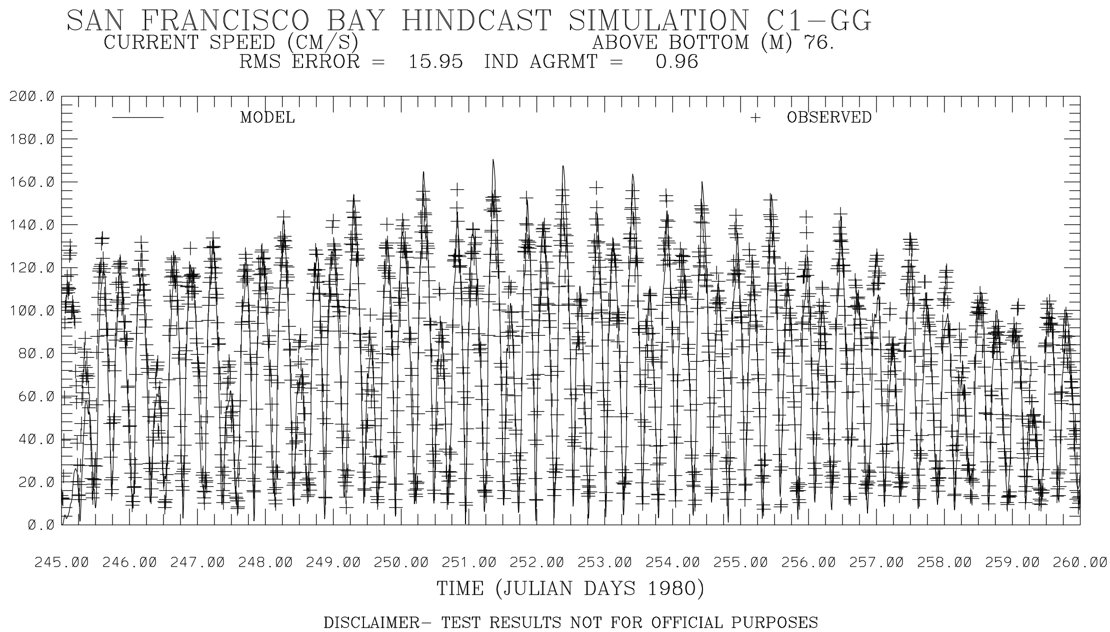

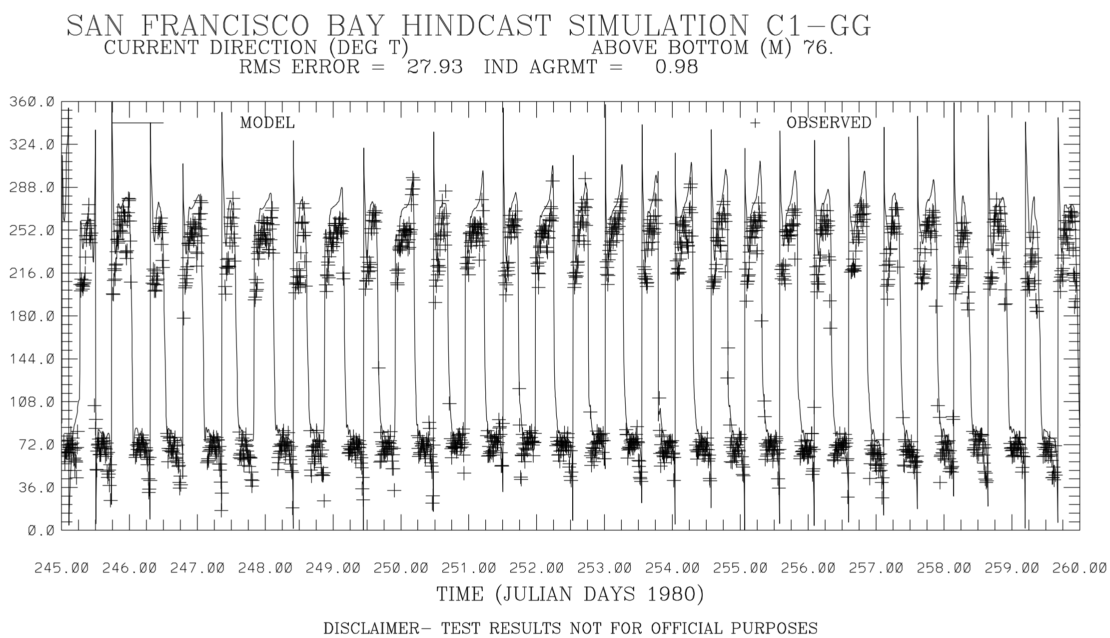

Figure 4.29. September 1-15, 1980 Hindcast: C-1 Current Speed and Direction at 91m above the bottom. Note IND AGRMT equals one minus Willmott et al. (1985) relative error.

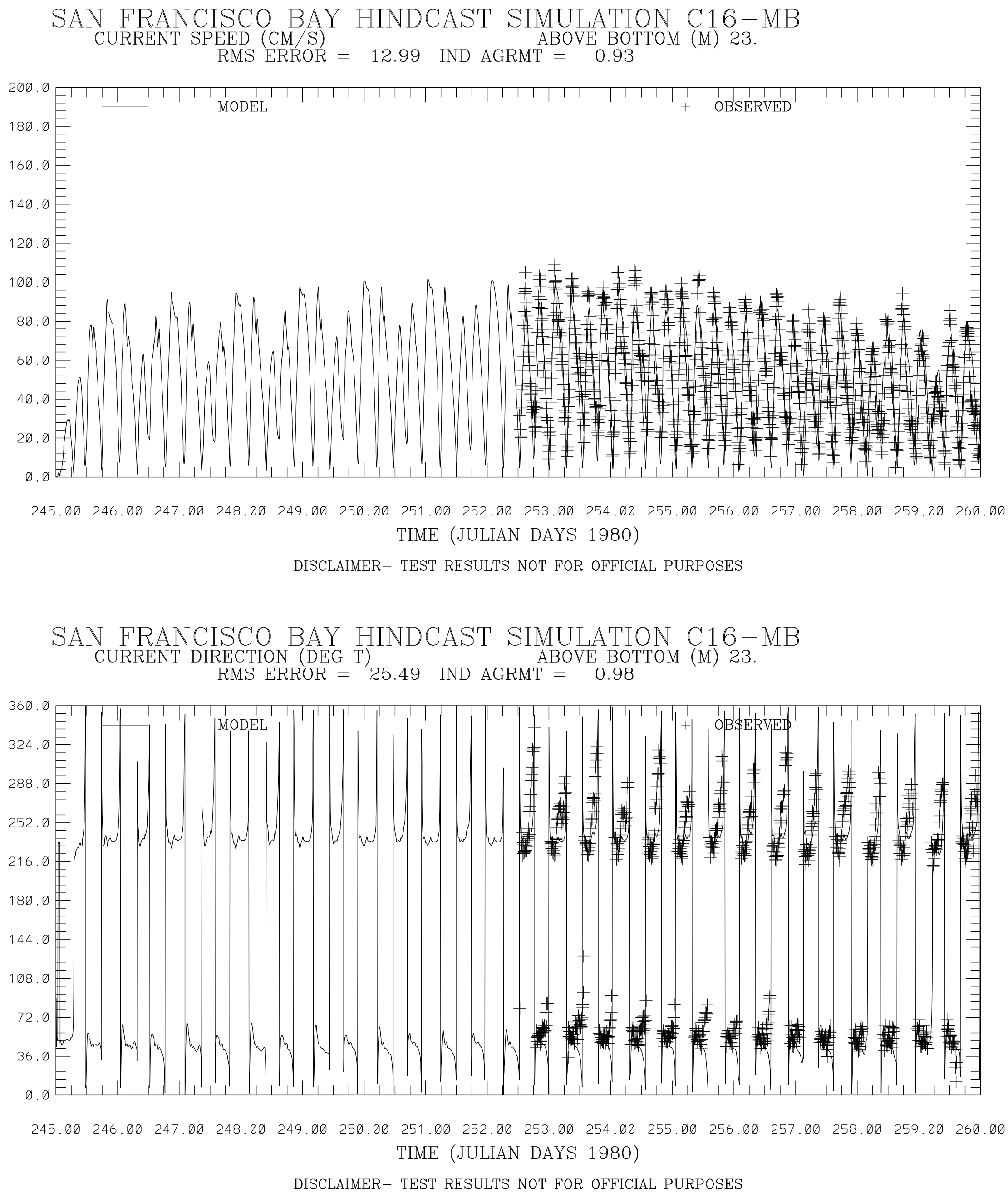

Figure 4.30. September 1-15, 1980 Hindcast: C-16 Current Speed and Direction at 23m above the bottom. Note IND AGRMT equals one minus Willmott et al. (1985) relative error.

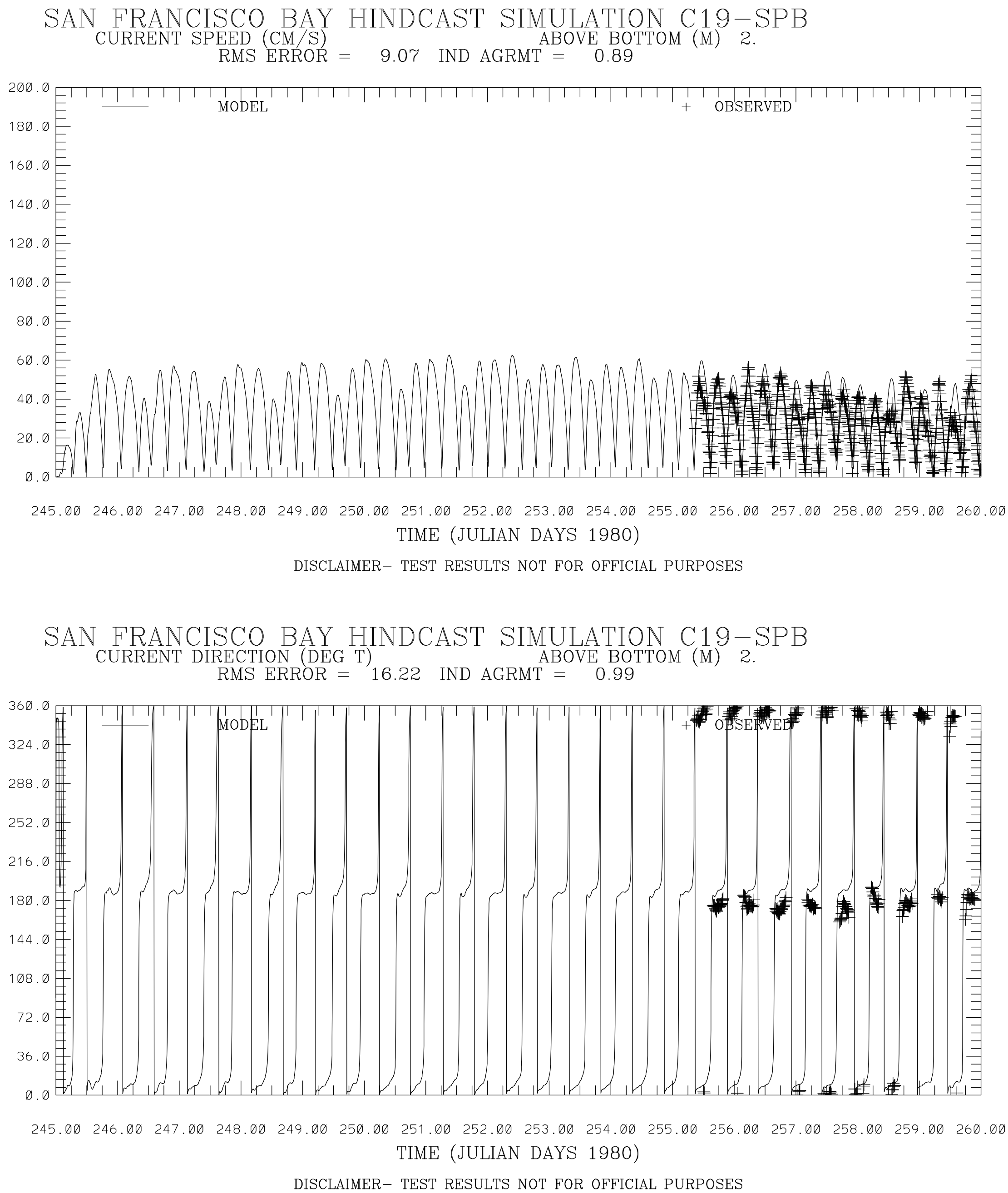

Figure 4.31. September 1-15, 1980 Hindcast: C-19 Current Speed and Direction at 2m above the bottom. Note IND AGRMT equals one minus Willmott et al. (1985) relative error.

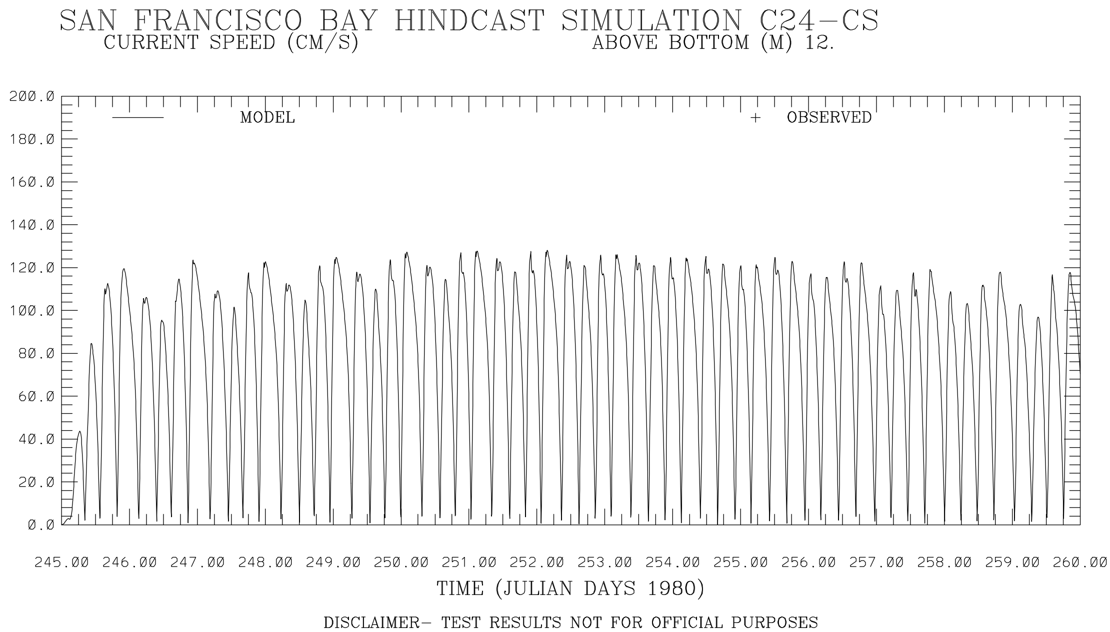

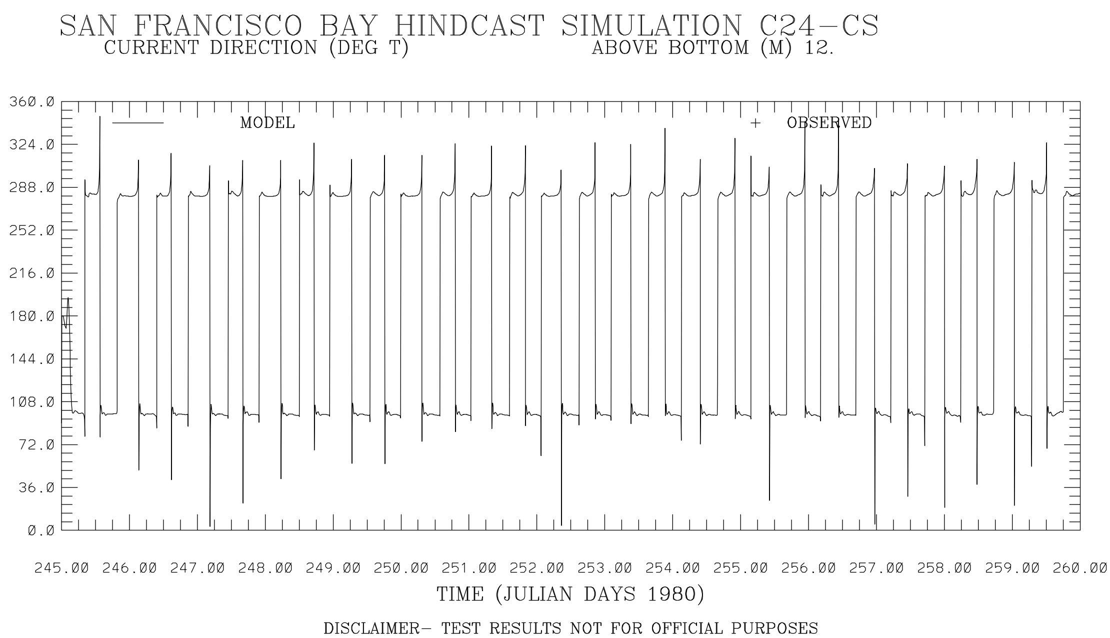

Figure 4.32. September 1-15, 1980 Hindcast: C-24 Current Speed and Direction at 12m above the bottom. Note IND AGRMT equals one minus Willmott et al. (1985) relative error.

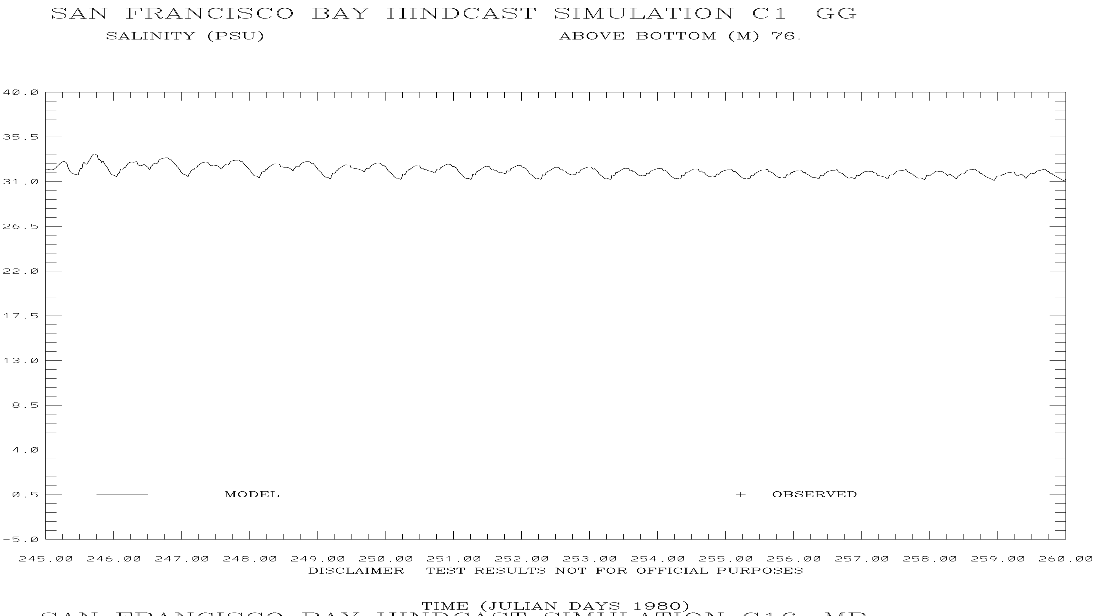

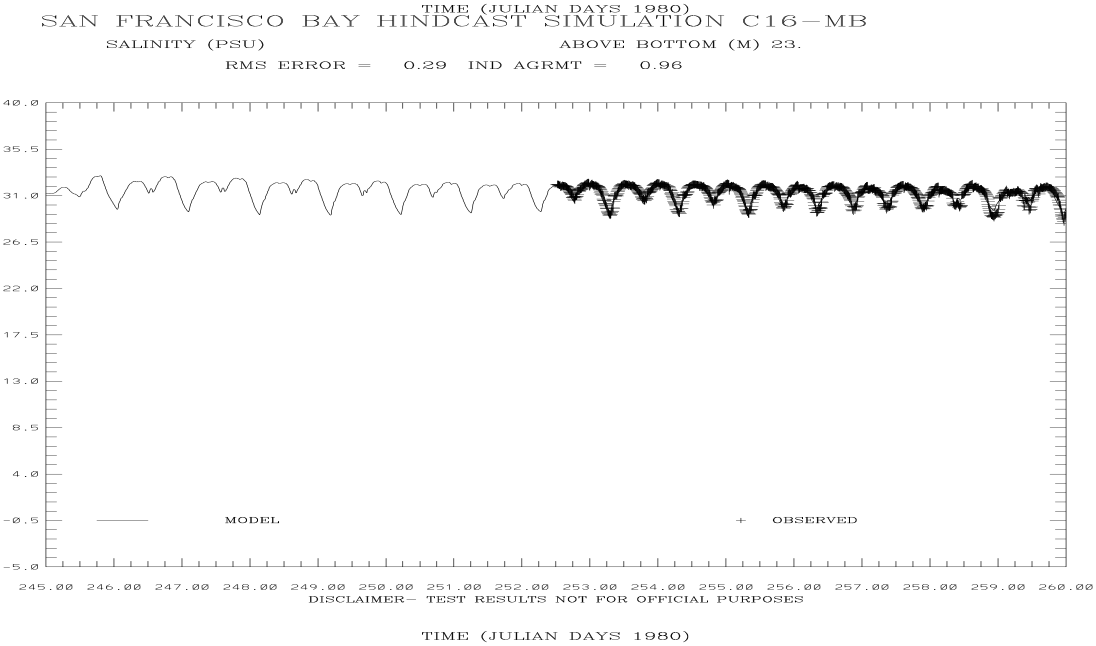

Figure 4.33. September 1-15, 1980 Hindcast: Salinity at C-1 at 46m and C-18 at 9m above the bottom. Note IND AGRMT equals one minus Willmott et al. (1985) relative error.

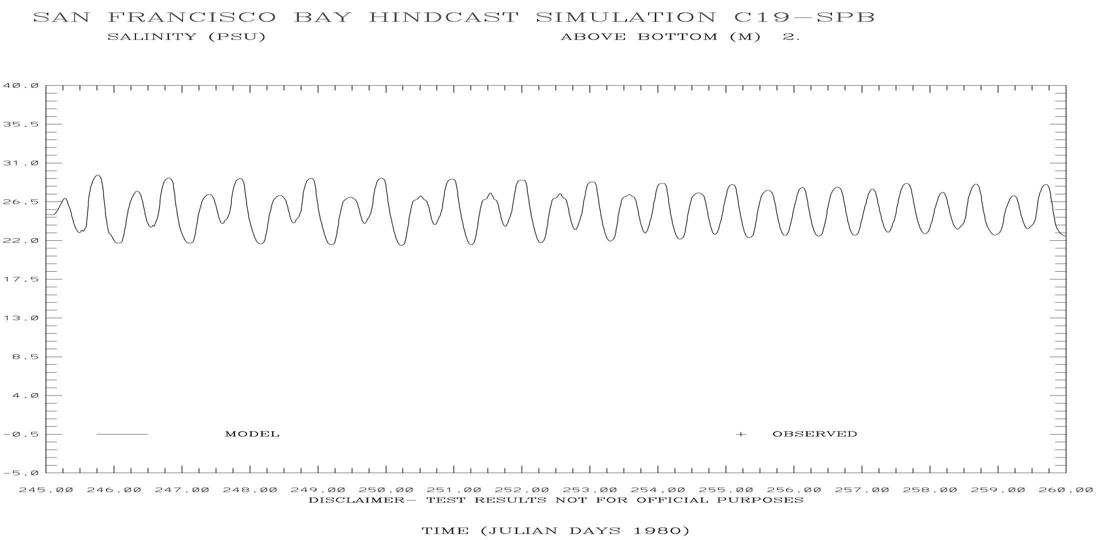

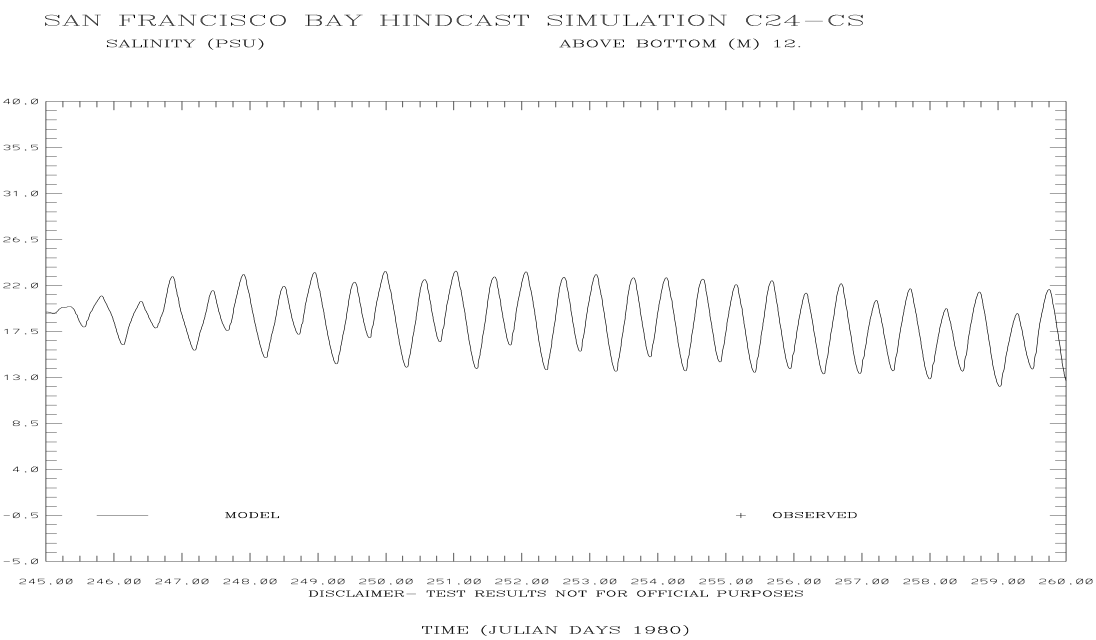

Figure 4.34. September 1-15, 1980 Hindcast: Salinity at C-22 at 2m and C-24 at 17m above the bottom. Note IND AGRMT equals one minus Willmott et al. (1985) relative error.

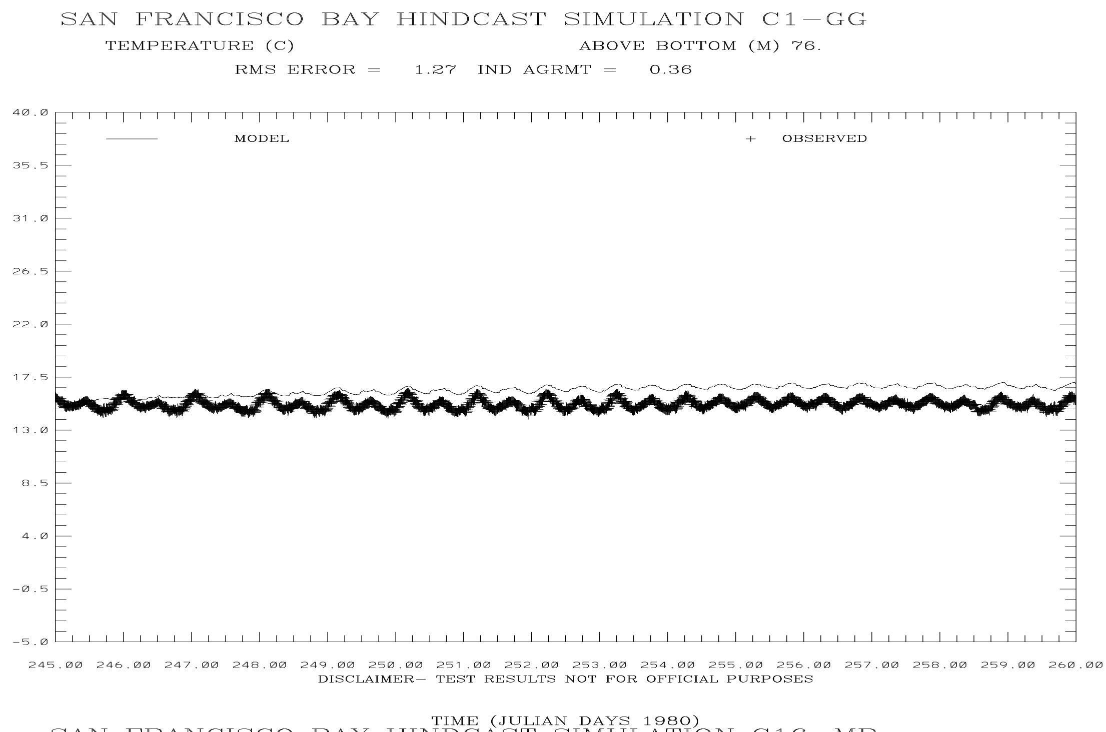

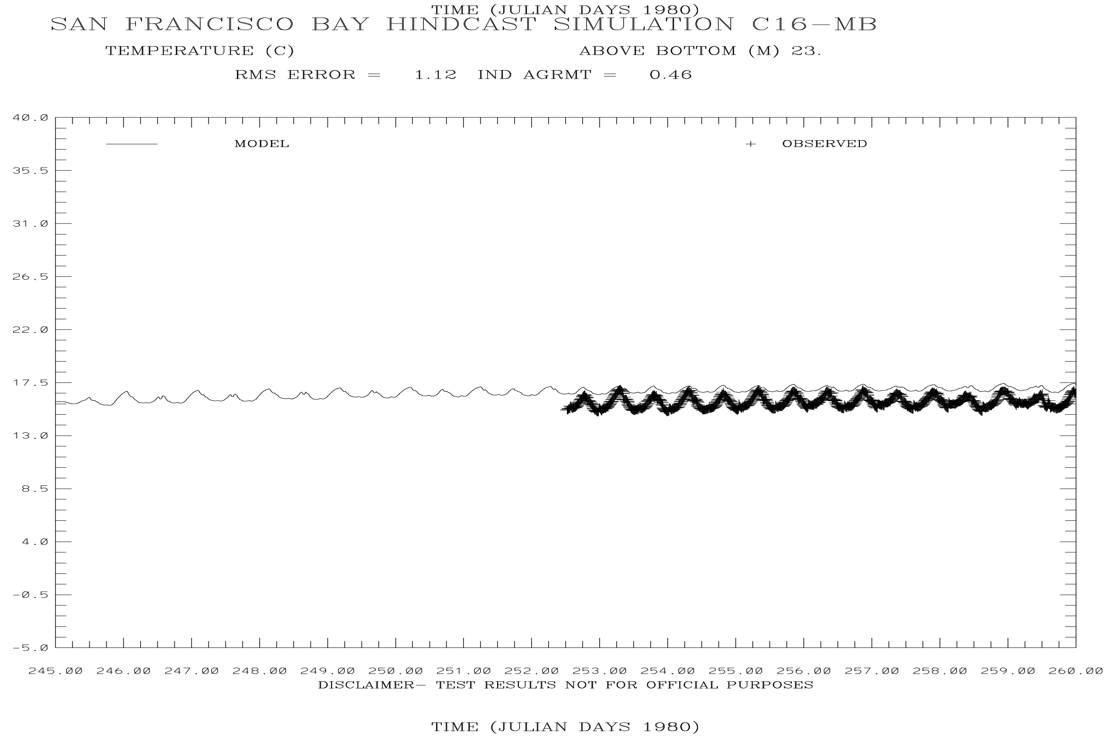

Figure 4.35. September 1-15, 1980 Hindcast: Temperature at C-1 at 76m and C-16 at 23m above the bottom. Note IND AGRMT equals one minus Willmott et al. (1985) relative error.

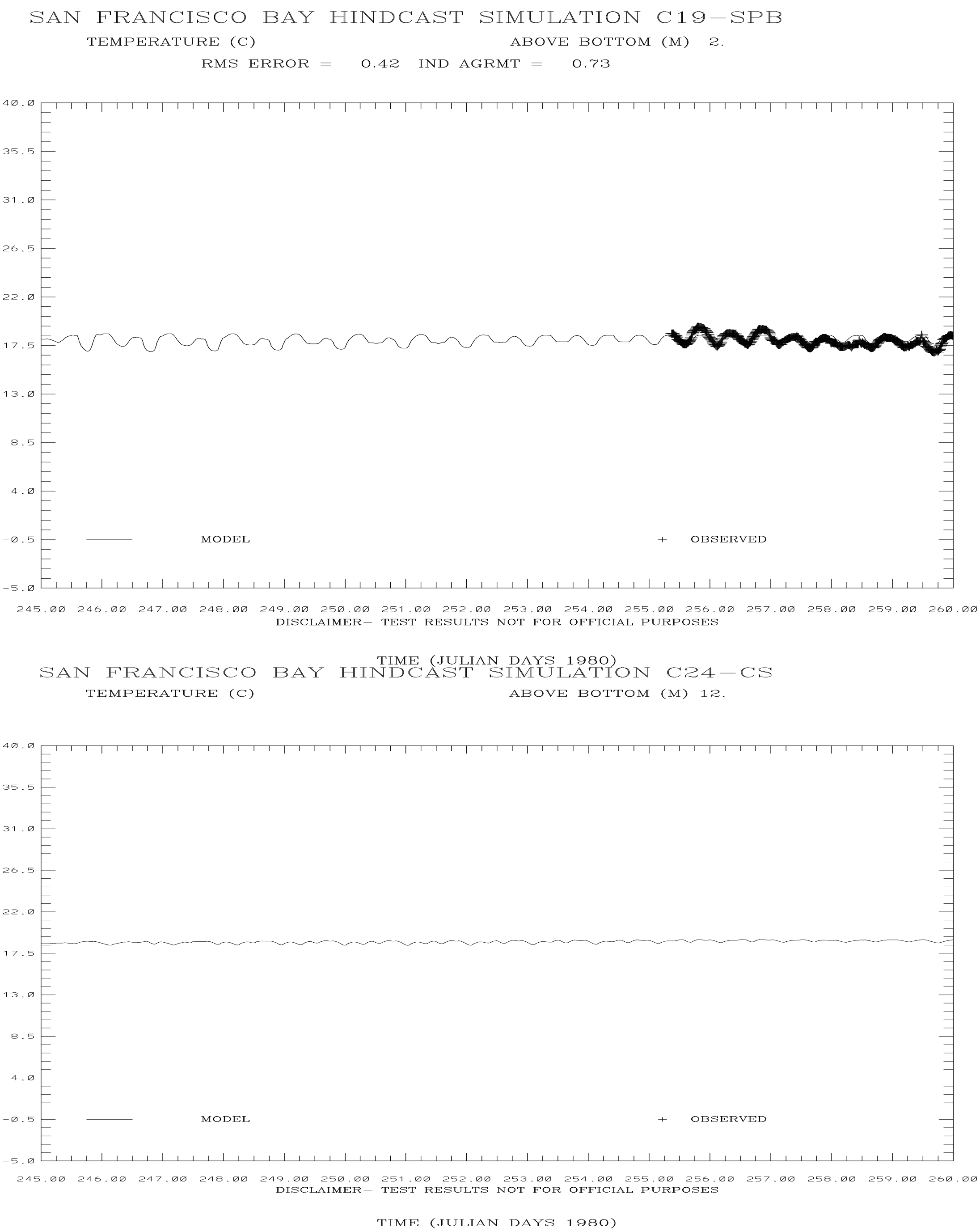

Figure 4.36. September 1-15, 1980 Hindcast: Temperature at C-19 at 2m and C-24 at 12m above the bottom. Note IND AGRMT equals one minus Willmott et al. (1985) relative error.

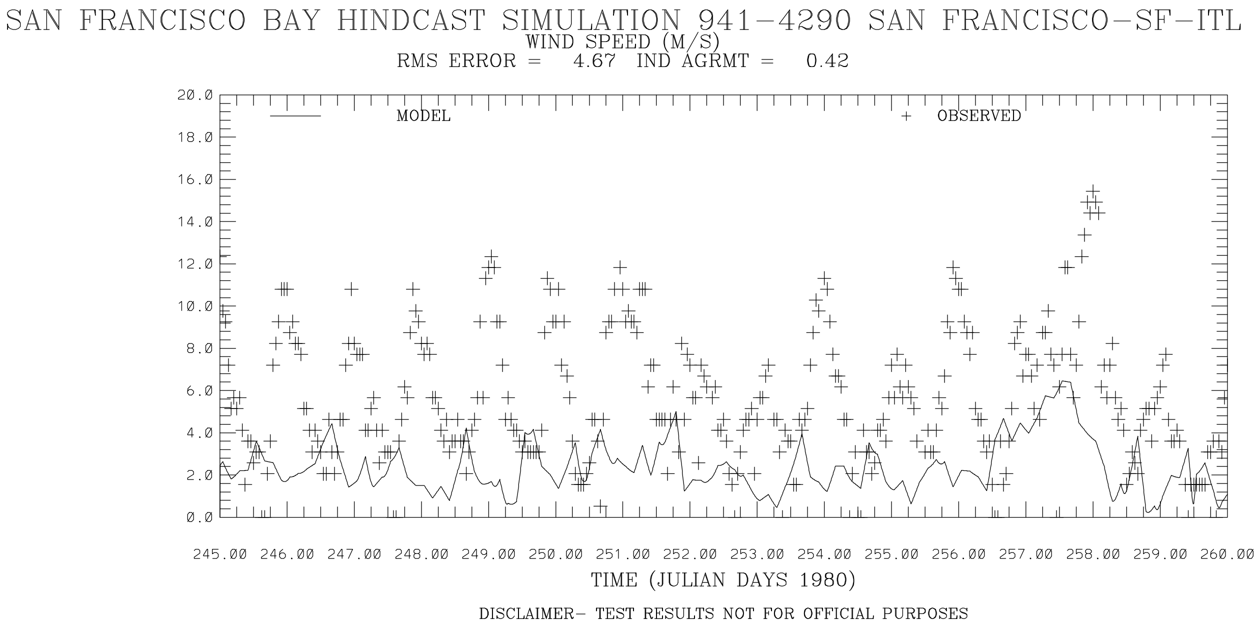

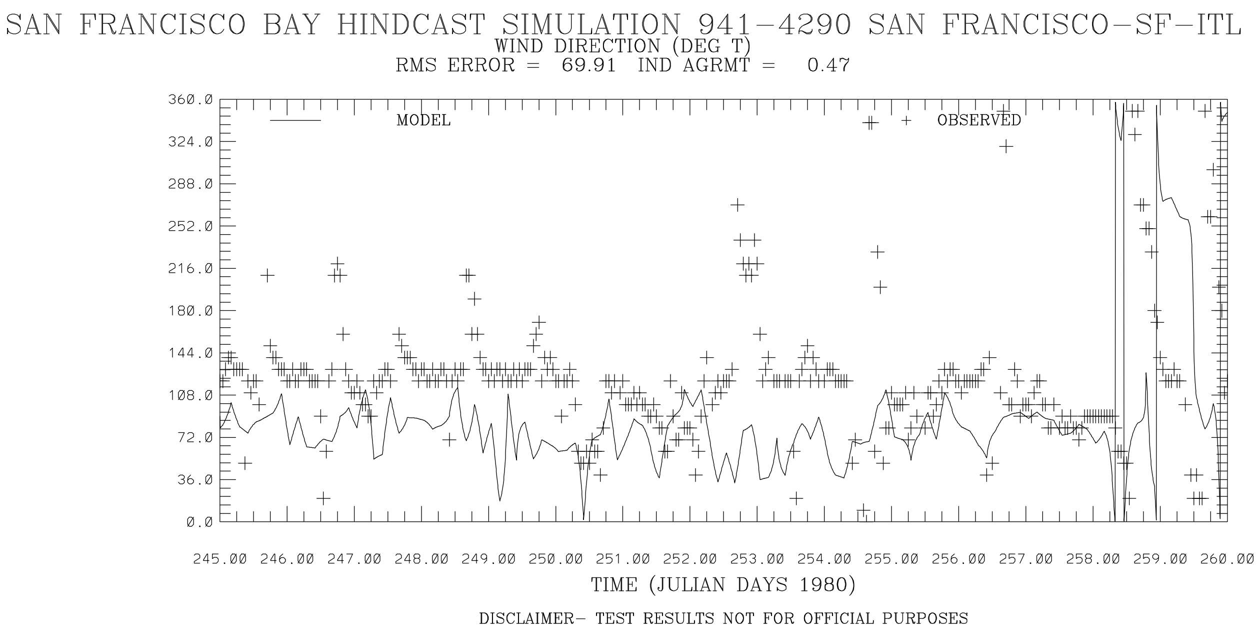

Figure 4.37. September 1-15, 1980 Hindcast: Wind speed and direction at San Francisco International Airport. Note IND AGRMT equals one minus Willmott et al. (1985) relative error.

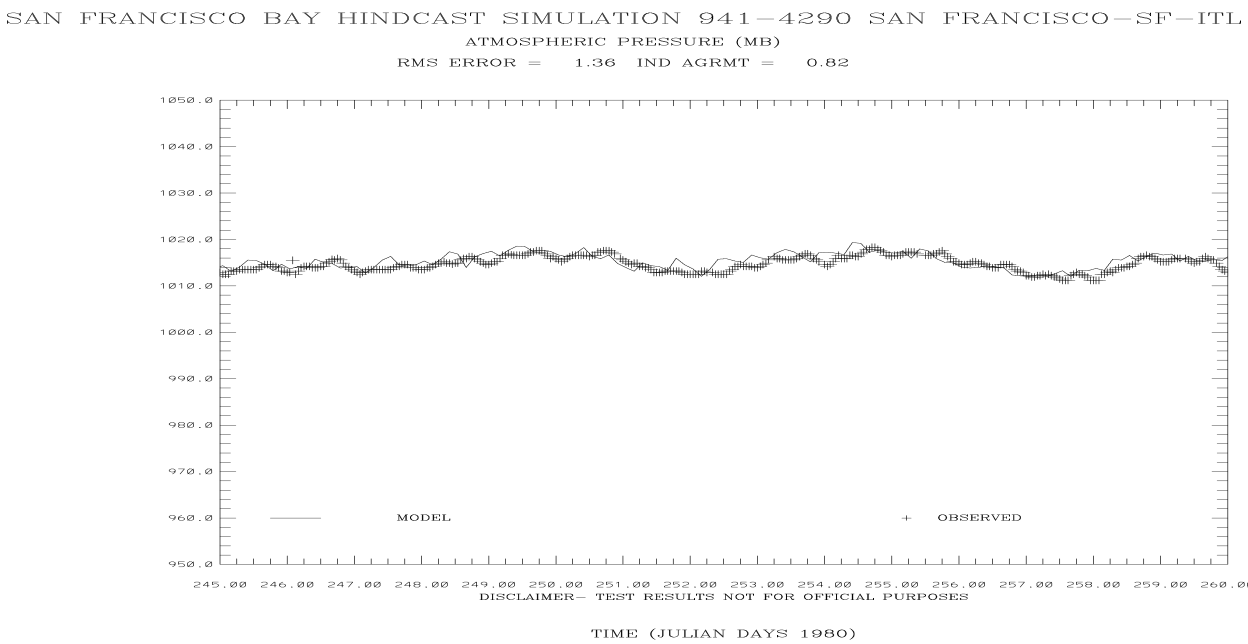

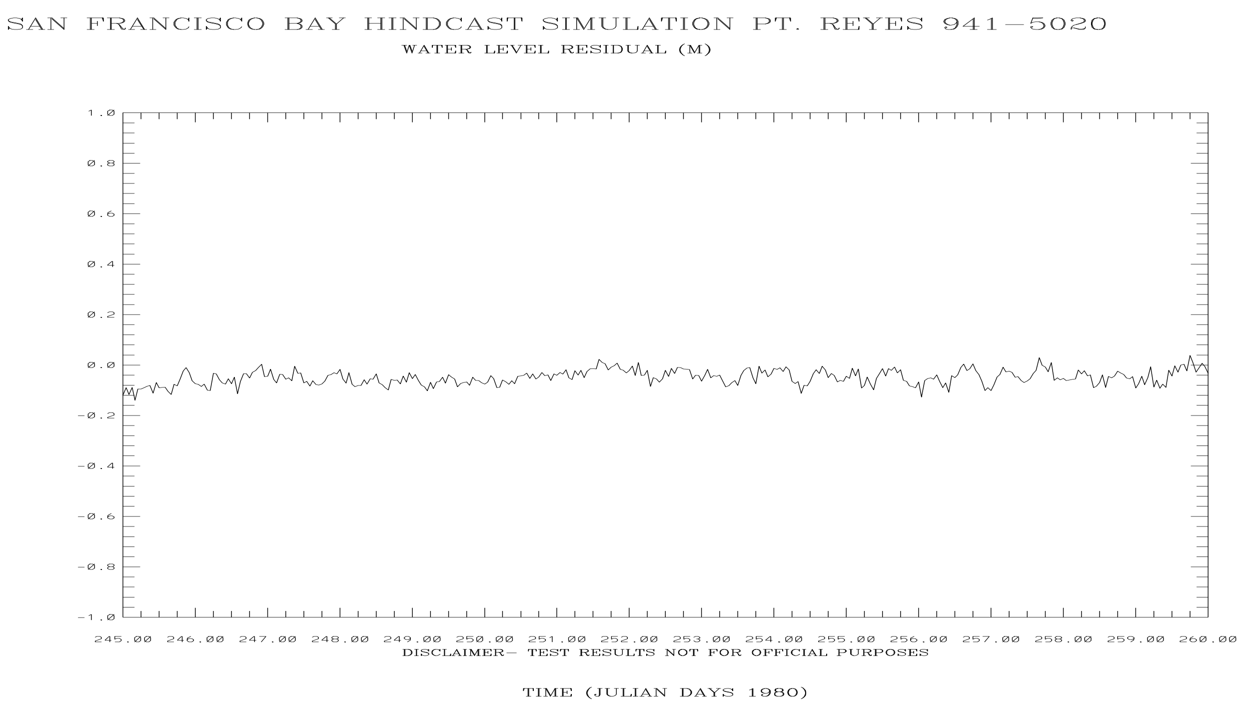

Figure 4.38. September 1-15, 1980 Hindcast: Atmospheric Pressure at San Francisco International Airport and Water Level Residual at Point Reyes. Note IND AGRMT equals one minus Willmott et al. (1985) relative error.

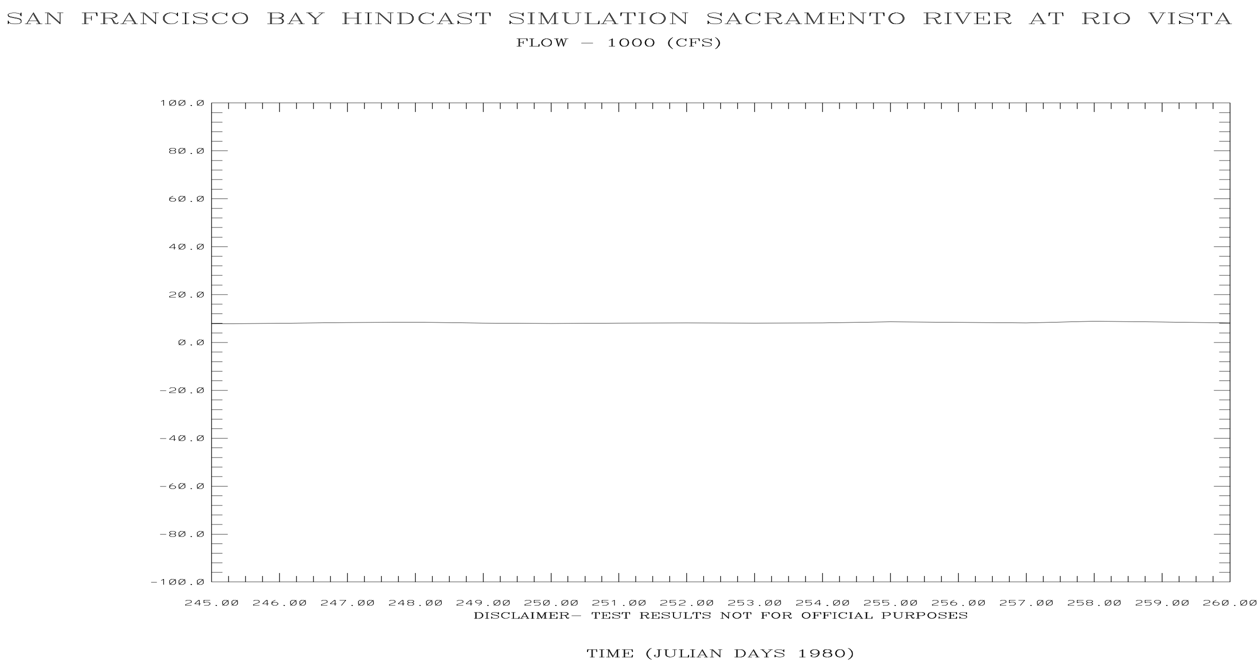

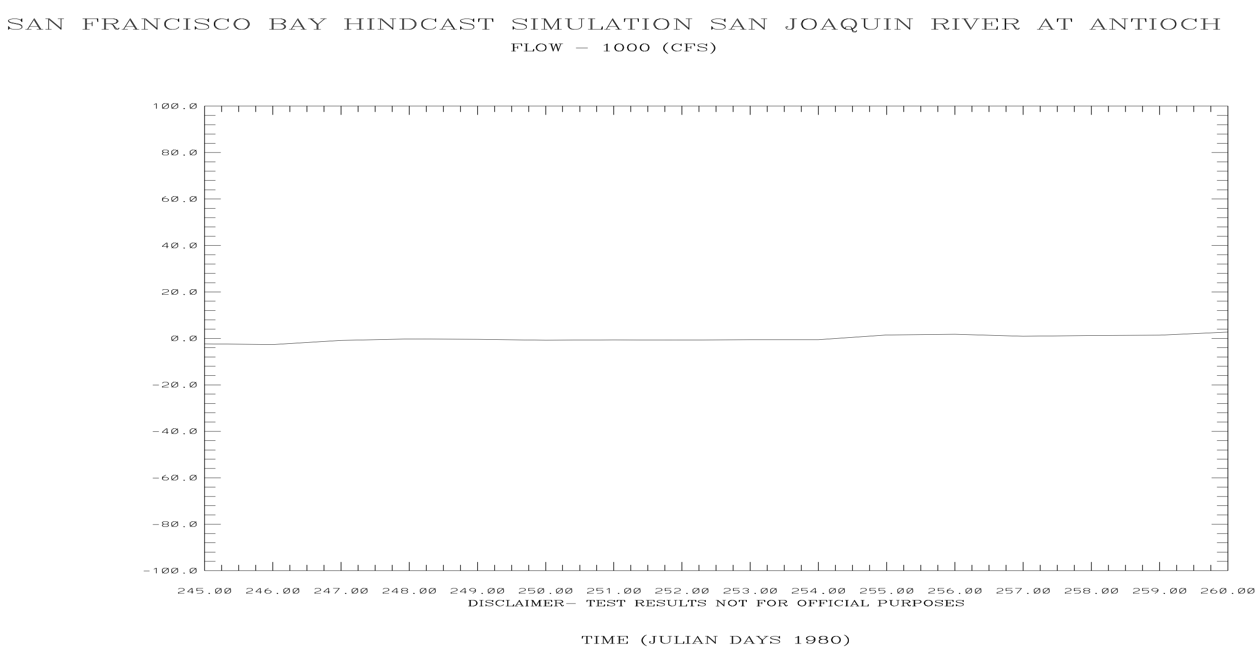

Figure 4.39. September 1-15, 1980 Hindcast: Flow (Thousands of CFS) on the Sacramento River at Rio Vista, CA and on the San Joaquin River at Antioch, CA

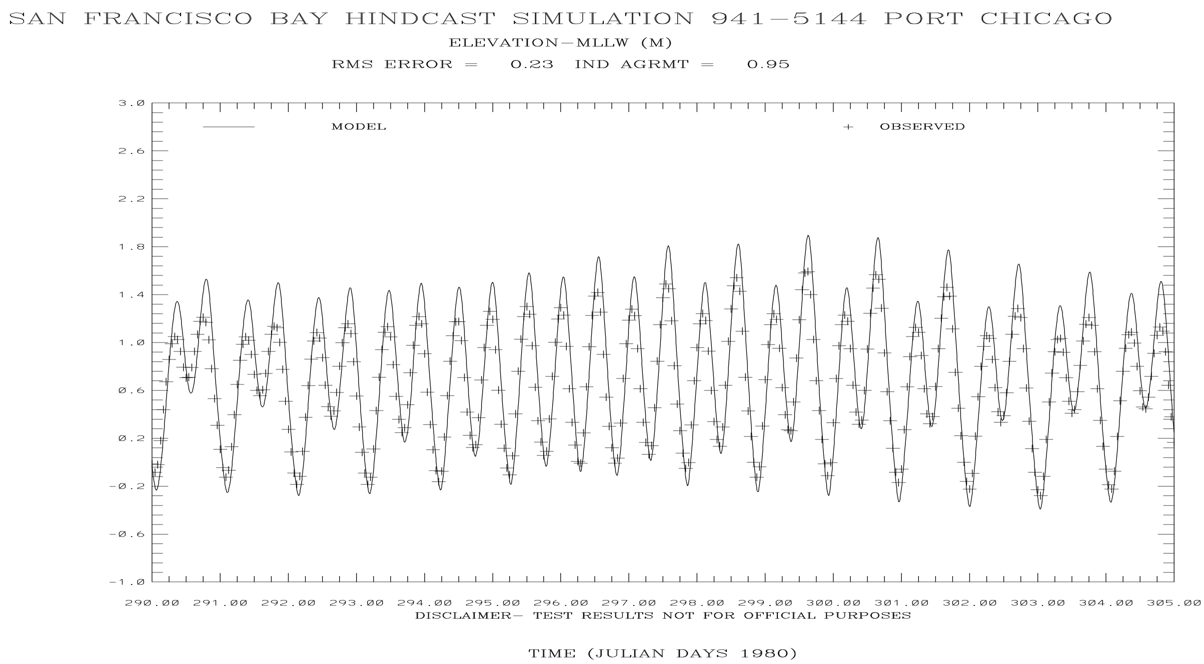

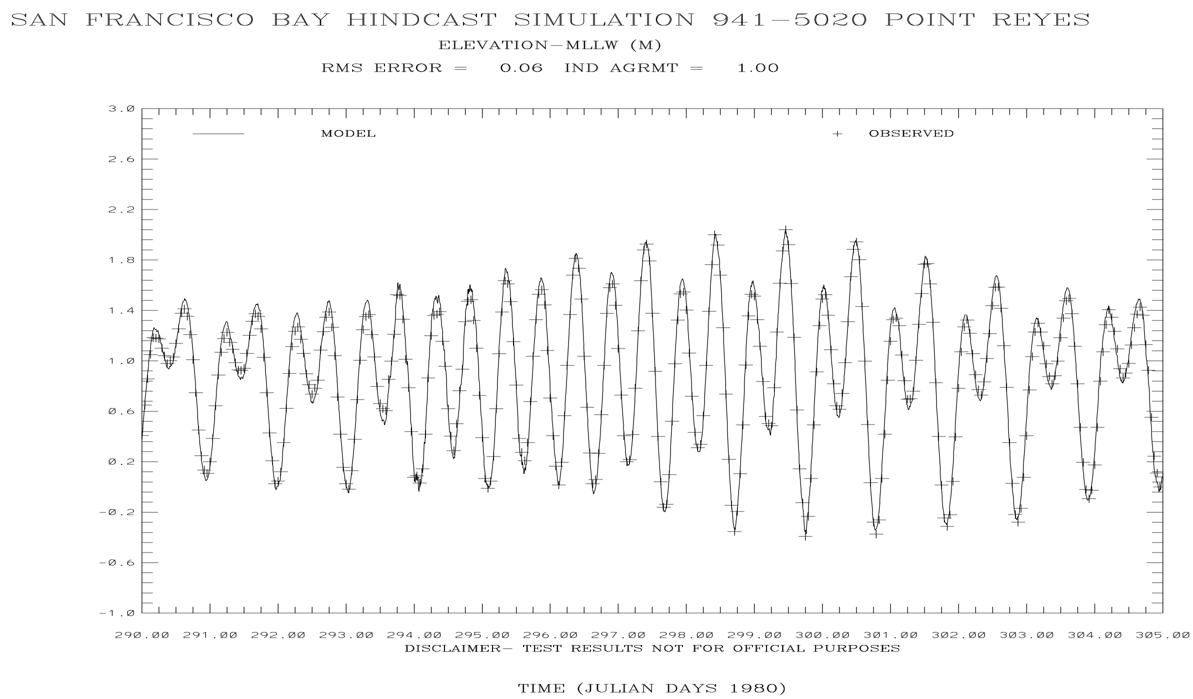

Figure 4.40. October 15-31, 1980 Hindcast: Port Chicago and Point Reyes Water Level Comparisons. Note IND AGRMT equals one minus Willmott et al. (1985) relative error.

SAN FRANCISCO BAY HINDCAST SIMULATION 941−4290 SAN FRANCISCO−SF−ITL
ELEVATION−MLLW (M)
RMS ERROR = 0.08 IND AGRMT = 1.00

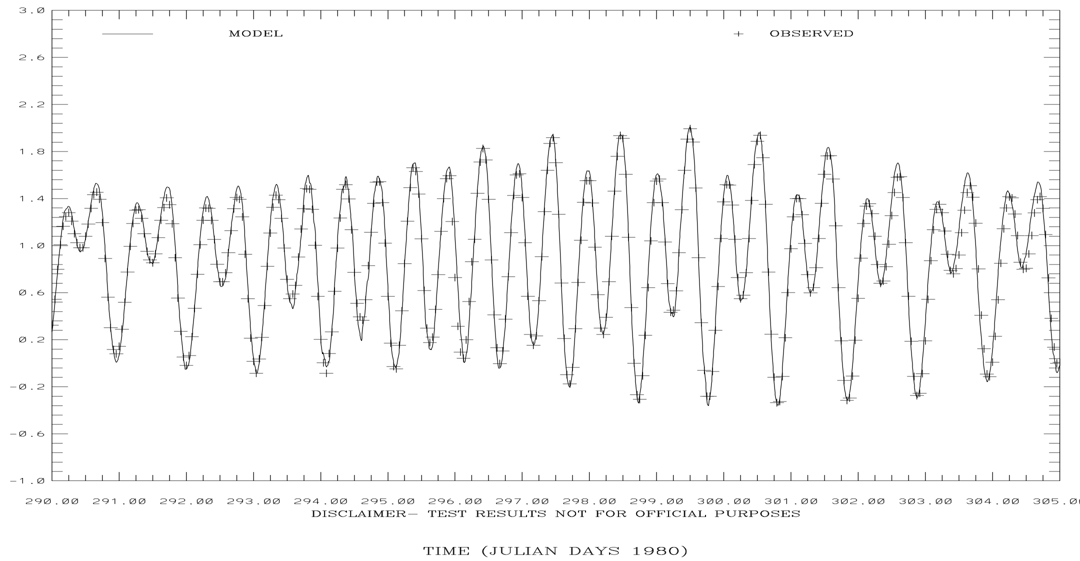

SAN FRANCISCO BAY HINDCAST SIMULATION 941−4458 SAN MATEO BRIDGE
ELEVATION−MLLW (M)

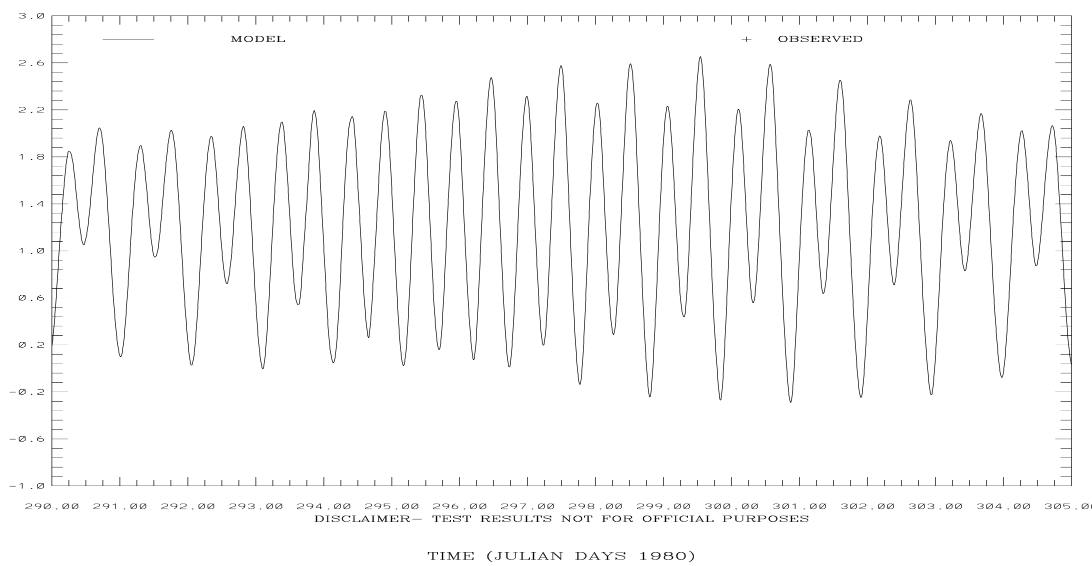

Figure 4.41. October 15-31, 1980 Hindcast: San Francisco and San Mateo Bridge Water Level Comparisons. Note IND AGRMT equals one minus Willmott et al. (1985) relative error.

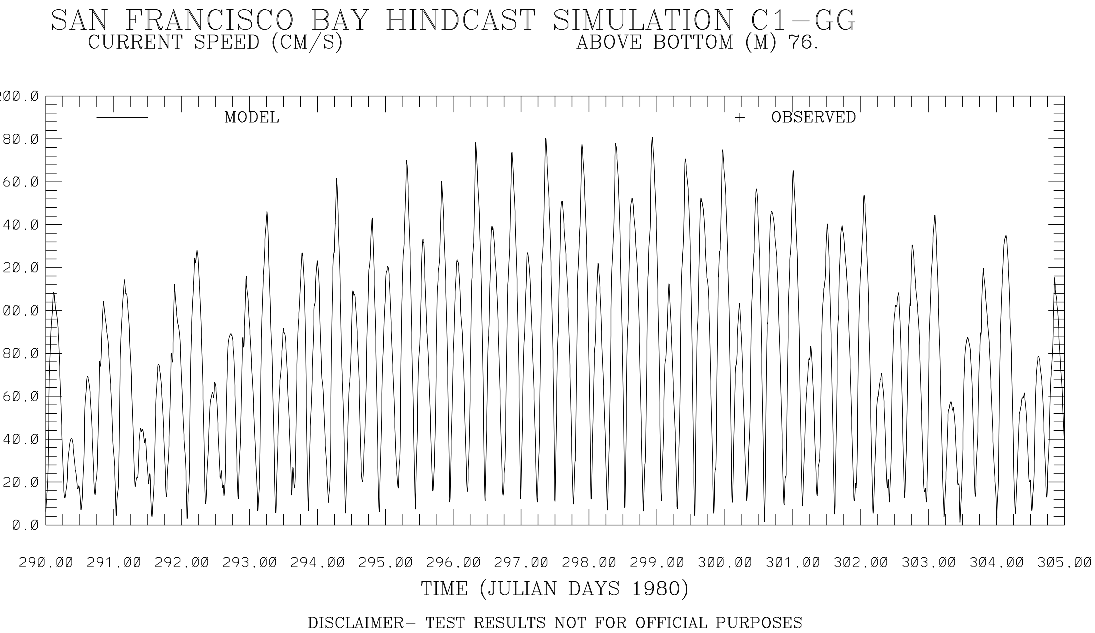

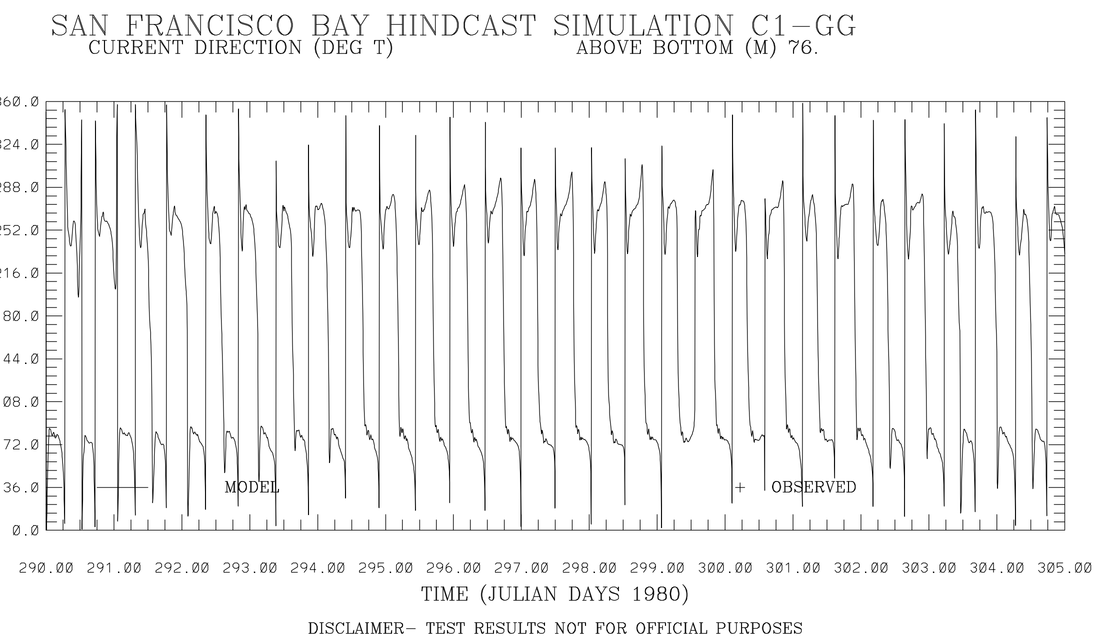

Figure 4.42. October 15-31, 1980 Hindcast: C-1 Current Speed and Direction at 76m above the bottom. Note IND AGRMT equals one minus Willmott et al. (1985) relative error.

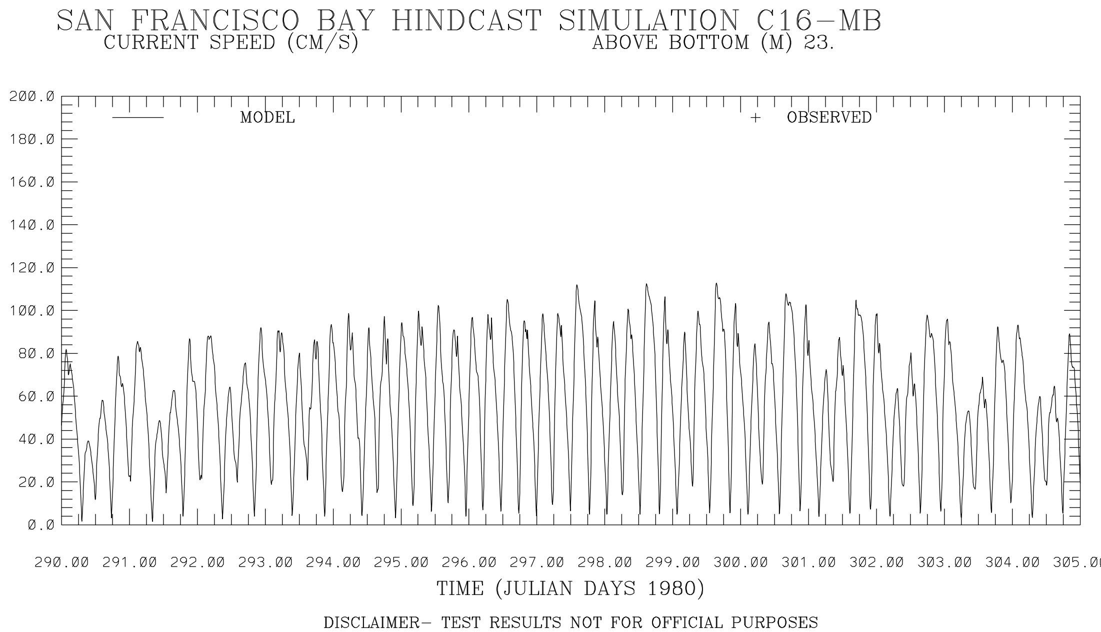

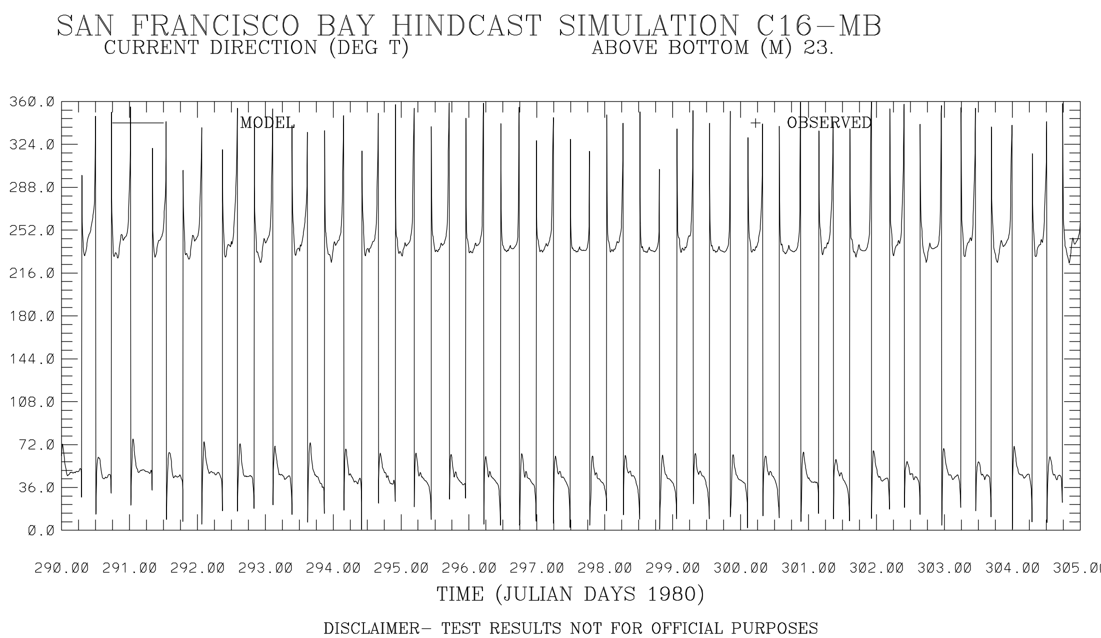

Figure 4.43. October 15-31, 1980 Hindcast: C-16 Current Speed and Direction at 23m above the bottom. Note IND AGRMT equals one minus Willmott et al. (1985) relative error.

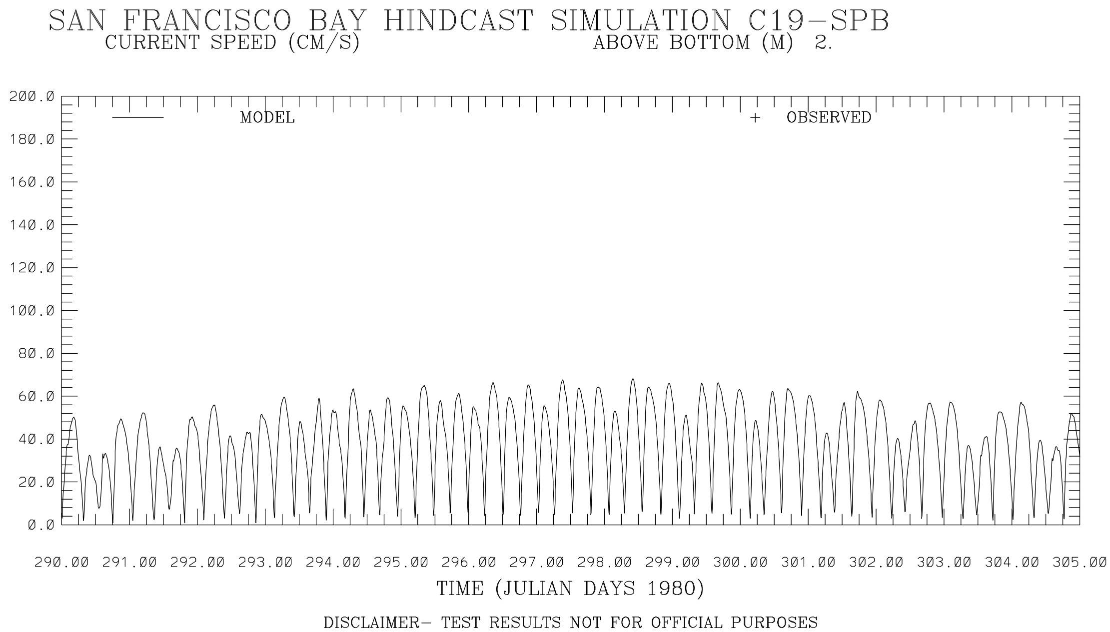

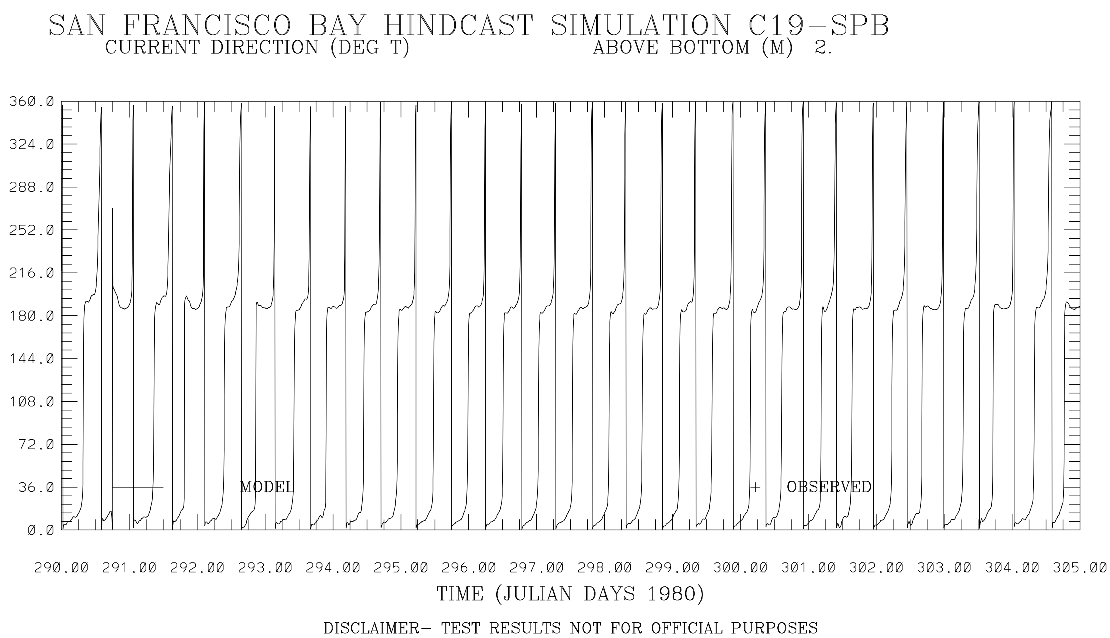

Figure 4.44. October 15-31, 1980 Hindcast: C-19 Current Speed and Direction at 2m above the bottom. Note IND AGRMT equals one minus Willmott et al. (1985) relative error.

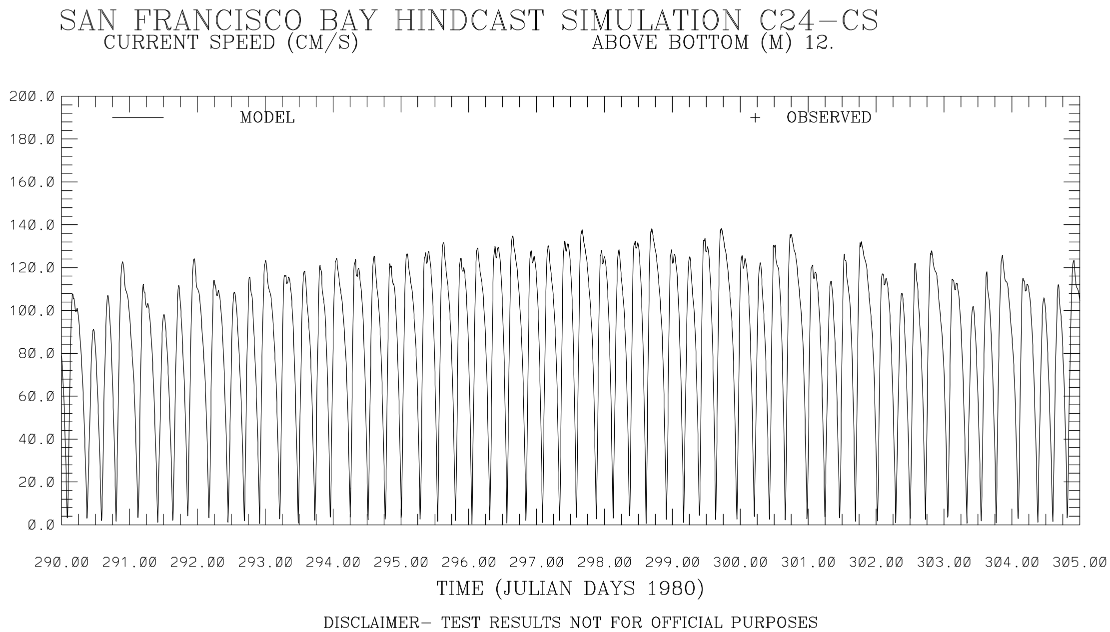

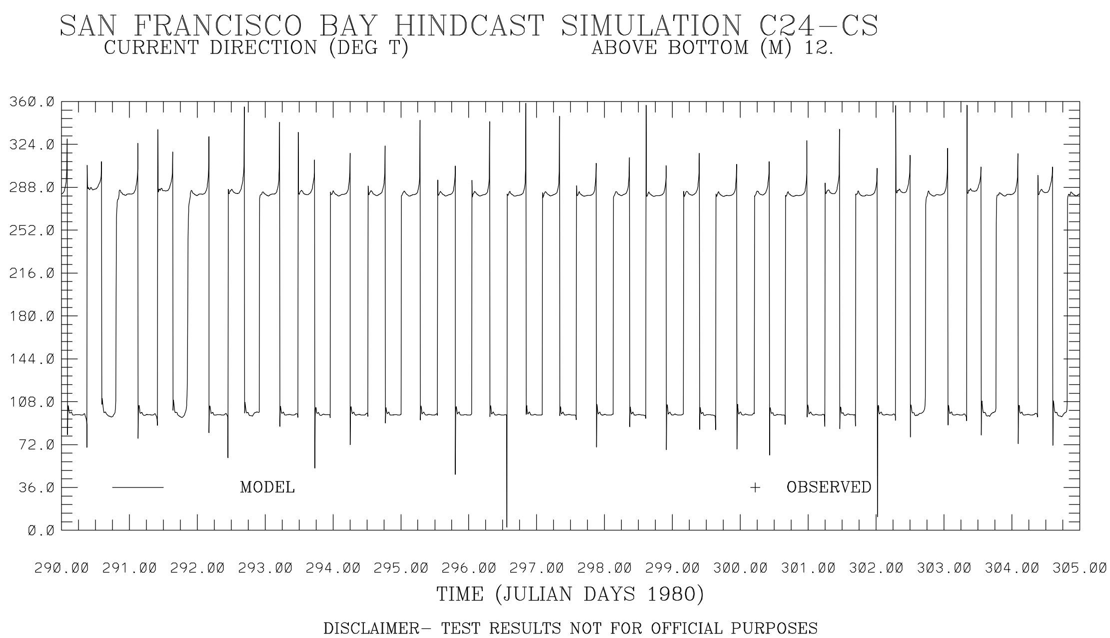

Figure 4.45. October 15-31, 1980 Hindcast: C-24 Current Speed and Direction at 12m above the bottom. Note IND AGRMT equals one minus Willmott et al. (1985) relative error.

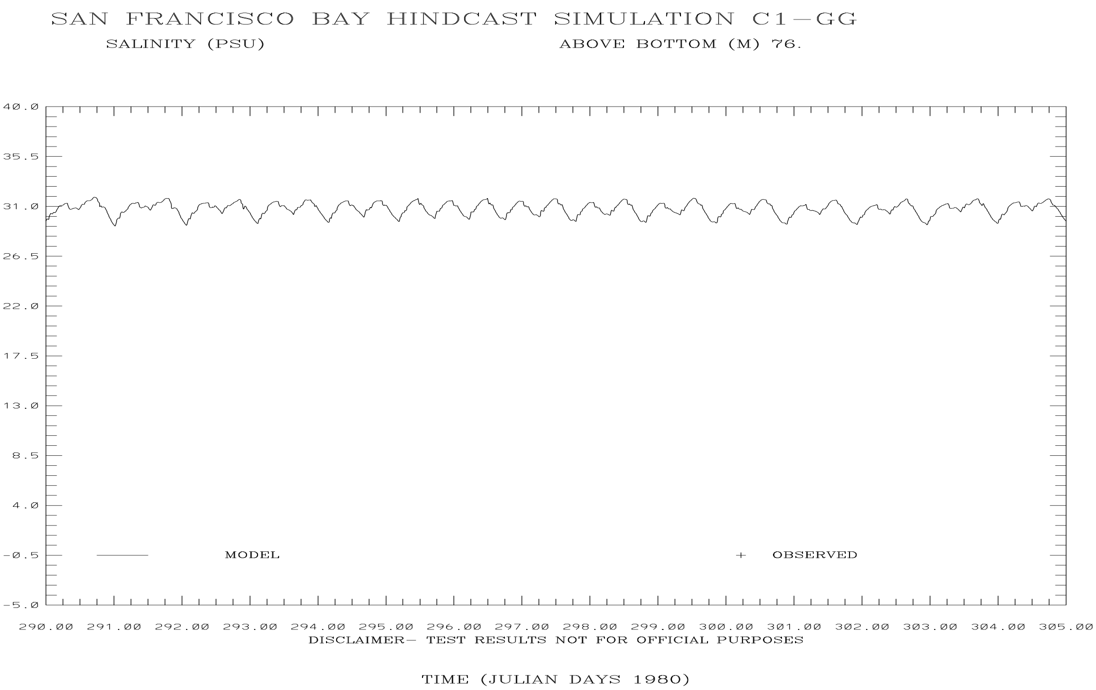

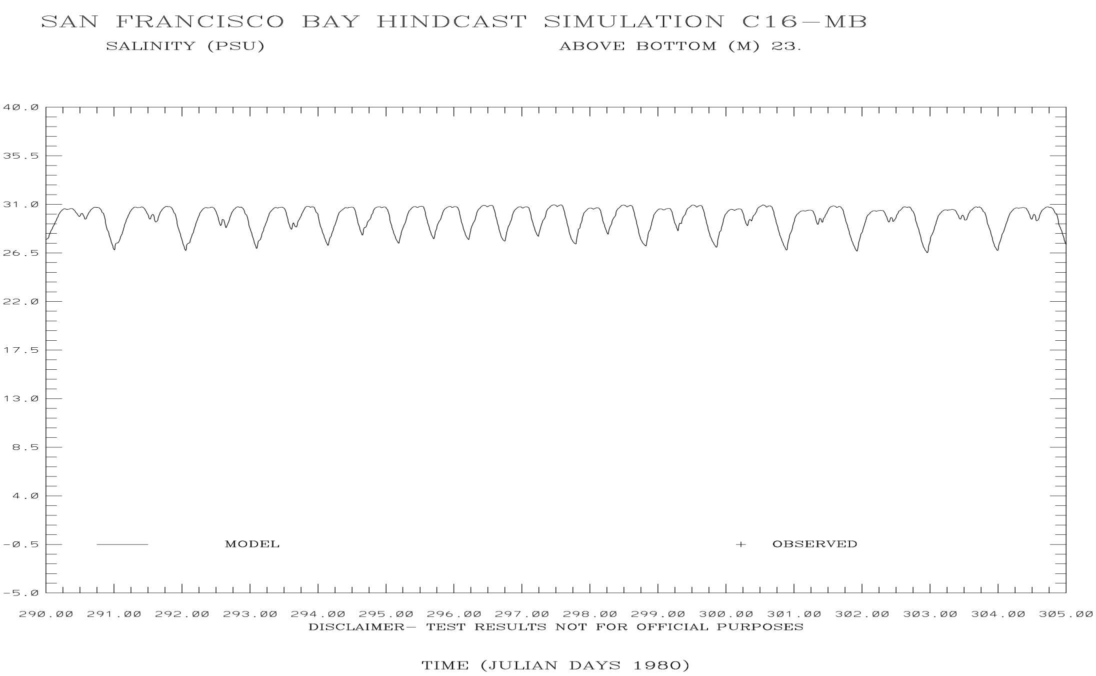

Figure 4.46. October 15-31, 1980 Hindcast: Salinity at C-1 at 76m and C-16 at 23m above the bottom. Note IND AGRMT equals one minus Willmott et al. (1985) relative error.

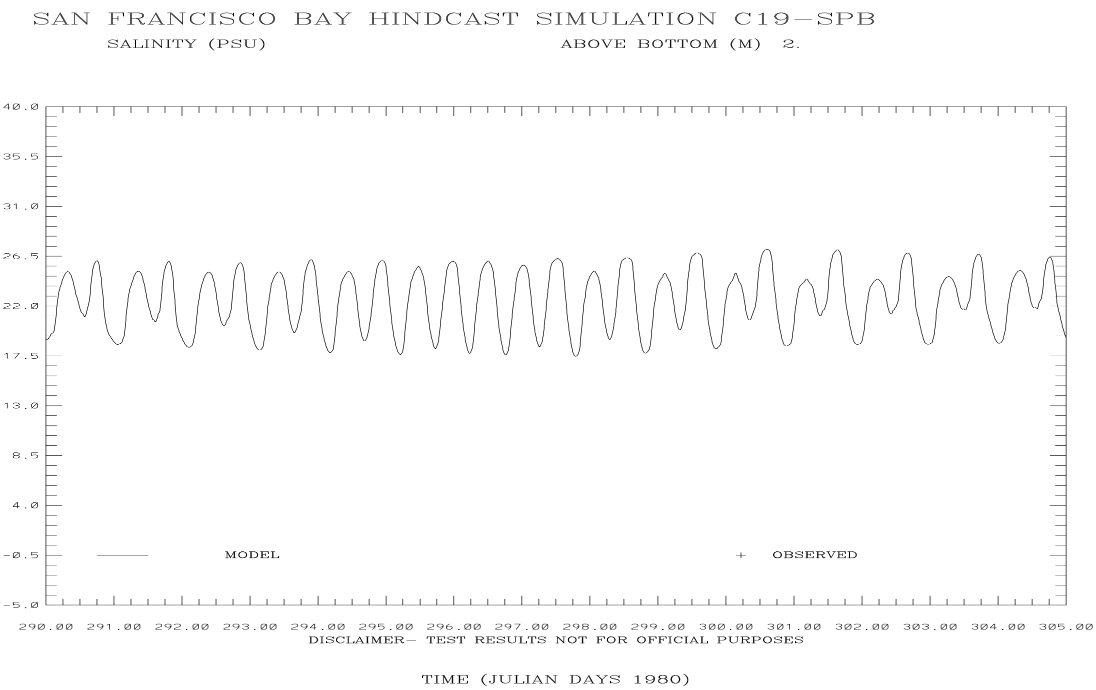

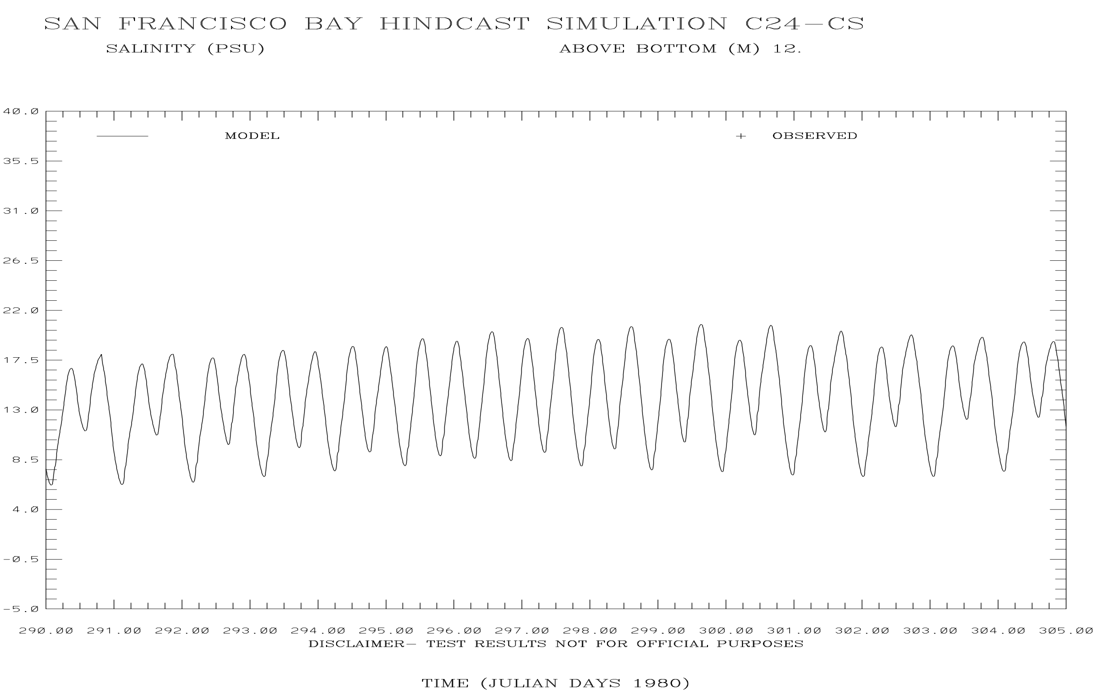

Figure 4.47. October 15-31, 1980 Hindcast: Salinity at C-19 at 2m and C-24 at 12m above the bottom. Note IND AGRMT equals one minus Willmott et al. (1985) relative error.

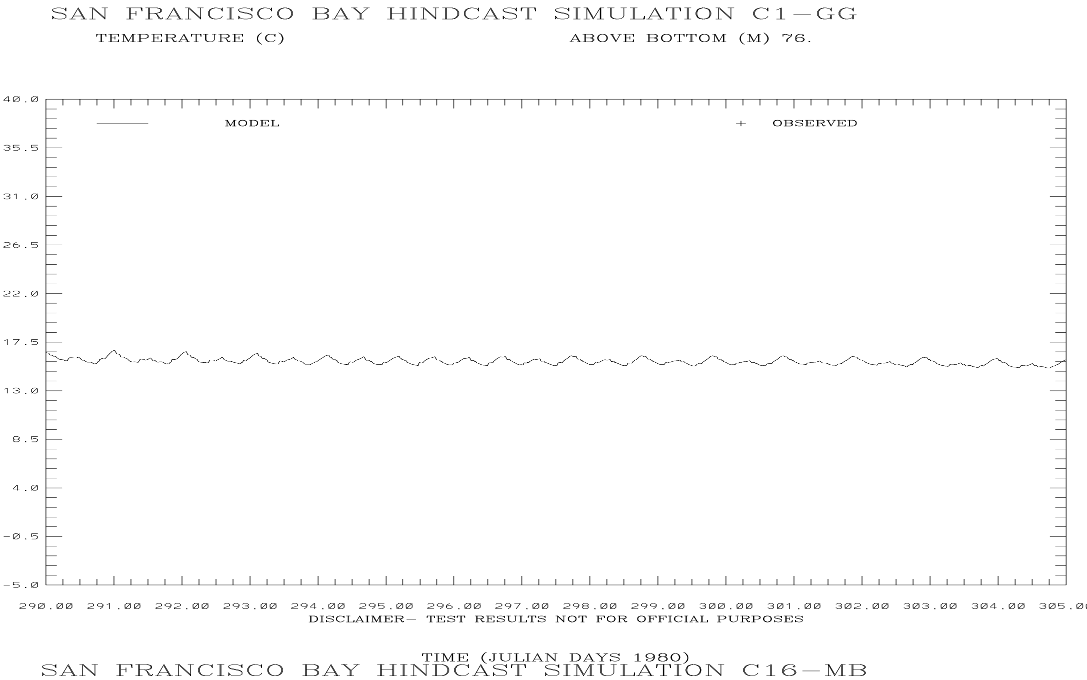

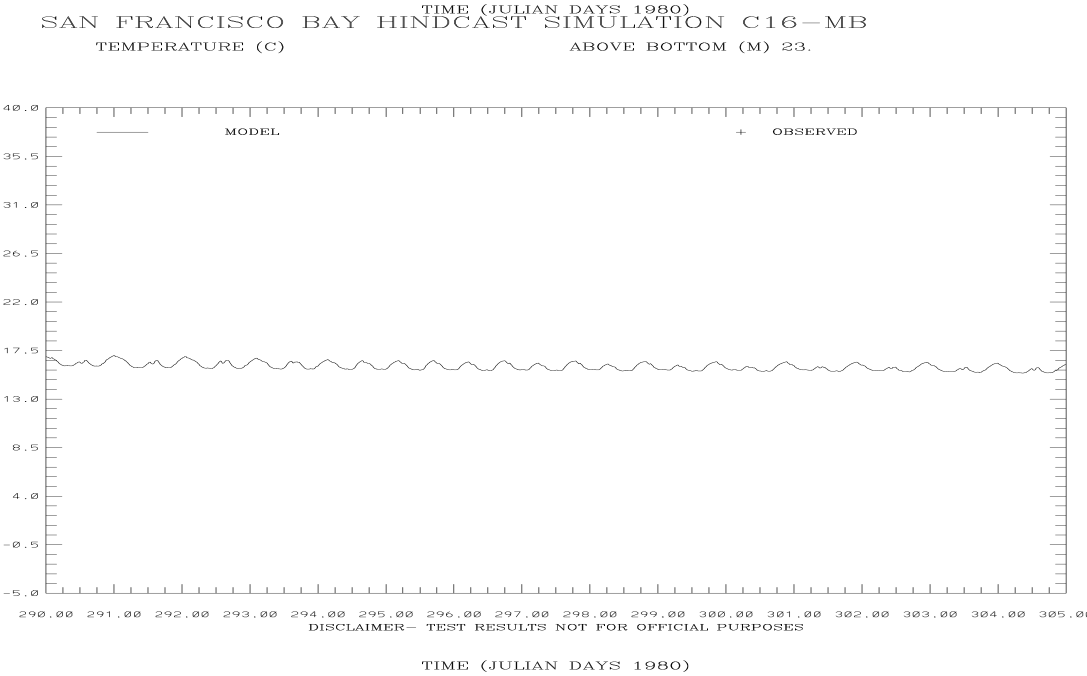

Figure 4.48. October 15-31, 1980 Hindcast: Temperature at C-1 at 76m and C-16 at 23m above the bottom. Note IND AGRMT equals one minus Willmott et al. (1985) relative error.

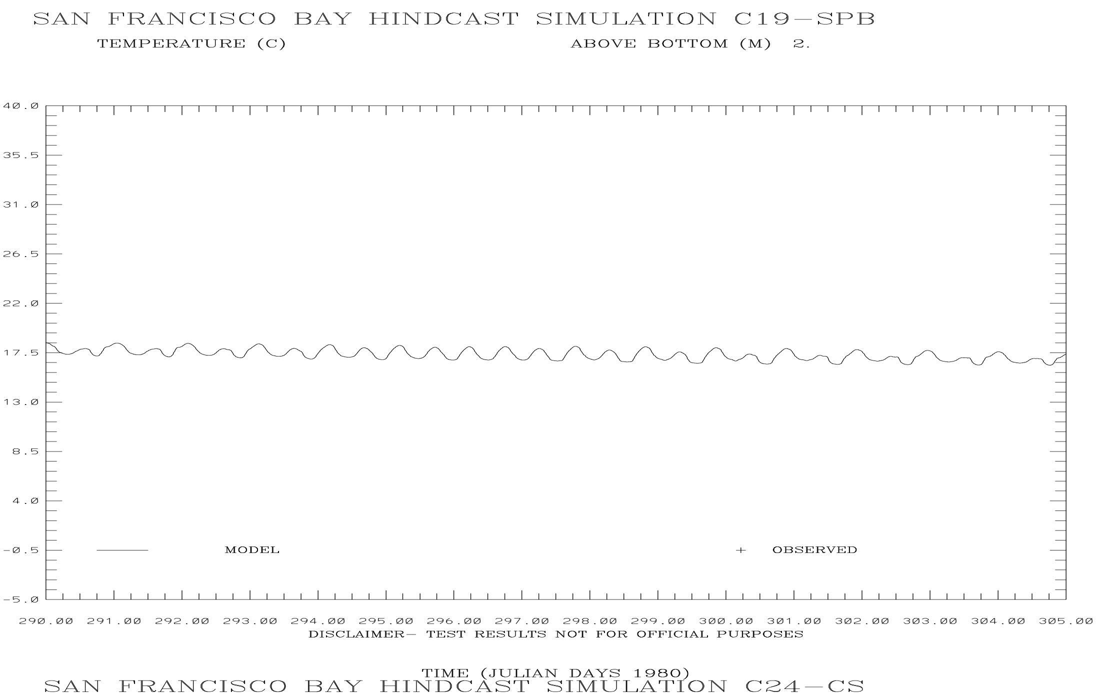

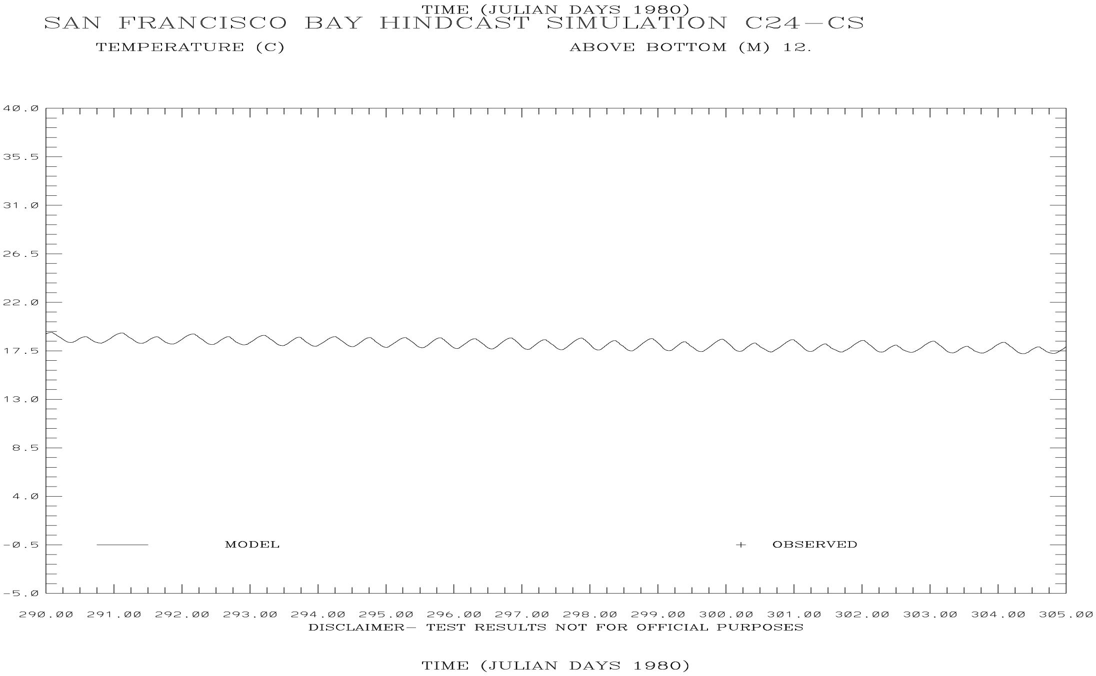

Figure 4.49. October 15-31, 1980 Hindcast: Temperature at C-19 at 2m and C-24 at 12m above the bottom. Note IND AGRMT equals one minus Willmott et al. (1985) relative error.

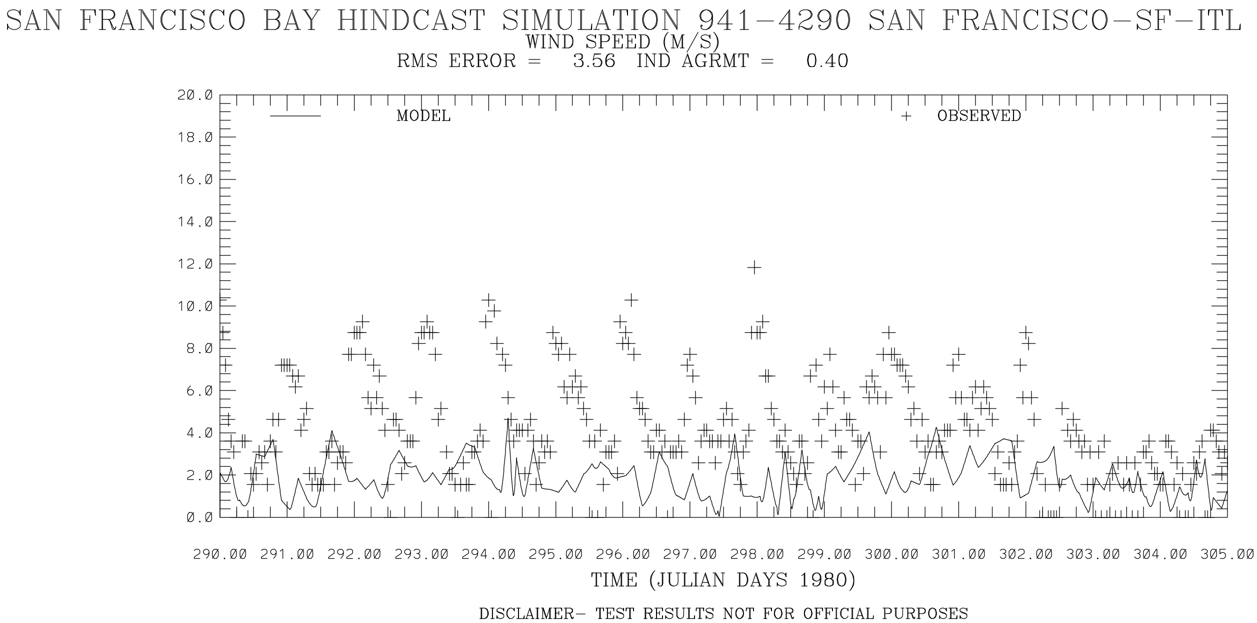

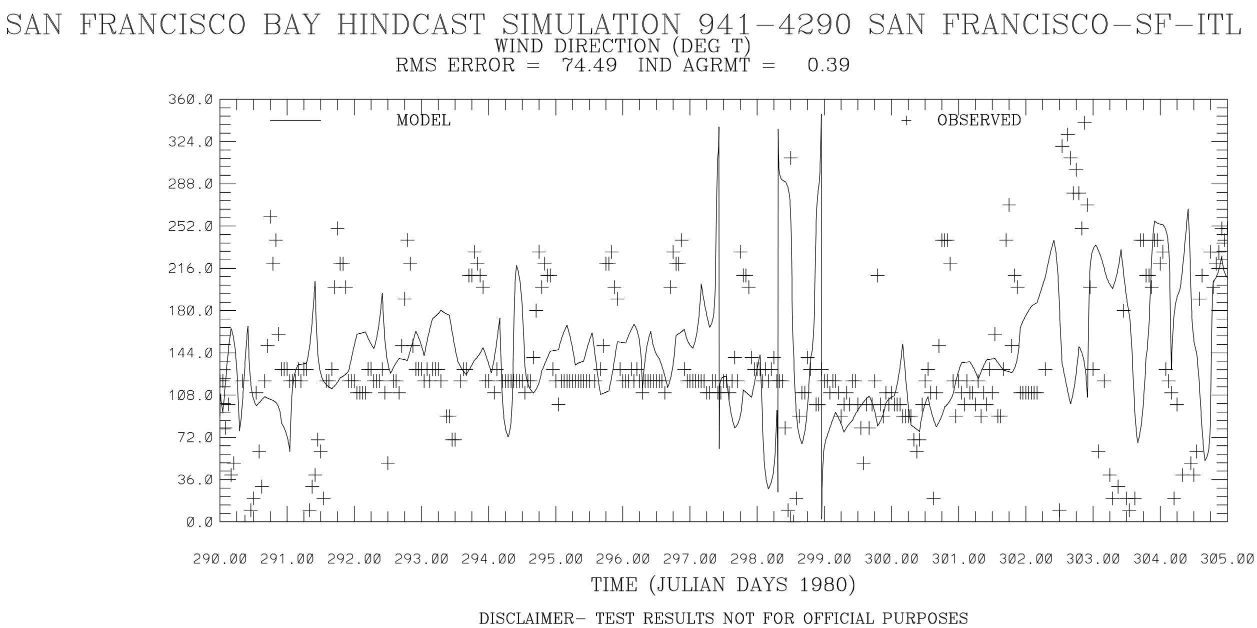

Figure 4.50. October 15-31, 1980 Hindcast: Wind speed and direction at San Francisco International Airport. Note IND AGRMT equals one minus Willmott et al. (1985) relative error.

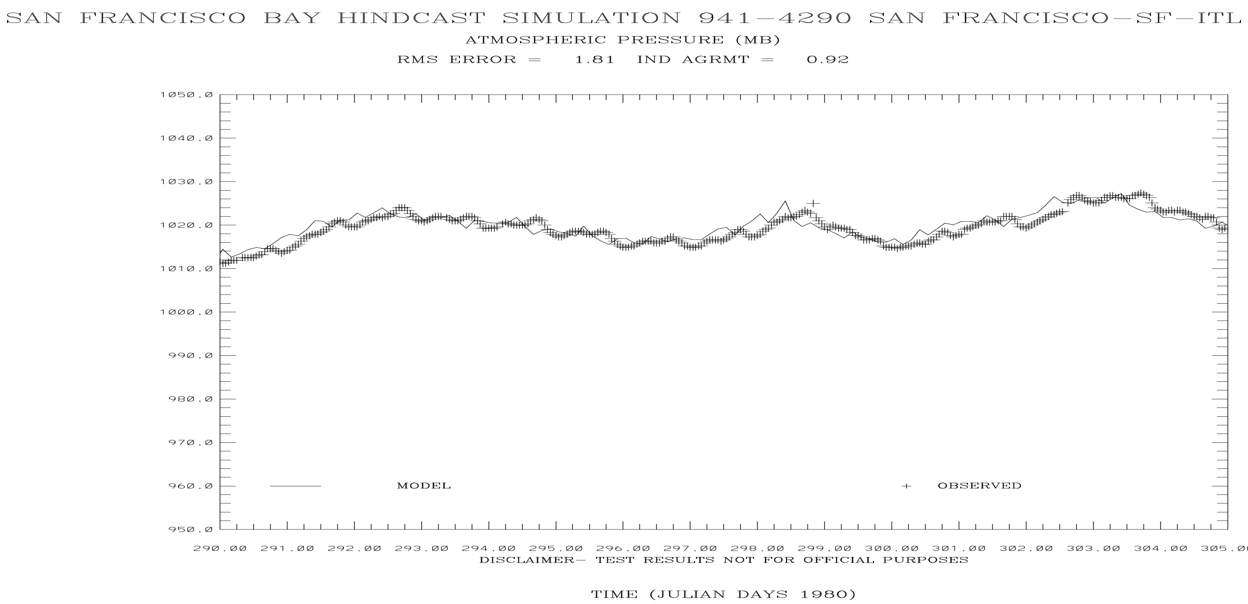

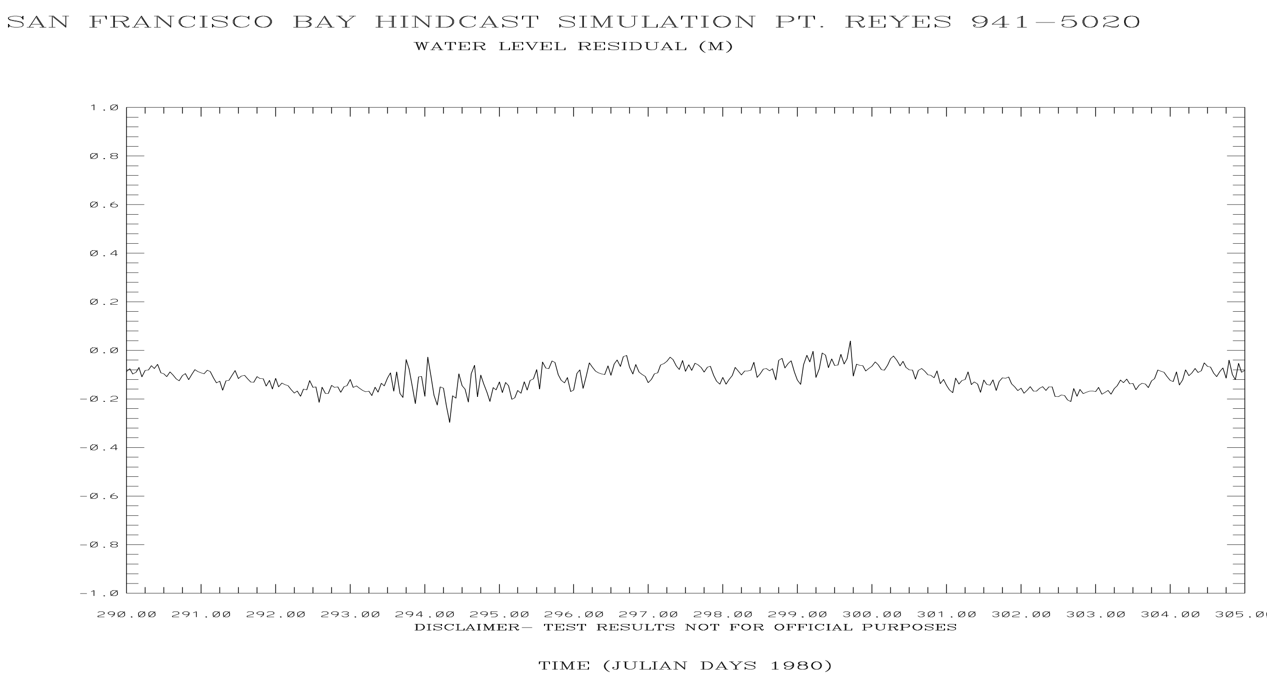

Figure 4.51. October 15-31, 1980 Hindcast: Atmospheric Pressure at San Francisco International Airport and Water Level Residual at Point Reyes. Note IND AGRMT equals one minus Willmott et al. (1985) relative error.

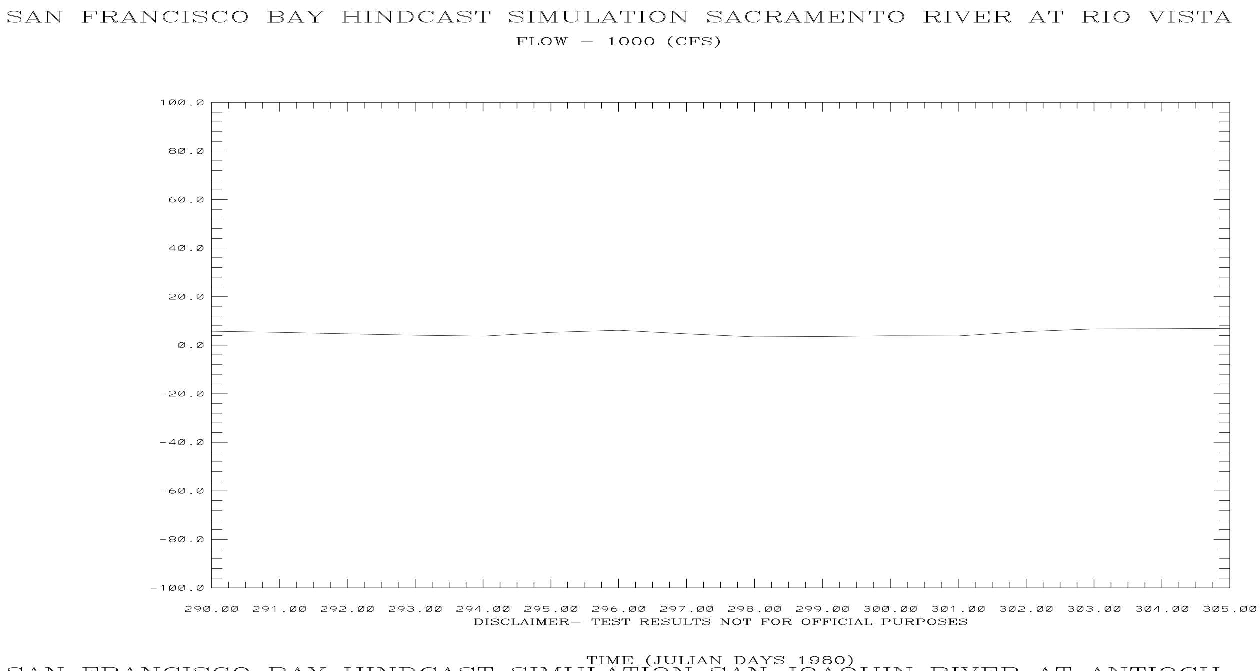

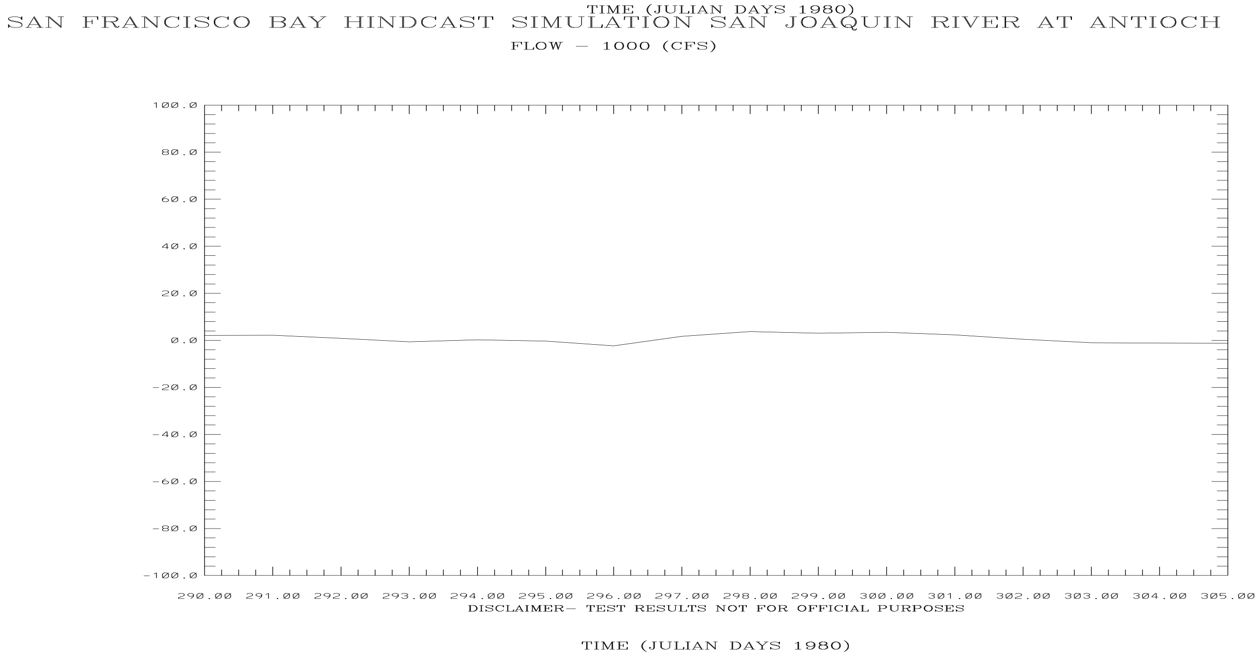

Figure 4.52. October 15-31, 1980 Hindcast: Flow (Thousands of CFS) on the Sacramento River at Rio Vista, CA and on the San Joaquin River at Antioch, CA.

4.3 April 1979 – October 1980 Extended Hindcast

An extended 19-month hindcast was performed with complete meteorological forcings to assess the ability of the model to perform heat flux computations over several seasons. The modified stage boundary condition was employed to specify the water levels on the Sacramento River at Rio Vista, CA and on the San Joaquin River at Antioch, CA. Our goal was to reduce the over prediction of the water level range at Port Chicago and in the upstream sections by reconstructing the water levels using the harmonic constant set in Table 3.8. Note no residual water level signal was specified.

Results are presented in 15 day increments in Table 4.2.1 for September 1-15, in Table 4.2.2 for September 15-30, in Table 4.2.3 for October 1-15, and in Table 4.2.4 for October 15-31. In general, there are fewer stations available with measured data for comparison than for the tidal simulation. For the offshore temperature and salinity a zero gradient boundary condition is used.

Water levels at Port Chicago and Point Reyes are shown in Figures 4.53, 4.63, 4.73, 4.83, 4.93, and 4.103. Water levels at San Francisco and the San Mateo Bridge are shown in Figures 4.54, 4.64, 4.74, 4.84, 4.94, and 4.104.

Current speed and direction are shown at Station C-1 (Golden Gate Bridge) in Figures 4.55, 4.65, 4.75, 4.85, 4.95, and 4.105 at Station C-18 (mid-Bay) in Figures 4.56, 4.66, 4.76, 4.86, 4.96 and 4.106. Current speed and direction at Station C-19 (San Pablo Bay) in Figures 4.57, 4.67, 4.77, 4.87, 4.97, and 4.107, and at C-24 (Carquinez Strait) are displayed in Figures 4.58, 4.68, 4.78, 4.88, 4.98, and 4.108.

Salinity is shown at Stations C-1 (Golden Gate Bridge) and C-18 (mid-Bay) in Figures 4.59, 4.69, 4.79, 4.89, 4.99, and 4.109. Salinity at Stations C-22 (San Pablo Bay) and C-24 (Carquinez Strait) is plotted in Figures 4.60, 4.70, 4.80, 4.90, 4.100, and 4.110.

Temperature is shown at Stations C-1 (Golden Gate Bridge) and C-18 (mid-Bay) in Figures 4.61, 4.71, 4.81, 4.91, 4.101, and 4.111. A at Stations C-22 (San Pablo Bay) and C-24 (Carquinez Strait) temperature is displayed in Figures 4.62, 4.72, 4.82, 4.92, 4.102, and 4.112.

We briefly characterize simulation results for months at the beginning, middle, and end of the extended hindcast in turn.

April 1979: There are datum issues associated with the observed water levels at San Francisco and at San Mateo Bridge. At Point Reyes the RMS error in water level is 7 cm with a Willmott relative error of 0.01. At San Francisco the RMS error in water level is near 20 cm with a Willmott et al. (1985) relative error of 0.03 for the second simulation segment. For salinity, temperature, and currents, the model response is examined at Station C-1 at the Golden Gate Bridge, at Stations C-5, C-17, and C-18 in the mid-Bay, at Stations C-19 and C-22 in San Pablo Bay, and at C-24 and C-25 in Carquinez Strait. For the San Pablo Bay stations the RMS errors are order 3 PSU, while in Carquinez Strait the RMS errors are above 4.5 PSU. In this region, there are large horizontal salinity gradients and the model tends to be too fresh by order 3 PSU.

Temperature comparisons are uniform throughout the Bay with RMS errors less than 1 ^{o}C. There are potential measurement issues at Stations C-20 and C-23. Currents speed RMS errors are near 26 cm/s. At Station C-1 at the Golden Gate Bridge near surface current strength is underestimated in the model by order 10 cm/s. Mean current directions are within 45 degrees with similar or reduced RMS errors. In general RMS wind speed errors are less than 5 m/s with direction RMS errors order 50 degrees. For sea level atmospheric pressure, the RMS errors are near 2 mb. The water level residual at Point Reyes is small relative to the tidal amplitude and is less than 20 cm. River inflow from the Delta into San Francisco Bay ranged from 30,000 to 40,000 cfs during the first simulation segment and was near zero during the second simulation segment.

May 1979: At Point Reyes, San Francisco, and San Mateo Bridge the RMS errors in water levels are near 5 cm with a Willmott et al. (1985) relative error of near zero. For salinity, temperature, and currents, the model response is examined at Station C-18 in the mid-Bay, at Stations C-28, C-29, C-30, C-31, and C-33 in Suisun Bay, and at C-24 in Carquinez Strait. For the Suisun Bay stations the RMS errors range from 0.5 to 6.0 PSU, while in Carquinez Strait the RMS errors are above 4.5 PSU. In this region, there are large horizontal salinity gradients and the model tends to be too fresh by order 3 PSU. Temperature comparisons are uniform throughout the Bay with RMS errors less than 1 ^{o}C. Currents speed RMS errors are near 26 cm/s at most stations Mean current directions are within 45 degrees with similar or reduced RMS errors. In general RMS wind speed errors are less than 5 m/s with direction RMS errors order 70 degrees. For sea level atmospheric pressure, the RMS errors are less than 3 mb. The water level residual at Point Reyes is small relative to the tidal amplitude and is less than 20 cm. River inflow from the Delta into San Francisco Bay ranged from 8,000 to 12,000 cfs.

December 1979: There are water level measurement problems at Port Chicago after the first three days and datum issues at Dumbarton Bridge. At Point Reyes, San Francisco, Pier 22.5 and Alameda the RMS errors in water levels are less than 9 cm with a Willmott et al. (1985) relative error of 0.01. At San Mateo Bridge, the RMS errors in water level range from12 cm to 14 cm. No salinity, temperature, and current data are available for model comparison. The water level residual at Point Reyes ranges from -20 to 40 cm. River inflow from the Delta into San Francisco Bay ranged from 12,000 to 50,000 cfs.

January 1980: There are water level datum issues at Dumbarton Bridge. At Point Reyes, San Francisco, Pier 22.5 and Alameda, the RMS errors in water levels are less than 6 cm with a Willmott et al. (1985) relative error of 0.01. At San Mateo Bridge, the RMS errors in water level range from 11 cm to 13 cm. At Port Chicago, during the first 15-day simulation segment, the water level RMS error is 13 cm with a Willmott relative error of 0.02. No salinity, temperature, and current data are available for model comparison. The water level residual at Point Reyes is small relative to the tidal amplitude and is less than 20 cm. River inflow from the Delta into San Francisco Bay was over 150,000 cfs during portions of the month, and the water level RMS error at Port Chicago was order 30 cm during these high flow periods.

September 1980: There are datum issues associated with the observed water levels at Oyster Point Marina, Pier 22.5, and at Dumbarton Bridge. At Point Reyes, San Francisco, and Alameda, the RMS errors in water levels are near 8 cm, with a Willmott et al. (1985) relative error of 0.01. At Port Chicago in Suisun Bay, water level RMS errors are much reduced from the previous hindcast and range from 6 to 7 cm. For salinity, temperature, and currents, the model response is examined at Stations C-16. C-211, and C-323 in the mid-Bay and at Station C-22 in San Pablo Bay. Salinity RMS errors are less than 0.5 PSU at most stations with temperature RMS errors less than 1.5 ^{o}C. Currents speed and direction RMS errors could not be assessed due to lack of observational data. In general RMS wind speed errors are less than 5 m/s with direction RMS errors order 70 degrees. For sea level atmospheric pressure, the RMS errors are less than 3.3 mb. The water level residual at Point Reyes is small relative to the tidal amplitude and is less than 15 cm. River inflow from the Delta into San Francisco Bay ranged from 8,000 to 12,000 cfs.

October 1980: There are datum issues associated with the observed water levels at Dumbarton Bridge. At Point Reyes, San Francisco, and Alameda the RMS errors in water levels are near 7 cm with a Willmott et al. (1985) relative error of 0.01. At Port Chicago in Suisun Bay, water level RMS errors are much reduced from the previous hindcast and are in the range of 6 to 10 cm. For salinity, temperature, and currents, the model response is examined at Station C-1 at the Golden Gate Bridge, at Station C-18 in the mid-Bay, at Stations C-19, C-23, and C-316 in San Pablo Bay, and at Station C-24 in Carquinez Strait. Salinity RMS errors are less than 1.0 PSU at all stations outside of Suisun Bay and Carquinez Strait where the model prediction is too fresh by order 3 to 4 PSU. With respect to temperature RMS errors less than 1.0 ^{o}C at most stations. Currents speed and direction RMS errors are order 26 cm/s and 30 degrees, respectively. In general RMS wind speed errors are less than 5 m/s, with direction RMS errors order 70 degrees. For sea level atmospheric pressure, the RMS errors are less than 3.3 mb. The water level residual at Point Reyes is small relative to the tidal amplitude and is less than 15 cm. River inflow from the Delta into San Francisco Bay ranged from 6,000 to 10,000 cfs.

Table 4.13 Water Surface Elevation Hindcast Validation: April 1979-October 1980. For each row in each month, the first entry corresponds to the first 15 days of the month, with the second entry denoting the remaining portion of the month. Row 1 corresponds to the RMSE in cm. Row 2 corresponds to the Willmott Relative Error in percent. Row 3 corresponds to the model mean in cm relative to MLLW with row 4 denoting the observed water level mean in cm with respect to MLLW. Bold italics indicate measurement errors and their associated model discrepancies. Note n/a denotes not applicable due to lack of measurements.

Station	Apr	May	Jun	Jul	Aug	Sep	Oct	Nov	Dec
Alameda	n/a n/a	n/a n/a	n/a n/a	n/a ***111***	8 ***36***	8 64	9 7	6 8	6 7
941-4750	n/a n/a	n/a n/a	n/a n/a	n/a ***85***	0 ***12***	0 35	1 0	0 0	0 0
	95 96	95 100	97 96	102 109	109 96	111 61	112 108	107 99	103 113
	n/a n/a	n/a n/a	n/a n/a	n/a ***10***	103 103	105 106	105 103	104 95	100 111
Dumbarton	n/a n/a	n/a n/a	n/a n/a	n/a n/a	n/a n/a	n/a n/a	n/a n/a	n/a n/a	n/a ***299***
Bridge	n/a n/a	n/a n/a	n/a n/a	n/a n/a	n/a n/a	n/a n/a	n/a n/a	n/a n/a	n/a ***61***
941-4509	131 132	131 136	133 132	144 132	144 130	145 95	146 143	141 133	137 146
	n/a n/a	n/a n/a	n/a n/a	n/a n/a	n/a n/a	n/a n/a	n/a n/a	n/a n/a	n/a ***-146***
Oyster Point	n/a n/a	n/a n/a	n/a n/a	n/a n/a	n/a n/a	n/a n/a	n/a n/a	n/a n/a	n/a n/a
Marina	n/a n/a	n/a n/a	n/a n/a	n/a n/a	n/a n/a	n/a n/a	n/a n/a	n/a n/a	n/a n/a
941-4392	106 107	106 111	107 106	119 106	119 106	121 71	122 118	117 109	113 123
	n/a n/a	n/a n/a	n/a n/a	n/a n/a	n/a n/a	n/a n/a	n/a n/a	n/a n/a	n/a n/a
Port	n/a n/a	n/a n/a	n/a n/a	n/a n/a	n/a n/a	n/a n/a	n/a n/a	n/a n/a	***80 95***
Chicago	n/a n/a	n/a n/a	n/a n/a	n/a n/a	n/a n/a	n/a n/a	n/a n/a	n/a n/a	***63 100***
941-5144	73 74	72 74	73 75	84 75	85 76	84 54	80 76	75 72	75 81
	n/a n/a	n/a n/a	n/a n/a	n/a n/a	n/a n/a	n/a n/a	n/a n/a	n/a n/a	***11 0***
Point Reyes	7 5	4 4	14 5	5 4	6 ***14***	6 ***25***	5 4	4 5	4 5
941-5020	1 0	0 0	1 0	0 0	0 ***2***	0 ***8***	0 0	0 0	0 0
	81 82	80 87	83 82	87 96	95 80	96 43	98 96	96 87	91 102
	80 79	78 85	80 79	85 94	93 ***73***	94 ***23***	96 94	95 85	90 102
San	14 18	5 5	31 7	8 8	8 33	8 59	7 6	3 4	5 6
Francisco	2 3	0 0	8 0	0 1	1 12	1 36	0 0	0 0	0 0
941-4290	84 84	83 88	85 84	90 98	97 84	98 51	99 96	96 88	92 102
	85 82	79 86	89 79	83 91	90 90	92 93	93 92	96 86	88 100
Pier 22.5	n/a n/a	n/a n/a	n/a n/a	n/a n/a	***51 38***	9 ***59***	10 9	7 7	6 6
941-4317	n/a n/a	n/a n/a	n/a n/a	n/a n/a	***18 12***	1 ***33***	1 1	0 0	0 0
	90 90	89 90	91 90	96 103	102 91	104 58	105 101	101 92	97 107
	n/a n/a	n/a n/a	n/a n/a	n/a n/a	***75 77***	97 97	96 94	96 86	93 104
San Mateo	***302 145***	9 8	34 8	11 11	21 43	19 65	17 12	12 12	12 14
Bridge	***69 40***	0 0	6 0	1 1	2 12	2 31	2 1	1 1	1 1
941-4458	117 118	117 122	118 117	124 130	130 117	132 81	133 128	127 120	124 133
	419 180	110 117	120 111	115 122	122 120	121 121	122 119	119 111	116 126

Table 4.13 (Cont.). Water Surface Elevation Hindcast Validation April 1979 –October 1980. For each row in each month, the first entry corresponds to the first 15 days of the month, with the second entry denoting the remaining portion of the month. Row 1 corresponds to the RMSE in cm. Row 2 corresponds to the Willmott Relative Error in percent. Row 3 corresponds to the model mean in cm with row 4 denoting the observed water level mean in cm. Bold italics indicate measurement errors and their associated model discrepancies. Note n/a denotes not applicable due to lack of measurements.

Station	Jan	Feb	Mar	Apr	May	Jun	Jul	Aug	Sep	Oct
Alameda 941-4750	6 11 0 1 117 107 118 115	7 13 0 1 109 126 111 134	12 8 1 1 112 91 119 97	7 5 0 0 94 96 95 98	7 4 0 0 97 95 98 96	7 3 0 0 98 101 98 101	6 4 0 0 99 109 97 107	5 6 0 0 112 109 110 105	6 7 0 0 110 110 105 107	6 6 0 0 109 101 107 98
Dumbarton Bridge 941-4509	329 329 69 65 150 142 -179 -186	335 330 69 66 144 159 -191 -171	328 330 70 66 146 129 -181 -200	334 333 67 67 129 132 -204 -201	330 330 65 67 132 132 -198 -198	335 335 65 68 134 136 -201 -198	336 335 65 68 134 144 -201 -191	335 339 66 68 146 144 -189 -195	336 336 68 67 144 144 -193 -192	***335 337*** ***69 66*** 143 136 ***-192 -201***
Oyster Point Marina 941-4392	n/a n/a n/a n/a 126 118 n/a n/a	n/a n/a n/a n/a 120 135 n/a n/a	n/a n/a n/a n/a 122 103 n/a n/a	15 10 1 1 104 106 104 107	13 10 1 1 107 106 106 103	14 8 1 0 108 111 106 108	14 9 1 0 110 119 105 118	10 9 1 0 122 119 121 116	***75*** n/a ***31*** n/a 119 120 ***89*** n/a	n/a n/a n/a n/a 119 112 n/a n/a
Port Chicago 941-5144	13 22 2 5 84 81 92 98	8 32 1 11 82 90 81 120	23 10 8 1 82 72 102 73	11 9 2 1 71 70 66 70	9 9 1 1 70 70 72 71	8 7 1 1 72 75 73 74	9 6 1 0 76 82 70 80	6 7 0 1 83 82 83 78	7 6 1 1 81 80 77 77	6 10 1 1 77 73 76 66
Point Reyes 941-5020	4 6 0 0 106 96 106 96	4 6 0 0 98 116 87 117	5 5 0 0 101 78 101 77	5 5 0 0 81 82 79 81	5 4 0 0 83 81 82 80	4 4 0 0 85 88 83 87	5 4 0 0 86 97 84 95	4 5 0 0 99 96 98 94	4 5 0 0 97 97 95 96	4 6 0 0 97 89 96 87
San Francisco 941-4290	5 9 0 1 106 96 106 101	5 11 0 1 99 116 99 120	10 8 1 1 101 80 107 83	6 5 0 0 83 85 83 85	6 3 0 0 85 84 86 85	5 3 0 0 86 90 86 89	6 5 0 0 88 98 84 95	5 5 0 0 100 97 99 94	6 5 0 0 99 98 95 96	6 8 0 0 98 90 96 87
Pier 22.5 941-4317	5 10 0 1 110 101 112 108	6 12 0 1 104 120 103 125	10 10 1 1 106 85 105 91	7 11 0 1 88 90 88 89	14 12 1 1 90 89 88 92	***47 57*** ***13 20*** 91 95 ***128 152***	***50 50*** ***13 16*** 93 103 ***142 154***	***89 50*** ***39 16*** 105 102 ***92 152***	***56*** n/a ***20*** n/a 103 103 ***146*** n/a	n/a n/a n/a n/a 103 95 n/a n/a
San Mateo Bridge 941-4458	11 13 1 1 137 129 135 134	10 23 1 3 130 146 129 146	***148 81*** ***100 29*** 133 114 ***0 76***	14 8 1 0 115 117 110 115	14 11 1 1 118 117 126 126	8 n/a 0 n/a 119 122 127 n/a	n/a n/a n/a n/a 121 130 n/a n/a	n/a n/a n/a n/a 132 130 n/a n/a	n/a n/a n/a n/a 130 130 n/a n/a	n/a n/a n/a n/a 129 122 n/a n/a

Table 4.14 Current Speed Hindcast Validation: April 1979-October 1980. For each row in each month, the first entry corresponds to the first 15 days of the month, with the second entry denoting the remaining portion. Row 1 corresponds to the RMSE in cm/s. Row 2 corresponds to the Willmott Relative Error in percent. Row 3 corresponds to the model mean in cm/s with row 4 denoting the observed mean current speed in cm/s. Note n/a denotes not applicable.

Station	Apr 1979	May 1979	Sep 1980	Oct 1980
C-1 (76) GG	n/a n/a n/a n/a n/a n/a n/a n/a	n/a n/a n/a n/a n/a n/a n/a n/a	15 15 4 8 67 73 77 50	n/a n/a n/a n/a 67 73 n/a n/a
C-1 (91) GG	38 n/a 26 n/a 63 75 80 n/a	n/a n/a n/a n/a 62 74 n/a n/a	n/a n/a n/a n/a n/a n/a n/a n/a	n/a n/a n/a n/a n/a n/a n/a n/a
C-5 (2) MB	30 n/a 50 n/a 34 39 29 n/a	n/a n/a n/a n/a 34 37 n/a n/a	n/a n/a n/a n/a n/a n/a n/a n/a	n/a n/a n/a n/a n/a n/a n/a n/a
C-5 (8) MB	33 n/a 42 n/a 46 52 34 n/a	n/a n/a n/a n/a 47 50 n/a n/a	n/a n/a n/a n/a n/a n/a n/a n/a	n/a n/a n/a n/a n/a n/a n/a n/a
C-5 (25) MB	26 n/a 34 n/a 43 51 35 n/a	n/a n/a n/a n/a 43 49 n/a n/a	n/a n/a n/a n/a n/a n/a n/a n/a	n/a n/a n/a n/a n/a n/a n/a n/a
C-16 (8) MB	n/a n/a n/a n/a n/a n/a n/a n/a	n/a n/a n/a n/a n/a n/a n/a n/a	12 15 9 11 46 47 45 47	n/a n/a n/a n/a 44 48 n/a n/a
C-16 (17) MB	n/a n/a n/a n/a n/a n/a n/a n/a	n/a n/a n/a n/a n/a n/a n/a n/a	14 15 9 9 51 52 49 49	n/a n/a n/a n/a 48 52 n/a n/a
C-16 (23) MB	n/a n/a n/a n/a n/a n/a n/a n/a	n/a n/a n/a n/a n/a n/a n/a n/a	13 15 8 9 53 53 50 50	n/a n/a n/a n/a 49 53 n/a n/a
C-17 (2) MB	13 n/a 17 n/a 31 36 33 n/a	n/a n/a n/a n/a 31 35 n/a n/a	n/a n/a n/a n/a n/a n/a n/a n/a	n/a n/a n/a n/a n/a n/a n/a n/a
C-17 (5) MB	25 n/a 27 n/a 41 48 49 n/a	n/a n/a n/a n/a 42 46 n/a n/a	n/a n/a n/a n/a n/a n/a n/a n/a	n/a n/a n/a n/a n/a n/a n/a n/a
C-18 (9) MB	22 17 13 8 60 65 68 63	n/a n/a n/a n/a 59 61 n/a n/a	n/a 24 n/a 14 57 59 n/a 74	20 19 12 12 54 59 63 52
C-18 (15) MB	21 19 8 6 68 76 75 74	17 n/a 7 n/a 68 75 55 n/a	n/a 20 n/a 7 70 71 n/a 83	18 18 7 9 67 72 71 55

Table 4.14 (Cont.). Current Speed Hindcast Validation April 1979 –October 1980. For each row in each month, the first entry corresponds to the first 15 days of the month, with the second entry denoting the remaining portion. Row 1 corresponds to the RMSE in cm/s. Row 2 corresponds to the Willmott Relative Error in percent. Row 3 corresponds to the model mean in cm/s with row 4 denoting the observed mean current speed in cm/s. Note n/a denotes not applicable.

Station	Apr 1979	May 1979	Sep 1980	Oct 1980
C-19 (1) SPB	10 n/a 25 n/a 22 26 23 n/a	n/a n/a n/a n/a 23 26 n/a n/a	6 12 5 14 33 34 28 29	9 n/a 12 n/a 32 34 25 n/a
C-20 (1) SPB	17 n/a 35 n/a 15 17 27 n/a	n/a n/a n/a n/a 15 17 n/a n/a	n/a n/a n/a n/a n/a n/a n/a n/a	n/a n/a n/a n/a n/a n/a n/a n/a
C-22 (2) SPB	11 n/a 14 n/a 33 38 29 n/a	n/a n/a n/a n/a 33 38 n/a n/a	10 11 9 6 40 42 36 39	n/a n/a n/a n/a 39 43 n/a n/a
C-23 (1) SPB	6 n/a 29 n/a 14 16 16 n/a	n/a n/a n/a n/a 15 16 n/a n/a	n/a 6 n/a 27 16 17 n/a 18	5 2 23 8 16 17 17 12
C-24 (2) CS	21 19 27 23 15 40 14 32	n/a n/a n/a n/a 36 40 n/a n/a	n/a 12 n/a 10 41 42 n/a 44	11 n/a 11 n/a 40 42 37 n/a
C-24 (17,11) CS	33 22 20 9 65 72 81 80	n/a n/a n/a n/a 66 71 n/a n/a	n/a 22 n/a 11 n/a 64 n/a 77	23 n/a 14 n/a 60 62 72 n/a
C-25 (2) CS	15 13 15 12 37 40 41 42	n/a n/a n/a n/a 36 38 n/a n/a	n/a n/a n/a n/a n/a n/a n/a n/a	n/a n/a n/a n/a n/a n/a n/a n/a
C-25 (8) CS	22 20 13 11 52 57 65 68	n/a n/a n/a n/a 53 59 n/a n/a	n/a n/a n/a n/a n/a n/a n/a n/a	n/a n/a n/a n/a n/a n/a n/a n/a
C-26 (2) SB	14 22 14 25 38 42 36 26	n/a n/a n/a n/a 38 40 n/a n/a	n/a n/a n/a n/a 39 40 n/a n/a	n/a 17 n/a 22 39 40 n/a 36

Table 4.15 Current Direction Hindcast Validation: April 1979-October 1980. For each row in each month, the first entry corresponds to the first 15 days of the month, with the second entry denoting the remaining portion. Row 1 corresponds to the RMSE in degrees. Row 2 corresponds to the Willmott Relative Error in percent. Row 3 corresponds to the model mean in degrees with row 4 denoting the observed mean current direction in degrees. Note n/a denotes not applicable.

Station	Apr 1979	May 1979	Sep 1980	Oct 1980
C-1 (76) GG	n/a n/a n/a n/a n/a n/a n/a n/a	n/a n/a n/a n/a n/a n/a n/a n/a	23 16 2 18 167 168 152 104	n/a n/a n/a n/a 168 168 n/a n/a
C-1 (91) GG	35 n/a 4 n/a 172 180 152 n/a	n/a n/a n/a n/a 174 182 n/a n/a	n/a n/a n/a n/a n/a n/a n/a n/a	n/a n/a n/a n/a n/a n/a n/a n/a
C-5 (2) MB	45 n/a 6 n/a 134 124 162 n/a	n/a n/a n/a n/a 138 121 n/a n/a	n/a n/a n/a n/a n/a n/a n/a n/a	n/a n/a n/a n/a n/a n/a n/a n/a
C-5 (8) MB	37 n/a 5 n/a 115 117 145 n/a	n/a n/a n/a n/a 114 119 n/a n/a	n/a n/a n/a n/a n/a n/a n/a n/a	n/a n/a n/a n/a n/a n/a n/a n/a
C-5 (25) MB	33 n/a 4 n/a 133 132 146 n/a	n/a n/a n/a n/a 133 133 n/a n/a	n/a n/a n/a n/a n/a n/a n/a n/a	n/a n/a n/a n/a n/a n/a n/a n/a
C-16 (8) MB	n/a n/a n/a n/a n/a n/a n/a n/a	n/a n/a n/a n/a n/a n/a n/a n/a	12 14 0 1 139 141 139 130	n/a n/a n/a n/a 143 143 n/a n/a
C-16 (17) MB	n/a n/a n/a n/a n/a n/a n/a n/a	n/a n/a n/a n/a n/a n/a n/a n/a	19 20 1 1 138 142 158 148	n/a n/a n/a n/a 141 143 n/a n/a
C-16 (23) MB	n/a n/a n/a n/a n/a n/a n/a n/a	n/a n/a n/a n/a n/a n/a n/a n/a	24 23 1 1 144 145 162 155	n/a n/a n/a n/a 147 148 n/a n/a
C-17 (2) MB	20 n/a 1 n/a 243 250 227 n/a	n/a n/a n/a n/a 248 248 n/a n/a	n/a n/a n/a n/a n/a n/a n/a n/a	n/a n/a n/a n/a n/a n/a n/a n/a
C-17 (5) MB	23 n/a 1 n/a 226 232 243 n/a	n/a n/a n/a n/a 227 233 n/a n/a	n/a n/a n/a n/a n/a n/a n/a n/a	n/a n/a n/a n/a n/a n/a n/a n/a
C-18 (9) MB	16 10 1 0 105 103 101 97	n/a n/a n/a n/a 102 101 n/a n/a	n/a 20 n/a 1 113 107 n/a 102	15 11 1 8 115 110 97 31
C-18 (15) MB	29 17 2 1 116 120 133 118	21 n/a 1 n/a 120 122 126 n/a	n/a 20 n/a 7 122 122 n/a 106	17 21 1 9 121 123 109 22

Table 4.15 (Cont.). Current Direction Hindcast Validation April 1979 –October 1980. For each row in each month, the first entry corresponds to the first 15 days of the month, with the second entry denoting the remaining portion. Row 1 corresponds to the RMSE in degrees. Row 2 corresponds to the Willmott Relative Error in percent. Row 3 corresponds to the model mean in degrees with row 4 denoting the observed mean current direction in degrees. Note n/a denotes not applicable.

Station	Apr 1979	May 1979	Sep 1980	Oct 1980
C-19 (1) SPB	15 n/a 1 n/a 113 116 105 n/a	n/a n/a n/a n/a 126 120 n/a n/a	13 16 0 1 116 117 237 246	15 n/a 1 n/a 117 114 227 n/a
C-20 (1) SPB	14 n/a 1 n/a 187 183 172 n/a	n/a n/a n/a n/a 186 184 n/a n/a	n/a n/a n/a n/a n/a n/a n/a n/a	n/a n/a n/a n/a n/a n/a n/a n/a
C-22 (2) SPB	17 n/a 1 n/a 136 138 139 n/a	n/a n/a n/a n/a 134 136 n/a n/a	35 29 4 3 145 143 149 156	n/a n/a n/a n/a 142 143 n/a n/a
C-23 (1) SPB	26 n/a 5 n/a 137 137 80 n/a	n/a n/a n/a n/a 136 140 n/a n/a	n/a 15 n/a 56 149 146 n/a 242	18 n/a 1 n/a 146 145 143 n/a
C-24 (2) CS	24 24 2 2 181 179 181 175	n/a n/a n/a n/a 176 174 n/a n/a	n/a 26 n/a 3 192 189 n/a 187	27 n/a 3 n/a 187 191 172 n/a
C-24 (17,11) CS	33 16 3 1 205 196 197 197	23 n/a 1 n/a 197 194 208 n/a	n/a 11 n/a 0 195 193 n/a 194	20 n/a 1 n/a 192 194 191 n/a
C-25 (2) CS	18 15 1 1 149 149 141 132	n/a n/a n/a n/a 145 137 n/a n/a	n/a n/a n/a n/a n/a n/a n/a n/a	n/a n/a n/a n/a n/a n/a n/a n/a
C-25 (8) CS	12 8 0 0 155 152 164 157	n/a n/a n/a n/a 151 146 n/a n/a	n/a n/a n/a n/a n/a n/a n/a n/a	n/a n/a n/a n/a n/a n/a n/a n/a
C-26 (2) SB	14 13 1 1 163 161 152 127	n/a n/a n/a n/a 162 155 n/a n/a	n/a n/a n/a n/a 162 160 n/a n/a	n/a 19 n/a 1 159 161 n/a 124

Table 4.16 Salinity Hindcast Validation: April 1979-October 1980. For each row in each month, the first entry corresponds to the first 15 days of the month, with the second entry denoting the remaining portion. Row 1 corresponds to the RMSE in PSU. Row 2 corresponds to the Willmott Relative Error in percent. Row 3 corresponds to the model mean in PSU with row 4 denoting the observed salinity mean in PSU. Note n/a denotes not applicable.

Station	Apr 1979	May 1979	Sep 1980	Oct 1980
C-1 (46) GG	2 3 41 56 30 29 31 32	n/a n/a n/a n/a 29 30 n/a n/a	n/a 2 n/a 58 30 30 n/a 32	1 n/a 55 n/a 31 31 32 n/a
C-1 (91,76) GG	3 4 46 61 28 27 30 31	n/a n/a n/a n/a 28 29 n/a n/a	n/a n/a n/a n/a 30 30 n/a n/a	n/a n/a n/a n/a 30 30 n/a n/a
C-5 (2) MB	1 n/a 37 n/a 29 28 30 n/a	n/a n/a n/a n/a 29 29 n/a n/a	n/a n/a n/a n/a n/a n/a n/a n/a	n/a n/a n/a n/a n/a n/a n/a n/a
C-5 (8) MB	1 n/a 35 n/a 29 28 29 n/a	n/a n/a n/a n/a 28 29 n/a n/a	n/a n/a n/a n/a n/a n/a n/a n/a	n/a n/a n/a n/a n/a n/a n/a n/a
C-5 (25) MB	2 n/a 21 n/a 28 27 28 n/a	n/a n/a n/a n/a 27 28 n/a n/a	n/a n/a n/a n/a n/a n/a n/a n/a	n/a n/a n/a n/a n/a n/a n/a n/a
C-16 (8) MB	n/a n/a n/a n/a n/a n/a n/a n/a	n/a n/a n/a n/a n/a n/a n/a n/a	3 4 72 59 29 29 32 32	n/a n/a n/a n/a 30 29 n/a n/a
C-16 (17) MB	n/a n/a n/a n/a n/a n/a n/a n/a	n/a n/a n/a n/a n/a n/a n/a n/a	3 2 65 43 29 29 31 31	n/a n/a n/a n/a 30 29 n/a n/a
C-16 (23) MB	n/a n/a n/a n/a n/a n/a n/a n/a	n/a n/a n/a n/a n/a n/a n/a n/a	3 2 59 36 29 29 31 31	n/a n/a n/a n/a 30 29 n/a n/a
C-17 (2) MB	1 n/a 10 n/a 25 24 26 n/a	n/a n/a n/a n/a 25 26 n/a n/a	n/a n/a n/a n/a n/a n/a n/a n/a	n/a n/a n/a n/a n/a n/a n/a n/a
C-17 (5) MB	2 n/a 10 n/a 25 23 25 n/a	n/a n/a n/a n/a 24 26 n/a n/a	n/a n/a n/a n/a n/a n/a n/a n/a	n/a n/a n/a n/a n/a n/a n/a n/a
C-18 (9) MB	4 5 42 50 22 21 25 26	5 n/a 58 n/a 22 24 27 n/a	n/a 1 n/a 12 26 26 n/a 27	1 1 11 10 27 27 27 28
C-18 (15) MB	4 6 38 46 20 19 22 25	5 n/a 46 n/a 20 23 25 n/a	n/a 1 n/a 11 25 26 n/a 27	1 1 12 17 27 26 27 26

Table 4.16 (Cont.). Salinity Hindcast Validation April 1979-October 1980. For each row in each month, the first entry corresponds to the first 15 days of the month, with the second entry denoting the remaining portion. Row 1 corresponds to the RMSE in PSU. Row 2 corresponds to the Willmott Relative Error in percent. Row 3 corresponds to the model mean in PSU with row 4 denoting the observed salinity mean in PSU. Note n/a denotes not applicable.

Station	Apr 1979	May 1979	Sep 1980	Oct 1980
C-19 (1) SPB	2 n/a 15 n/a 16 15 18 n/a	n/a n/a n/a n/a 16 19 n/a n/a	n/a n/a n/a n/a 23 24 n/a n/a	n/a n/a n/a n/a 25 24 n/a n/a
C-20 (1) SPB	n/a n/a n/a n/a 17 13 n/a n/a	n/a n/a n/a n/a 10 9 n/a n/a	n/a n/a n/a n/a n/a n/a n/a n/a	n/a n/a n/a n/a n/a n/a n/a n/a
C-22 (2) SPB	3 n/a 31 n/a 18 17 22 n/a	n/a n/a n/a n/a 18 21 n/a n/a	2 1 61 15 24 25 27 25	n/a n/a n/a n/a 26 25 n/a n/a
C-23 (1) SPB	n/a n/a n/a n/a 9 8 n/a n/a	n/a n/a n/a n/a 9 15 n/a n/a	n/a 2 n/a 86 22 23 n/a 21	3 4 71 89 24 23 21 19
C-24 (2,6) CS	10 10 57 60 6 6 15 13	9 n/a 55 n/a 7 13 17 n/a	n/a 3 n/a 52 22 22 n/a 20	3 n/a 46 n/a 23 22 20 n/a
C-24 (17,11) CS	8 10 61 56 4 5 11 14	7 n/a 51 n/a 6 11 14 n/a	n/a 4 n/a 51 22 22 n/a 19	4 n/a 49 n/a 23 22 19 n/a
C-25 (2) CS	n/a n/a n/a n/a 2 2 n/a n/a	n/a n/a n/a n/a 2 7 n/a n/a	n/a n/a n/a n/a n/a n/a n/a n/a	n/a n/a n/a n/a n/a n/a n/a n/a
C-25 (8) CS	7 10 50 59 2 1 7 10	n/a n/a n/a n/a 2 7 n/a n/a	n/a n/a n/a n/a n/a n/a n/a n/a	n/a n/a n/a n/a n/a n/a n/a n/a
C-26(2) SB	n/a n/a n/a n/a 1 0 n/a n/a	n/a n/a n/a n/a 0 4 n/a n/a	n/a n/a n/a n/a 22 22 n/a n/a	n/a 10 n/a 65 22 22 n/a 13

Table 4.17 Temperature Hindcast Validation: April 1979- October 1980. For each row in each month, the first entry corresponds to the first 15 days of the month, with the second entry denoting the remaining portion. Row 1 corresponds to the RMSE in ^oC. Row 2 corresponds to the Willmott Relative Error in percent. Row 3 corresponds to the model mean in ^oC with row 4 denoting the observed temperature mean in ^oC. Note n/a denotes not applicable.

Station	Apr 1979	May 1979	Sep 1980	Oct 1980
C-1 (46,76) GG	1 1 57 58 13 13 12 12	n/a n/a n/a n/a 13 14 n/a n/a	2 1 66 46 17 16 15 15	1 n/a 50 n/a 16 15 15 n/a
C-1 (91) GG	1 2 56 59 13 13 12 12	n/a n/a n/a n/a 13 14 n/a n/a	n/a n/a n/a n/a n/a n/a n/a n/a	n/a n/a n/a n/a n/a n/a n/a n/a
C-5 (2) MB	1 n/a 61 n/a 13 13 12 n/a	n/a n/a n/a n/a 13 14 n/a n/a	n/a n/a n/a n/a n/a n/a n/a n/a	n/a n/a n/a n/a n/a n/a n/a n/a
C-5 (8) MB	1 n/a 59 n/a 13 13 12 n/a	n/a n/a n/a n/a 13 14 n/a n/a	n/a n/a n/a n/a n/a n/a n/a n/a	n/a n/a n/a n/a n/a n/a n/a n/a
C-5 (25) MB	0 n/a 37 n/a 13 13 13 n/a	n/a n/a n/a n/a 14 14 n/a n/a	n/a n/a n/a n/a n/a n/a n/a n/a	n/a n/a n/a n/a n/a n/a n/a n/a
C-16 (8) MB	n/a n/a n/a n/a n/a n/a n/a n/a	n/a n/a n/a n/a n/a n/a n/a n/a	2 1 67 49 17 17 16 16	n/a n/a n/a n/a 17 16 n/a n/a
C-16 (17) MB	n/a n/a n/a n/a n/a n/a n/a n/a	n/a n/a n/a n/a n/a n/a n/a n/a	2 1 62 42 17 17 16 16	n/a n/a n/a n/a 17 16 n/a n/a
C-16 (23) MB	n/a n/a n/a n/a n/a n/a n/a n/a	n/a n/a n/a n/a n/a n/a n/a n/a	2 1 60 39 18 17 16 16	n/a n/a n/a n/a 17 16 n/a n/a
C-17 (2) MB	0 n/a 33 n/a 13 14 13 n/a	n/a n/a n/a n/a 14 15 n/a n/a	n/a n/a n/a n/a n/a n/a n/a n/a	n/a n/a n/a n/a n/a n/a n/a n/a
C-17 (5) MB	0 n/a 22 n/a 13 14 13 n/a	n/a n/a n/a n/a 14 15 n/a n/a	n/a n/a n/a n/a n/a n/a n/a n/a	n/a n/a n/a n/a n/a n/a n/a n/a
C-18 (9) MB	0 1 29 35 13 14 13 13	0 n/a 17 n/a 14 15 14 n/a	n/a 1 n/a 29 19 19 n/a 17	1 2 24 65 18 17 17 16
C-18 (15) MB	0 1 28 35 14 14 14 14	0 n/a 24 n/a 15 15 15 n/a	n/a 1 n/a 27 20 19 n/a 18	1 1 18 59 18 18 18 16

Table 4.17 (Cont.). Temperature Hindcast Validation April 1979–October 1980. For each row in each month, the first entry corresponds to the first 15 days of the month, with the second entry denoting the remaining portion. Row 1 corresponds to the RMSE in ^{o}C. Row 2 corresponds to the Willmott Relative Error in percent. Row 3 corresponds to the model mean in ^{o}C with row 4 denoting the observed temperature mean in ^{o}C. Bold italics indicate measurement errors and their associated model discrepancies. Note n/a denotes not applicable.

Station	Apr 1979	May 1979	Sep 1980	Oct 1980
C-19 (1) SPB	0 n/a 34 n/a 14 14 14 n/a	n/a n/a n/a n/a 15 16 n/a n/a	3 2 73 59 21 20 18 18	1 n/a 20 n/a 19 19 19 n/a
C-20 (1) SPB	4 n/a 59 n/a 13 14 17 n/a	n/a n/a n/a n/a 14 15 n/a n/a	n/a n/a n/a n/a n/a n/a n/a n/a	n/a n/a n/a n/a n/a n/a n/a n/a
C-22 (2) SPB	0 n/a 17 n/a 14 14 13 n/a	n/a n/a n/a n/a 15 16 n/a n/a	2 2 78 69 20 20 18 18	n/a n/a n/a n/a 19 19 n/a n/a
C-23 (1) SPB	***11*** n/a ***93*** n/a 14 15 ***3*** n/a	n/a n/a n/a n/a 16 16 n/a n/a	n/a 1 n/a 58 21 21 n/a 19	1 3 51 92 20 20 19 17
C-24 (2,6) CS	1 1 41 59 15 15 14 14	0 n/a 48 n/a 16 17 n/a n/a	n/a 3 n/a 83 22 21 n/a 18	2 n/a 75 n/a 21 20 19 n/a
C-24 (17,11) CS	1 0 36 34 15 15 15 15	0 n/a 55 n/a 16 17 16 n/a	n/a 3 n/a 84 22 21 n/a 19	2 n/a 76 n/a 21 20 19 n/a
C-25 (2) CS	1 1 57 67 15 16 15 15	n/a n/a n/a n/a 16 17 n/a n/a	n/a n/a n/a n/a n/a n/a n/a n/a	n/a n/a n/a n/a n/a n/a n/a n/a
C-25 (8) CS	0 1 51 65 15 16 15 15	n/a n/a n/a n/a 16 17 n/a n/a	n/a n/a n/a n/a n/a n/a n/a n/a	n/a n/a n/a n/a n/a n/a n/a n/a
C-26 (2) SB	0 1 52 57 15 16 15 15	n/a n/a n/a n/a 17 18 n/a n/a	n/a n/a n/a n/a 22 22 n/a n/a	n/a 4 n/a 95 21 20 n/a 16

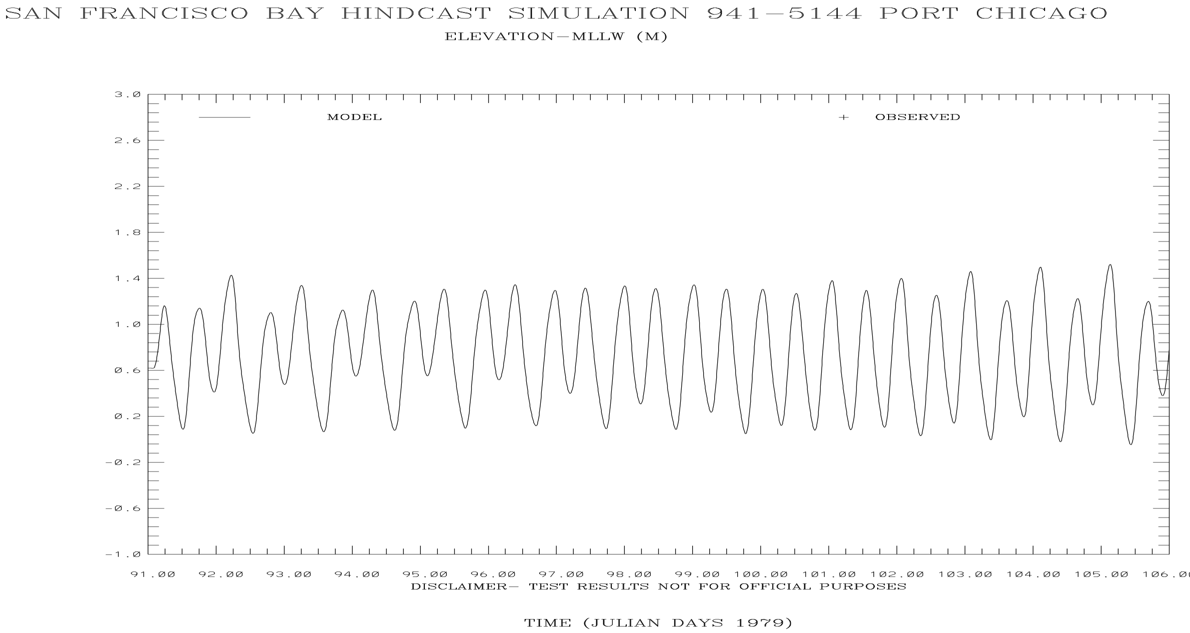

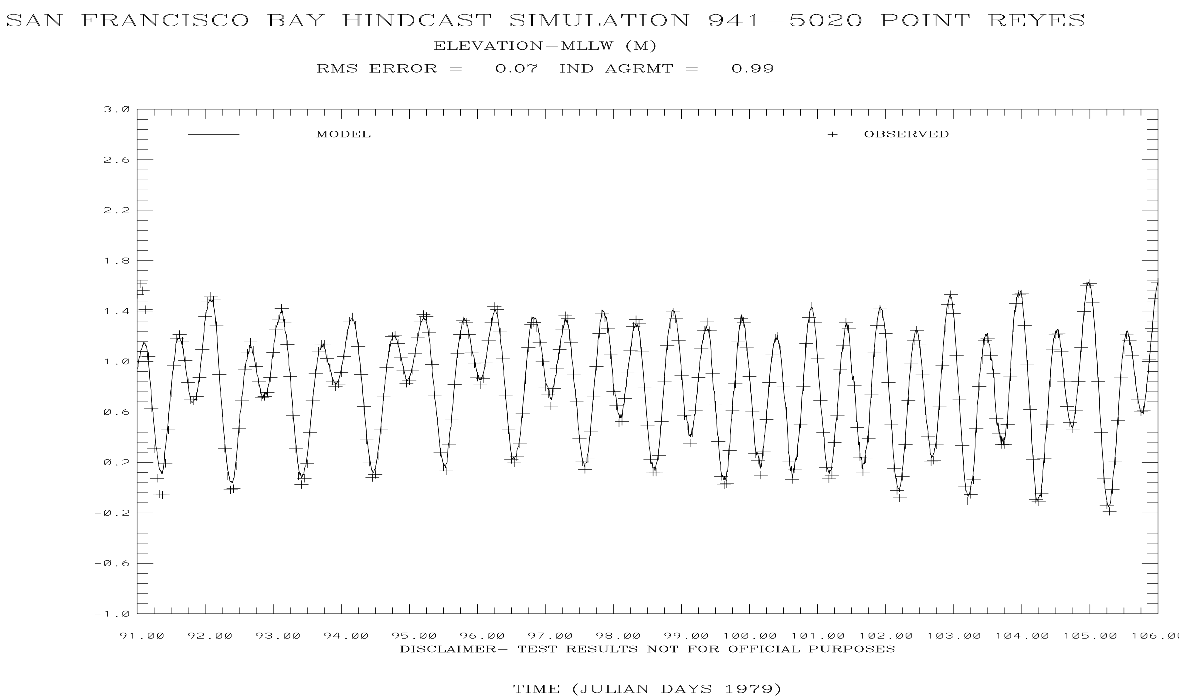

Figure 4.53. April 1-15, 1979 Hindcast: Port Chicago and Point Reyes Water Level Comparisons. Note IND AGRMT equals one minus Willmott et al. (1985) relative error.

SAN FRANCISCO BAY HINDCAST SIMULATION 941-4290 SAN FRANCISCO-SF-ITL
ELEVATION-MLLW (M)
RMS ERROR = 0.14 IND AGRMT = 0.98

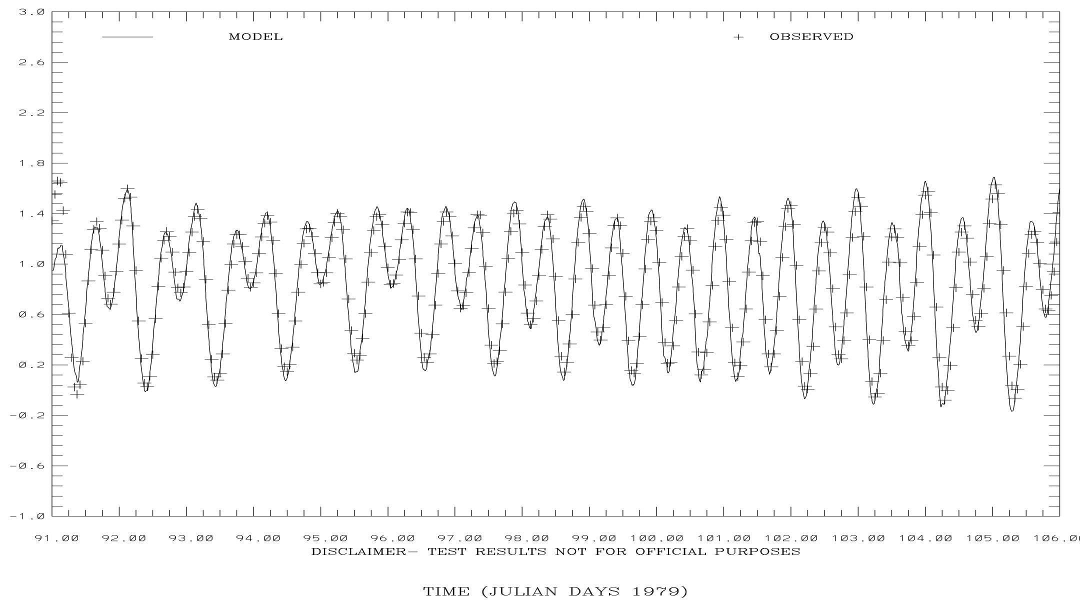

SAN FRANCISCO BAY HINDCAST SIMULATION 941-4458 SAN MATEO BRIDGE
ELEVATION-MLLW (M)
RMS ERROR = 3.02 IND AGRMT = 0.31

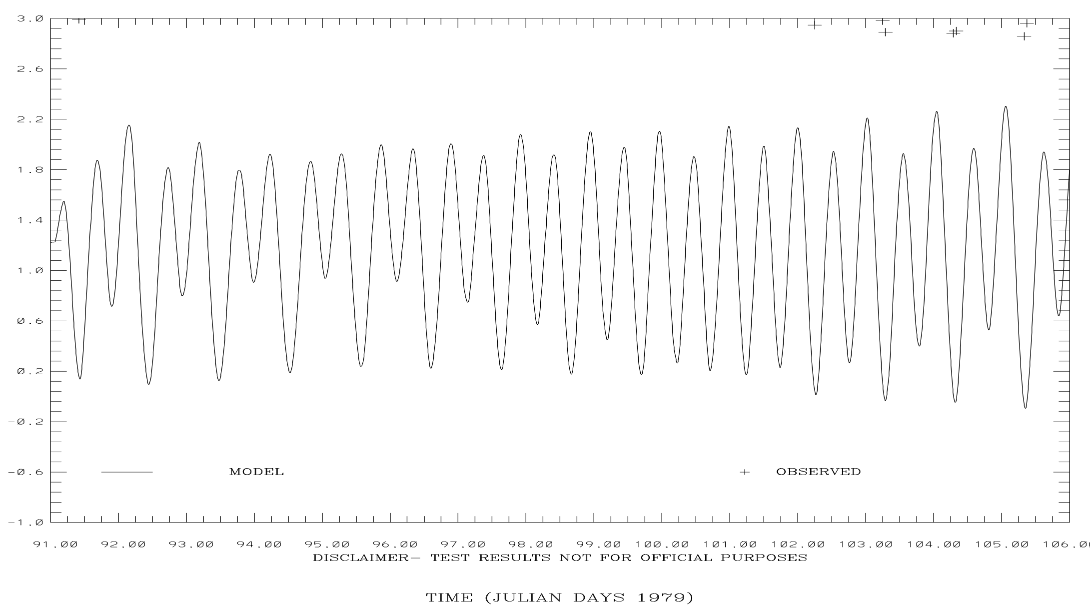

Figure 4.54. April 1-15, 1979 Hindcast: San Francisco and San Mateo Bridge Water Level Comparisons. Note IND AGRMT equals one minus Willmott et al. (1985) relative error.

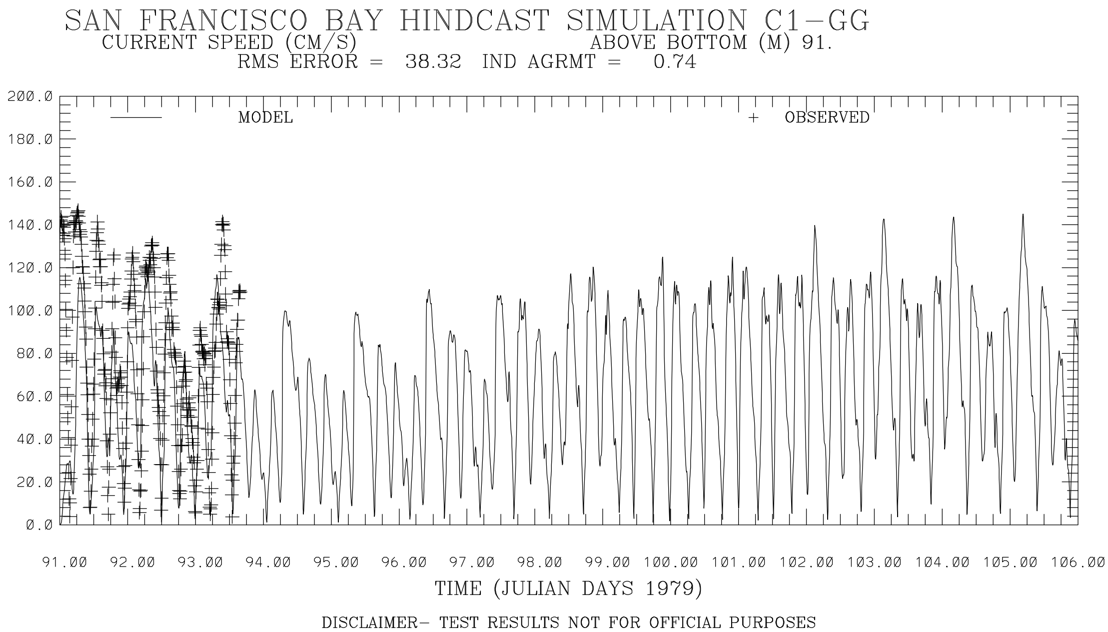

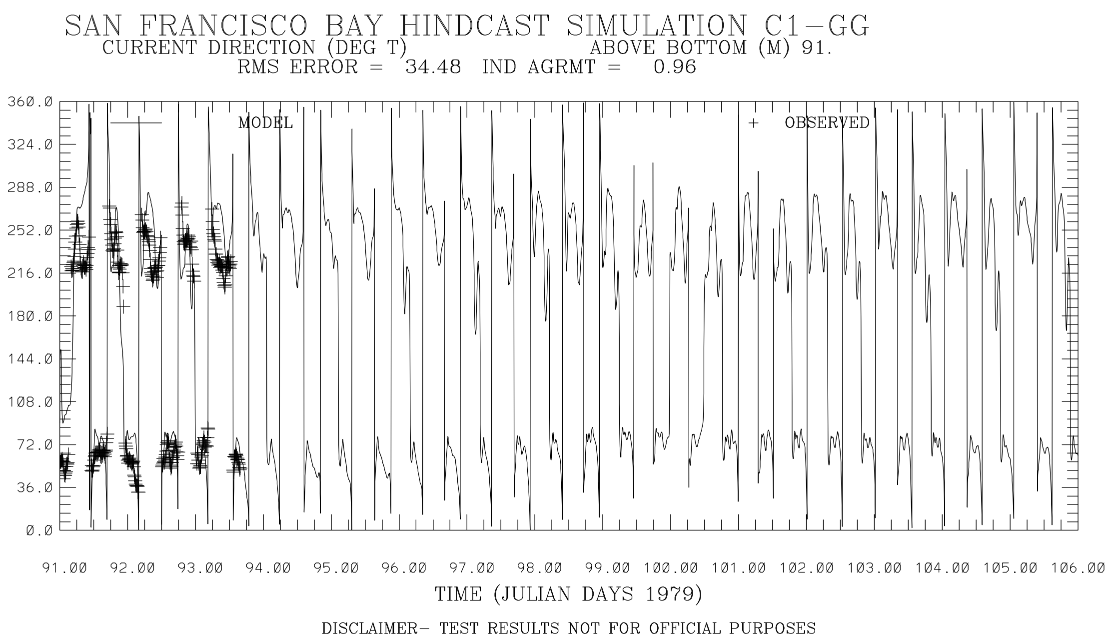

Figure 4.55. April 1-15, 1979 Hindcast: C-1 Current Speed and Direction at 91m above the bottom. Note IND AGRMT equals one minus Willmott et al. (1985) relative error.

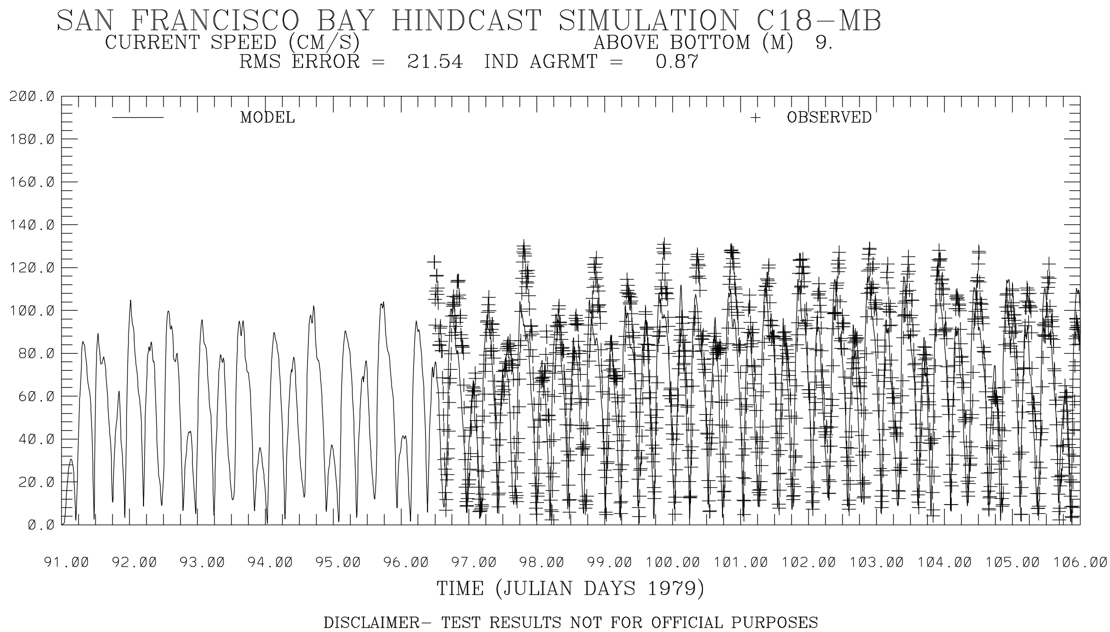

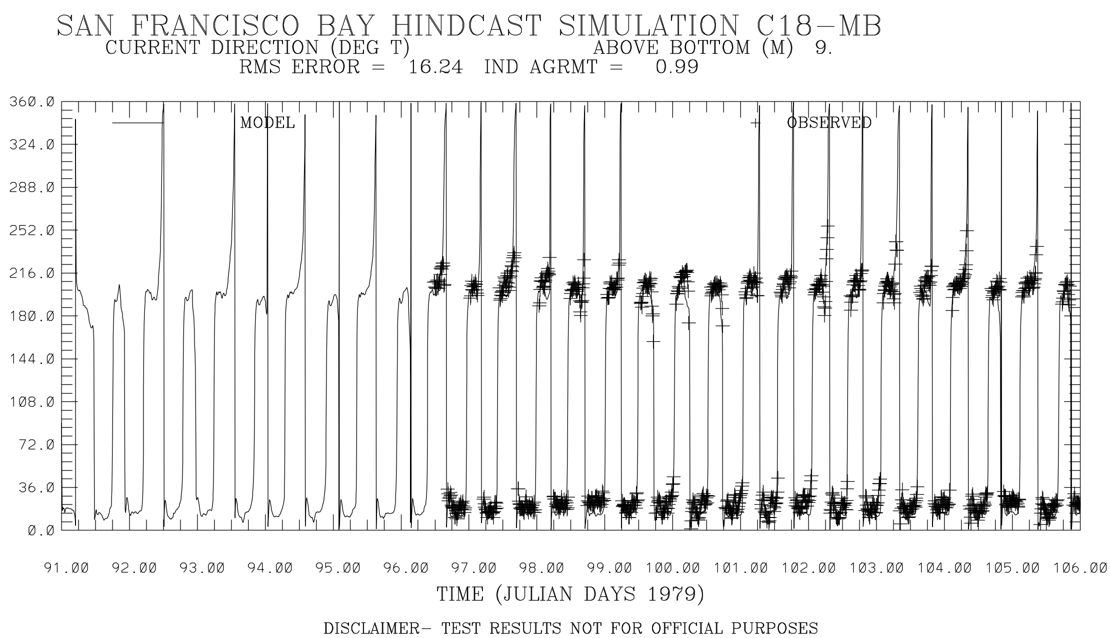

Figure 4.56. April 1-15, 1979 Hindcast: C-18 Current Speed and Direction at 9m above the bottom. Note IND AGRMT equals one minus Willmott et al. (1985) relative error.

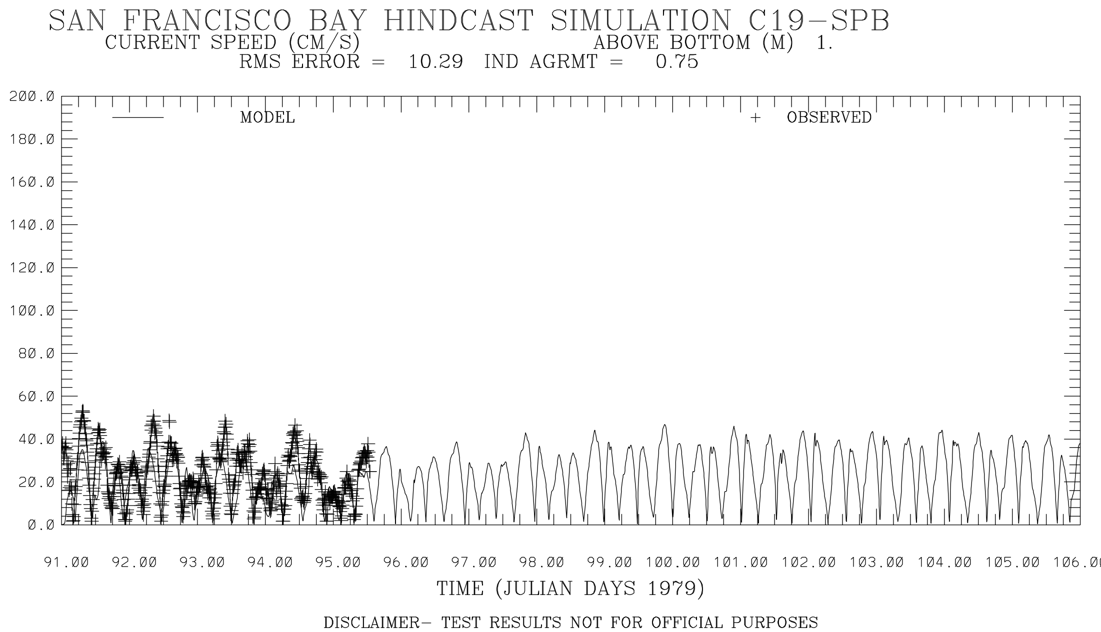

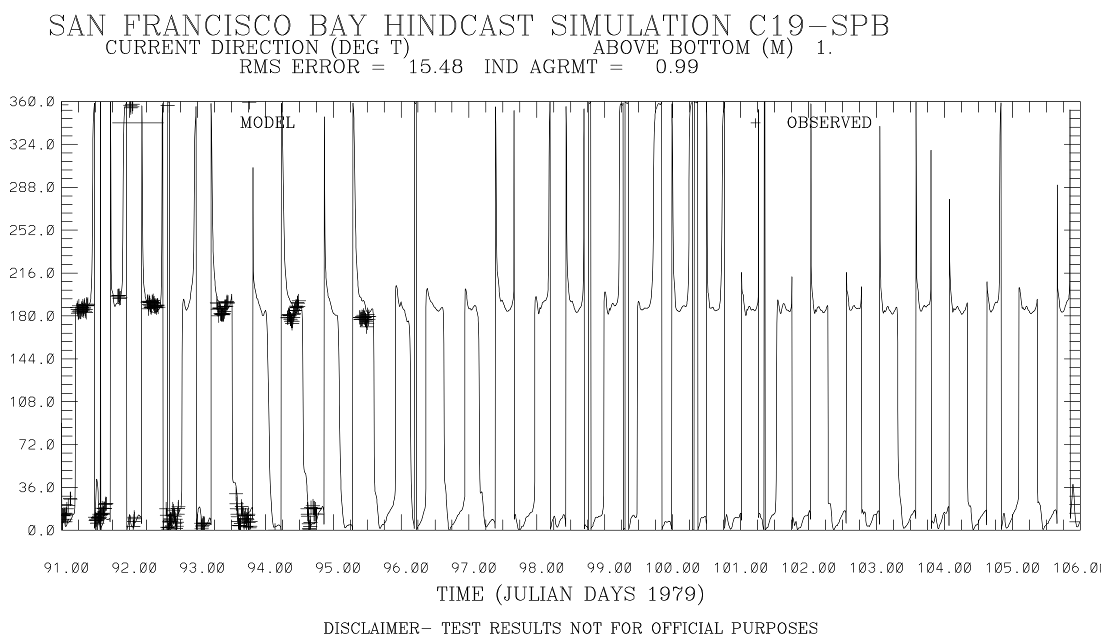

Figure 4.57. April 1-15, 1979 Hindcast: C-19 Current Speed and Direction at 1m above the bottom. Note IND AGRMT equals one minus Willmott et al. (1985) relative error.

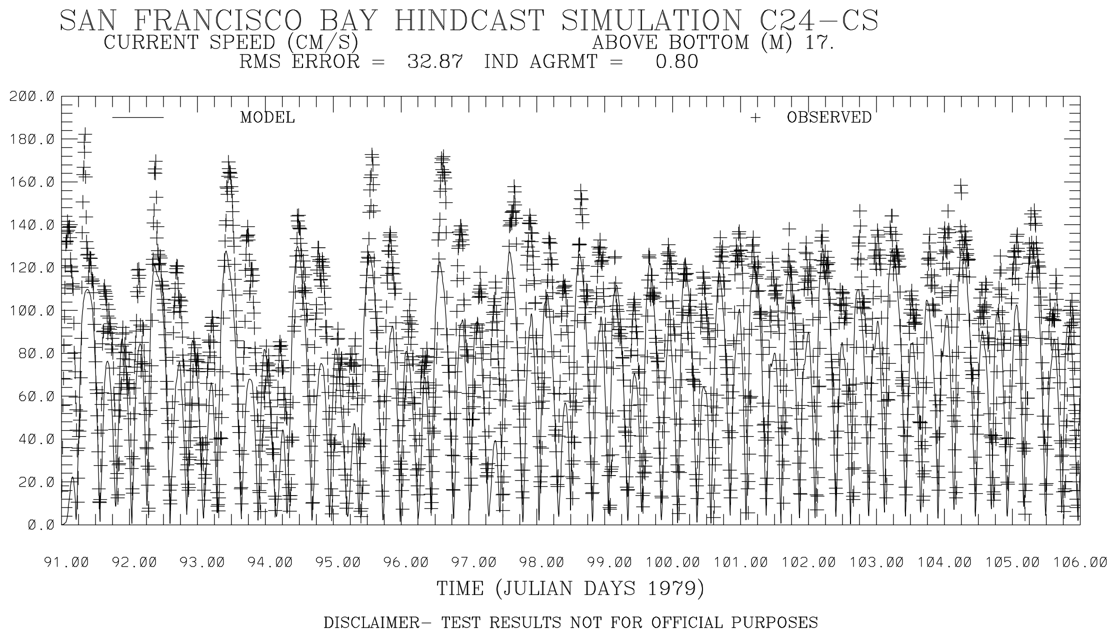

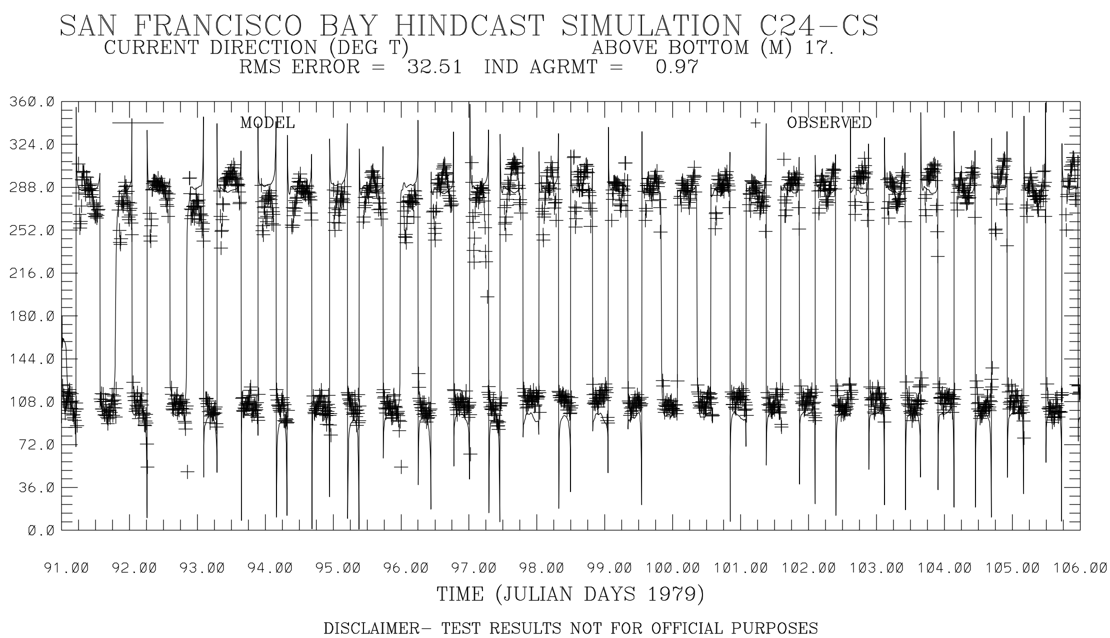

Figure 4.58. April 1-15, 1979 Hindcast: C-24 Current Speed and Direction at 17m above the bottom. Note IND AGRMT equals one minus Willmott et al. (1985) relative error.

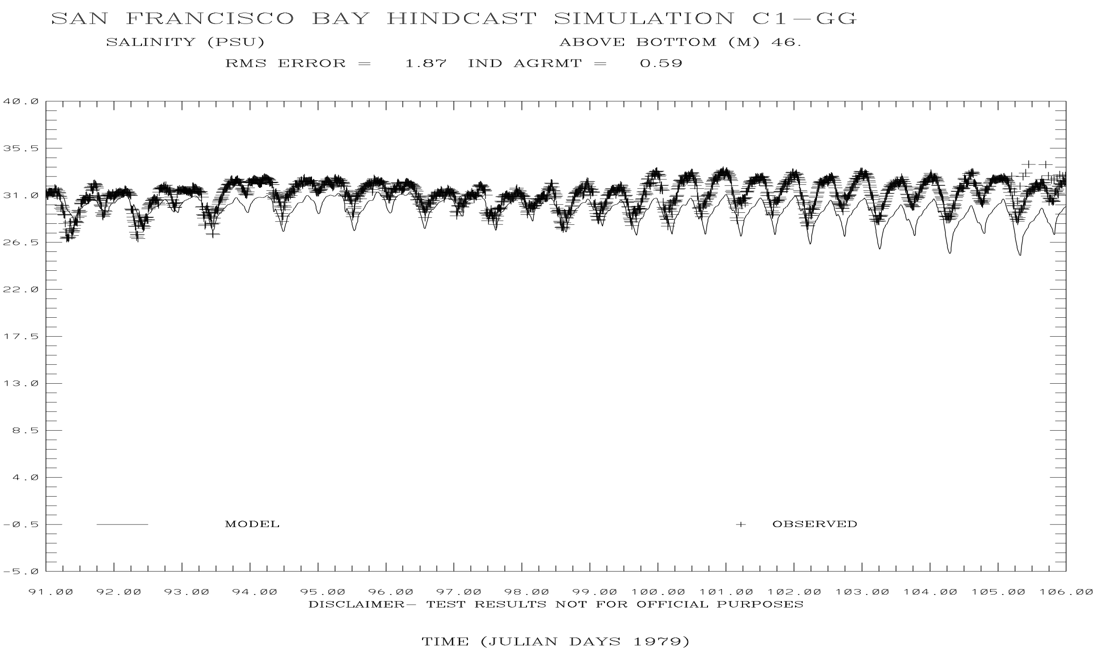

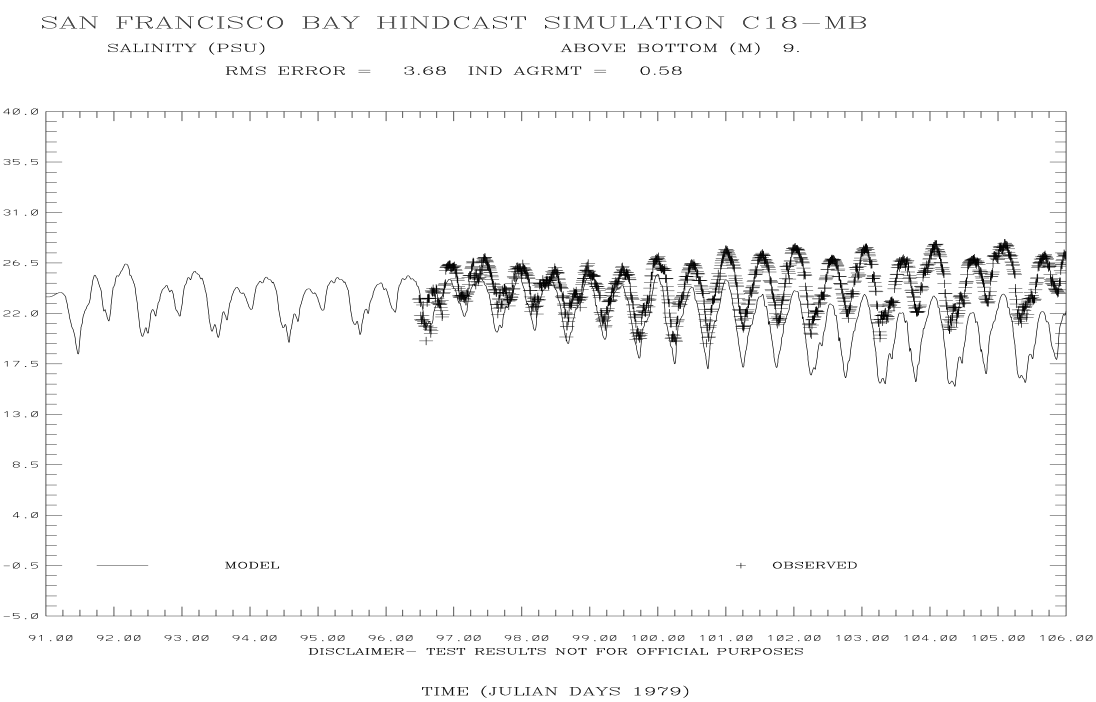

Figure 4.59. April 1-15, 1979 Hindcast: Salinity at C-1 at 46m and C-18 at 9m above the bottom. Note IND AGRMT equals one minus Willmott et al. (1985) relative error.

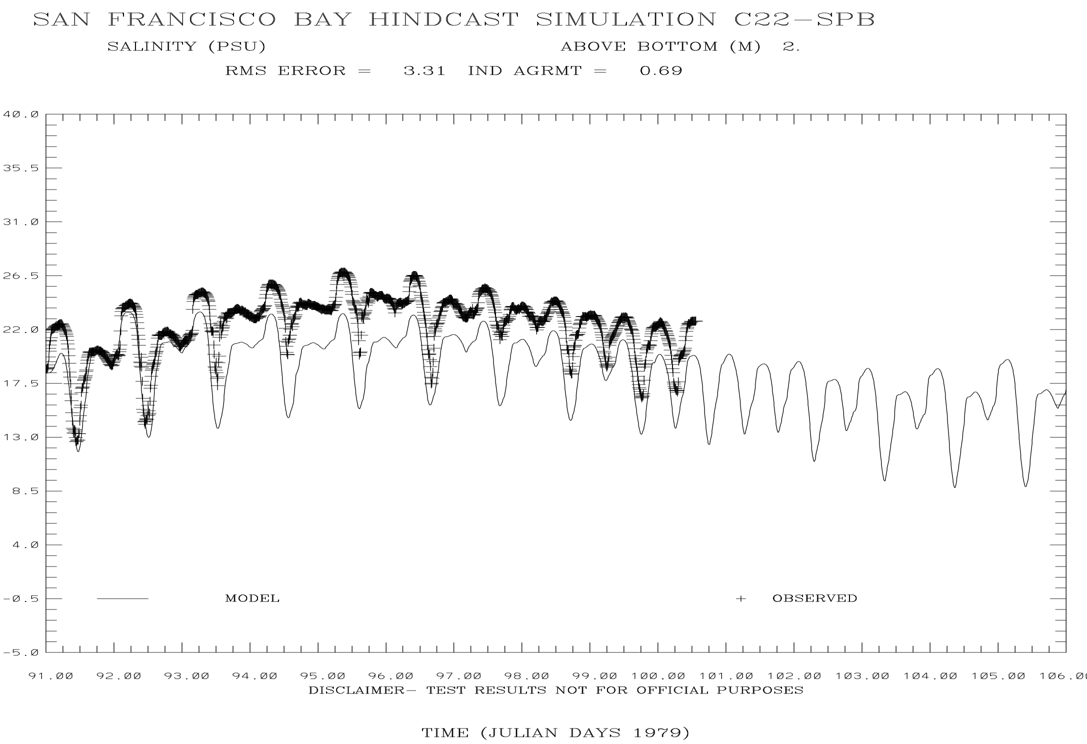

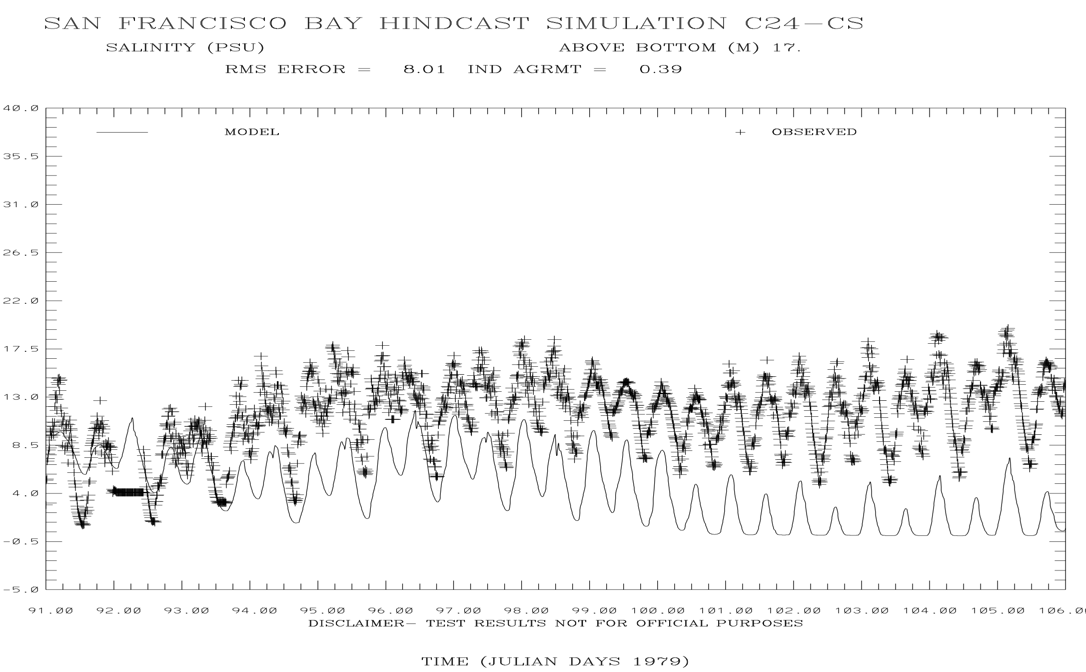

Figure 4.60. April 1-15, 1979 Hindcast: Salinity at C-22 at 2m and C-24 at 17m above the bottom. Note IND AGRMT equals one minus Willmott et al. (1985) relative error.

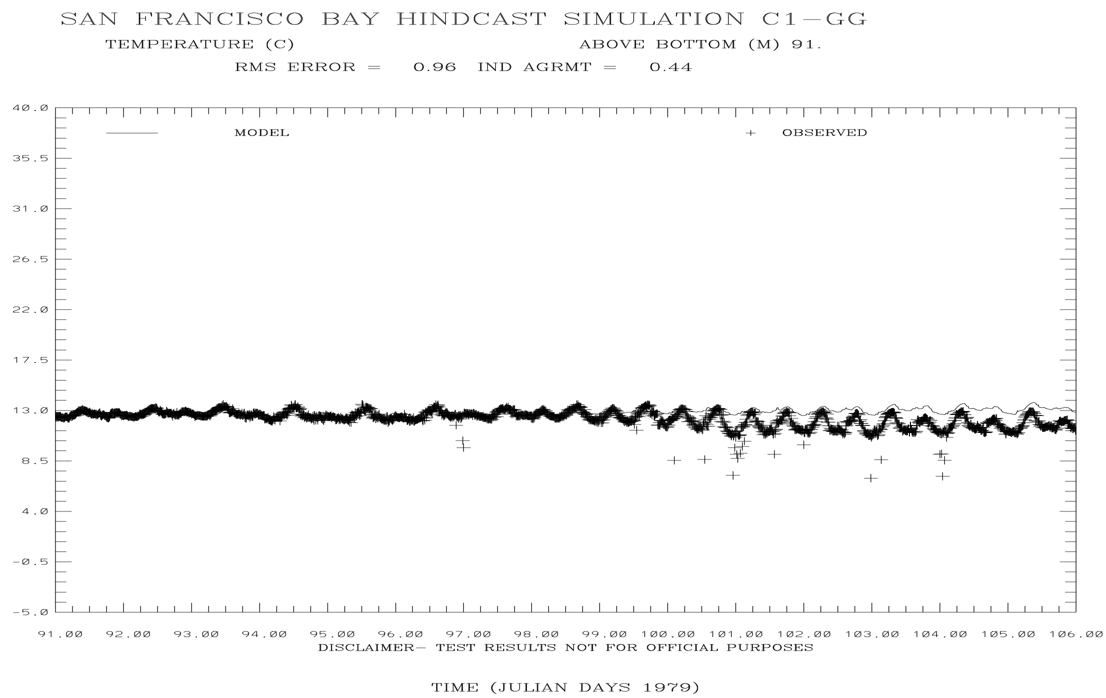

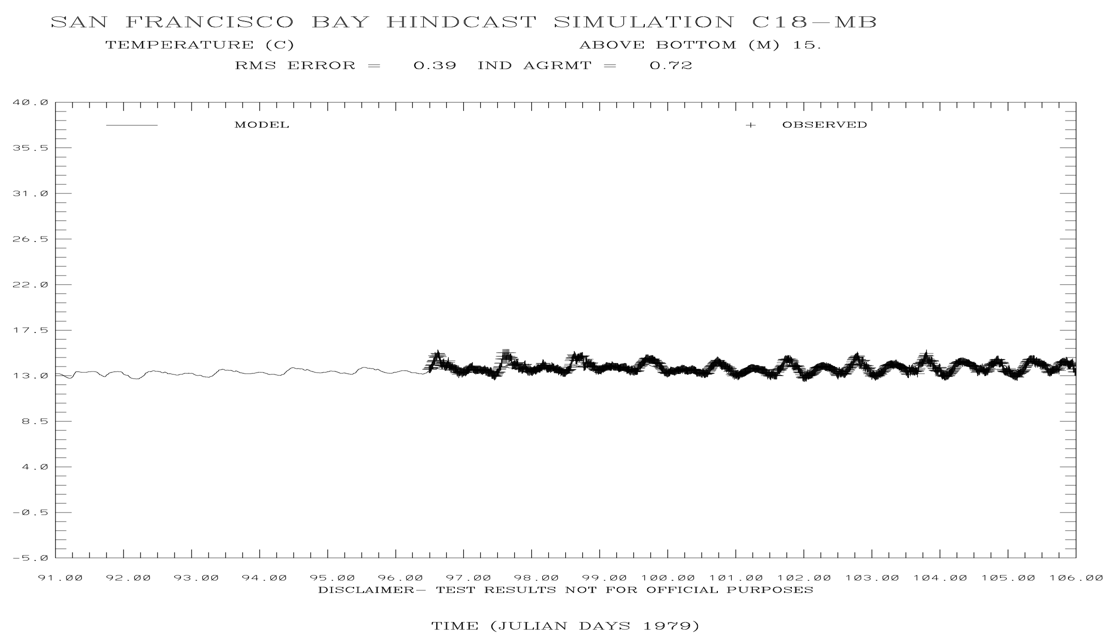

Figure 4.61. April 1-15, 1979 Hindcast: Temperature at C-1 at 91m and C-18 at 15m above the bottom. Note IND AGRMT equals one minus Willmott et al. (1985) relative error.

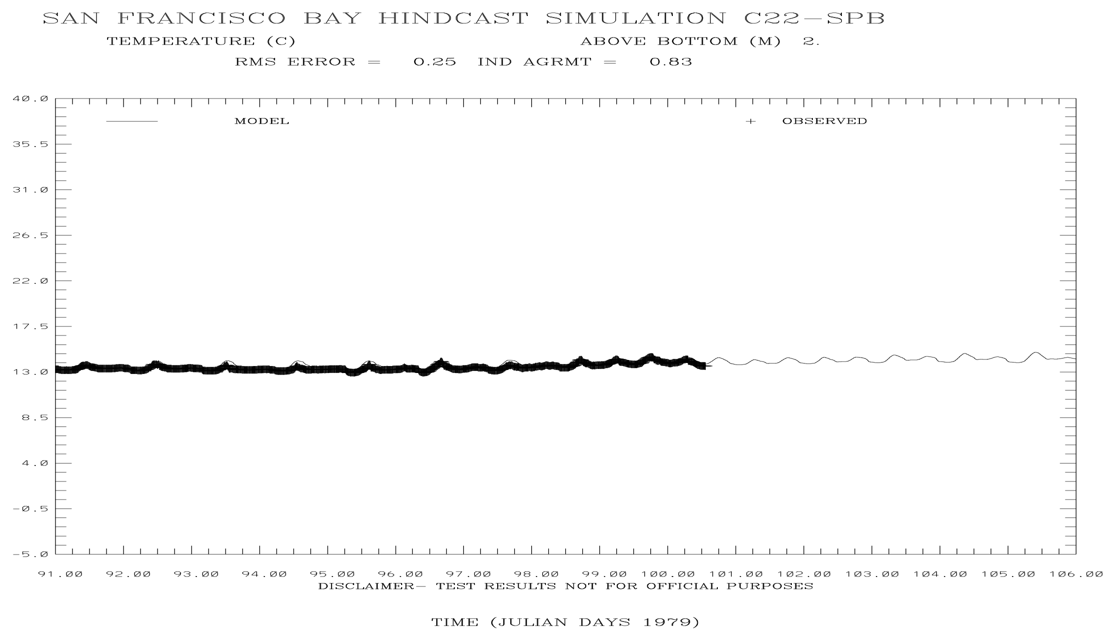

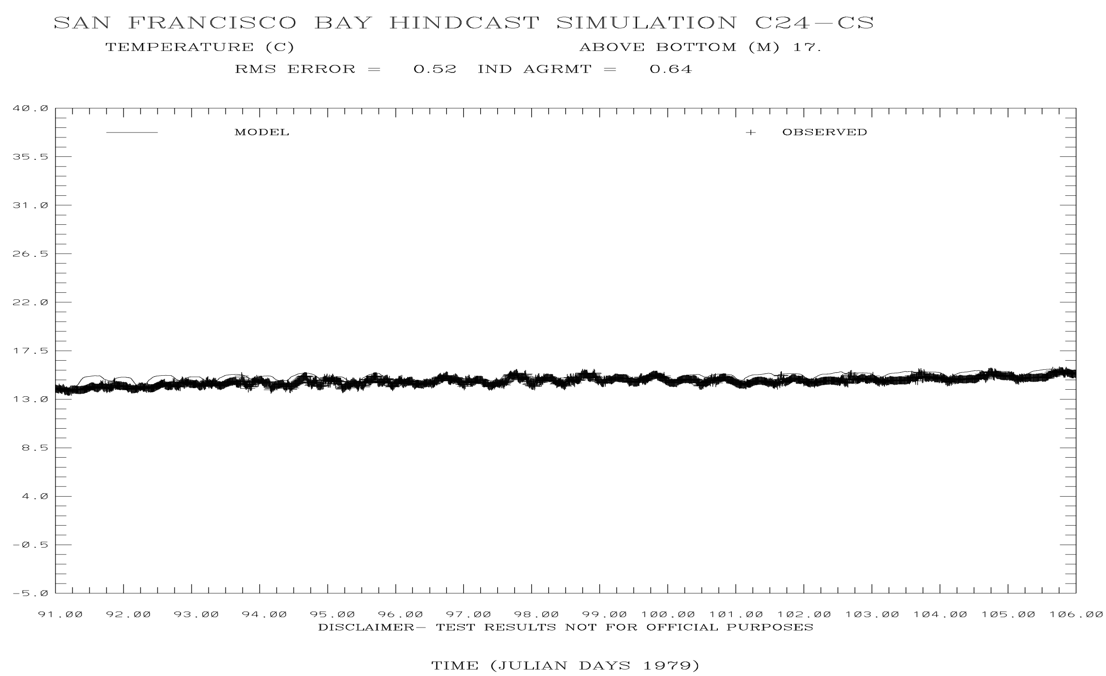

Figure 4.62. April 1-15, 1979 Hindcast: Temperature at C-22 at 2m and C-24 at 17m above the bottom. Note IND AGRMT equals one minus Willmott et al. (1985) relative error.

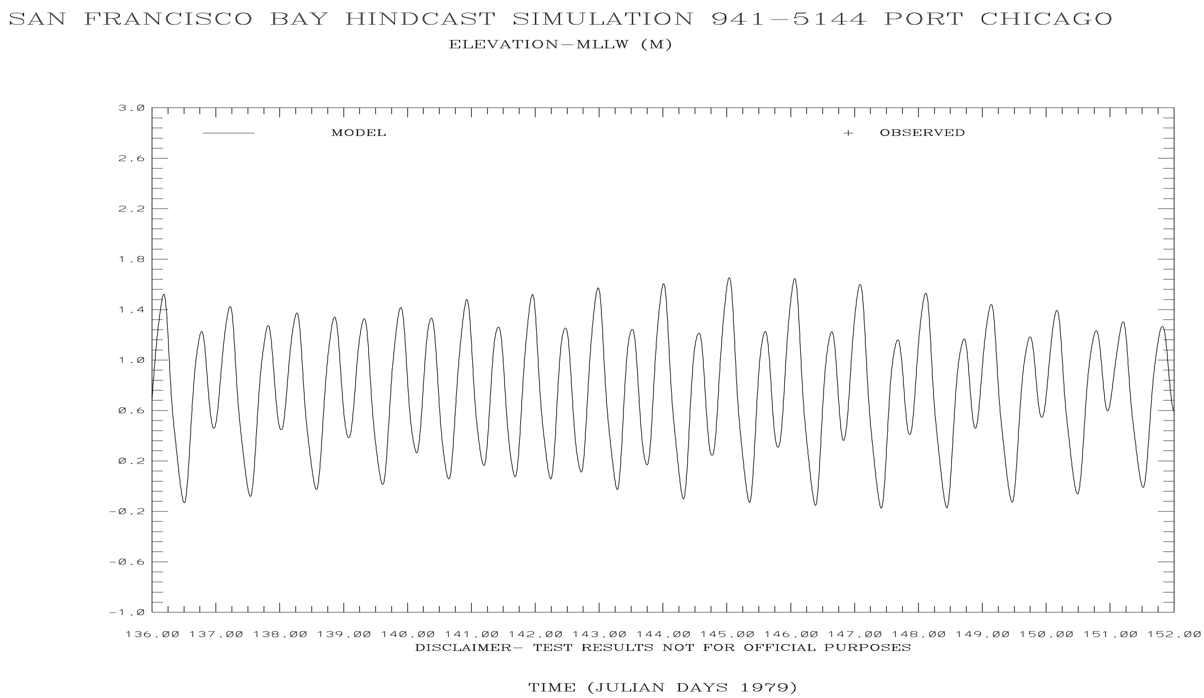

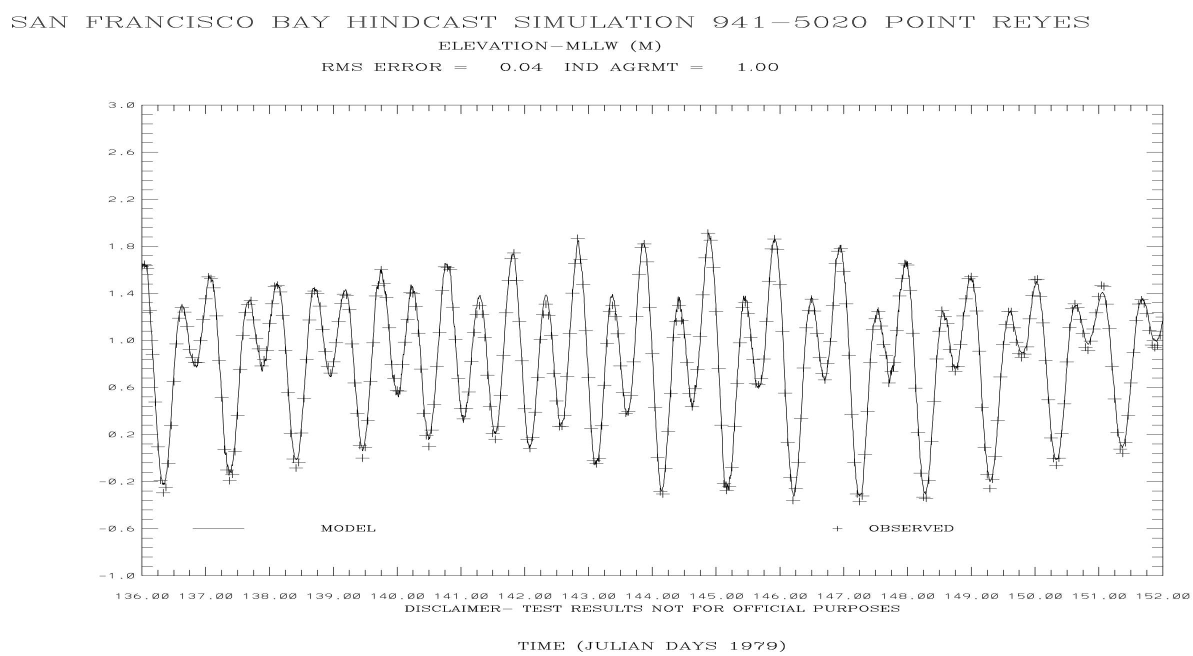

Figure 4.63. May 15-31, 1979 Hindcast: Port Chicago and Point Reyes Water Level Comparisons. Note IND AGRMT equals one minus Willmott et al. (1985) relative error.

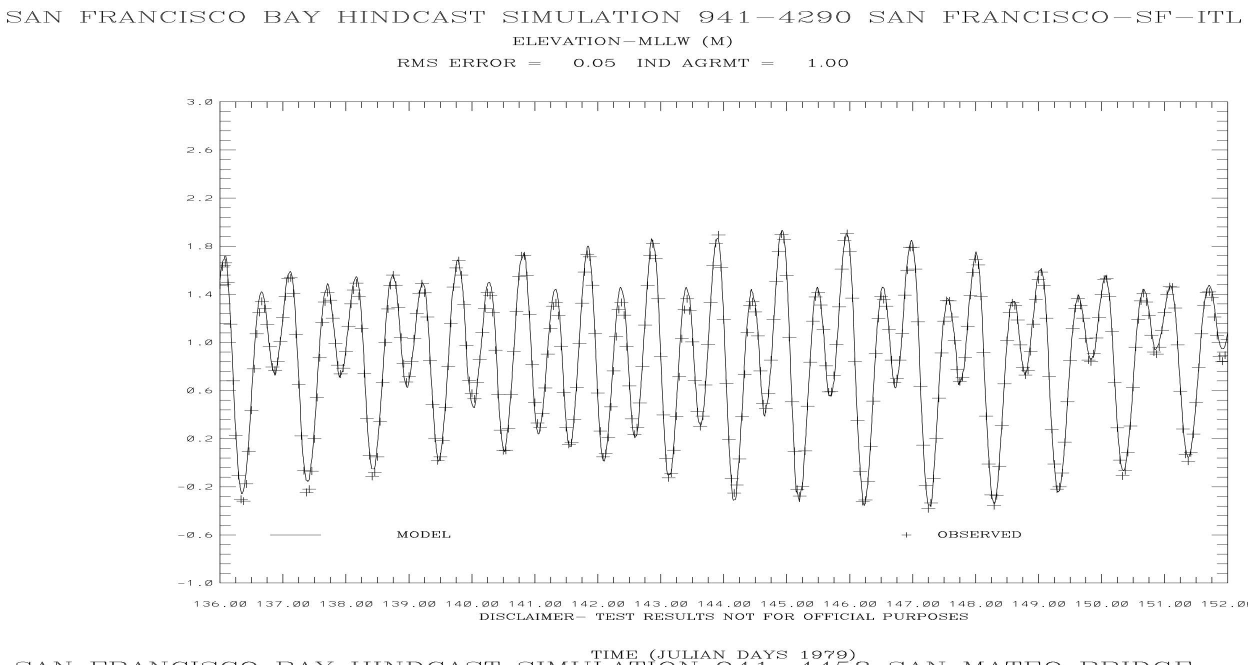

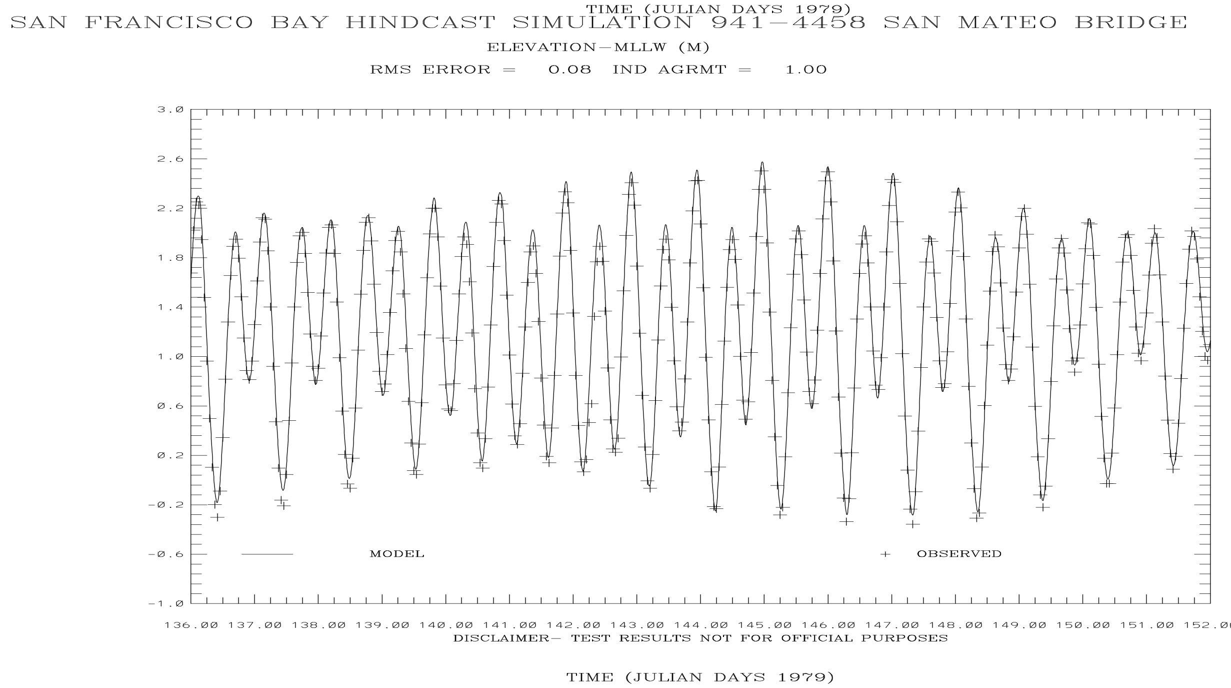

Figure 4.64. May 15-31, 1979 Hindcast: San Francisco and San Mateo Bridge Water Level Comparisons. Note IND AGRMT equals one minus Willmott et al. (1985) relative error.

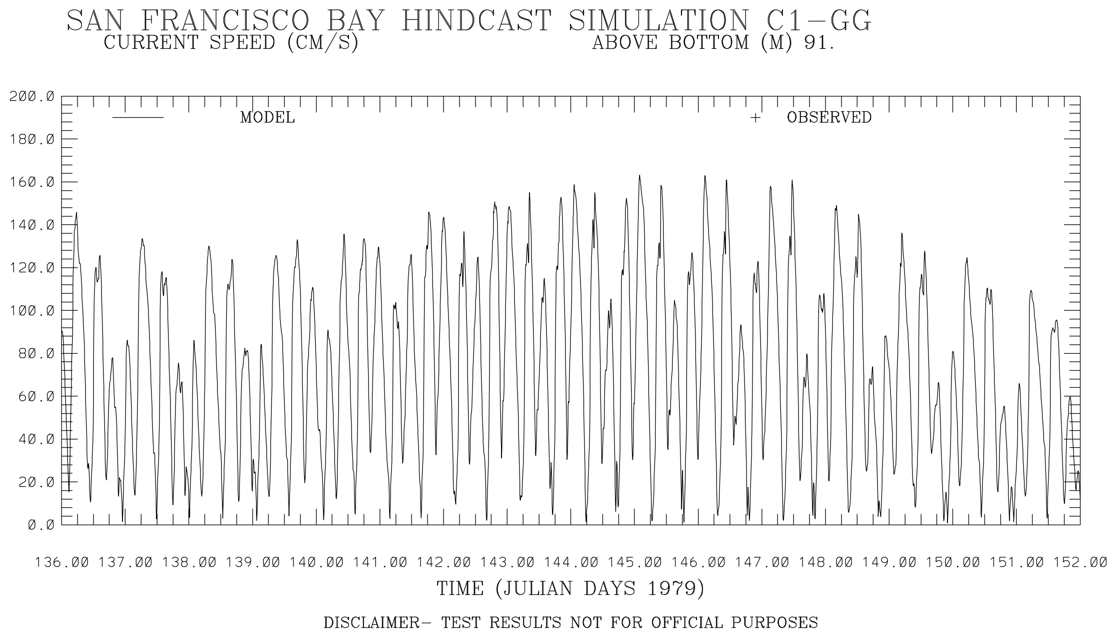

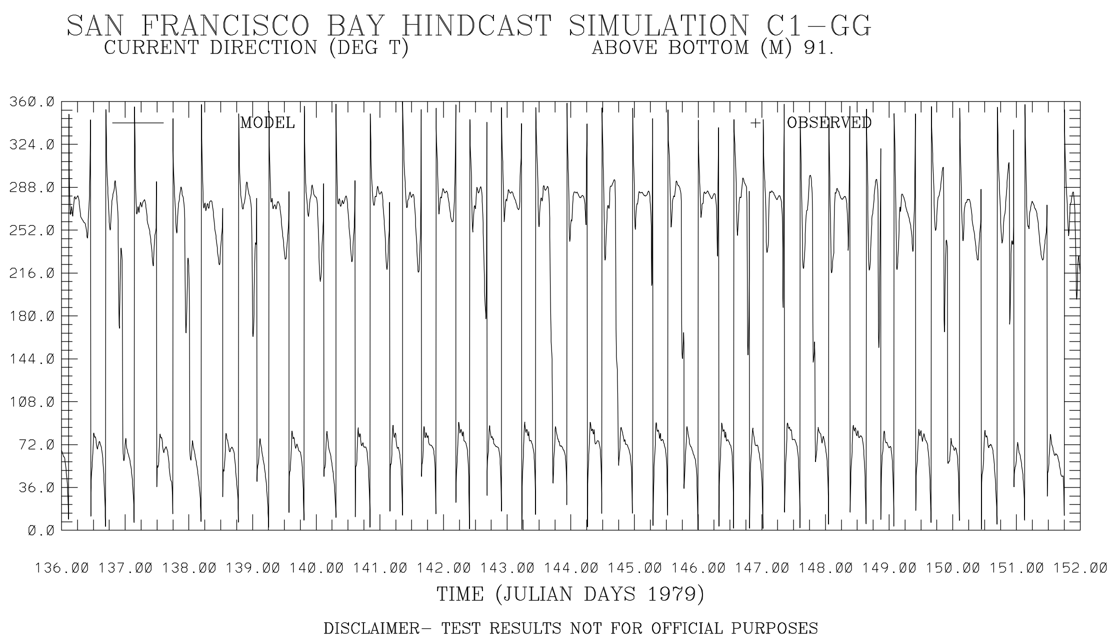

Figure 4.65. May 15-31, 1979 Hindcast: C-1 Current Speed and Direction at 91m above the bottom. Note IND AGRMT equals one minus Willmott et al. (1985) relative error.

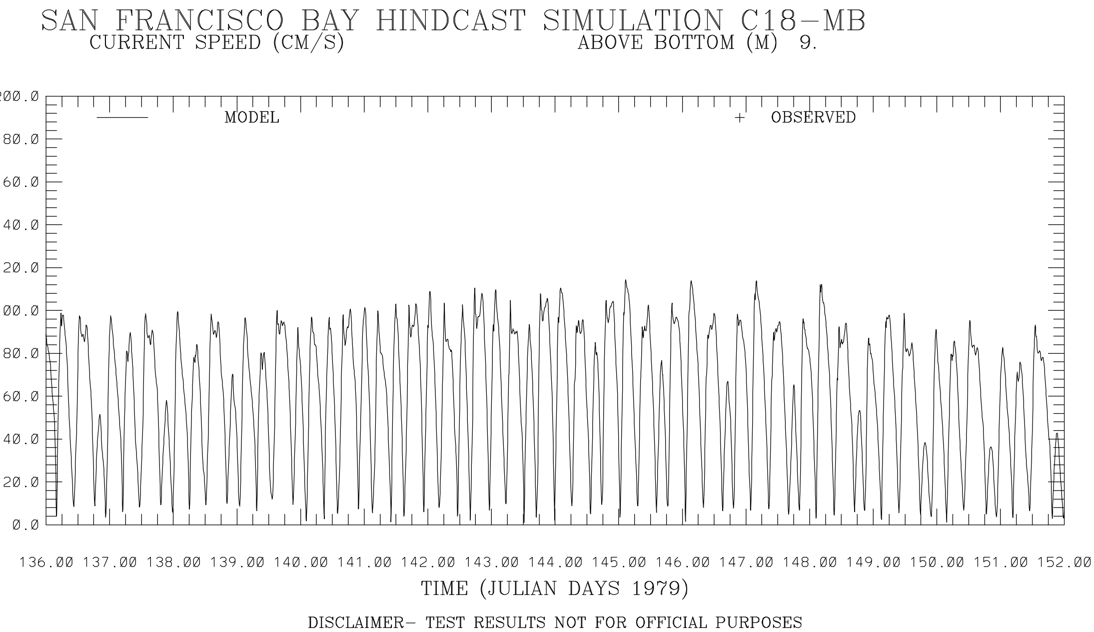

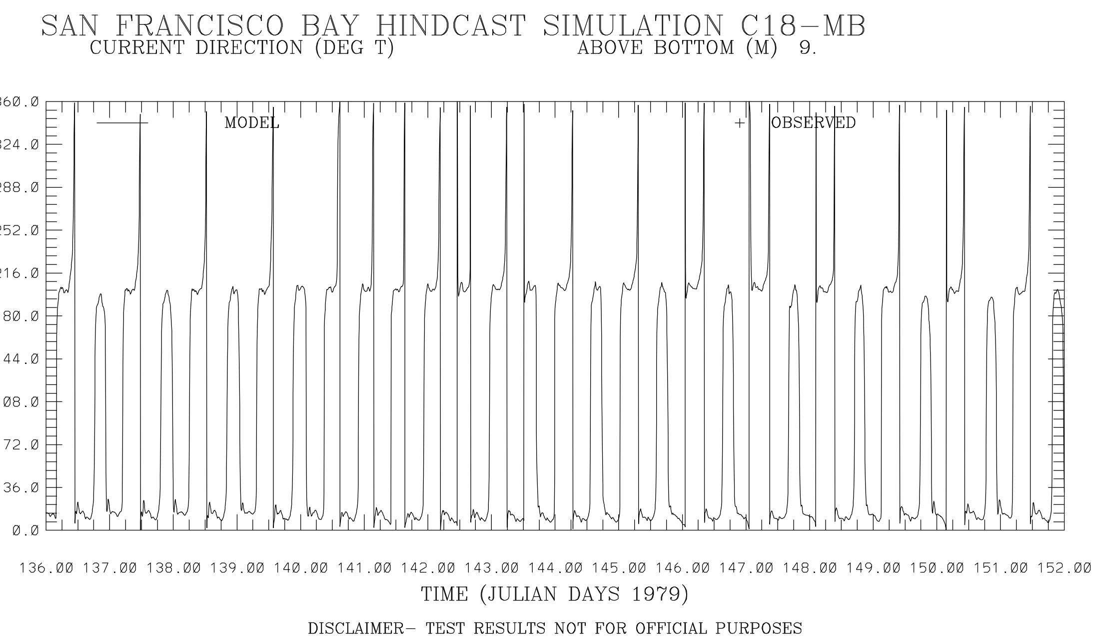

Figure 4.66. May 15-31, 1979 Hindcast: C-18 Current Speed and Direction at 9m above the bottom. Note IND AGRMT equals one minus Willmott et al. (1985) relative error.

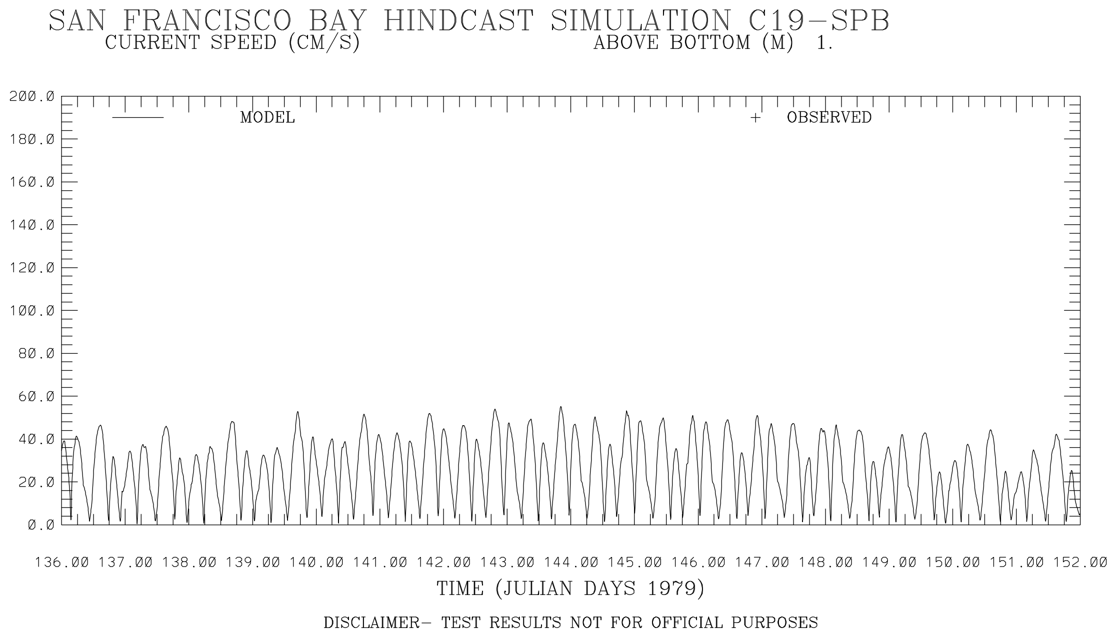

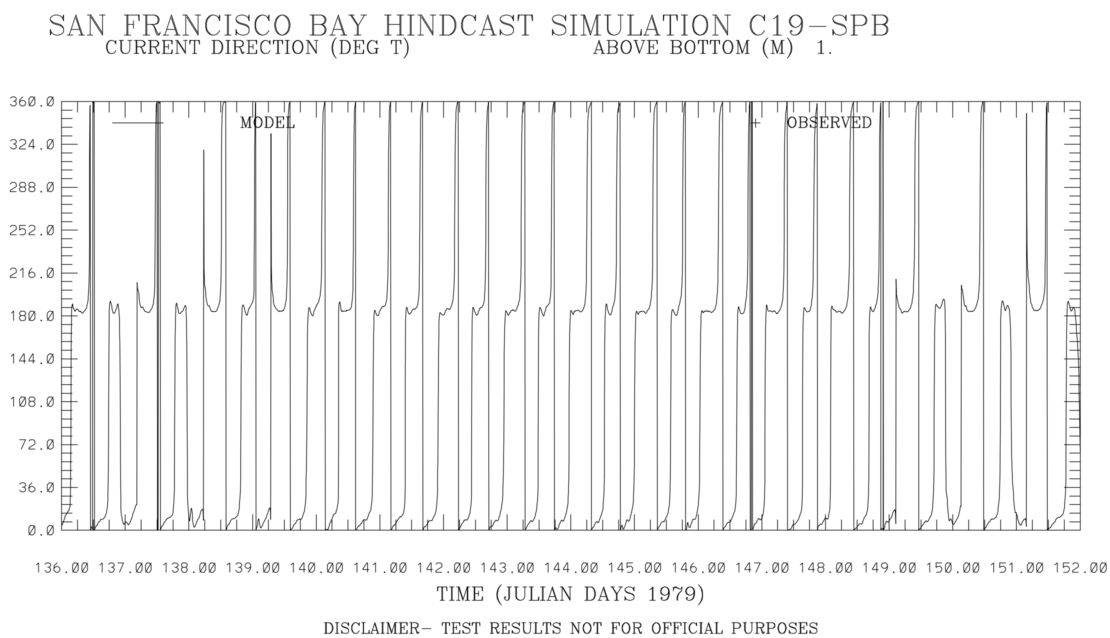

Figure 4.67. May 15-31, 1979 Hindcast: C-19 Current Speed and Direction at 1m above the bottom. Note IND AGRMT equals one minus Willmott et al. (1985) relative error.

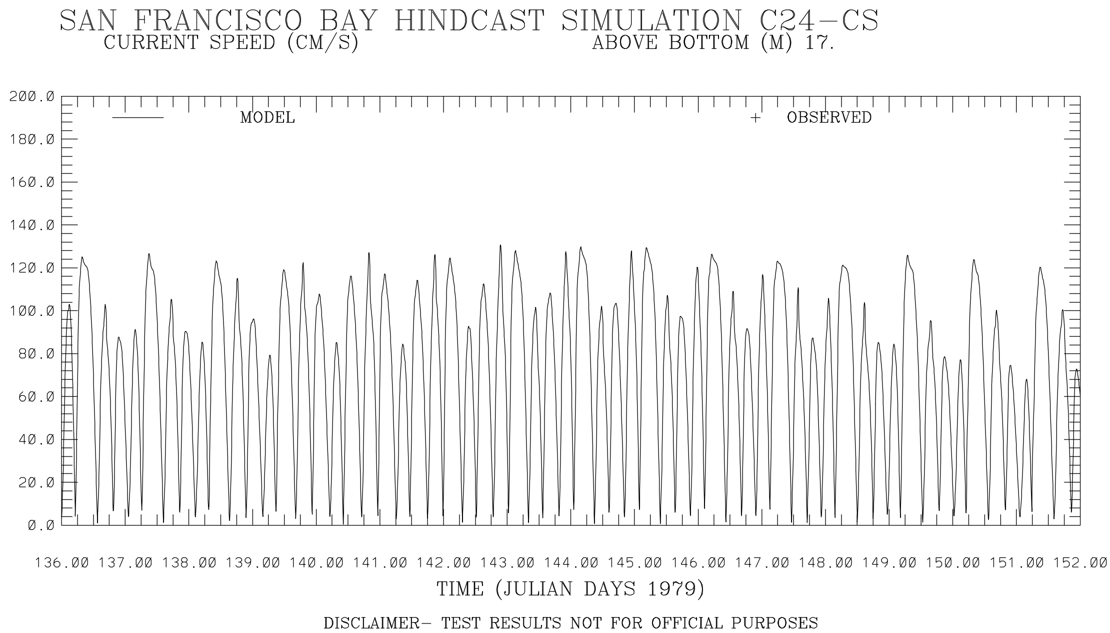

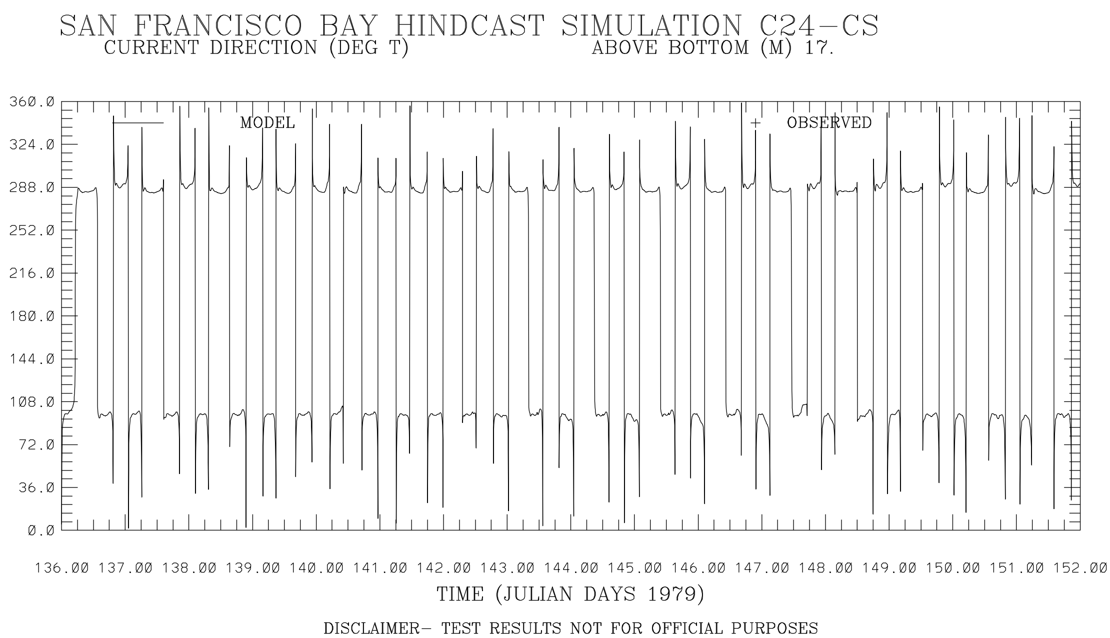

Figure 4.68. May 15-31, 1979 Hindcast: C-24 Current Speed and Direction at 17m above the bottom. Note IND AGRMT equals one minus Willmott et al. (1985) relative error.

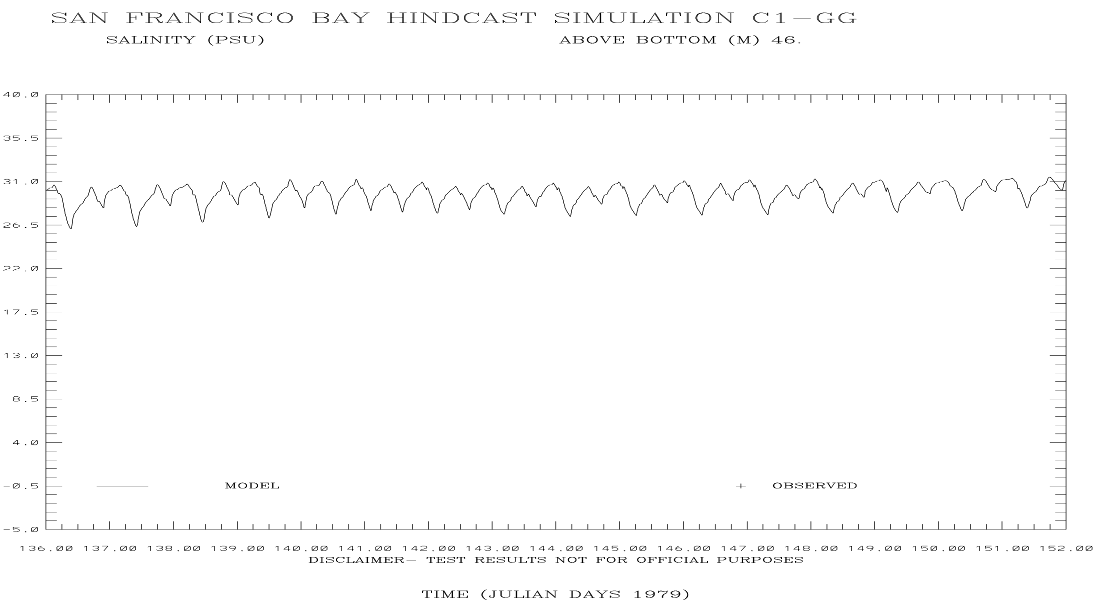

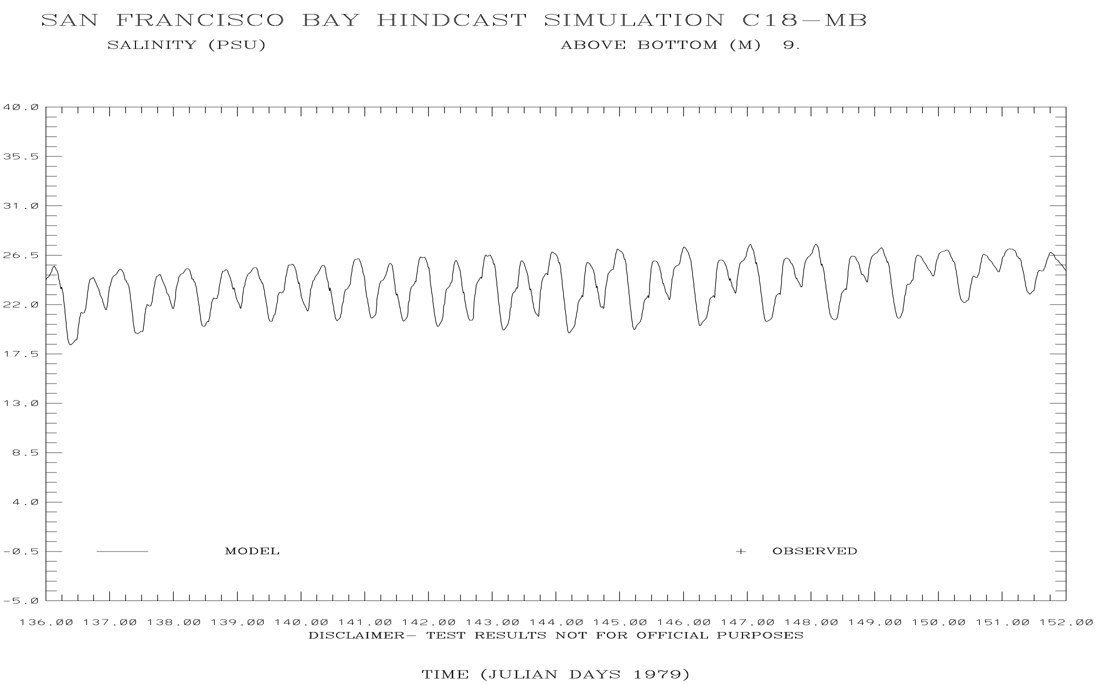

Figure 4.69. May 15-31, 1979 Hindcast: Salinity at C-1 at 91m and C-18 at 9m above the bottom. Note IND AGRMT equals one minus Willmott et al. (1985) relative error.

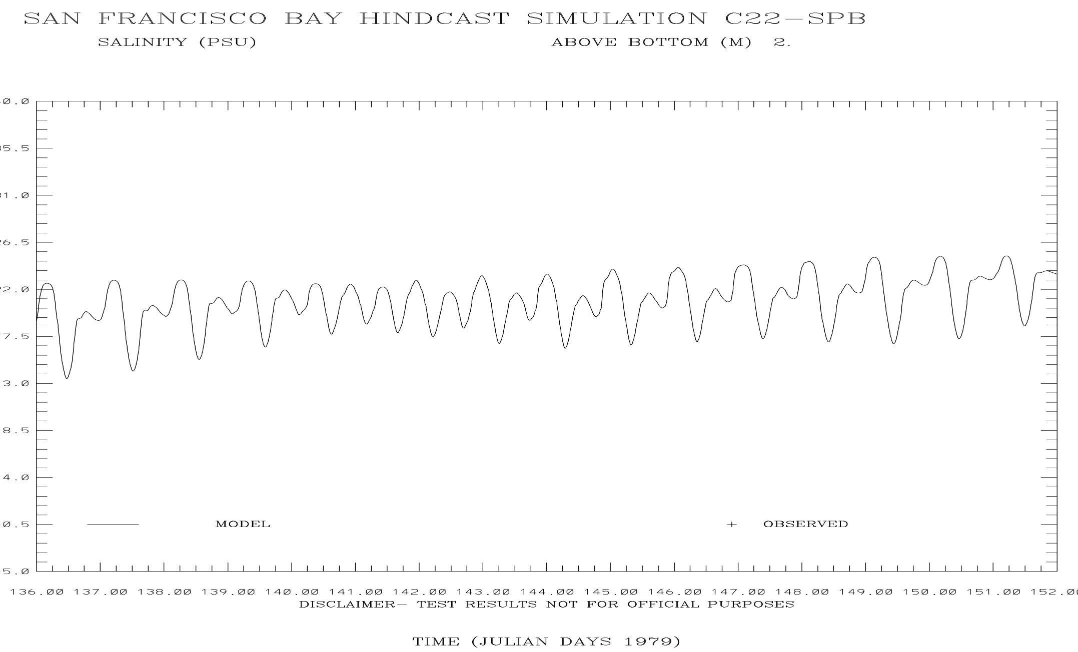

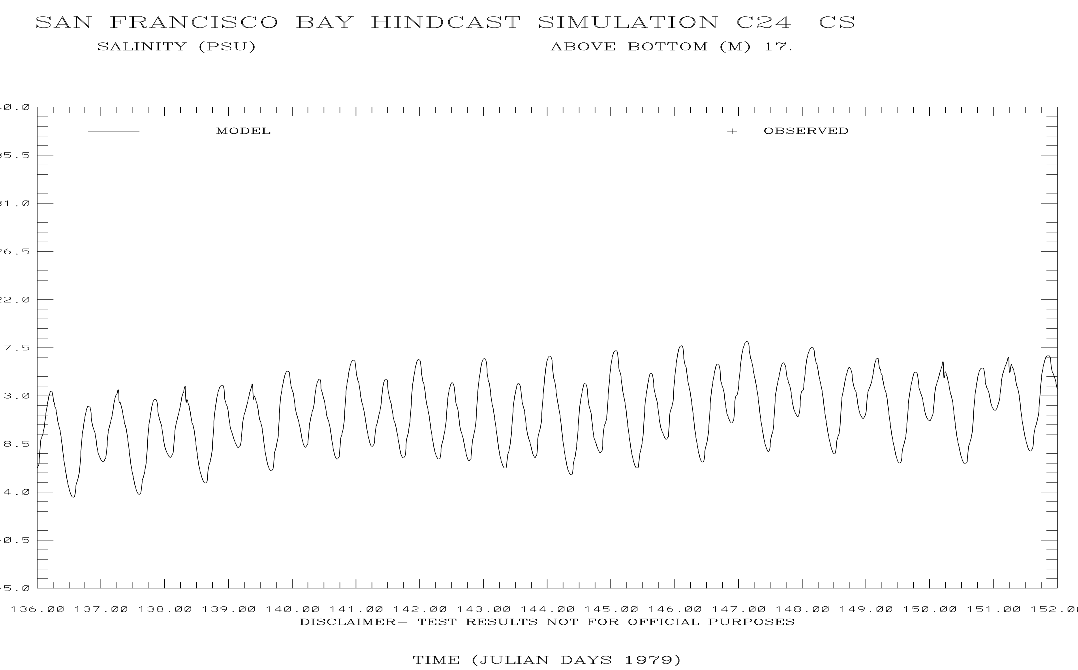

Figure 4.70. May 15-31, 1979 Hindcast: Salinity at C-22 at 2m and C-24 at 17m above the bottom. Note IND AGRMT equals one minus Willmott et al. (1985) relative error.

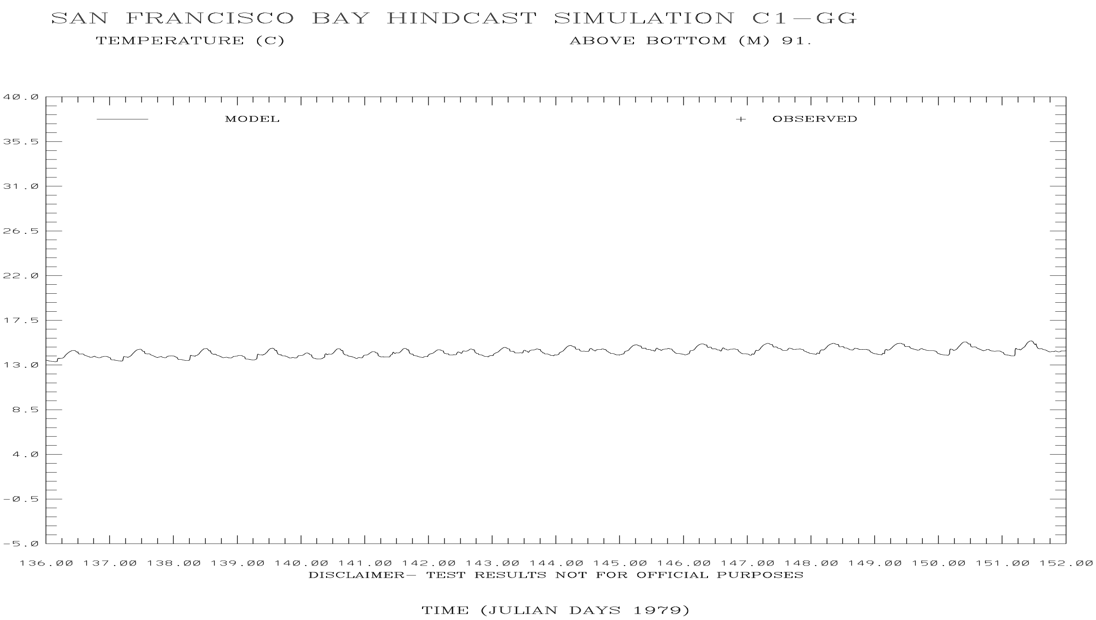

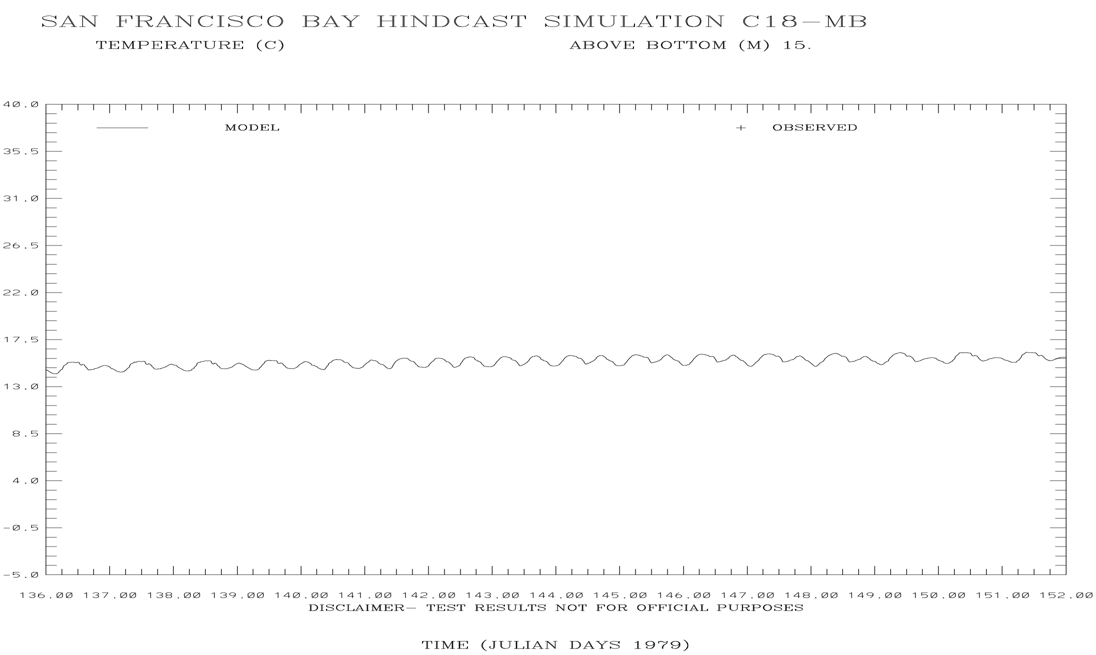

Figure 4.71. May 15-31, 1979 Hindcast: Salinity at C-1 at 91m and C-18 at 15m above the bottom. Note IND AGRMT equals one minus Willmott et al. (1985) relative error.

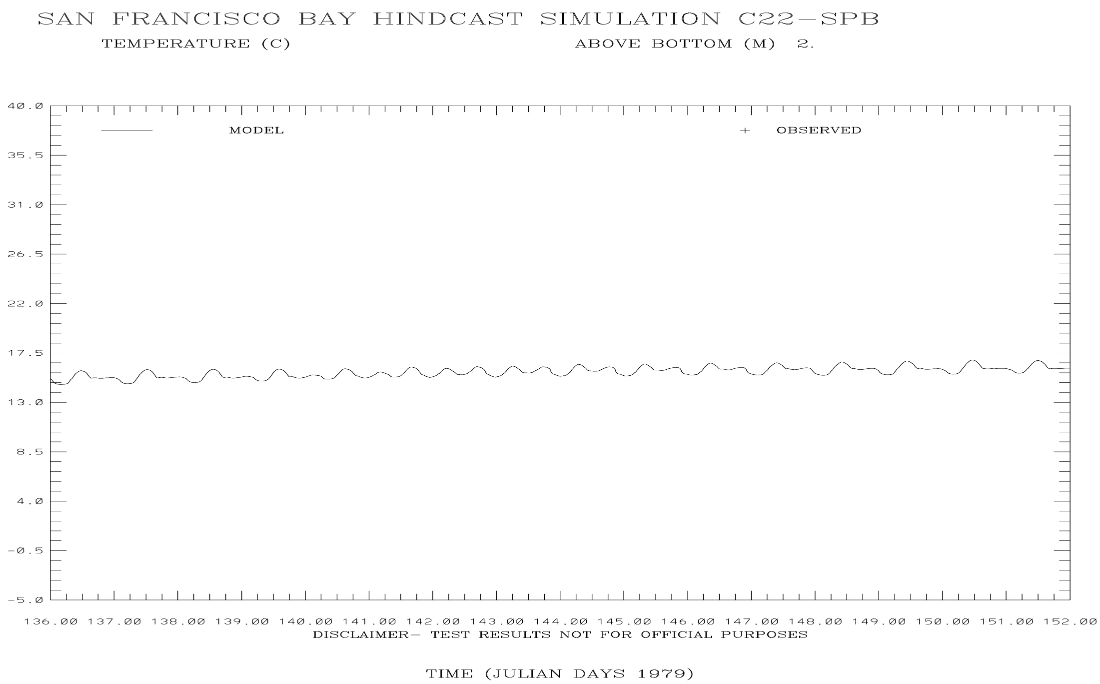

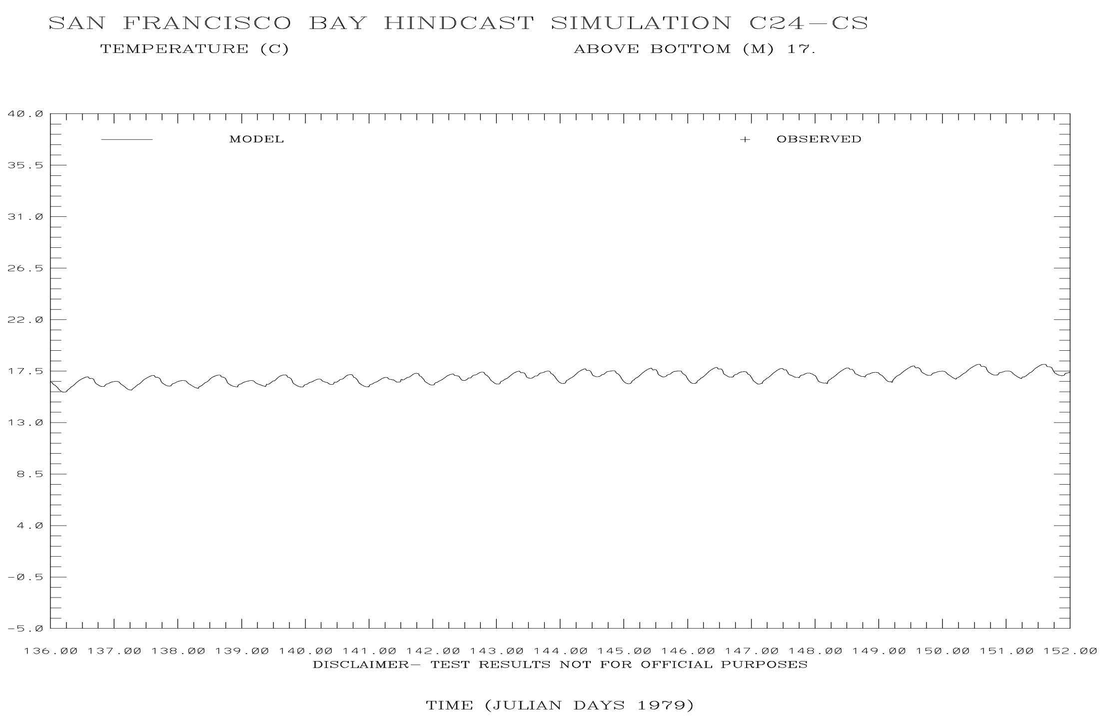

Figure 4.72. May 15-31, 1979 Hindcast: Temperature at C-22 at 2m and C-24 at 17m above the bottom. Note IND AGRMT equals one minus Willmott et al. (1985) relative error.

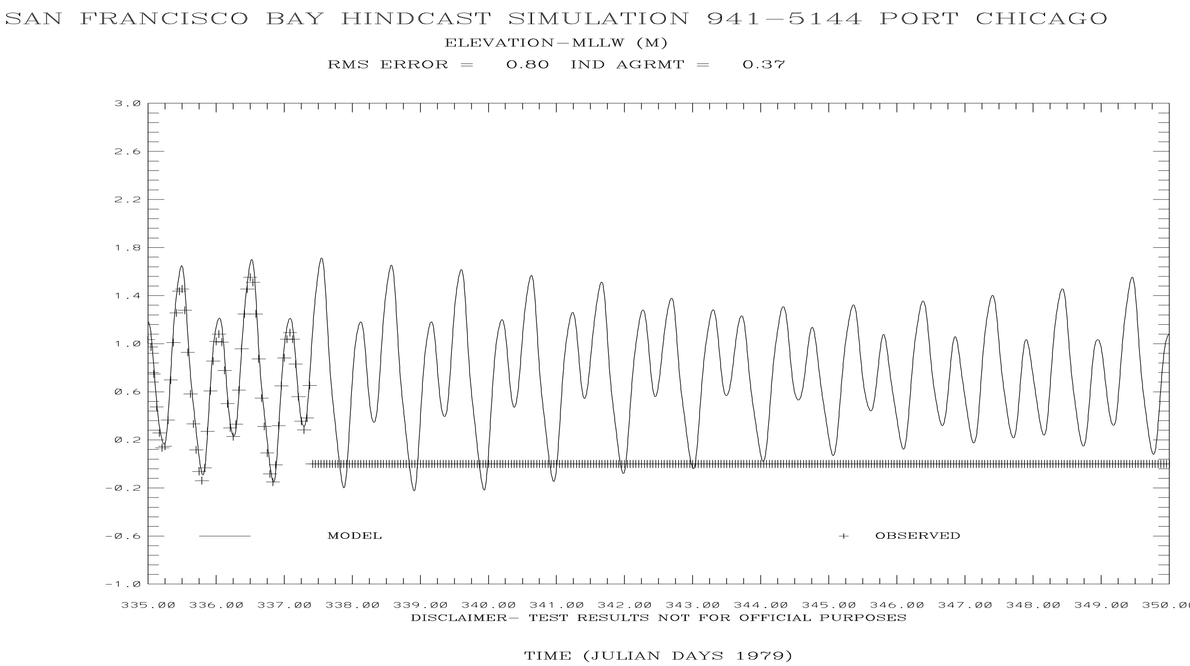

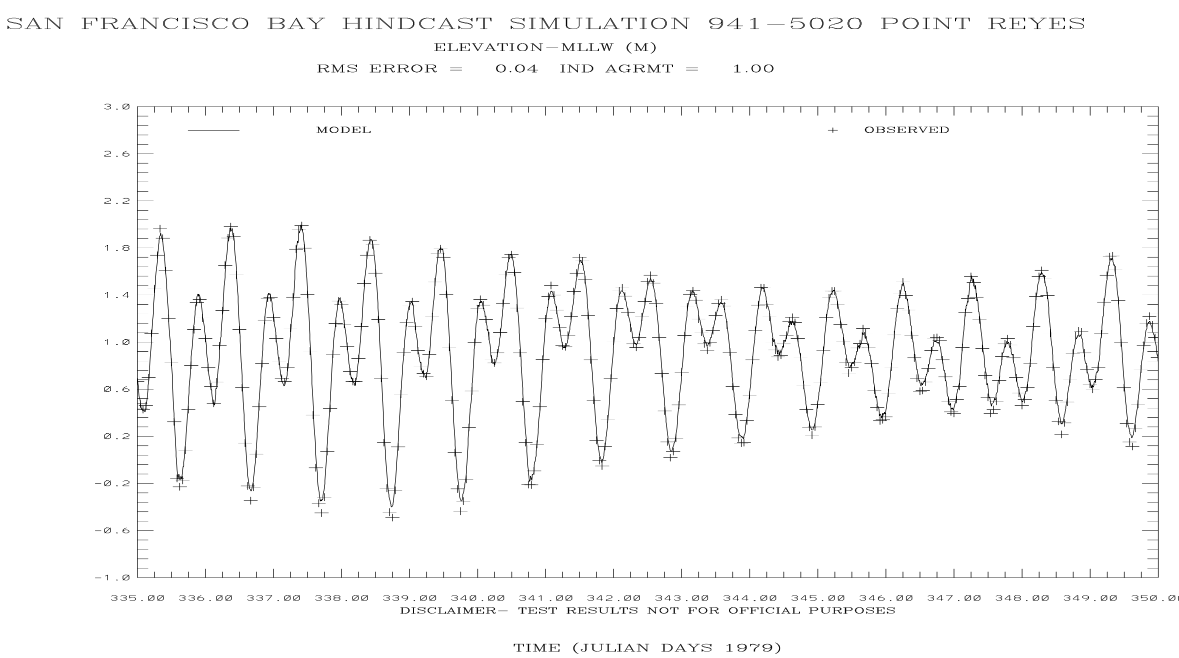

Figure 4.73. December 1-15, 1979 Hindcast: Port Chicago and Point ReyesWater Level Comparisons. Note IND AGRMT equals one minus Willmott et al. (1985) relative error.

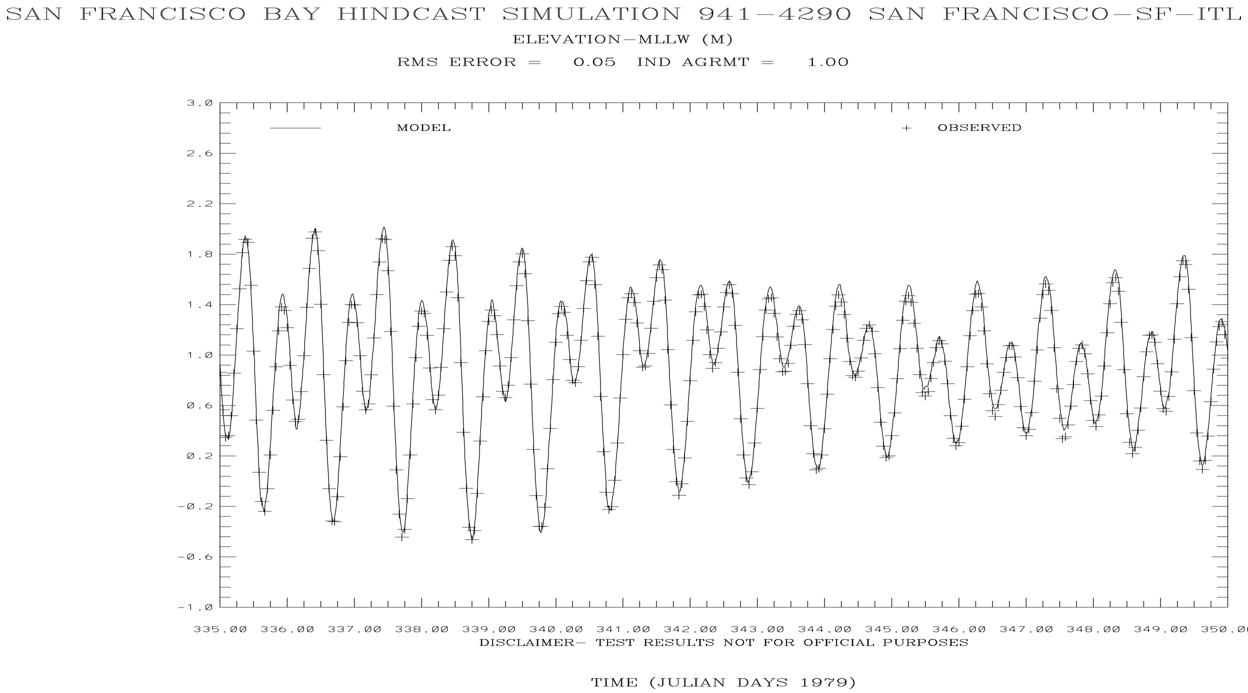

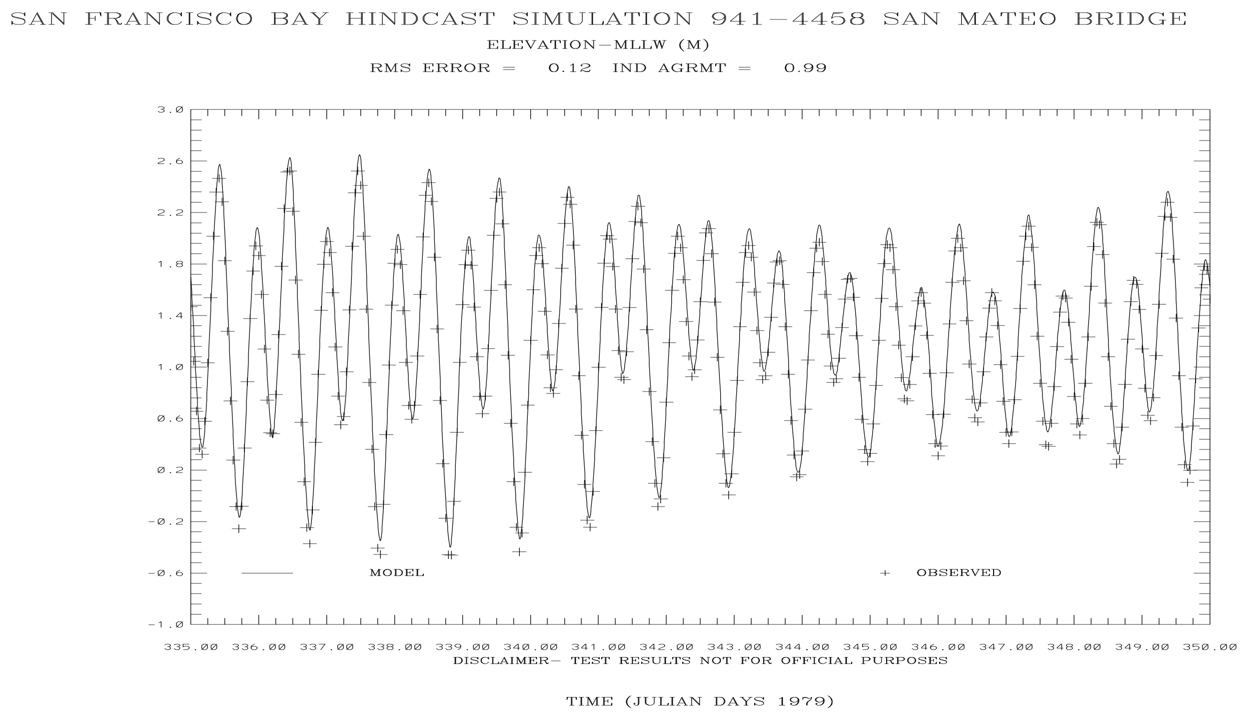

Figure 4.74. December 1-15, 1979 Hindcast: San Francisco and San Mateo Bridge Water Level Comparisons. Note IND AGRMT equals one minus Willmott et al. (1985) relative error.

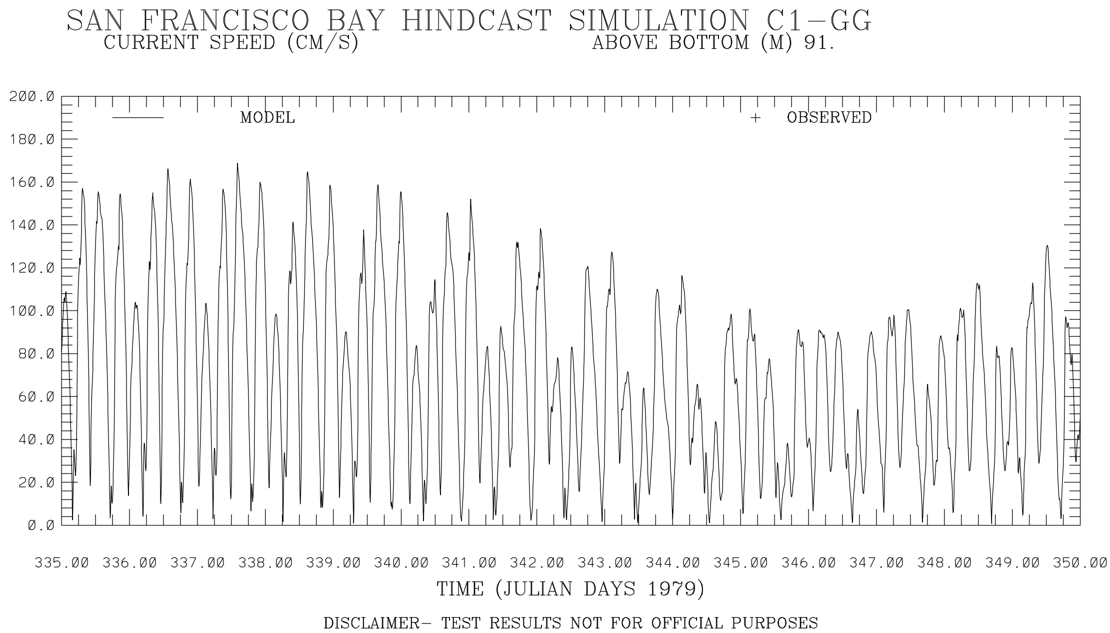

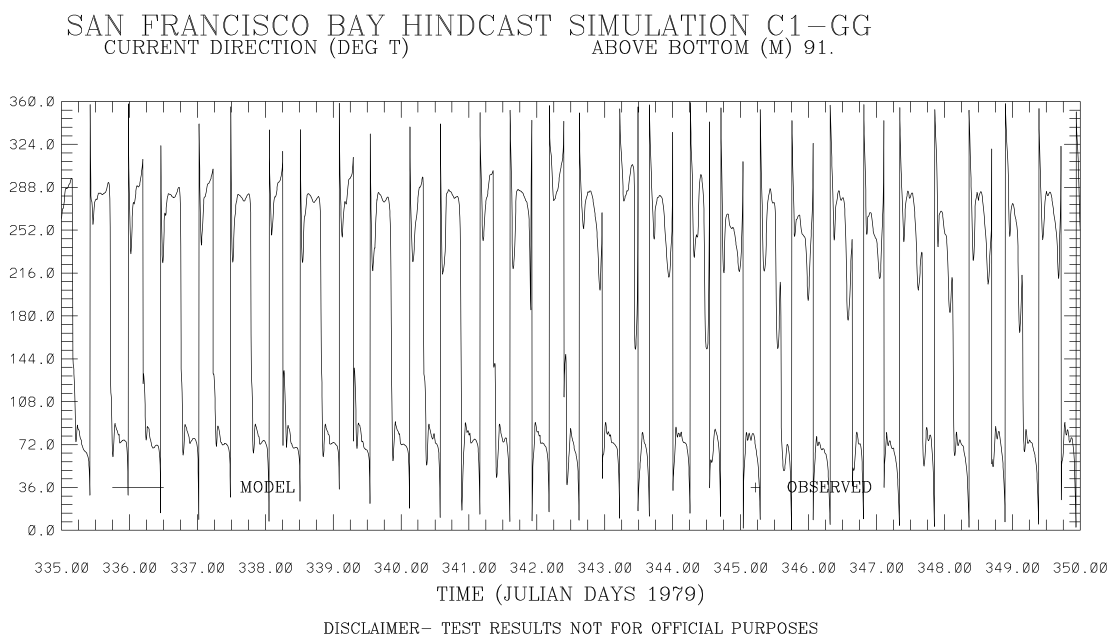

Figure 4.75. December 1-15, 1979 Hindcast: C-1 Current Speed and Direction at 91m above the bottom. Note IND AGRMT equals one minus Willmott et al. (1985) relative error.

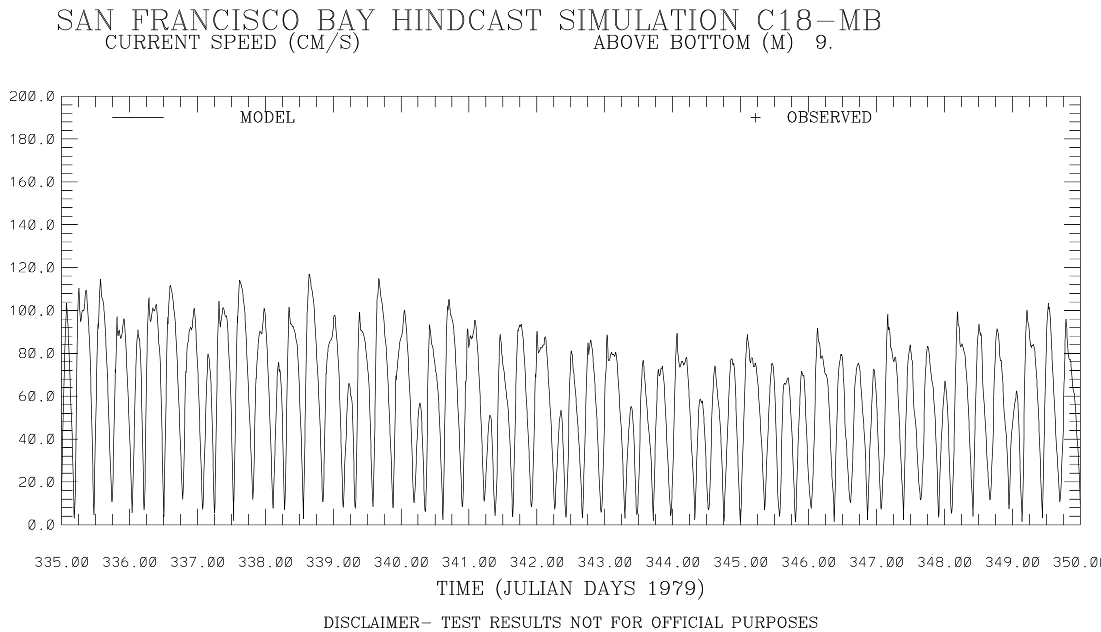

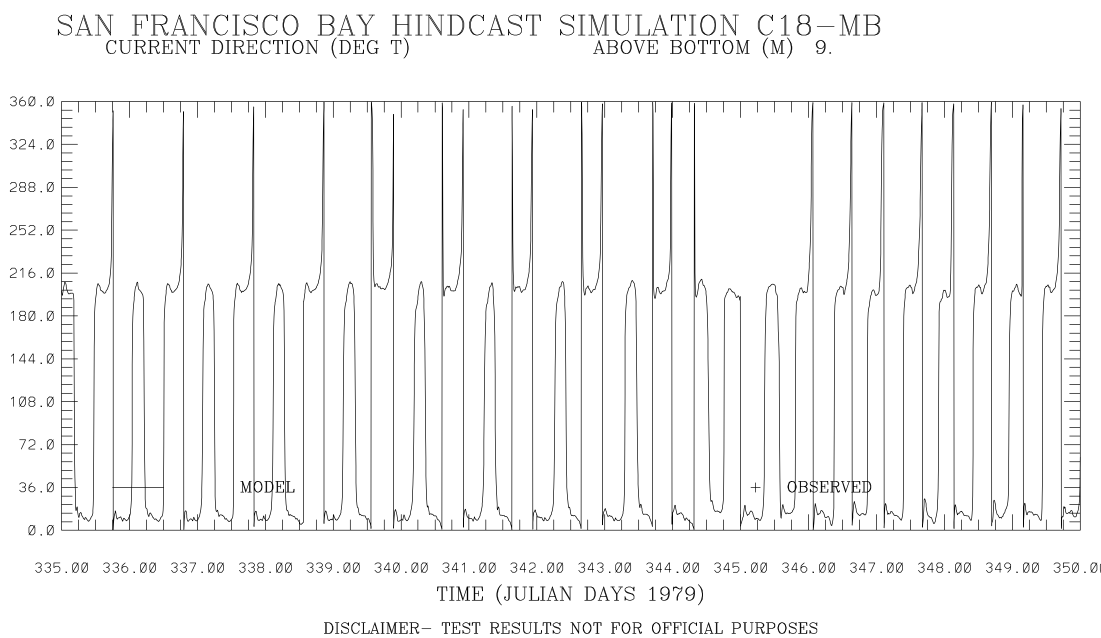

Figure 4.76. December 1-15, 1979 Hindcast: C-18 Current Speed and Direction at 9m above the bottom. Note IND AGRMT equals one minus Willmott et al. (1985) relative error.

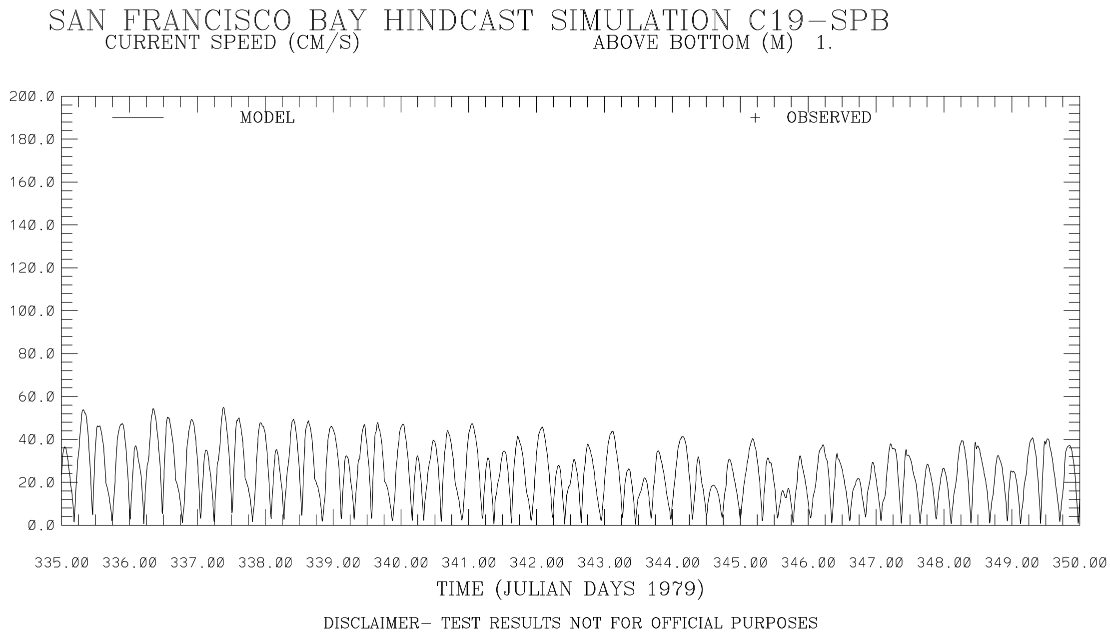

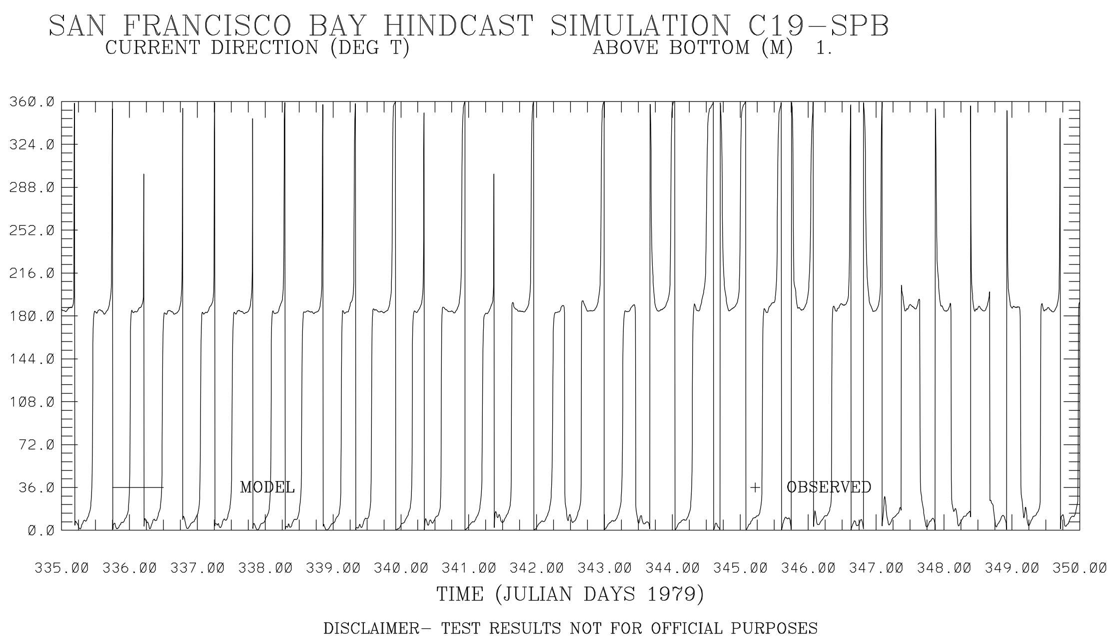

Figure 4.77. December 1-15, 1979 Hindcast: C-19 Current Speed and Direction at 1m above the bottom. Note IND AGRMT equals one minus Willmott et al. (1985) relative error.

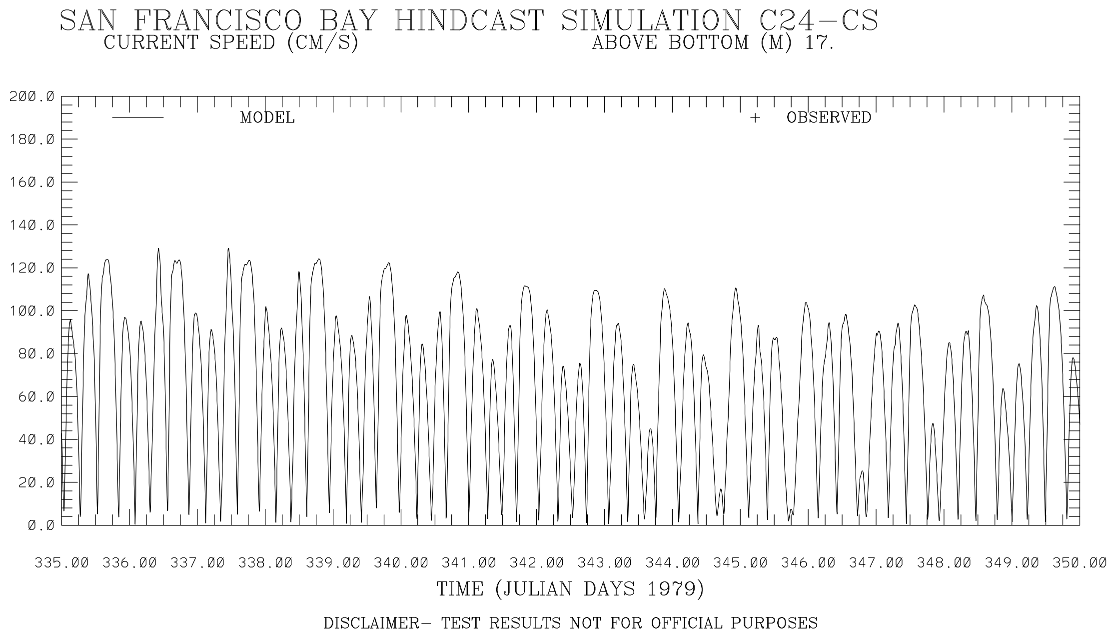

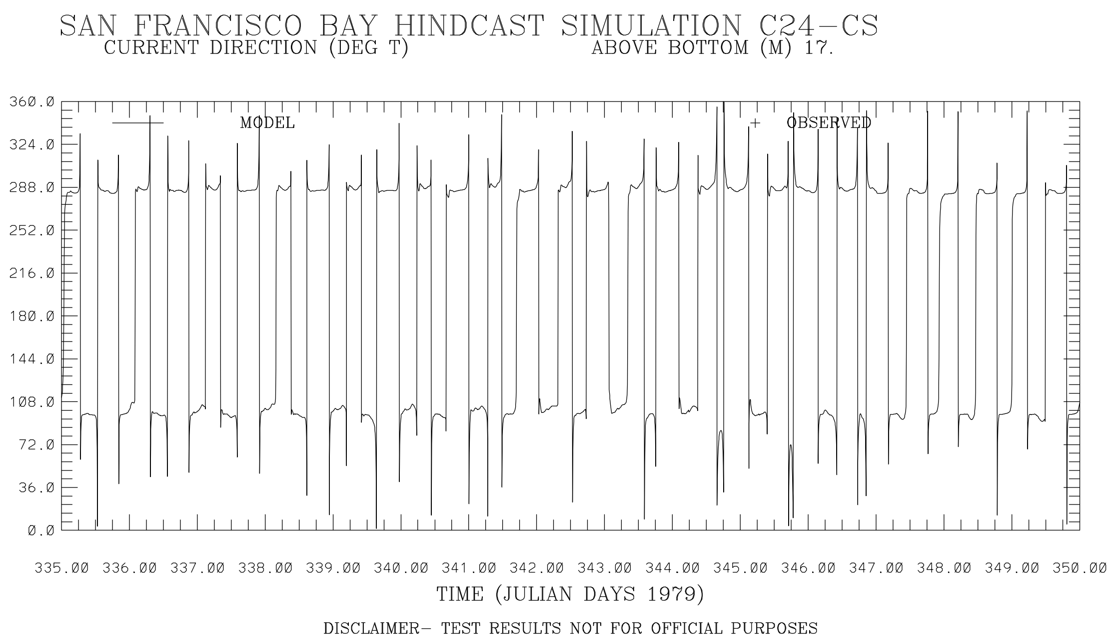

Figure 4.78. December 1-15, 1979 Hindcast: C-24 Current Speed and Direction at 17m above the bottom. Note IND AGRMT equals one minus Willmott et al. (1985) relative error.

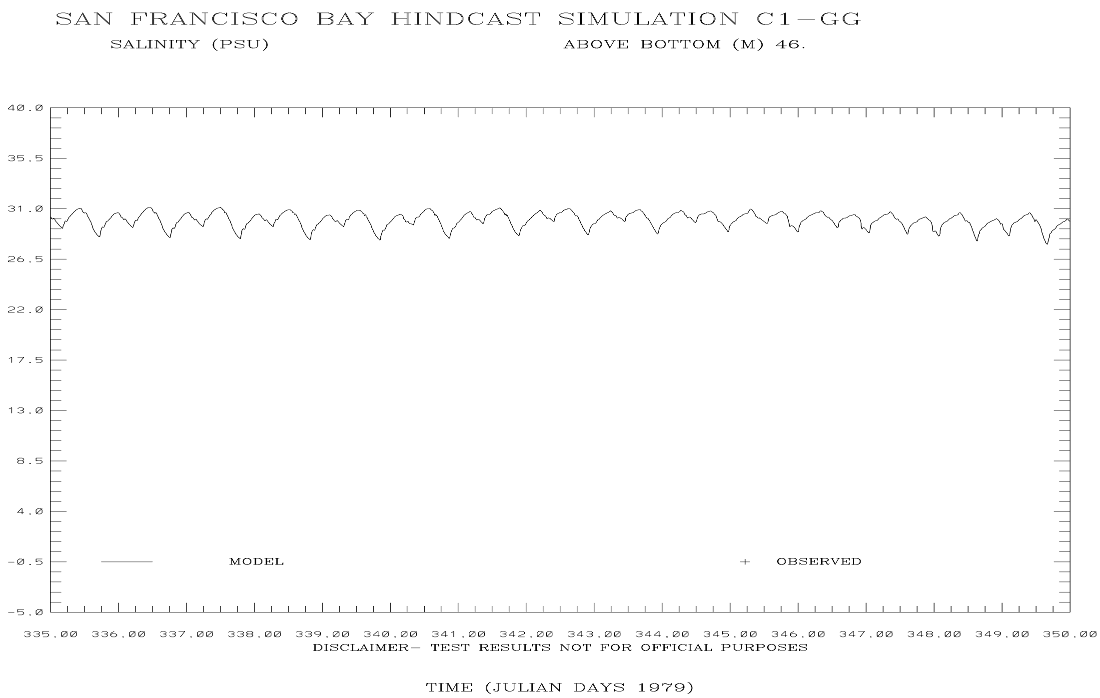

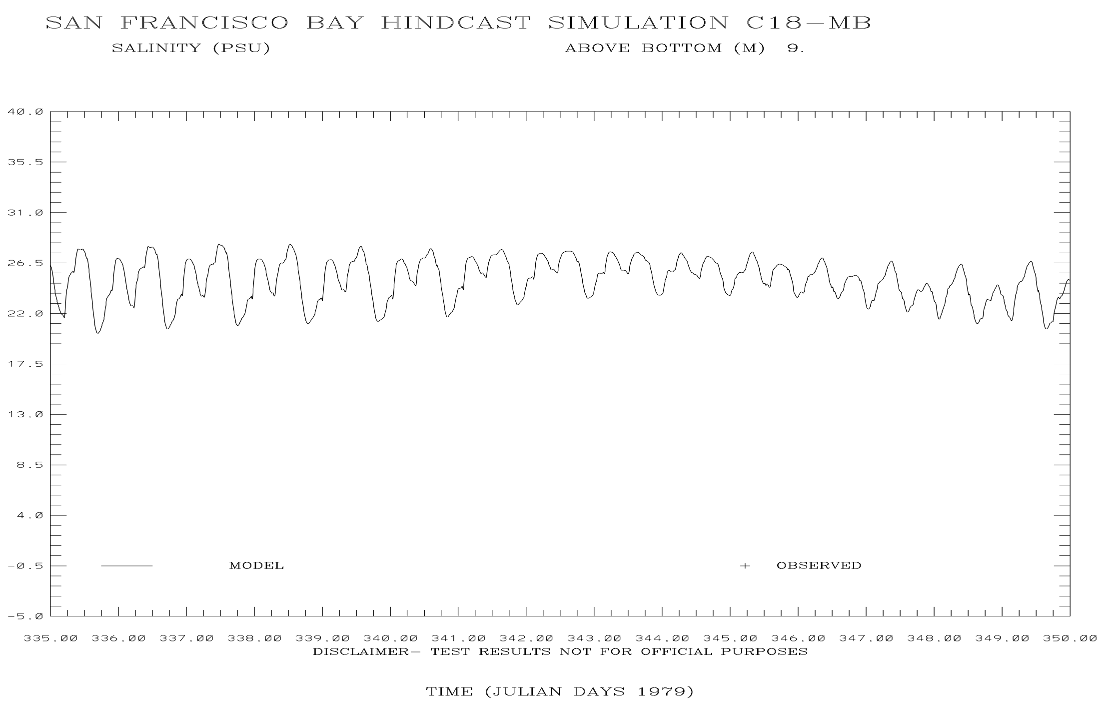

Figure 4.79. December 1-15, 1979 Hindcast: Salinity at C-1 at 91m and at C-18 at 9 m above the bottom. Note IND AGRMT equals one minus Willmott et al. (1985) relative error.

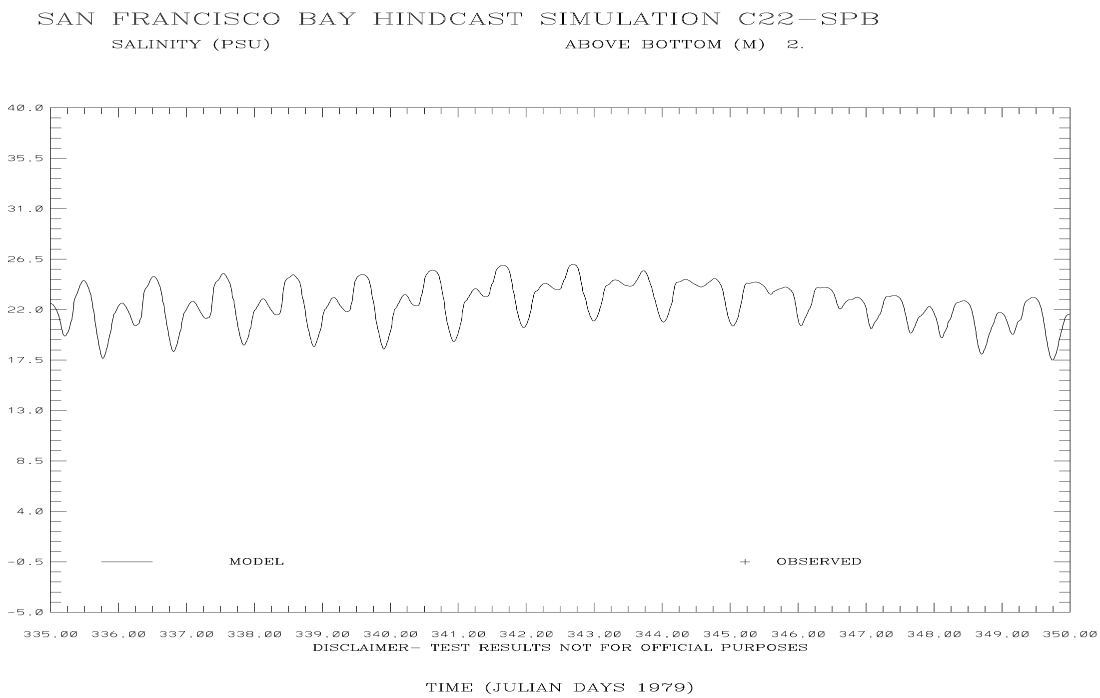

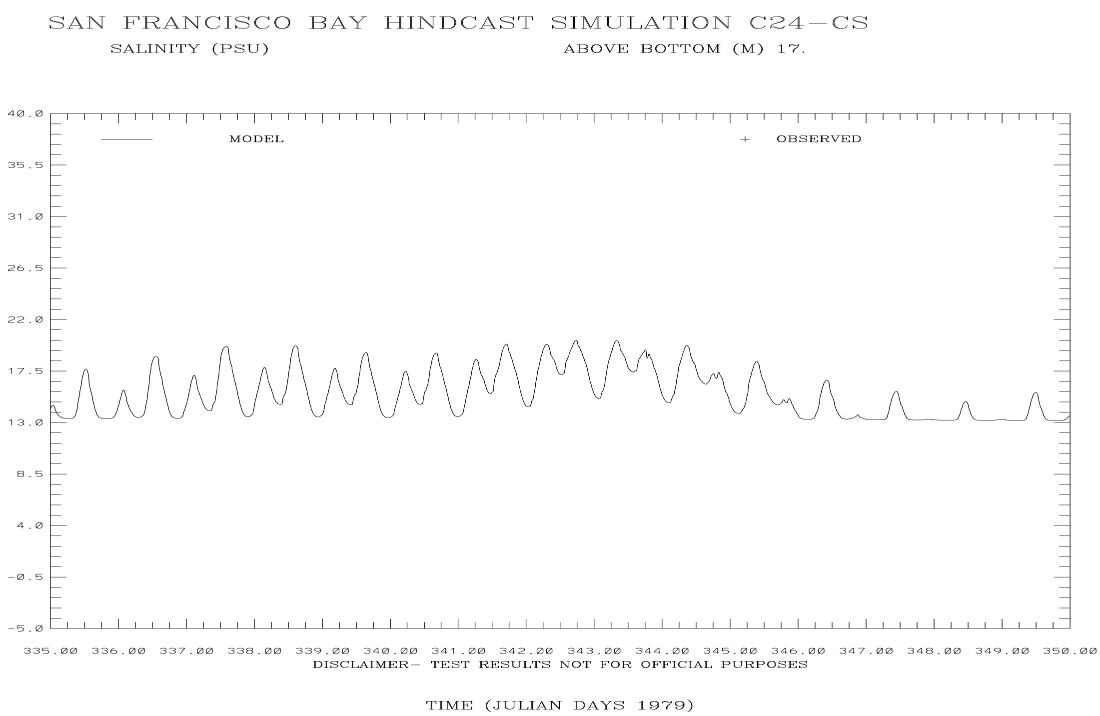

Figure 4.80. December 1-15, 1979 Hindcast: Salinity at C-22 at 2m and at C-24 at 17m above the bottom. Note IND AGRMT equals one minus Willmott et al. (1985) relative error.

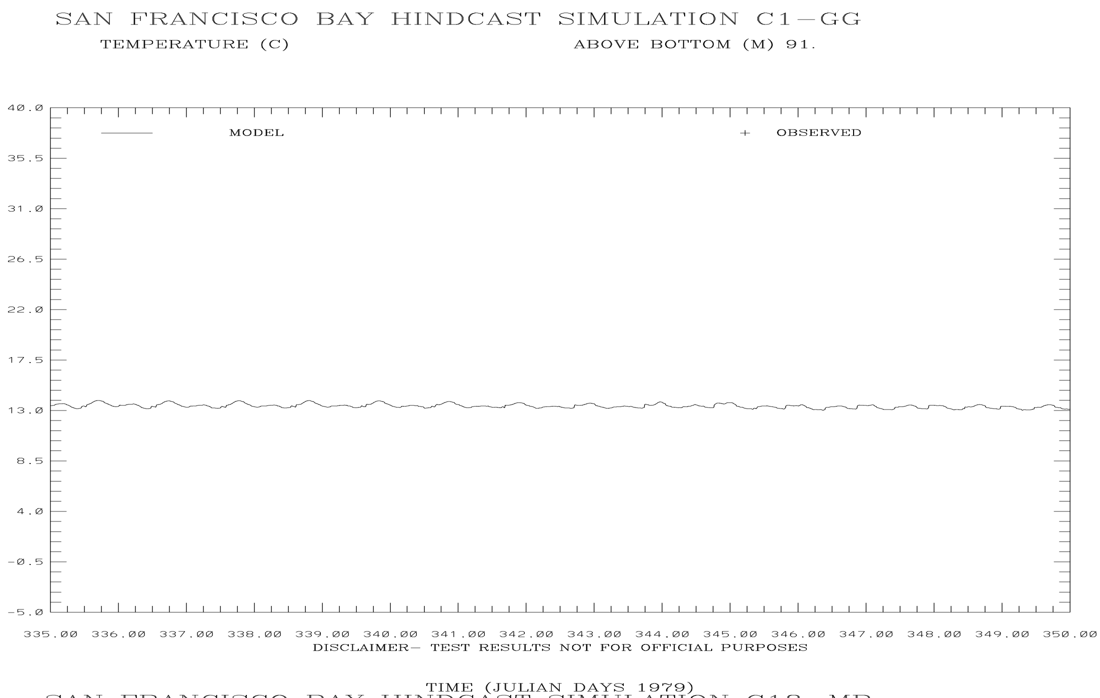

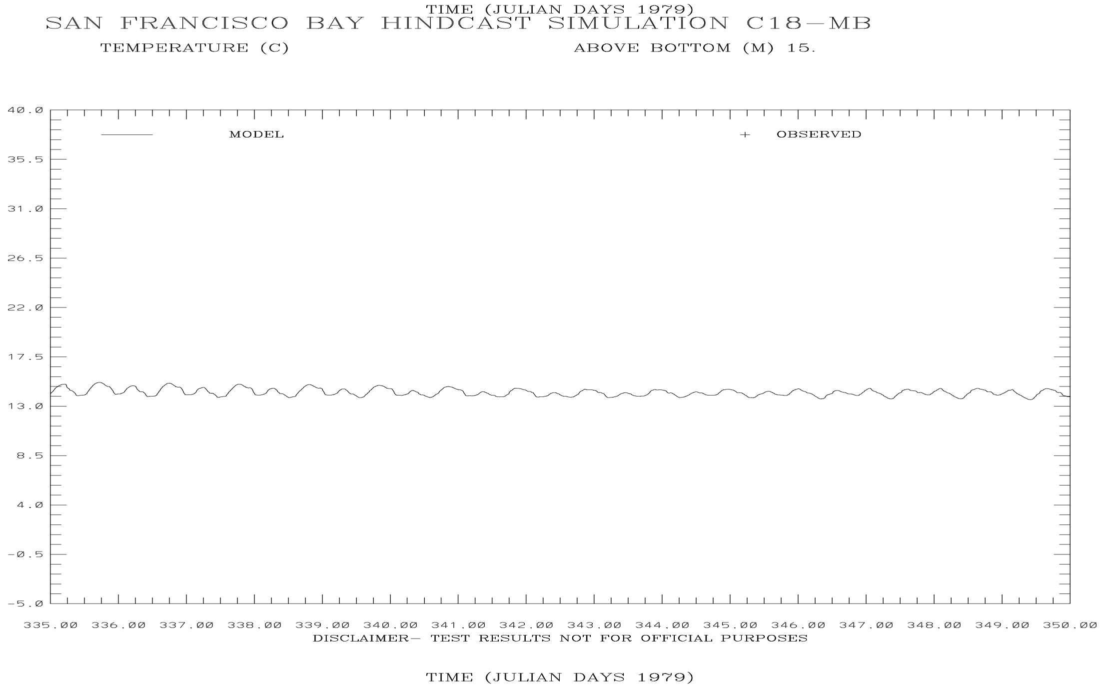

Figure 4.81. December 1-15, 1979 Hindcast: Temperature at C-1 at 91m and at C-18 at 9 m above the bottom. Note IND AGRMT equals one minus Willmott et al. (1985) relative error.

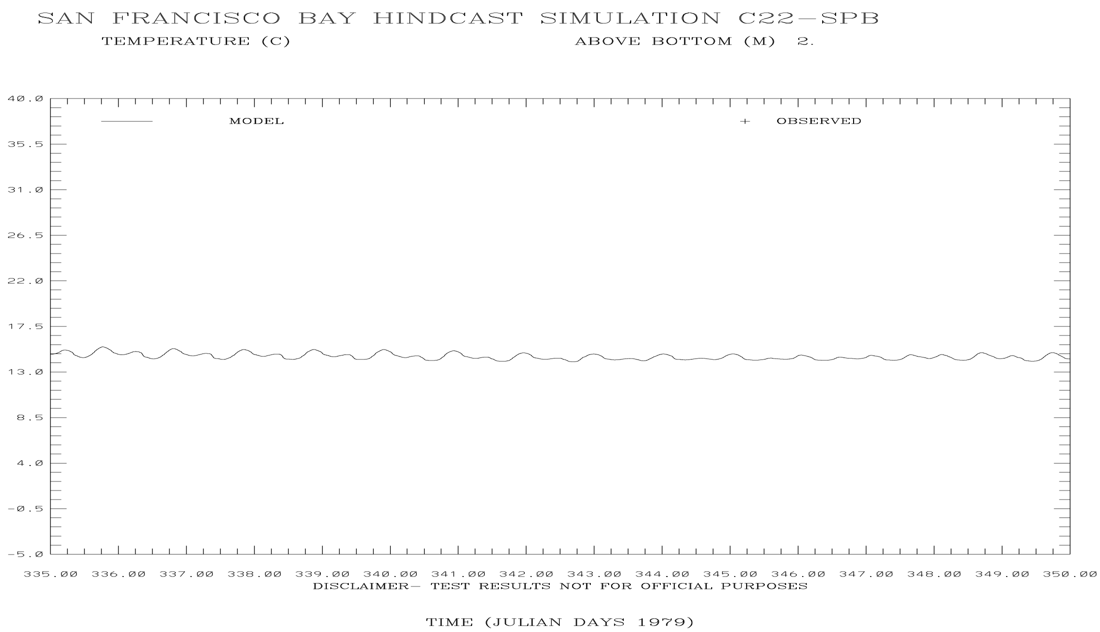

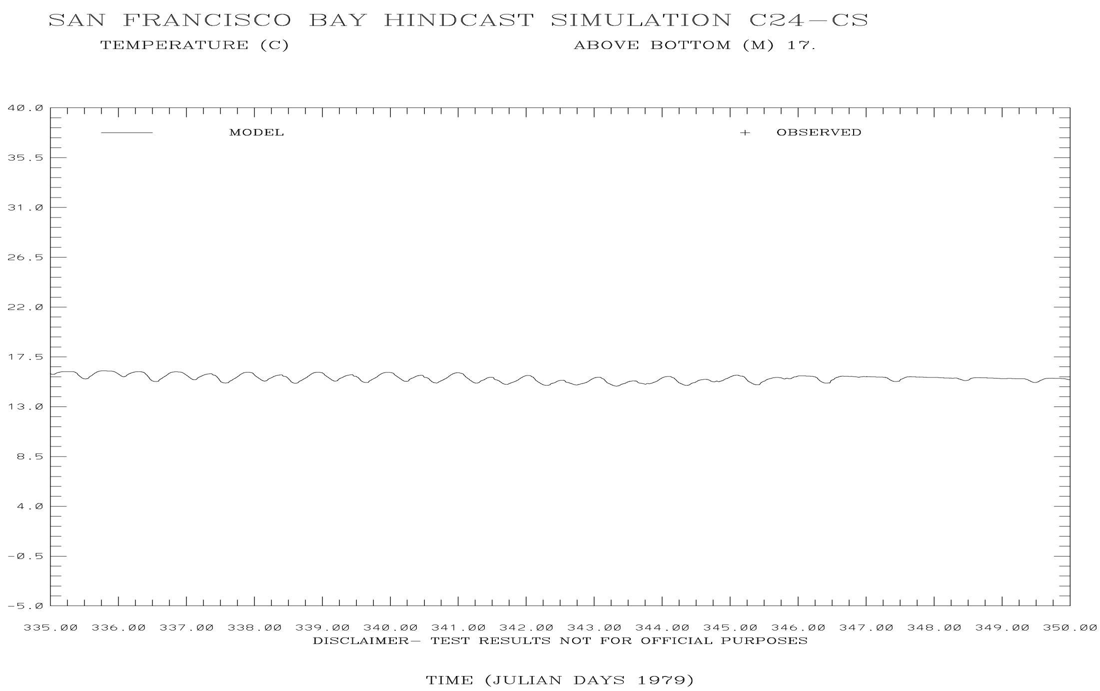

Figure 4.82. December 1-15, 1979 Hindcast: Temperature at C-22 at 2m and at C-24 at 17m above the bottom. Note IND AGRMT equals one minus Willmott et al. (1985) relative error.

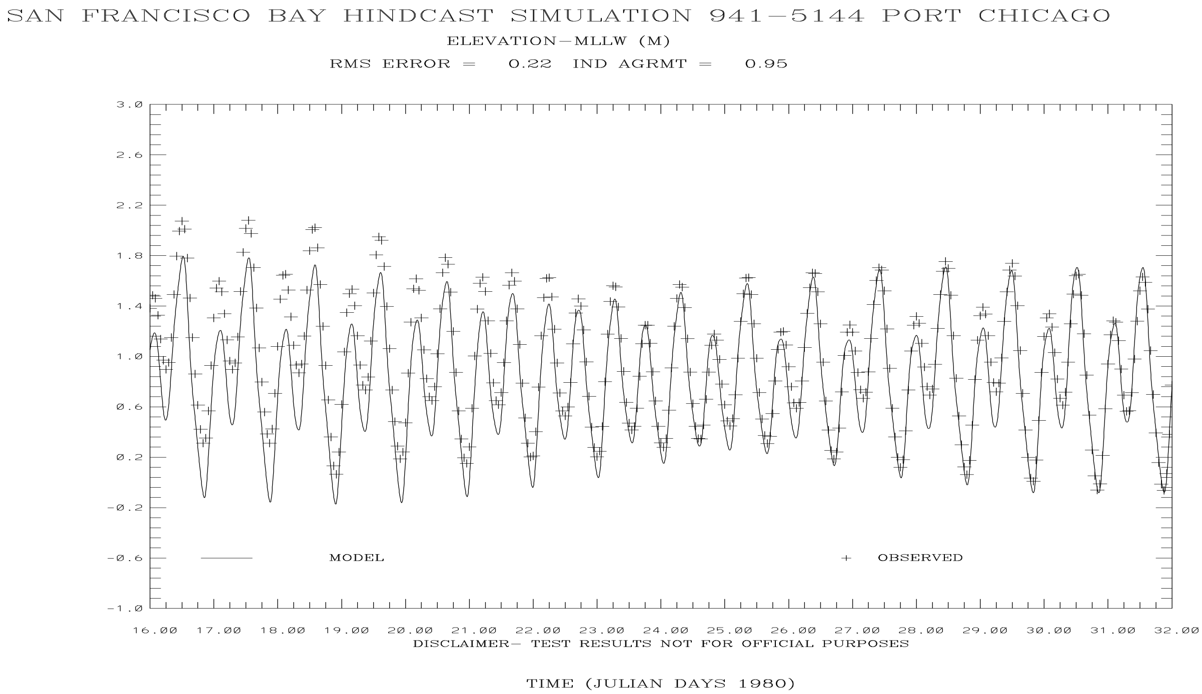

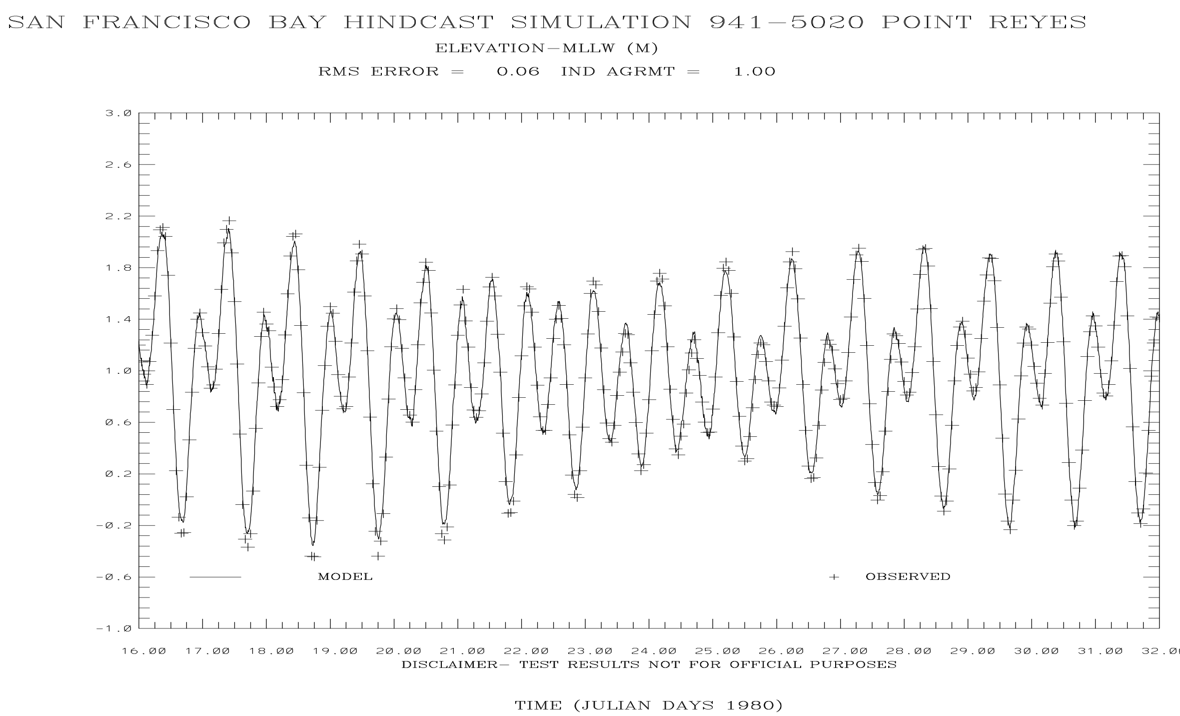

Figure 4.83. January 15-31, 1980 Hindcast: Port Chicago and Point Reyes Water Level Comparisons. Note IND AGRMT equals one minus Willmott et al. (1985) relative error.

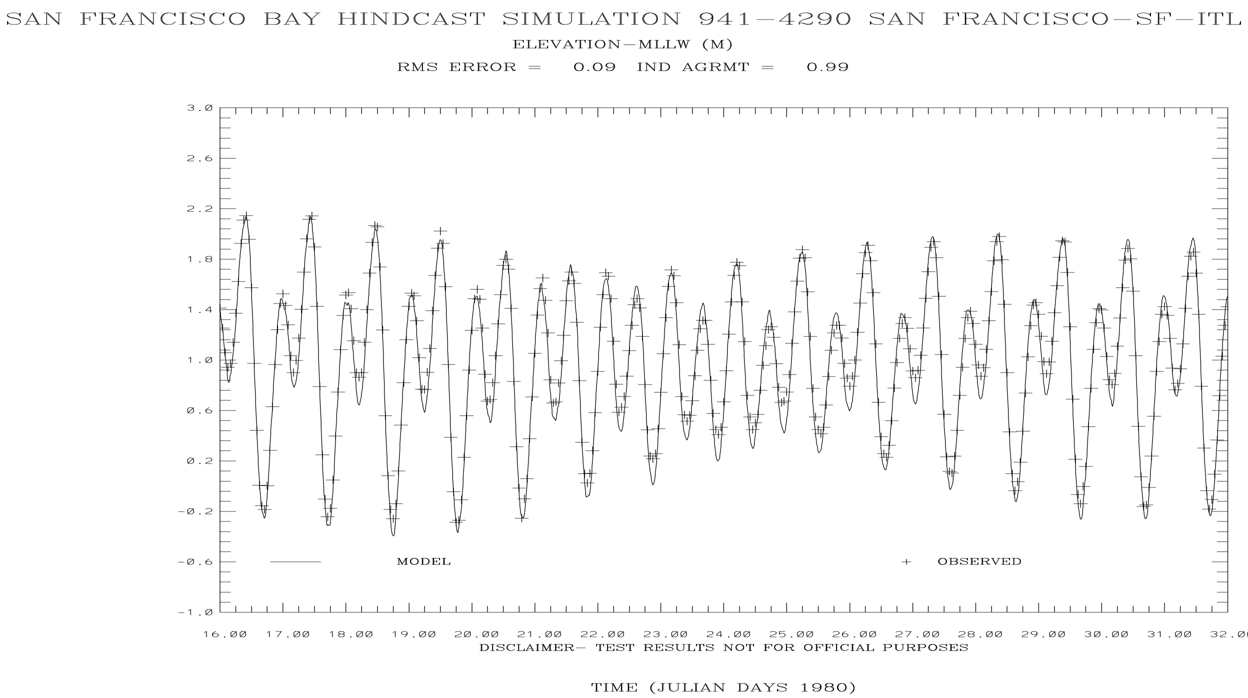

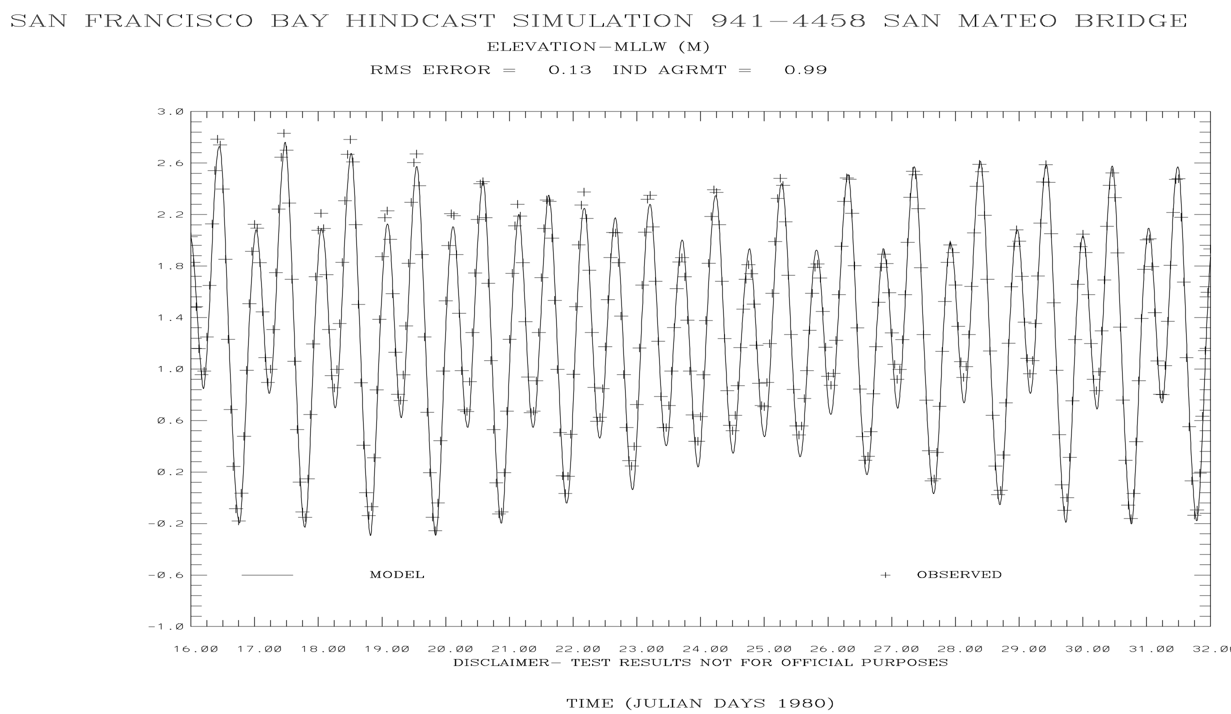

Figure 4.84. January 15-31, 1980 Hindcast: San Francisco and San Mateo Bridge Water Level Comparisons. Note IND AGRMT equals one minus Willmott et al. (1985) relative error.

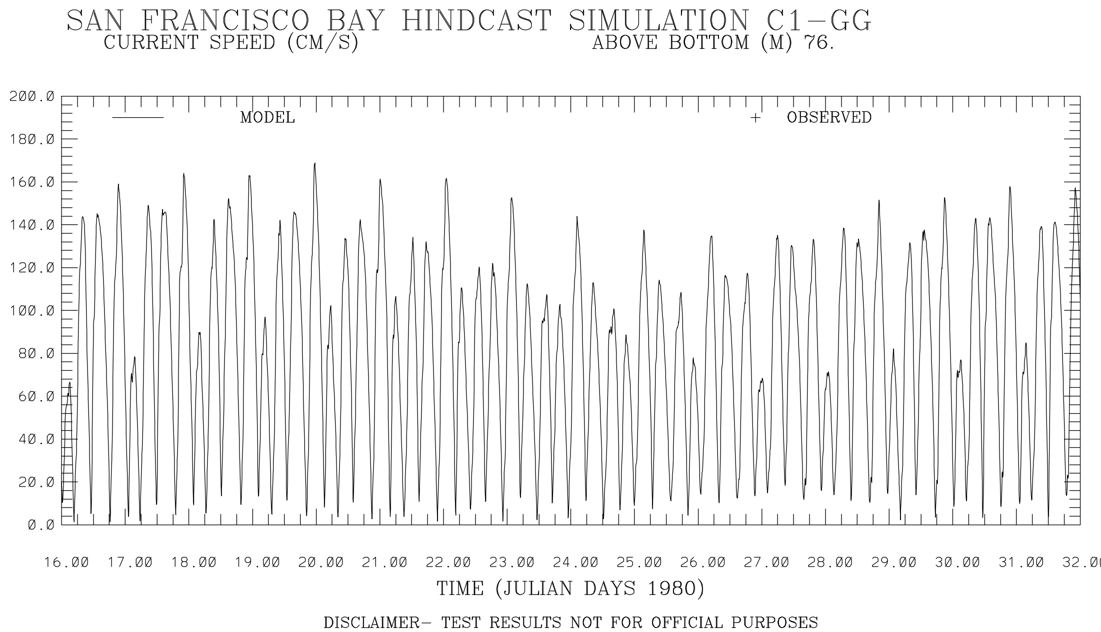

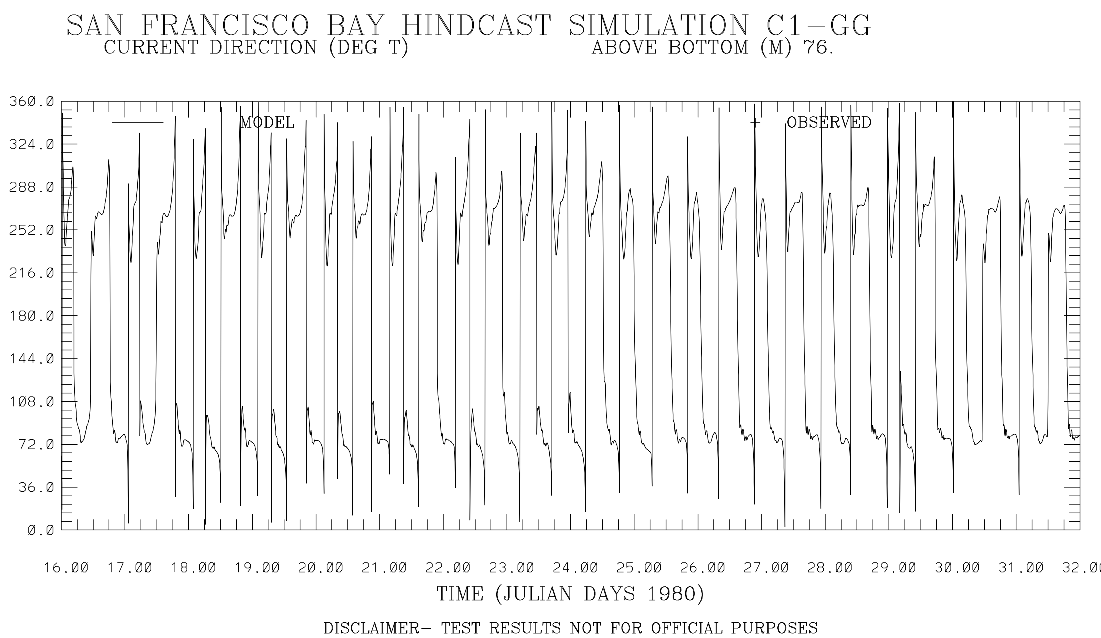

Figure 4.85. January 15-31, 1980 Hindcast: C-1 Current Speed and Direction at 76m above the bottom. Note IND AGRMT equals one minus Willmott et al. (1985) relative error.

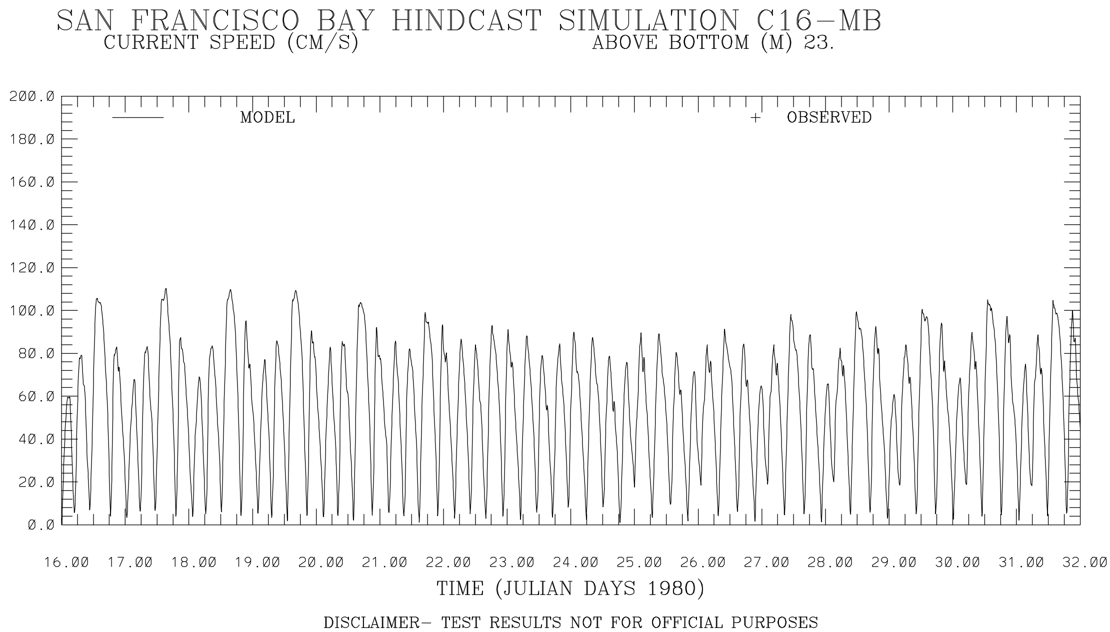

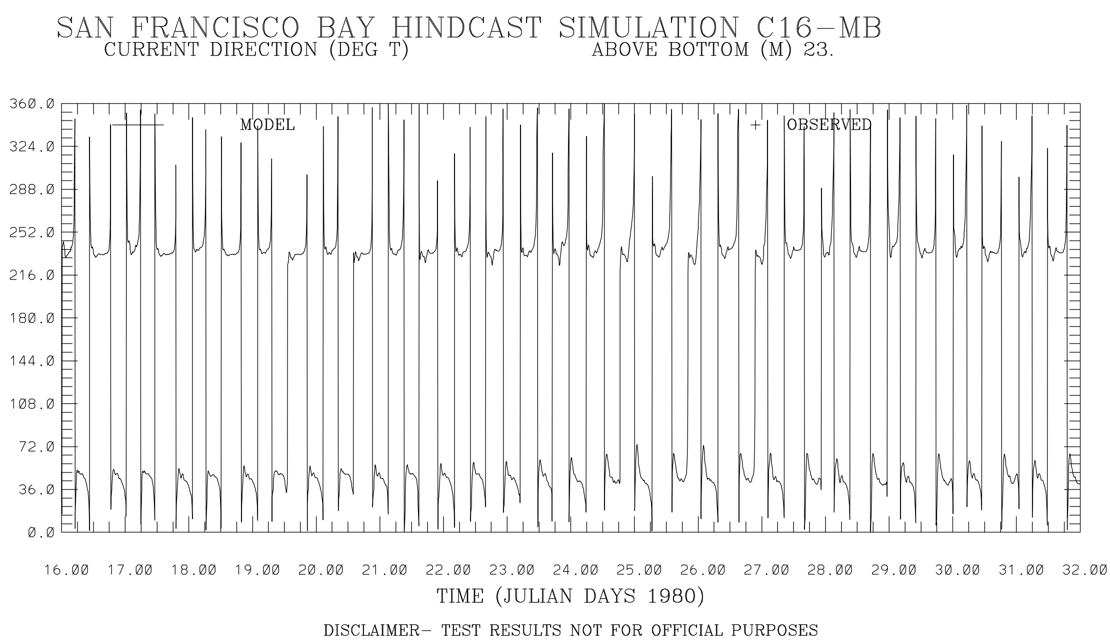

Figure 4.86. January 15-31, 1980 Hindcast: C-16 Current Speed and Direction at 23m above the bottom. Note IND AGRMT equals one minus Willmott et al. (1985) relative error.

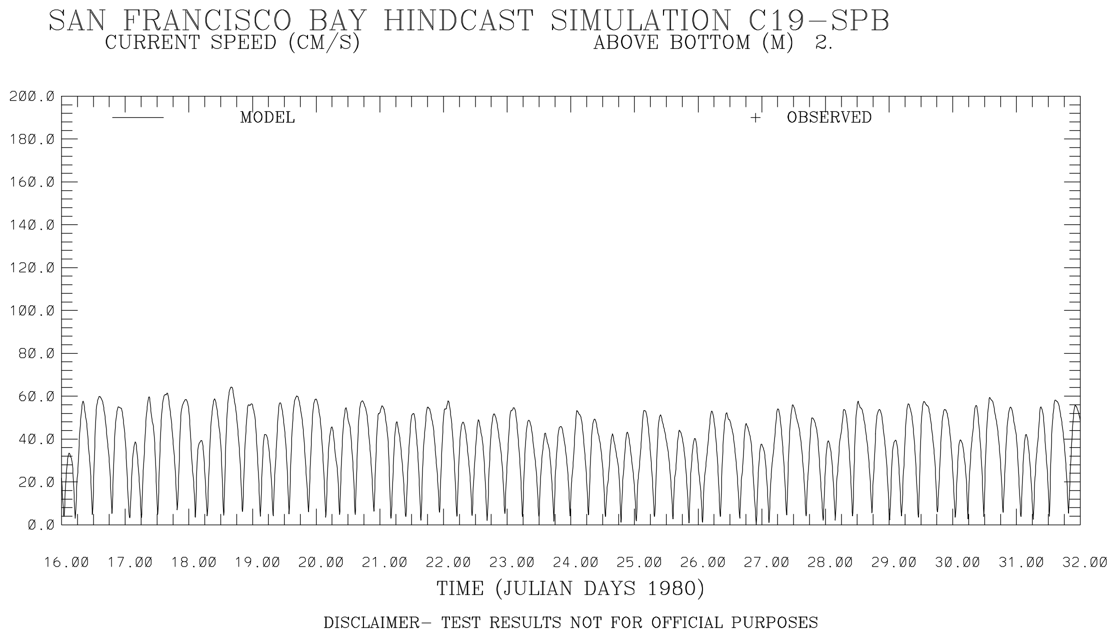

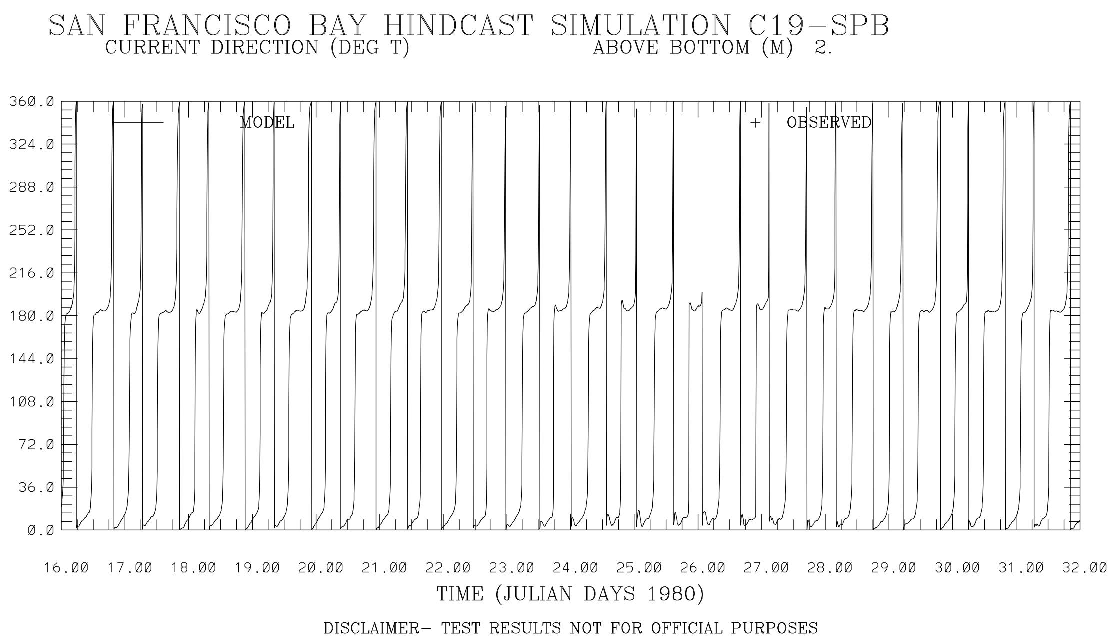

Figure 4.87. January 15-31, 1980 Hindcast: C-19 Current Speed and Direction at 2m above the bottom. Note IND AGRMT equals one minus Willmott et al. (1985) relative error.

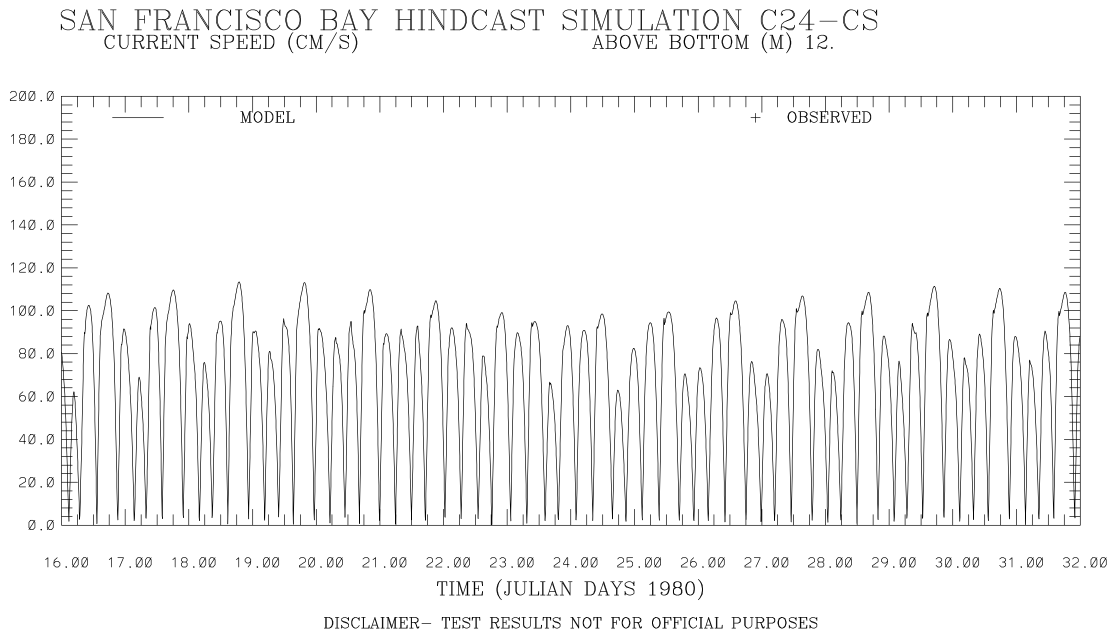

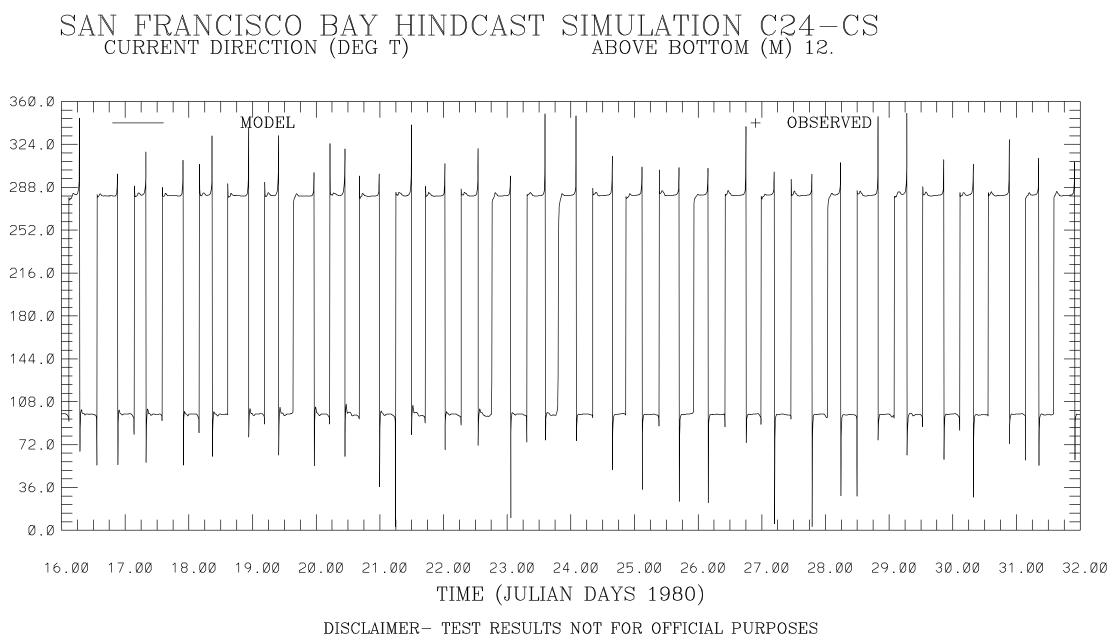

Figure 4.88. January 15-31, 1980 Hindcast: C-24 Current Speed and Direction at 12m above the bottom. Note IND AGRMT equals one minus Willmott et al. (1985) relative error.

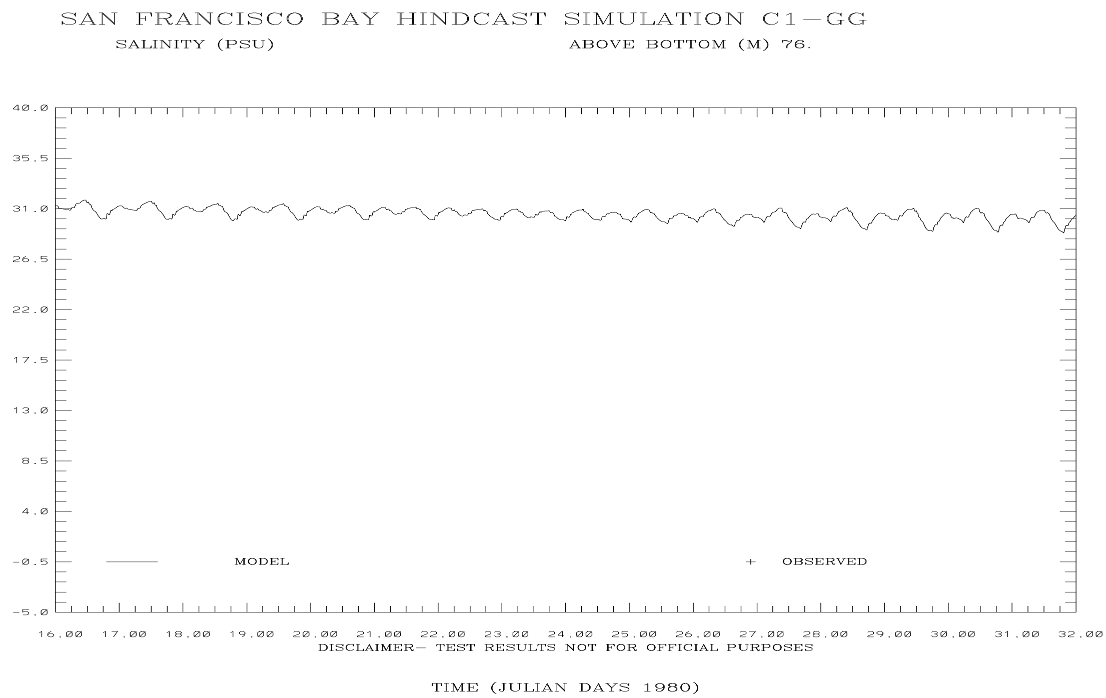

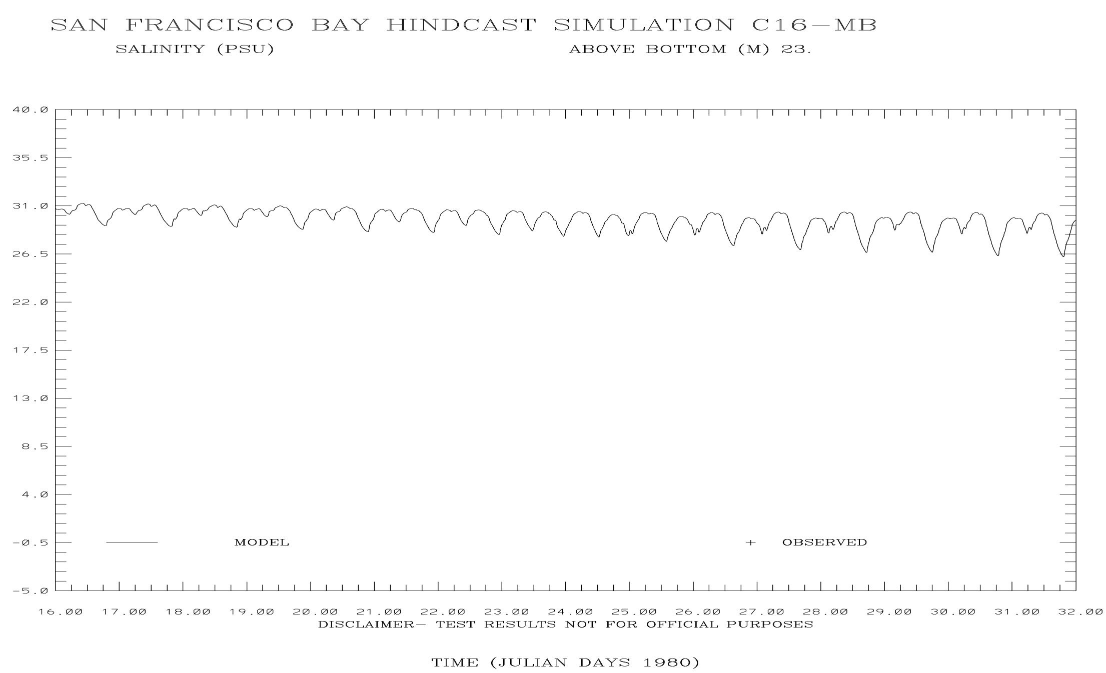

Figure 4.89. January 15-31, 1980 Hindcast: Salinity at C-1 at 76m and at C-16 at 23m above the bottom. Note IND AGRMT equals one minus Willmott et al. (1985) relative error.

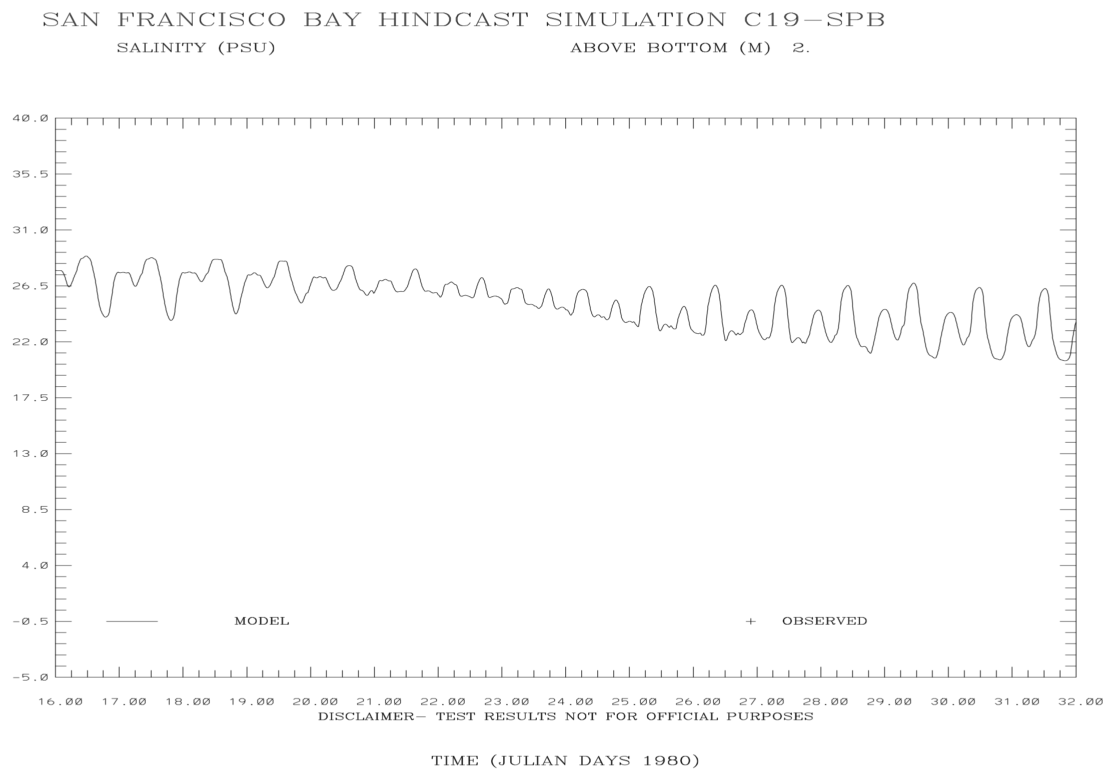

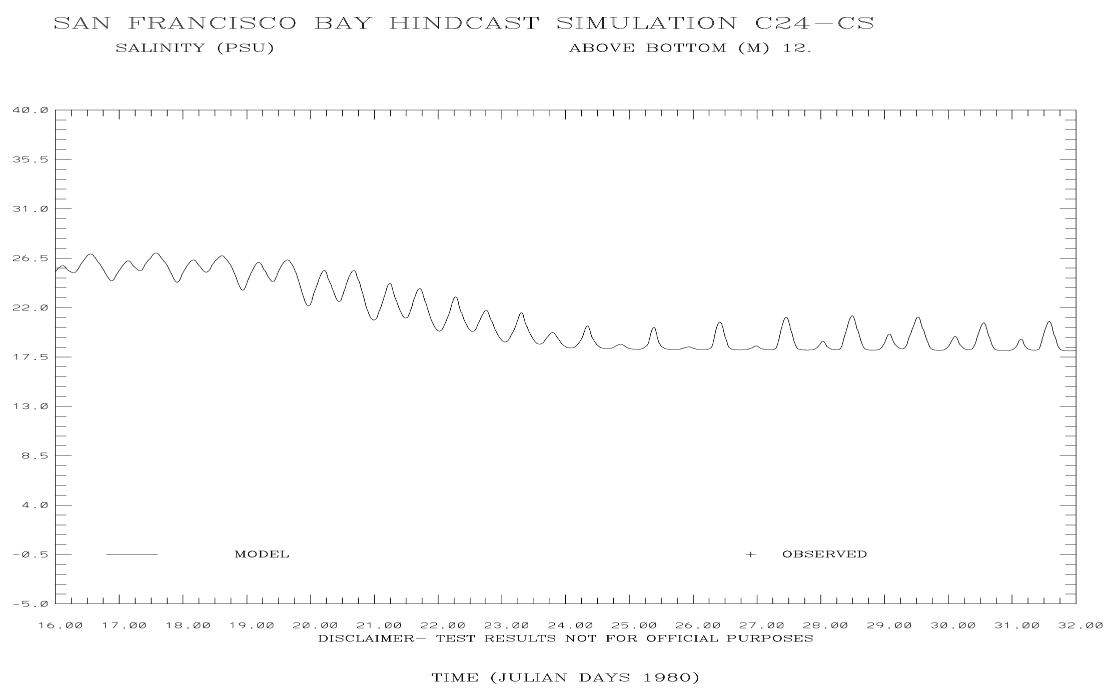

Figure 4.90. January 15-31, 1980 Hindcast: Salinity at C-19 at 2m and at C-24 at 12m above the bottom. Note IND AGRMT equals one minus Willmott et al. (1985) relative error.

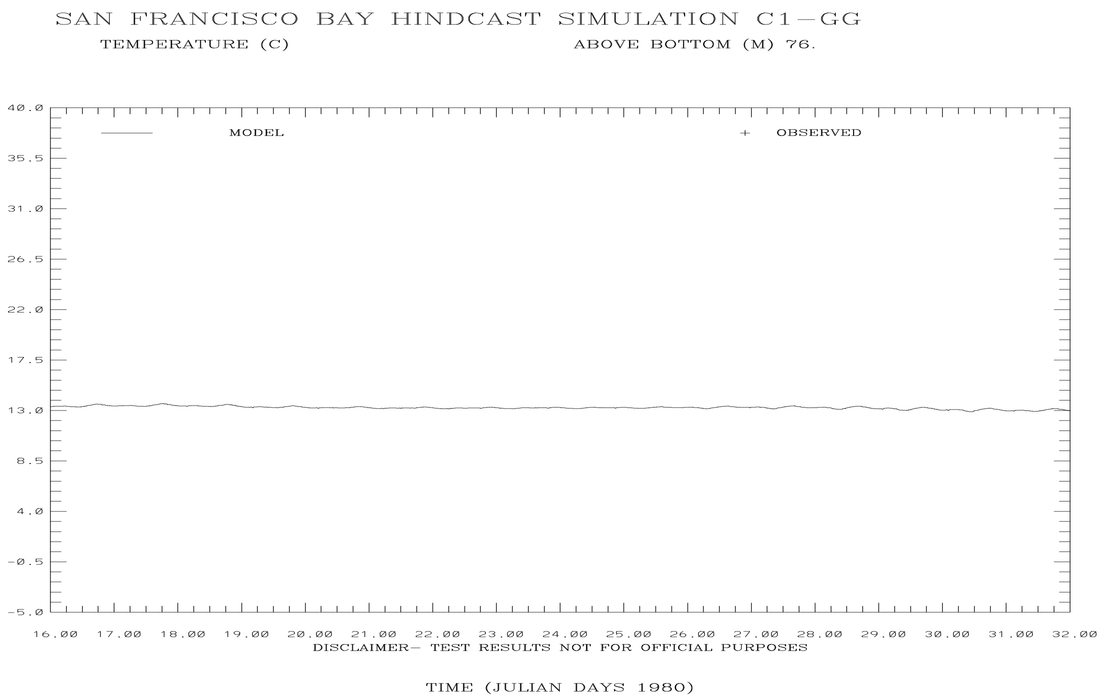

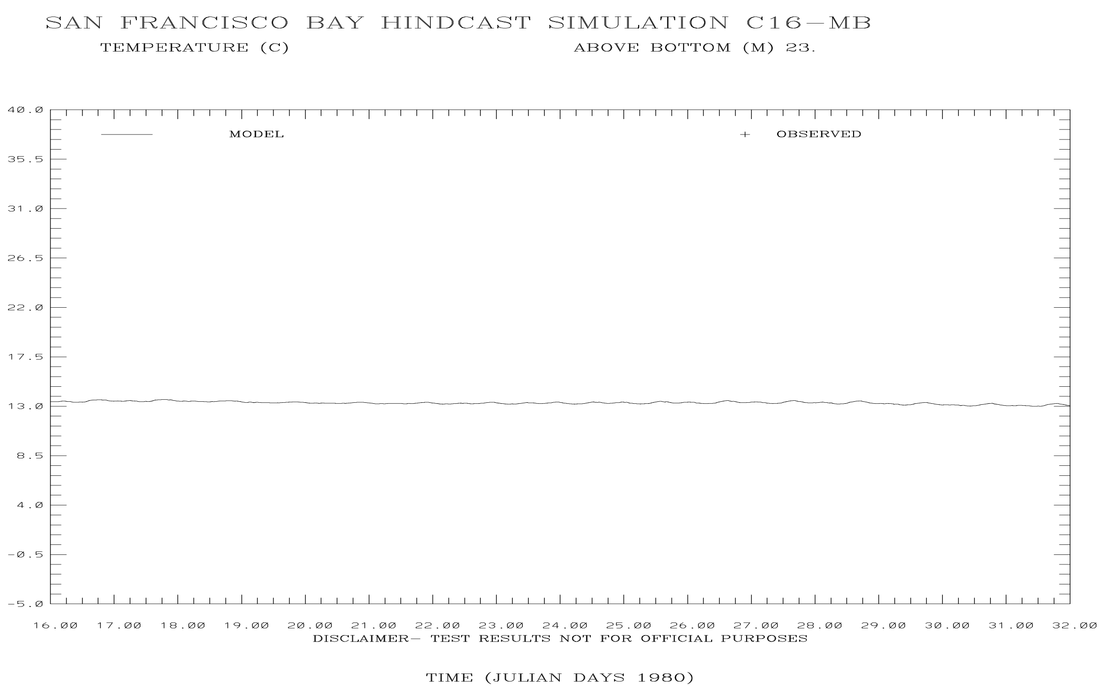

Figure 4.91. January 15-31, 1980 Hindcast: Temperature at C-1 at 76m and at C-16 at 23m above the bottom. Note IND AGRMT equals one minus Willmott et al. (1985) relative error.

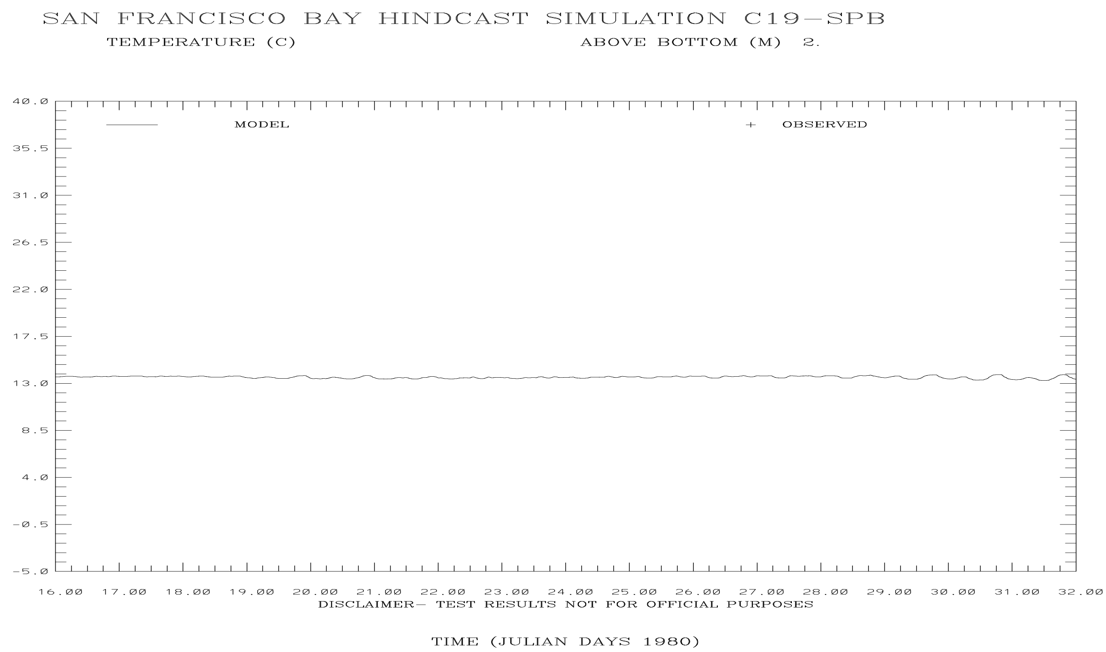

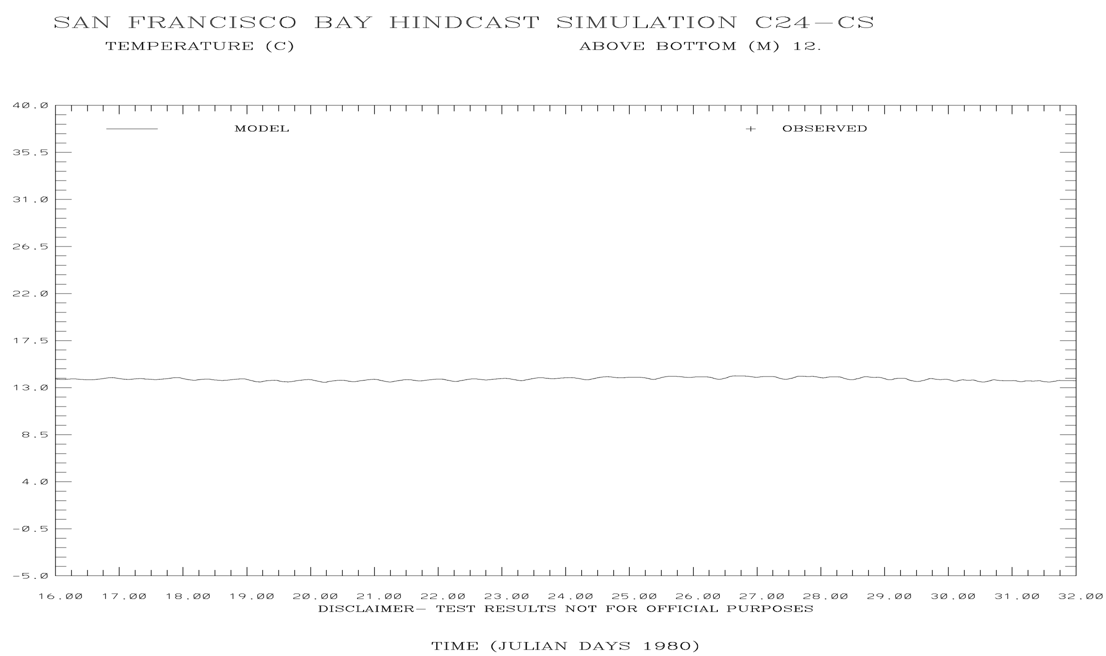

Figure 4.92. January 15-31, 1980 Hindcast: Temperature at C-19 at 2m and at C-24 at 12m above the bottom. Note IND AGRMT equals one minus Willmott et al. (1985) relative error.

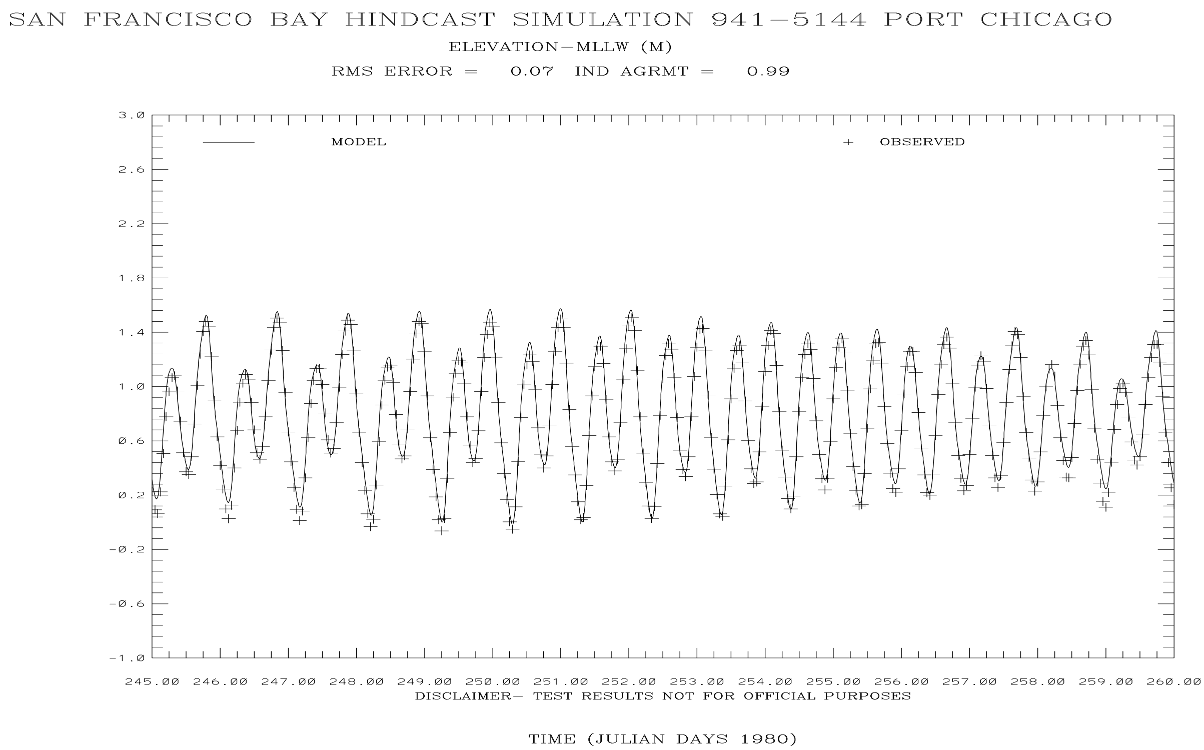

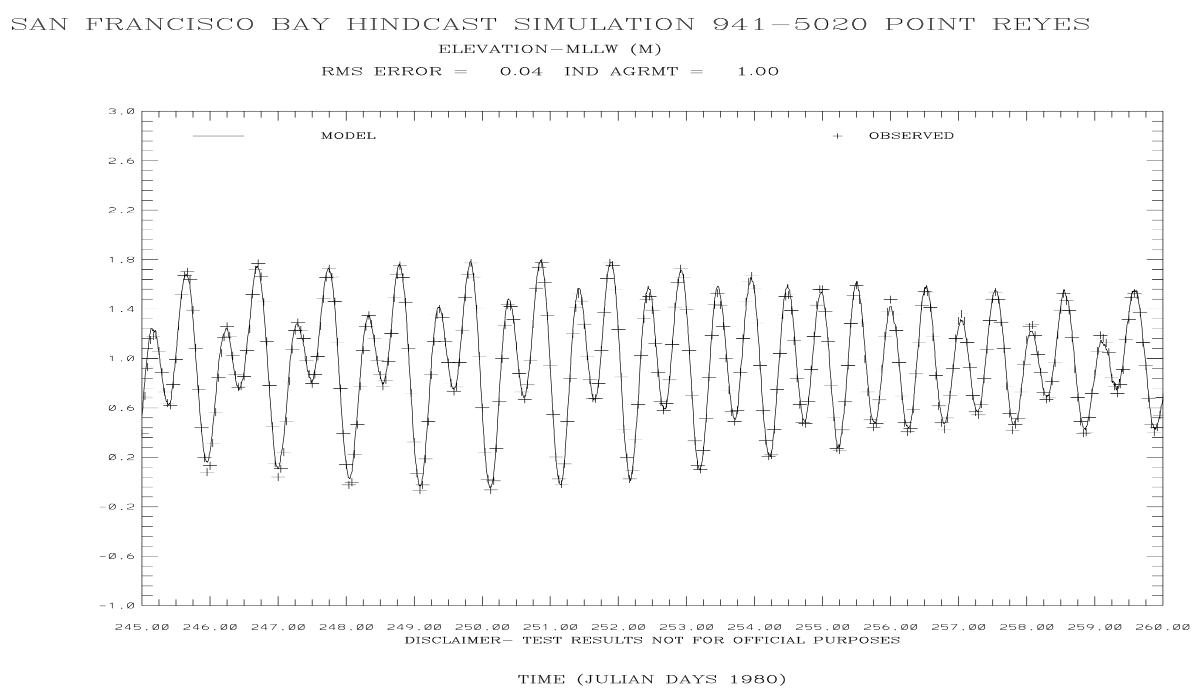

Figure 4.93. September 1-15, 1980 Hindcast: Port Chicago and Point Reyes Water Level Comparisons. Note IND AGRMT equals one minus Willmott et al. (1985) relative error.

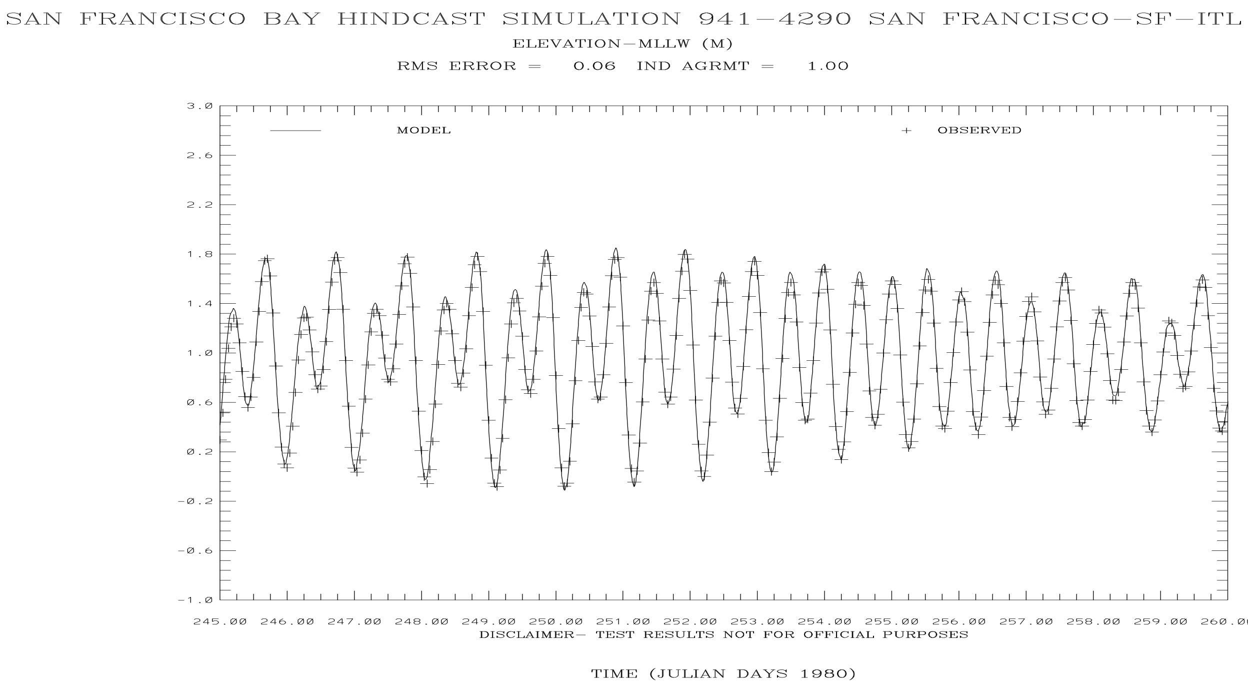

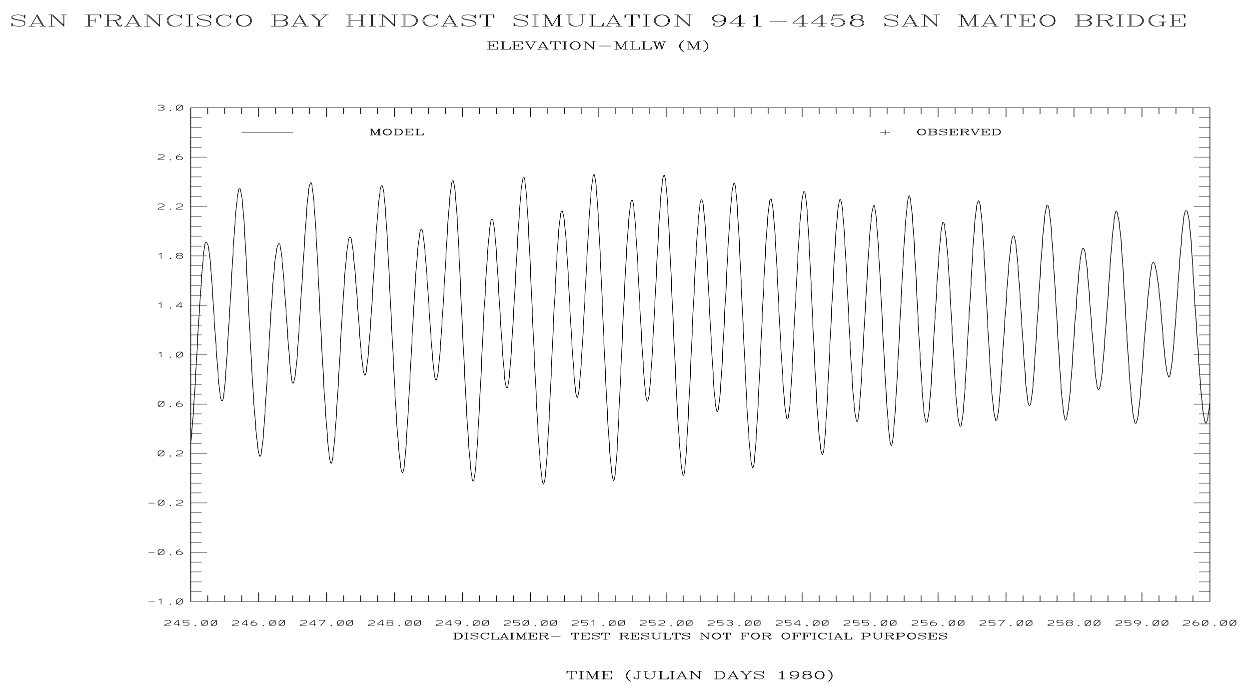

Figure 4.94. September 1-15, 1980 Hindcast: San Francisco and San Mateo Bridge Water Level Comparisons. Note IND AGRMT equals one minus Willmott et al. (1985) relative error.

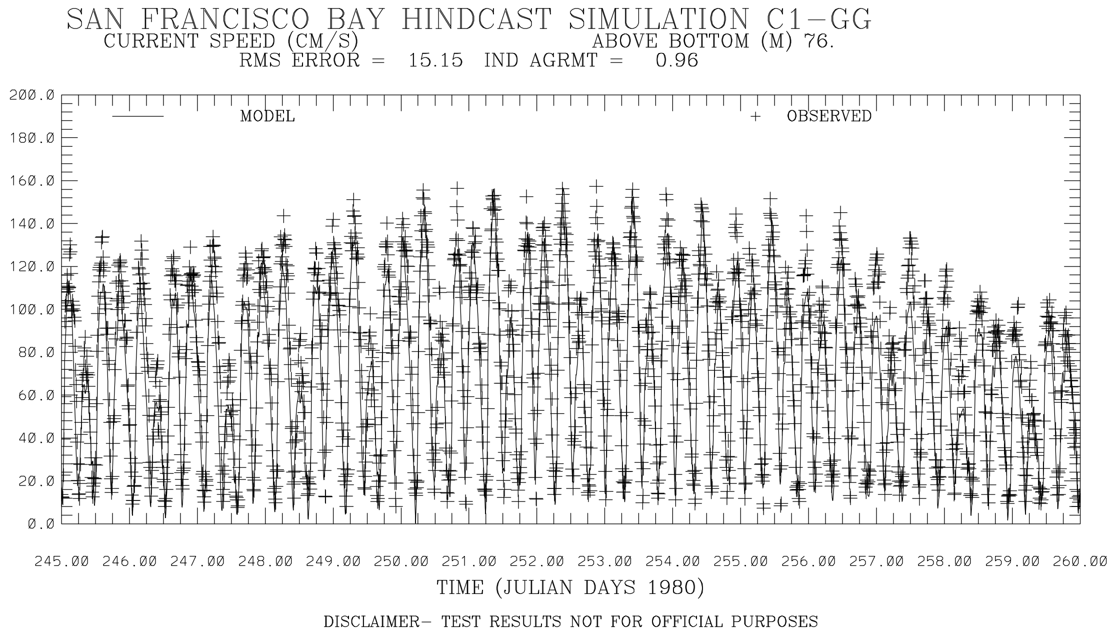

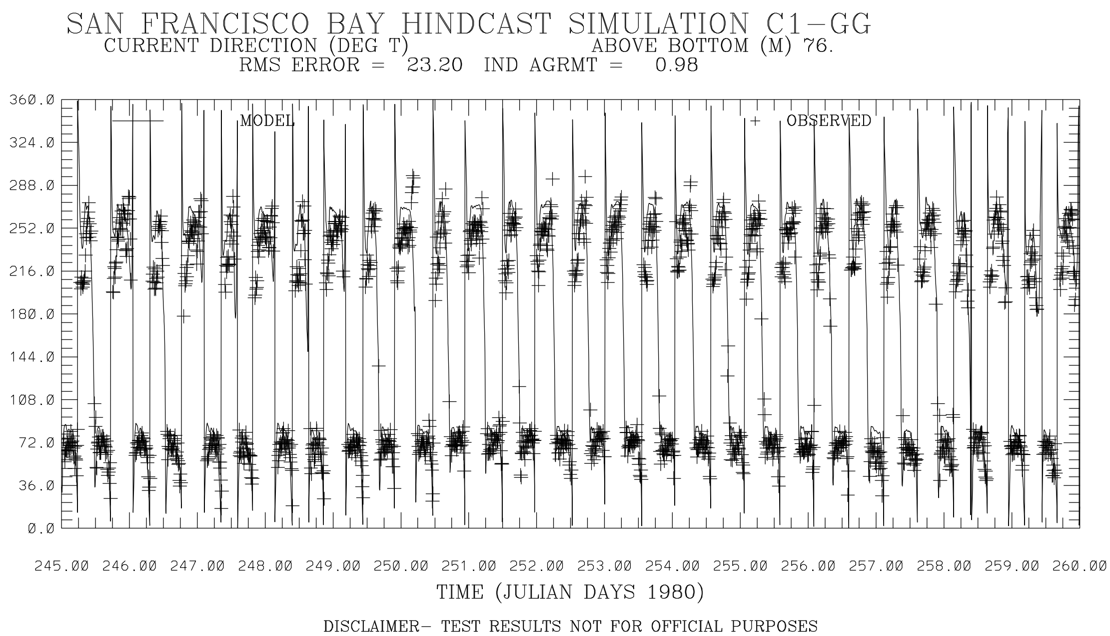

Figure 4.95. September 1-15, 1980 Hindcast: C-1 Current Speed and Direction at 91m above the bottom. Note IND AGRMT equals one minus Willmott et al. (1985) relative error.

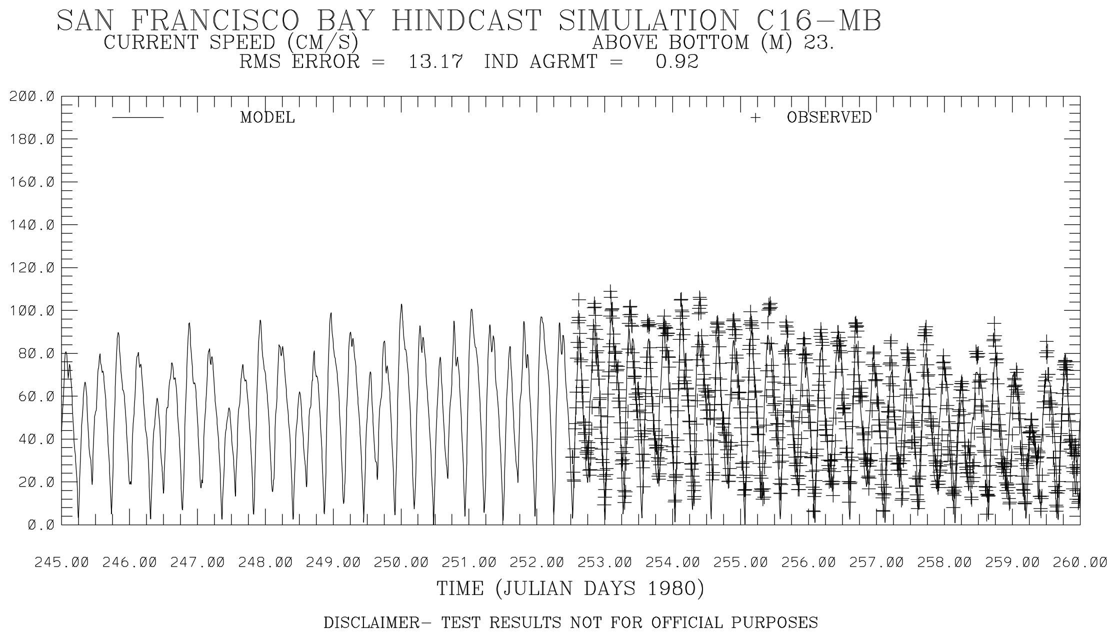

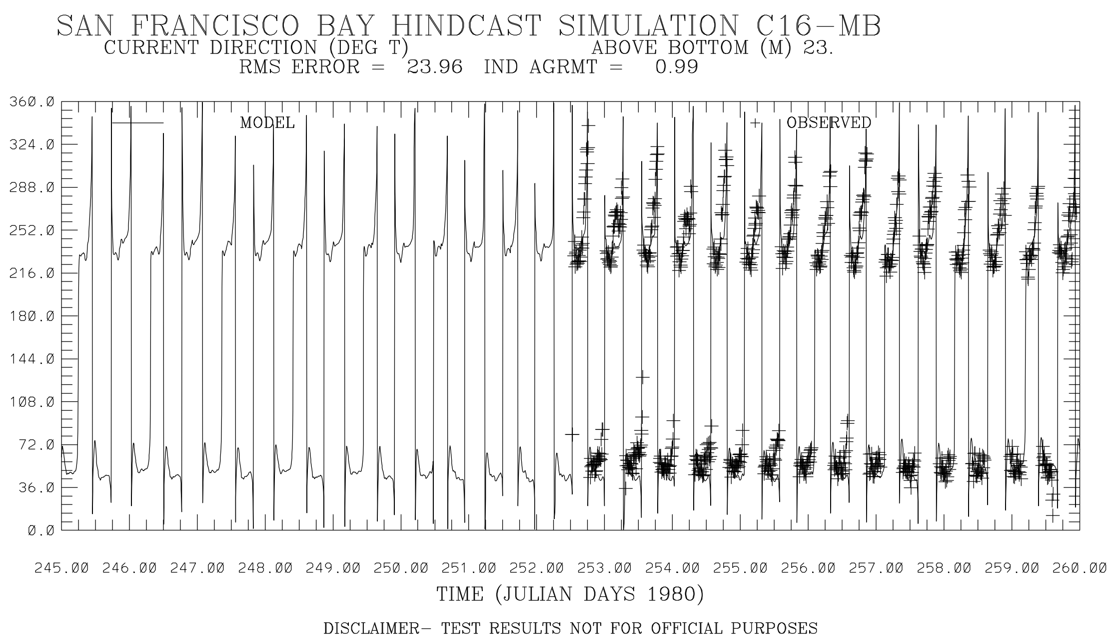

Figure 4.96. September 1-15, 1980 Hindcast: C-16 Current Speed and Direction at 23m above the bottom. Note IND AGRMT equals one minus Willmott et al. (1985) relative error.

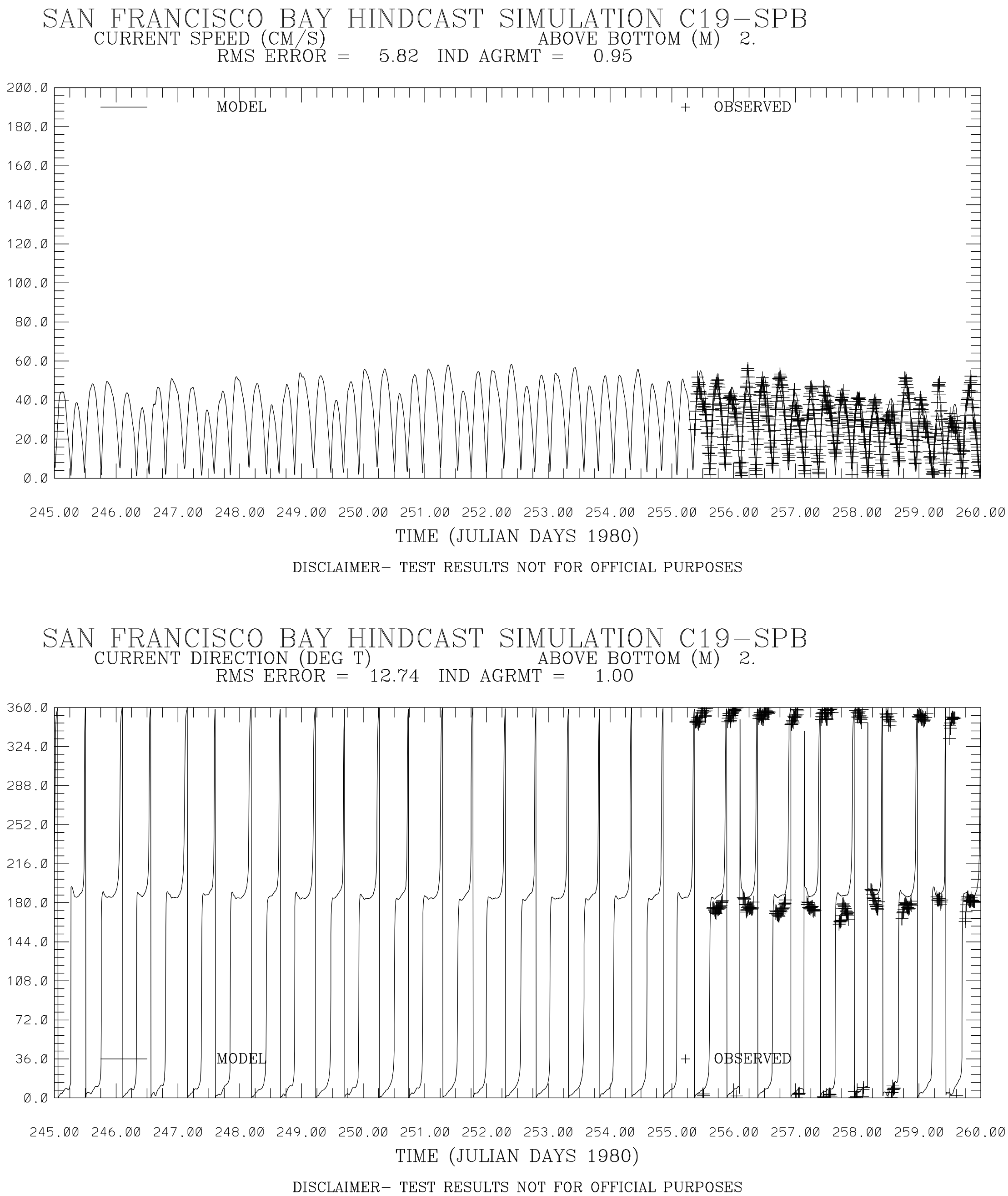

Figure 4.97. September 1-15, 1980 Hindcast: C-19 Current Speed and Direction at 2m above the bottom. Note IND AGRMT equals one minus Willmott et al. (1985) relative error.

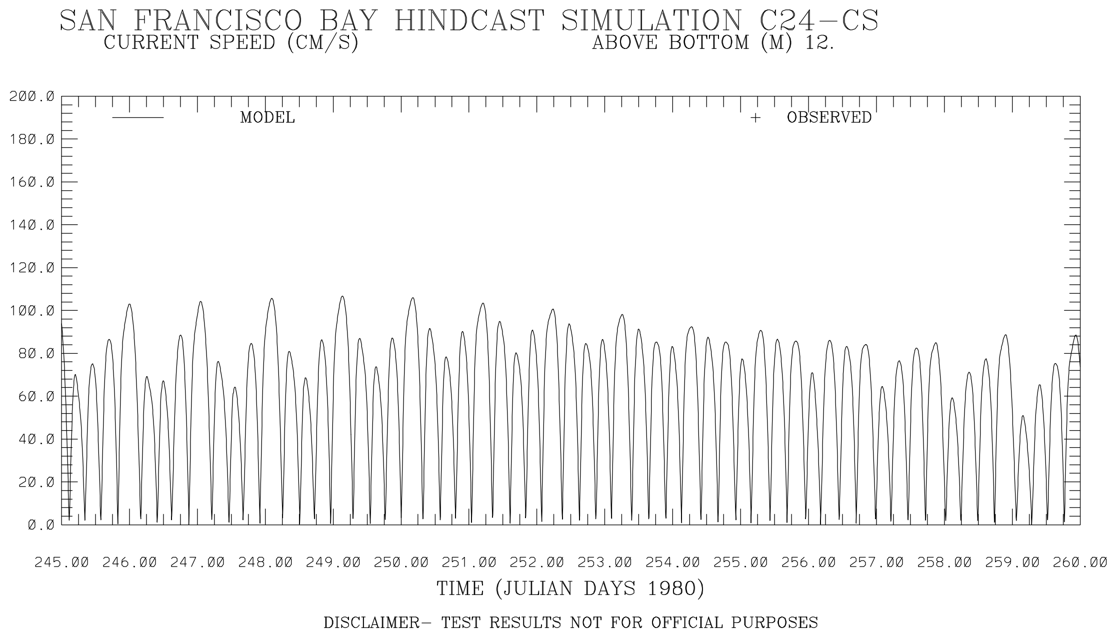

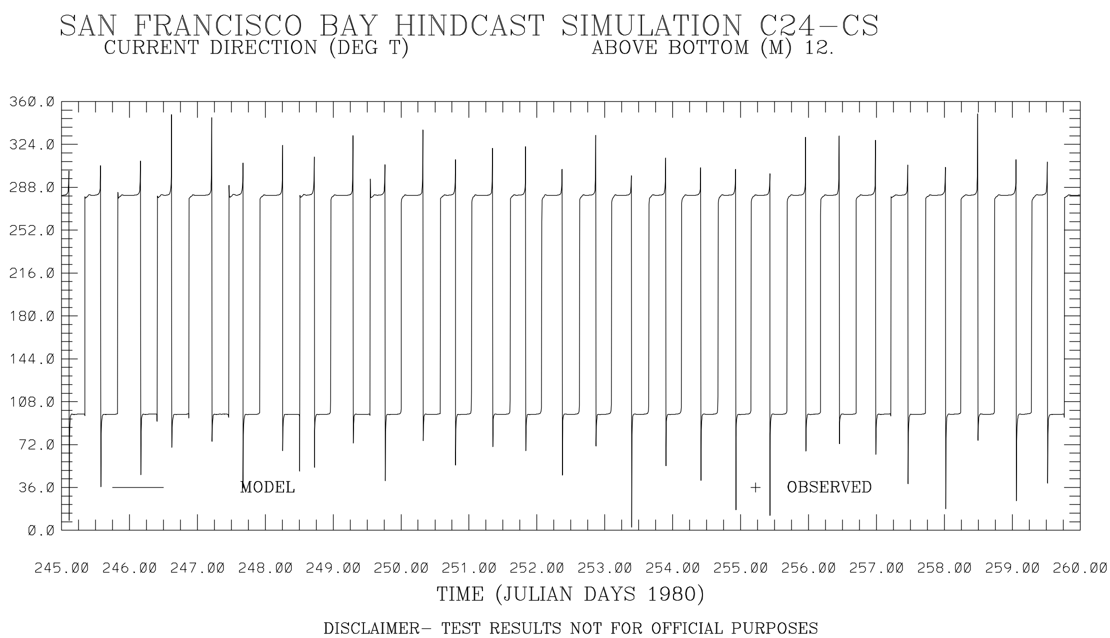

Figure 4.98. September 1-15, 1980 Hindcast: C-24 Current Speed and Direction at 12m above the bottom. Note IND AGRMT equals one minus Willmott et al. (1985) relative error.

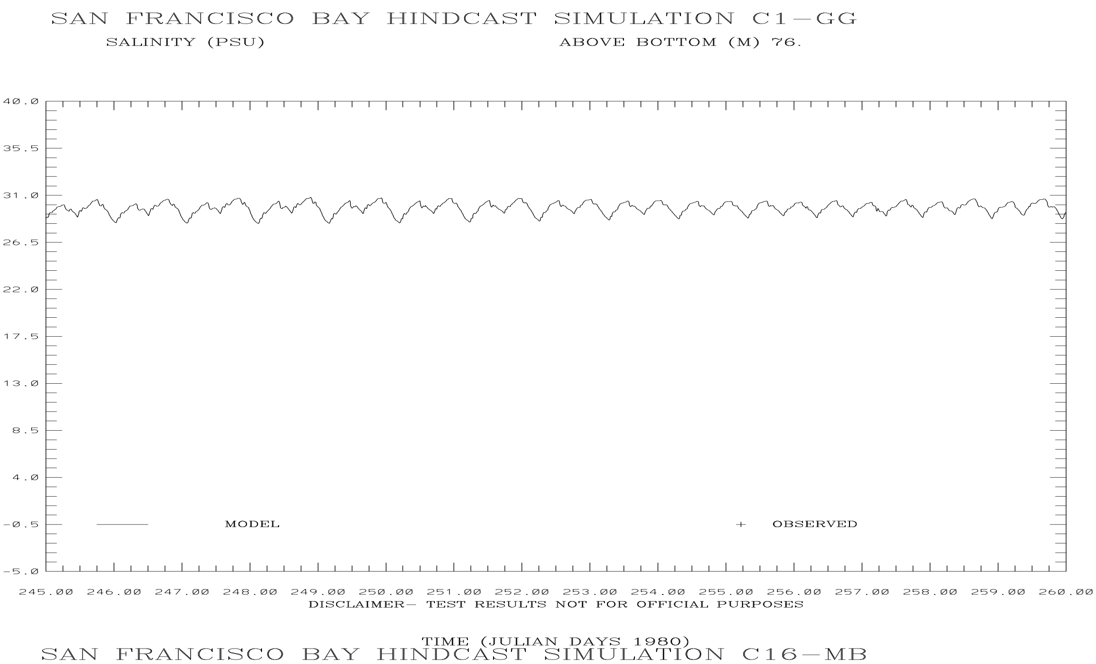

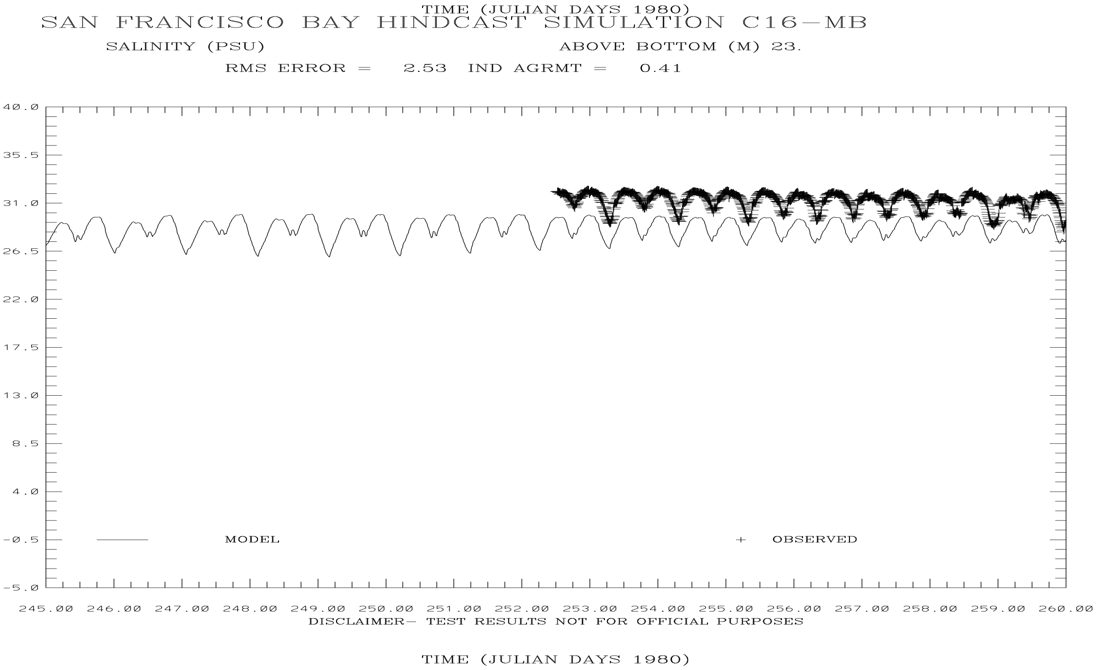

Figure 4.99. September 1-15, 1980 Hindcast: Salinity at C-1 at 46m and C-18 at 9m above the bottom. Note IND AGRMT equals one minus Willmott et al. (1985) relative error.

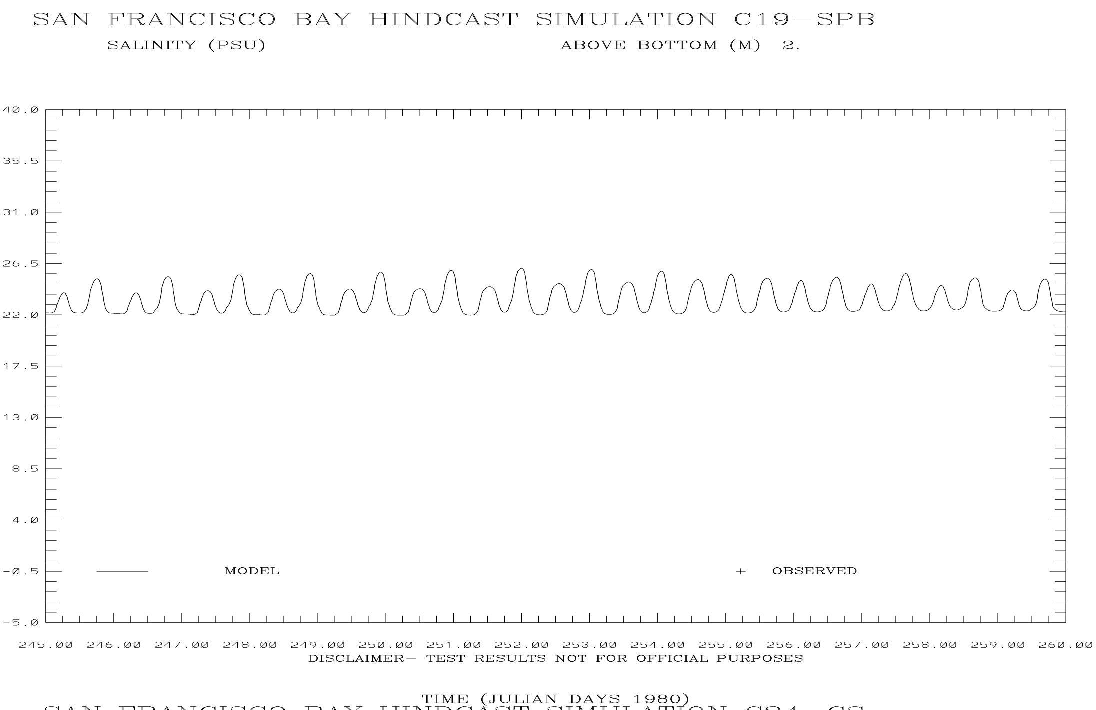

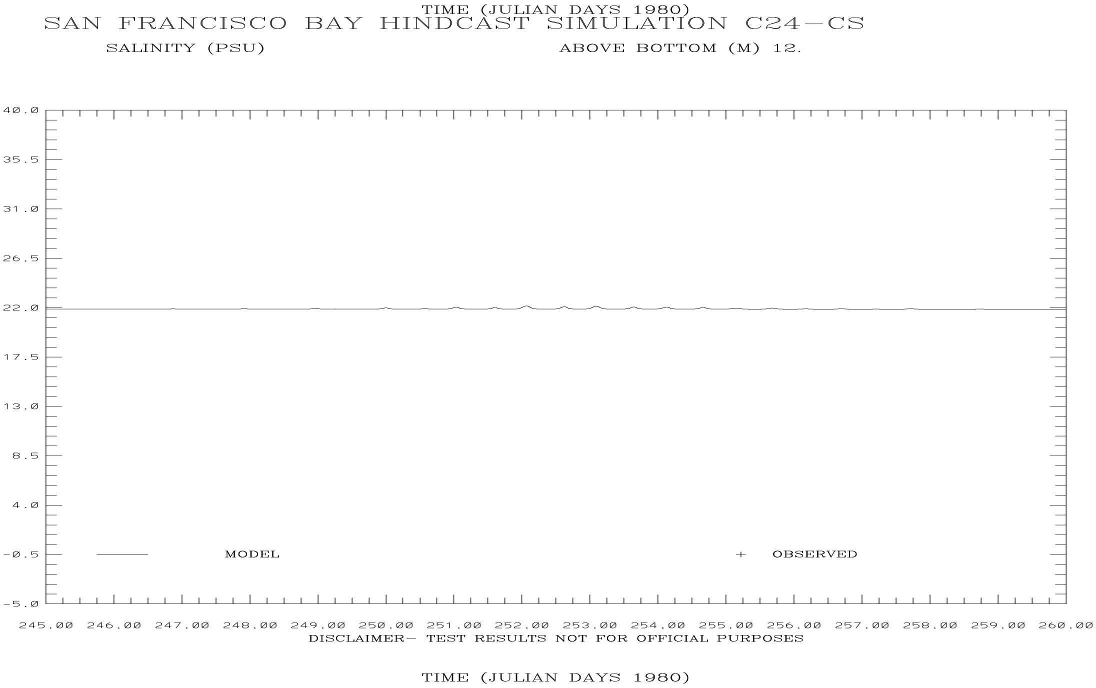

Figure 4.100. September 1-15, 1980 Hindcast: Salinity at C-22 at 2m and C-24 at 17m above the bottom. Note IND AGRMT equals one minus Willmott et al. (1985) relative error.

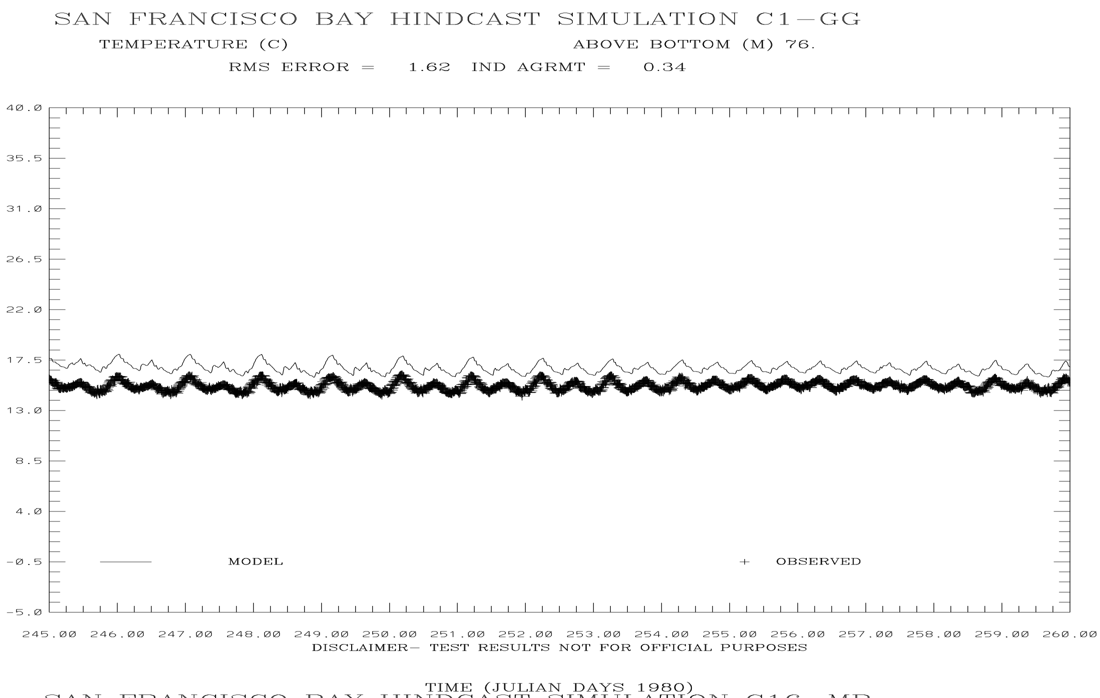

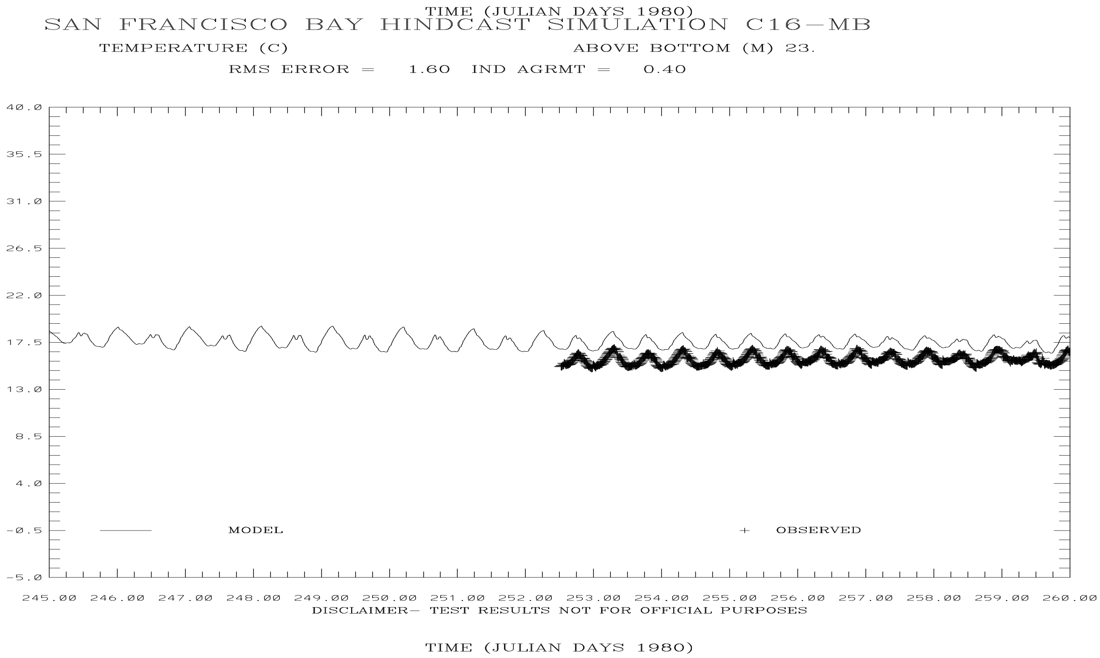

Figure 4.101. September 1-15, 1980 Hindcast: Temperature at C-1 at 76m and C-16 at 23m above the bottom. Note IND AGRMT equals one minus Willmott et al. (1985) relative error.

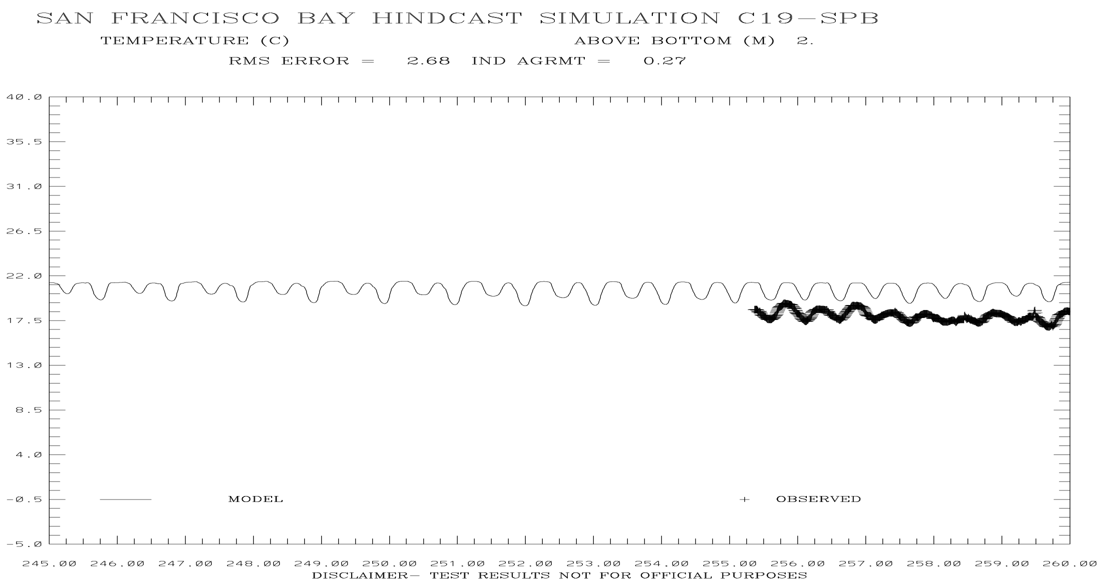

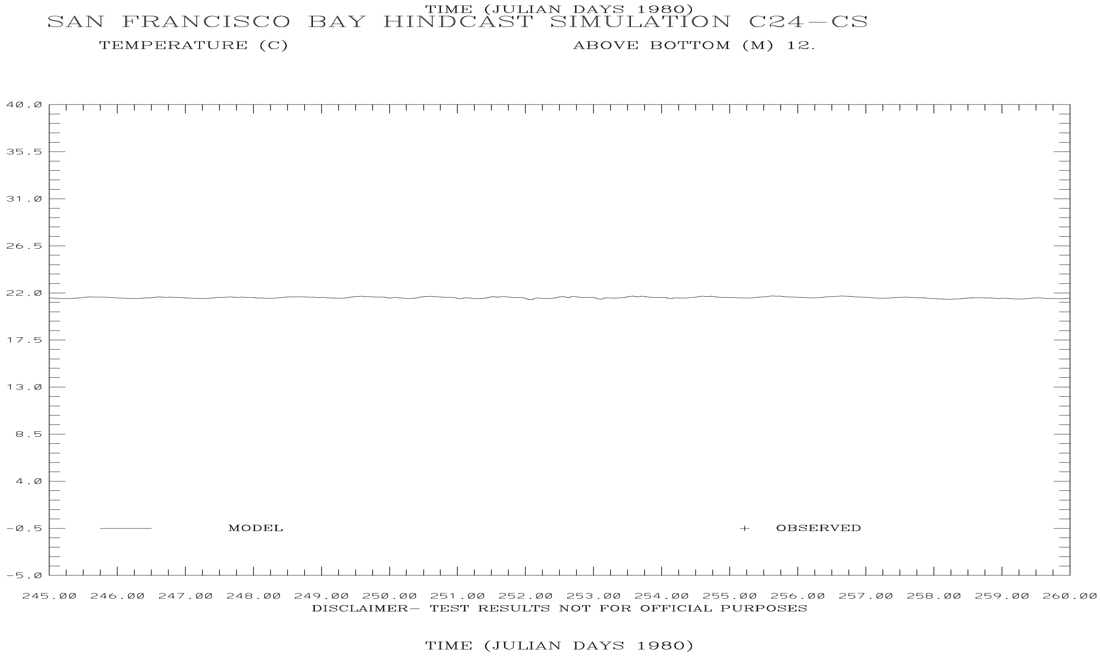

Figure 4.102. September 1-15, 1980 Hindcast: Temperature at C-19 at 2m and C-24 at 17m above the bottom. Note IND AGRMT equals one minus Willmott et al. (1985) relative error.

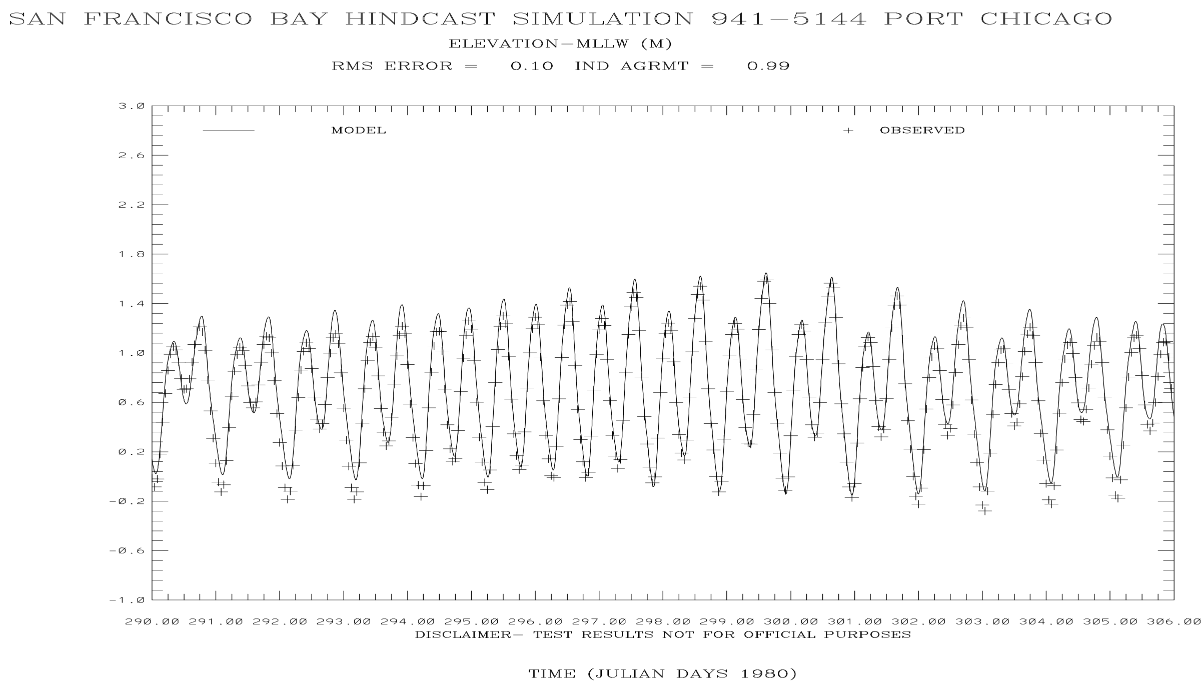

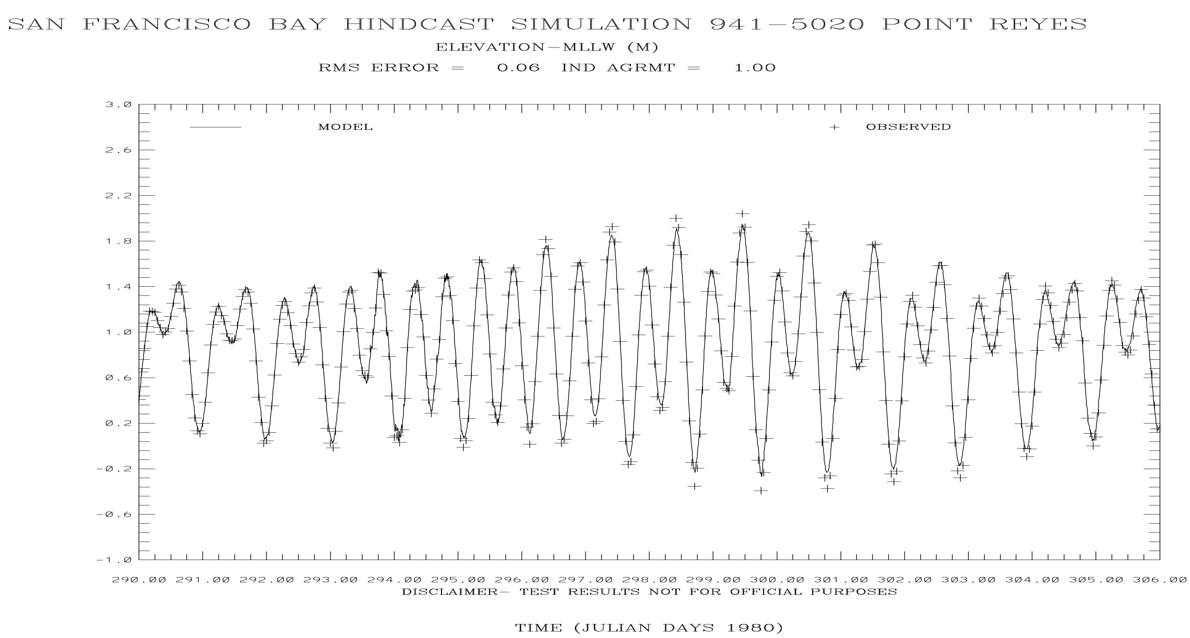

Figure 4.103. October 15-31, 1980 Hindcast: Port Chicago and Point Reyes Water Level Comparisons. Note IND AGRMT equals one minus Willmott et al. (1985) relative error.

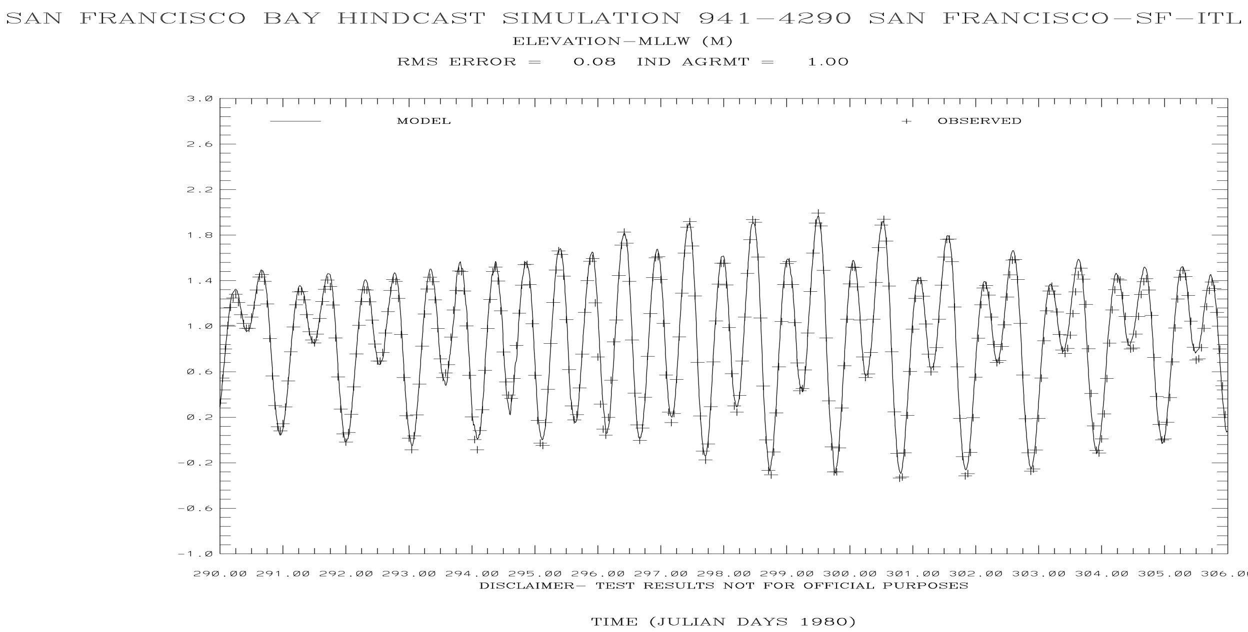

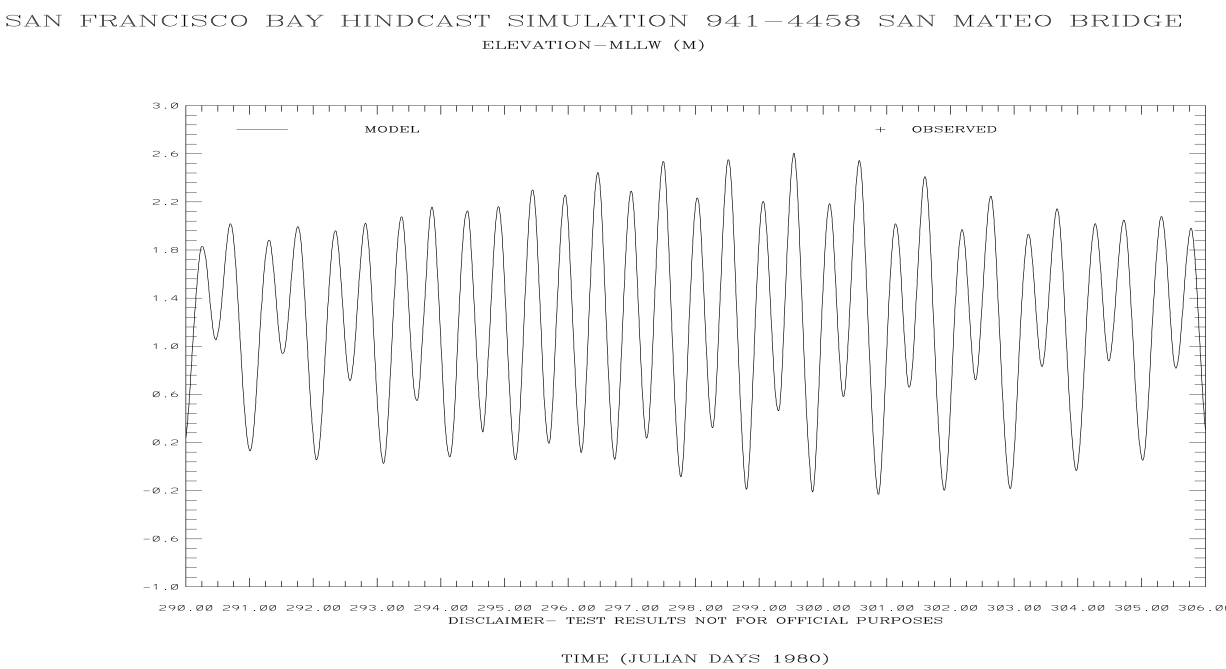

Figure 4.104. October 15-31, 1980 Hindcast: San Francisco and San Mateo Bridge Water Level Comparisons. Note IND AGRMT equals one minus Willmott et al. (1985) relative error.

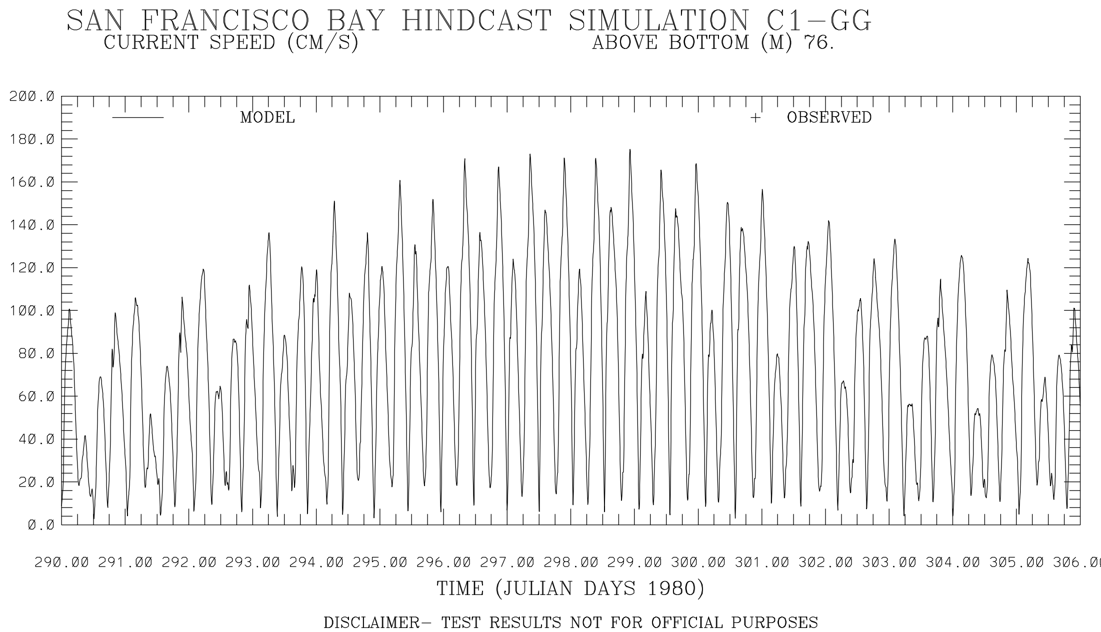

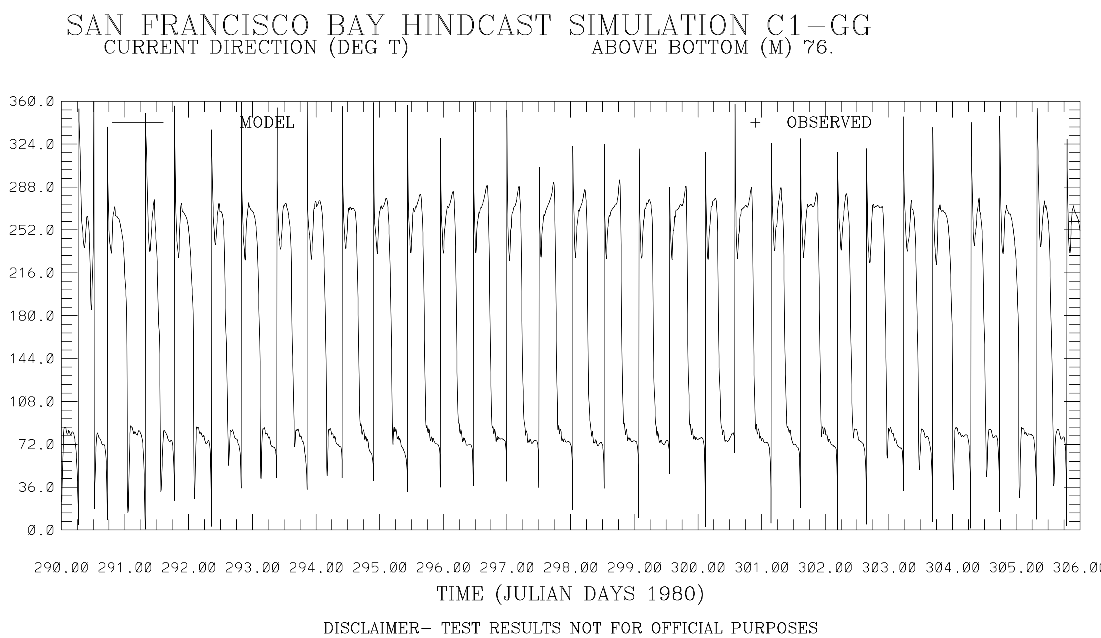

Figure 4.105. October 15-31, 1980 Hindcast: C-1 Current Speed and Direction at 76m above the bottom. Note IND AGRMT equals one minus Willmott et al. (1985) relative error.

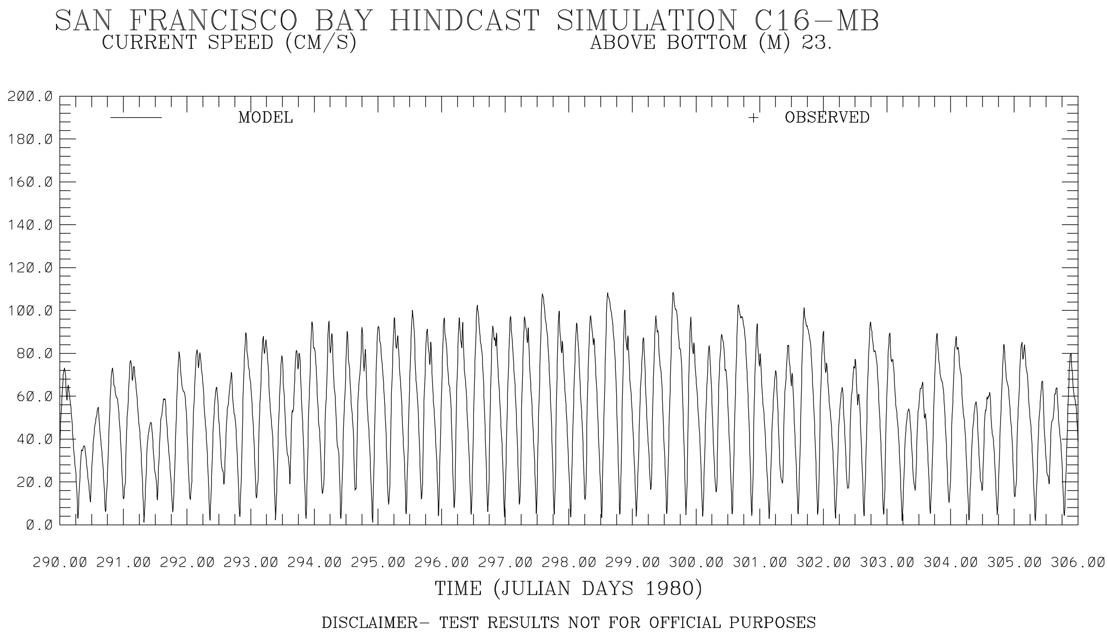

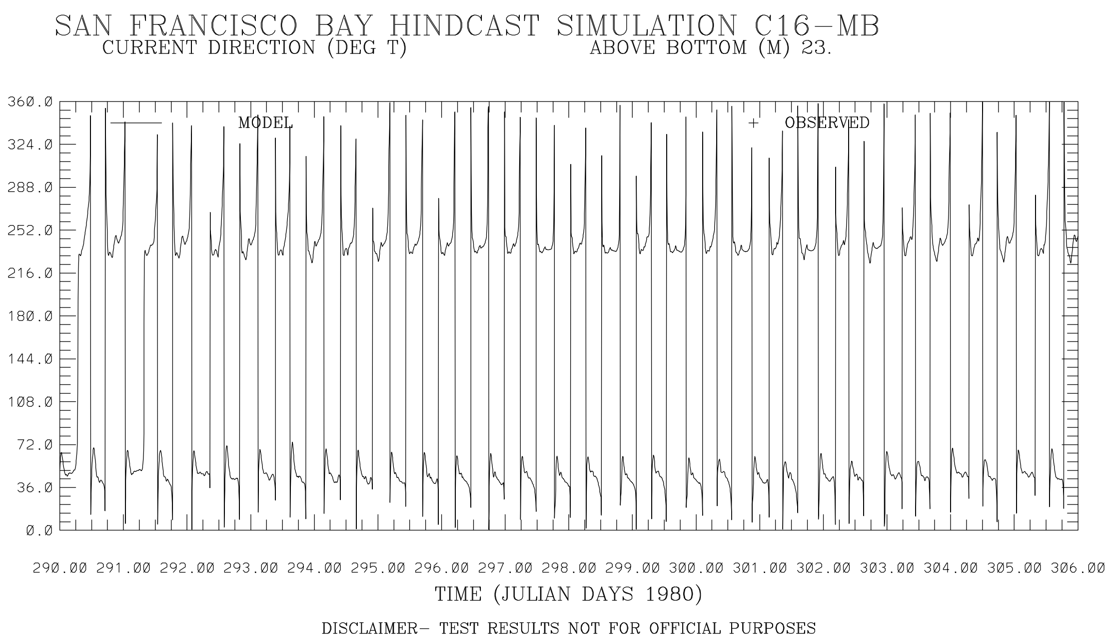

Figure 4.106. October 15-31, 1980 Hindcast: C-16 Current Speed and Direction at 23m above the bottom. Note IND AGRMT equals one minus Willmott et al. (1985) relative error.

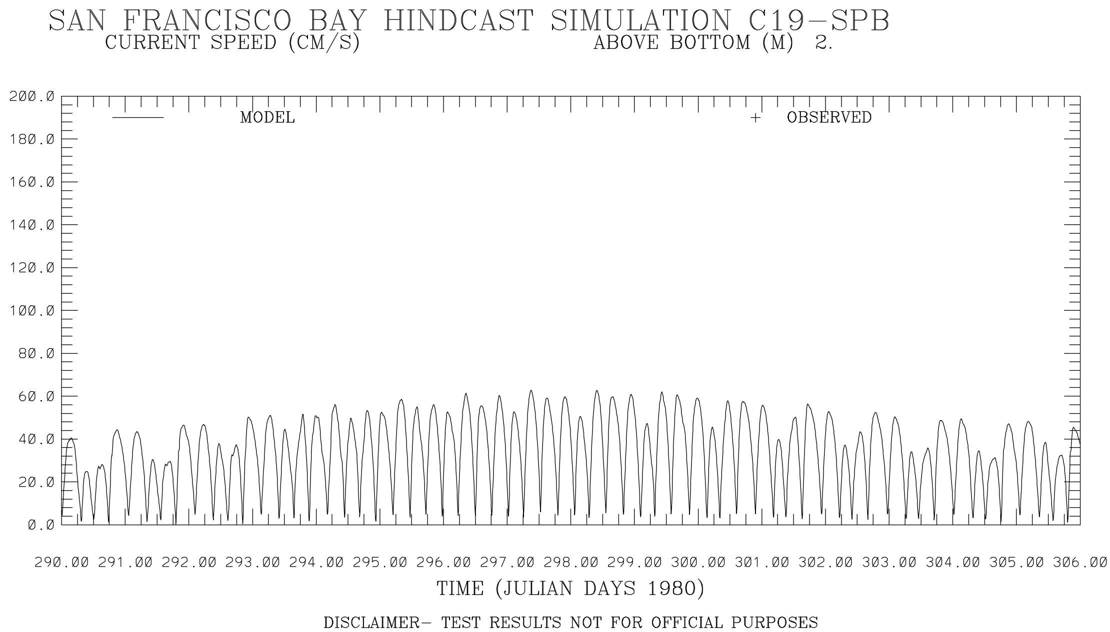

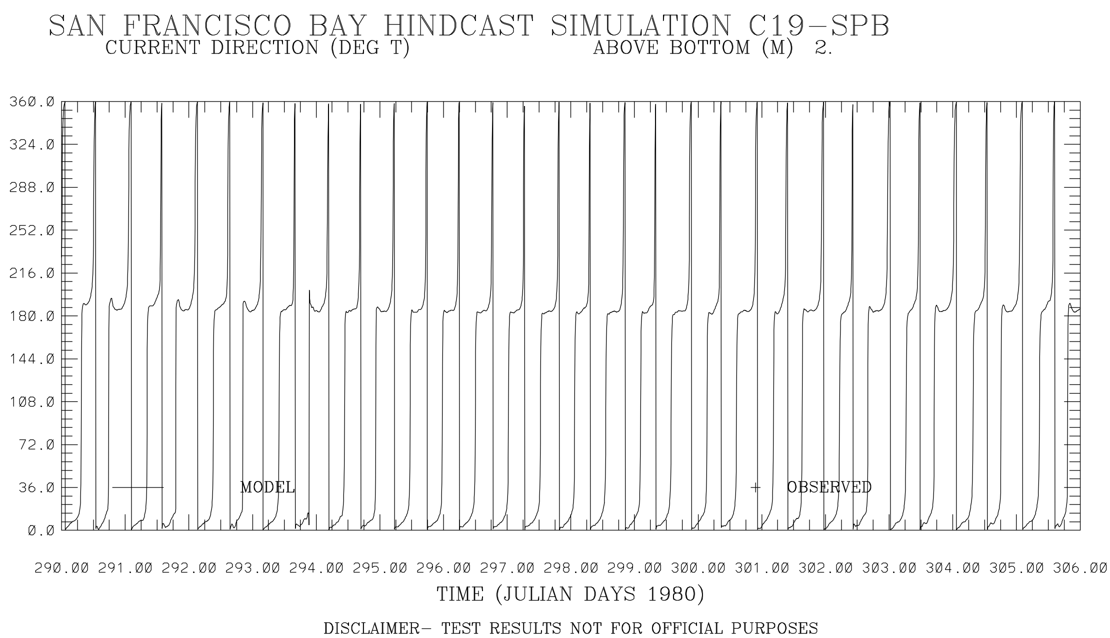

Figure 4.107. October 15-31, 1980 Hindcast: C-19 Current Speed and Direction at 2m above the bottom. Note IND AGRMT equals one minus Willmott et al. (1985) relative error.

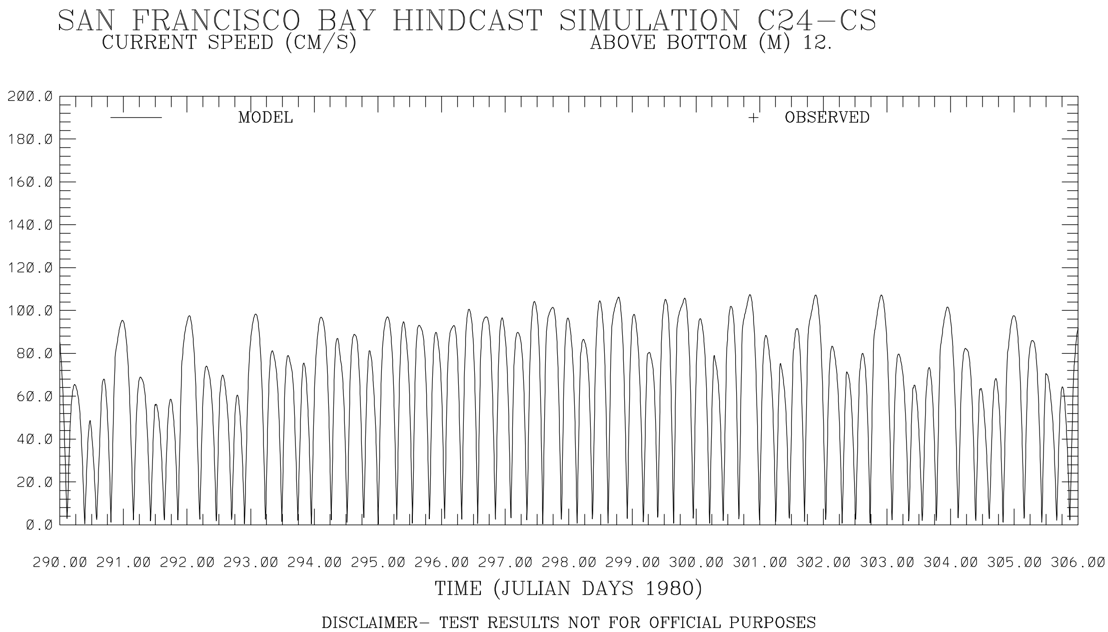

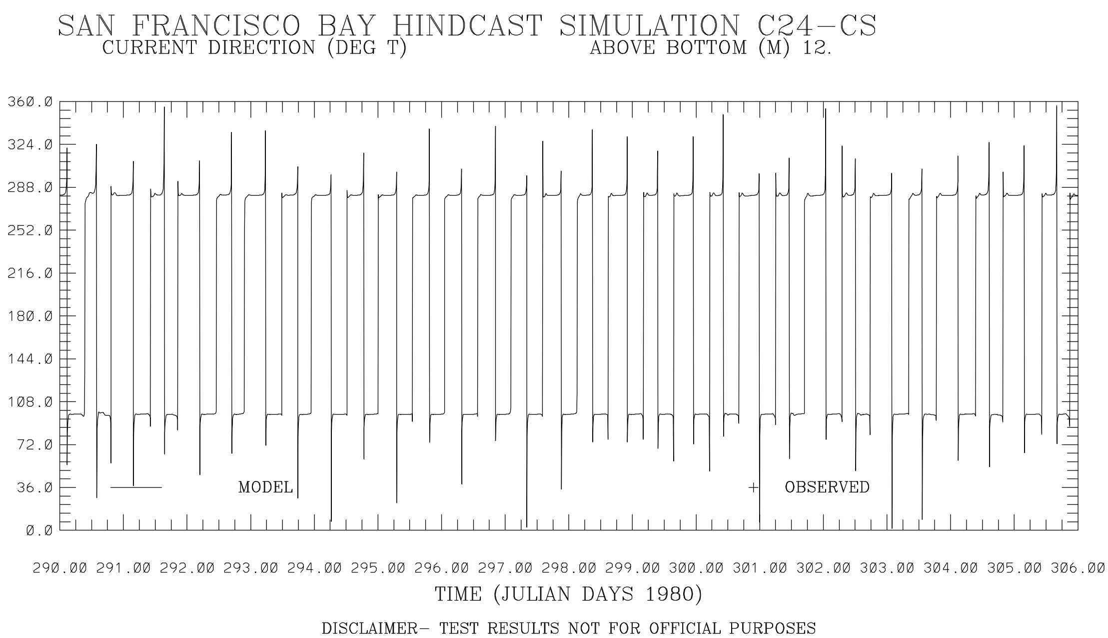

Figure 4.108. October 15-31, 1980 Hindcast: C-24 Current Speed and Direction at 12m above the bottom. Note IND AGRMT equals one minus Willmott et al. (1985) relative error.

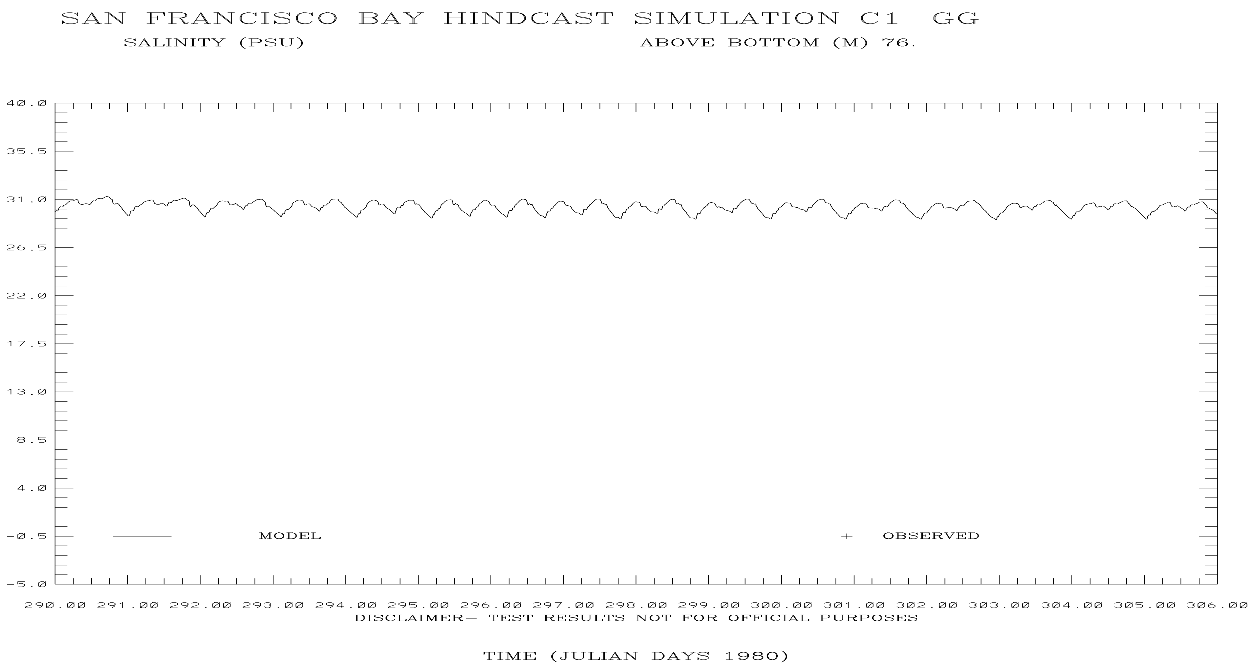

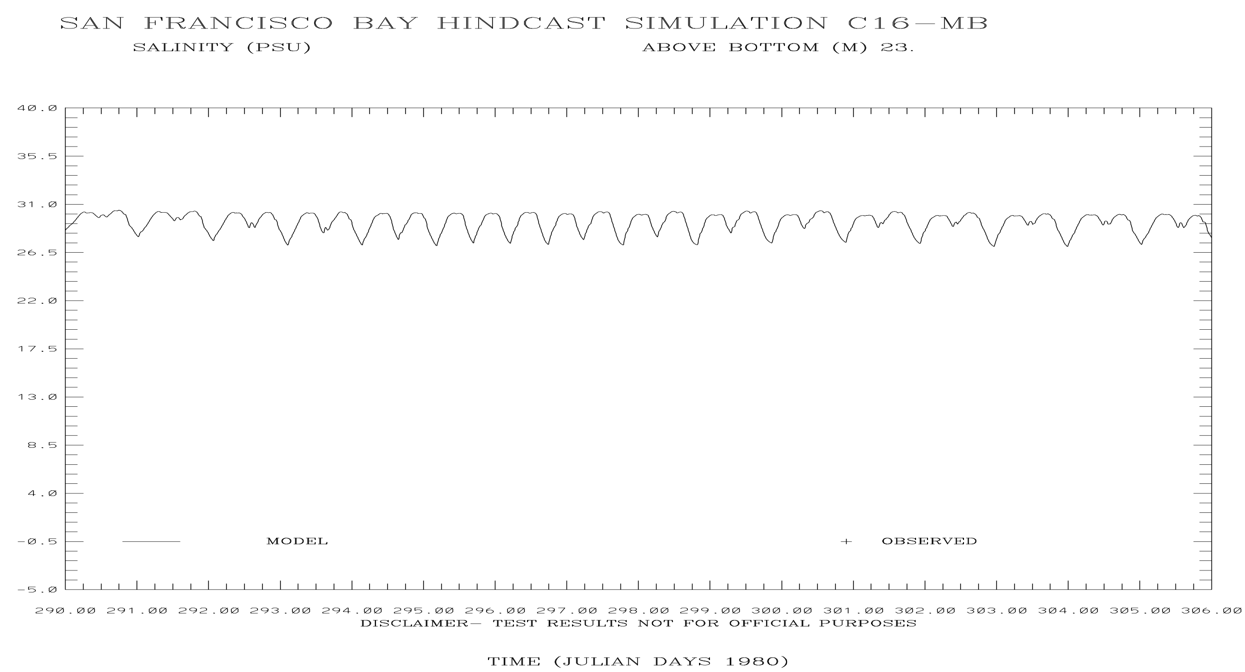

Figure 4.109. October 15-31, 1980 Hindcast: Salinity at C-1 at 76m and C-16 at 23m above the bottom. Note IND AGRMT equals one minus Willmott et al. (1985) relative error.

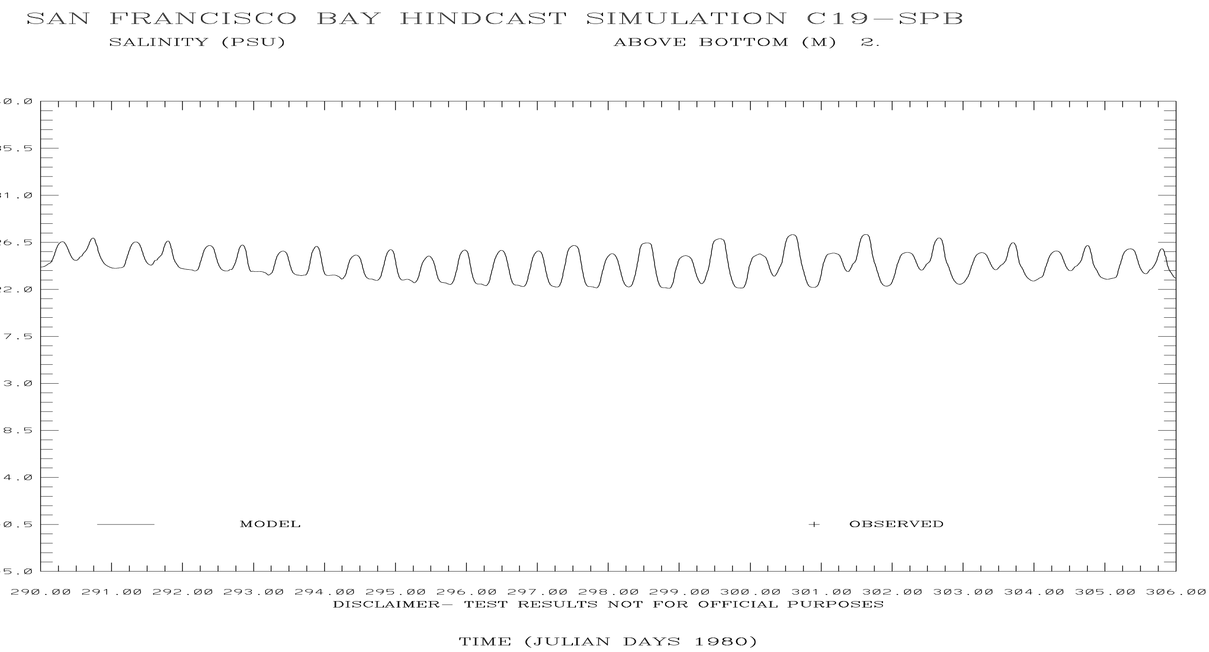

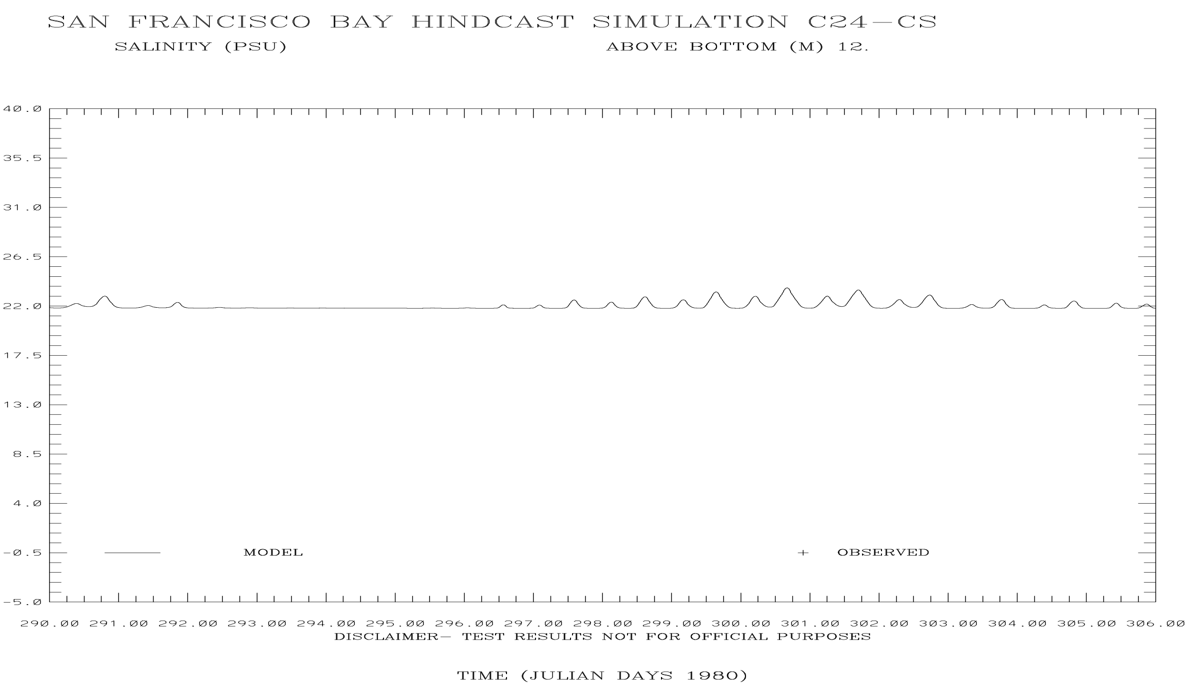

Figure 4.110. October 15-31, 1980 Hindcast: Salinity at C-19 at 2m and C-24 at 12m above the bottom. Note IND AGRMT equals one minus Willmott et al. (1985) relative error.

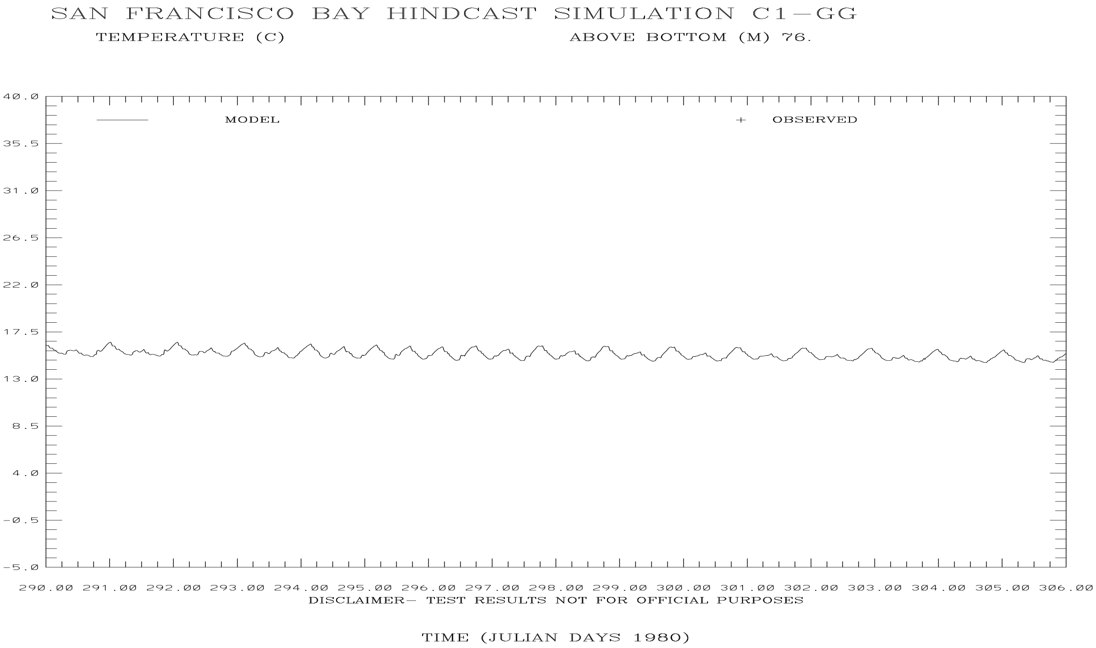

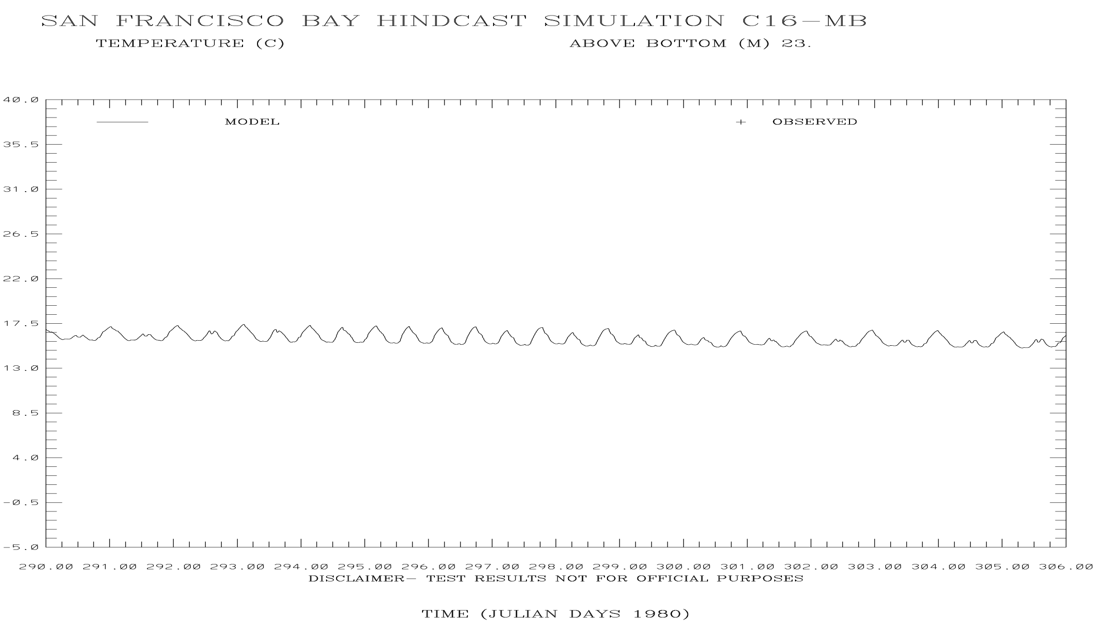

Figure 4.111. October 15-31, 1980 Hindcast: Temperature at C-1 at 76m and C-16 at 23m above the bottom. Note IND AGRMT equals one minus Willmott et al. (1985) relative error.

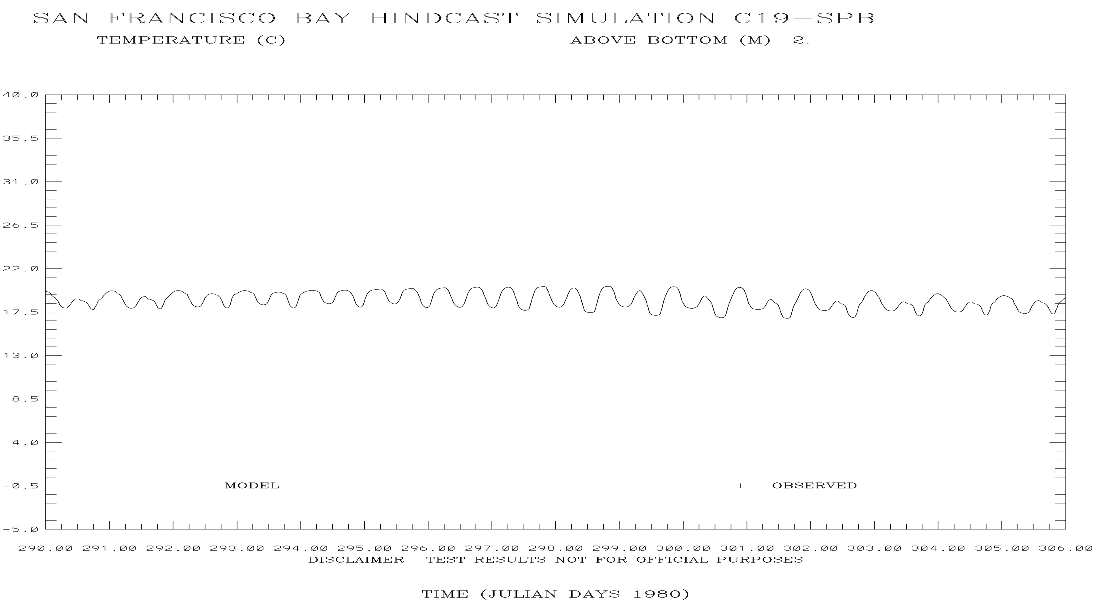

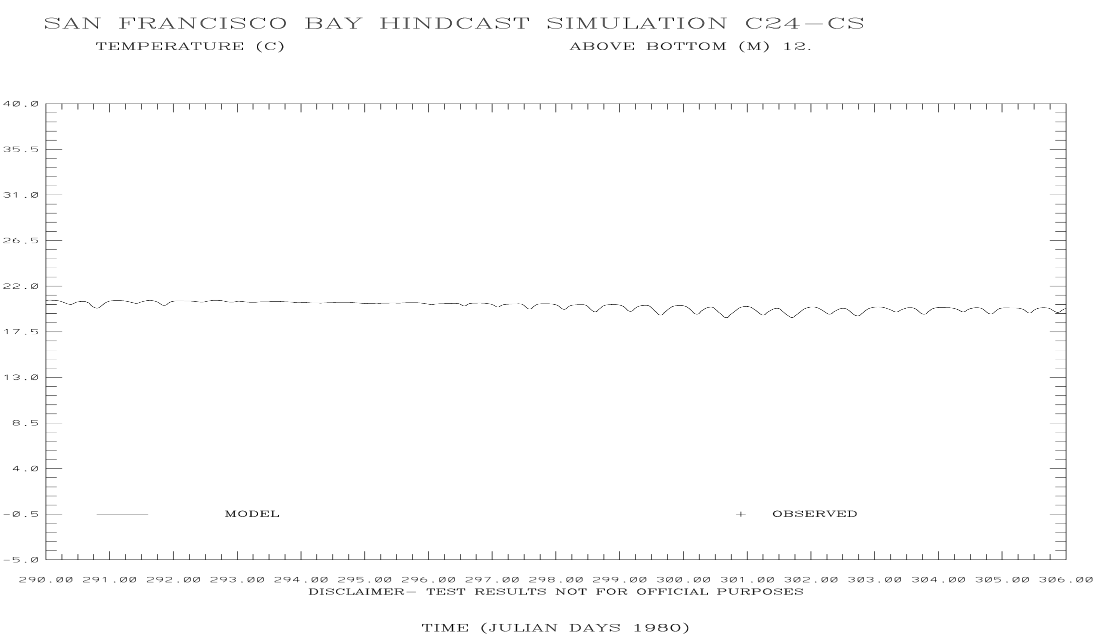

Figure 4.112. October 15-31, 1980 Hindcast: Temperature at C-19 at 2m and C-24 at 12m above the bottom. Note IND AGRMT equals one minus Willmott et al. (1985) relative error.

4.4 Summary and Discussion

The revised stage boundary condition with the 22 cm offset for the Sacramento River at Rio Vista and the 20 cm offset for the San Joaquin River at Antioch improved the water level response in both the tide and hindcast simulations throughout the Bay. This improvement was most evident at Port Chicago in Suisun Bay.

During the high flow periods in January and February 1980, the water level RMS errors were larger, since the specified offsets were not consistent with the inflow conditions. In general, it is necessary to specify the river offsets as a function of river inflow to first order and as a function of water level residual offshore to second order. In Table 4.18, we note the inflow conditions during April through December 1979 and in Table 4.19 during January through October 1980 simulation period. The inflows can be very large (over 100,000 cfs) during the winter rainy season. During most of the year, the inflows are on the order of 15,000 cfs.

To obtain the offshore water level residual signal, the predicted tide at Point Reyes was subtracted from the observed water level. No filtering of the resulting signal was performed and as a result there was significant high frequency content. However, the revised sponge layer algorithm served to effectively damp any high frequency oscillations in the water levels. In addition, the observed water level at Point Reyes exhibited datum issues as well as periods when the observations were constant. As a result, the water level residual signal exhibited periods of sinusoidal behavior as well as many significant spikes. This served as a sensitivity test of the model to large swings in offshore subtidal water levels. The model ran seamlessly through these periods and proved to be very robust with the time step and minimum depth selection.

Table 4.18 April – December 1979 Hindcast Characteristics. The first line represents the first 15 days of the month, while the second line show results for the remainder of the month. Note the water levels at Port Chicago are relative to MLLW. Note * means less than given value. Note ** means less than given value with sinusoidal behavior. Note *** denotes high frequency content (spikes).

Parameter	Apr	May	Jun	Jul	Aug	Sep	Oct	Nov	Dec
Delta Inflow (10^3 cfs)	30 8	12 12	8 4	6 6	4 4	2 7	6 10	8 12	14 50
Offshore Water Level Residual (cm)	-15 -10	-10 0	-100* -10	-8 -4	-6 -100**	-4 -100**	-8 4	-4 -8***	-8 16
Port Chicago RMSE (cm)	n/a	n/a	n/a	n/a	n/a	n/a	n/a 69	8 12	80 95
Port Chicago Model Water Level Mean (cm)	73 74	72 74	73 75	80 84	85 76	84 54	80 76	75 72	75 81
Port Chicago Observed Water Level Mean (cm)	n/a	n/a	n/a	n/a	n/a	n/a	n/a- 18	70 63	11 0
Point Reyes Model Water Level Mean (cm)	81 82	80 87	83 82	87 96	95 80	96 43	98 96	96 87	91 102

Table 4.19 January – October 1980 1979 Hindcast Characteristics. The first line represents the first 15 days of the month, while the second line show results for the remainder of the month. Note the water levels at Port Chicago are relative to MLLW. Note * means less than given value. Note ** means less than given value with sinusoidal behavior. Note *** denotes high frequency content (spikes).

Parameter	Jan	Feb	Mar	Apr	May	Jun	Jul	Aug	Sep	Oct
Delta Inflow (10^3 cfs)	100+ 100+	60 100+	100+ 90	35 30	20 25	16 14	11 10	6 5	6 14	9 10
Offshore Water Level Residual (cm)	20 0	20 60	40 -20	-10 -10	0 -4	0 0	-20 0	0 0	-8 -12	-4 -10
Port Chicago RMSE (cm)	13 22	8 32	23 10	11 9	9 9	8 7	9 6	6 7	7 6	6 10
Port Chicago Model Water Level Mean (cm)	84 81	82 90	82 72	71 70	70 70	72 75	76 82	83 82	81 80	77 73
Port Chicago Observed Water Level Mean (cm)	92 98	81 120	102 73	66 70	72 71	73 74	70 80	83 78	77 77	76 66
Point Reyes Model Water Level Mean (cm)	106 96	98 116	101 78	81 82	83 81	85 88	86 97	99 96	97 97	97 89

5. SEMI-OPERATIONAL NOWCAST/FORECAST SYSTEM CONSTRUCTION

To develop a semi-operational nowcast/forecast system, it was necessary to utilize the Coastal Ocean Modeling Framework for High Performance Computing (COMF-HPC) for implementation at NCEP. In this effort, it was necessary to standardize the initial condition, boundary condition, and forcing files for the operational nowcast forecast systems to be run at NCEP. To support this effort several templates were developed to aid in the development of the appropriate fixed files.

5.1 River Template

To specify the lateral (river) boundary conditions the template given in Table 5.1 was developed for SFBOFS.

Table 5.1. Template of River Control File for SFBOFS.

```
Section 1: Information about USGS or NOS gages where real-time discharges
and/or water temperature observations are available

RiverID STATION_ID NWS_ID AGENCY_ID Q_min Q_max Q_mean  T_min  T_max  T_mean  Q_Flag TS_Flag
River_Name
  1     11459150   XXXXX    USGS    0.0  280.0    2.0       9.5    25.0  20.    1     1
"Petaluma River at Petaluma, CA
     "
  2     11180700   XXXXX    USGS    0.0  430.0    3.0       9.5    25.0  20.    1     1
"Alameda Creek at Union City, CA      "

  3     11458000   XXXXX    USGS    0.0 1000.0  100.0      10.0    23.0  20.    1     1
"Napa River near Napa, CA             "

  4     11172175   XXXXX    USGS    0.0  100.0    2.0       9.5    25.0  20.    1     1
"Coyote Creek at Milpitas, CA         "

  5     11169025   XXXXX    USGS    0.0  170.0    3.0       9.5    25.0  20.    1     1
"Guadalupe River at San Jose, CA      "

Section 2: Information of FVCOM grids/locations to specify river inputs
GRID_ID NODE_ID ELE_ID DIR    FLAG RiverID_Q  Q_Scale RiverID_T T_Scale   River_Basin_Name

  1      46752      1   0      3      3     0.15       3       1.0    Napa River near Napa, CA

  2      46753      2   0      3      3     0.20       3       1.0    Napa River near Napa, CA

  3      46804      3   0      3      3     0.30       3       1.0    Napa River near Napa, CA

  4      46805      4   0      3      3     0.20       3       1.0    Napa River near Napa, CA

  5      46850      5   0      3      3     0.15       3       1.0    Napa River near Napa, CA

  6      45345      6   0      3      1     1.0        1       1.0    Petaluma R. at Petaluma, CA

  7      45670      18   0     3      2     1.0        2       1.0    Alameda Cr.at Union Cy, CA

  8      52543      19   0     3      5     1.0        5       1.0    Guadalupe R.at San Jose, CA

  9      52308      20   0     3      4     1.0        4       1.0    Coyote Cr.at Milpitas, CA


Note min, max, and mean flows are in m3/s.
```

5.2 Open Boundary Condition Template

For the open boundary condition, the template given in Table 5.2 was constructed, which seeks to use secondary and backup water level gages for subtidal water level. In general the A and B coefficients would need to be determined via linear regression of at least one month of subtidal water levels.

Table 5.2. Template of Open Boundary Condition Control File for SFBOFS.

```
SECTION 1:  WATER LEVEL and WATER TEMPERATURE INFORMATION FOR LATERAL OPEN BOUNDARY
SID   NOS_ID  NWS_ID  AGENCY_ID DATUM  FLAG TS_FLAG BACKUP_SID GRIDID_STA  AS     GAUGE NAME
1   9415020   PRYC1   NOAA     0.946   0      1          0         1      1.0  Point Reyes, Ca
2   4602699   46026   NOAA     -9999.  0      1          0       183      1.0  NDBC Buoy 46026
3   11337190  ATIC1   USGS    -0.955   0      1          0        92      1.0  SAN JOAQUIN RIVER
4   11455420  RVBC1   USGS    -0.955   0      1          0        98      1.0  SACRAMENTO RIVER

Note for subtidal water level: SEC_WL_ID is the secondary water level station
id and BKP_WL is the backup water level station id.

A(s,b) and B(s,b) are used to estimate the water level at the NOS_ID as
follows:
WL(NOS_ID)= As*WL(SEC_WL_ID) + Bs, and WL(NOS_ID)= Ab*WL(BKP_WL_ID) + Bb.

Note ids equal to 99 indicate no stations for secondary or backup water
level.

Note for T and S: PORTS_SIG_ID and CLIM_SIG_ID equal zero corresponds to
Levitus climatology. If PORTS_SIG_ID is not
zero, specify PORTS signal information in Section 2. If CLIM_SIG_ID is not
zero then you must provide
T and S information in Section 3 as follows. Note ids equal to 99 indicate no
stations for PORTS or climatology, these are water level backup stations
only.

SECTION 2: CONFIGURATION OF LATERAL OPEN BOUNDARY
 GRIDID  NODE_ID WL_STA WL_SID_1 WL_S_1 WL_SID_2 WL_S_2 TS_STA TS_SID_1 TS_S_1 TS_SID_2 TS_S_2
     1     1       1       1     1.00       0     0.00     1         1    1.00       0    0.00
     .
    20    20       1       1     1.00       0     0.00     1         1    1.00       0    0.00
    21    21       1       1     1.00       0     0.00     2         1    0.975      2    0.025
    22    22       1       1     1.00       0     0.00     2         1    0.950      2    0.050
     .
    59    59       1       1     1.00       0     0.00     2         1    0.025      2    0.975
    60    60       1       1     1.00       0     0.00     1         2    1.00       0    0.00

    91    91       1       1     1.00       0     0.00     1         2    1.00       0    0.00
    92 53503       1       3     1.00       0     0.00     1         2    1.00       0    0.00
    93 53502       1       3     1.00       0     0.00     1         2    1.00       0    0.00
    94 53500       1       3     1.00       0     0.00     1         2    1.00       0    0.00
    95 53499       1       3     1.00       0     0.00     1         2    1.00       0    0.00
    96 53481       1       3     1.00       0     0.00     1         2    1.00       0    0.00
    97 53482       1       3     1.00       0     0.00     1         2    1.00       0    0.00
    98 54120       1       4     1.00       0     0.00     1         2    1.00       0    0.00
    99 54119       1       4     1.00       0     0.00     1         2    1.00       0    0.00
   100 54118       1       4     1.00       0     0.00     1         2    1.00       0    0.00
   102 54116       1       4     1.00       0     0.00     1         2    1.00       0    0.00
   103 54117       1       4     1.00       0     0.00     1         2    1.00       0    0.00
```

Table 5.2. (Cont.) Template of Open Boundary Condition Control File for SFBOFS.

```
SECTION 3: CONFIGURATION OF LATERAL OPEN BOUNDARY
SeqNumber      ElementID     CU_STA      CU_1    CU_2
        1          1           0          0       0
        .
        184        184         0          0       0
        185     101177         0          0       0
        186     101178         0          0       0
        187     101207         0          0       0
        188     101208         0          0       0
        189     101209         0          0       0
        190     101210         0          0       0
        191     101248         0          0       0
        192     101213         0          0       0
        193     101214         0          0       0
        194     101258         0          0       0
        195     101259         0          0       0
        196     101260         0          0       0
        197     101261         0          0       0
        198     101262         0          0       0
        199     101263         0          0       0
        200     101264         0          0       0
```

To standardize the specification of the tidal boundary conditions at each open boundary cell, a harmonic constituent netCDF file for water level amplitude and phase and East and North vertically integrated horizontal current amplitudes and phases was constructed, such that all phases are in GMT. The COMF-HPC software accesses this netCDF harmonic constituent file to use in providing the tidal boundary forcings required by FVCOM. The software also computes the node factors and equilibrium arguments and adjusts the harmonic constants for each nowcast/forecast cycle.

5.3 Vertical Datum Considerations

Model datum specification is made to be consistent with the VDatum Project utilizing the following approach. In SFBOFS, we assume that the model datum equal to the North American Vertical Datum of 1988 (NAVD88) minus 0.955m. Therefore, an additional field, model datum minus mean sea level, was developed. For the majority of the coastal estuaries, the values in this file will be zero. For the Delaware Estuary, nonzero values were added as one proceeded up the river above Marcus Hook, Pennsylvania, to the head of tide at Trenton, New Jersey. In San Francisco Bay, NAVD88 data were available from Monterey up to river inflow locations as shown in Table 5.3, which allowed via Barnes (1973) interpolation for a complete specification. There is an intensive effort to obtain additional land gravity measurements as well as make use of additional satellite altimeter observations to update the coastal geoid, which will allow further adjustment of the model datum to MSL field.

A program was developed to access the VDatum database and to interpolate onto the SFBOFS grid the following four datum fields: MLLW to MSL, MLW to MSL, MHHW to MSL, and MHW to MSL. The MLLW to MSL field is shown in Figure 5.1 and exhibits a smooth transition of contours out on to the continental shelf from the lower Bay region.

Table 5.3. Water Level Vertical Datums. Note tidal datums and NAVD88 are with respect to gage zero. Tidal datums are with respect to the 1983-2001 tidal epoch. Model Datum (MD) is given with respect to MSL. Note at the up estuary stations MSL is above the model datum, while at the entrance to the Bay, MSL and the model datum are coincident. Using the table it is possible to determine MLLW with respect to MD. Values are in meters.

Station Number	Station Name	MHHW	MHW	MSL	MLW	MLLW	NAVD88	MSL-MD
941-3450	Monterey	2.657	2.433	1.893	1.364	1.031	0.988	-0.050
941-5020	Point Reyes	2.964	2.760	2.152	1.567	1.206	1.214	-0.017
941-4290	San Francisco	3.602	3.416	2.773	2.168	1.822	1.804	0.014
941-4317	Pier 22.5	2.970	2.779	2.057	1.403	1.062	1.068	0.034
941-4358	Hunters Point	2.850	2.661	1.863	1.126	0.778	n/a	0.026
941-4392	Oyster Point Marina	2.749	2.555	1.711	0. 909	0.561	n/a	0.026
941-4458	San Mateo Bridge	6.838	6.644	5.737	4.846	4.484	n/a	0.026
941-4509	Dumbarton Bridge	6.271	6.079	5.071	4.043	3.678	n/a	0.026
941-4523	Redwood City	4.539	4.346	3.378	2.398	2.033	n/a	0.026
941-4575	Coyote Creek	2.632	2.453	1.388	0.265	-0.112	n/a	0.026
941-4632	Alameda Creek	2.488	2.299	1.488	0.693	0.597	n/a	0.026
941-4750	Alameda	3.027	2.838	2.067	1.361	1.016	1.086	0.026
941-4863	Richmond	5.372	5.188	4.520	3.870	3.528	3.530	0.035
941-5218	Mare Island	2.685	2.513	1.864	1.214	0.922	0.784	0.125
941-5144	Port Chicago	2.713	2.558	1.996	1.441	1.215	0.880	0.161

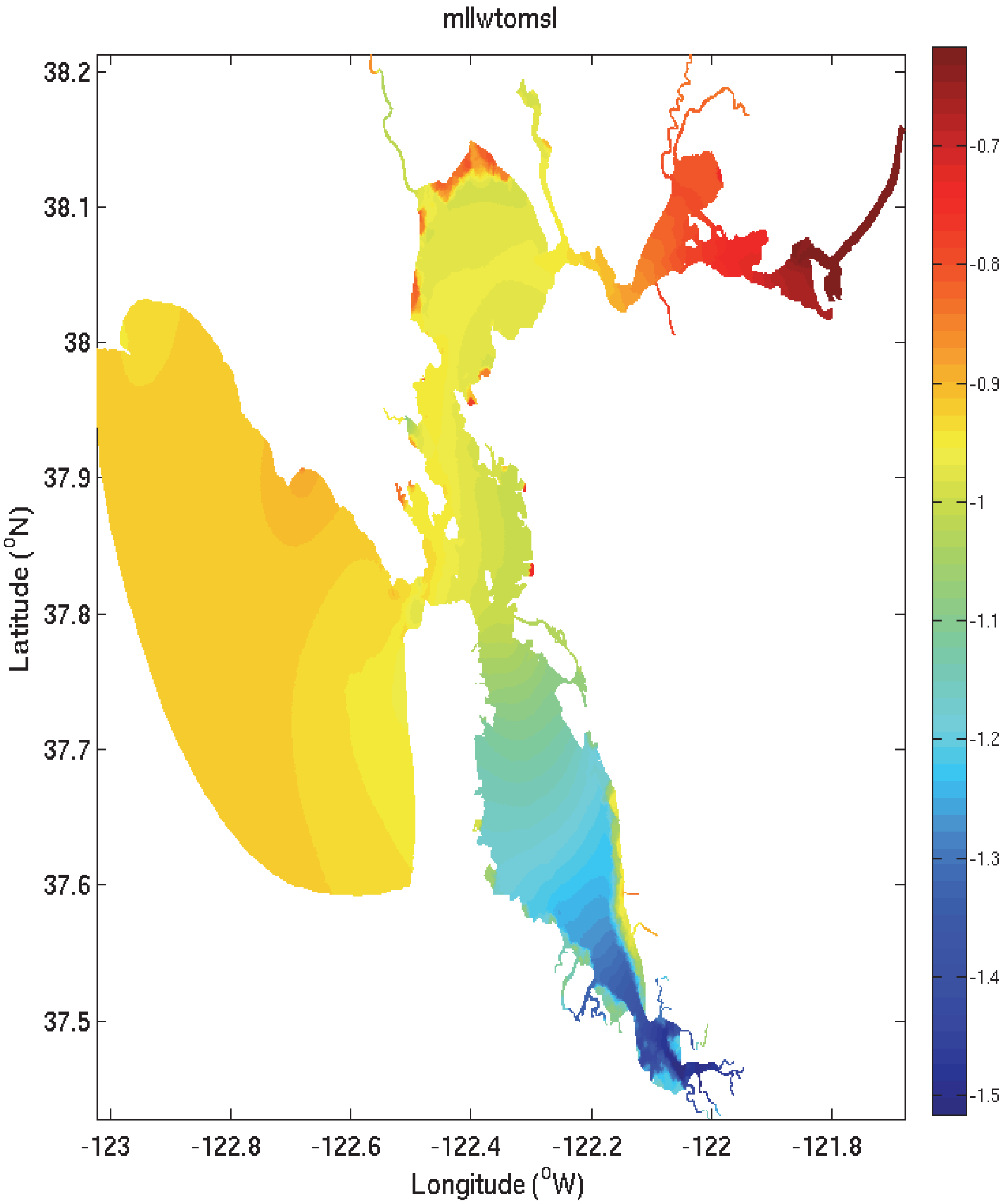

Figure 5.1 SFBOFS MLLW to MSL Datum Conversion (m).

5.4 Operational Summary

In late July 2012, SFBOFS Version 1.0 was provided to CO-OPS for implementation in the development mode at NCEP. This version employed a flow inflow specification for the Delta inflows on the Sacramento and San Joaquin rivers and a specified net heat flux.

Additional simulations outlined in Chapters 3 and 4 indicated that the water level response in the Suisun Bay and in the two rivers was over-predicted. As a result, an alternative stage boundary condition was developed at the upstream river inflows. In addition, the full bulk flux surface boundary condition was used. Based on the 19-month hindcast results presented in Chapter 4, the hydrodynamic simulations proved very stable under large excursions in subtidal water levels along the open ocean boundary. As result in late November 2012, SFBOFS Version 2.0 was provided to CO-OPS implementing the above modifications as the final SFBOFS. The improvement in the water level response is given in Table 5.4 in terms of RMS error. As a result of the improvement, SFBOFS Version 2.0 will be transitioned to CO-OPS for implementation of SFBOFS.

SFBOFS will operate within the COMF-HPC and is anticipated to have four daily nowcast and forecast cycles at 0, 6, 12, and 18 UTC; however, alternate protocols are under consideration as well. For the SFBOFS nowcast cycle, the meteorological forcing will be provided by the nested, high resolution (4 km) NCEP North American Mesoscale (NAM) weather prediction model. River discharge is estimated using near-real-time observations from U.S. Geological Survey (USGS) river gauges. Oceanographic conditions of subtidal water levels, currents, water temperature and salinity on the SFBOFS lateral open boundary on the shelf are estimated based on forecast guidance from Global-RTOFS (Global-RTOFS, NWS, http://polar.ncep.noaa.gov/global/about) and adjusted by real-time observations at NOS water level gauges. Tides are derived from the OSU West Coast 2010 tide database. Subtidal water level forecasts from the National Weather Service (NWS) Extra-Tropical Storm Surge (ETSS) model (Chen et al., 1993) are used as a backup if Global-RTOFS is not available.

For the SFBOFS forecast cycle, the meteorological forcing is provided by the nested, high resolution (4 km) NCEP NAM weather prediction model. River discharge is estimated by persistence of the most recent near-real-time observations from USGS river gauges. Oceanographic conditions of subtidal water levels, currents, water temperature and salinity on SFBOFS' lateral open boundary on the shelf are estimated based on forecast guidance from Global-RTOFS. Tides are derived from the OSU West Coast 2010 tide database. Subtidal water level forecasts from the NWS ETSS model are used as a backup if Global-RTOFS is not available.

Table 5.4. Comparison of SFBOFS Version 1.0 and Version 2.0 Water Level RMS Errors: April - May 1979 and September - October 1980. The first two lines correspond to the Version 1.0 tidal and hindcast simulation. The next two lines correspond to the Version 2.0 tidal and hindcast simulation. Note n/a denotes periods when either data were not available or were suspect. Values are in cm.

Station	April 1979	May 1979	September 1980	October 1980
Alameda 941-4750	10 7 n/a n/a 9 6 n/a n/a	6 7 n/a n/a 5 6 n/a n/a	8 7 8 7 7 7 6 7	7 6 7 6 6 7 6 6
Dumbarton Bridge 941-4509	13 10 n/a n/a 13 11 n/a n/a	9 11 n/a n/a 9 10 n/a n/a	11 11 n/a n/a 8 11 n/a n/a	8 11 n/a n/a 7 11 n/a n/a
Oyster Point Marina 941-4392	10 8 n/a n/a 10 7 n/a n/a	7 9 n/a n/a 4 7 n/a n/a	10 9 n/a n/a 8 8 n/a n/a	8 8 n/a n/a 7 8 n/a n/a
Port Chicago 941-5144	20 20 n/a n/a 9 7 n/a n/a	18 18 n/a n/a 7 7 n/a n/a	19 21 20 23 7 7 7 6	20 22 20 23 7 6 6 10
Point Reyes 941-5020	8 6 7 6 7 4 7 5	5 7 5 7 4 4 4 4	7 5 7 5 4 5 4 5	6 5 7 6 4 5 4 6
San Francisco 941-4290	9 7 n/a n/a 7 4 n/a n/a	6 7 5 7 4 4 5 5	7 5 8 6 6 5 6 5	7 5 7 8 6 5 6 8
Pier 22.5 941-4317	9 6 n/a n/a 8 5 n/a n/a	5 6 n/a n/a 4 5 n/a n/a	7 6 n/a n/a 6 5 n/a n/a	7 5 n/a n/a 6 6 n/a n/a
San Mateo Bridge 941-4458	10 7 n/a n/a 10 8 n/a n/a	5 7 6 8 6 7 9 8	9 8 n/a n/a 6 8 n/a n/a	6 5 n/a n/a 6 9 n/a n/a

6. CONCLUSIONS AND RECOMMENDATIONS

A review of previous and current three-dimensional modeling efforts in San Francisco Bay was conducted prior to the selection of FVCOM as the hydrodynamic modeling component of the SFBOFS. Three grids were developed and populated with the latest available bathymetric and topographic information. Initial simulations on the original grid, without the inclusion of the river inflows, indicated a ratio of approximately 1:60 simulation to real time using 256 processors on the NCEP CCS. This computational requirement is near the upper limit of the present operational time allotment and therefore SFBOFS uses the original grid.

Utilizing the tidal stage boundary conditions at the Delta inflow locations and a 22 cm water level offset at Rio Vista on the Sacramento River and a 20 cm water level offset at Antioch on the San Joaquin River, an extended 19-month baroclinic tidal simulation from April 1979 through October 1980 was performed. For this extended simulation, nudging to climatological salinity and temperature was used for the offshore boundary condition. Water level RMS errors were consistent from month to month and were below 15 cm at the majority of the stations. Principal component current strengths were in close agreement with predictions, with RMS errors less than 35 cm/s at the majority of the stations.

When one compares the simulated tidal baroclinic structure to the observed structure, the salinity was overestimated in the northern portion of San Pablo Bay and throughout Suisun Bay. This is due to the fact that in the tidal simulation the offsets were held constant and did not reflect the increased levels during the high flow months. This in effect, limited the amount of freshwater entering the Bay through the Delta. The temperature response exhibited a normal seasonal response, but at the end of the simulation in October 1980 there was some evidence of overheating by order 2 ^{o}C in the shallow water areas in Suisun Bay.

Over this same 19-month period, an extended hindcast utilizing full meteorological forcing was also performed. Water level RMS errors were similar to those in the extended tidal simulation, although there were fewer stations available for comparison. During the high flow periods in January and February 1980, the water level RMS errors were larger since the specified offsets were not consistent with the inflow conditions. In general, it is necessary to specify the river offsets as a function of river inflow to first order and as a function of water level residual offshore to second order. On comparing the hindcast baroclinic structure to the observations results similar to the baroclinic tidal simulation were obtained due to the effect of using the constant offsets.

Within the SFBOFS, real-time stage observations with respect to NAVD88 are available at Rio Vista on the Sacramento River and at Antioch on the San Joaquin River, so that the appropriate influences will be directly observed. These measurements were not available during the hindcast period. Due to problems at the Point Reyes water level gauge, the offshore boundary water level residual signal exhibited periods of sinusoidal behavior as well as many significant spikes. This served as a sensitivity test of the model to large swings in offshore subtidal water levels. The model ran seamlessly through these periods and proved to be very robust.

Based on the extended tidal simulation and hindcast simulation, it is recommended that Version 2.0 of SFBOFS be implemented in quasi-operational status and based on further evaluation transferred to operational status. Version 2.0 is sufficient to provide navigation guidance throughout San Francisco Bay to Port Chicago.

Future improvements are suggested via a set of short term and longer term activities, which are itemized as follows:

Short Term Activities:

1. Extend the PORTS to include salinity measurements to provide additional density information in real-time.
2. Extend the model grid to include the entire Delta region building on the work of MacWilliams et al. (2008) and to include control structures within FVCOM to construct SFBOFS Version 3.0.
3. Further evaluate SFBOFS Version 2.0 based on high frequency radar data and current meter data from San Francisco Bay 2012 and 2013 survey to include internal waves.
4. Refine the heat flux algorithms in shallow water to include contributions from the bottom sediments.
5. Investigate the further use of the supplemental grids described in Chapter 2.

Long Term Activities:

6. Include short period gravity waves using SWAN wave module within FVCOM.
7. Include water quality-biological interactions using the water quality module within FVCOM.
8. Include sediment transport dynamics using the sediment module within FVCOM

Note the development of both the short and long term activities will allow non-navigational areas of concern to be addressed to further manage the Bay as raised by Williams (1989) and Kimmerer (2002).

ACKNOWLEDGMENTS

Dr. Frank Aikman, Chief of Marine Modeling and Analysis Programs, Coast Survey Development Laboratory (CSDL) provided project guidance and support during the development of the SFBOFS. Dr. Richard Patchen, Chief Science Officer (retired), CSDL, provided several insights on model grid development. Special thanks to Dr. Jiangtao Xu, CSDL, for all her assistance on the development of the grids and in providing support on the use of the SMS software. Special thanks to Jason Greenlaw, CSDL, for providing the high resolution graphics in Figures 2.11 and 2.12. Thanks to Philip Richardson, CSDL, for reviewing the California Current references. Thanks to Dr.Yuji Funakoshi for providing guidance on using SMS to develop the animations.

REFERENCES

Aikman III, F., M.S. Vincent, and R.C. Patchen, 2008: Development and Evolution of Operational Forecast Systems for the Coastal and Estuarine Environment in NOAA's National Ocean Service, *Proceedings of the 10th International Conference on Estuarine and Coastal Modeling, ASCE*, 671-684.

Barnard, P.L., D.M. Hanes, D.M. Rubin, and R.G. Kvitek, 2006: Giant Sand Waves at the Mouth of San Francisco Bay, *EOS Transactions of the AGU*, 87, No. 29, p285, 289.

Barnard, P.L., J.L. Eshleman, L.H. Erikson,and D.M. Hanes, 2007: Coastal Processes Study at Ocean Beach, San Francisco, CA: Summary of Data Collection 2004- 2006, *USGS, Open File Report 2007-1217*, Reston, VA.

Barnard, P.L., B. O'Reilly, M. van Ormondt, E. Elias, P. Ruggiero, L.H. Erikson, C. Hapke, B.D. Collins, R.T. Guza, P.N. Adams, and J. Thomas, The Framework of a coastal Hazards Model-A Tool for Predicting the Impact of Severe Storms, 2009: *USGS, Open File Report 2009-1073*, Reston, VA.

Barnes, S. L., 1973: Mesoscale Objective Map Analysis Using Weighted Time Series Observations, *NOAA Technical Memorandum ERL NSSl-62*, National Severe Storms Laboratory, Norman, OK.

Brigham Young University Environmental Modeling Research Laboratory, 2006: The Surface-water Modeling System (SMS) – Version 9.2, *SMS Tutorials*, Salt Lake City, UT.

California Department of Water Resources, DAYFLOW: An Estimate of Daily Average Delta Outflow, http://www.water.ca.gov/dayflow/documentation/dayflowDoc.cfm#Introduction.

Carter, G.S., 2010: Barotropic and Baroclinic M_2 Tides in the Monterey Bay Region*, Journal of Physical Oceanography*, 40(8), 1766-1783.

Carter, G.S., O.B. Fringer, and E.D. Zaron, 2012: Regional Models of Internal Tides, *Special Issue on Internal Tides, Oceanography* 25(2), 56-65.

Carignan, K.S., L.A. Taylor, B.W. Eakins, R.J. Caldwell, D.Z. Friday, P.R. Grothe, and E. Lim, 2010: Digital Elevation Models of Central California and San Francisco Bay: Procedures, Data Sources and Analysis, *NOAA/NGDC Special Report*, prepared for NOAA/PMEL Center for Tsunami Research, Boulder, CO.

Cassuli, V., 1990: Semi-Implicit Finite Difference Methods For The Two-Dimensional Shallow Water Equations, *Journal of Computational Physics*, 86, 56-74.

Casulli, V., and E. Cattani, 1994: Stability, Accuracy and Efficiency of A Semi-Implicit Method for Three-Dimensional Shallow Water Flow, *Applied Mathematics and Computation*, 27,99-112.

Casulli, V. and R.A. Walters, 2000: An Unstructured Grid, Three-Dimensional Model Based On The Shallow Water Equations, *International Journal of Numerical Methods in Fluids*, 32, 331-348.

Chen, C., H. Liu, and R.C. Beardsley, 2003: An Unstructured, Finite-Volume, Three-Dimensional, Primitive Equation Ocean Model: Application to Coastal Ocean and Estuaries. *Journal of Atmospheric and Oceanic Technology*, 20, 159-186.

Chen, C., R.C. Beardsley, and G.W. Cowles, 2006a: FVCOM, *Oceanography*, Vol. 19, No 1.

Chen, C., R.C. Beardsley, and G.W. Cowles, 2006b: An Unstructured Grid, Finite- Volume Coastal Ocean Model FVCOM User Manual, *SMAST/UMASSD-06-0602*, University of Massachusetts-Dartmouth, New Bedford, MA.

Chen, C., R. C. Beardsley, and G. Cowles, 2006c: An unstructured grid, finite-volume ocean model (FVCOM) system. Special Issue entitled “Advances in Computational Oceanography”, *Oceanography*, vol. 19, No. 1, 78-89.

Chen, J., W.A. Shafer, and S.C. Kim, 1993: A Forecast Model for Extratropical Storm Surge, Advances in Hydro-Science and Engineering, (ed.) Sam S.Y. Wang, Volume I Part B, University of Mississippi, 1437-1444.

Cheng, R.T. and J.W. Gartner, 1984: Tides, Tidal and Residual Currents in San Francisco Bay California – Results of the Measurement, 1979-1980, *USGS, Water Resources Investigation Report 84-4339*, Menlo Park, CA.

Cheng, R.T., V. Casulli, and J.W. Gartner, 1993: Tidal, Residual, Intertidal Mudflat (TRIM) Model and Its Applications to San Francisco Bay California, *Estuarine, Coastal and Shelf Science*, 36, 235-280.

Cheng, R.T. and R.E. Smith, 1998: A Nowcast Model for Tides and Tidal Currents in San Francisco Bay, California, Proceedings of Ocean Community Conference, Marine Technology Society,537-543.

Chua, V.P. and O.B. Fringer, 2011: Sensitivity Analysis of Three-Dimensional Salinity Simulations in North San Francisco Bay Using the Unstructured-Grid SUNTANS Model, *Ocean Modelling*, 39, 332-350.

Delft Hydraulics, 2007: User Manual Delft3D-FLOW: WL, Deltares, Delft, Netherlands.

Fang, X. and H.G. Stefan, 1996: Dynamics of Heat Exchange Between Sediment and Water in a Lake, *Water Resources Research*, 32(6), 1719-1727.

Fringer, O.B., M. Gerritsen, and R.L. Street, 2006: An Unstructured-Grid, Finite Volume, Nonhydrostatic, Parallel Coastal Ocean Simulator, *Ocean Modelling*, 14, 139-173.

Global-RTOFS, NWS, http://polar.ncep.noaa.gov/global/about.

Gross, T.F, H. Lin, Z. Bronder, M.S. Vincent, 2006: Coastal Ocean Modeling Framework: COMF, *NOAA Technical Report NOS CS 22*, Silver Spring, MD.

Gross, E.S, M.L. MacWilliams, and W.J. Kimmerer, 2010: Three-Dimensional Modeling of Tidal Hydrodynamics in the San Francisco Estuary, *San Francisco Estuary and Watershed Science*, 7, 1-37.

Hess, K.W., T.F. Gross, R.A. Schmalz, J.G.W. Kelley, F. Aikman, E. Wei, and M.S. Vincent, 2003: NOS Standards for Evaluating Operational Nowcast and Forecast Hydrodynamic Model Systems*, NOAA Technical Report NOS CS 17*, Silver Spring, MD.

Kimmerer, W.J., 2002: Physical, Biological, and Management Responses to Variable Freshwater Flow into the San Francisco Estuary, *Estuaries*, Vol. 25, No 6B, 1275- 1290.

Lettman, K., 2012: Personal Communication: Newtonian Damping Sponge Layer, provided by FVCOM Group, June 25, 2012.

Loeper, T., 2006: Restoration of CTD Data from the 1984-1985 Delaware River and Bay Circulation Survey, *NOAA/NOS/CSDL Informal Technical Note No. 6*, Silver Spring, MD.

MacWilliams, M.L. and R.T. Cheng, 2006: Three-Dimensional Hydrodynamic Modeling of San Pablo Bay On An Unstructured Grid, *Proceedings of the 7th International Conference on Hydroscience and Engineering, (ICHE-2006)*, Philadelphia, PA.

MacWilliams, M.L., E.S. Gross, J.F. DeGeorge, and R.R. Rachielle, 2007: Three- Dimensional Hydrodynamic Modeling of the San Francisco Estuary On An Unstructured Grid, IAHR, 32nd Congress, Venice, Italy, July 1-6, 2007.

MacWilliams, M.L, F.G. Salcedo, E.S. Gross, 2008: San Francisco Bay-Delta UnTRIM *Model Calibration Report, POD 3-D Particle Tracking Modeling Study*, California Department of Water Resources, Sacramento, CA.

Marchesiello P., J.C. McWilliams, and A. Shchepetkin, 2003: Equilibrium Structure and Dynamics of the California Current System, *Journal of Physical Oceanography*, 33, 753-783.

NOAA National Geophysical Data Center, NOS Hydrographic Survey Data, Bathymetry Attributed Grid (BAG) Conversion to XYZ Text Data, http://surveys.ngdc.noaa.gov.

NOAA National Geophysical Data Center, San Francisco Bay, CA 1/3 Arc-Second MHW DEM, http://ngdc.noaa.gov/dem.

North American Regional Reanalysis (NARR), 2007: http://www.emc.ncep.noaa.gov/mmb/rreanl/index.html.

North American Model (NAM) Weather Research and Forecasting Model, http://wrf-model.org.

NOS, 1999: NOS Procedures for Developing and Implementing Operational Nowcast and Forecast Systems for PORTS, *NOAA Technical Report NOS CO-OPS 0020*, Silver Spring, MD.

Oey, L., 2005: A Wetting-Drying Scheme for POM*, Ocean Modeling*, 9, 133-150.

Oey, L., 2006: An OGCM with Movable Land-Sea Boundaries, *Ocean Modeling*, 13, 176-195.

Oey, L., T. Ezer, C. Hu, F.E. Muller-Karger, 2007: Baroclinic Tidal Flow and Inundation Processes in Cook Inlet, Alaska: Numerical Modeling and satellite Observations, *Ocean Dynamics*, 57, 205-221.

Oltmann, R.N., 1998: Indirect Measurement of Delta Outflow using Ultrasonic Velocity Meters and Comparison with Mass-Balance Calculated Outflow, Interagency Ecological Program (IEP) for the Sacramento-San Joaquin Estuary Newsletter, 11(1).

Oregon State University Tidal Data Inversion, OTIS Regional Tide Solutions, 2010: West Coast of the USA, http://volkov.oce.orst.edu/tides/WC.html.

Penven, P., L. Debreu, P. Marchesiello, and J.C. McWilliams, 2006: Evaluation and Application of the ROMS 1-way Embedding Procedure to the Central California Upwelling System, *Ocean Modelling*, 12, 157-187.

Richardson, P.H. and R. A. Schmalz, 2006: Restoration of Delaware River and Bay Circulation Survey, Current Meter and CTD Observations 1984-1985, *NOAA/NOS/CSDL Informal Technical Note No. 5*, Silver Spring, MD.

Richardson, P.H. and R. A. Schmalz, 2008: NOS Historical Circulation Survey Restoration: Chesapeake Bay (1981-1983), Columbia (1981), San Francisco Bay (1979-1980), and New York Harbor (1980-1981), *NOAA/NOS/CSDL Informal Technical Note No. 9*, Silver Spring, MD.

Schmalz, R.A., 2011: Three-dimensional Free-Surface Flow Model Verification and Validation: Past, Present, and Future Directions, CDROM, *Proceedings of the World Environmental and Water Congress: Bearing Knowledge for Sustainability*, ASCE, Reston, VA.

Shureman, P., 1958. Manual of Harmonic Analysis and Prediction of Tides, *Special Publication 98, U.S. Government Printing Office*, Washington, DC.

Smith, N., 2002: Observations and Simulations of Water-Sediment Heat Exchange in a Shallow Coastal Lagoon*, Estuaries*, 25(3), 483-487.

Uchiyama, Y., 2005: Modeling Three-dimensional Cohesive Sediment Transport and Associated Morphological Variation in Estuarine Intertidal Mudflats, *Report of the Port and Airport Research Institute 44 No. 1*, Yokosuka, Japan.

Uslu, B., D. Arcas, V.V. Titov, and A.J. Venturato, 2010: PMEL Tsunami Forecast Series: Vol. 3 A Tsunami Forecast Model for San Francisco, California, *NOAA/OAR Special Report, NOAA/PMEL Contribution No. 3342*, prepared for NOAA/PMEL Center for Tsunami Research, Seattle, WA.

Warner, J., 2012: Re: Problem with ROMS Wetting/Drying and Turbulence Model(s), ROMS Discussion Group, February 6, 2012.

Welch, J.M., J.W. Gartner, and S.K. Gill, 1985: San Francisco Bay Area Circulation Survey: 1979-1980, *NOS Oceanographic Circulation Survey Report No. 7*, Rockville, MD.

Williams, P.B., 1989: Managing Freshwater Inflow to the San Francisco Bay Estuary, *Regulated Rivers: Research and Management*, 4, 285-298.

Willmott, C. J., S. G. Ackleson, R. E. Davis, J. J. Feddema, K. M. Klink, D.R. Legates, J. O′Donnell, and C. M. Rowe, 1985: Statistics for the evaluation and comparison of models, *Journal of Geophysical Research*, 90, 8995-9005.

Xu, J., E.P. Myers, and S.A. White, 2009: VDATUM for the Coastal Waters of North/Central California, Oregon and Western Washington: Tidal Datums and Sea Surface Topography, NOAA Technical Memorandum, NOS CS 22, Silver Spring, MD.

Xue, H. and Y. Due, 2010: Implementation of a Wetting-and-Drying Model in Simulating the Kennebec-Androscoggin Plume and the Circulation in Casco Bay, *Ocean Dynamics*, 60, 341-357.

Zamani, K, F.A. Bombardelli, S. Wuertz, and P.E. Smith, 2010: Towards a 3-Dimensional Numerical Modeling of Tidal Currents in San Francisco Bay, *Proceedings of the World Environmental and Water Resources Congress: Challenges of Change*, CDROM, ASCE, Reston, VA.

Zhang, A., K.W. Hess, E. Wei, and E. Myers, 2006: Implementation of Model Skill Assessment Software for Water Level and Current in Tidal Regions*, NOAA Technical Report NOS CS 24*, Silver Spring, MD. (Note an updated version is in preparation.)

Zhang, A., K.W. Hess and F. Aikman, 2010: User-based Skill Assessment Techniques for Operational Hydrodynamic Forecast Systems, *Journal of Operational Oceanography*, Volume 3, Number 2, 11-24(14).

Appendix A. SMS Grid Development Procedures

1. Grid modification method: Node(s) deletion
   a. Select Node on LHS screen toolbar in mesh module
   b. Use Magnifying Glass to define box within which to delete the nodes.
   c. Press delete

2. Select Node on top toolbar, then select Disjoint to find and display disjoint nodes then press delete.

3. Grid boundary definition
   a. Select Nodestring on LHS screen toolbar in mesh module
   b. click on first node
   c. double click on final boundary node

4. Reprojection (Note shoreline data and initial grid are in Cartesian coordinates
   a. Select Edit mode on top toolbar
   b. Current Projection Window on LHS—click specify, global and UTM Zone 10 for San Francisco Bay Region
   c. New Projection Window on RHS----click global and select geographic (lat,lon)

Note: The original shoreline is usually in geographic coordinate (lat, lon). For precision consideration, it's usually a good practice to convert the geographic coordinate to a Cartesian coordinates with a proper map projection before generating the mesh. After the mesh is generated and finalized, the coordinate can be converted back.

5. To copy an image into a MS Word document under Edit mode on top toolbar select copy to clipboard.

6. It is possible to open two sessions of SMS at once and place one on each monitor screen for a dual monitor system. Then you may load *.grd files and *.xyz sounding files and compare using both screens.

7. Note when you load a grid file use select ADCIRC *.grd type. Use scatter module for *.xyz sounding files.

8. For developing images select Display mode on top tool bar and select display options. Remove all and select contour, then select range (0. – 107) then select contour interval (5m) and select color fill for contour method.

9. You can use the hand to pan on LHS toolbar and the Magnifying Glass on the top toolbar to reset the view.

10. To create the mesh, one loads and edits the shoreline data to create the map file. It is necessary to create connected node strings to outline the domain. One then goes to the Map module and selects Feature Objects from the top toolbar. Then selects build polygons. Select the polygon for mesh generation, then select the menu Feature Objects and then attributes to set the mesh type to pave. Then go back the Feature objects menu and select Map → 2D Mesh. We used the Paving Method to generate the grid, which starts from the distribution of nodes along the node strings and paves into the interior.

11. We did use node create and node select to move and create nodes to improve grid quality, which can be displayed under Display options for 2D Mesh. One just selects the "Options…" button next to Mesh quality to set the quality options.

12. To generate the final mesh file, it is necessary to complete the following steps: 1) convert to (lat,lon) geographical coordinates, 2) define boundaries, and 3) renumber the nodes. The default value for nodal bathymetry is set to -999. in the interpolate_xyz_to_mesh_fill.f90 program.

The San Francisco Bay Grid Development was performed in conjunction with SMS 10.1 in P:\Jiangtao\SFBay. Two grids were initially developed:

1) stage grid (ModelGrid.ras.stg.1.grd-->sfb.stg.grd) included both San Joaquin and Sacramento Rivers
2) flow grid (ModelGrid.ras.flw.3.grd-->sfb.flw.grd) was truncated below Antioch, CA.

Sounding files *.xyz (lon, lat, depth) were obtained from CGTP. Note sounding_SFB.xyz was the file used in the VDATUM Project and included all sounding data through 1996.

SFbay_Surveys70s_80s.xyz contained all sounding data during the 70s and 80s and was obtained to reflect the hindcast conditions 1979-1980.

san_francisco_bay.xyz contained the latest sounding data from 1985 - 2000. It contained data for 1999 and 2000.

sounding_SFBe.xyz contains sounding_SFB.xyz and 1999 and 2000 data in san_francisco_bay.xyz

Note SFbay_Surveys70s_80s.txt and san_francisco_bay.txt were the original files obtained from CGTP and were processed using the appropriate awk scripts.

Program interpolate_xyz_to_mesh.f90 was obtained to interpolate bathymetry onto an ADCIRC grid. This program was modified to include the FVCOM Tracer Control Element concept for interpolating the sounding data to an FVCOM node.

Program bathy2all.f90 was obtained to further fill the ADCIRC grid following the interpolation. This program was incorporated as a subroutine within the revised program interpolate_xyz_to_mesh_fill.f90.

Note the programs are run by executing the interp_xyz.sh and the interp_xyz.fill.sh scripts. The scripts produce printout* and printfout* files, respectively. The revised *bathy files are *.grd type files in SMS 10.1 with the grid denoted by (stg or flw) and the sounding files obtained in bathy.*.list. The bathy.0.list file and the fvcom.gstg.b0.bathy are the final files produced and used in the future modeling work with FVCOM. Note corresponding ADCIRC style files are also produced for work with ADCIRC.

The NED files are from NGDC and are 3 arc second DEM data for use in future inundation studies.

The following inventory of files is given:

```
/disks/NASWORK/sfops/bathy
total 445088
drwxrwxrwx    4 hgops    games        4096 Feb  8 20:03 ./
drwxrwxrwx   15 hgops    games        4096 Dec 29 16:07 ../
-rw-r--r--    1 hgops    games    12879364 Feb  8 18:39 adcirc.gflw.b1.bathy
-rw-r--r--    1 hgops    games     6439719 Feb  2 18:32 adcirc.gflw.b2.bathy
-rw-r--r--    1 hgops    games     6439719 Feb  2 18:33 adcirc.gflw.b3.bathy
-rw-r--r--    1 hgops    games    13256523 Feb  8 21:30 adcirc.gstg.b0.bathy
-rw-r--r--    1 hgops    games    13256523 Feb  2 20:45 adcirc.gstg.b1.bathy
-rw-r--r--    1 hgops    games     6628299 Feb  2 18:21 adcirc.gstg.b2.bathy
-rw-r--r--    1 hgops    games     6628299 Feb  2 18:24 adcirc.gstg.b3.bathy
-rw-r--r--    1 hgops    games          23 Feb  8 19:41 bathy.0.list
-rw-r--r--    1 hgops    games          22 Jan 31 18:29 bathy.1.list
-rwxr--r--    1 nobody   nobody       5395 Oct  3  2008 bathy2all.f90*
-rw-r--r--    1 hgops    games          53 Feb  2 16:22 bathy.2.list
-rw-r--r--    1 hgops    games          53 Feb  2 16:22 bathy.3.list
-rwxr-xr-x    1 hgops    games         104 Feb  7 17:54 bathy.awk.70s_80s.sh*
-rwxr-xr-x    1 hgops    games         104 Feb  7 18:07 bathy.awk.san_francisco_bay.sh*
-rw-r--r--    1 hgops    games     6439719 Feb  8 20:18 fvcom.gflw.b1.bathy
-rw-r--r--    1 hgops    games     6439719 Feb  2 18:32 fvcom.gflw.b2.bathy
-rw-r--r--    1 hgops    games     6439719 Feb  2 18:33 fvcom.gflw.b3.bathy
-rw-r--r--    1 hgops    games     6628299 Feb  8 19:51 fvcom.gstg.b0.bathy
-rw-r--r--    1 hgops    games     6628299 Feb  2 20:56 fvcom.gstg.b1.bathy
-rw-r--r--    1 hgops    games     6628299 Feb  2 18:21 fvcom.gstg.b2.bathy
-rw-r--r--    1 hgops    games     6628299 Feb  2 18:24 fvcom.gstg.b3.bathy
-rw-r--r--    1 hgops    games         388 Feb  8 21:22 grid.mod
-rwxr--r--    1 hgops    games       16385 Feb  2 18:04 interpolate_xyz_to_mesh.f90*
-rwxr--r--    1 hgops    games       15218 Jan 20 15:55 interpolate_xyz_to_mesh.f90.org*
-rwxr--r--    1 hgops    games       20019 Feb  2 20:39 interpolate_xyz_to_mesh_fill.f90*
-rwxr-xr-x    1 hgops    games         472 Feb  8 21:42 interp_xyz_fill.sh*
-rwxr-xr-x    1 hgops    games         442 Feb  8 21:42 interp_xyz.sh*
-rwxr--r--    1 hgops    games     5999512 Jan 31 19:35 ModelGrid.ras.flw.3.grd*
-rwxr--r--    1 hgops    games     6198715 Jan 31 19:35 ModelGrid.ras.stg.1.grd*
drwxr-xr-x    2 hgops    games        4096 Jan 20 16:58 NED_44942250/
-rwxr--r--    1 nobody   nobody   66087697 Jul  7  2010 NED_44942250.zip*
drwxr-xr-x    2 hgops    games        4096 Jan 20 16:41 NED_95312720/
-rwxr--r--    1 nobody   nobody   28187992 Jul  7  2010 NED_95312720.zip*
-rw-r--r--    1 hgops    games        4525 Feb  8 18:39 printfout.gflw.b1.bathy.out
-rw-r--r--    1 hgops    games        4526 Feb  8 21:30 printfout.gstg.b0.bathy.out
-rw-r--r--    1 hgops    games        4526 Feb  2 20:45 printfout.gstg.b1.bathy.out
-rw-r--r--    1 hgops    games        1091 Feb  2 20:06 printout.gflw.b1.bathy.out
-rw-r--r--    1 hgops    games        1189 Feb  2 20:09 printout.gflw.b2.bathy.out
-rw-r--r--    1 hgops    games        1189 Feb  2 20:11 printout.gflw.b3.bathy.out
-rw-r--r--    1 hgops    games        1092 Jan 31 21:50 printout.gstg.b1.bathy.out
-rw-r--r--    1 hgops    games        1190 Feb  2 19:58 printout.gstg.b2.bathy.out
-rw-r--r--    1 hgops    games        1190 Feb  2 18:24 printout.gstg.b3.bathy.out
-rwxr--r--    1 hgops    games    45974143 Jan 31 18:33 san_francisco_bay.txt*
-rw-r--r--    1 hgops    games    33481964 Feb  7 18:07 san_francisco_bay.xyz
-rwxr--r--    1 hgops    games    20859782 Jan 31 18:32 SFbay_Surveys70s_80s.txt*
-rw-r--r--    1 hgops    games    17494984 Feb  7 17:56 SFbay_Surveys70s_80s.xyz
-rwxr--r--    1 hgops    games     5999545 Jan 31 17:59 sfb.flw.grd*
-rwxr--r--    1 hgops    games     6198749 Jan 31 17:59 sfb.stg.grd*
-rw-r--r--    1 hgops    games    54488109 Feb  8 21:19 sounding_SFBe.xyz
-rwxr--r--    1 hgops    games    52600868 Jan 31 18:32 sounding_SFB.xyz*
```

Appendix B. SMS Animation Procedures

To view FVCOM hydrodynamic fields in SMS, one first reformats the fields to ADCIRC fort.* file formats. We considered two-dimensional fields for water surface elevation, 10m winds, and sea level atmospheric pressure. For the three-dimensional fields, surface and bottom levels were written as separate two-dimensional field files.

A program was written to convert the FVCOM netCDF field file to the individual two-dimensional ASCII ADCIRC format files. Field values are written at NSPOOLGE time steps at each grid node. Since FVCOM velocity components are at the element centers, one constructs a node average based on values within all elements connected to the given node.

We summarize the required ADCIRC formats below, which are described more completely in http://adcirc.org/documentv49/Output_file_descript.

Fort.63----Water Surface Elevation (m) File

```
RUNDES, RUNID, AGRID
NDSETSE, NP, DTDP*NSPOOLGE, NSPOOLGE, IRTYPE
TIME, IT
for k=1, NP
k, ETA2(k)
end k loop
```

Fort.64----2D Horizontal Velocity Components (m/s) File

```
RUNDES, RUNID, AGRID
NDSETSE, NP, DTDP*NSPOOLGE, NSPOOLGE, IRTYPE
TIME, IT
for k=1, NP
k, UU(k),VV(k)
end k loop
```

Fort.73----Atmospheric Pressure (mb) File

```
RUNDES, RUNID, AGRID
NDSETSE, NP, DTDP*NSPOOLGE, NSPOOLGE, IRTYPE
TIME, IT
for k=1, NP
k, PR2(k)
end k loop
```

Fort.74----Wind Velocity Components (m/s) File

```
RUNDES, RUNID, AGRID
NDSETSE, NP, DTDP*NSPOOLGE, NSPOOLGE, IRTYPE
TIME, IT
for k=1, NP
k, WVNXOUT(k),WVNYOUT(k)
end k loop
```

Note for salinity and temperature one constructs a separate 2D fort.63 file for the surface and bottom sigma layers. Similarly for the horizontal velocity one constructs a separate 2D fort.64 file for the surface and bottom sigma layers.

To process these files within SMS, grid information is required, so that the sfbm.grd file must be imported along with either the fort.63, fort.64, fort.73 or fort.74 file. The appropriate fort.* file is then converted to HXML format as file datasetn.h5, where n is the number of the current HXML file.

One may then select the appropriate time to display, but first must set the DISPLAY options.
Best options are select nodes and elements and Contours for scalar field or Vectors for vector fields. Within the appropriate tab at the top, one then selects:

Contours: Color Fill, Color Ramp, etc. Note one can also set the legend using the legend options; e.g., WSE (m) DS:TS, Surface salinity (psu) DS:TS.
Vectors: Node spacing for plotting vectors etc. Note one can also set the legend using the legend options; e.g., Surface velocity (m/s) DS:TS.

Note one can plot scalar fields on top of the vector fields for additional analysis. This is useful for water surface elevation and velocity fields and for atmospheric pressure fields and wind fields.

One can then step through the time steps and view the results using the pan and zoom features to explore details of the fields in different regions. Once can then use the Edit/copy to clipboard feature to import these into MS Word or Power Point.

One can also make an animation by selecting the Data tab and clicking film loop. I have used just the default setting, which creates and AVI file in the directory of the imported files. One then goes to next to set the film loop time options. I use days, since the fields are presently at daily intervals over each 15 day simulation. A separate window is opened with film controls at the top. One can set the speed of the frames (frame rate) and advance frame by frame.

For additional controls, one may also use the AVI player embedded within SMS (C:/Program Files/SMS11.0/pavia) or use Windows Media Player to access the *.avi file previously saved.

The *.avi files can be imported into Power Point for presentation by using insert video from file. One then resizes the window and clicks twice to play the video. Power Point uses Windows Media Player.